

NACA
C-560

UNCLASSIFIED



Copy No. 119
ACR No. L5C05

NATIONAL ADVISORY COMMITTEE
FOR AERONAUTICS

~~Summary of Airfoil Data~~

SUMMARY OF AIRFOIL DATA

By Ira H. Abbott, Albert E. von Doenhoff,
and Louis S. Stivers, Jr.

Langley Memorial Aeronautical Laboratory
Langley Field, Va.

Washington
March 1945



UNCLASSIFIED

[REDACTED]

✓

✓

✓

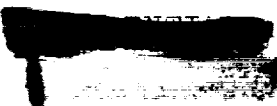
[REDACTED]

TABLE OF CONTENTS

	Page
SUMMARY	1
INTRODUCTION	2
SYMBOLS	3
HISTORICAL DEVELOPMENT	7
DESCRIPTION OF AIRFOILS	10
Method of Combining Mean Lines and Thickness Distributions	10
NACA Four-Digit Series Airfoils	11
Numbering system	11
Thickness distributions	12
Mean lines	12
NACA Five-Digit Series Airfoils	13
Numbering system	13
Thickness distributions	13
Mean lines	13
NACA 1-Series Airfoils	14
Numbering system	14
Thickness distributions	14
Mean lines	14
NACA 6-Series Airfoils	14
Numbering system	14
Thickness distributions	16
Mean lines	16
NACA 7-Series Airfoils	17
Numbering system	17
Thickness distributions	18
THEORETICAL CONSIDERATIONS	19
Pressure Distributions	19
Methods of derivation of thickness distributions	19
Rapid estimation of pressure distributions	23
Numerical examples	27
Effect of camber on pressure distribution	31
Critical Mach Number	32
Moment Coefficients	33
Methods of calculation	33
Numerical examples	33
Angle of Zero Lift	34
Methods of calculation	34
Numerical examples	35
Description of Flow around Airfoils	36



	Page
EXPERIMENTAL CHARACTERISTICS	39
Sources of Data	39
Drag Characteristics of Smooth Airfoils	39
Drag characteristics in low-drag range	39
Drag characteristics outside low-drag range	41
Effects of type of section on drag characteristics	42
Effective aspect ratio	42
Effect of Surface Irregularities on Drag	44
Permissible roughness	44
Permissible waviness	46
Drag with fixed transition	47
Drag with practical construction methods	47
Effects of propeller slipstream and air-plane vibration	49
Lift Characteristics of Smooth Airfoils	50
Two-dimensional data	50
Three-dimensional data	53
Lift Characteristics of Rough Airfoils	53
Two-dimensional data	53
Three-dimensional data	54
Unconservative Airfoils	55
Pitching Moment	57
Critical Speed	57
High-Lift Devices	60
Lateral-Control Devices	60
Leading-Edge Air Intakes	62
Interference	63
APPLICATION TO WING DESIGN	64
Application of Section Data	64
Selection of Root Section	66
Selection of Tip Section	68
CONCLUSIONS	69
APPENDIX - METHODS OF OBTAINING DATA IN THE LANGLEY	
TWO-DIMENSIONAL LOW-TURBULENCE TUNNELS	73
Description of Tunnels	73
List of Symbols	74
Measurement of Lift	77
Measurement of Drag	81
Tunnel-Wall Corrections	82
Correction for Blocking at High Lifts	87
Comparison with Experiment	89





	Page
REFERENCES	90
TABLES	100
FIGURES (NUMBERED)	
SUPPLEMENTARY DATA	
	Supplement page
I.- Basic Thickness Forms	S1
II.- Mean Lines	S40
III.- Airfoil Ordinates	S64
IV.- Predicted Critical Mach Numbers	S79
V.- Aerodynamic Characteristics	S111





ADVANCE CONFIDENTIAL REPORT

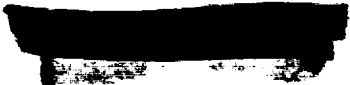
SUMMARY OF AIRFOIL DATA

By Ira H. Abbott, Albert E. von Doenhoff,
and Louis S. Stivers, Jr.

SUMMARY

Recent airfoil data for both flight and wind-tunnel tests have been collected and correlated insofar as possible. The flight data consist largely of drag measurements made by the wake-survey method. Most of the data on airfoil section characteristics were obtained in the Langley two-dimensional low-turbulence pressure tunnel. Detail data necessary for the application of NACA 6-series airfoils to wing design are presented in supplementary figures, together with recent data for the NACA 24-, 44-, and 230-series airfoils. The general methods used to derive the basic thickness forms for NACA 6- and 7-series airfoils and their corresponding pressure distributions are presented. Data and methods are given for rapidly obtaining the approximate pressure distributions for NACA four-digit, five-digit, 6-, and 7-series airfoils.

The report includes an analysis of the lift, drag, pitching-moment, and critical-speed characteristics of the airfoils, together with a discussion of the effects of surface conditions. Available data on high-lift devices are presented. Problems associated with lateral-control devices, leading-edge air intakes, and interference are briefly discussed. The data indicate that the effects of surface condition on the lift and drag characteristics are at least as large as the effects of the airfoil shape and must be considered in airfoil selection and the prediction of wing characteristics. Airfoils permitting extensive laminar flow, such as the NACA 6-series airfoils, have much lower drag coefficients at high speed and cruising lift coefficients than earlier types of airfoils if, and only if, the wing surfaces are sufficiently smooth and fair. The NACA 6-series airfoils also have favorable critical-speed characteristics and do not appear to present unusual problems associated with the application of high-lift and lateral-control devices.



Much of the data given in the NACA Advance Confidential Report entitled "Preliminary Low-Drag-Airfoil and Flap Data from Tests at Large Reynolds Number and Low Turbulence," by Eastman N. Jacobs, Ira H. Abbott, and Milton Davidson, March 1942 has been corrected and included in the present paper, which supersedes the previously published paper.

INTRODUCTION

A considerable amount of airfoil data has been accumulated since the issuance of reference 1, which presented airfoil characteristics obtained in the Langley two-dimensional low-turbulence tunnels. The data have been obtained from tests both in wind tunnels and in flight and include the effects of high-lift devices, surface irregularities, and interference. Some data are also available on the effects of airfoil section on aileron characteristics and on the effects of high Mach numbers on airfoil characteristics. Although a large amount of these data has been published, the scattered nature of the data and the limited objectives of the reports have prevented adequate analysis and interpretation of the results. The purpose of this report is to summarize these data and to correlate and interpret them insofar as possible. In addition, much of the data given in reference 1 has been corrected and is included in the present paper, which supersedes reference 1.

Recent information on the aerodynamic characteristics of NACA airfoils is presented. The historical development of NACA airfoils is briefly reviewed. New data are presented that permit the rapid calculation of the approximate pressure distributions for the older NACA four-digit and five-digit airfoils by the same methods used for the NACA 6-series airfoils. The general methods used to derive the basic thickness forms for NACA 6- and 7-series airfoils together with their corresponding pressure distributions are presented. Detail data necessary for the application of the airfoils to wing design are presented in supplementary figures placed at the end of the paper. The report includes an analysis of the lift, drag, pitching-moment, and critical-speed characteristics of the airfoils, together with a discussion of the effects of surface conditions. Available data on high-lift devices are presented. Problems associated with lateral-

control devices, leading-edge air intakes, and interference are briefly discussed, together with aerodynamic problems of application.

The report has been prepared in loose-leaf form to facilitate additions or revisions. As new data become available, additional or replacement pages will be forwarded to holders of the report for insertion in their copies. Numbered figures are used to illustrate the text and to present miscellaneous data. Supplementary figures and tables are not numbered but are conveniently arranged at the end of the report according to the numerical designation of the airfoil section within the following headings:

I.- Basic thickness forms

II.- Mean lines

III.- Airfoil ordinates

IV.- Predicted critical Mach numbers

V.- Aerodynamic characteristics

These supplementary figures and tables present the basic data for the airfoils. New figures of this type will be forwarded as soon as data become available.

SYMBOLS

- A aspect ratio
- A_n, B_n Fourier series coefficients
- a mean-line designation, fraction of chord from leading edge over which design load is uniform; in derivation of thickness distributions, basic length usually considered unity
- b wing span
- b_{f_i} flap span, inboard
- b_{f_o} flap span, outboard

C_D	drag coefficient
$C_{D_{L=0}}$	drag coefficient at zero lift
C_L	lift coefficient
ΔC_{L_f}	increment of maximum lift caused by flap deflection
c	chord
c_a	aileron chord
c_d	section drag coefficient
$c_{d_{min}}$	minimum section drag coefficient
c_{f_i}	flap chord, inboard
c_{f_o}	flap chord, outboard
$\frac{c_f}{c}$	flap-chord ratio
C_H	section aileron hinge-moment coefficient $\left(\frac{h}{q_0 c^2}\right)$
ΔC_H	increment of aileron hinge-moment coefficient at constant lift
$\Delta C_H \delta$	hinge-moment parameter
c_l	section lift coefficient
c_{l_i}	design section lift coefficient
$c_{m_{a.c.}}$	moment coefficient about aerodynamic center
$c_{m_c/4}$	moment coefficient about quarter-chord point
c_n	section normal-force coefficient
D	drag
ΔH	loss of total pressure
H_0	free-stream total pressure
h	section aileron hinge moment

h_e	exit height
k	constant
L	lift
M	Mach number
M_{cr}	critical Mach number
O_U, O_L	typical points on upper and lower surfaces of airfoil
P	pressure coefficient $\left(\frac{p - p_o}{q_o} \right)$
P_{cr}	critical pressure coefficient
P_R	resultant pressure coefficient; difference between local upper- and lower-surface pressure coefficients
p	local static pressure; also, angular velocity in roll in $pb/2V$
p_o	free-stream static pressure
$pb/2V$	helix angle of wing tip
q_o	free-stream dynamic pressure
R	Reynolds number
R_{cr}	critical Reynolds number
S	pressure coefficient $\left(\frac{H_o - p}{q_o} \right)$
t_1	first airfoil thickness ratio
t_2	second airfoil thickness ratio
V	free-stream velocity
V_i	inlet velocity
v	local velocity
Δv	increment of local velocity

Δv_a	increment of local velocity caused by additional type of load distribution
$\left(\frac{v}{V}\right)_{t_1}$	velocity ratio corresponding to thickness t_1
$\left(\frac{v}{V}\right)_{t_2}$	velocity ratio corresponding to thickness t_2
x	distance along chord
x_c	mean-line abscissa
x_L	abscissa of lower surface
x_U	abscissa of upper surface
$\left(\frac{x}{c}\right)_{tr}$	chordwise position of transition
y	distance perpendicular to chord
y_c	mean-line ordinate
y_L	ordinate of lower surface
y_t	ordinate of symmetrical thickness distribution
y_U	ordinate of upper surface
z	complex variable in circle plane
z'	complex variable in near-circle plane
α	angle of attack
$\frac{\Delta \alpha_o}{\Delta \delta}$	section aileron effectiveness parameter, ratio of change in section angle of attack to increment of aileron deflection at a constant value of lift coefficient
α_{l_0}	angle of zero lift
α_o	section angle of attack
$\Delta \alpha_o$	increment of section angle of attack
α_i	section angle of attack corresponding to design lift coefficient

- δ flap or aileron deflection; down deflection is positive
- δ_{f_i} flap deflection, inboard
- δ_{f_o} flap deflection, outboard
- ϵ airfoil parameter ($\phi - \theta$)
- ϵ_{TE} value of ϵ at trailing edge
- ζ complex variable in airfoil plane
- θ angular coordinate of z' ; also, angle whose tangent is slope of mean line
- λ taper ratio $\left(\frac{\text{Tip chord}}{\text{Root chord}} \right)$
- τ turbulence factor $\left(\frac{\text{Effective Reynolds number}}{\text{Test Reynolds number}} \right)$
- ϕ angular coordinate of z
- ψ airfoil parameter determining radial coordinate of z
- ψ_0 average value of ψ , $\left(\frac{1}{2\pi} \int_0^{2\pi} \psi d\phi \right)$

HISTORICAL DEVELOPMENT

The development of types of NACA airfoils now in common use was started in 1929 with a systematic investigation of a family of airfoils in the Langley variable-density tunnel. Airfoils of this family were designated by numbers having four digits, such as the NACA 4412 airfoil. All airfoils of this family had the same basic thickness distribution (reference 2), and the amount and type of camber was systematically varied to produce the family of related airfoils. This investigation of the NACA airfoils of the four-digit series produced airfoil sections having higher maximum lift coefficients and lower minimum drag coefficients than those of sections developed before that time. The investigation also provided information on the changes in aerodynamic characteristics resulting from variations of geometry of the mean line and thickness ratio (reference 2).

The investigation was extended in references 3 and 4 to include airfoils with the same thickness distribution but with positions of the maximum camber far forward on the airfoil. These airfoils were designated by numbers having five digits, such as the NACA 23012 airfoil. Some airfoils of this family showed favorable aerodynamic characteristics except for a large sudden loss in lift at the stall.

Although these investigations were extended to include a limited number of airfoils with varied thickness distributions (references 2 and 4 to 7), no extensive investigations of thickness distribution were made. Comparison of experimental drag data at low lift coefficients with the skin-friction coefficients for flat plates indicated that nearly all of the profile drag under such conditions was attributable to skin friction. It was therefore apparent that any pronounced reduction of the profile drag must be obtained by a reduction of the skin friction through increasing the relative extent of the laminar boundary layer.

Decreasing pressures in the direction of flow and low air-stream turbulence were known to be favorable for laminar flow. An attempt was accordingly made to increase the relative extent of laminar flow by the development of airfoils having favorable pressure gradients over a greater proportion of the chord than the airfoils developed in references 2, 3, 4, and 7. The actual attainment of extensive laminar boundary layers at large Reynolds numbers was a previously unsolved experimental problem requiring the development of new test equipment with very low air-stream turbulence. This work was greatly encouraged by the experiments of Jones (reference 8), who demonstrated the possibility of obtaining extensive laminar layers in flight at relatively large Reynolds numbers. Uncertainty with regard to factors affecting separation of the turbulent boundary layer required experiments to determine the possibility of making the rather sharp pressure recoveries required over the rear portion of the new type of airfoil.

New wind tunnels were designed specifically for testing airfoils under conditions closely approaching flight conditions of air-stream turbulence and Reynolds number. The resulting wind tunnels, the Langley two-dimensional low-turbulence tunnel (LTT) and the Langley two-dimensional low-turbulence pressure tunnel (TDT),

[REDACTED]

and the methods used for obtaining and correcting data are briefly described in the appendix. In these tunnels the models completely span the comparatively narrow test sections; two-dimensional flow is thus provided, which obviates difficulties previously encountered in obtaining section data from tests of finite-span wings and in correcting adequately for support interference (reference 9).

Difficulty was encountered in attempting to design airfoils having desired pressure distributions because of the lack of adequate theory. The Theodorsen method (reference 10), as ordinarily used for calculating the pressure distributions about airfoils, was not sufficiently accurate near the leading edge for prediction of the local pressure gradients. In the absence of a suitable theoretical method, the 9-percent-thick symmetrical airfoil of the NACA 16-series (reference 11) was obtained by empirical modification of the previously used thickness distributions (reference 5). These NACA 16-series sections represented the first family of the low-drag high-critical-speed sections.

Successive attempts to design airfoils by approximate theoretical methods led to families of airfoils designated NACA 2- to 5-series sections (references 1 and 12). Experience with these sections showed that none of the approximate methods tried was sufficiently accurate to show correctly the effect of changes in profile near the leading edge. Wind-tunnel and flight tests of these airfoils showed that extensive laminar boundary layers could be maintained at comparatively large values of the Reynolds number if the airfoil surfaces were sufficiently fair and smooth. These tests also provided qualitative information on the effects of the magnitude of the favorable pressure gradient, leading-edge radius, and other shape variables. The data also showed that separation of the turbulent boundary layer over the rear of the section, especially with rough surfaces, limited the extent of laminar layer for which the airfoils should be designed. The airfoils of these early families generally showed relatively low maximum lift coefficients and, in many cases, were designed for a greater extent of laminar flow than is practical. It was learned that, although sections designed for an excessive extent of laminar flow gave extremely low drag coefficients near the design lift coefficient when smooth, the drag of such sections became unduly large when rough, particularly at lift

coefficients higher than the design lift. These families of airfoils are accordingly considered obsolete.

The NACA 6-series basic thickness forms were derived by new and improved methods described herein in the section "Methods of Derivation of Thickness Distributions," in accordance with design criteria established with the objective of obtaining desirable drag, critical Mach number, and maximum-lift characteristics. The present report deals largely with the characteristics of these sections. The development of the NACA 7-series family has also been started. This family of airfoils is characterized by a greater extent of laminar flow on the lower than on the upper surface. These sections permit low pitching-moment coefficients with moderately high design lift coefficients at the expense of some reduction in maximum lift and critical Mach number.

Acknowledgement is gratefully expressed for the expert guidance and many original contributions of Mr. Eastman N. Jacobs, who supervised this work.

DESCRIPTION OF AIRFOILS

Method of Combining Mean Lines and Thickness Distributions

The cambered airfoil sections of all NACA families considered herein are obtained by combining a mean line and a thickness distribution. The necessary geometric data and some theoretical aerodynamic data for the mean lines and thickness distributions may be obtained from the supplementary figures by the methods described for each family of airfoils.

The process for combining a mean line and a thickness distribution to obtain the desired cambered airfoil section is illustrated in figure 1. The leading and trailing edges are defined as the forward and rearward extremities, respectively, of the mean line. The chord line is defined as the straight line connecting the leading and trailing edges. Ordinates of the cambered airfoil are obtained by laying off the thickness distribution perpendicular to the mean line. The abscissas, ordinates, and slopes of the mean line are designated as x_c , y_c , and $\tan \theta$, respectively. If x_U and y_U represent,

respectively, the abscissa and ordinate of a typical point of the upper surface of the airfoil and y_t is the ordinate of the symmetrical thickness distribution at chordwise position x , the upper-surface coordinates are given by the following relations:

$$x_U = x - y_t \sin \theta \quad (1)$$

$$y_U = y_c + y_t \cos \theta \quad (2)$$

The corresponding expressions for the lower-surface coordinates are

$$x_L = x + y_t \sin \theta \quad (3)$$

$$y_L = y_c - y_t \cos \theta \quad (4)$$

The center for the leading-edge radius is found by drawing a line through the end of the chord at the leading edge with the slope equal to the slope of the mean line at that point and laying off a distance from the leading edge along this line equal to the leading-edge radius. This method of construction causes the cambered airfoils to project slightly forward of the leading-edge point. Because the slope at the leading edge is theoretically infinite for the mean lines having a theoretically finite load at the leading edge, the slope of the radius through the end of the chord for such mean lines is usually taken as the slope of the mean line at $\frac{x}{c} = 0.005$. This procedure is justified by the manner in which the slope increases to the theoretically infinite value as x/c approaches 0. The slope increases slowly until very small values of x/c are reached. Large values of the slope are thus limited to values of x/c very close to 0 and may be neglected in practical airfoil design.

Tables of ordinates are included in the supplementary data for all airfoils for which standard characteristics are presented.

NACA Four-Digit-Series Airfoils

Numbering system.- The numbering system for the NACA airfoils of the four-digit series (reference 2) is based

on the airfoil geometry. The first integer indicates the maximum value of the mean-line ordinate y_c in percent of the chord. The second integer indicates the distance from the leading edge to the location of the maximum camber in tenths of the chord. The last two integers indicate the airfoil thickness in percent of the chord. Thus, the NACA 2415 airfoil has 2-percent camber at 0.4 of the chord from the leading edge and is 15 percent thick.

The first two integers taken together define the mean line, for example, the NACA 24 mean line. Symmetrical sections are designated by zeros for the first two integers, as in the case of the NACA 0015 airfoil and the last two integers represent the thickness distribution for the family of airfoils.

Thickness distributions.- Data for the NACA 0006, 0009, 0012, 0015, 0018, 0021, and 0024 thickness distributions are presented in the supplementary figures. Ordinates for intermediate thicknesses may be obtained correctly by scaling the tabulated ordinates in proportion to the thickness ratio (reference 2). The leading-edge radius varies as the square of the thickness ratio. Values of $(v/V)^2$, which is equivalent to the low-speed pressure distribution, and of v/V are also presented. These data were obtained by Theodorsen's method (reference 10). Values of the velocity increments $\Delta v_a/V$ induced by changing angle of attack (see section "Rapid Estimation of Pressure Distribution") are also presented for an additional lift coefficient of approximately unity. Values of the velocity ratio v/V for intermediate thickness ratios may be obtained approximately by linear scaling of the velocity increments obtained from the tabulated values of v/V for the nearest thickness ratio; thus,

$$\left(\frac{v}{V}\right)_{t_2} = \left[\left(\frac{v}{V}\right)_{t_1} - 1 \right] \frac{t_2}{t_1} + 1 \quad (5)$$

Values of the velocity-increment ratio $\Delta v_a/V$ may be obtained for intermediate thicknesses by interpolation.

Mean lines.- Data for the NACA 62, 63, 64, 65, 66, and 67 mean lines are presented in the supplementary figures. The data presented include the mean-line

ordinates y_c , the slope dy_c/dx , the design lift coefficient c_{l_i} and the corresponding design angle of attack α_i , the moment coefficient $c_{m_c/4}$, the resultant pressure coefficient P_R , and the velocity ratio $\Delta v/V$. The theoretical aerodynamic characteristics were obtained from thin-airfoil theory. All tabulated values for each mean line, accordingly, vary linearly with the maximum ordinate y_c , and data for similar mean lines with different amounts of camber within the usual range may be obtained simply by scaling the tabulated values. Data for the NACA 22 mean line may thus be obtained by multiplying the data for the NACA 62 mean line by the ratio 2:6, and for the NACA 44 mean line by multiplying the data for the NACA 64 mean line by the ratio 4:6.

NACA Five-Digit-Series Airfoils

Numbering system.- The numbering system for airfoils of the NACA five-digit series is based on a combination of theoretical aerodynamic characteristics and geometric characteristics (references 3 and 4). The first integer indicates the amount of camber in terms of the relative magnitude of the design lift coefficient; the design lift coefficient in tenths is thus three-halves of the first integer. The second and third integers together indicate the distance from the leading edge to the location of the maximum camber; this distance in percent of the chord is one-half the number represented by these integers. The last two integers indicate the airfoil thickness in percent of the chord. The NACA 23012 airfoil thus has a design lift coefficient of approximately 0.3, has its maximum camber at 15 percent of the chord, and has a thickness ratio of 12 percent.

Thickness distributions.- The thickness distributions for airfoils of the NACA five-digit series are the same as those for airfoils of the NACA four-digit series.

Mean lines.- Data for the NACA 210, 220, 230, 240, and 250 mean lines are presented in the supplementary figures in the same form as for the mean lines given herein for the four-digit series. All tabulated values for each mean line vary linearly with the maximum ordinate or with the design lift coefficient. Thus, data for the NACA 430 mean line may be obtained by

multiplying the data for the NACA 230 mean line by the ratio 4:2 and for the NACA 640 mean line by multiplying the data for the NACA 240 mean line by the ratio 6:2.

NACA 1-Series Airfoils

Numbering system.- The NACA 1-series airfoils are designated by a five-digit number - as, for example, the NACA 16-212 section. The first integer represents the series designation. The second integer indicates the distance in tenths of the chord from the leading edge to the position of minimum pressure for the symmetrical section at zero lift. The first number following the dash indicates the amount of camber expressed in terms of the design lift coefficient in tenths, and the last two numbers together indicate the thickness in percent of the chord. The commonly used sections of this family have minimum pressure at 0.6 of the chord from the leading edge and are usually referred to as the NACA 16-series sections.

Thickness distributions.- Data for the NACA 16-006, 16-009, 16-012, 16-015, 16-018, and 16-021 thickness distributions (reference 11) are presented in the supplementary figures. These data are similar in form to those for airfoils of the NACA four-digit series, and data for intermediate thickness ratios may be obtained in the same manner.

Mean lines.- The NACA 16-series airfoils as commonly used are cambered with a mean line of the uniform-load type ($a = 1.0$), which is described under the section for the NACA 6-series airfoils that follows. If any other type of mean line is used, this fact should be stated in the airfoil designation.

NACA 6-Series Airfoils

Numbering system.- The NACA 6-series airfoils are usually designated by a six-digit number together with a statement showing the type of mean line used. For example, in the designation NACA 65,3-218, $a = 0.5$, the "6" is the series designation. The "5" denotes the chordwise position of minimum pressure in tenths of the chord behind the leading edge for the basic symmetrical

section at zero lift. The "3" following the comma gives the range of lift coefficient in tenths above and below the design lift coefficient in which favorable pressure gradients exist on both surfaces. The "2" following the dash gives the design lift coefficient in tenths. The last two digits indicate the airfoil thickness in percent of the chord. The designation "a = 0.5" shows the type of mean line used. When the mean-line designation is not given, it is understood that the uniform-load mean line (a = 1.0) has been used.

When the mean line used is obtained by combining more than one mean line, the design lift coefficient used in the designation is the algebraic sum of the design lift coefficients of the mean lines used, and the mean lines are described in the statement following the number as in the following case:

$$\text{NACA } 65,3-218 \left\{ \begin{array}{l} a = 0.5, \quad c_{l_1} = 0.3 \\ a = 1.0, \quad c_{l_1} = -0.1 \end{array} \right\}$$

Airfoils having a thickness distribution obtained by linearly increasing or decreasing the ordinates of one of the originally derived thickness distributions are designated as in the following example:

$$\text{NACA } 65(318)-217, \quad a = 0.5$$

The significance of all of the numbers except those in the parentheses is the same as before. The first number and the last two numbers enclosed in the parentheses denote, respectively, the low-drag range and the thickness in percent of the chord of the originally derived thickness distribution.

The more recent NACA 6-series airfoils are derived as members of thickness families having a simple relationship between the conformal transformations for airfoils of different thickness ratios but having minimum pressure at the same chordwise position. These airfoils are distinguished from the earlier individually derived airfoils by writing the number indicating the low-drag range as a subscript; for example,

$$\text{NACA } 65_3-218, \quad a = 0.5$$

Ordinates for the basic thickness distributions designated by a subscript are slightly different from those for the corresponding individually derived thickness distributions. As before, if the ordinates of the basic thickness distribution have been changed by a factor, the low-drag range and thickness ratio of the original thickness distribution are enclosed in parentheses as follows:

NACA 65(318)-217, $a = 0.5$

If the design lift coefficient in tenths or the airfoil thickness in percent of chord are not whole integers, the numbers giving these quantities are usually enclosed in parentheses as in the following designation:

NACA 65(318)-(1.5)(16.5), $a = 0.5$

Some early experimental airfoils are designated by the insertion of the letter x immediately preceding the hyphen as in the designation 66,2x-116.

Thickness distributions.- Data for available NACA 6-series thickness forms are presented in the supplementary figures. These data are comparable with the similar data for airfoils of the NACA four-digit series, except that ordinates for intermediate thicknesses may not be correctly obtained by scaling the tabulated ordinates proportional to the thickness ratio. This method of changing the ordinates by a factor will, however, produce shapes satisfactorily approximating members of the family if the change in thickness ratio is small. Values of v/V and $\Delta v_a/V$ for intermediate thickness ratios may be approximated as described for the NACA four-digit series.

Mean lines.- The mean lines commonly used with the NACA 6-series airfoils produce a uniform chordwise loading from the leading edge to the point $\frac{x}{c} = a$ and a linearly decreasing load from this point to the trailing edge. Data for NACA mean lines with values of a equal to 0, 0.1, 0.2, 0.3, 0.4, 0.5, 0.6, 0.7, 0.8, 0.9, and 1.0 are presented in the supplementary figures. The ordinates were computed by the following formula, which represents a simplification of the original expression for mean-line ordinates given in reference 12:

$$\frac{y_c}{c} = \frac{c_{l_1}}{2\pi(a+1)} \left\{ \frac{1}{1-a} \left[\frac{1}{2} \left(a - \frac{x}{c} \right)^2 \log_e \left| a - \frac{x}{c} \right| \right. \right. \\ \left. \left. - \frac{1}{2} \left(1 - \frac{x}{c} \right)^2 \log_e \left(1 - \frac{x}{c} \right) + \frac{1}{4} \left(1 - \frac{x}{c} \right)^2 - \frac{1}{4} \left(a - \frac{x}{c} \right)^2 \right] \right. \\ \left. - \frac{x}{c} \log_e \frac{x}{c} + g - h \frac{x}{c} \right\} \quad (6)$$

where

$$g = -\frac{1}{1-a} \left[a^2 \left(\frac{1}{2} \log_e a - \frac{1}{4} \right) + \frac{1}{4} \right]$$

$$h = \frac{1}{1-a} \left[\frac{1}{2} (1-a)^2 \log_e (1-a) - \frac{1}{4} (1-a)^2 \right] + g$$

The data are presented for a design lift coefficient c_{l_1} equal to unity. All tabulated values vary directly with the design lift coefficient. Corresponding data for similar mean lines with other design lift coefficients may accordingly be obtained simply by multiplying the tabulated values by the desired design lift coefficient.

In order to camber NACA 6-series airfoils, mean lines are usually used having values of a equal to or greater than the distance from the leading edge to the location of minimum pressure for the selected thickness distribution at zero lift. For special purposes, load distributions other than those corresponding to the simple mean lines may be obtained by combining two or more types of mean line having positive or negative values of the design lift coefficient. The geometric and aerodynamic characteristics of such combinations may be obtained by algebraic addition of the values for the component mean lines.

NACA 7-Series Airfoils

Numbering system.—The NACA 7-series airfoils are designated by a number of the following type (reference 13):

NACA 747A315

CONFIDENTIAL

The first number "7" indicates the series number. The second number "4" indicates the extent over the upper surface, in tenths of the chord from the leading edge, of the region of favorable pressure gradient at the design lift coefficient. The third number "7" indicates the extent over the lower surface, in tenths of the chord from the leading edge, of the region of favorable pressure gradient at the design lift coefficient. The significance of the last group of three numbers is the same as for the previous NACA 6-series airfoils. The letter "A" which follows the first three numbers is a serial letter to distinguish different airfoils having parameters that would correspond to the same numerical designation. For example, a second airfoil having the same extent of favorable pressure gradient over the upper and lower surfaces, the same design lift coefficient, and the same maximum thickness as the original airfoil but having a different mean-line combination or thickness distribution would have the serial letter "B". Mean lines used for the NACA 7-series airfoils are obtained by combining two or more of the previously described mean lines. A list of the thickness distributions and mean lines used to form these airfoils are presented in table I. The extra columns in table I have been provided to facilitate the listing of additional information for subsequent airfoils. The basic thickness distribution is given a designation similar to those of the final cambered airfoils. For example, the basic thickness distribution for the NACA 747A315 and 747A415 airfoils is given the designation NACA 747A015 even though minimum pressure occurs at 0.4c on both upper and lower surfaces at zero lift. Combination of this thickness distribution with the mean lines listed in table I for the NACA 747A315 airfoil changes the pressure distribution to the desired type as shown in figure 2.

Thickness distributions.- Data for available NACA 7-series thickness distributions are presented in the supplementary figures. These thickness distributions are individually derived and do not form thickness families. The thickness ratio may, however, be changed a moderate amount - say 2 or 3 percent - by multiplying the tabulated ordinates by a suitable factor without seriously altering their characteristic features. Values of $(v/v)^2$ and of v/v for thinner or thicker thickness distributions may be approximated by the method of equation (5). If the change in thickness ratio is

small, tabulated values of $\Delta v_a/V$ may be applied directly with reasonable accuracy.

THEORETICAL CONSIDERATIONS

Pressure Distributions

A knowledge of the pressure distribution over an airfoil is desirable for structural design and for estimation of the critical Mach number and moment coefficient if tests are not available. The pressure distribution also exerts a strong or predominant influence on the boundary-layer flow and, hence, on the airfoil characteristics. It is therefore usually advisable to relate the airfoil characteristics to the pressure distribution rather than directly to the airfoil geometry.

Methods of derivation of thickness distributions.-
As mentioned in the section "Historical Development," the basic symmetrical thickness distributions of the NACA 6- and 7-series airfoils, together with their corresponding pressure distributions, are derived by means of conformal transformations. The transformations used to relate the known flow about a circle to that about an airfoil section were developed by Theodorsen in reference 10. Figure 3 shows schematically the significance of the various phases of the process.

The circle about which the flow is originally calculated has its center at the origin and a radius of ae^{ψ_0} . The equation of this circle in complex coordinates is

$$z = ae^{\psi_0 + i\phi} \quad (7)$$

where

- z complex variable in circle plane
- ϕ angular coordinate of z .
- a basic length usually considered unity
- ψ_0 constant determining radius of circle

This true circle is transformed into an arbitrary, almost circular curve by the relation

$$\frac{z'}{z} = e^{(\psi - \psi_0) + i(\theta - \phi)} \quad (8)$$

The equation of the almost circular curve is

$$z' = ae^{\psi + i\theta} \quad (9)$$

where

z' complex variable in near-circle plane

ae^{ψ} radial coordinate of z'

θ angular coordinate of z'

In order for the transformation (8) to be conformal, it is necessary that the quantity $(\theta - \phi)$ (given the symbol $-\epsilon$) be the conjugate function of $(\psi - \psi_0)$; that is, if ϵ is represented by a Fourier series of the form

$$\epsilon = \sum_1^{\infty} A_n \sin n\phi - \sum_1^{\infty} B_n \cos n\phi$$

then $(\psi - \psi_0)$ is given by the relation

$$(\psi - \psi_0) = \sum_1^{\infty} A_n \cos n\phi + \sum_1^{\infty} B_n \sin n\phi$$

This relationship indicates that, if the function $\epsilon(\phi)$ is given, $(\psi - \psi_0)$ can be calculated as a function of ϕ . Means of performing this calculation are presented in reference 14. The transformation relating the almost circular curve to the airfoil shape is

$$\zeta = z' + \frac{a^2}{z'} \quad (10)$$

where ζ is the complex variable in the airfoil plane. The coordinates of the airfoil x and y are the real and imaginary parts of ζ , respectively. These coordinates are given by the relations

$$x = 2a \cosh \psi \cos \theta \quad (11)$$

$$y = 2a \sinh \psi \sin \theta \quad (12)$$

The velocity distribution in terms of the airfoil parameters ψ and ϵ is given exactly for perfect fluid flow by the expression

$$\frac{v}{V} = \frac{\sin(\alpha_0 + \theta) + \sin(\alpha_0 + \epsilon_{TE})e^{\psi_0}}{\sqrt{(\sinh^2 \psi + \sin^2 \theta) \left[\left(1 - \frac{d\epsilon}{d\theta}\right)^2 + \left(\frac{d\psi}{d\theta}\right)^2 \right]}} \quad (13)$$

where

v local velocity over surface of airfoil

V free-stream velocity

α_0 section angle of attack

ψ_0 average value of ψ $\left(\frac{1}{2\pi} \int_0^{2\pi} \psi d\theta \right)$

ϵ_{TE} value of ϵ at trailing edge

The basic symmetrical shapes were derived by assuming suitable values of $d\epsilon/d\theta$ as a function of θ . These values were chosen on the basis of previous experience and are subject to the conditions that

$$\int_0^\pi \frac{d\epsilon}{d\theta} = 0$$

and $d\epsilon/d\theta$ at θ is equal to $d\epsilon/d\theta$ at $-\theta$. These conditions are necessary for obtaining closed symmetrical shapes. Values of $\epsilon(\theta)$ were obtained simply by integrating $\frac{d\epsilon}{d\theta} d\theta$. Values of $\psi(\theta)$ were found by

obtaining the conjugate of the curve of $\epsilon(\theta)$ and adding a value ψ_0 sufficient to make the value of ψ equal to zero at $\theta = \pi$. This condition assures a sharp trailing-edge shape.

Inasmuch as small changes in the velocity distribution at any point of the surface are approximately proportional to $1 + \frac{d\epsilon}{d\theta}$ (see reference 15), the initially assumed values of $d\epsilon/d\theta$ were altered by a process of successive approximations until the desired type of velocity distribution was obtained. After the final values of ψ and ϵ were obtained, the ordinates of the basic thickness distribution were computed by equations (11) and (12).

When these computations were made, it appeared that there was an optimum value of the leading-edge radius dependent upon the airfoil thickness and the position of minimum pressure. If the leading-edge radius was too small, a premature peak in the pressure distribution occurred in the immediate vicinity of the leading edge as the angle of attack was increased. If the leading-edge radius was too large, a premature peak occurred a few percent of the chord behind the leading edge. With the correct leading-edge radius, the pressure distribution became nearly flat over the forward portion of the airfoil before the normal leading-edge peak formed at the higher lift coefficients. Curves of the parameters ψ , ϵ , $d\psi/d\theta$, $d\epsilon/d\theta$ plotted against θ for the NACA 643-018 airfoil section are given in figure 4.

Experience has shown that, when the thickness ratio of an originally derived basic form was increased merely by multiplying all the ordinates by a constant factor, an unnecessarily large decrease in the critical speed of the resulting section occurred. Reducing the thickness ratio in a similar manner caused an unnecessarily large decrease in the low-drag range. For this reason, each of the earlier NACA 6-series sections was individually derived. It was later found that it was possible to derive basic airfoil parameters ψ and ϵ that could be multiplied by a constant factor to obtain airfoils of various thickness ratios, without having the aforementioned limitations in the resulting sections. Each of the more recent families of NACA 6-series airfoils, in which numerical subscripts are used in the designation, having minimum pressure at a given chordwise position

was obtained by scaling up and down the basic values of the airfoil parameters ψ and ϵ .

Theoretical pressure distributions (indicated by $(\frac{v}{V})^2$) for a family of NACA 65-series airfoils covering a range of thickness ratios are given in figure 5(a). This figure shows the typical increase in the magnitude of the favorable pressure gradient, increase in maximum velocity over the surface, and increase in the relative pressure recovery over the rear portion of the airfoil with increase in thickness ratio. Figure 5(b) shows the pressure distribution for a series of basic thickness forms having a thickness ratio of 0.15 and having minimum pressure at various chordwise positions. The value of the minimum pressure coefficient is seen to decrease and the magnitude of the pressure recovery over the rear portion of the airfoil to increase with rearward movement of the point of minimum pressure.

The pressure distribution for one of the basic symmetrical thickness distributions at various lift coefficients is shown in figure 6. At zero lift the pressure distributions over the upper and lower surfaces are the same. As the lift coefficient is increased, the slope of the pressure distribution over the forward portion of the upper surface decreases until it becomes flat at a lift coefficient of 0.22 (the end of the low-drag range). As the lift coefficient is increased beyond this value, the usual peak in the pressure distribution forms at the leading edge.

Rapid estimation of pressure distributions.- In the discussion that follows, the term "pressure distribution" is used to signify the distribution of the static pressures on the upper and lower surfaces of the airfoil along the chord. The term "load distribution" is used to signify the distribution along the chord of the normal force resulting from the difference in pressure on the upper and lower surfaces.

The pressure distribution about any airfoil in potential flow may be calculated accurately by a generalization of the methods of the previous section. Although this method is not unduly laborious, the computations required are too long to permit quick and easy calculations for large numbers of airfoils. The need for a simple method of quickly obtaining pressure distributions with engineering accuracy has led to the

development of a method (reference 16) combining features of thin- and thick-airfoil theory. This simple method makes use of previously calculated characteristics of a limited number of mean lines and thickness distributions that may be combined to form large numbers of airfoils.

Thin-airfoil theory (references 17 to 19) shows that the load distribution of a thin airfoil may be considered to consist of: (1) a basic distribution at the ideal angle of attack and (2) an additional distribution proportional to the angle of attack as measured from the ideal angle of attack.

The first load distribution is a function only of the shape of the thin airfoil, or (if the thin airfoil is considered to be a mean line) of the mean-line geometry. Integration of this load distribution along the chord results in a normal-force coefficient which, at small angles of attack, is substantially equal to a lift coefficient c_{l_i} , which is designated the ideal or design lift coefficient. If, moreover, the camber of the mean line is changed by multiplying the mean-line ordinates by a constant factor, the resulting load distribution, the ideal or design angle of attack α_i and the design lift coefficient c_{l_i} may be obtained simply by multiplying the original values by the same factor. The characteristics of a large number of mean lines are presented in both graphical and tabular form in the supplementary figures. The load-distribution data are presented both in the form of the resultant pressure coefficient P_R and in the form of the corresponding velocity-increment ratios $\Delta v/V$. For positive design lift coefficients, these velocity-increment ratios are positive on the upper surface and negative on the lower surface; the opposite is true for negative design lift coefficients.

The second load distribution, which results from changing the angle of attack, is designated herein the "additional load distribution" and the corresponding lift coefficient is designated the "additional lift coefficient." This additional load distribution contributes no moment about the quarter-chord point and, according to thin-airfoil theory, is independent of the airfoil geometry except for angle of attack. The additional load distribution obtained from thin-airfoil theory is of limited practical application, however,

because this simple theory leads to infinite values of the velocity at the leading edge. This difficulty is obviated by the exact thick-airfoil theory (reference 10), which also shows that the additional load distribution is neither completely independent of the airfoil shape nor exactly a linear function of the lift coefficient. For this reason, the additional load distribution has been calculated by the methods of reference 10 for each of the thickness distributions presented in the supplementary figures. These data are presented in the form of velocity-increment ratios $\Delta v_a/V$ corresponding to an additional lift coefficient of approximately unity. For positive additional lift coefficients, these velocity-increment ratios are positive on the upper surface and negative on the lower surface; the opposite is true for negative additional lift coefficients.

In addition to the pressure distributions associated with these two load distributions, another pressure distribution exists which is associated with the basic symmetrical thickness form or thickness distribution of the airfoil. This pressure distribution has been calculated by the methods described in the previous section for the condition of zero lift and is presented in the supplementary figures as $\left(\frac{v}{V}\right)^2$, which is equivalent at low Mach numbers to the pressure coefficient S , and as the local velocity ratio v/V . This local velocity ratio is always positive and is the same for corresponding points on the upper and lower surfaces of the thickness form.

The velocity distribution about the airfoil is thus considered to be composed of three separate and independent components as follows:

- (1) The distribution corresponding to the velocity distribution over the basic thickness form at zero angle of attack
- (2) The distribution corresponding to the design load distribution of the mean line
- (3) The distribution corresponding to the additional load distribution associated with angle of attack

The velocity-increment ratios $\Delta v/V$ and $\Delta v_a/V$ corresponding to components (2) and (3) are added to the velocity ratio corresponding to component (1) to obtain the total velocity at one point, from which the pressure coefficient S is obtained; thus,

$$S = \left(\frac{v}{V} \pm \frac{\Delta v}{V} \pm \frac{\Delta v_a}{V} \right)^2 \quad (14)$$

When this formula is used, values of the ratios corresponding to one value of x are added together and the resulting value of the pressure coefficient S is assigned to the airfoil surface at the same value of x .

The values of v/V and of $\Delta v/V$ in equation (14) should, of course, correspond to the airfoil geometry. Methods of obtaining the proper values of these ratios from the values tabulated in the supplementary figures are presented in the previous section "Description of Airfoils."

When the ratio $\Delta v_a/V$ has the value of zero, the resulting pressure coefficient S will correspond approximately to the design lift coefficient c_{l_1} of the mean line, and the lift coefficient may be assigned this value as a first approximation. If the pressure-distribution diagram is integrated, however, the value of c_l will be found to be greater than c_{l_1} by an amount dependent on the thickness ratio of the basic thickness form.

The pressure distribution will usually be desired at some specified lift coefficient not corresponding to c_{l_1} . For this purpose the ratio $\Delta v_a/V$ must be assigned some value obtained by multiplying the tabulated value of this ratio by a factor $f(\alpha)$. For a first approximation this factor may be assigned the value

$$f(\alpha) = c_l - c_{l_1} \quad (15)$$

where c_l is the lift coefficient for which the pressure distribution is desired. If greater accuracy is desired, the value of $f(\alpha)$ may be adjusted by trial and error to produce the actual desired lift coefficient as determined by integration of the pressure-distribution diagram.

Although this method of superposition of velocities has inadequate theoretical justification, experience has shown that the results obtained are adequate for engineering use. In fact, the results of even the first approximations agree well with experimental data and are adequate for at least preliminary consideration and selection of airfoils. A comparison of a first-approximation theoretical pressure distribution with an experimental distribution is shown in figure 7. Some discrepancy naturally occurs between the results of experiment and of any theoretical method based on potential flow because of the presence of the boundary layer. These effects are small, however, over the range of lift coefficients for which the boundary layer is thin and the drag coefficient is low.

Numerical examples.- The following numerical examples are included to illustrate the method of obtaining the first-approximation pressure distributions:

Example 1: Find the pressure coefficient S at the station $x = 0.50$ on the upper and lower surfaces of the NACA 65₃-418 airfoil at a lift coefficient of 0.2.

From the description of the NACA 6-series airfoils, it is determined that this airfoil is obtained by combining the NACA 65₃-018 basic thickness form with the $a = 1.0$ type mean line cambered to a design lift coefficient of 0.4. The following data are obtained from the supplementary figures for this thickness form and mean line at $x = 0.50$:

$$\frac{v}{V} = 1.235$$

$$\frac{\Delta v_a}{V} = 0.157$$

$$\frac{\Delta v}{V} = 0.250$$

The desired value of $\Delta v_a/V$ is computed as follows by use of equation (15):

$$\begin{aligned}\frac{\Delta v_a}{V} &= (0.157)(0.2 - 0.4) \\ &= -0.031\end{aligned}$$

The desired value of $\Delta v/V$ is obtained by multiplying the tabulated value by the design lift coefficient as stated in the description of the NACA 6-series airfoils. Thus,

$$\begin{aligned}\frac{\Delta v}{V} &= (0.250)(0.4) \\ &= 0.100\end{aligned}$$

Substituting these values in equation (14) gives the following values of S :

For the upper surface

$$\begin{aligned}S &= (1.235 + 0.100 - 0.031)^2 \\ &= 1.700\end{aligned}$$

For the lower surface

$$\begin{aligned}S &= (1.235 - 0.100 + 0.031)^2 \\ &= 1.360\end{aligned}$$

Example 2: Find the pressure coefficient S at the station $x = 0.25$ on the upper and lower surfaces of the NACA 65(215)-214, $a = 0.5$ airfoil at a lift coefficient of 0.6.

The airfoil designation shows that this airfoil was obtained by combining a thickness form obtained by multiplying the ordinates of the NACA 652-015 form by the factor 14/15 with the $a = 0.5$ type mean line cambered to a design lift coefficient of 0.2.

The supplementary figures give a value of 1.182 for v/V at $x = 0.25$ for the NACA 652-015 basic thickness form. The desired value of v/V is obtained by applying formula (5) as follows:

$$\frac{v}{V} = (1.182 - 1) \frac{14}{15} + 1$$

$$= 1.170$$

From the supplementary figures the following values of $\Delta v_a/V$ are obtained at $x = 0.25$ for the following basic thickness forms:

Thickness form	$\frac{\Delta v_a}{V}$ at $x = 0.25$
NACA 65 ₂ -015	0.290
NACA 65 ₁ -012	.282

By interpolation the value of $\Delta v_a/V$ of 0.287 may be assigned to the 14-percent-thick form. The desired value of $\Delta v_a/V$ is then computed as follows by use of equation (15):

$$\frac{\Delta v_a}{V} = (0.287)(0.6 - 0.2)$$

$$= 0.115$$

Data presented in the supplementary figures for the $a = 0.5$ type mean lines give the value of 0.333 for $\Delta v/V$ at $x = 0.25$. As stated in the description of the NACA 6-series airfoils, the desired value of $\Delta v/V$ is obtained by multiplying the tabulated value by the design lift coefficient. Thus,

$$\frac{\Delta v}{V} = (0.333)(0.2)$$

$$= 0.067$$

Substituting the foregoing values in equation (14) gives the values of S as follows:

For the upper surface

$$s = (1.170 + 0.067 + 0.115)^2$$

$$= 1.828$$

For the lower surface

$$S = (1.170 - 0.067 - 0.115)^2 \\ = 0.976$$

Example 3: Find the pressure coefficient S at the station $x = 0.30$ on the upper and lower surfaces of the NACA 2412 airfoil at a lift coefficient of 0.5.

The description of airfoils of the NACA four-digit series shows that the necessary data may be found from the NACA 0012 thickness form and 64 mean line in the supplementary figures. From these figures the following data are obtained:

At $x = 0.30$

$$\frac{v}{V} = 1.162$$

At $x = 0.30$

$$\frac{\Delta v_a}{V} = 0.239$$

For the NACA 64 mean line at $x = 0.30$

$$\frac{\Delta v}{V} = 0.260$$

For the NACA 64 mean line

$$c_{l_i} = 0.76$$

The values of $\Delta v/V$ and c_{l_i} corresponding to the airfoil geometry are obtained by multiplying the foregoing values by the factor $2/6$ as explained in the description of these airfoils; thus,

$$\frac{\Delta v}{V} = (0.260) \left(\frac{2}{6} \right) \\ = 0.087 \\ c_{l_i} = (0.76) \left(\frac{2}{6} \right) \\ = 0.253$$

The desired value of $\Delta v_a/V$ is obtained from equation (15) as follows:

$$\frac{\Delta v_a}{V} = (0.239)(0.5 - 0.253) \\ = 0.059$$

Substituting the proper values in equation (14) gives the values of S as follows:

For the upper surface

$$S = (1.162 + 0.087 + 0.059)^2 \\ = 1.712$$

For the lower surface

$$S = (1.162 - 0.087 - 0.059)^2 \\ = 1.032$$

Effect of camber on pressure distribution.- At zero lift the pressure distributions over the upper and lower surfaces of a basic symmetrical thickness distribution are, of course, identical. The effect of camber on the pressure distribution at the design lift coefficient is to separate the pressures on the upper and lower surfaces by an amount corresponding approximately to the design load distribution of the mean line. When the local value of the design load distribution is positive, the pressure coefficient S on the upper surface is increased (decreased absolute pressure) whereas that on the lower surface is decreased. This effect is shown in figure 8(a) for various amounts of camber.

The maximum value of the pressure coefficient on the upper surface at the design lift coefficient increases with the design lift coefficient and for a given design lift coefficient increases with decreasing values of a . The result is to cause the critical Mach number at the design lift coefficient to decrease with increasing camber or with the use of types of mean line concentrating the load near the leading edge. Figure 8(b) shows that the location of minimum pressure on both surfaces is not

affected if a type of mean line is used having a value of a at least as large as the value of x/c at the position of minimum pressure on the basic thickness distribution. If a mean line with a smaller value of a is used, the possible extent of laminar flow along the upper surface will be reduced.

Critical Mach Number

If the maximum value of the low-speed pressure coefficient S is known either experimentally or from theoretical methods, the critical Mach number may be predicted approximately by the von Kármán method (reference 20). A curve relating the critical Mach number and the low-speed pressure coefficient S has been calculated from the equations of reference 20 and included in the supplementary figures. These predicted critical Mach numbers are useful for preliminary considerations in the absence of test data and appear to correspond fairly well to the Mach numbers at which the local velocity of sound is reached in the high-critical-speed range of lift coefficient. This criterion does not, however, appear to predict accurately the Mach numbers at which large changes in airfoil characteristics occur, especially when sharp pressure peaks exist at the leading edge.

For convenience, curves of predicted critical Mach number plotted against the low-speed section lift coefficient have been included in the supplementary figures for a number of airfoils. These figures are somewhat similar to those of Heaslet (reference 21) but are plotted against the low-speed lift coefficient rather than against the high-speed lift coefficient, as in reference 21. High-speed lift coefficients corresponding to those of Heaslet may be obtained by multiplying the

low-speed lift coefficient by the factor $\frac{1}{\sqrt{1 - M^2}}$.

The critical Mach numbers have been predicted from theoretical pressure distributions. For airfoils of the NACA four- and five-digit series and for the NACA 7-series airfoils, the theoretical pressure distributions were obtained by Theodorsen's method. For the other airfoils, the theoretical pressure distributions were obtained by the approximate method described in the preceding section.

In order to select an airfoil section suitable for high-speed applications, it is necessary that the expected range of operating conditions be known. For purposes of airfoil selection, these conditions may be conveniently expressed in terms of the variation of Mach number with lift coefficient at various altitudes. A set of such curves based on the United States standard atmosphere (reference 22) corresponding to wing loadings of 30, 40, 50, 60, 70, and 80 pounds per square foot are included in the supplementary figures. These curves are plotted against low-speed section lift coefficient to correspond to the figures giving critical Mach numbers for various airfoil sections. The low-speed section lift coefficients were obtained by applying the Glauert compressibility factor $\sqrt{1 - M^2}$ to the high-speed lift coefficient obtained by dividing the wing loading by the dynamic pressure. Use of the Glauert factor, and hence of these charts, is justifiable only if the wing is operating at Mach numbers not much higher than the critical Mach number for the wing. Direct application of these data is based on the assumption that the entire wing is uniformly loaded. A comparison of the curve representing the required flight conditions for a given airplane on these charts with the curves of critical Mach number plotted against lift coefficient for various airfoil sections will assist in selection of the airfoil sections for the application.

Moment Coefficients

Methods of calculation.- Theoretical moment coefficients may be approximated directly from the values presented in the supplementary figures for the various mean lines. These values were obtained from thin-airfoil theory and may be scaled up or down linearly with the design lift coefficient or with the mean-line ordinates. These theoretical values are sufficiently accurate for preliminary considerations, but experimental values should be used for stability and control calculations.

Numerical examples.- The following numerical examples illustrate the methods of calculating the moment coefficients:

Example 1: Find the theoretical moment coefficient about the quarter-chord point for the NACA 65₂-215, $a = 0.5$ airfoil.

The designation of the airfoil shows that the design lift coefficient of this airfoil is 0.2. From the data on the NACA $a = 0.5$ type mean line included in the supplementary figures, the value of $c_{m_c/4}$ is -0.139 for a design lift coefficient of 1.0. The desired value of the moment coefficient is accordingly

$$\begin{aligned} c_{m_c/4} &= (-0.139)(0.2) \\ &= -0.028 \end{aligned}$$

Example 2: Find the theoretical moment coefficient about the quarter-chord point for the NACA 4415 airfoil.

From the description of the NACA four-digit series airfoils, the required data is found to be presented for the NACA 64 mean line in the supplementary figures. The moment coefficient for this mean line is -0.157. The required value is then

$$\begin{aligned} c_{m_c/4} &= (-0.157)\frac{4}{6} \\ &= -0.105 \end{aligned}$$

Angle of Zero Lift

Methods of calculation.— Values of the ideal or design angle of attack α_1 corresponding to the design lift coefficient c_{l_1} are included among the data for the various mean lines presented in the supplementary figures. The approximate values of the angle of zero lift may be obtained from the data by using the theoretical value of the lift-curve slope for thin airfoils, 2π per radian. The value of α_{l_0} in degrees is then

$$\alpha_{l_0} = \alpha_1 - \frac{57.3}{2\pi} c_{l_1} \quad (16)$$

The tabulated values of α_1 may be scaled linearly with the design lift coefficient or with the mean-line ordinates.

Although these theoretical angles of zero lift may be useful in preliminary design, they should not be used without experimental verification for such purposes as establishing the washout of a wing.

Numerical examples.- The method of computing α_{l_0} is illustrated in the following examples:

Example 1: Find the theoretical angle of zero lift of the NACA 65₂-515, $a = 0.5$ airfoil.

This airfoil number indicates a design lift coefficient of 0.5. Data for the NACA $a = 0.5$ mean line indicate that $\alpha_1 = 3.04^\circ$ when $c_{l_1} = 1.0$. The desired value of α_1 is then

$$\begin{aligned}\alpha_1 &= (3.04)(0.5) \\ &= 1.52^\circ\end{aligned}$$

Substituting in equation (16) gives

$$\begin{aligned}\alpha_{l_0} &= 1.52 - \frac{(57.3)(0.5)}{2\pi} \\ &= -3.0^\circ\end{aligned}$$

Example 2: Find the theoretical angle of zero lift for the NACA 2415 airfoil.

The description of the NACA four-digit-series airfoils shows that the required values of α_1 and c_{l_1} may be obtained by multiplying the corresponding values for the NACA 64 mean line (see supplementary figs.) by a factor $2/6$; then

$$\begin{aligned}\alpha_1 &= (0.74)\left(\frac{2}{6}\right) \\ &= 0.25^\circ\end{aligned}$$

$$\begin{aligned}c_{l_1} &= (0.76)\left(\frac{2}{6}\right) \\ &= 0.253\end{aligned}$$

and from equation (16)

$$\begin{aligned} \alpha_{l_0} &= 0.25 - \frac{(57.3)(0.253)}{2\pi} \\ &= -2.0^\circ \end{aligned}$$

Description of Flow around Airfoils

Perfect-fluid theory postulates that the flow follow the airfoil contour smoothly at all angles of attack with no loss of energy. Consequently, perfect-fluid theory itself gives no information concerning the profile drag or the maximum lift of airfoil sections. The explanation of these phenomena is found from a consideration of the effects of viscosity, which are of primary importance in a thin region near the surface of the airfoil called the boundary layer.

Boundary layers in general are of two types, namely, laminar and turbulent. The flow in the laminar layer is smooth and free from any eddying motion. The flow in the turbulent layer is characterized by the presence of a large number of relatively small eddies. Because the eddies in the turbulent layer produce a transfer of momentum from the relatively fast-moving outer parts of the boundary layer to the portions closer to the surface, the distribution of average velocity is characterized by relatively higher velocities near the surface and a greater total boundary-layer thickness in a turbulent boundary layer than in a laminar boundary layer developed under otherwise identical conditions. Skin friction is therefore higher for turbulent boundary-layer flow than for laminar flow.

When the pressures along the airfoil surface are increasing in the direction of flow, a general deceleration takes place. At the outer limits of the boundary layer this deceleration takes place in accordance with Bernoulli's law. Closer to the surface, no such simple law can be given because of the action of the viscous forces within the boundary layer. In general, however, the relative loss of speed is somewhat greater for particles of fluid within the boundary layer than for those at the outer limits of the layer because the reduced kinetic energy of the boundary-layer air limits

its ability to flow against the adverse pressure gradient. If the rise in pressure is sufficiently great, portions of the fluid within the boundary layer may actually have their direction of motion reversed and may start moving upstream. When this reversal occurs, the flow in the boundary layer is said to be "separated." Because of the increased interchange of momentum from different parts of the layer, turbulent boundary layers are much more resistant to separation than are laminar layers. Laminar boundary layers can only exist for a relatively short distance in a region in which the pressure increases in the direction of flow. Formulas for calculating many of the boundary-layer characteristics are given in references 23 to 25.

After laminar separation occurs, the flow may either leave the surface permanently or reattach itself in the form of a turbulent boundary layer. Not much is known concerning the factors controlling this phenomenon. Laminar separation on wings is usually not permanent at flight values of the Reynolds number except when it occurs near the leading edge under conditions corresponding to maximum lift. The size of the locally separated region that is formed when the laminar boundary layer separates and the flow returns to the surface decreases with increasing Reynolds number at a given angle of attack.

The flow over aerodynamically smooth airfoils at low and moderate lift coefficients is characterized by laminar boundary layers from the leading edge back to approximately the location of the first minimum-pressure point on both upper and lower surfaces. If the region of laminar flow is extensive, separation occurs immediately downstream from the location of minimum pressure (reference 23) and the flow returns to the surface almost immediately at flight Reynolds numbers as a turbulent boundary layer. This turbulent boundary layer extends to the trailing edge. If the surfaces are not sufficiently smooth and fair, if the air stream is turbulent, or perhaps if the Reynolds number is sufficiently large, transition from laminar to turbulent flow may occur anywhere upstream of the calculated laminar separation point.

For low and moderate lift coefficients where inappreciable separation occurs, the airfoil profile drag is largely caused by skin friction and the value of the drag coefficient depends mainly on the relative amounts of laminar and turbulent flow. If the location of

transition is known or assumed, the drag coefficient may be calculated with reasonable accuracy from boundary-layer theory by use of the methods of references 26 to 28.

As the lift coefficient of the airfoil is increased by changing the angle of attack, the resulting application of the additional type of lift distribution moves the minimum-pressure point upstream on the upper surface, and the possible extent of laminar flow is thus reduced. The resulting greater proportion of turbulent flow, together with the larger average velocity of flow over the surfaces, causes the drag to increase with lift coefficient.

In the case of many of the older types of airfoils, this forward movement of transition is gradual and the resulting variation of drag with lift coefficient occurs smoothly. The pressure distributions for NACA 6-series airfoils are such as to cause transition to move forward suddenly at the end of the low-drag range of lift coefficients. A sharp increase in drag coefficient to the value corresponding to a forward location of transition on the upper surface results. Such sudden shifts in transition give the typical drag curve for these airfoils with a "sag" or "bucket" in the low-drag range. The same characteristic is shown to a smaller degree by some of the earlier airfoils such as the NACA 23015 when tested in a low-turbulence air stream.

At high lift coefficients, a large part of the drag is contributed by pressure or form drag resulting from separation of the flow from the surface. The flow over the upper surface is characterized by a negative pressure peak near the leading edge, which causes laminar separation. The onset of turbulence causes the flow to return to the surface as a turbulent boundary layer. High Reynolds numbers are favorable to the development of turbulence and aid in this process. If the lift coefficient is sufficiently high or if the reestablishment of flow following laminar separation is unduly delayed by low Reynolds numbers, the turbulent layer will separate from the surface near the trailing edge and will cause large drag increases. The eventual loss in lift with increasing angle of attack may result either from relatively sudden permanent separation of the laminar boundary layer near the leading edge or from progressive forward movement of turbulent separation. Under the latter condition, the flow over a relatively

large portion of the surface may be separated prior to maximum lift. A more extended discussion of the flow conditions associated with maximum lift is given in reference 6.

EXPERIMENTAL CHARACTERISTICS

Sources of Data

The primary source of the wind-tunnel data presented is from tests in the Langley two-dimensional low-turbulence pressure tunnel (TDT). The methods used to obtain and correct the data are summarized in the appendix. Some changes in the corrections have been made since the issuance of reference 1, with the result that the data presented herein will not exactly agree with those of reference 1 and some other early reports. Design data obtained from tests of 2-foot-chord models in this tunnel are presented in the supplementary figures.

Some wind-tunnel data presented were obtained in other NACA wind tunnels. In each case, the source of the data is indicated and the testing techniques and corrections used were conventional unless otherwise indicated.

Most of the flight data consist of drag measurements made by the wake-survey method on either the airplane wing or a "glove" fitted over the wing as the test specimen. Whenever the measurements were obtained for a glove, this fact is indicated in the presentation of the data. All data obtained at high speeds have been reduced to coefficient form by compressible-flow methods. In the case of all such NACA flight data, precautions have been taken to ensure that the results presented are not invalidated by cross flows of low-energy air into or out of the survey plane.

Drag Characteristics of Smooth Airfoils

Drag characteristics in low-drag range.- The value of the drag coefficient in the low-drag range for smooth airfoils is mainly a function of the Reynolds number and the relative extent of the laminar layer and is moderately affected by the airfoil thickness ratio and camber. The

effect on minimum drag of the position of minimum pressure which determines the possible extent of laminar flow is shown in figure 9 for some NACA 6-series airfoils. Although lack of data prevented the selection of airfoils having the same thickness and camber for this comparison, the data show a regular decrease of drag coefficient with rearward movement of minimum pressure.

The variation of minimum drag coefficient with Reynolds number for several airfoils is shown in figure 10. The drag coefficient generally decreases with increasing Reynolds number up to Reynolds numbers of the order of 20×10^6 . Above this Reynolds number the drag coefficient of the NACA 65(421)-420 airfoil remained substantially constant up to a Reynolds number of nearly 4.0×10^6 . The earlier increase in drag coefficient shown by the NACA 66,2x-116 airfoil may be caused by surface irregularities because the specimen tested was a practical-construction model. It may be noted that the drag coefficient for the NACA 65₃-418 airfoil at low Reynolds numbers is substantially higher than that of the NACA 0012, whereas at high Reynolds numbers the opposite is the case. The higher drag of the NACA 65₃-418 airfoil section at low Reynolds numbers is caused by a relatively extensive region of laminar separation downstream of the point of minimum pressure. This region decreases in size with increasing Reynolds number. These data illustrate the inadequacy of low Reynolds number test data either to estimate the full-scale characteristics or to determine the relative merits of airfoil sections at flight Reynolds numbers (references 29 and 30).

Figure 11 shows the variation of minimum drag coefficient with thickness for smooth NACA airfoils. The variation of minimum drag coefficient with camber is shown in figure 12 for a number of 18-percent-thick NACA 65-series airfoils.

The data presented in the supplementary figures for the NACA 6-series thickness forms show that the range of lift coefficients for low drag varies markedly with airfoil thickness. It has been possible to design airfoils of 12-percent thickness with a total theoretical low-drag range of lift coefficients of 0.2. This theoretical range increases by approximately 0.2 for each 3-percent increase of airfoil thickness. Figure 13

shows that the theoretical extent of the low-drag range is approximately realized at a Reynolds number of 9×10^6 . Figure 13 also shows a characteristic tendency for the drag to increase to some extent toward the upper end of the low-drag range for moderately cambered airfoils, particularly for the thicker airfoils. All data for the NACA 6-series airfoils show a decrease in the extent of the low-drag range with increasing Reynolds number. Extrapolation of the rate of decrease observed at Reynolds numbers below 9×10^6 would indicate a vanishingly small low-drag range at flight values of the Reynolds number. Tests of a carefully constructed model of the NACA 65(421)-420 airfoil showed, however, that the rate of reduction of the low-drag range with increasing Reynolds number decreased markedly at Reynolds numbers above 9×10^6 (fig. 14). These data indicate that the extent of the low-drag range of this airfoil is reduced to about one-half the theoretical value at a Reynolds number of 35×10^6 .

The values of the lift coefficient for which low drag is obtained are determined largely by the amount of camber. The lift coefficient at the center of the low-drag range corresponds approximately to the design lift coefficient of the mean line. The effect on the drag characteristics of various amounts of camber is shown in figure 15. Section data indicate that the location of the low-drag range may be shifted by even such crude camber changes as those caused by small deflections of a plain flap (references 1 and 31).

The location of the low-drag range shows some variation from that predicted by simple thin-airfoil theory. This departure appears to be a function of the type of mean line used (reference 32) and the airfoil thickness. The effect of airfoil thickness is shown in figure 13, from which the center of the low-drag range is seen to shift to higher lift coefficients with increasing airfoil thickness. This shift is partly explained by the increase in lift coefficient above the design lift coefficient for the mean line obtained when the velocity increments caused by the mean line are combined with the velocity distribution for the basic thickness form according to the approximate methods previously described.

Drag characteristics outside low-drag range.- At the end of the low-drag range the drag increases rapidly

with increase in lift coefficient. For symmetrical and low-cambered airfoils, for which the lift coefficient at the upper end of the low-drag range is moderate, this high rate of increase does not continue. (See fig. 15.) For highly cambered sections, for which the lift at the upper end of the low-drag range is already high, the drag coefficient shows a continued rapid increase.

Comparison of data for airfoils cambered with a uniform-load mean line with data for airfoils cambered to carry the load farther forward shows that the uniform-load mean line is favorable for obtaining low drag coefficients at high lift coefficients (fig. 16 and reference 32).

Data for many of the airfoils given in the supplementary figures show large reductions in drag with increasing Reynolds number at high lift coefficients. This scale effect is too large to be accounted for by the normal variation in skin friction and appears to be associated with the effect of Reynolds number on the onset of turbulent flow following laminar separation near the leading edge (reference 33).

Effects of type of section on drag characteristics.- A comparison of the drag characteristics of the NACA 23012 and of three NACA 6-series airfoils is presented in figure 17. The drag for the NACA 6-series sections is substantially lower than for the NACA 23012 section in the range of lift coefficients corresponding to high-speed flight, and this margin may usually be maintained through the range of lift coefficients useful for cruising by suitable choice of camber. The NACA 6-series sections show the higher maximum values of the lift-drag ratio. At high values of the lift coefficient, however, the earlier NACA sections have generally lower drag coefficients than the NACA 6-series airfoils.

Effective aspect ratio.- The combination of high drags at high lift coefficients, low drags at moderate lift coefficients, and the nonregular variation of drag with lift coefficient shown by the NACA 6-series airfoils may lead to paradoxical results when the span-efficiency concept (reference 34) is used for the calculation of airplane performance. In the usual application of this concept, the airplane drag characteristics are approximated by a curve of the type

$$C_D = C_{D_{L=0}} + kC_L^2 \quad (17)$$

This curve is usually matched to the actual drag characteristics at a rather low and at a moderately high value of the lift coefficient (reference 35).

The application of this concept to two hypothetical airplanes with NACA 230- and 65-series sections, respectively, is illustrated in figure 18(a). The wing drags of the airplanes have been calculated by adding the induced drags corresponding to an aspect ratio of 10 with elliptical loading to the profile-drag coefficients of the NACA 23018 and 653-418 airfoils. These sections are considered representative of average wing sections for a large airplane of this aspect ratio. Ordinate scales are given in figure 18(a) for the wing drag and for the total airplane drag coefficients obtained by adding a representative constant value of 0.0150 to the wing drag coefficients. The resulting drag coefficients have been approximated by two curves corresponding to equation (17) and matched to the drag curves at lift coefficients of 0.2 and 1.0. These two curves correspond to effective aspect ratios of 9.29 for the airplane with NACA 23018 sections and of 8.30 for the airplane with NACA 653-418 sections and illustrate the typical large reduction in the effective aspect ratio obtained with such sections.

It should be noted, however, that although equation (17) provides a reasonably satisfactory approximation to the drag of the airplane with NACA 23018 sections, such is not the case for the airplane with the NACA 653-418 section. The most important reason for using high aspect ratios on large airplanes is to reduce the drag at cruising lift coefficients and to obtain high maximum values of the lift-drag ratio. For the two wings considered, the maximum value of this ratio is appreciably higher for the airplane with NACA 653-418 sections (19.8 as compared with 18.5) despite the fact that this airplane shows the lower effective aspect ratio. Figure 18(b) shows a similar comparison with similar results for two airplanes of aspect ratio 8 and NACA 2415 and 652-415 airfoils. It is accordingly concluded that the effective aspect ratio is not a satisfactory criterion for use in airfoil selection.

Effect of Surface Irregularities on Drag

Permissible roughness.- Previous work has shown large drag increments resulting from surface roughness (reference 36). Although a large part of these drag increments were shown to result from forward movement of transition, substantial drag increments resulted from surface roughness in the region of turbulent flow. It is accordingly important to maintain smooth surfaces even when extensive laminar flow cannot be expected, but the gains that may be expected from maintaining smooth surfaces are greater for NACA 6- or 7-series airfoils when extensive laminar flows are possible.

No accurate method of specifying the surface condition necessary for extensive laminar flow at high Reynolds numbers has been developed, although some general conclusions have been reached. It may be presumed that for a given Reynolds number, the size of the permissible roughness will vary directly with the chord of the airfoil. It is known, at one extreme, that the surfaces do not have to be polished or optically smooth. Such polishing or waxing has shown no improvement in tests in the Langley two-dimensional low-turbulence tunnels when applied to satisfactorily sanded surfaces. Polishing or waxing a surface that is not aerodynamically smooth will, of course, result in improvement and such finishes may be of considerable practical value because deterioration of the finish may be easily seen and possibly postponed. Large models having chord lengths of 5 to 8 feet tested in the Langley two-dimensional low-turbulence tunnels are usually finished by sanding in the chordwise direction with No. 320 carborundum paper when an aerodynamically smooth surface is desired. Experience has shown the resulting finish to be satisfactory at flight values of the Reynolds number. Any rougher surface texture should be considered as a possible source of transition, although slightly rougher surfaces have appeared to produce satisfactory results in some cases.

Wind-tunnel experience in testing NACA 6-series sections and unpublished data show that small protuberances extending above the general surface level of an otherwise satisfactory surface are more likely to cause transition than small depressions. Dust particles, for example, are more effective than small scratches in producing transition if the material at the edges of the scratches is not forced above the general surface level. Dust

particles adhering to the oil left on airfoil surfaces by fingerprints may be expected to cause transition at high Reynolds numbers.

Transition spreads from an individual disturbance with an included angle of about 15° (references 36 and 37). A few scattered specks, especially near the leading edge, will cause the flow to be largely turbulent. This fact makes necessary an extremely thorough inspection if low drags are to be realized. Specks sufficiently large to cause premature transition on full-size wings can be felt by hand. The inspection procedure used in the Langley two-dimensional low-turbulence tunnels is to feel the entire surface by hand after which the surface is thoroughly wiped with a dry cloth.

It has been noticed that transition resulting from individual small sharp protuberances, in contrast to waves, tends to occur at the protuberance. Transition caused by surface waviness appears to approach the wave gradually as the Reynolds number or wave size is increased. The height of a small cylindrical protuberance necessary to cause transition when located at 5 percent of the chord with its axis normal to the surface is shown in figure 19. These data were obtained at rather low values of the Reynolds number and show a large decrease in allowable height with increase in Reynolds number. This effect of Reynolds number on permissible surface roughness is also evident in figure 20, in which a sharp increase in drag at a Reynolds number of approximately 20×10^6 occurs for the model painted with camouflage lacquer.

The magnitude of the favorable gradient appears to have a small effect on the permissible surface roughness for laminar flow. Figure 21 shows that the roughness becomes more important at the extremities of the low-drag range where the favorable pressure gradient is reduced on one surface. The effect of increasing the Reynolds number for a surface of marginal smoothness, which has an effect similar to increasing the surface roughness for a given Reynolds number, is to reduce rapidly the extent of the low-drag range and then to increase the minimum drag coefficient (fig. 21). The data of figure 21 were specially chosen to show this effect. In most cases, the effect of Reynolds number predominates over the effect of decreasing the magnitude of the favorable pressure gradient to such an extent.

that the only effect is the elimination of the low-drag range (reference 38).

Permissible waviness.- More difficulty is generally encountered in reducing the waviness to permissible values for the maintenance of laminar flow than in obtaining the required surface smoothness. In addition, the specification of the required surface waviness is more difficult than that of the required surface smoothness. The problem is not limited merely to finding the minimum wave size that will cause transition under given conditions because the number of waves and the shape of the waves require consideration.

If the wave is sufficiently large to affect the pressure distribution in such a manner that laminar separation is encountered, there is little doubt that such a wave will cause premature transition at all useful Reynolds numbers. A relation between the dimensions of a wave and the pressure distribution may be found by the methods of reference 39. The size of the wave required to reverse the favorable pressure gradient increases with the pressure gradient. Large negative pressure gradients would therefore appear to be favorable for wavy surfaces. Experimental results have shown this conclusion to be qualitatively correct.

Little information is available on waves too small to cause laminar separation or even reversal of the pressure gradient. Uncertainty exists as to the method of applying Fages's relations (reference 40) to waves on convex surfaces. An attempt to apply these relations to experimental results (fig. 22) showed that premature transition occurred at a much higher Reynolds number than that predicted. On the other hand, transition has been caused at comparatively low Reynolds numbers by a series of small waves with a wave height of the order of a few ten-thousandths of an inch and a wave length of the order of 2 inches on the same 60-inch-chord model.

For the types of wave usually encountered on practical-construction wings, the test of rocking a straightedge over the surface in a chordwise direction is a fairly satisfactory criterion. The straightedge should rock smoothly without jarring or clicking. The straightedge test will not show the existence of waves that leave the surface convex, such as the wave of figure 22 and the series of small waves previously

mentioned. Tests of a large number of practical-construction models, however, have shown that those models which passed the straightedge test were sufficiently free of small waves to permit low drags to be obtained at flight values of the Reynolds number.

It is not feasible to specify construction tolerances on airfoil ordinates with sufficient accuracy to ensure adequate freedom from waviness. If care is taken to obtain fair surfaces, normal tolerances may be used without causing serious alteration of the drag characteristics.

Drag with fixed transition.- If the airfoil surface is sufficiently rough to cause transition near the leading edge, large drag increases are to be expected. Figure 23 shows that, although the degree of roughness has some effect, the increment in minimum drag coefficient caused by the smallest roughness capable of producing transition is nearly as great as that caused by much larger grain roughness when the roughness is confined to the leading edge. The degree of roughness has a much larger effect on the drag at high lift coefficients. If the roughness is sufficiently large to cause transition at all Reynolds numbers considered, the drag of the airfoil with roughness only at the leading edge decreases with increasing Reynolds number (fig. 10 and reference 41).

The effect of fixing transition by means of a roughness strip of carborundum of 0.011-inch grain is shown in figure 24. The minimum-drag increases progressively with forward movement of the roughness strip. The effect on the drag at high lift coefficients is not progressive; the drag increases rapidly when the roughness is at the leading edge. Figure 25 shows that the drag coefficients for the NACA 65(223)-422 and 63(420)-422 airfoils were nearly the same throughout most of the lift range when the extent of laminar flow was limited to 0.30c.

Drag with practical construction methods.- The section drag coefficients of several airplane wings have been measured in flight by the wake-survey method (reference 42), and a number of practical-construction wing sections have been tested in the Langley two-dimensional low-turbulence pressure tunnel at flight values of the Reynolds number. Flight data obtained by the NACA

48
June 1, 1945

CONFIDENTIAL

NACA ACR No. L5C05

(reference 42) are summarized in figure 26 and some data obtained by the Consolidated Vultee Aircraft Corporation are presented in figure 27. Data obtained in the Langley two-dimensional low-turbulence pressure tunnel for typical practical-construction sections are presented in figures 28 to 32. Figure 33 presents a comparison of the drag coefficients obtained in this wind tunnel for a model of the NACA 0012 section and in flight for the same model mounted on an airplane. For this case, the wind-tunnel and flight data agree to within the experimental error.

All wings for which flight data are presented in figure 26 were carefully finished to produce smooth surfaces. Great care was taken to reduce surface waviness to a minimum for all the sections except the NACA 2415.5, N-22, Republic S-3,13, and the NACA 27-212. Curvature-gage measurements of surface waviness for some of these airfoils are presented in reference 42. Surface conditions corresponding to the data of figure 27 are described in the figure. These data show that the sections permitting extensive laminar flow had substantially lower drag coefficients when smooth than the other sections.

The wind-tunnel tests of practical-construction wing sections as delivered by the manufacturer showed minimum drag coefficients of the order of 0.0070 to 0.0080 in nearly all cases regardless of the airfoil section used (figs. 28 to 32). Such values may be regarded as typical for good current construction practice. Finishing the sections to produce smooth surfaces always produced substantial drag reductions although considerable waviness usually remained. None of the sections tested had fair surfaces at the front spar. Unless special care is taken to produce fair surfaces at the front spar, the resulting wave may be expected to cause transition either at the spar location or a short distance behind it. One practical-construction specimen tested with smooth surfaces maintained low drags up to Reynolds numbers above 30×10^6 (NACA 66,2x-116 airfoil of fig. 10). This specimen had no spar forward of about 35-percent chord from the leading edge and no spanwise stiffeners forward of the spars. This type of construction resulted in unusually fair surfaces and is being used on some modern high-performance airplanes.

A comparison of the effect of airfoil section on the minimum drag with practical-construction surfaces is

CONFIDENTIAL

very difficult because the quality of the surface has more effect on the drag than the type of section. Probably the best comparison can be obtained from pairs of models constructed at the same time by the same manufacturers. Data for such pairs of models are presented in figures 30 to 32. The results indicate that as long as current construction practices are used the type of section has relatively little effect at flight values of the Reynolds number for military airplanes.

Important savings in drag may be obtained at high Reynolds numbers by keeping the surfaces smooth even if extensive laminar flow is not realized. Drag increments resulting from surface roughness in turbulent flow have been shown to be important (reference 36). The effects of surface roughness on the variation of drag with Reynolds number are shown in figure 29, in which the favorable scale effect usually expected at high Reynolds numbers was not realized. This type of scale effect may be compared with that shown for the NACA 63(420)-422 airfoil with rough leading edge but otherwise smooth surfaces (fig. 10). Drag increments obtained in flight resulting from roughness in the turbulent boundary layer with fixed transition are presented in reference 43, and large variations in airplane speed are reported to result from applications of different kinds of camouflage paint in reference 44.

The effect of the application of de-icers to the leading edge of two smooth airfoils is shown in figure 34. The de-icer "boots" were installed in both cases by the manufacturer to represent good typical installations. The minimum drag coefficients for both sections with de-icers installed were of the order of 0.0070 at high Reynolds numbers.

Effects of propeller slipstream and airplane vibration.- Very few data are available on the effect of propeller slipstream on transition or airfoil drag; the data that are available do not show consistent results. This inconsistency may result from variations in lift coefficient, surface condition, air-stream turbulence, propeller advance-diameter ratio, and number of blades. British results (references 45 to 47) show transition occurring from 5 to 10 percent of the chord from the leading edge. Similar results are indicated from tests in the Langley 8-foot high-speed tunnel

(reference 48). Drag measurements made in the Langley 19-foot pressure tunnel (fig. 35) indicated only moderate drag increments resulting from a windmilling propeller. Although the data of figure 35 may not be very accurate because of the difficulty of making wake surveys in the slipstream, these data seem to preclude very large drag increments such as would result from movement of the transition to a position close to the leading edge. These data also seem to be confirmed by recent NACA flight data (fig. 36), which show transition as far back as 20 percent of the chord in the slipstream. Other unpublished NACA flight data on transition on an S-3,14.6 airfoil in the slipstream indicated that laminar flow occurred as far back as 0.2c.

Even less data are available on the effects of vibration on transition. Tests in the Langley 8-foot high-speed tunnel (reference 48) showed negligible effects but the range of frequencies tested may not have been sufficiently wide. Some unpublished flight data showed small but consistent rearward movements of transition outside the slipstream when the propellers were feathered. This effect was noticed even when the propeller on the opposite side of the airplane from the survey plane was feathered and was accordingly attributed to vibration. Recent tests in the Ames full-scale tunnel showed premature adverse scale effect on drag coefficients measured by the wake-survey method when a model-support strut vibrated.

Lift Characteristics of Smooth Airfoils

Two-dimensional data.- As explained in the section "Angle of Zero Lift," the angle of zero lift of an airfoil is largely determined by the camber. Thin-airfoil theory provides a means for computing the angle of zero lift from the mean-line data presented in the supplementary figures. The agreement between the calculated and the experimental angle of zero lift will depend on the type of mean line used (fig. 37). The agreement appears to be good except for the uniform-load type ($a = 1.0$) of mean line. The angles of zero lift for this type of mean line are generally closer to 0° than predicted. The airfoil thickness appears to have little effect on the angle of zero lift.

The lift-curve slopes for airfoils tested in the Langley two-dimensional low-turbulence pressure tunnel (see supplementary figs.) are higher than those previously obtained in the tests reported in reference 9. It is not clear whether this difference in slope is caused by the difference in air-stream turbulence or by the differences in test methods, since the section data of reference 9 were inferred from tests of models of aspect ratio 6. The lift-curve slopes for the NACA 6-series airfoils are only slightly higher than those for the NACA 24-, 44-, and 230-series airfoils and usually exceed the theoretical value for thin airfoils (2π per radian). There appears to be little systematic variation of the lift-curve slope of smooth NACA 6-series sections with thickness ratio, at least for airfoils in the range from 12- to 21-percent thickness (fig. 38) or with Reynolds number in the range from 3 to 9×10^6 . For the NACA 24-, 44-, and 230-series airfoils, however, the lift-curve slope increases slightly with increasing Reynolds number for airfoils of 21-percent thickness or more (see supplementary figs.) and decreases with increasing thickness ratio for airfoils of more than 18-percent thickness. (See fig. 38.)

Some NACA 6-series airfoils show jogs in the lift curve at the end of the low-drag range, especially at low Reynolds numbers. This jog becomes more pronounced with increase of camber or thickness and with rearward movement of the position of minimum pressure on the basic thickness form. This jog decreases rapidly in severity with increasing Reynolds number, becomes merely a change in lift-curve slope, and is practically non-existent at a Reynolds number of 9×10^6 for most airfoils that would be considered for practical application. This jog may be a consideration in the selection of airfoils for small low-speed airplanes. An analysis of the flow conditions leading to this jog is presented in reference 33.

The maximum lift coefficient of moderately cambered sections increases with increasing camber (fig. 39). Comparatively few data are available for sections cambered to design lift coefficients higher than 0.4. The data indicate that, although further increases in camber may be favorable at high Reynolds numbers, this may not be the case at Reynolds numbers of 6×10^6 or less. It should be noticed from figure 39 that cambering the airfoil with the $a = 0.5$ type of mean line resulted in

little increase in maximum lift over that of the symmetrical section. The variation of maximum lift with type of camber is shown in figure 40 for one condition. Unfortunately, no systematic data are available for mean lines with values of a less than 0.5. It should be noted, however, that airfoils such as the NACA 230-series with the maximum camber far forward show large increments of maximum lift as compared with symmetrical sections. Sections with maximum camber far forward and with normal thickness ratios stall from the leading edge with large sudden losses of lift. A more desirable gradual stall is obtained when the location of maximum camber is farther back as with the NACA 24-, 44-, and 6-series sections with normal types of camber.

The variation of maximum lift coefficient with airfoil thickness ratio is shown in figure 41 for several NACA sections. No recent data are available for thickness ratios of less than 12 percent. For all the series shown in figure 41, the highest maximum lift is obtained for 12-percent-thick sections. The rate of decrease of maximum lift coefficient with increasing thickness ratio is less for the NACA 6-series sections than for the others shown, especially at the higher thickness ratios. Figure 41 shows that the maximum lift coefficients of the NACA 64- and 65-series sections cambered for a design lift coefficient of 0.4 are at least as high as those for the NACA 24- and 44-series sections. The NACA 230-series sections have somewhat higher maximum lift coefficients except for thickness ratios above 20 percent.

A sufficient amount of systematic data is not available to permit detailed conclusions to be drawn with regard to the magnitude of the scale effect for all airfoils likely to be used. The scale effect on maximum lift coefficient up to Reynolds numbers of 10×10^6 for several NACA 6-series sections are presented in figure 42. All the sections show large favorable scale effects at Reynolds numbers less than 6×10^6 . The scale effect at Reynolds numbers above 6×10^6 becomes more favorable with increasing thickness ratio (figs. 42(a) and 42(b)) and increasing camber (fig. 42(c)) for NACA 64- and 65-series airfoils. The data of figures 42(d) and 42(e) show that position of minimum pressure at 60 percent of the chord produces a less favorable scale effect at Reynolds numbers between 6×10^6 and 9×10^6 than positions of minimum pressure farther forward on the airfoil. The data (fig. 42(e)) do not, however,

show a progressive change in type of scale effect with location of minimum pressure. The data of figure 43 show that the maximum lift coefficient for the NACA 63(420)-422 airfoil continues to increase with Reynolds number up to values of at least 26×10^6 .

Three-dimensional data.- No recent systematic three-dimensional wing data obtained at high Reynolds numbers are available, so that it is difficult to make any comparison with the section data. When the maximum-lift data for three-dimensional wings are compared with section data, account should be taken of the span load distribution over the wing. The predicted maximum lift coefficient for the wing will be somewhat lower than the maximum lift coefficients of the sections used because of the nonuniformity of the spanwise distribution of lift coefficient. The difference amounts to about 4 to 7 percent for a rectangular wing with an aspect ratio of 6.

Maximum-lift data obtained from tests of a number of wings and airplane models in the Langley 19-foot pressure tunnel are presented in table II. Although section data at the Reynolds numbers necessary to permit a detailed comparison are not available, the maximum lift coefficient for plain wings given in table II appears to be in general agreement with values expected from section data. The data for the airplane models are presented to indicate the maximum lift coefficients obtained with various airfoils and configurations.

Lift Characteristics of Rough Airfoils

Two-dimensional data.- Most recent airfoil tests, especially of airfoils with the thicker sections, have included tests with roughened leading edge (references 1 and 49), and the available data are included in the supplementary figures. The standard roughness selected for 24-inch-chord models consists of 0.011-inch carborundum grains applied to the airfoil surface at the leading edge over a surface length of $0.03c$ measured from the leading edge on both surfaces. The grains are thinly spread to cover 5 to 10 percent of this area.

The effect on maximum lift coefficient of various degrees of roughness applied to the leading edge of the NACA 63(420)-422 airfoil is shown in figure 23. The

maximum lift coefficient decreases progressively with increasing roughness (reference 41). For a given surface condition at the leading edge, the maximum lift coefficient increases slowly with increasing Reynolds number (fig. 44). Few data are available on the effect of leading-edge roughness on the maximum lift of flapped airfoils. Figure 45 shows that the decrement in maximum lift coefficient was about the same for the flapped and the plain airfoil in one case. The effect of the same leading-edge roughness on several thick airfoils is shown in figure 46. For thickness ratios of about 21 percent, the NACA 63- and 65-series sections showed higher maximum lift coefficients with rough leading edges than the NACA 24-, 44-, and 230-series sections. The data of figure 46 and the supplementary figures indicate that maximum lift coefficients with rough leading edges at a Reynolds number of 6×10^6 do not exceed 1.3 and may be less than 1.0. Figure 24 shows that roughness strips located more than 0.20c from the leading edge have little effect on the maximum lift coefficient or the lift-curve slope.

The maximum lift coefficient may be lowered by failure to maintain the true airfoil contour near the leading edge, but no systematic data on this effect have been obtained. Examples of this effect that were accidentally encountered are presented in figure 47, in which lift characteristics are given for accurate and slightly inaccurate models. The model inaccuracies were so small that they were not found previous to the tests. Such difficulties have not yet been encountered for models of NACA 6-series airfoils built in the same shop by the same methods.

Three-dimensional data.- Tests of several airplanes in the Langley full-scale tunnel (reference 50) show that many factors besides the airfoil sections affect the maximum lift coefficient of airplanes. Such factors as roughness, leakage, leading-edge air intakes, armament installations, nacelles, and fuselages make it difficult to correlate the airplane maximum lift with the airfoils used, even when the flaps are retracted. The various flap configurations used make such a correlation even more difficult when the flaps are deflected. When the flaps were retracted, both the highest and the lowest maximum lift coefficients obtained in recent tests of airplanes and complete mock-ups of conventional configuration in the Langley full-scale tunnel were those obtained with NACA 6-series airfoils.

Results obtained from tests of a model of an airplane in the Langley 19-foot pressure tunnel and of the airplane in the Langley full-scale tunnel are presented in figure 48. Both tests were made at approximately the same Reynolds number. The results show that the airplane in the service condition had a maximum lift coefficient more than 0.2 lower than that of the model, as well as a lower lift-curve slope. Some improvement in the airplane lift characteristics was obtained by sealing leaks. These results show that airplane lift characteristics are strongly affected by details not reproduced on large-scale smooth models.

Lift characteristics obtained in the Langley 19-foot pressure tunnel for two airplane models in the smooth condition and with transition fixed at the front spar are presented in figures 49 and 50. In both cases, the lift-curve slope was decreased throughout most of the lift range with fixed transition. The maximum lift coefficient was decreased in one case but was increased in the other case.

Unconservative Airfoils

The attempt to obtain low drags, especially for long-range airplanes, leads to high wing loadings together with relatively low span loadings. This tendency results in wings of high aspect ratio that require large spar depths for structural efficiency. The large spar depths require the use of thick root sections.

This trend to thick root sections has been encouraged by the relatively small increase in drag coefficient with thickness ratio of smooth airfoils (fig. 11). Unfortunately, airplane wings are not usually constructed with smooth surfaces and, in any case, the surfaces cannot be relied upon to stay smooth under all service conditions. The effect of roughening the leading edges of thick airfoils is to cause large increases in the drag coefficient at high lift coefficients. The resulting drag coefficients may be excessive at cruising lift coefficients for heavily loaded, high-altitude airplanes. Airfoil sections that have suitable characteristics when smooth but have excessive drag coefficients when rough at lift coefficients corresponding to cruising or climbing conditions are classified as unconservative.

As an aid in judging whether the sections are conservative, most recent airfoil investigations (especially tests of the thicker sections) have included tests with a standard roughness (described in the preceding section) applied to the leading edge. This standard roughness is considerably more severe than that caused by usual manufacturing irregularities or deterioration in service but is considerably less severe than that likely to be encountered in service as a result of accumulations of ice, mud, or damage in military combat.

The decision as to whether a given airfoil section is conservative will depend upon the power and the wing loading of the airplane. The decision may be affected by expected service and operating conditions. For example, the ability of a multiengine airplane to fly with one or more engines inoperative in icing conditions or after suffering damage in combat may be a consideration.

Although systematic tests have not been made, data presented in the supplementary figures show that thickness is probably the most important factor in determining the lift coefficient at which the drag increases rapidly. Most airfoils with a thickness ratio larger than 20 percent appear to be definitely unconservative if used on airplanes with high wing loadings. Increasing the camber of thick sections in an attempt to decrease the drag coefficients at the higher lift coefficients only makes such sections even less conservative. Nearly all the tests with the standard roughness applied to the leading edge have been made at a Reynolds number of 6×10^6 . The data of figure 51 show that the drag coefficients at flight values of the Reynolds number may be considerably lower than at a Reynolds number of 6×10^6 if the roughness is confined to the leading edge.

Figure 52 indicates that NACA 6-series sections with minimum pressure far forward are more conservative than those with minimum pressures farther back. The data of the supplementary figures and of reference 32 show that the uniform-load type of mean line is favorable. Figure 46 shows that the drag characteristics at moderately high lift coefficients with rough leading edges of the NACA 24-, 44-, and 230-series sections are intermediate to those for the NACA 63- and 65-series sections.

Pitching Moment

As discussed in a previous section, the pitching moment of an airfoil section is primarily a function of its camber and thin-airfoil theory provides a means for estimating the pitching moment from the mean-line data presented in the supplementary figures. A comparison of the experimental moment coefficient and theoretical values for the mean lines is presented in figure 53 (reference 32). The experimental moment coefficients for airfoils cambered with the uniform-load type of mean line and for NACA 24-, 44-, and 230-series airfoils are less than the values obtained from thin-airfoil theory. The NACA 6-series airfoils having mean lines with values of a less than 1.0 usually have slightly higher moment coefficients than those indicated by theory.

The variation of measured moment coefficients with thickness ratio is shown in figure 54 for some NACA airfoils. Changes in thickness ratio appear to have comparatively little effect on the moment characteristics of the NACA 6-series airfoils that have cusped trailing edges. The moment coefficients for the NACA 24-, 44-, and 230-series airfoils, however, become more positive as the thickness is increased. The trailing-edge angles for these airfoils increase with the thickness ratio. The data of reference 51 show important forward movements of the aerodynamic center with increasing trailing-edge angle. These results suggest that the chief effects of thickness on the moment characteristics are associated with the trailing-edge angle.

Critical Speed

The critical speed is defined as the speed at which the velocity over the surface of the airfoil reaches the local velocity of sound. At speeds slightly in excess of the critical speed, important changes occur in the airfoil characteristics. As discussed in a previous section, the critical speed or Mach number may be predicted approximately from low-speed pressure distributions. Predicted critical Mach numbers are presented in reference 21 for some airfoils and in the supplementary figures for all airfoils for which other data are presented.

For any one type of airfoil, the maximum critical Mach number decreases rapidly as the thickness is

increased. For NACA 6-series airfoils, the range of lift coefficients for high critical Mach numbers is the same as the low-drag range. This range decreases with decreasing thickness ratio. The effect of camber is to lower the maximum critical Mach number and to shift the range of high critical Mach numbers in the same manner as for the low-drag range. For common types of camber, the minimum reduction in critical speed for a given design lift coefficient is obtained with a uniform-load type of mean line.

A discussion of the effect of thickness distribution on the critical Mach number is given in reference 21. Comparison of the data presented in the supplementary figures shows that NACA 6-series sections have considerably higher maximum critical Mach numbers than NACA 24-, 44-, and 230-series airfoils. This superiority is maintained throughout the high critical Mach number range of the NACA 6-series sections. At high lift coefficients, however, the NACA 24-, 44-, and 230-series sections have higher predicted critical Mach numbers than the 6-series sections. The higher cambered and thicker sections tend to have higher critical Mach numbers at high lift coefficients. For the NACA 6-series airfoils, the maximum critical Mach number increases slowly with rearward movement of the position of minimum pressure.

It is especially desirable for the airfoil section to have high critical Mach numbers for the lift coefficients corresponding to high-speed unaccelerated flight in order to avoid excessive drags. The NACA 6-series airfoils are favorable in this respect. Slightly higher maximum critical Mach numbers than those for the NACA 6-series sections can be obtained by different thickness distributions. This slight gain in maximum critical Mach number is offset, however, by a large reduction in the range of lift coefficient within which the critical Mach number is high. This range is already small for the thinner sections required for high-speed applications, and too limited a range will result in difficulties with normal variations of wing loadings and altitude. The NACA 6-series sections are considered to offer a desirable compromise between the maximum critical Mach number and the range of lift coefficients for high critical Mach numbers.

High critical Mach numbers at high lift coefficients are of interest for high-speed accelerated flight

such as pull-outs. All high-speed highly maneuverable airplanes may be expected to exceed the critical Mach number at high lift coefficients (reference 52). The airfoil characteristics at high Mach numbers and moderately high lift coefficients are therefore of interest. The lower predicted critical Mach numbers of the NACA 6-series sections at high lift coefficients would be expected to be unfavorable, but limited experience with a fighter airplane using these sections fails to show any disadvantage.

Some data obtained at high Mach numbers in the Langley rectangular high-speed tunnel for the NACA 23015, 66,2-015, and 66,2-215 airfoils are presented in figures 55 to 60. Although these data are uncorrected for tunnel-wall effects, the comparisons indicated are believed to be substantially correct at the Mach numbers considered. These data show that the adverse effect of Mach numbers up to 0.725 on the shape of the normal-force curve is much less for the NACA 66-series sections than for the NACA 23015 airfoil. At an angle of attack of 6° , the normal-force coefficient for the NACA 23015 airfoil reaches a maximum of about 0.76 at a Mach number of only 0.55. At the same angle of attack, a maximum normal-force coefficient of about 0.88 is reached for the NACA 66,2-215 airfoil at a Mach number of over 0.675. These limited data would seem to indicate a greater loss in maneuverability for the NACA 23015 airfoil than for the NACA 66,2-215 despite the lower predicted critical Mach numbers for the NACA 66,2-215 section at moderately high lift coefficients.

The results of tests in the Ames 16-foot high-speed tunnel of a complete model of a fighter-type airplane with two alternate wings are summarized in figure 61. Figure 61(a) shows that the use of the NACA 66-series wing would result in large drag reductions at a Mach number of 0.7, especially at the higher lift coefficients. Figure 61(b) shows the limits of the usable range of lift coefficients for the model equipped with each of the two wings. The limits were selected as the lift coefficients at which large changes in stability and trim occurred and excessive movement of the elevator was required. The results indicate that the NACA 66-series wing would permit level flight without excessive control difficulties at higher Mach numbers and altitudes than the NACA 230-series wing and would permit a greater degree of maneuverability.

High-Lift Devices

Lift characteristics for two NACA 6-series airfoils equipped with plain flaps are presented in figure 62 and in references 31 and 53. These data show that the maximum lift coefficient increases less rapidly with flap deflection for the more highly cambered section. Lift characteristics of three NACA 6-series airfoils with split flaps are presented in reference 54 and figure 63. The maximum-lift increments for the 12-percent-thick sections were only about three-fourths of that for the 16-percent-thick section. The maximum lift coefficient for the thicker section with flap deflected is about the same as those obtained for the NACA 23012 airfoil in the now obsolete Langley variable-density tunnel (reference 55) and in the Langley 7- by 10-foot tunnel (reference 56).

Tests of a number of slotted flaps on NACA 6-series airfoils (references 53, 57, and 58) indicate that the design parameters necessary to obtain high maximum lifts are essentially similar to those for the NACA 230-series sections (references 59 and 60). Lift data obtained for typical hinged single-slotted 0.25c flaps (fig. 64(a)) on the NACA 63,4-420 airfoil are presented in figure 64(b). A maximum lift coefficient of approximately 2.95 was obtained for one of the flaps. Lift characteristics for the NACA 653-118 airfoil fitted with a double-slotted flap (reference 58 and fig. 65(a)) are presented in figure 65(b). A maximum lift coefficient of 3.28 was obtained. It may be concluded that no special difficulties exist in obtaining high maximum lift coefficients with slotted flaps on moderately thick NACA 6-series sections.

Tests of airplanes in the Langley full-scale tunnel (reference 50) have shown that expected increments of maximum lift coefficient are obtained for split flaps (fig. 66) but not for slotted flaps (fig. 67). This failure to obtain the expected maximum-lift increments with slotted flaps may be attributed to inaccuracies of flap contour and location, roughness near the flap leading edge, leakage, interference from flap supports, and deflection of flap and lip under load.

Lateral-Control Devices

An adequate discussion of lateral-control devices is outside the scope of this report. The following

brief discussion is therefore limited to considerations of effects of airfoil shape on aileron characteristics.

The effect of airfoil shape on aileron effectiveness may be inferred from the data of figure 68 and reference 61. The section flap-effectiveness parameter $\Delta\alpha_0/\Delta\delta$ is plotted against the flap-chord ratio c_f/c for a number of airfoils of different type in figure 68. Table III, which presents supplementary information regarding the data, is placed opposite figure 68 to facilitate its use. Also shown in this figure are the theoretical values of the parameter for thin airfoils. The data show no large consistent trends of aileron-effectiveness variation with airfoil section for a wide range of thickness distributions and thickness ratios. In order to evaluate aileron characteristics from section data, a method of analysis is necessary that will lead to results comparable to the usual curves of stick force against helix angle $pb/2V$ for three-dimensional data. The analysis that follows is considered suitable for comparing the relative merits of ailerons from two-dimensional data.

Two-dimensional data are presented in the form of the equivalent change in section angle of attack $\Delta\alpha_0$ required to maintain a constant section lift coefficient for various deflections of the aileron from neutral. This equivalent change in angle of attack is plotted against the hinge-moment parameter $\Delta c_H\delta$, which is the product of the aileron deflection from neutral and the resulting increment of hinge-moment coefficient based on the wing chord. This method of analysis takes into account the aileron effectiveness, the hinge moments, and the possible mechanical advantage between the controls and the ailerons. The span of the ailerons and possible three-dimensional-flow effects are not considered. The larger the value of $\Delta\alpha_0$ for a given value of the hinge-moment parameter, the more advantageous the combination should be for providing a large value of $pb/2V$ for a given control force.

For the purpose of evaluating the effect of airfoil shape on the aileron characteristics, it is desirable to make the comparison with unbalanced ailerons to avoid confusion. Plots of the parameters for plain unbalanced flaps of true airfoil contour on three airfoil sections are shown in figure 69. The characteristics of the NACA 66(215)-216, $a = 0.6$ section are essentially the

same as those for the NACA 0009 airfoil within the range of deflections for which data are available. The NACA 64,2-(1.4)(13.5) airfoil shows appreciably smaller values of $\Delta C_H \delta$ for a given value of $\Delta \alpha_0$ than the other sections. No explanation for this difference can be offered, although some of the difference may result from the slightly smaller chord of the flap for this combination.

The effects of using straight-sided ailerons instead of ailerons of true airfoil contour are shown in figure 70 for two NACA 6-series airfoils. One of the two combinations for which data are available was provided with an internal balance whereas the other combination was without balance. This difference prevents any comparison between the two combinations but does not affect comparison of the two contours for each case. For the NACA 66(215)-216, $a = 0.6$ airfoil, the straight-sided aileron has more desirable characteristics for the range of deflections for which data are available. It appears, however, that the straight-sided aileron would be less advantageous than the aileron of true contour for positive deflections greater than 12° . In the case of the NACA 63,4-4(17.8) airfoil, the straight-sided aileron appears to have no advantage over the aileron of true airfoil contour. The advantage of using straight-sided ailerons appears to depend markedly on the airfoil used but sufficient data are not available to determine the significant airfoil parameters. Figure 71 shows that in one case the effect of leading-edge roughness on the aileron characteristics is unfavorable.

Leading-Edge Air Intakes

The problem of designing satisfactory leading-edge air intakes is to maintain the lift, drag, and critical-speed characteristics of the sections while providing low intake losses over a wide range of lift coefficients and intake velocity ratios. The data of references 76 and 77 show that desirable intake, drag, and critical-speed characteristics can easily be maintained over a rather small range of lift coefficients for NACA 6-series airfoils. The data of reference 76 show that the intake losses increase rapidly at moderately high lift coefficients for the shapes tested. Unpublished data taken at the Langley Laboratory indicate that shapes such as

those of reference 76 have low maximum-lift coefficients. Recent data show that air-intake shapes can be provided for such airfoil sections with desirable air-intake characteristics and without loss in maximum lift coefficient (fig. 72). Some pressure-distribution data for the air intakes shown in figure 72 indicate that the critical speed of the section has been lowered only slightly and that falling pressures in the direction of flow were maintained for some distance from the leading edge on both surfaces at lift coefficients near the design lift coefficient for the section. Sufficient information is not available to permit such desirable configurations to be designed without experimental development.

Interference

The main problem of interference at low Mach numbers is considered to be that of avoiding boundary-layer separation resulting from rapid flow expansions caused by the addition of induced velocities about bodies and the boundary-layer accumulations near intersections. No recent systematic investigations of interference such as the investigation of reference 78 have been made.

Some tests have been made of airfoil sections with intersecting flat plates (reference 79). These configurations may be considered to represent approximately the condition of a wing intersection with a large flat-sided fuselage. In this case, the interference may be considered to result from the effect on the wing of the fully developed turbulent boundary layer on the fuselage or flat plate and the accumulation of boundary layer in the intersection. These tests showed little interference except in cases for which the boundary layer on the airfoil alone was approaching conditions of separation such as was noted with the less conservative airfoils at moderately high lift coefficients.

Some scattered data on the characteristics of nacelles mounted on airfoils permitting extensive laminar flow are presented in references 80 to 82. The data appear to indicate that the interference problems for conservative NACA 6-series sections are similar to those encountered with other types of airfoils. The detail shapes for optimum interfering bodies and fillets

may, however, be different for various sections if local excessive expansions in the flow are to be avoided.

Some lift and drag data for an airfoil with pusher-propeller-shaft housings are presented in reference 83. These results indicate that protuberances near the trailing edge of wings should be carefully designed to avoid unnecessary drag increments.

Another type of interference of particular importance for high-speed airplanes results in the reduction of the critical Mach number of the combination because of the addition of the induced velocities associated with each body (reference 34). This effect may be kept to a minimum by the use of bodies with low induced velocities, by separation of interfering bodies to the greatest possible extent, and by such selection and arrangement of combinations that the points of maximum induced velocity for each body do not coincide.

APPLICATION TO WING DESIGN

Detail consideration of the various factors affecting wing design lies outside the scope of this report. The following discussion is therefore limited to some important aerodynamic features that must be considered in the application of the data presented.

Application of Section Data

Wing characteristics are usually predicted from airfoil-section data by use of methods based on simple lifting-line theory (references 85 to 88). Application of such methods to wings of conventional plan form without spanwise discontinuities yields results of reasonable engineering accuracy (reference 89), especially with regard to such important characteristics as the angle of zero lift, the lift-curve slope, the pitching moment, and the drag. Basically similar methods not requiring the assumption of linear section lift characteristics (references 90 and 91) appear capable of yielding results of greater accuracy, especially at high lift coefficients. Further refinement may be made by consideration of the chordwise distribution of lift

(reference 92). Wings with large amounts of sweep require special consideration (reference 93).

The usual wing theory assumes that the resultant air force and moment on any wing section are functions of only the section lift coefficient (or angle of attack) and the section shape. According to this assumption, the air forces and moments on any section are not affected by adjacent sections or other features of the wing except as such sections or features affect the lift distribution and thus the local lift of the section under consideration. These assumptions obviously are not valid near wing tips, near discontinuities in deflected flaps or ailerons, near disturbing bodies, or for wings with pronounced sweep or sudden changes in plan form, section, or twist. Under such circumstances, cross flows result in a breakdown of the concept of two-dimensional flow over the airfoil sections. In addition to these cross flows, induced effects exist that are equivalent to a change in camber. Such effects are particularly marked near the wing tips for wings of normal plane form and for wings of low aspect ratio or unusual plan form. Lifting-surface theory (see, for example, reference 93) provides a means for calculating wing characteristics more accurately than the simple lifting-line theory.

Although span load distributions calculated for wings with discontinuities such as are found with partial-span flaps (references 94 and 95) may be sufficiently accurate for structural design, such distributions are not suitable for predicting maximum-lift and stalling characteristics. Until sufficient data are obtained to permit the prediction of the maximum-lift and stalling characteristics of wings with discontinuities, these characteristics may best be estimated from previous results with similar wings or, in the case of unusual configurations, should be obtained by test.

The characteristics of intermediate wing sections must be known for the application of wing theory, but data for such sections are seldom available. Tests of a number of such intermediate sections obtained by several manufacturers for wings formed by straight-line fairing have indicated that the characteristics of such sections may be obtained with reasonable accuracy by interpolation of the root and tip characteristics according to the thickness variation.

Selection of Root Section

The characteristics of a wing are affected to a large extent by the root section. In the case of tapered wings formed by straight-line fairing, the resulting nonlinear variation of section along the span causes the shapes of the sections to be predominantly affected by the root section over a large part of the wing area. The desirability of having a thick wing that provides space for housing fuel and equipment and reduces structural weight or permits large spans usually leads to the selection of the thickest root section that is aerodynamically feasible. The comparatively small variation of minimum drag coefficient with thickness ratio for smooth airfoils in the normal range of thickness ratios and the maintenance of high lift coefficient for thick sections with flaps deflected usually result in limitation of thickness ratio by characteristics other than maximum lift and minimum drag.

The critical Mach number of the section is the most serious limitation of thickness ratio for high-speed airplanes. It is desirable to select a root section with a critical Mach number sufficiently high to avoid serious drag increases resulting from compressibility effects at the highest level-flight speed of the airplane, allowance being made for the increased velocity of flow over the wing resulting from interference of bodies and slipstream. Available data indicate that a small margin exists between the critical Mach number and the Mach number at which the drag increases sharply. As airplane speeds increase, it becomes increasingly difficult and finally impossible to avoid the drag increases resulting from compressibility effects by reduction of the airfoil thickness ratio. The use of small airfoil thickness ratios to obtain high critical speed results in a reduction in the lift-coefficient range for high critical Mach numbers. Greater difficulty is consequently experienced with thin airfoil sections in avoiding compressibility shock over the range of lift coefficients required by normal changes in airplane weight and altitude of flight, especially with high wing loadings. This effect is expected to be one of the factors limiting the wing loadings of very high-speed, high-altitude airplanes traveling at subsonic speeds.

In the cases of airplanes of such low speeds that compressibility considerations do not limit the thickness ratio to values less than about 0.20, the maximum thickness ratio is limited by excessive drag coefficients at moderate and high lift coefficients with the surfaces rough. In these cases, the actual surface conditions expected for the airplane should be considered in selecting the section. Consideration should also be given to unusual conditions such as ice, mud, and damage caused in military combat, especially in the case of multiengine airplanes for which ability to fly under such conditions is desired with one or more engines inoperative. In cases for which root sections having large thickness ratios are under consideration to permit the use of high aspect ratios, a realistic appraisal of the drag coefficients of such sections with the expected surface conditions at moderately high lift coefficients will indicate an optimum aspect ratio beyond which corresponding increases in aspect ratio and root thickness ratio will result in reduced performance.

Inboard sections of wings on conventional airplanes are subject to interference effects and may be in the propeller slipstream. The wing surfaces are likely to be roughened by access doors, landing-gear retraction wells, and armament installations. Attainment of extensive laminar flows is, therefore, less likely on the inboard wing panels than on the outboard panels. Unless such effects are minimized, little drag reduction is to be expected from the use of sections permitting extensive laminar flow. Under these conditions, the use of sections such as the NACA 63-series will provide advantages if the sections are thick, because such sections are more conservative than those permitting more extensive laminar flow. If the thickness ratio is limited to moderate values, however, by critical-speed requirements, the use of NACA 65- or 66-series sections will provide favorable critical-speed characteristics without imposing drag penalties.

It is usually advisable to camber the root section the minimum amount consistent with low drag for the cruising conditions. This amount of camber is usually only a little more than that corresponding to the highest critical Mach number for the high-speed condition. For very high-speed high-altitude airplanes

with heavy wing loadings, it may be impossible to select an amount of camber that will provide high critical speed for all the desired operating conditions. The amount of camber must then be selected from consideration of the flight conditions at which good performance is most desired.

Selection of Tip Section

In order to promote desirable stalling characteristics, the tip section should have a high maximum lift coefficient and a large range of angle of attack between zero and maximum lift as compared with the root section. It is also desirable that the tip section stall without a large sudden loss in lift. The attainment of a high maximum lift coefficient is more difficult at the tip section than at the root section for tapered wings because of the lower Reynolds number of the tip section. For wings with small camber, the most effective way of increasing the section maximum lift coefficient is to increase the camber. The amount of camber used will be limited in most cases by either the critical-speed requirements or by the requirement that the section have low drag at the high-speed lift coefficient.

The selection of the optimum type of camber for the tip section presents problems for which no categorical answers can be given on the basis of existing data. The use of a type of camber that imposes heavy loads on the ailerons complicates the design of the lateral-control system and increases its weight. The use of a type of camber that carries the lift farther forward on the section and thus relieves the ailerons will, however, have little effect on the maximum lift coefficient of the section unless the maximum-camber position is well forward, as for the NACA 230-series sections. In this case a sudden loss of lift at the stall may be expected. The effects on the camber of modifications to the airfoil contour near the trailing edge, which may be made in designing the ailerons, should not be overlooked in estimating the characteristics of the wing.

If the root sections are at least moderately thick, it is usually desirable to select a tip section with a somewhat reduced thickness ratio. This reduction in thickness ratio, together with the absence of induced

velocities from interfering bodies, gives a margin in critical speed that permits the camber of the tip section to be increased. This reduction in thickness ratio will be limited either by the loss in maximum lift coefficient resulting from too thin a section or by the reduction in angular range of the low-drag, high-critical-speed region to a value too small to cover the desired flight conditions.

A small amount of aerodynamic washout may also be useful as an aid in the avoidance of tip stalling. The permissible amount of washout may not be limited by the increase in induced drag, which is small for 1° or 2° of washout (reference 85). The limiting washout may be that which causes the tip section to operate outside the low-drag, high-critical-speed range at the high-speed lift coefficient. This limitation may be so severe as to require some adjustment of the camber to permit the use of any washout.

A change in airfoil section between the root and tip may be desirable to obtain favorable stalling characteristics or to take advantage of the greater extent of laminar flow that may be possible on the outboard sections. Thus, such combinations as an NACA 230-series root section with an NACA 44-series tip section or an NACA 63-series root section with an NACA 65-series tip section may be desirable.

It should be noted that the tip sections may easily be so heavily loaded by the use of an unfavorable plan form as to cause tip stalling with any reasonable choice of section and washout. Both high taper ratios and large amounts of sweepback are unfavorable in this respect and are particularly bad when used together, because the resulting tip stall promotes longitudinal instability at the stall in addition to the usual lateral instability.

CONCLUSIONS

The following conclusions may be tentatively drawn from the data presented. Most of the data, particularly for the lift and moment characteristics, were obtained at Reynolds numbers from 3 to 9×10^6 .

CONFIDENTIAL

Although some of these conclusions may be modified when more systematic data are available, they are believed to be essentially correct:

1. Airfoil sections permitting extensive laminar flow, such as the NACA 6- and 7-series sections, result in substantial reductions in drag at high-speed and cruising lift coefficients as compared with other sections if, and only if, the wing surfaces are fair and smooth.
2. Experience with full-size wings has shown that extensive laminar flows are obtainable if the surface finish is as smooth as that provided by sanding in the chordwise direction with No. 320 carborundum paper and if the surface is free from small scattered defects and specks. Satisfactory results are usually obtained if the surface is sufficiently fair to permit a straight-edge to be rocked smoothly in the chordwise direction without jarring or clicking.
3. For wings of moderate thickness ratios with surface conditions corresponding to those obtained with current construction methods, minimum drag coefficients of the order of 0.0080 may be expected. The values of the minimum drag coefficient for such wings depend primarily on the surface condition rather than on the airfoil section.
4. Substantial reductions in drag coefficient at high Reynolds numbers may be obtained by smoothing the wing surfaces, even if extensive laminar flow is not obtained.
5. The maximum lift coefficients for moderately cambered smooth NACA 6-series airfoils with the uniform-load type of mean line are as high as those for NACA 24- and 44-series airfoils. The NACA 230-series airfoils have somewhat higher maximum lift coefficients for thickness ratios less than 0.20.
6. The maximum lift coefficients of airfoils with flaps are about the same for moderately thick NACA 6-series sections as for the NACA 23012 section but appear to be considerably lower for thinner NACA 6-series sections.

7. The lift-curve slopes for smooth NACA 6-series airfoils are slightly higher than for NACA 24-, 44-, and 230-series airfoils and usually exceed the theoretical value for thin airfoils.

8. Leading-edge roughness causes large reductions in maximum lift coefficient and a moderate reduction in lift-curve slope for all good airfoil sections.

9. Characteristics of airfoil sections with the expected surface conditions must be known or estimated to provide a satisfactory basis for the prediction of the characteristics of practical-construction wings and the selection of airfoils for such wings.

10. The NACA 6-series airfoils provide higher critical Mach numbers for high-speed and cruising lift coefficients than earlier types of sections and have a reasonable range of lift coefficients within which high critical Mach numbers may be obtained.

11. The NACA 6-series sections provide lower predicted critical Mach numbers at moderately high lift coefficients than the earlier types of sections. The limited data available suggest, however, that the NACA 6-series sections retain satisfactory lift characteristics up to higher Mach numbers than the earlier sections.

12. The NACA 6-series airfoils do not appear to present unusual problems with regard to the application of ailerons.

13. Problems associated with the avoidance of boundary-layer separation caused by interference are expected to be similar for conservative NACA 6-series sections and other good airfoils. Detail shapes for optimum interfering bodies and fillets may be different for various sections if local excessive expansions in the flow are to be avoided.

14. Satisfactory leading-edge air intakes may be provided for NACA 6-series sections, but insufficient

information exists to allow such intakes to be designed without experimental development.

Langley Memorial Aeronautical Laboratory
National Advisory Committee for Aeronautics
Langley Field, Va.

APPENDIX

METHODS OF OBTAINING DATA IN THE LANGLEY
TWO-DIMENSIONAL LOW-TURBULENCE TUNNELS

By Milton M. Klein

Description of Tunnels

The Langley two-dimensional low-turbulence tunnels are closed-throat wind tunnels having rectangular test sections 3 feet wide and $7\frac{1}{2}$ feet high and are designed to test models completely spanning the width of the tunnel in two-dimensional flow. The low-turbulence level of these tunnels, amounting to only a few hundredths of 1 percent, is achieved by the large contraction ratio in the entrance cone (approx. 20:1) and by the introduction of a number of fine-wire small-mesh turbulence-reducing screens in the widest part of the entrance cone. The chord of models tested in these tunnels is usually about 2 feet, although the characteristics at low lift coefficients of models having chords as large as 8 feet may be determined.

The Langley two-dimensional low-turbulence tunnel operates at atmospheric pressure and has a maximum speed of approximately 155 miles per hour. The Langley two-dimensional low-turbulence pressure tunnel operates at pressures up to 10 atmospheres absolute and has a maximum speed of approximately 300 miles per hour at atmospheric pressure. Standard airfoil tests in this tunnel are made of 2-foot-chord wooden models up to Reynolds numbers of approximately 9×10^6 at a pressure of 4 atmospheres absolute.

The lift and drag characteristics of airfoils tested in these tunnels are usually measured by methods other than the use of balances. The lift is evaluated from measurements of the pressure reactions on the floor and ceiling of the tunnel. The drag is obtained from measurements of static and total pressures in the wake. Moments are usually measured by a balance.

CONFIDENTIAL

Symbols

A_1, A_2, \dots, A_n	coefficients of potential function for a symmetrical body
a	fraction of chord from leading edge over which design load is uniform
B	dimensionless constant determining width of wake
c	chord
c_d	drag coefficient corrected for tunnel-wall effects
c_d'	drag coefficient uncorrected for tunnel-wall effects
c_{dT}	drag coefficient measured in tunnel
c_l	section lift coefficient corrected for tunnel-wall effects
c_l'	section lift coefficient uncorrected for tunnel-wall effects
c_{li}	design lift coefficient
c_{lT}	lift coefficient measured in tunnel
$c_{m_c/4}$	moment coefficient about quarter-chord point corrected for tunnel-wall effects
$c_{m_c/4}'$	moment coefficient about quarter-chord point measured in tunnel
F	average of velocity readings of orifices on floor and ceiling used to measure blocking at high lifts
F_0	average value of F in low-lift range
f	potential function used to obtain η -factor
H_0	total pressure in front of airfoil

H_1	total pressure in wake of airfoil
H_c	coefficient of loss of total pressure in the wake $\left(\frac{H_0 - H_1}{q_0}\right)$
$H_{c_{max}}$	maximum value of H_c
h_T	tunnel height
$K = \frac{c_d'}{c_{dT}}$	
L	true lift resulting from a point vortex
L'	lift associated with a point vortex as measured by integrating manometers
m	upstream limit of integration of floor and ceiling pressures
n	downstream limit of integration of floor and ceiling pressures
P_R	resultant pressure coefficient; difference between local upper- and lower-surface pressure coefficients
p_1	static pressure in the wake
q_0	free-stream dynamic pressure
S	static-pressure coefficient $\left(\frac{H_0 - p}{q_0}\right)$
S_1	static-pressure coefficient in the wake $\left(\frac{H_0 - p_1}{q_0}\right)$
s	distance along airfoil surface
u	velocity, due to row of vortices, at any point along tunnel walls
V	free-stream velocity
ΔV	increment in free-stream velocity due to blocking

V'	corrected indicated tunnel velocity
V''	tunnel velocity measured by static-pressure orifices
v	local velocity at any point on airfoil surface
w	potential function for flow past a symmetrical body
x	distance along chord or center line of tunnel
Y	variable of integration $\left(\frac{By_w}{c}\right)$
y	distance perpendicular to stream direction
y_t	ordinate of symmetrical thickness distribution
y_w	distance perpendicular to stream direction from position of $H_{c_{max}}$
$\frac{dy_t}{dx}$	slope of surface of symmetrical thickness distribution
z	complex variable $(x + iy)$
α_{l_0}	angle of zero lift
α_0	section angle of attack corrected for tunnel-wall effects
α_0'	section angle of attack measured in tunnel
Γ	strength of a single vortex
η	ratio of measured lift to actual lift for any type of lift distribution
η_a	η -factor for additional-type loading
η_b	η -factor for basic mean-line loading

η_x	η -factor applying to a point vortex
Λ	component of blocking factor dependent on shape of body
ξ	quantity used for correcting effect of body upon velocity measured by static-pressure orifices
σ	component of blocking factor dependent on size of body
ϕ	potential function
ψ	stream function

Measurement of Lift

The lift carried by the airfoil induces an equal and opposite reaction upon the floor and ceiling of the tunnel. The lift may therefore be obtained by integrating the pressure distribution along the floor and ceiling of the tunnel, the integration being accomplished with an integrating manometer. Because the pressure field theoretically extends to infinity in both the upstream and the downstream directions, not all the lift is included in the length over which the integration is performed. It is therefore necessary to apply a correction factor η that gives the ratio of the measured lift to the actual lift for any lift distribution. The calculation was performed by first finding the correction factor η_x applying to a point vortex and then determining the weighted average of this factor over the chord of the model.

The factor η_x was obtained as follows: The image system which gives only a tangential component of velocity along the tunnel walls is made up of an infinite vertical row of vortices of alternating sign as shown in figure 73. If the sign of the vortex at the origin is assumed to be positive, the complex potential function f for this image system is

$$f = \frac{i\Gamma}{2\pi} \log \sinh \frac{\pi z}{2h_T} - \frac{i\Gamma}{2\pi} \log \sinh \pi \left(\frac{z - ih_T}{2h_T} \right) \quad (18)$$

where

Γ strength of a single vortex

z complex variable ($x + iy$)

h_T tunnel height

The velocity u , due to the row of vortices, at any point along the tunnel walls where

$$y = \frac{h_T}{2}$$

is then obtained as

$$u = \frac{\Gamma}{2h_T} \operatorname{sech} \frac{\pi x}{h_T} \quad (19)$$

where x is the horizontal distance from the point on the wall to the origin. The resultant pressure coefficient P_R is then given by

$$\begin{aligned} P_R &= \frac{4u}{V} \\ &= \frac{2\Gamma}{h_T V} \operatorname{sech} \frac{\pi x}{h_T} \end{aligned} \quad (20)$$

where V is the free-stream velocity.

The lift manometers integrate the pressure distribution along the floor and ceiling from the downstream position n to the upstream position m (fig. 73). For a point vortex located a distance x from the origin along the center line of the tunnel, the limits of integration become $n - x$ and $m - x$. The lift L' associated with a point vortex, as measured by the integrating manometers, is given by

$$L' = \int_{m-x}^{n-x} q_0 P_R dx \quad (21)$$

where q_0 is the free-stream dynamic pressure.

The true lift L resulting from the point vortex is given by

$$L = \frac{2q_0'}{\Gamma V}$$

The correction factor η_x is then

$$\begin{aligned} \eta_x &= \frac{L'}{L} \\ &= \frac{1}{h_T} \int_{m-x}^{n-x} \operatorname{sech} \frac{\pi x}{h_T} dx \end{aligned}$$

which yields

$$\eta_x = \frac{2}{\pi} \tan^{-1} \left[\frac{e^{-\pi x/h_T} (e^{m/h_T} - e^{n/h_T})}{1 + e^{-2\pi x/h_T} e^{\pi(m+n)/h_T}} \right] \quad (22)$$

In the Langley two-dimensional low-turbulence tunnels, the orifices in the floor and ceiling of the tunnel used to measure the lift extend over a length of approximately 13 feet. A plot of η_x against x for the Langley two-dimensional low-turbulence pressure tunnel is shown in figure 74. The η -factor for a given lift distribution is obtained from the expression

$$\eta = \frac{\int_{\text{chord}} P_R \eta_x d\left(\frac{x}{c}\right)}{\int_{\text{chord}} P_R d\left(\frac{x}{c}\right)} \quad (23)$$

The values of η_b and η_a for the Langley two-dimensional low-turbulence pressure tunnel are given in the following table for a model having a chord length of 2 feet, where η_b is the η -factor corresponding to the basic mean-line loading (indicated by the value of a) and η_a is the η -factor for the additional type of loading as given by thin-airfoil theory:

a	η_b
1.0	0.9347
.8	.9342
.6	.9336
.4	.9330
.2	.9325
0	.9322

$$\eta_a = 0.9296$$

In order to check the variation of η_a with variations in the additional type of lift distribution, the value of η_a was recalculated for the class C additional lift distribution given in figure 6 of reference 86. The value of η_a for this case was 0.9304, as compared with 0.9296 for a thin airfoil. Because of the small variation of η_a with the type of additional lift, the value for thin-airfoil additional lift was used for all calculations. The lift coefficient of the model in the tunnel uncorrected for blocking $c_{l'}$ is given in terms of the lift coefficient measured in the tunnel c_{l_T} and the design lift coefficient of the airfoil c_{l_1} by the following expression:

$$c_{l'} = \frac{c_{l_T}}{\eta_a} - \left(\frac{\eta_b}{\eta_a} - 1 \right) c_{l_1} \quad (24)$$

Because η_b does not differ much from η_a , it is not necessary that the basic loading or the design lift coefficient be known with great accuracy.

Because of tunnel-wall and other effects, the lift distribution over the airfoil in the tunnel does not agree exactly with the assumed lift distribution. Because of the small variations of η with lift distribution, errors caused by this effect are considered negligible. It can also be shown that errors caused by neglecting the effect of airfoil thickness on the distribution of the lift reaction along the tunnel walls are small.

Measurement of Drag

The drag of an airfoil may be obtained from observations of the pressures in the wake (reference 96). An approximation to the drag is given by the loss in total pressure of the air in the wake of the airfoil. The loss of total pressure is measured by a rake of total-pressure tubes in the wake. When the total pressures in front of the airfoil and in the wake are represented by H_0 and H_1 , respectively, the drag coefficient obtained from loss of total pressure c_{dT} is

$$c_{dT} = \int_{\text{wake}} H_c \frac{dy_w}{c} \quad (25)$$

where

H_c coefficient of loss of total pressure in the wake $\left(\frac{H_0 - H_1}{q_0} \right)$

y_w distance perpendicular to stream direction from position of $H_{c_{max}}$

If the static pressure in the wake is represented by p_1 , the true drag coefficient uncorrected for blocking c_d' may be shown to be (reference 96)

$$c_d' = \int_{\text{wake}} 2\sqrt{S_1 - H_c} (1 - \sqrt{1 - H_c}) \frac{dy_w}{c} \quad (26)$$

where S_1 is the static-pressure coefficient in the wake $\frac{H_0 - p_1}{q_0}$. The assumption is made that the variation

of total pressure across the wake can be represented by a normal probability curve. The drag coefficient c_d' is then easily obtainable from measurements of c_{dT} by means of a factor K , the ratio of c_d' to c_{dT} , which depends only on S_1 and the maximum value of H_c .

If the maximum value of H_c is represented by $H_{c_{max}}$, the equation of the normal probability curve is

$$H_c = H_{c_{max}} e^{-\left(\frac{By_w}{c}\right)^2}$$

where B is a dimensionless constant that determines the width of the wake. If a convenient variable of integration $Y = \frac{By_w}{c}$ is used, the ratio K is

$$K = \frac{c_d'}{c_{dT}}$$

$$= \frac{2}{\sqrt{\pi}} \frac{1}{H_{c_{max}}} \int_{-\infty}^{\infty} \sqrt{S_1 - H_c} (1 - \sqrt{1 - H_c}) dY \quad (27)$$

and is independent of the width of the wake. The quantity K has been evaluated for various values of $H_{c_{max}}$ and S_1 by assuming S_1 to be constant across the wake. The drag coefficient c_d' may thus be obtained from tunnel measurements of c_{dT} , $H_{c_{max}}$, and S_1 . A plot of K as a function of $H_{c_{max}}$ with S_1 as parameter is given in figure 75. A parallel treatment of this problem is given in reference 97.

Tunnel-Wall Corrections

In two-dimensional flow, the tunnel walls may be conveniently considered as having two distinct effects upon the flow over a model in a tunnel: (1) an increase in the free-stream velocity in the neighborhood of the model because of a constriction of the flow and (2) a distortion of the lift distribution from the induced curvature of the flow.

The increase in free-stream velocity caused by the tunnel walls (blocking effect) is obtained from consideration of an infinite vertical row of images of

a symmetrical body as given in reference 98; the images represent the effect of the tunnel walls.

The potential function w for a symmetrical body is given by

$$w = Vz + \frac{A_1}{z} + \frac{A_2}{z^2} + \dots + \frac{A_n}{z^n} \quad (28)$$

where V is the free-stream velocity and the coefficients A_1, A_2, \dots are complex. If the tunnel height is large compared to the size of the body, powers of $1/z$ greater than 1 may be neglected and

$$w = Vz + \frac{A_1}{z} \quad (29)$$

This operation is equivalent to replacing the body by a circle of which the doublet strength is $2\pi A_1$; the term A_1/z represents the disturbance to the free-stream flow. The total induced velocity at the center of the body due to all the images is expressed in reference 98 as

$$\Delta V = \frac{A_1}{h_T^2} \frac{\pi^2}{3} \quad (30)$$

where the term A_1 is the same as the term $\frac{1}{4}\lambda t^2 V$ of reference 98.

For convenience in tunnel calculations, the expression for ΔV may be written

$$\frac{\Delta V}{V} = \Lambda \sigma \quad (31)$$

where

$$\sigma = \frac{\pi^2}{48} \left(\frac{c}{h_T} \right)^2 \quad (32)$$

$$\Lambda = \frac{16A_1}{c^2V} \quad (33)$$

The factor σ depends only on the size of the body and is easily calculated. The factor Λ depends on the shape of the body and is more difficult to calculate. For bodies such as Rankine ovals and ellipses, simple formulas may be obtained for calculating Λ . In the general case, the value of Λ may be obtained from the velocity distribution over the body by the expression

$$\Lambda = \frac{16}{\pi} \int_0^1 \frac{y}{c} \frac{v}{V} \sqrt{1 + \left(\frac{dy_t}{dx}\right)^2} d\left(\frac{x}{c}\right) \quad (34)$$

where v is the velocity at any point on the airfoil surface and dy_t/dx is the slope of the airfoil surface at any point of which the ordinate is y_t .

In order to obtain this expression, consider the flow past a symmetrical body as shown in figure 76. The potential function for this flow is given by equation (28). Differentiating and multiplying equation (28) by z gives

$$z \frac{dw}{dz} = Vz - \frac{A_1}{z} - \frac{2A_2}{z^2} \dots - \frac{nA_n}{z^n}$$

The line integral about a closed curve $\int_C z \frac{dw}{dz} dz$ will depend only on the term $-A_1/z$ and, from the theory of residues, is given by

$$\int_C z \frac{dw}{dz} dz = -2\pi i A_1$$

but

$$\begin{aligned} z \frac{dw}{dz} dz &= z dw \\ &= (x + iy)(d\phi + i d\psi) \end{aligned}$$

where ϕ is the potential function and ψ is the stream function. On the surface of the body $d\psi = 0$, so that

$$\int_C z \frac{dw}{dz} dz = \int_C x d\phi + i \int_C y d\phi \quad (35)$$

Since the body is symmetrical, the term $x d\phi$ will have equal numerical values but opposite signs at corresponding points of the upper and lower surfaces, and $\int_C x d\phi$ will vanish. The term $y d\phi$ will have equal values at corresponding points of the upper and lower surfaces, and $\int_C y d\phi$ may be replaced by an integration over the upper surface; therefore,

$$\int_C z \frac{dw}{dz} dz = 2i \int y d\phi \text{ (counterclockwise direction)}$$

or

$$A_1 = -\frac{1}{\pi} \int y d\phi$$

Reversing the path of integration, replacing $d\phi$ by $v ds$, replacing ds by $\sqrt{1 + \left(\frac{dy_t}{dx}\right)^2} dx$, and solving for $\Lambda = \frac{16A_1}{c^2 v}$ gives

$$\Lambda = \frac{16}{\pi} \int_0^1 \frac{y}{c} \frac{v}{V} \sqrt{1 + \left(\frac{dy_t}{dx}\right)^2} d\left(\frac{x}{c}\right)$$

where the integration is taken from the leading edge to the trailing edge over the upper surface.

In addition to the error caused by blocking, an error exists in the measured tunnel velocity because of the interference effects of the model upon the velocity indicated by the static-pressure orifices located a few

feet upstream of the model and halfway between floor and ceiling. In order to correct for this error an analysis was made of the velocity distribution along the streamline halfway between the upper and the lower tunnel walls for Rankine ovals of various sizes and thickness ratios. The analysis showed that the correction could be expressed, within the range of conventional-airfoil thickness ratios, as a product of a thickness factor given by the blocking factor Λ and a factor ξ - which depended upon the size of the model and the distance from the static-pressure orifices to the midchord point of the model. The corrected indicated tunnel velocity V' could then be written

$$V' = V''(1 + \Lambda\xi) \quad (36)$$

where V'' is the velocity measured by the static-pressure orifices. In the Langley two-dimensional low-turbulence tunnels, the distance from the static-pressure orifices to the midchord point of the model is approximately 5.5 feet; the corresponding value of ξ for a 2-foot-chord model is approximately 0.002.

In order to calculate the effect of the tunnel walls upon the lift distribution, a comparison is made of the lift distribution of a given airfoil in a tunnel and in free air on the basis of thin-airfoil theory. It is assumed that the flow conditions in the tunnel correspond most closely to those in free air when the additional lift in the tunnel and in free air are the same (reference 99). On this basis, the following corrections are derived (reference 99), in which the primed quantities refer to the coefficients measured in the tunnel:

$$c_l = [1 - 2\Lambda(\sigma + \xi) - \sigma]c_l' \quad (37)$$

$$\alpha_0 = (1 + \sigma)\alpha_0' + \frac{4\sigma c_{m_c/4}'}{dc_l'/d\alpha_0'} - \sigma\alpha_{l_0} \quad (38)$$

$$c_{m_c/4} = [1 - 2\Lambda(\sigma + \xi)]c_{m_c/4}' + \sigma\frac{c_l'}{4} \quad (39)$$

In the foregoing equations, the terms $\frac{4\sigma c_{mc}/4}{dc_l'/d\alpha_0'}$, a_{l_0} , and $\sigma c_l'/4$ are usually negligible for 2-foot-chord models in the Langley two-dimensional low-turbulence tunnels.

When the effect of the tunnel walls on the pressure distribution over the model is small, the wall effect on the drag is merely that corresponding to an increase in the tunnel speed. The correction to the drag coefficient is therefore given by the following relation:

$$c_d = [1 - 2A(\sigma + \xi)]c_d' \quad (40)$$

Similar considerations have been applied to the development of corrections for the pressure distribution in reference 99.

Equation (40) neglects the blocking due to the wake, such blocking being small at low to moderate drags. The effect of a pressure gradient in the tunnel upon loss of total pressure in the wake is not easily analyzed but is estimated to be small. The effect of the pressure gradient upon the drag has therefore been disregarded. When the drag is measured by a balance, the effect of the pressure gradient upon the drag is directly additive and a correction should be applied. For large models, especially at high lift coefficients, the effect of the tunnel walls is to distort the pressure distribution appreciably. Such distortions of the pressure distribution may cause large changes in the boundary flow and no adequate corrections to any of the coefficients, particularly the drag, can be found.

Correction for Blocking at High Lifts

So long as the flow follows the airfoil surface, the foregoing relations account for the effects of the tunnel walls with sufficient accuracy. When the flow leaves the surface, the blocking increases because of the predominant effect of the wake upon the free-stream velocity. Since the wake effect shows up primarily in the drag, the increase in blocking would logically be expressed in terms of the drag. The accurate measurement of drag under these conditions by means of a rake is impractical because of spanwise movements of low-energy air. A method of correcting for increased blocking at

high angles of attack without drag measurements has therefore been devised for use in the Langley two-dimensional low-turbulence tunnels.

Readings of the floor and ceiling velocities are taken a few inches ahead of the quarter-chord point and averaged to remove the effect of lift. This average F , which is a measure of the effective tunnel velocity, is essentially constant in the low-lift range. The quantity F/F_0 , where F_0 is the average value of F in the low-lift range, however, shows a variation from unity in the high-lift range for any airfoil tested in the tunnel; this variation indicates a change in blocking at high lifts. A plot of F/F_0 against angle of attack α_0' for a 2-foot-chord model of the NACA 643-418 airfoil is given in figure 77. The quantity F/F_0 is nearly constant for values of α_0' up to 12° ; but for values of α_0' greater than 12° , F/F_0 increases and the increase is particularly noticeable at and over the stall.

A theoretical comparison was made of the blocking factor $\Lambda\sigma$, and the velocity measured by the floor and ceiling orifices for a series of Rankine ovals of various sizes and thickness ratios. The quarter-chord point of each oval was located at the pivot point, the usual position of an airfoil in the tunnel. The analysis showed the relation between the blocking factor $\Lambda\sigma$ and the change in F to be unique for chord lengths up to 50 inches in that different bodies having the same blocking factor $\Lambda\sigma$ gave approximately the same value of F . For chords up to 50 inches, the relationship is

$$\frac{\Delta V}{V} = 0.45 \left(\frac{F}{F_0} - 1 \right) \quad (41)$$

where $\Delta V/V$ is the true increment in tunnel velocity due to blocking. The foregoing relation was adopted to obtain the correction to the blocking in the range of lifts where $\frac{F}{F_0} > 1$.

Considerable uncertainty exists regarding the correct numerical value of the coefficient occurring in equation (41). If a row of sources, rather than the Rankine ovals used in the present analysis, is considered to represent the effect of the wake, the value

of the coefficient in equation (41) would be approximately twice the value used. Fortunately, the correction amounts to only about 2 percent at maximum lift for an extreme condition with a 2-foot-chord model. Further refinement of this correction has therefore not been attempted.

Comparison with Experiment

A check of the validity of the tunnel-wall corrections has been made in reference 99, which gives lift and moment curves for models having various ratios of chord to tunnel height, uncorrected and corrected for tunnel-wall effects. The general agreement of the corrected curves shows that the method of correcting the lifts and moments is valid.

A comparison is made in reference 99 between the theoretical correction factor (equation (40)) and the experimentally derived corrections of reference 100. The theoretical correction factors were found to be in good agreement with those obtained experimentally.

In order to check the validity of the η -factor, a comparison has been made of lift values obtained from pressure distributions with those obtained from the integration of the floor and ceiling pressures in the tunnel. A comparison for two airfoils given in figure 78 shows that the two methods of measuring lift give results that are in good agreement. The η -factor has also been checked by comparison of the lift obtained from balance measurements with the integrating-manometer values in figure 79.

Finally, a check has been made of the method of correcting pressure distributions (reference 99) for NACA 6-series airfoils of two chord lengths at zero angle of attack in figure 80, in which the pressure coefficients are plotted against chordwise position x/c . The agreement between the corrected pressure distributions for both models verifies the method of making the tunnel-wall corrections.

REFERENCES

1. Jacobs, Eastman N., Abbott, Ira H., and Davidson, Milton: Preliminary Low-Drag-Airfoil and Flap Data from Tests at Large Reynolds Numbers and Low Turbulence, and Supplement. NACA ACR, March 1942.
2. Jacobs, Eastman N., Ward, Kenneth E., and Pinkerton, Robert M.: The Characteristics of 78 Related Airfoil Sections from Tests in the Variable-Density Wind Tunnel. NACA Rep. No. 460, 1933.
3. Jacobs, Eastman N., and Pinkerton, Robert M.: Tests in the Variable-Density Wind Tunnel of Related Airfoils Having the Maximum Camber Unusually Far Forward. NACA Rep. No. 537, 1935.
4. Jacobs, Eastman N., Pinkerton, Robert M., and Greenberg, Harry: Tests of Related Forward-Camber Airfoils in the Variable-Density Wind Tunnel. NACA Rep. No. 610, 1937.
5. Stack, John, and von Doenhoff, Albert E.: Tests of 16 Related Airfoils at High Speeds. NACA Rep. No. 492, 1934.
6. Jacobs, Eastman N., and Sherman, Albert: Airfoil Section Characteristics as Affected by Variations of the Reynolds Number. NACA Rep. No. 586, 1937.
7. Pinkerton, Robert M., and Greenberg, Harry: Aerodynamic Characteristics of a Large Number of Airfoils Tested in the Variable-Density Wind Tunnel. NACA Rep. No. 628, 1938.
8. Jones, B. Melvill: Flight Experiments on the Boundary Layer. Jour. Aero. Sci., vol. 5, no. 3, Jan. 1938, pp. 81-94.
9. Jacobs, Eastman N., and Abbott, Ira H.: Airfoil Section Data Obtained in the N.A.C.A. Variable-Density Tunnel as Affected by Support Interference and Other Corrections. NACA Rep. No. 669, 1939.

10. Theodorsen, Theodore: Theory of Wing Sections of Arbitrary Shape. NACA Rep. No. 411, 1931.
11. Stack, John : Tests of Airfoils Designed to Delay the Compressibility Burble. NACA TN No. 976, Dec. 1944. (Reprint of NACA ACR, June 1939.)
12. Jacobs, Eastman N.: Preliminary Report on Laminar-Flow Airfoils and New Methods Adopted for Airfoil and Boundary-Layer Investigations. NACA ACR, June 1939.
13. von Doenhoff, Albert E., and Stivers, Louis S., Jr.: Aerodynamic Characteristics of the NACA 747A315 and 747A415 Airfoils from Tests in the NACA Two-Dimensional Low-Turbulence Pressure Tunnel. NACA CB No. L4I25, 1944.
14. Naiman, Irven: Numerical Evaluation of the ϵ -Integral Occurring in the Theodorsen Arbitrary Airfoil Potential Theory. NACA ARR No. L4D27a, 1944.
15. Theodorsen, Theodore: Airfoil-Contour Modification Based on ϵ -Curve Method of Calculating Pressure Distribution. NACA ARR No. L4G05, 1944.
16. Allen, H. Julian: A Simplified Method for the Calculation of Airfoil Pressure Distribution. NACA TN No. 708, 1939.
17. Munk, Max M.: Elements of the Wing Section Theory and the Wing Theory. NACA Rep. No. 191, 1924.
18. Glauert, H.: The Elements of Aerofoil and Airscrew Theory. Cambridge Univ. Press, 1926, pp. 87-93.
19. Theodorsen, Theodore: On the Theory of Wing Sections with Particular Reference to the Lift Distribution. NACA Rep. No. 383, 1931.
20. von Kármán, Th.: Compressibility Effects in Aerodynamics. Jour. Aero. Sci., vol. 8, no. 9, July 1941, pp. 337-356.
21. Heaslet, Max. A.: Critical Mach Numbers of Various Airfoil Sections. NACA ACR No. L4G18, 1944.

22. Brombacher, W. G.: Altitude-Pressure Tables Based on the United States Standard Atmosphere. NACA Rep. No. 538, 1935.
 23. von Doenhoff, Albert E.: A Method of Rapidly Estimating the Position of the Laminar Separation Point. NACA TN No. 671, 1938.
 24. Jacobs, E. N., and von Doenhoff, A. E.: Formulas for Use in Boundary-Layer Calculations on Low-Drag Wings. NACA ACR, Aug. 1941.
 25. von Doenhoff, Albert E., and Tetervin, Neal: Determination of General Relations for the Behavior of Turbulent Boundary Layers. NACA ACR No. 3G13, 1943.
 26. Squire, H. B., and Young, A. D.: The Calculation of the Profile Drag of Aerofoils. R & M No. 1838, British A.R.C., 1938.
 27. Nitzberg, Gerald E.: A Concise Theoretical Method for Profile-Drag Calculation. NACA ACR No. 4B05, 1944.
 28. Tetervin, Neal: A Method for the Rapid Estimation of Turbulent Boundary-Layer Thicknesses for Calculating Profile Drag. NACA ACR No. 14G14, 1944.
 29. Quinn, John H., Jr., and Tucker, Warren A.: Scale and Turbulence Effects on the Lift and Drag Characteristics of the NACA 653-418, $a = 1.0$ Airfoil Section. NACA ACR No. 14H11, 1944.
 30. Tucker, Warren A., and Wallace, Arthur R.: Scale-Effect Tests in a Turbulent Tunnel of the NACA 653-418, $a = 1.0$ Airfoil Section with 0.20-Airfoil-Chord Split Flap. NACA ACR No. 14I22, 1944.
 31. Abbott, Ira H., and Miller, Ralph B.: Tests of a Highly Cambered Low-Drag Airfoil Section with a Lift-Control Flap. NACA ACR, Dec. 1942.
- Abbott, Ira H. and Miller, Ralph B.: Supplement to Advance Confidential Report, Tests of a Highly Cambered Low-Drag-Airfoil Section with a Lift-Control Flap. NACA ACR No. 3D30, 1943.

32. Davidson, Milton, and Turner, Harold R., Jr.:
Effects of Mean-Line Loading on the Aerodynamic
Characteristics of Some Low-Drag Airfoils.
NACA ACR No. 3I27, 1943.
33. von Doenhoff, Albert E., and Tetervin, Neal: Investi-
gation of the Variation of Lift Coefficient with
Reynolds Number at a Moderate Angle of Attack on
a Low-Drag Airfoil. NACA CB, Nov. 1942.
34. Oswald, W. Bailey: General Formulas and Charts for
the Calculation of Airplane Performance. NACA
Rep. No. 408, 1932.
35. Millikan, Clark B.: Aerodynamics of the Airplane.
John Wiley & Sons, 1941, pp. 108-109.
36. Hood, Manley J.: The Effects of Some Common Sur-
face Irregularities on Wing Drag. NACA TN No. 695,
1939.
37. Charters, Alex C.: Transition between Laminar and
Turbulent Flow by Transverse Contamination.
NACA TN No. 891, 1943.
38. Braslow, Albert L.: Investigation of Effects of
Various Camouflage Paints and Painting Procedures
on the Drag Characteristics of an NACA 65(421)-420,
a $\alpha = 1.0$ Airfoil Section. NACA CB No. L4G17, 1944.
39. Allen, H. Julian: Notes on the Effect of Surface
Distortions on the Drag and Critical Mach Number
of Airfoils. NACA ACR No. 3I29, 1943.
40. Fage, Arthur: The Smallest Size of a Surface Bulge,
Ridge or Hollow, Which Affects the Drag of a
Laminar-Flow Aerofoil. 6443, Ae. 2148, British A.R.C.,
Jan. 22, 1943.
41. Abbott, Frank T., Jr., and Turner, Harold R., Jr.:
The Effects of Roughness at High Reynolds Numbers
on the Lift and Drag Characteristics of Three
Thick Airfoils. NACA ACR No. L4H21, 1944.
42. Zalovcik, John A.: Profile-Drag Coefficients of
Conventional and Low-Drag Airfoils as Obtained
in Flight. NACA ACR No. L4E31, 1944.

43. Zalovecik, John A., and Wood, Clotaire: A Flight Investigation of the Effect of Surface Roughness on Wing Profile Drag with Transition Fixed. NACA ARR No. L4I25, 1944.
44. Smelt, R., and Higton, D. J.: Measurements of the Drag of Rough Painted Surfaces on a Mustang. Rep. No. Aero 1849, British R.A.E., Aug. 1943.
45. Young, A. D.: Note on the Effect of Slipstream on Boundary Layer Flow. Rep. No. B.A. 1404, British R.A.E., May 1937.
46. Young, A. D.: Further Note on the Effect of Slipstream on Boundary Layer Flow. Rep. No. B.A. 1404a, British R.A.E., Oct. 1938.
47. Young, A. D., and Morris, D. E.: Further Note on Flight Tests on the Effect of Slipstream on Boundary Layer Flow. Rep. No. B.A. 1404b, British R.A.E., Sept. 1939.
48. Hood, Manley J., and Gaydos, M. Edward: Effects of Propellers and of Vibration on the Extent of Laminar Flow on the N.A.C.A. 27-212 Airfoil. NACA ACR, Oct. 1939.
49. Jacobs, Eastman N., Abbott, Ira H., and Davidson, Milton: Investigation of Extreme Leading-Edge Roughness on Thick Low-Drag Airfoils to Indicate Those Critical to Separation. NACA CB, June 1942.
50. Sweberg, Harold H., and Dingeldein, Richard C.: Summary of Measurements in the Langley Full-Scale Tunnel of Maximum Lift Coefficients and Stalling Characteristics of Airplanes. NACA ACR (to be published).
51. Purser, Paul E., and Johnson, Harold S.: Effects of Trailing-Edge Modifications on Pitching-Moment Characteristics of Airfoils. NACA CB No. L4I30, 1944.
52. Rhode, Richard V.: Correlation of Flight Data on Limit Pressure Coefficients and Their Relation to High-Speed Bubbling and Critical Tail Loads. NACA ACR No. L4I27, 1944.

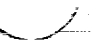
53. Davidson, Milton, and Turner, Harold R., Jr.: Tests of an NACA 66,2-216, $a = 0.6$ Airfoil Section with a Slotted and Plain Flap. NACA ACR No. 3J05, 1943.
54. Fullmer, Felicien F., Jr.: Wind-Tunnel Investigation of NACA 66(215)-216, 66,1-212, and 65₁-212 Airfoils with 0.20-Airfoil-Chord Split Flaps. NACA CB No. L4G10, 1944.
55. Abbott, Ira H., and Greenberg, Harry: Tests in the Variable-Density Wind Tunnel of the N.A.C.A. 23012 Airfoil with Plain and Split Flaps. NACA Rep. No. 661, 1939.
56. Wenzinger, Carl J., and Harris, Thomas A.: Wind-Tunnel Investigation of NACA 23012, 23021, and 23030 Airfoils with Various Sizes of Split Flap. NACA Rep. No. 668, 1939.
57. Abbott, Ira H., and Fullmer, Felicien F., Jr.: Wind-Tunnel Investigation of NACA 63,4-420 Airfoil with 25-Percent-Chord Slotted Flap. NACA ACR No. 3I21, 1943.
58. Bogdonoff, Seymour M.: Wind-Tunnel Investigation of a Low-Drag Airfoil Section with a Double Slotted Flap. NACA ACR No. 3I20, 1943.
59. Wenzinger, Carl J., and Harris, Thomas A.: Wind-Tunnel Investigation of an N.A.C.A. 23012 Airfoil with Various Arrangements of Slotted Flaps. NACA Rep. No. 664, 1939.
60. Wenzinger, Carl J., and Harris, Thomas A.: Wind-Tunnel Investigation of an N.A.C.A. 23021 Airfoil with Various Arrangements of Slotted Flaps. NACA Rep. No. 677, 1939.
61. Swanson, Robert S., and Crandall, Stewart M.: Analysis of Available Data on the Effectiveness of Ailerons without Exposed Overhang Balance. NACA ACR No. L4E01, 1944.
62. Street, William B., and Ames, Milton B., Jr.: Pressure-Distribution Investigation of an N.A.C.A. 0009 Airfoil with a 50-Percent-Chord Plain Flap and Three Tabs. NACA TN No. 734, 1939.

63. Ames, Milton B., Jr., and Sears, Richard I.: Pressure-Distribution Investigation of an NACA 0009 Airfoil with an 80-Percent-Chord Plain Flap and Three Tabs. NACA TN No. 761, 1940.
64. Ames, Milton B., Jr., and Sears, Richard I.: Pressure-Distribution Investigation of an NACA 0009 Airfoil with a 30-Percent-Chord Plain Flap and Three Tabs. NACA TN No. 759, 1940.
65. Sears, Richard I.: Wind-Tunnel Investigation of Control-Surface Characteristics. I - Effect of Gap on the Aerodynamic Characteristics of an NACA 0009 Airfoil with a 30-Percent-Chord Plain Flap. NACA ARR, June 1941.
66. Jones, Robert T., and Ames, Milton B., Jr.: Wind-Tunnel Investigation of Control-Surface Characteristics. V - The Use of a Beveled Trailing Edge to Reduce the Hinge Moment of a Control Surface. NACA ARR, March 1942.
67. Sears, Richard I., and Liddell, Robert B.: Wind-Tunnel Investigation of Control-Surface Characteristics. VI - A 30-Percent-Chord Plain Flap on the NACA 0015 Airfoil. NACA ARR, June 1942.
68. Wenzinger, Carl J., and Delano, James B.: Pressure Distribution over an N.A.C.A. 23012 Airfoil with a Slotted and a Plain Flap. NACA Rep. No. 633, 1938.
69. Gillis, Clarence L., and Lockwood, Vernard E.: Wind-Tunnel Investigation of Control-Surface Characteristics. XIII - Various Flap Overhangs Used with a 30-Percent-Chord Flap on an NACA 66-009 Airfoil. NACA ACR No. 3G20, 1943.
70. Rogallo, F. M.: Collection of Balanced-Aileron Test Data. NACA ACR No. 4A11, 1944.
71. Denaci, H. G., and Bird, J. D.: Wind-Tunnel Tests of Ailerons at Various Speeds. II - Ailerons of 0.20 Airfoil Chord and True Contour with 0.60 Aileron-Chord Sealed Internal Balance on the NACA 66,2-216 Airfoil. NACA ACR No. 3F18, 1943.

72. Purser, Paul E., and Riebe, John M.: Wind-Tunnel Investigation of Control-Surface Characteristics. XV - Various Contour Modifications of a 0.30-Airfoil-Chord Plain Flap on an NACA 66(215)-014 Airfoil. NACA ACR No. 3L20, 1943.
73. Braslow, Albert L.: Wind-Tunnel Investigation of Aileron Effectiveness of 0.20-Airfoil-Chord Plain Ailerons of True Airfoil Contour on NACA 65₂-415, 65₃-418, and 65₄-421 Airfoil Sections. NACA CB No. 14H12, 1944.
74. Sears, Richard I., and Purser, Paul E.: Wind-Tunnel Investigation of Control-Surface Characteristics. XIV - NACA 0009 Airfoil with a 20-Percent-Chord Double Plain Flap. NACA ARR No. 3F29, 1943.
75. Crane, Robert M., and Holtzclaw, Ralph W.: Wind-Tunnel Investigation of Ailerons on a Low-Drag Airfoil. I - The Effect of Aileron Profile. NACA ACR No. 4A14, 1944.
76. von Doenhoff, Albert E., and Horton, Elmer A.: Preliminary Investigation in the NACA Low-Turbulence Tunnel of Low-Drag-Airfoil Sections Suitable for Admitting Air at the Leading Edge. NACA ACR, July 1942.
77. Smith, Norman F.: High-Speed Investigation of Low-Drag Wing Inlets. NACA ACR No. 14I18, 1944.
78. Jacobs, Eastman N., and Ward, Kenneth E.: Interference of Wing and Fuselage from Tests of 209 Combinations in the N.A.C.A. Variable-Density Tunnel. NACA Rep. No. 540, 1935.
79. Abbott, Ira H.: Interference Effects of Longitudinal Flat Plates on Low-Drag Airfoils. NACA CB, Nov. 1942.
80. Ellis, Macon C., Jr.: Some Lift and Drag Measurements of a Representative Bomber Nacelle on a Low-Drag Wing - II. NACA CB, Sept. 1942.

81. Ellis, Macon C., Jr.: Effects of a Typical Nacelle on the Characteristics of a Thick Low-Drag Airfoil Critically Affected by Leading-Edge Roughness. NACA CB No. 3D27, 1943.
82. Allen, H. Julian, and Frick, Charles W., Jr.: Experimental Investigation of a New Type of Low-Drag Wing-Nacelle Combination. NACA ACR, July 1942.
83. Abbott, Frank T., Jr.: Lift and Drag Data for 30 Pusher-Propeller Shaft Housings on an NACA 65,3-018 Airfoil Section. NACA ACR No. 3K13, 1943.
84. Robinson, Russell G., and Wright, Ray H.: Estimation of Critical Speeds of Airfoils and Streamline Bodies. NACA ACR, March 1940.
85. Anderson, Raymond F.: Determination of the Characteristics of Tapered Wings. NACA Rep. No. 572, 1936.
86. Jacobs, Eastman N., and Rhode, R. V.: Airfoil Section Characteristics as Applied to the Prediction of Air Forces and Their Distribution on Wings. NACA Rep. No. 631, 1938.
87. Soulé, H. A., and Anderson, R. F.: Design Charts Relating to the Stalling of Tapered Wings. NACA Rep. No. 703, 1940.
88. Harmon, Sidney M.: Additional Design Charts Relating to the Stalling of Tapered Wings. NACA ARR, Jan. 1943.
89. Anderson, Raymond F.: The Experimental and Calculated Characteristics of 22 Tapered Wings. NACA Rep. No. 627, 1938.
90. Tani, Itiro: A Simple Method of Calculating the Induced Velocity of a Monoplane Wing. Rep. No. 111 (Vol. IX,3), Aero. Res. Inst., Tokyo Imperial Univ., Aug. 1934.
91. Sherman, Albert: A Simple Method of Obtaining Span Load Distributions. NACA TN No. 732, 1939.

92. Jones, Robert T.: Correction of the Lifting-Line Theory for the Effect of the Chord. NACA TN No. 817, 1941.
93. Cohen, Doris: Theoretical Distribution of Load over a Swept-Back Wing. NACA ARR, Oct. 1942.
94. Pearson, H. A.: Span Load Distribution for Tapered Wings with Partial-Span Flaps. NACA Rep. No. 585, 1937.
95. Pearson, Henry A., and Anderson, Raymond F.: Calculation of the Aerodynamic Characteristics of Tapered Wings with Partial-Span Flaps. NACA Rep. No. 665, 1939.
96. The Cambridge University Aeronautics Laboratory: The Measurement of Profile Drag by the Pitot-Traverse Method. R. & M. No. 1633, British A.R.C., 1936.
97. Silverstein, A., and Katzoff, S.: A Simplified Method for Determining Wing Profile Drag in Flight. Jour. Aero. Sci., vol. 7, no. 7, May 1940, pp. 295-301.
98. Glauert, H.: Wind Tunnel Interference on Wings, Bodies and Airscrews. R. & M. No. 1566, British A.R.C., 1933.
99. Allen, H. Julian, and Vincenti, Walter G.: Wall Interference in a Two-Dimensional-Flow Wind Tunnel with Consideration of the Effect of Compressibility. NACA ARR No. 4K03, 1944.
100. Fage, A.: On the Two-Dimensional Flow past a Body of Symmetrical Cross-Section Mounted in a Channel of Finite Breadth. R. & M. No. 1223, British A.R.C., 1929.



CONFIDENTIAL

TABLE I
ANALYSIS OF AIRFOIL DERIVATION

Airfoil designation	Basic thickness form	Mean-line combination ¹														
		a = 0	a = 0.1	a = 0.2	a = 0.3	a = 0.4	a = 0.5	a = 0.6	a = 0.7	a = 0.8	a = 0.9	a = 1.0				
747A315	747A015				0.763				-0.463							
747A415	747A015				0.763				-0.463							0.100

¹The numbers in the various columns headed "Mean-line combination" indicate the magnitude of the design lift coefficient used.

CONFIDENTIAL



CONFIDENTIAL

TABLE II

MAXIMUM LIFT AND STALLING CHARACTERISTICS OF MODELS TESTED IN THE NACA 19-FOOT PRESSURE TUNNEL

Model	Configuration		Geometric characteristics	Flap		Flap angle (deg)		Flap chord (percent)		Flap span (percent)		R	C _{Lmax}	Stalling characteristics		
	Plan View	Front view		Inboard	Outboard	δ _{f1}	δ _{f0}	c _{f1}	c _{f0}	b _{f1}	b _{f0}					
I			Sections: Root: NACA 66(215)-216 Tip: NACA 66(215)-216 A = 7.00 λ = 1.00 Geometric washout, 0.0°	None	None	---	---	None	None	None	None	2.6 × 10 ⁶	1.26	Abrupt stall progresses from root toward tip for flaps neutral and partial-span flaps deflected; no data for full-span flaps		
				Split	Split	60	---	10	---	53	---	---	2.6		1.26	
				Split	Split	---	---	---	---	---	---	---	---		4.5	1.01
				Split	Split	---	---	---	---	---	---	---	---		2.6	1.72
II			Sections: Root: NACA 66(215)-116 Tip: NACA 66(215)-216 A = 7.0 λ = 0.5 Geometric washout, 1.5°	None	None	---	---	None	None	None	None	2.6 × 10 ⁶	2.07	With flaps neutral, satisfactory; with flaps deflected, extremely abrupt stall envelopes entire wing		
				Split	Split	60	---	10	---	37	---	---	2.6		1.94	
				Split	Split	---	---	---	---	---	---	---	---		4.6	2.01
				Split	Split	---	---	---	---	---	---	---	---		2.6	2.06
III			Sections: Root: NACA 65(318)-019 Tip: NACA 65(318)-015 A = 7.56 λ = 0.25 Geometric washout, 3.6°	None	None	---	---	None	None	None	None	3.0 × 10 ⁶	1.18	Abrupt stall with satisfactory progression toward tips		
				None	None	---	---	---	---	---	---	---	---		5.1	1.37
				None	None	---	---	---	---	---	---	---	---		7.4	1.43
				None	None	---	---	---	---	---	---	---	---		2.1	1.17
IV			Sections: Root: NACA 65(318)-019 Tip: NACA 65(318)-015 A = 7.36 λ = 0.25 Geometric washout, 4.0° Sweepback of 0.25 chord line, 21.93°	None	None	---	---	None	None	None	None	3.0 × 10 ⁶	1.17	Unsatisfactory stall; a strong out-flow resulted in severe tip stall		
				None	None	---	---	---	---	---	---	---	---		5.1	1.31
				None	None	---	---	---	---	---	---	---	---		7.2	1.34
				None	None	---	---	---	---	---	---	---	---		2.1	1.17

NATIONAL ADVISORY COMMITTEE FOR AERONAUTICS

CONFIDENTIAL



TABLE II - Continued

MAXIMUM LIFT AND STALLING CHARACTERISTICS OF MODELS - Continued

CONFIDENTIAL

Model	Configuration		Geometric characteristics	Flap		Flap angle (deg)		Flap chord (percent)		Flap span (percent)		R	C _{lmax}	Stalling characteristics
	Plan view	Front view		Inboard	Outboard	δ_{f1}	δ_{f0}	α_{f1}	α_{f0}	b_{f1}	b_{f0}			
V			Sections: Root: NACA 66(215)-(1.8)(15.5), $\lambda = 0.6$ Tip: NACA 66(215)-(1.8)12, $\lambda = 0.6$ Geometric washout, 2.5°	Plain ↓ None ↓	None ↓	0 ↓ 50 ↓	25 ↓ 25 ↓	25 ↓ 25 ↓	60 ↓ 60 ↓	60 ↓ 60 ↓	3.2×10^6 5.4 ↓ 3.3 ↓ 5.8 ↓ 7.0	1.40 1.52 1.55 2.10 2.19 2.21 2.23	Abrupt stall with satisfactory progression toward tips	
VI			Sections: Root: NACA 66(215)-(1.8)(15.5), $\lambda = 0.6$ Tip: NACA 66(215)-(1.8)12, $\lambda = 0.6$ Geometric washout, 2.5°	Plain ↓ None ↓	None ↓	0 ↓ 50 ↓	25 ↓ 25 ↓	25 ↓ 25 ↓	60 ↓ 60 ↓	60 ↓ 60 ↓	3.3×10^6 5.3 ↓ 6.0 ↓ 3.3 ↓ 5.1 ↓ 5.8	1.34 1.39 1.39 1.87 1.91 1.92	Abrupt stall with satisfactory progression toward tips	
VII			Sections: Root: Mod. NACA 65,3-318, $\lambda = 0.8$ Tip: Mod. NACA 65(318)-316, $\lambda = 0.8$ Geometric washout, 0.0°	Double slotted ↓ Double slotted ↓	Double slotted ↓	0 ↓ 55 ↓	0 ↓ 30 ↓	25 ↓ 25 ↓	25 ↓ 25 ↓	48 ↓ 48 ↓	5.1×10^6 5.1	1.33 2.85	Satisfactory	
VIII			Sections: Root: NACA 67(115)-116 Tip: NACA 67,1-115 $\lambda = 0.4$ Geometric washout, 2.0°	Zap ↓ Split ↓ None ↓ Split ↓	Zap ↓ None ↓ Split ↓	0 ↓ 48 ↓ 60 ↓	0 ↓ 48 ↓ 60 ↓	35 ↓ 35 ↓ 20 ↓	35 ↓ 35 ↓ 20 ↓	60 ↓ 60 ↓ 60 ↓	2.4×10^6 2.4 ↓ 2.4 ↓ 2.5 ↓ 2.5	1.32 2.27 2.07 1.91 2.22	No data	

CONFIDENTIAL

NATIONAL ADVISORY COMMITTEE FOR AERONAUTICS

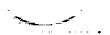


TABLE II - Continued
 MAXIMUM LIFT AND STALLING CHARACTERISTICS OF MODELS - Continued

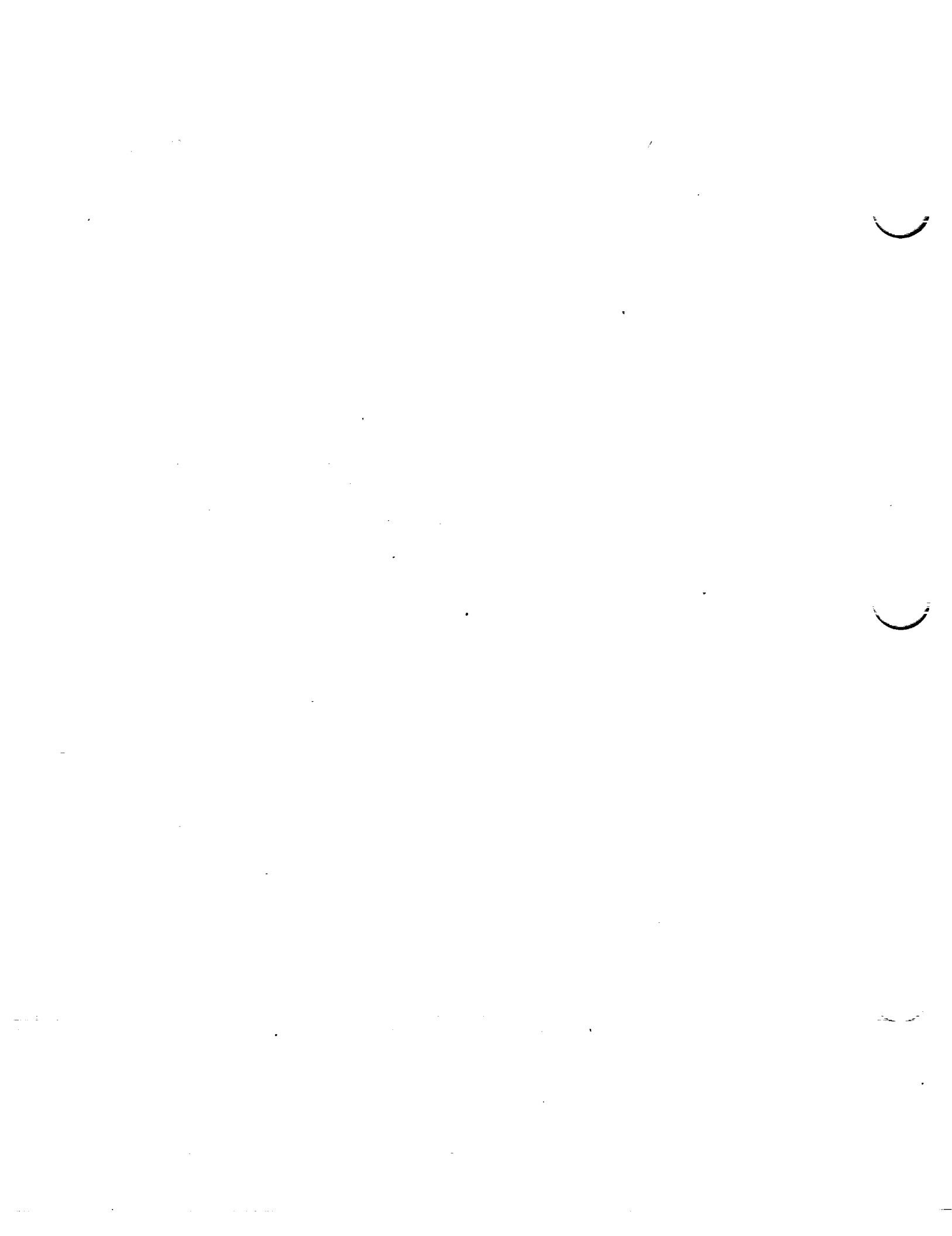
CONFIDENTIAL

Model	Configuration		Geometric characteristics	Flap		Flap angle (deg)		Flap chord (percent c)		Flap span (percent b)		R	C _l max	Stalling characteristics
	Plan view	Front view		Inboard	Outboard	α _{f1}	α _{f0}	c _{f1}	c _{f0}	b _{f1}	b _{f0}			
IX			Sections: NACA 64(215)-418 Root: NACA 66,21-415 A = 8.92 λ = 0.53 Geometric washout, 1.0°	None	None	---	---	---	---	---	---	3.5 × 10 ⁶	1.38	Satisfactory
				Split	↓	55	---	20	---	60	---			
X			Sections: NACA 64(215)-418 Root: NACA 66,21-415 A = 8.92 λ = 0.53 Geometric washout, 1.0°	None	None	---	---	---	---	---	---	3.5 × 10 ⁶	1.42 1.87 2.11	Satisfactory
				Split	↓	55	---	20	---	60	---			
XI			Sections: NACA 64(215)-418 Root: NACA 66,21-415 A = 8.92 λ = 0.53 Geometric washout, 1.0°	None	None	---	---	---	---	---	---	4.0 × 10 ⁶	1.47	Satisfactory
				Split	↓	55	---	20	---	60	---			
XII			Sections: NACA 65(420)-418 Root: NACA 66,21-415 A = 7.77 λ = 0.50 Geometric washout, 2.8°	Extensible slotted	None	0	---	25	---	---	---	3.1 × 10 ⁶	2.37 2.42 2.45	Satisfactory
				↓	↓	35	---	---	---	---				
XIII			Sections: NACA 66(215)-016 Root: NACA 66(215)-016 A = 5.24 λ = 0.88 Geometric washout, 0.0°	None	None	---	---	---	---	---	---	3.4 × 10 ⁶	1.21 1.27 1.45 1.76 1.86 1.96	Satisfactory
				Split	↓	60	---	20	---	65	---			
XIII			Sections: NACA 66(215)-016 Root: NACA 66(215)-016 A = 5.24 λ = 0.88 Geometric washout, 0.0°	Extensible	Split	45	---	---	---	---	---	3.4 × 10 ⁶	1.72 1.86 1.98	Satisfactory
				↓	↓	60	---	20	---	30	---			

NATIONAL ADVISORY
 COMMITTEE FOR AERONAUTICS

CONFIDENTIAL

*Propellers windmilling.



CONFIDENTIAL

TABLE II - Continued
MAXIMUM LIFT AND STALLING CHARACTERISTICS OF MODELS - Continued

Model	Configuration		Geometric characteristics	Flap		Flap angle (deg)			Flap chord (percent)		Flap span (percent)		R	$C_{l_{max}}$	Stalling characteristics
	Plan view	Front view		Inboard	Outboard	δ_{r1}	δ_{r0}	δ_{f1}	δ_{f0}	b_{r1}	b_{r0}	b_{f1}			
XIV			Sections: $MACA\ 65(218)-11(18.5)$ Root: $MACA\ 65(215)-216$ Tip: $MACA\ 65(215)-216$ $\lambda = 5.52$ $\lambda = 0.46$ Geometric washout, 3.0°	Extensible slotted ↓	None ↓	0	---	20	---	60	---	3.6 × 10 ⁶ 5.1 6.1	1.32 1.42 1.46	Abrupt stall with satisfactory progression toward tips	
XV			Sections: $MACA\ 23015-6$ Root: $MACA\ 23009$ Tip: $MACA\ 23009$ $\lambda = 5.52$ $\lambda = 0.52$ Geometric washout, 3.0°	Slotted ↓	None ↓	0	---	20	---	60	---	2.4 × 10 ⁶ 4.8 5.6	1.55 1.58 1.60 2.46 2.50 2.52	Very abrupt stall, left wing stalling very rapidly, for all conditions	
XVI			Sections: $MACA\ 66, 2-118$ Root: $MACA\ 66(215)-116$ Tip: $MACA\ 66(215)-116$ $\lambda = 6.9$ Geometric washout, 2.0°	Extensible slotted ↓	None ↓	0	---	24	---	50	---	3.0 × 10 ⁶ 5.0	1.34 1.47 1.50	Extremely abrupt stall, left wing stalls first for the extensible slotted flap, satisfactory for split flap	
XVII			Sections: $MACA\ 65(216)-215$ Root: $MACA\ 65(216)-215$ Tip: $MACA\ 65(216)-215$ $\lambda = 9.08$ $\lambda = 0.45$ Geometric washout, 1.0° 0.2 chord line straight	Double slotted ↓	Double slotted ↓	0	0	25	↑	65	↑	3.6 × 10 ⁶ 3.1	1.38 2.45	Satisfactory	
XVIII			Sections: $MACA\ 65(216)-215$ Root: $MACA\ 65(216)-215$ Tip: $MACA\ 65(216)-215$ $\lambda = 9.08$ $\lambda = 0.45$ Geometric washout, 1.0° -0.10 chord line straight	Double slotted ↓	Double slotted ↓	0	0	25	↑	65	↑	3.6 × 10 ⁶ 3.1	1.37 2.44	Satisfactory	
XIX			Sections: $MACA\ 65(216)-215$ Root: $MACA\ 65(216)-215$ Tip: $MACA\ 65(216)-215$ $\lambda = 9.08$ $\lambda = 0.45$ Geometric washout, 1.0° 1.1 chord line straight	Double slotted ↓	Double slotted ↓	0	0	25	↑	65	↑	3.6 × 10 ⁶ 3.1	1.45 2.57	Unsatisfactory, severe tip stall for all conditions except full-span flap	

NATIONAL ADVISORY COMMITTEE FOR AERONAUTICS

CONFIDENTIAL

b-pilots removed.



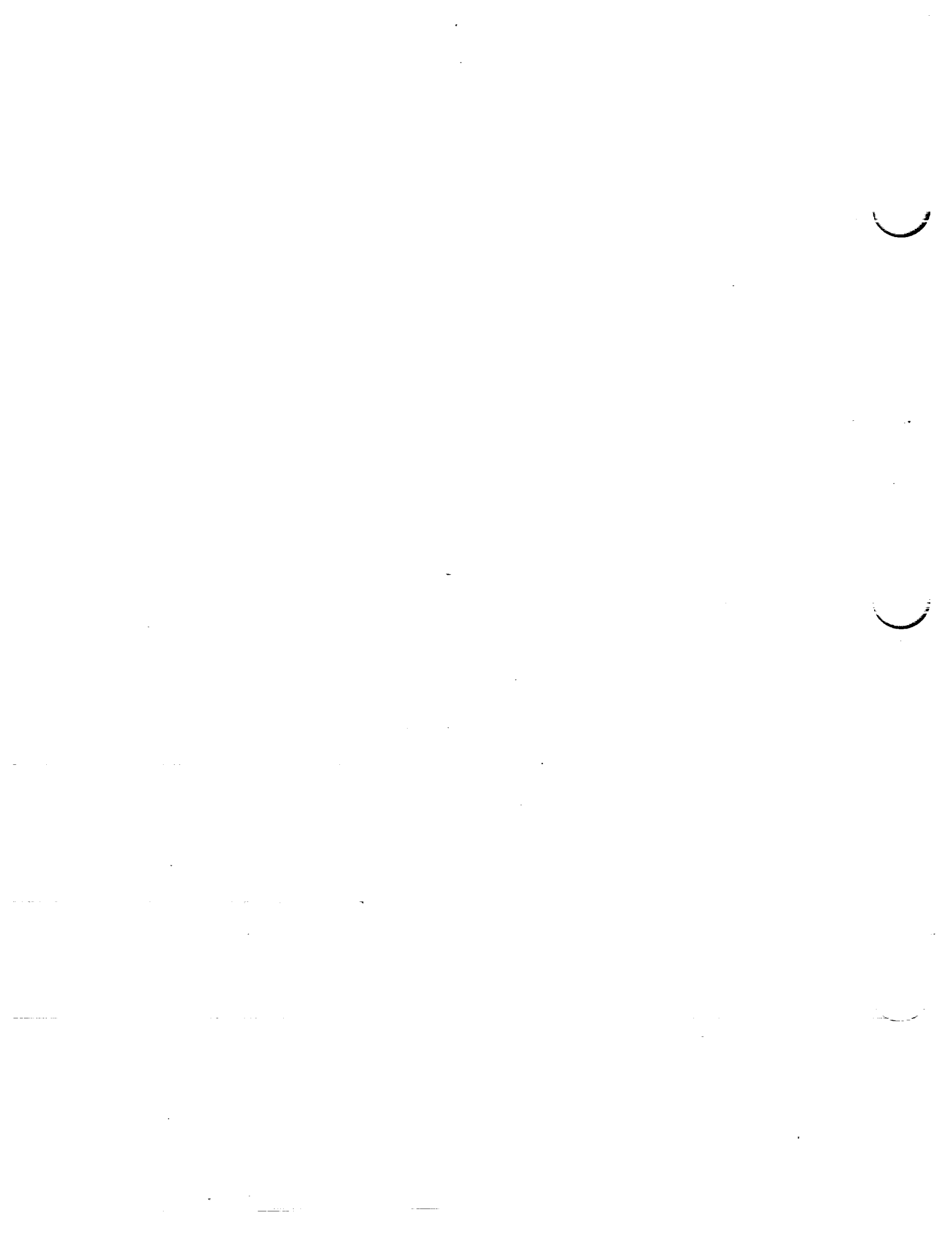
CONFIDENTIAL

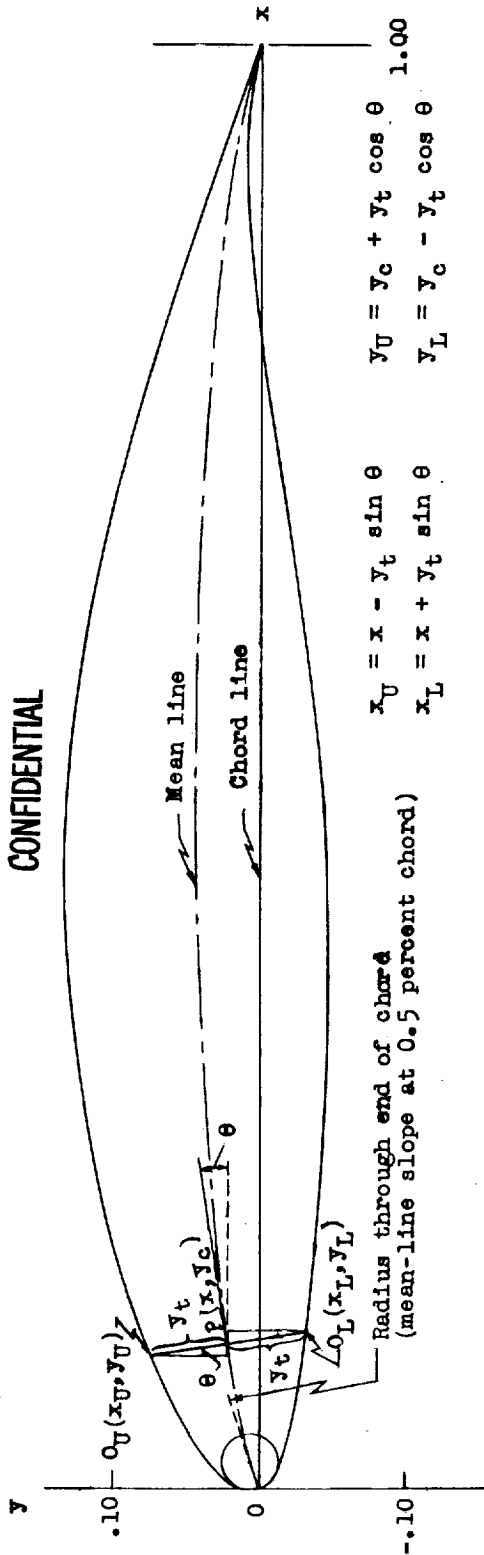
TABLE II - Concluded
MAXIMUM LIFT AND STALLING CHARACTERISTICS OF MODELS - Concluded

Model	Configuration		Geometric characteristics	Flap		Flap angle (deg)		Flap chord (percent)		Flap span (percent)		R	C _{Lmax}	Stalling characteristics
	Plan view	Front view		Inboard	Outboard	δ _f	δ _{f0}	α _{f1}	α _{f0}	b _{f1}	b _{f0}			
XX			Sections: Root: NACA 65(216)-215, Tip: NACA 65(216)-215, λ = 0.5 A = 9.08 Geometric washout, 1.0° 0.20 chord line straight	Double slotted	Double slotted	0	0	25	25	65	31	5.5 × 10 ⁶	1.45 2.37 2.65	Satisfactory
XXI			Sections: Root: NACA 66,2-118 Tip: NACA 66(2x15)-116 λ = 0.5 A = 6.25 Geometric washout, 2.5° 0.375 chord line straight	None	Split	45	---	20	---	50	---	2.9 × 10 ⁶	1.23 1.43 1.51 1.80 1.82 1.98	Satisfactory
XXII			Sections: Root: NACA 66,2-118 Tip: NACA 66(2x15)-116 λ = 0.5 A = 6.25 Geometric washout, 2.5° 0.375 chord line straight	None	Split	---	---	---	---	---	---	4.1 × 10 ⁶	1.50 1.60 2.02	Satisfactory
XXIII			Sections: Root: NACA 66,2-118 Tip: NACA 66(2x15)-116 λ = 0.5 A = 6.25 Geometric washout, 2.5° 0.375 chord line straight	None	Split	45	---	20	---	50	---	2.9 × 10 ⁶	1.38 1.57 1.61 1.83 1.82 2.02	Satisfactory
XXIV			Sections: Root: NACA 66,2-118 Tip: NACA 66(2x15)-116 λ = 0.47 A = 6.1 Geometric washout, 2.5° 0.375 chord line straight	None	Split	---	---	---	---	---	---	2.9 × 10 ⁶	1.34 1.56 1.63 1.85 1.92 2.01	Satisfactory
XXV			Sections: Root: NACA 65(223)-221, Tip: NACA 66(215)-316, λ = 0.6 A = 12.8 Geometric washout, 0.0°	Powder	Split	0	---	18	---	53	---	1.5 × 10 ⁶	1.17 1.27 1.37 2.21 2.29 2.50	Poor, initial stall occurs at tips

NATIONAL ADVISORY
COMMITTEE FOR AERONAUTICS

CONFIDENTIAL





**SAMPLE CALCULATIONS FOR DERIVATION OF THE
NACA 65,3-818 AIRFOIL (a = 1.0)**

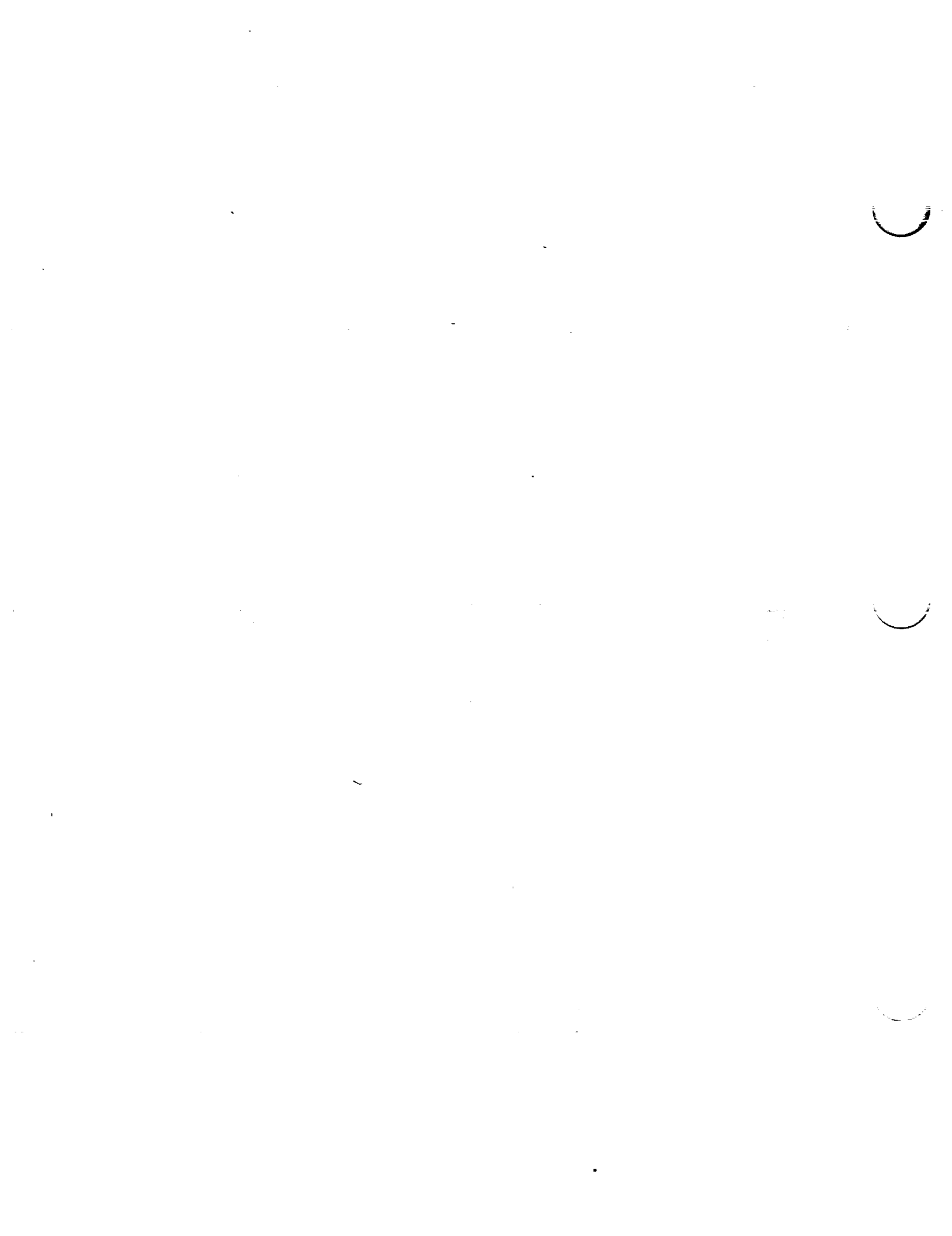
x	y _t (a)	y _c (b)	tan θ	sin θ	cos θ	y _t sin θ	y _t cos θ	x _U	y _U	x _L	y _L
0	0	0	0	0	1.00000	0	0	0	0	0	0
.005	.01324	.00200	.33696	.31932	.94765	.00423	.01255	.00077	.01455	.00923	-.01055
.05	.03851	.01264	.18744	.18422	.98288	.00706	.03765	.04294	.05029	.05706	-.02501
.25	.08093	.03580	.06979	.06979	.99756	.00565	.08073	.24435	.11653	.25565	-.04493
.50	.08593	.04412	0	0	1.00000	0	.08593	.50000	.13005	.50000	-.04181
.75	.04456	.03580	-.06996	-.06979	.99756	-.00311	.04445	.75311	.08025	.74689	-.00865
1.00	0	0	0	0	1.00000	0	0	1.00000	0	1.00000	0

^aThickness distribution obtained from ordinates of the NACA 65,3-018 airfoil.
^bOrdinates of the mean line, 0.8 of the ordinate for c_{t1}
^cSlope of radius through end of chord.

CONFIDENTIAL

NATIONAL ADVISORY
COMMITTEE FOR AERONAUTICS.

Figure 1.- Method of combining mean lines and basic thickness forms.



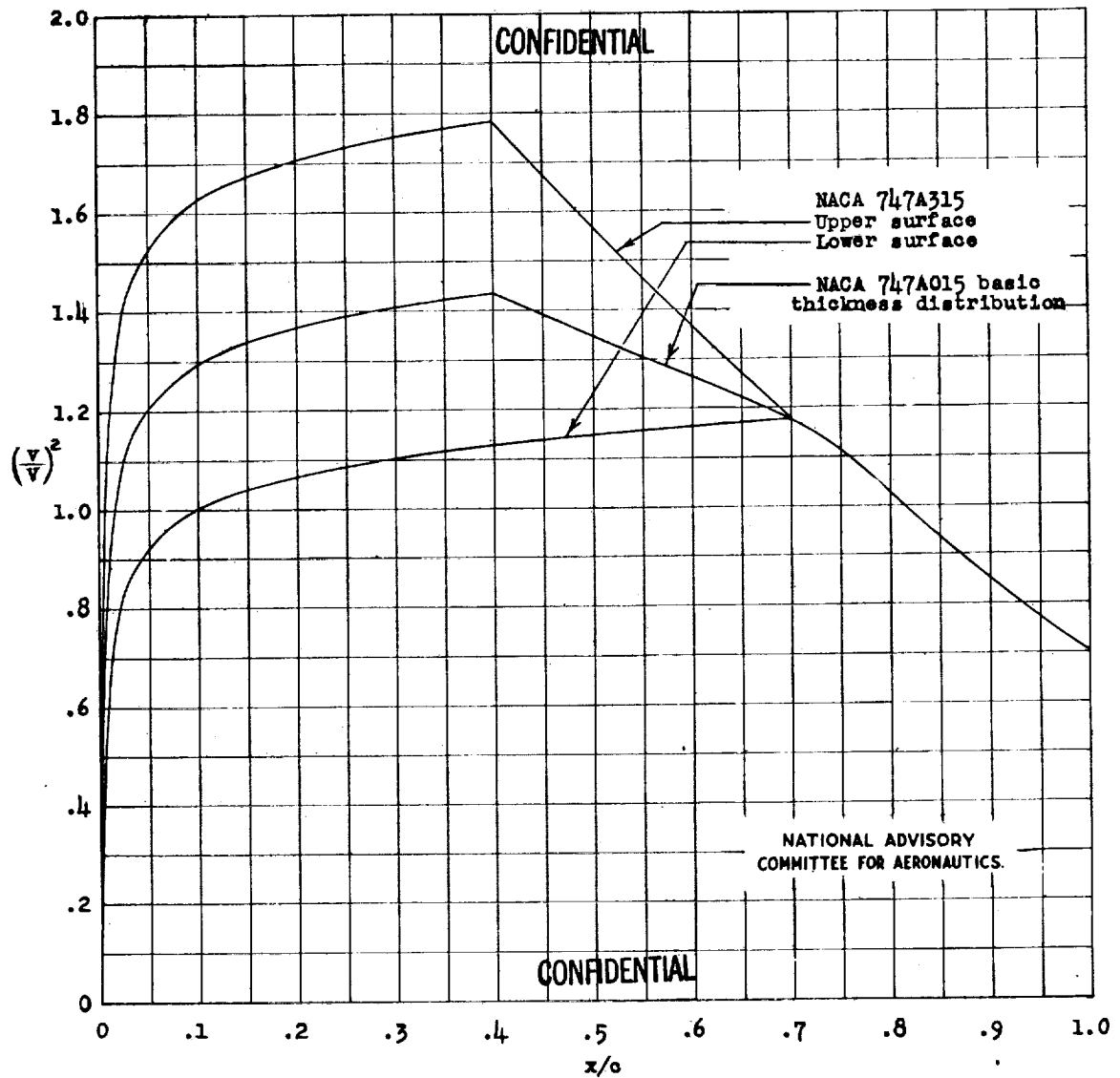
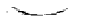


Figure 2.- Theoretical pressure distribution for the NACA 747A315 airfoil section at the design lift coefficient and the NACA 747A015 basic thickness distribution.



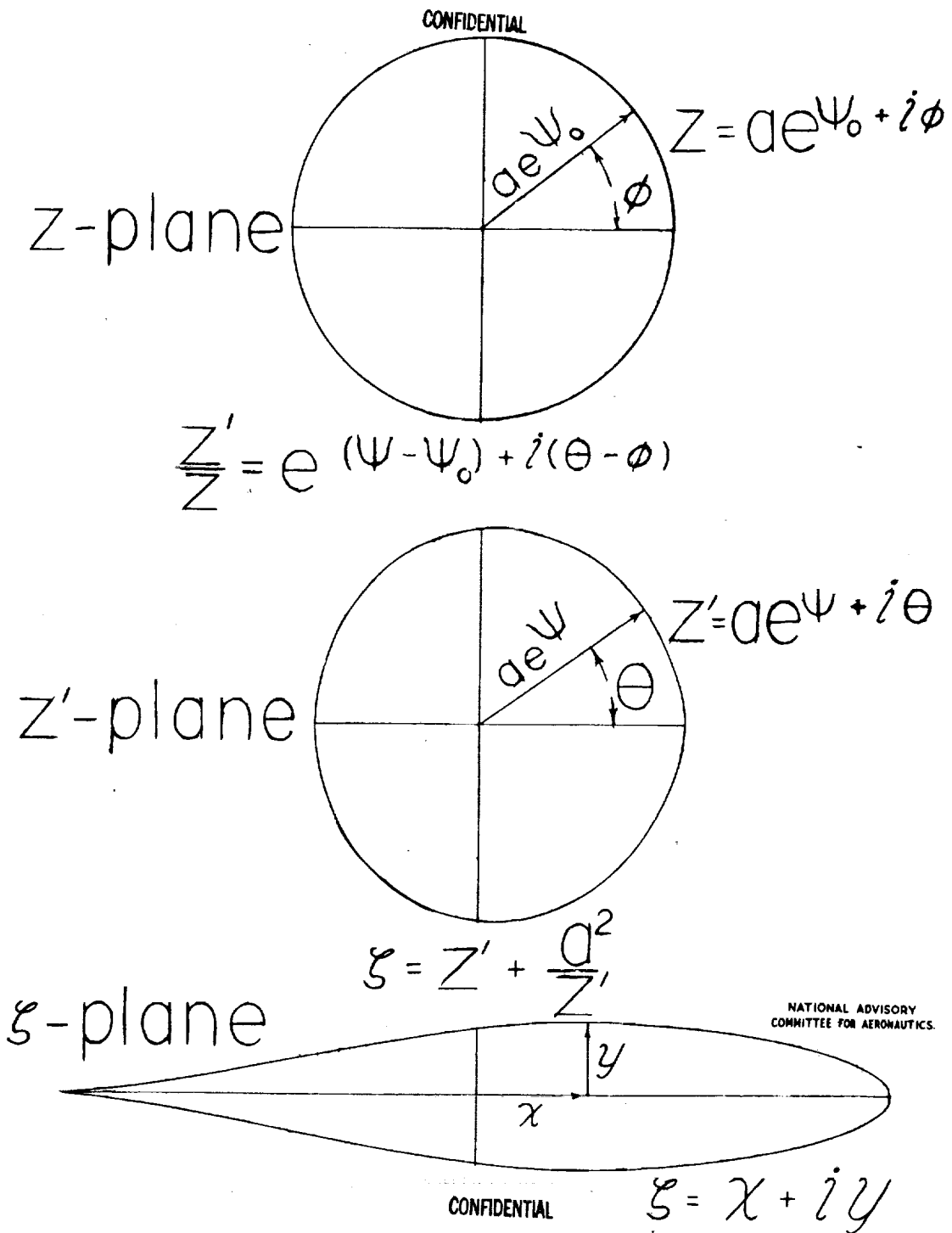


Figure 3.-Illustration of transformations used to derive airfoils and calculate pressure distributions.



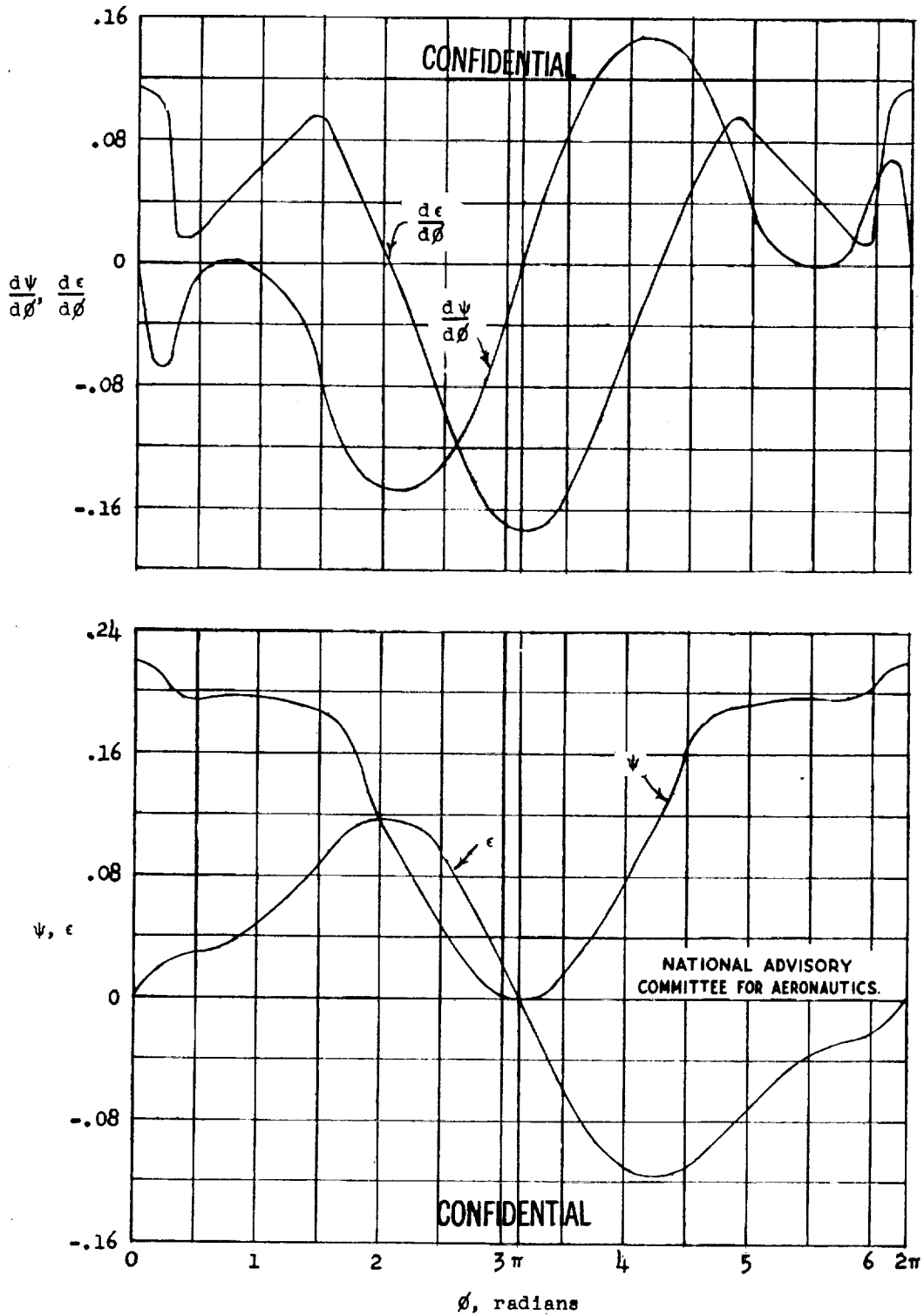
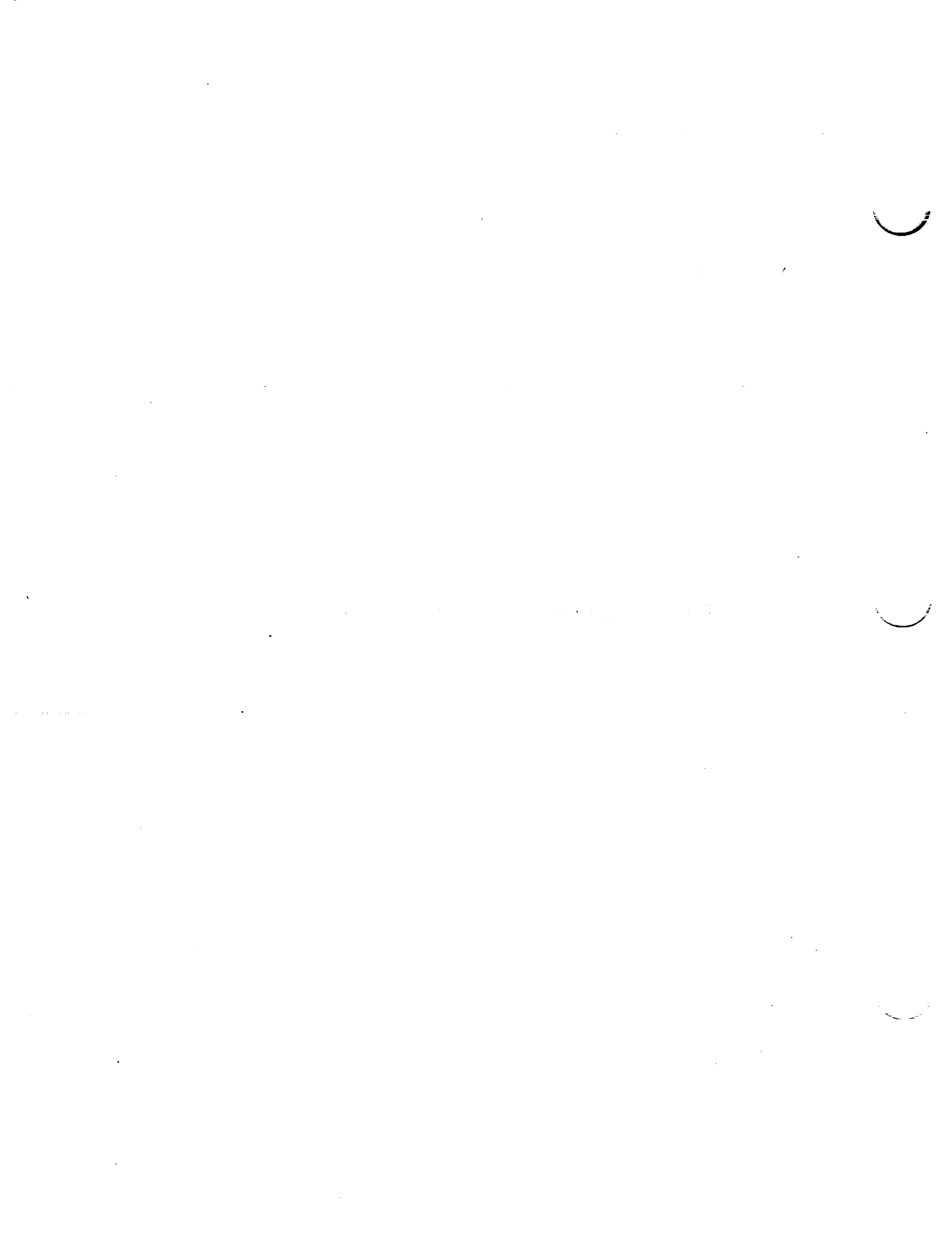
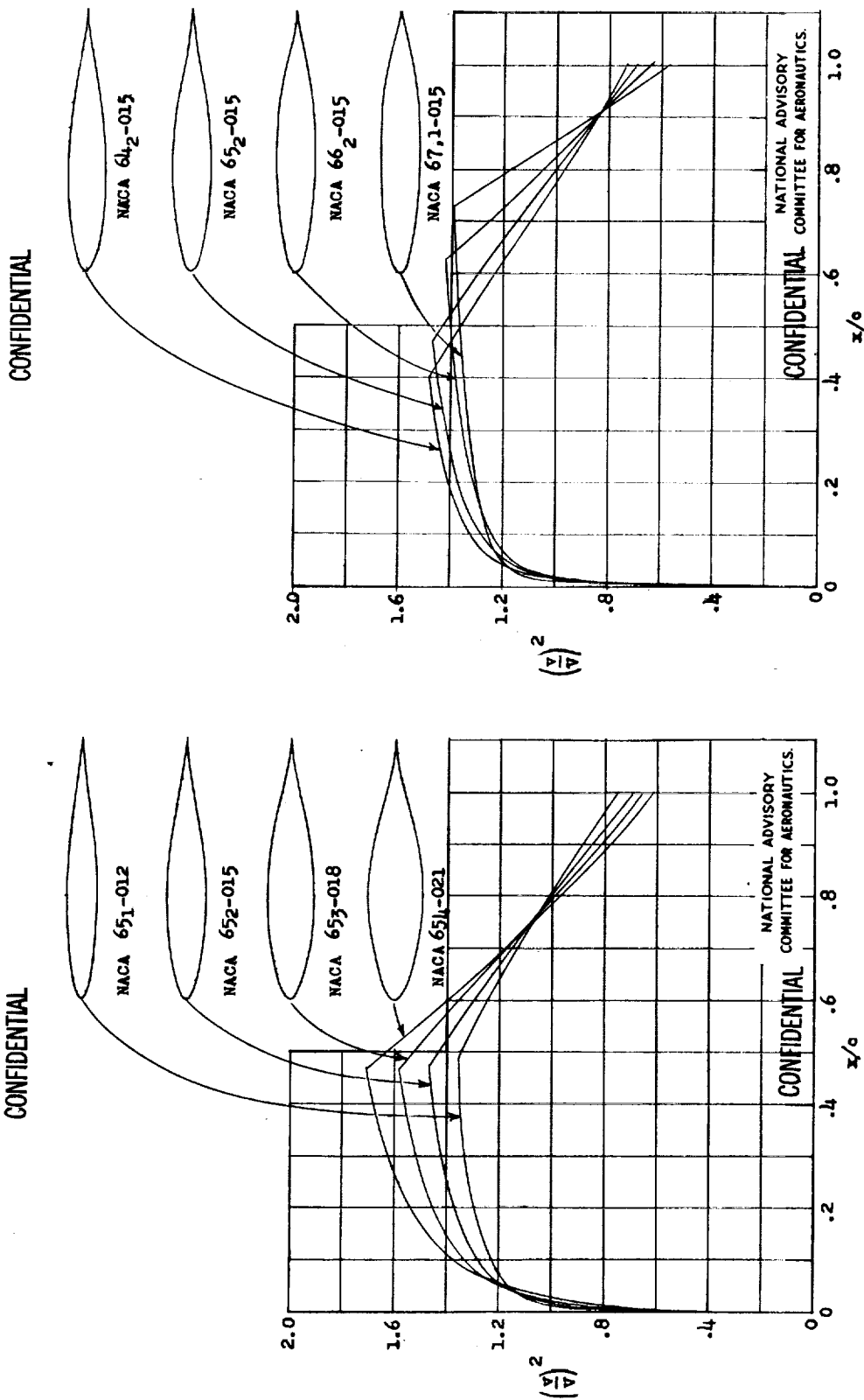


Figure 4.- Variation of airfoil parameters ψ , ϵ , $\frac{d\psi}{d\phi}$, $\frac{d\epsilon}{d\phi}$ with ϕ for the NACA 64₃-018 airfoil-section basic thickness form.



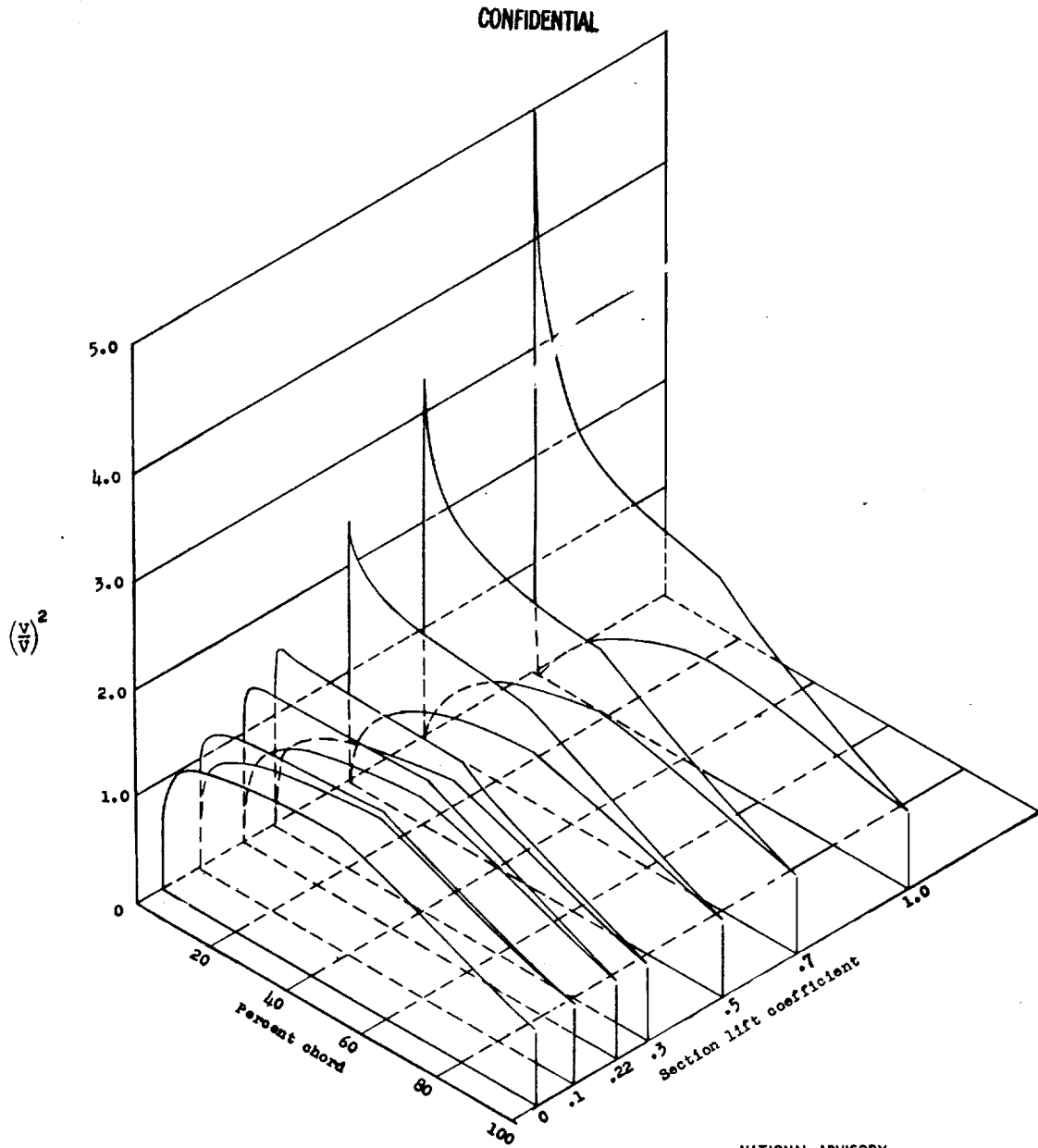


(a) Variation with thickness.

(b) Variation with position of minimum pressure.

Figure 5.- Theoretical pressure distributions for some basic symmetrical NACA 6-series airfoils at zero lift.



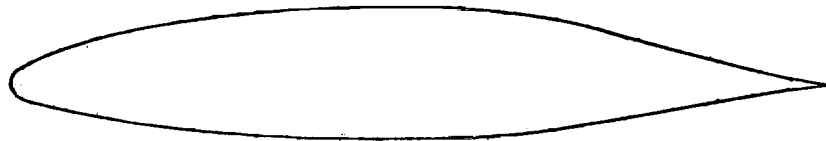


NATIONAL ADVISORY
COMMITTEE FOR AERONAUTICS.

Figure 6.- Theoretical pressure distributions for the NACA 65₂-015 airfoil at several lift coefficients.



CONFIDENTIAL



NACA 66(215)-216, $\alpha = 0.6$

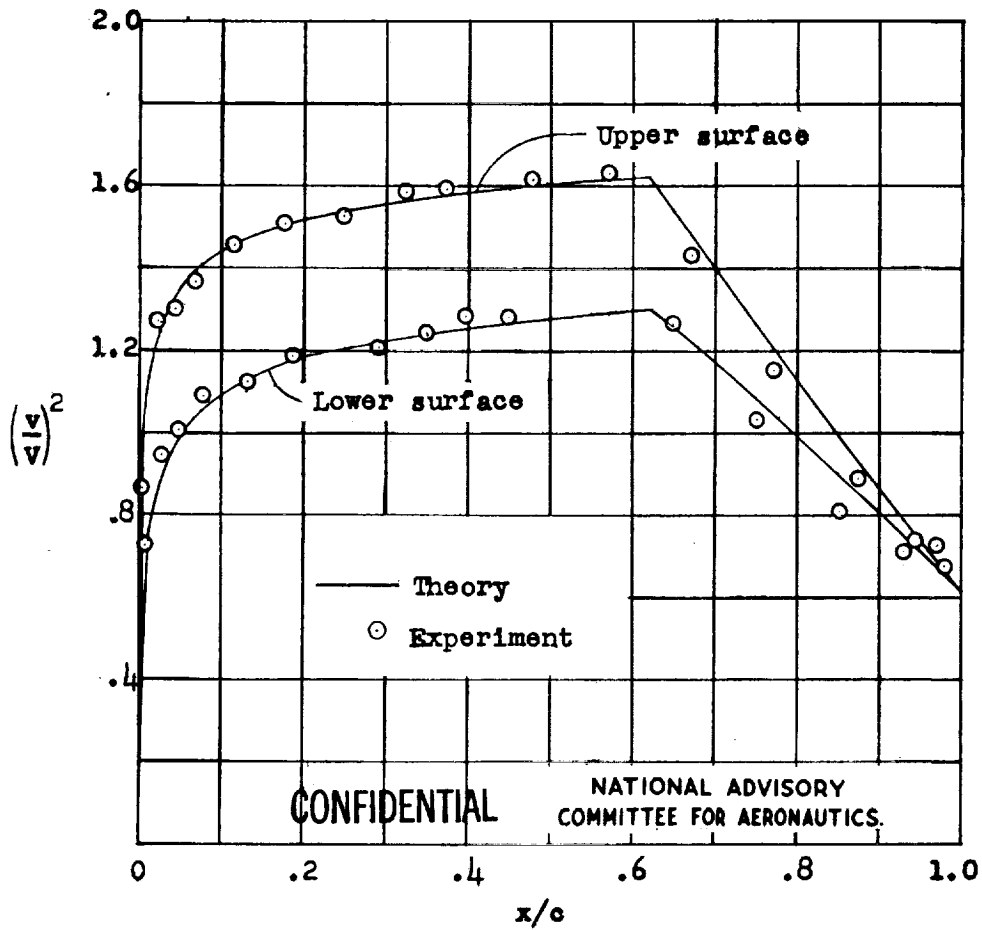


Figure 7.- Comparison of theoretical and experimental pressure distributions for the NACA 66(215)-216, $\alpha = 0.6$ airfoil; $c_l = 0.23$.



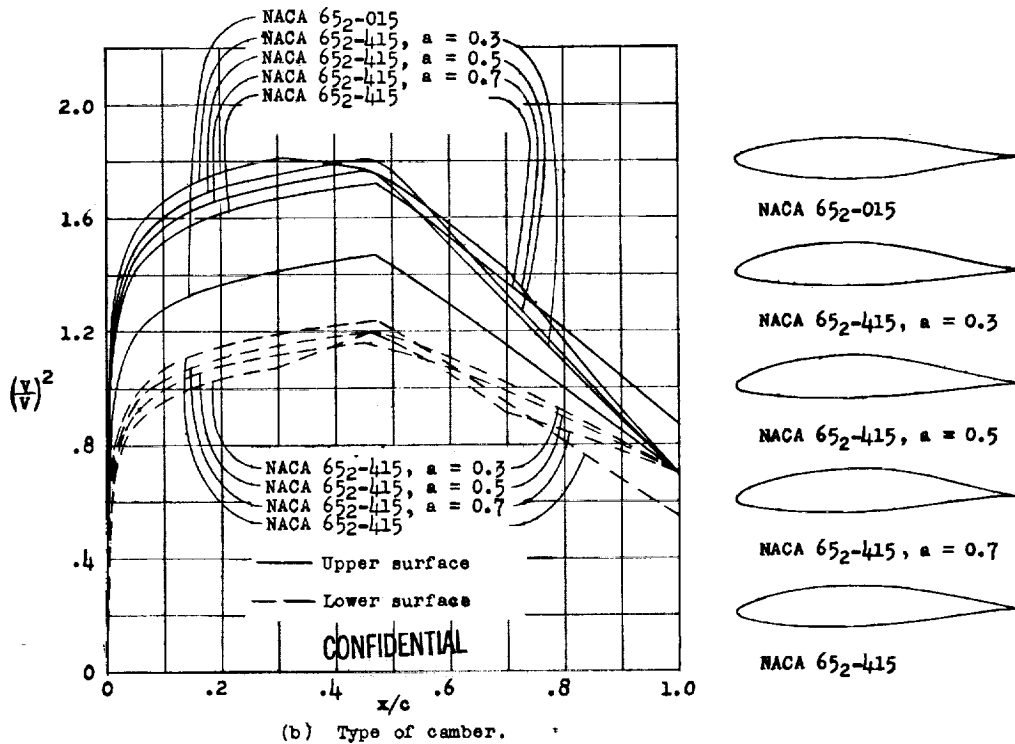
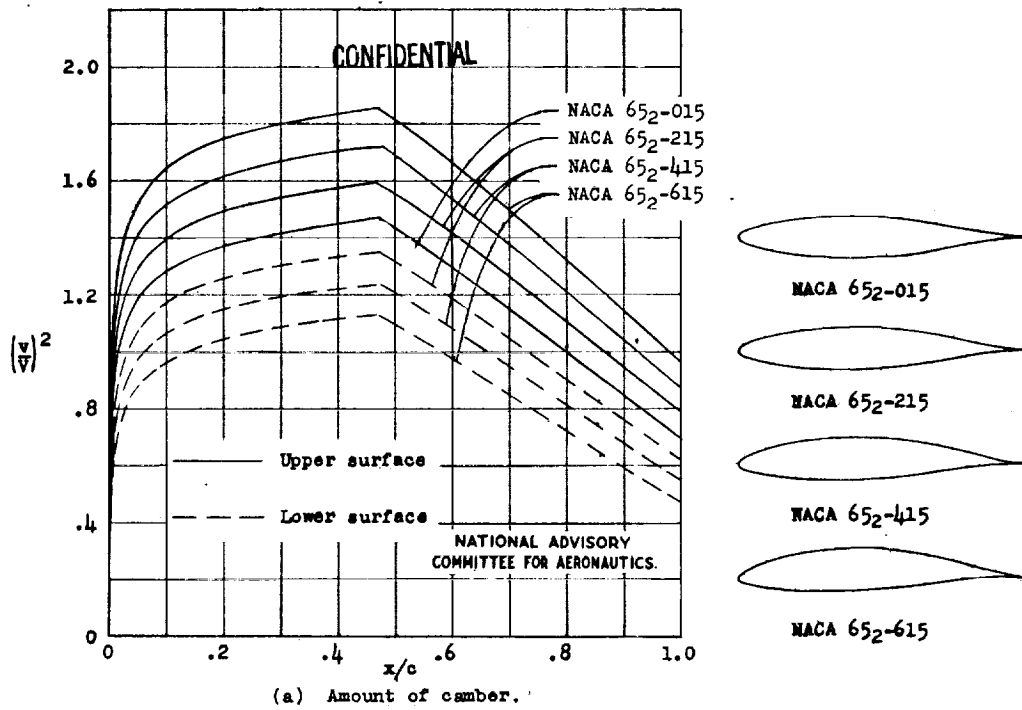


Figure 8.- Effect of amount and type of camber on pressure distribution at design lift.



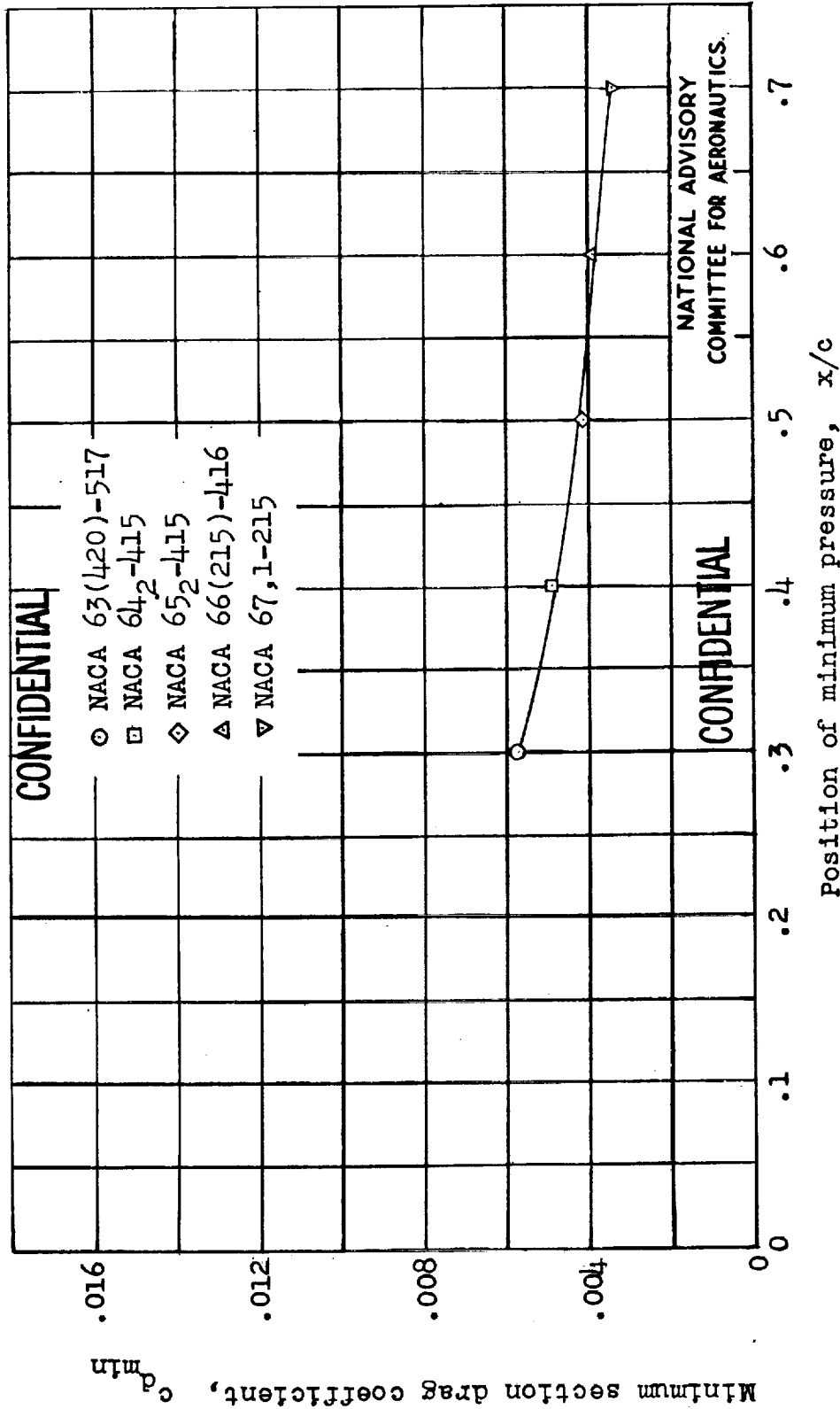
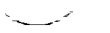


Figure 9.- Variation of minimum drag coefficient with position of minimum pressure for some NACA 6-series airfoils from tests in the Langley two-dimensional low-turbulence pressure tunnel at a Reynolds number of 6×10^6 .



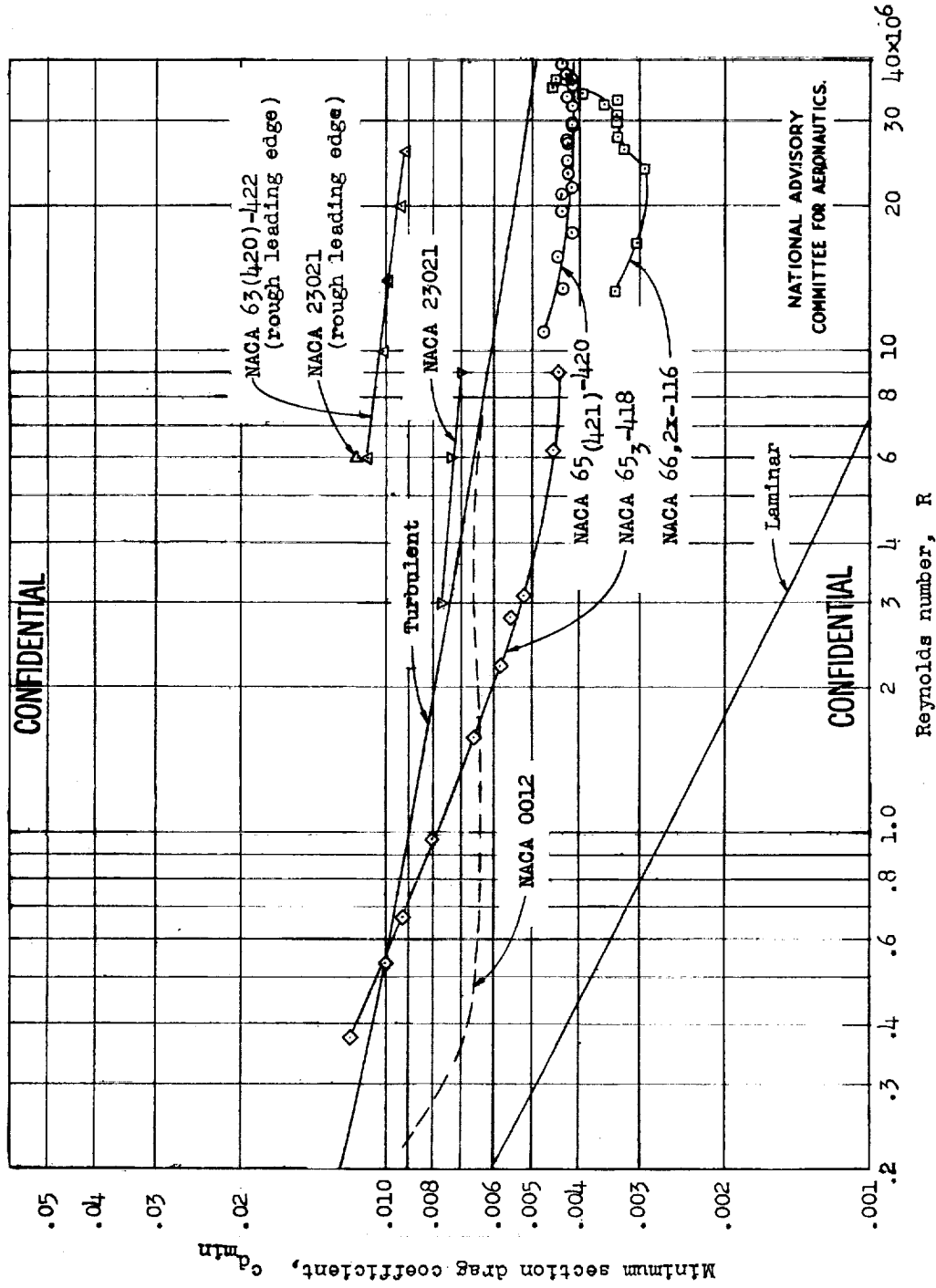


Figure 10.- Variation of minimum drag coefficient with Reynolds number for several airfoils together with laminar and turbulent skin-friction coefficients for a flat plate.

CONFIDENTIAL

CONFIDENTIAL

NATIONAL ADVISORY
COMMITTEE FOR AERONAUTICS.



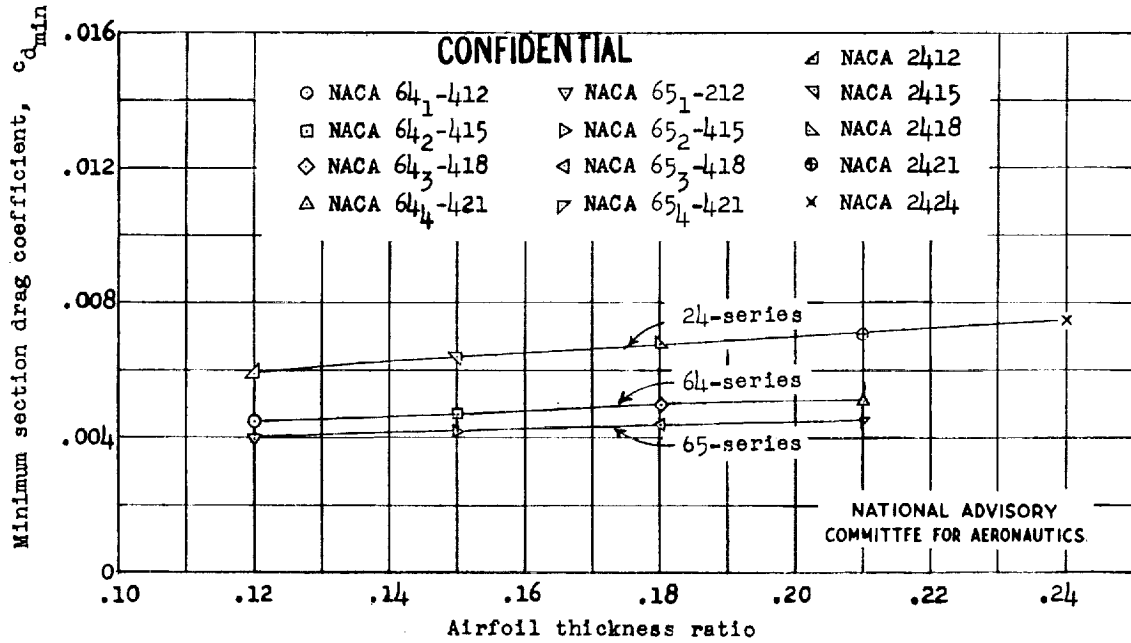


Figure 11.- Variation of minimum drag coefficient with airfoil thickness for some NACA airfoils from tests in the Langley two-dimensional low-turbulence pressure tunnel at a Reynolds number of 9×10^6 .

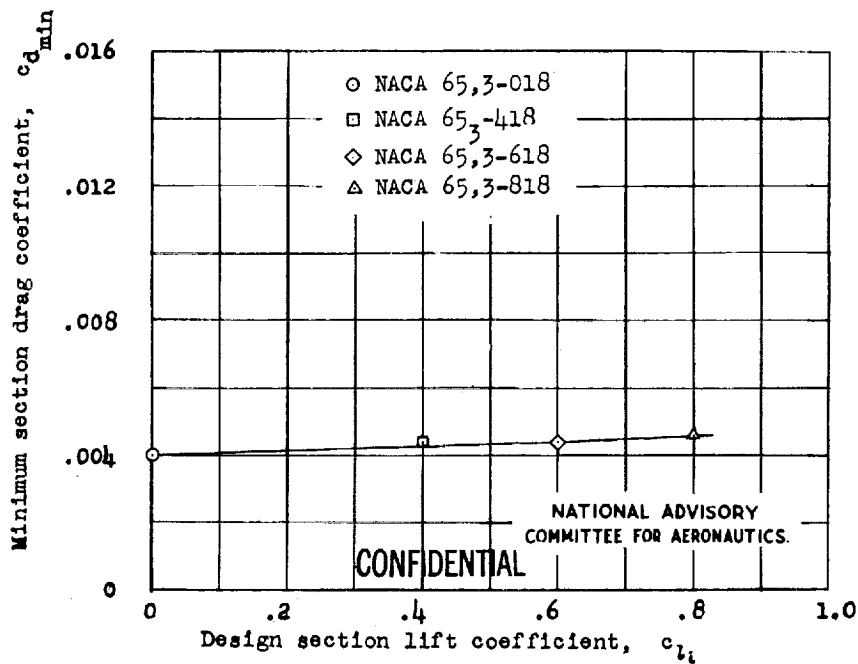
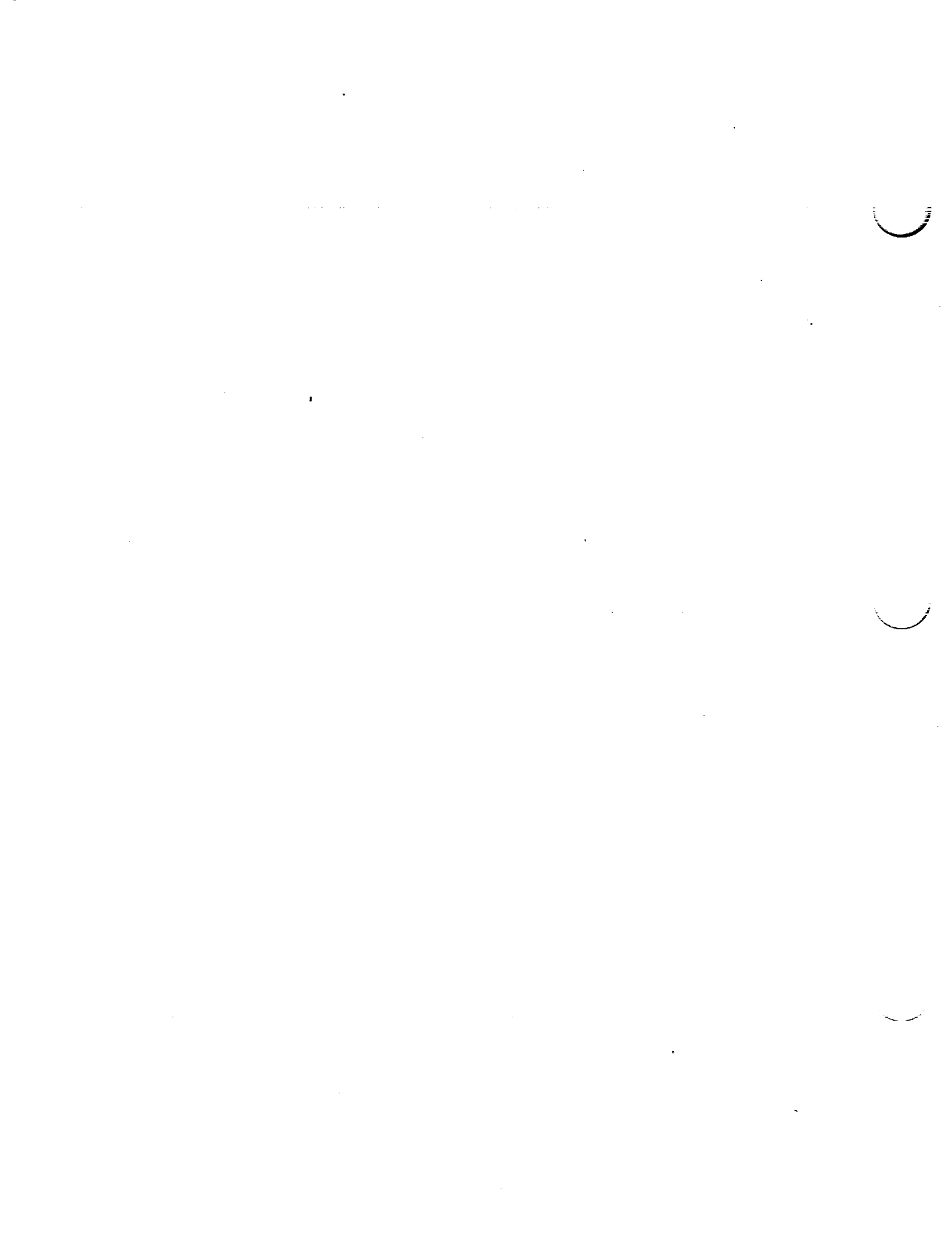


Figure 12.- Variation of minimum drag coefficient with camber for the NACA 65,3-018, 65,3-418, 65,3-618, and 65,3-818 airfoils from tests in the Langley two-dimensional low-turbulence pressure tunnel at a Reynolds number of 9×10^6 .



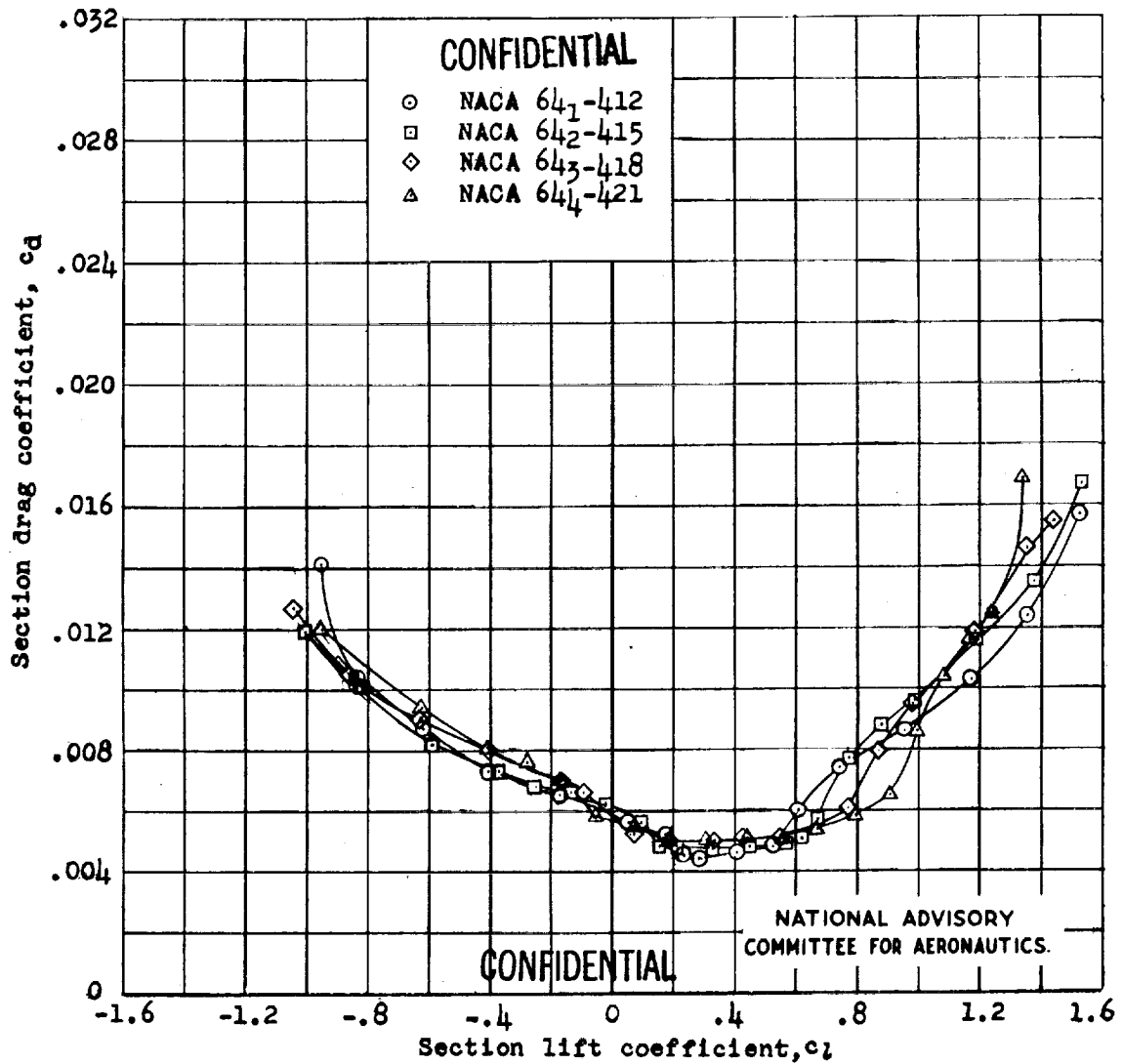
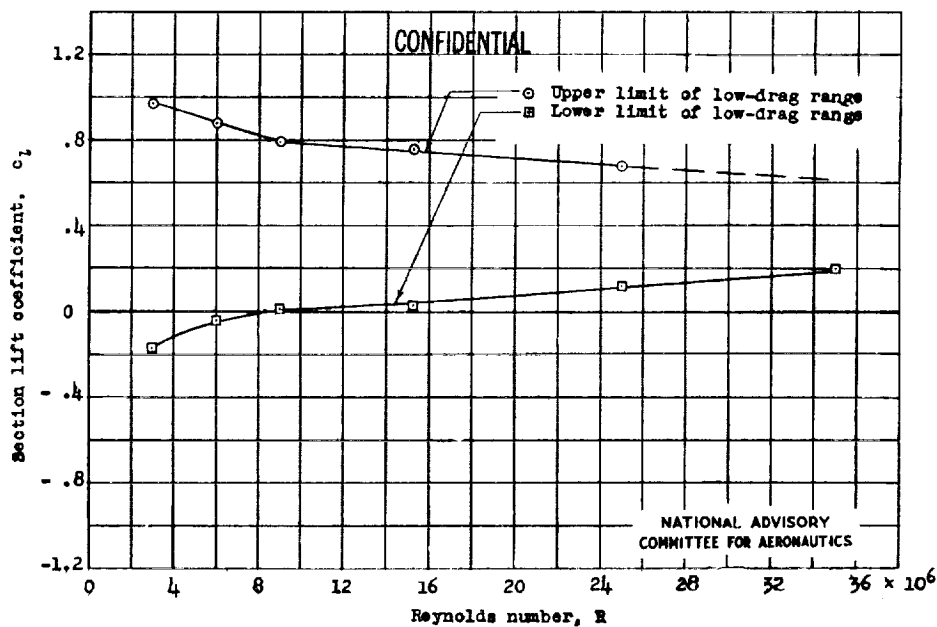
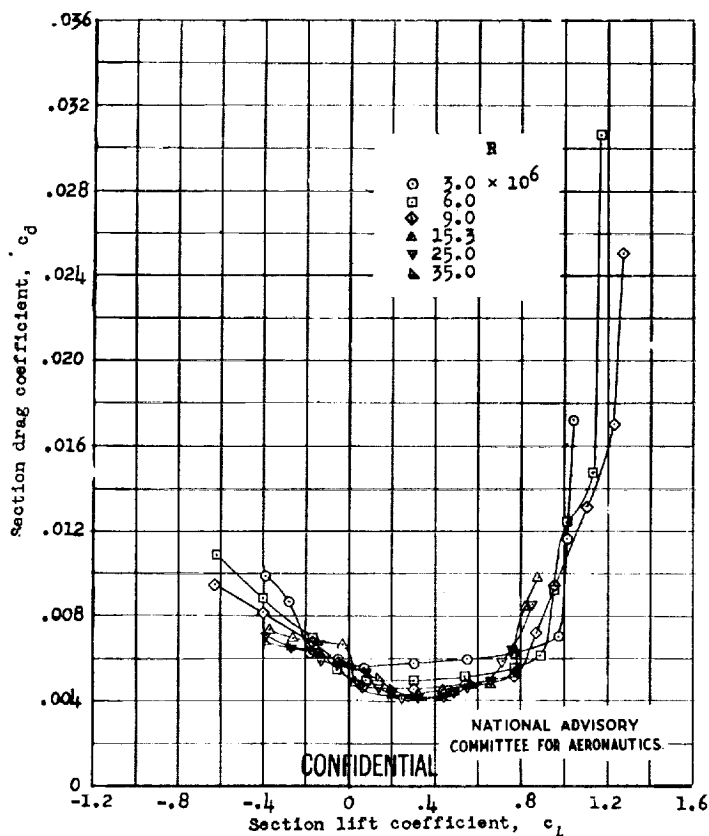


Figure 13.- Drag characteristics of some NACA 64-series airfoil sections of various thicknesses, cambered to a design lift coefficient of 0.4; $R, 9 \times 10^6$, TDT tests 682, 733, 735, and 691.





(a) Variation of upper and lower limits of low-drag range with Reynolds number.



(b) Section drag characteristics at various Reynolds numbers.

Figure 14.- Variation of low-drag range with Reynolds number for the NACA 65₍₄₂₁₎-420 airfoil; TDT tests 300, 312, and 328.



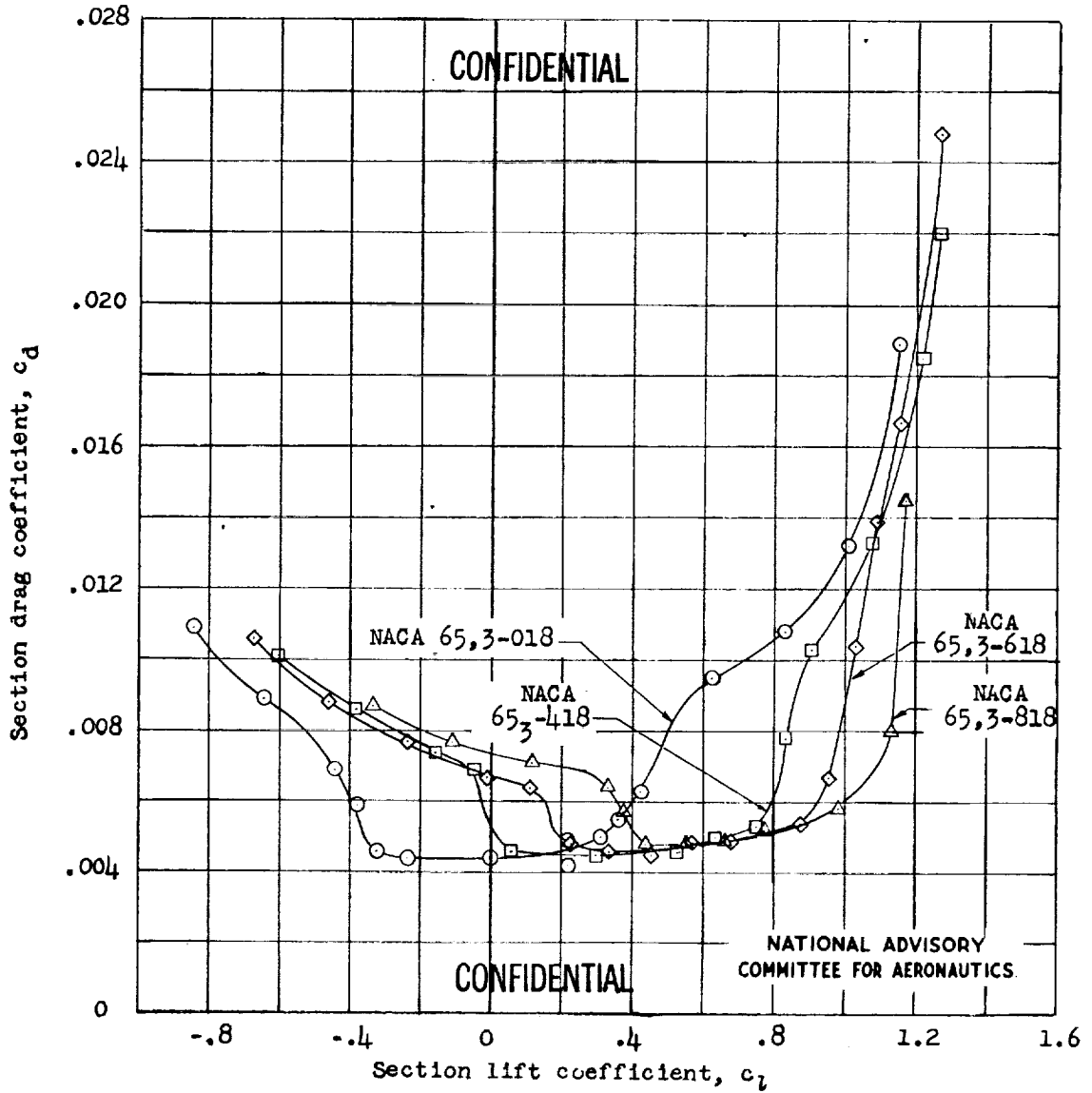


Figure 15.- Drag characteristics of some NACA 65-series airfoil sections of 18-percent thickness, with various amounts of camber; $R, 6 \times 10^6$; TDT tests 159, 314, 195, and 163.



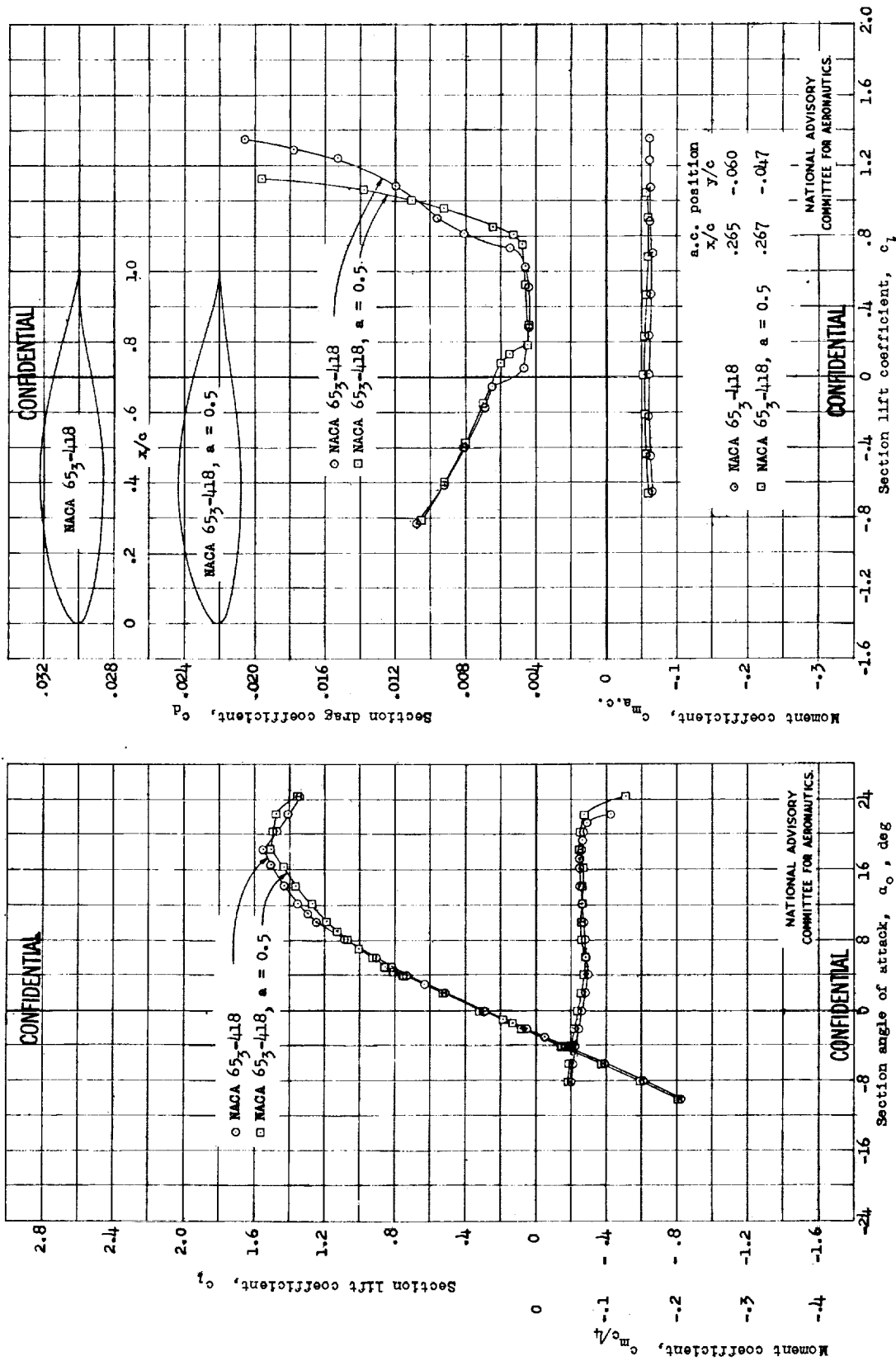
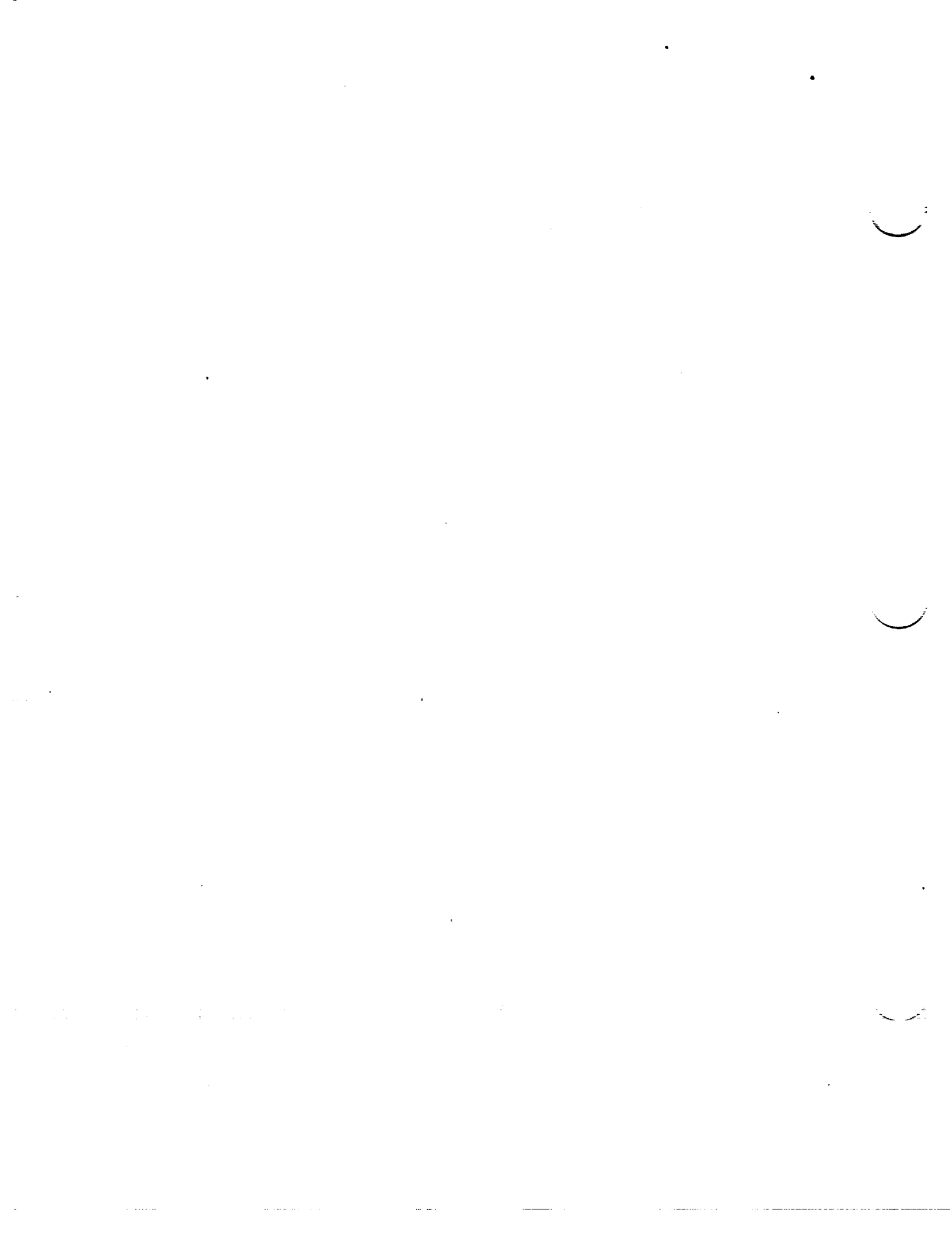


Figure 16.- Comparison of the aerodynamic characteristics of the MACA 653-418 and MACA 653-418, $\alpha = 0.5$ airfoils at a Reynolds number of 9×10^6 , TDT tests 311, 320, 406, and 411.



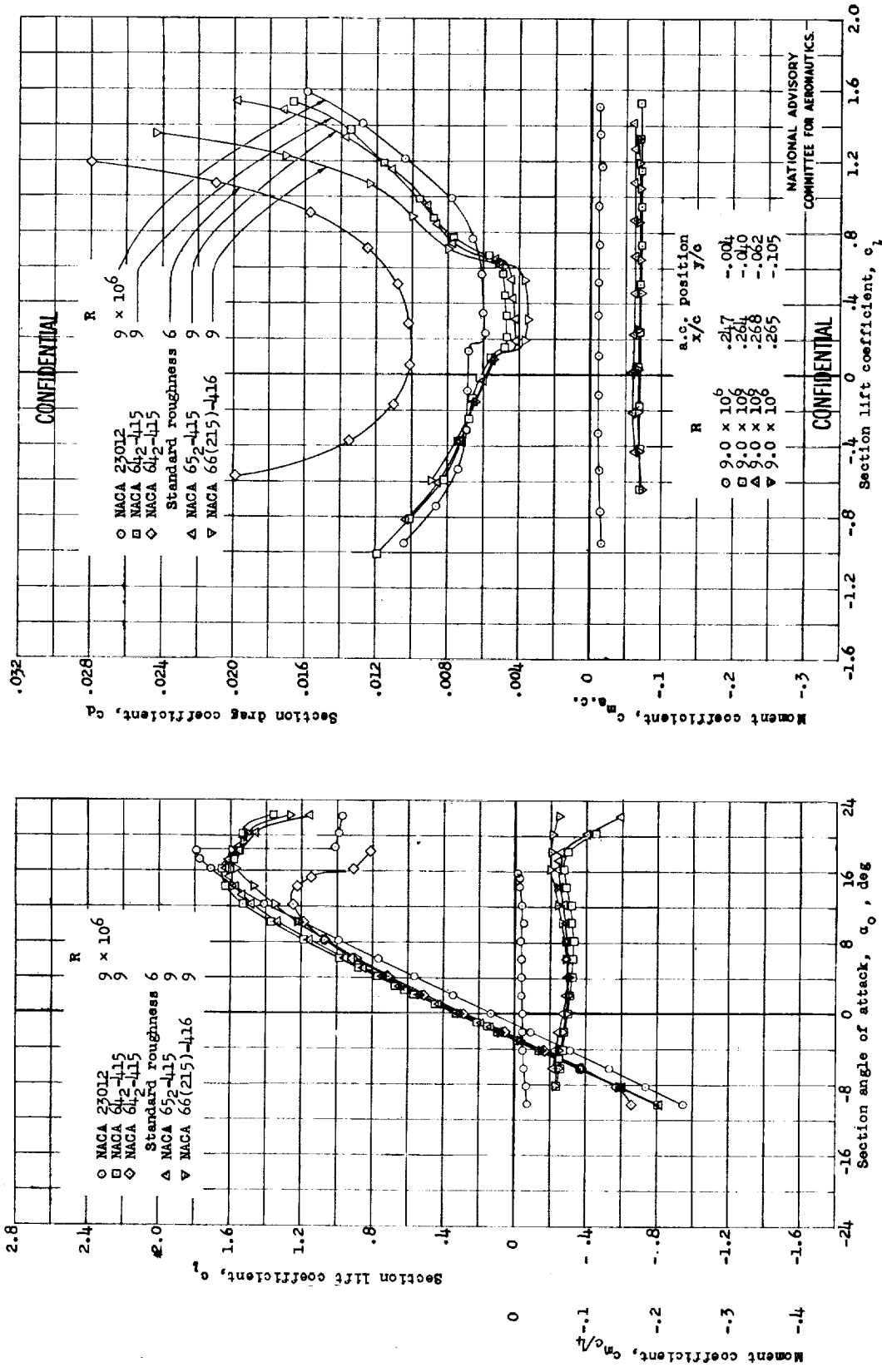
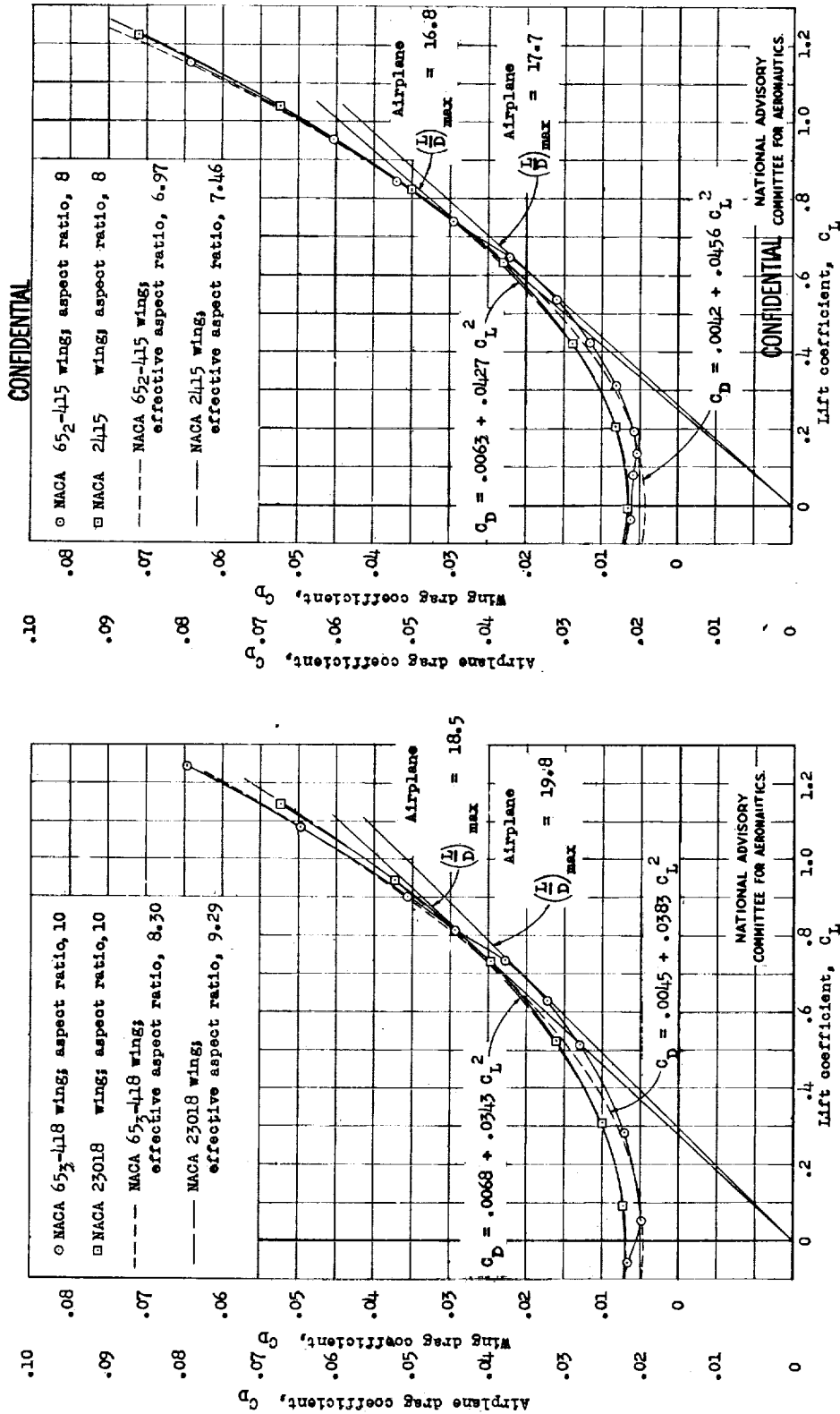


Figure 17.- Comparison of the aerodynamic characteristics of some NACA airfoils from tests in the Langley two-dimensional low-turbulence pressure tunnel.





(a) NACA 65₃-418 and 25018 wings of aspect ratio 10.
 Figure 18.- Comparison of finite aspect-ratio drag characteristics for two types of airfoils obtained by adding the induced drag corresponding to an elliptical span loading to the section drag coefficients.

(b) NACA 65₂-415 and 2415 wings of aspect ratio 8.



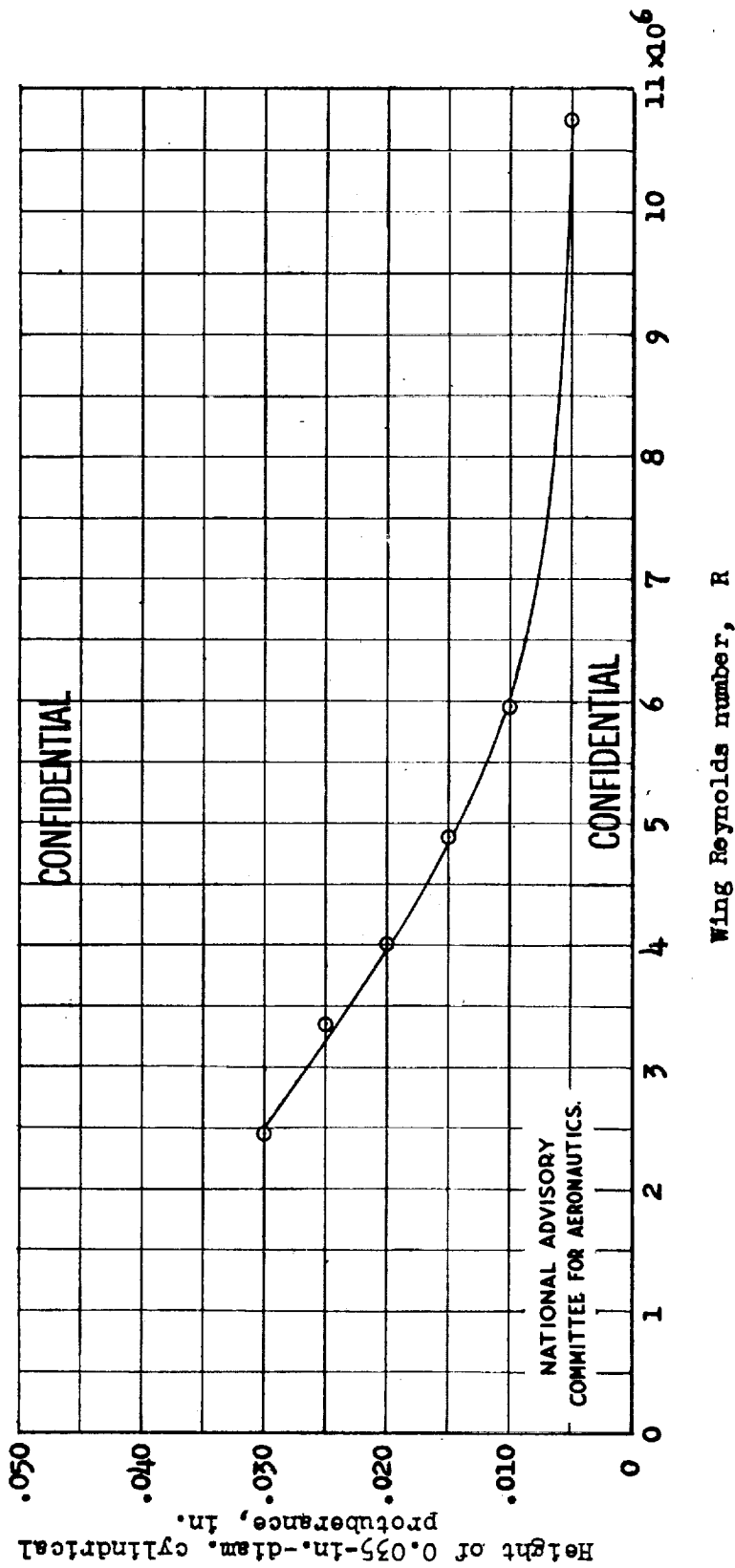
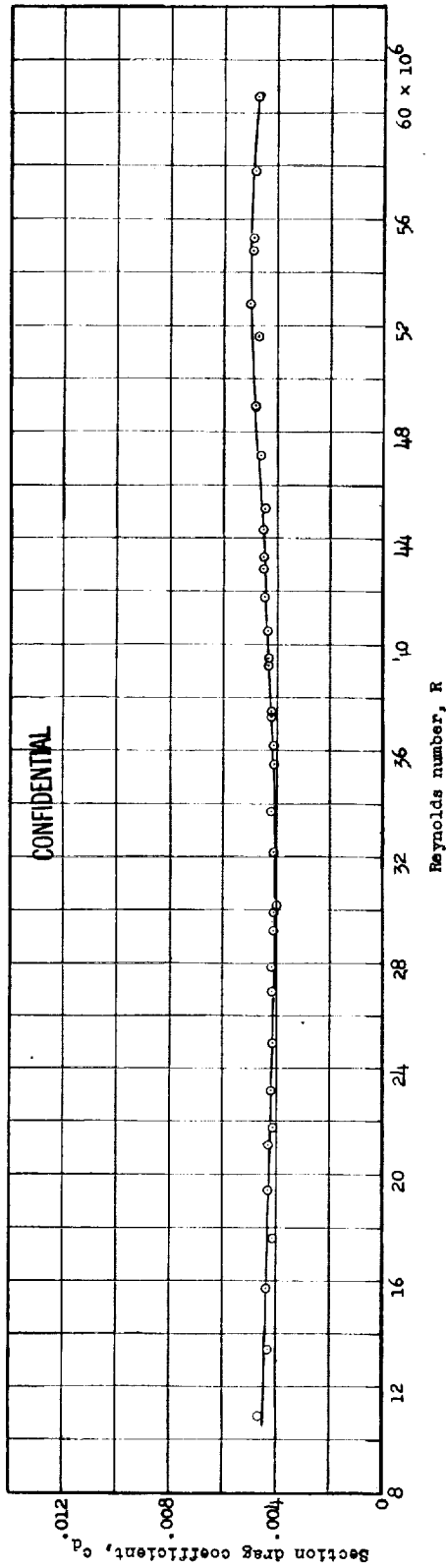
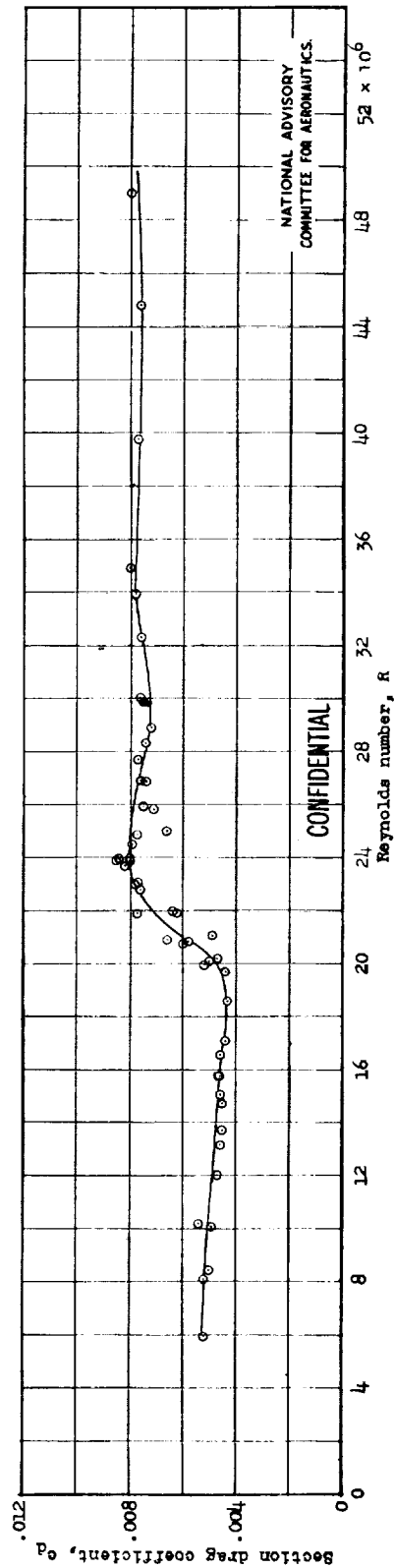


Figure 19.- Variation with wing Reynolds number of the minimum height of a cylindrical protuberance necessary to cause premature transition. Protuberance has 0.035-inch diameter with axis normal to wing surface and is located at 5-percent-chord of a 90-inch-chord symmetrical 6-series airfoil section of 15-percent thickness and with minimum pressure at 70-percent chord.

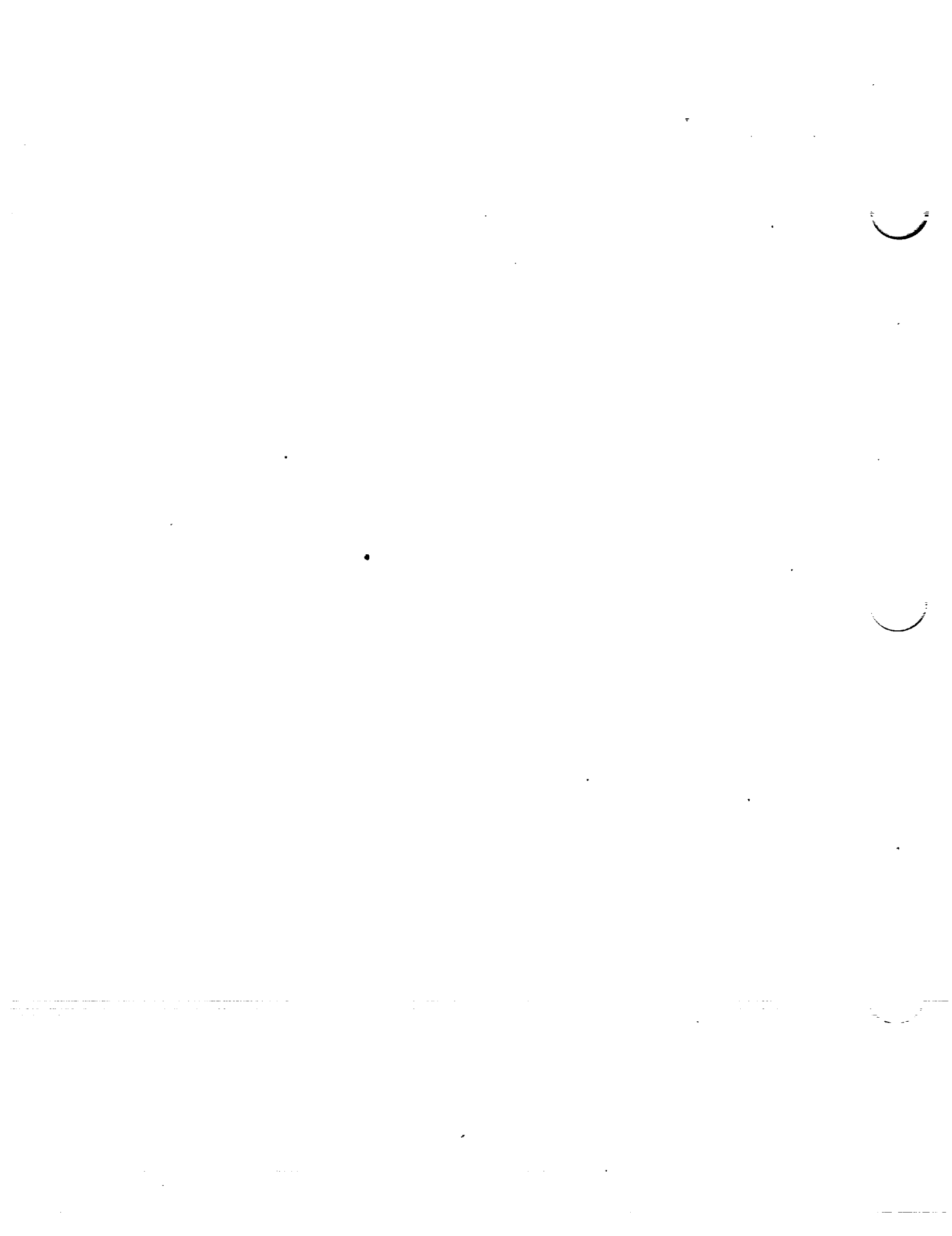




(a) Smooth condition; TDT test 328.



(b) Lacquer camouflage unimproved after painting; TDT test 461.
 Figure 20.- Variation of drag coefficient with Reynolds number for a 60-inch-chord model of the
 NACA 65(421)-420 airfoil for two surface conditions.



CONFIDENTIAL

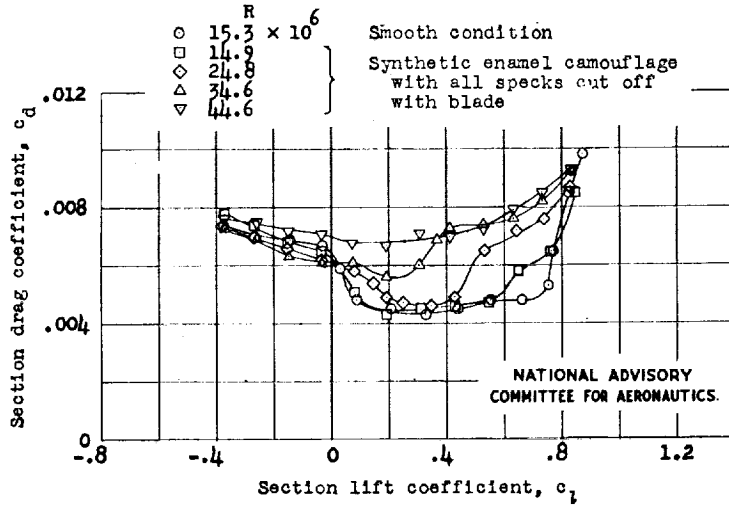


Figure 21.- Drag characteristics of NACA 65(421)-420 airfoil for two surface conditions; TDT tests 300 and 486.

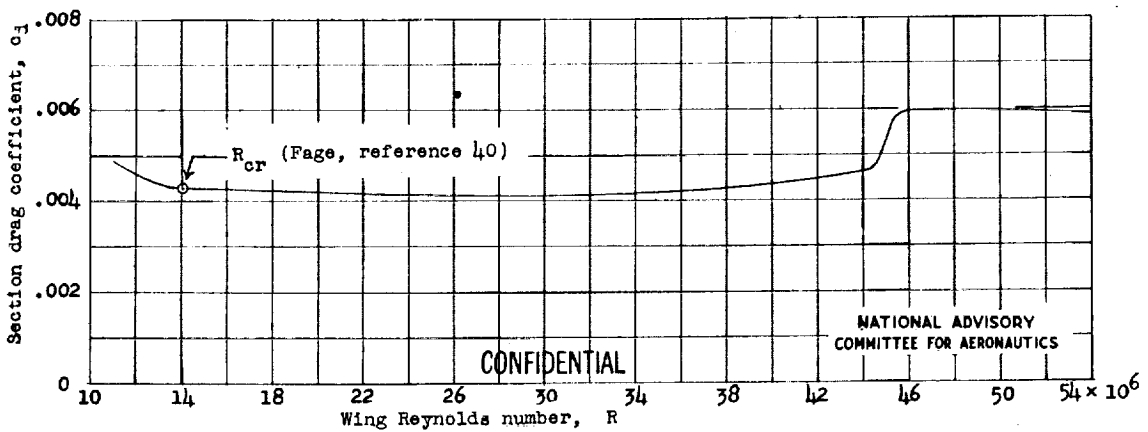
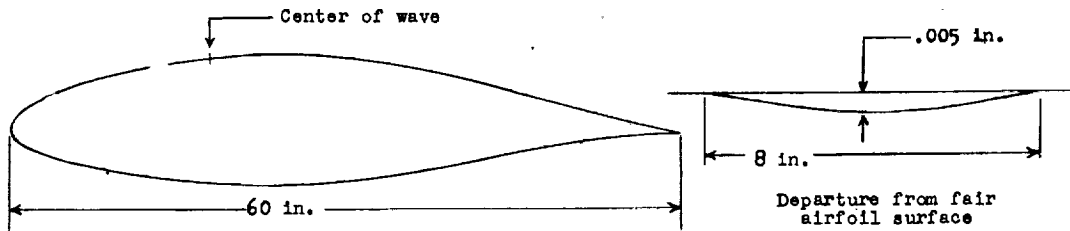


Figure 22.- Experimental curve showing variation of drag coefficient with Reynolds number for the NACA 65(421)-420 airfoil section with a small amount of surface waviness.



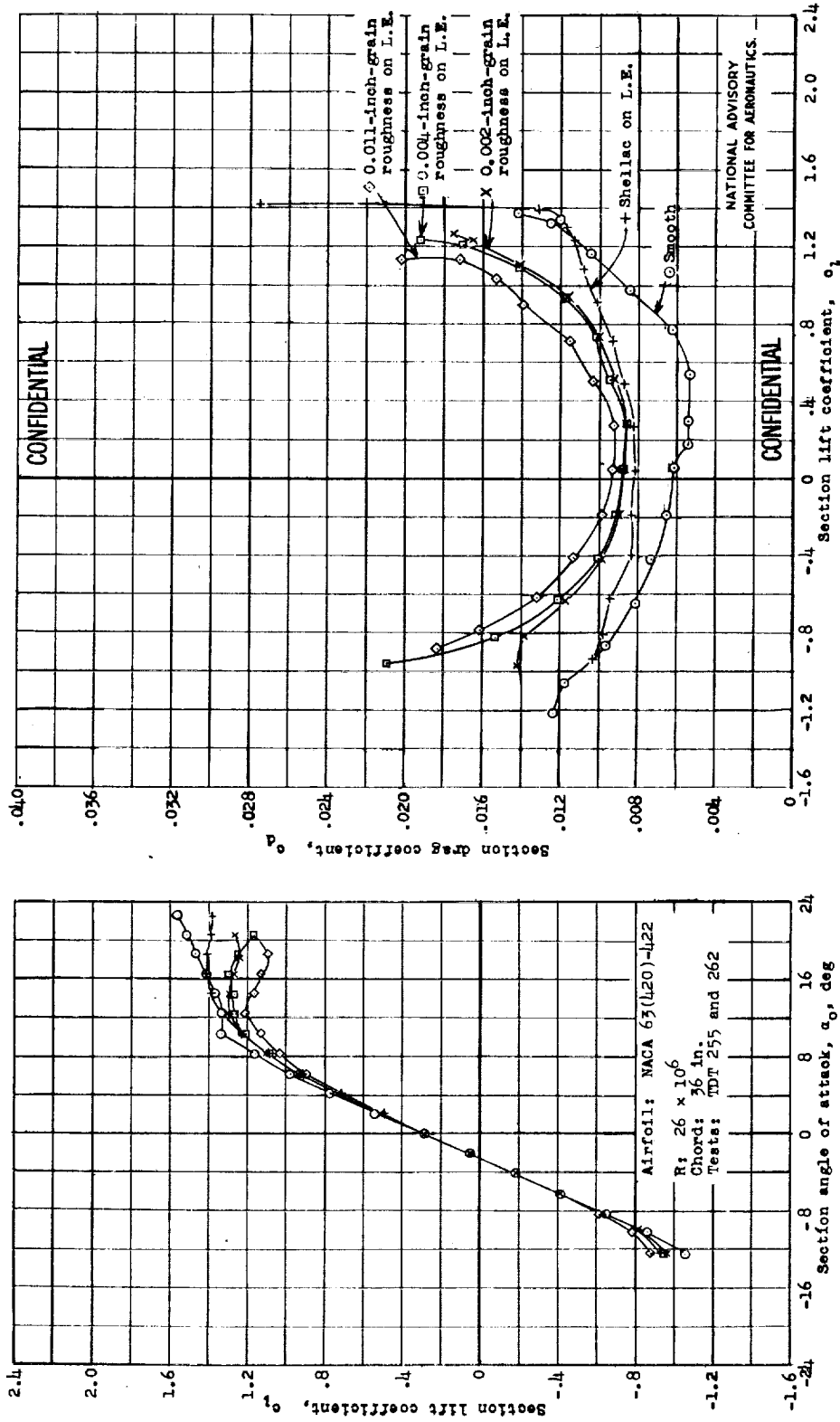
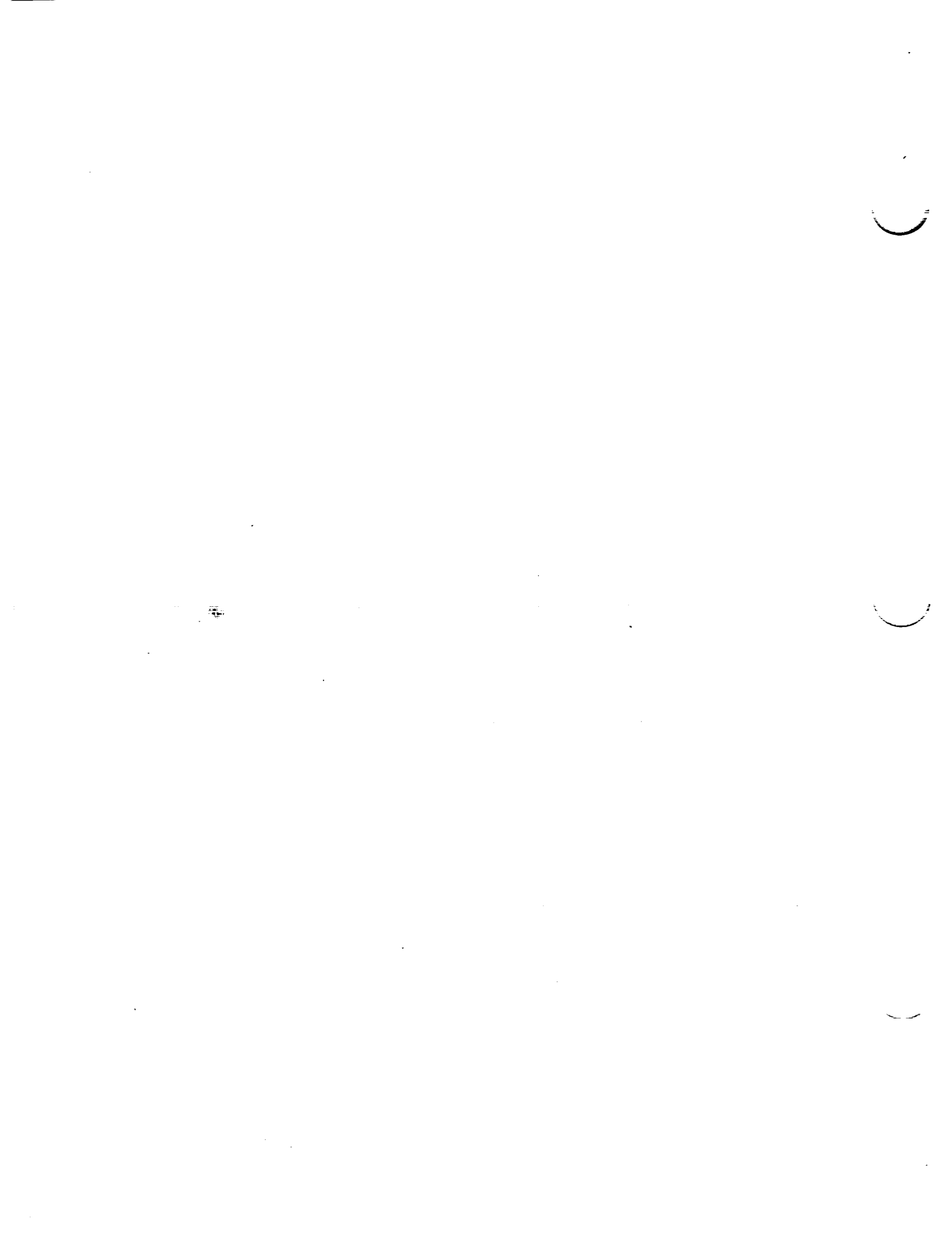


Figure 23.- Lift and drag characteristics of an NACA 63(420)-422 airfoil with various degrees of roughness at the leading edge.



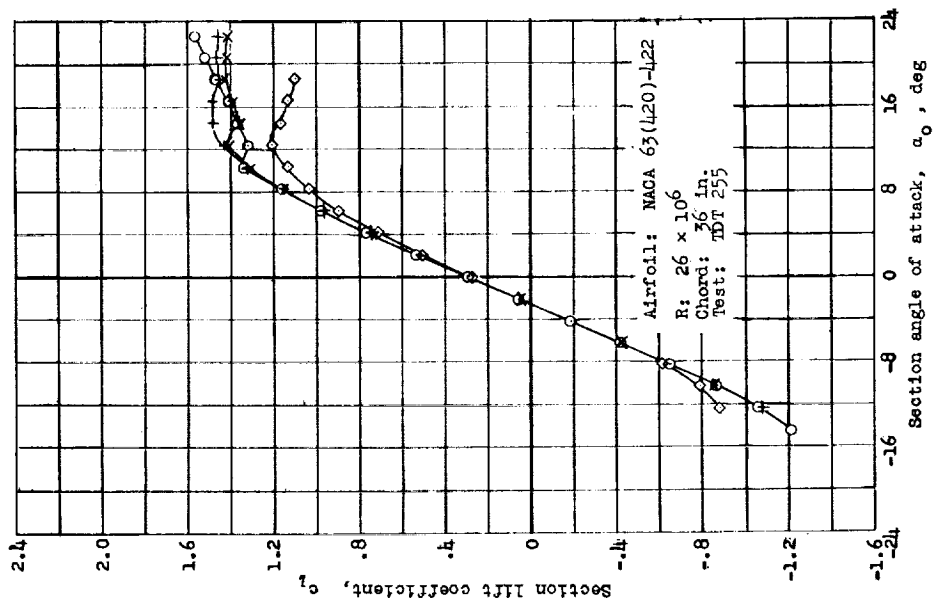
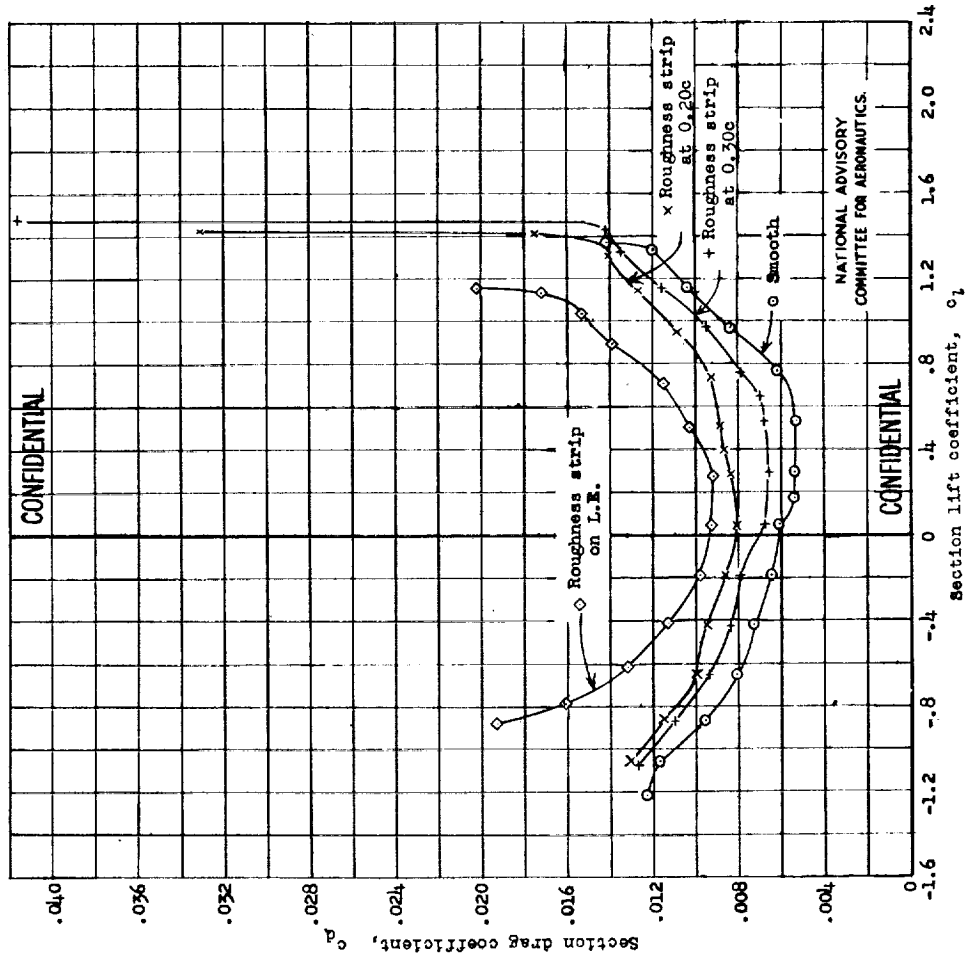
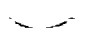


Figure 24.- Lift and drag characteristics of an NACA 63(420)-422 airfoil with 0.011-in.-grain roughness at various chordwise locations.

NATIONAL ADVISORY
COMMITTEE FOR AERONAUTICS.



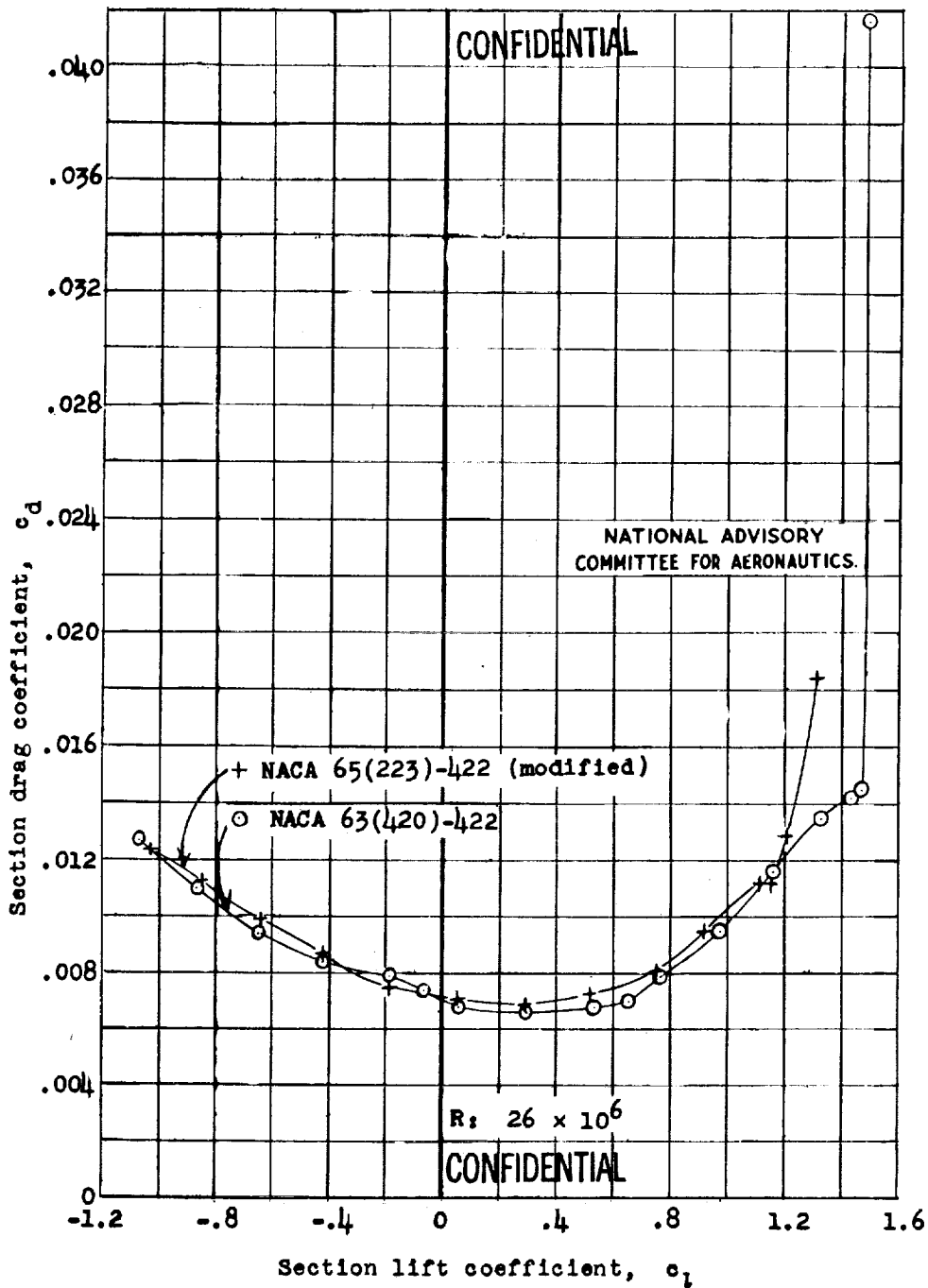
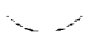


Figure 25.- Drag characteristics of two NACA 6-series airfoils with 0.011-inch-grain roughness at 0.30c.



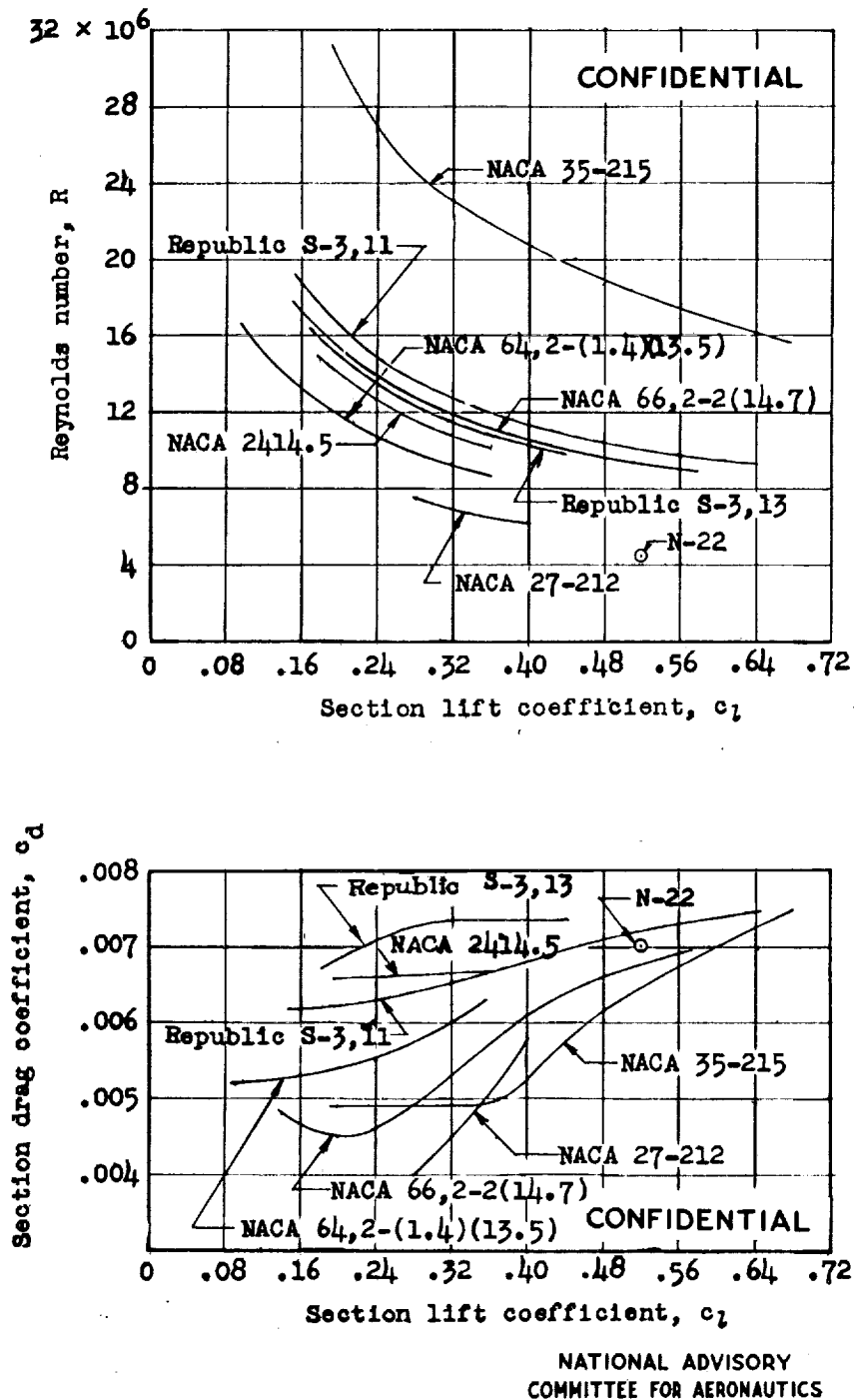


Figure 26.- Comparison of section drag coefficients obtained in flight on various airfoils. Tests of NACA 27-212 and 35-215 sections made on gloves.



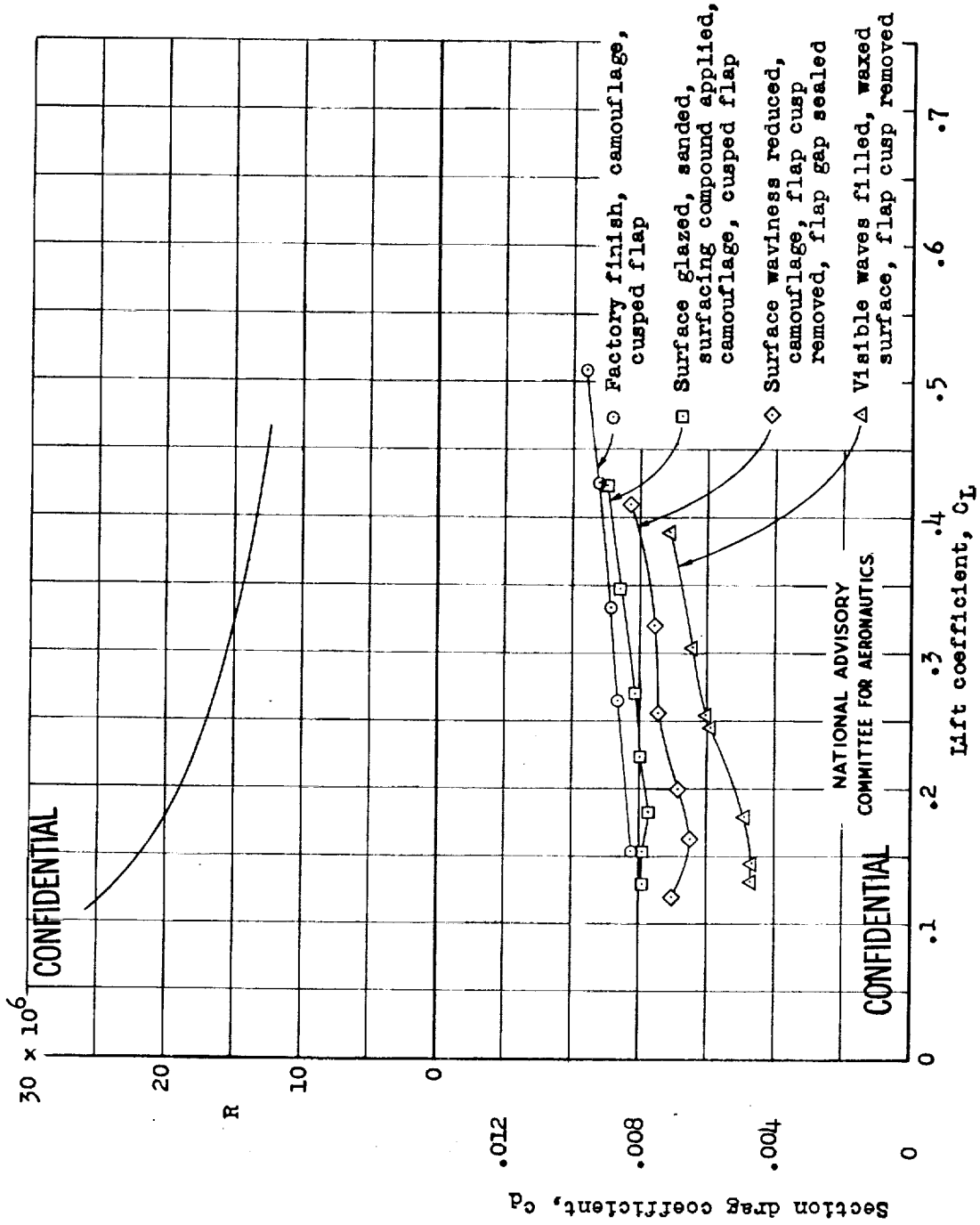
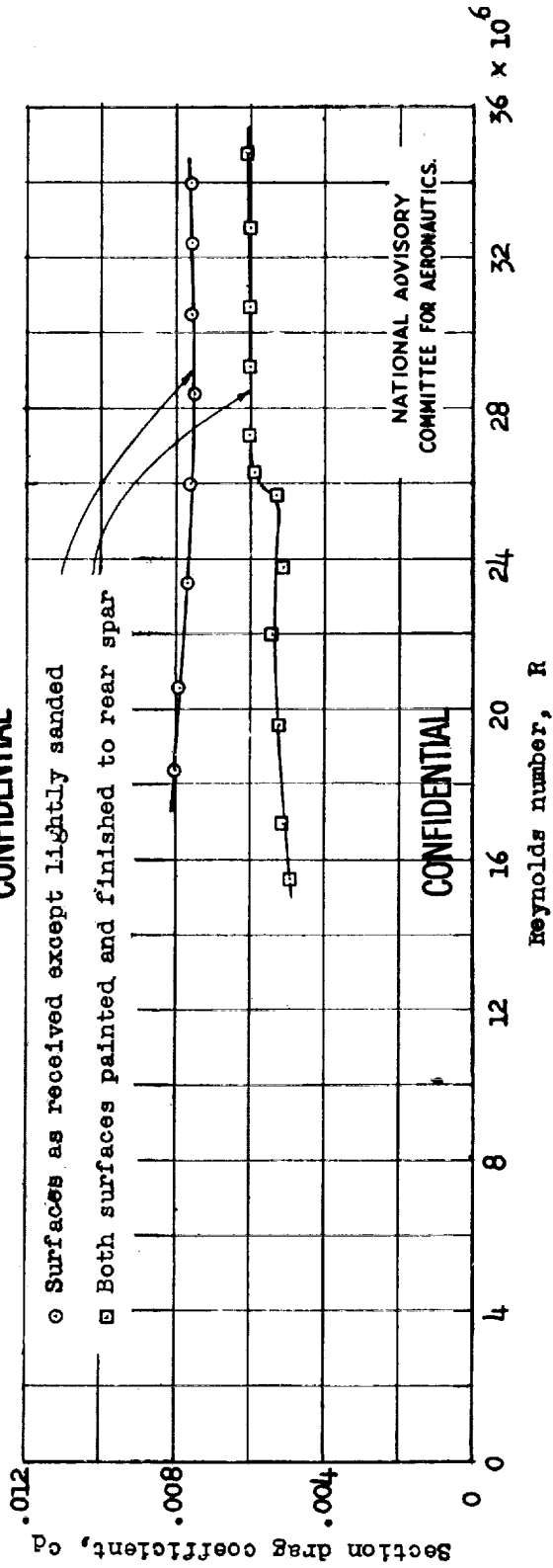


Figure 27.- Consolidated-Vultee flight measurements of the effect of wing surface condition on drag of an NACA 66(215)-1(14.5) wing section.





CONFIDENTIAL



NATIONAL ADVISORY
COMMITTEE FOR AERONAUTICS.

CONFIDENTIAL

Figure 28.- Drag scale effect on 100-inch-chord practical-construction model of the NACA 65(216)-3(16.5)(approx.) airfoil section. $c_l = 0.2$ (approx.).



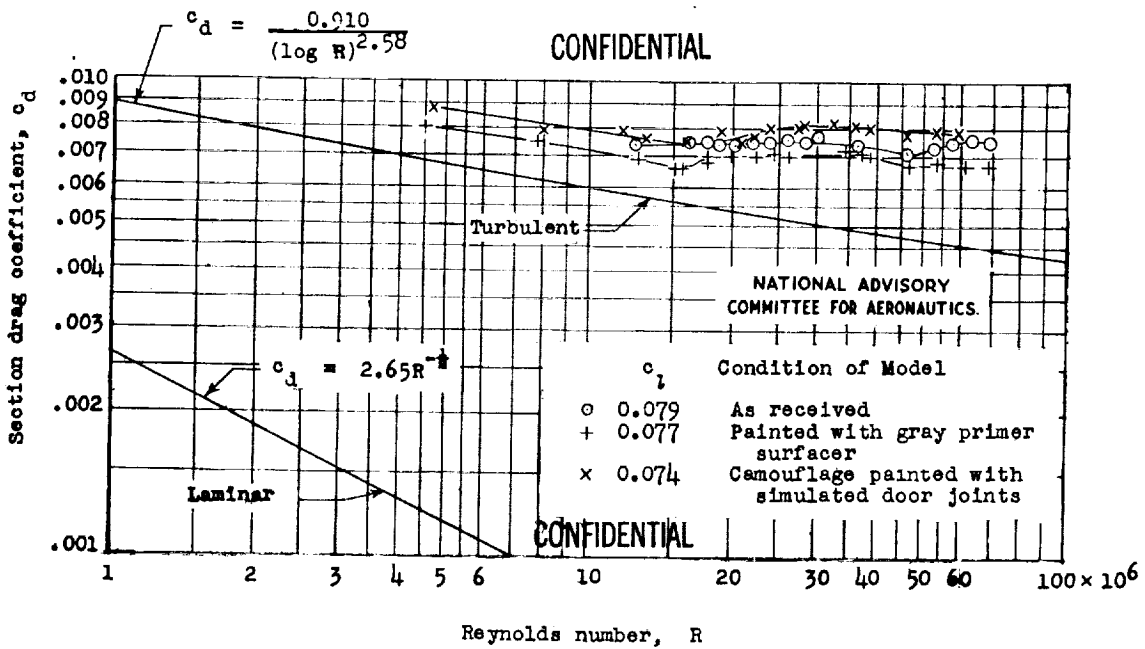
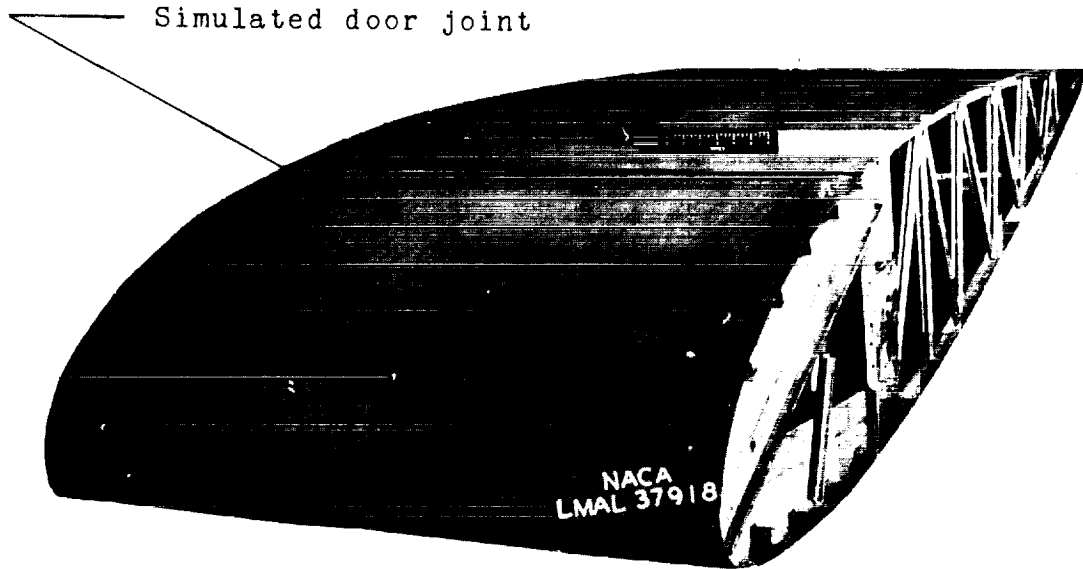


Figure 29.- Variation of the drag coefficient with Reynolds number for the NACA 23016 airfoil section together with laminar and turbulent skin-friction coefficients for a flat plate.



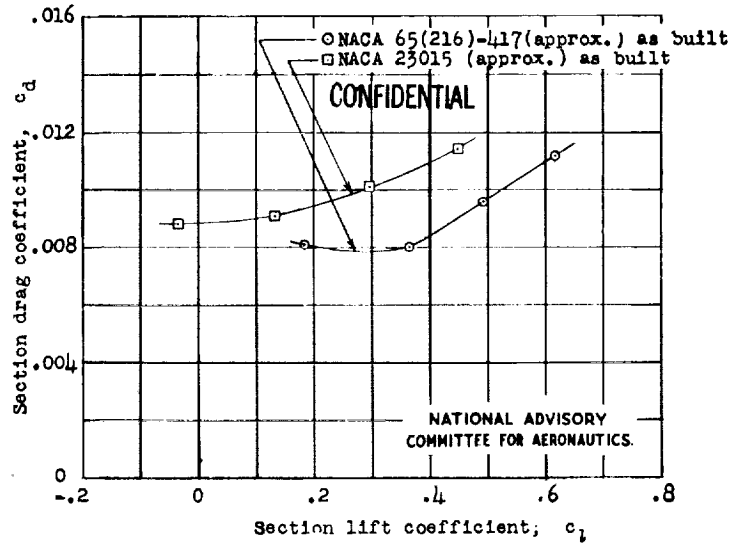


Figure 30.- Drag characteristics of the NACA 65,2-417 (approx.) and NACA 23015 (approx.) airfoil sections built by practical-construction methods by the same manufacturer. $R = 10.23 \times 10^6$.

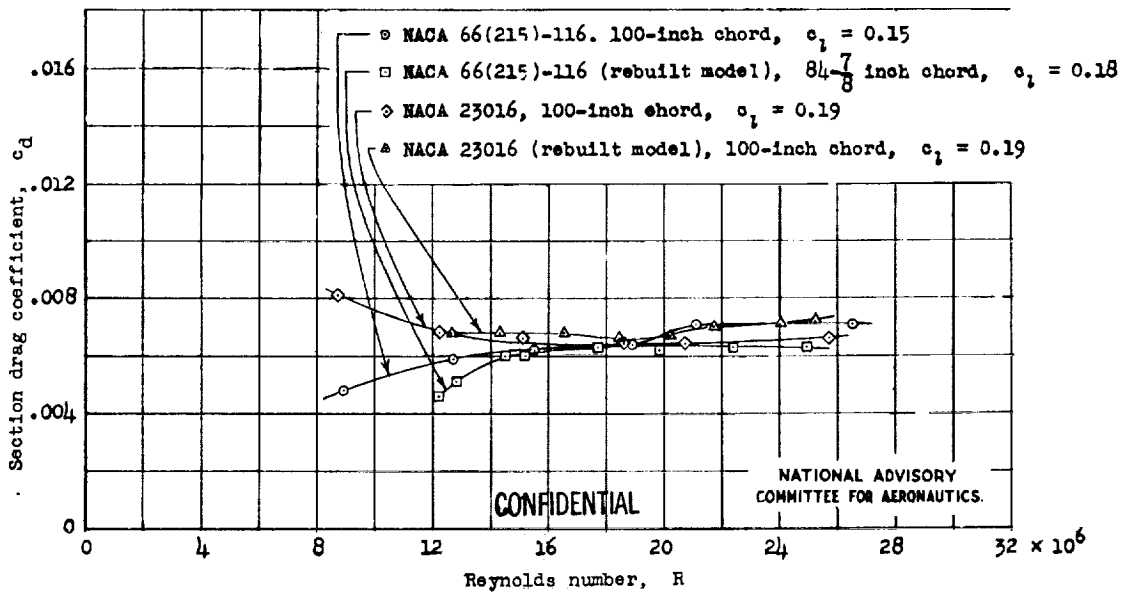


Figure 31.- Scale effect on drag of the NACA 66(215)-116 and NACA 23016 airfoil sections built by practical-construction methods by the same manufacturer and tested as received.



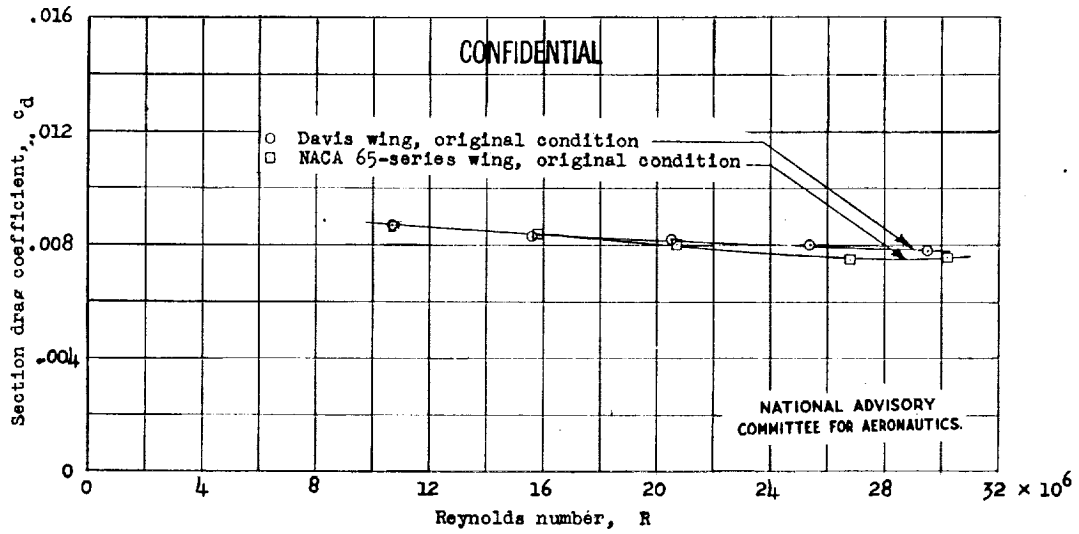


Figure 32.- Drag scale effect for a model of the NACA 65-series airfoil section 18.27 percent thick and the Davis airfoil section 18.27 percent thick, built by practical-construction methods by the same manufacturer. $c_l = 0.46$ (approx.).

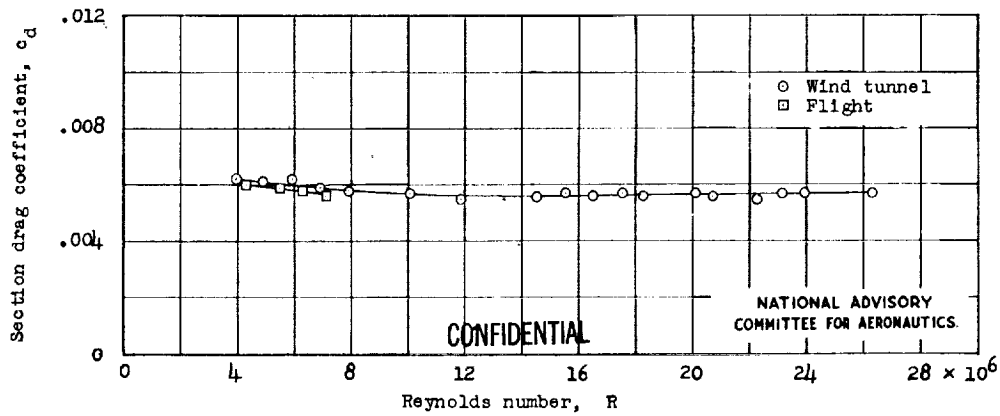
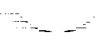


Figure 33.- Comparison of drag coefficients measured in flight and wind tunnel for the NACA 0012 airfoil section at zero lift.



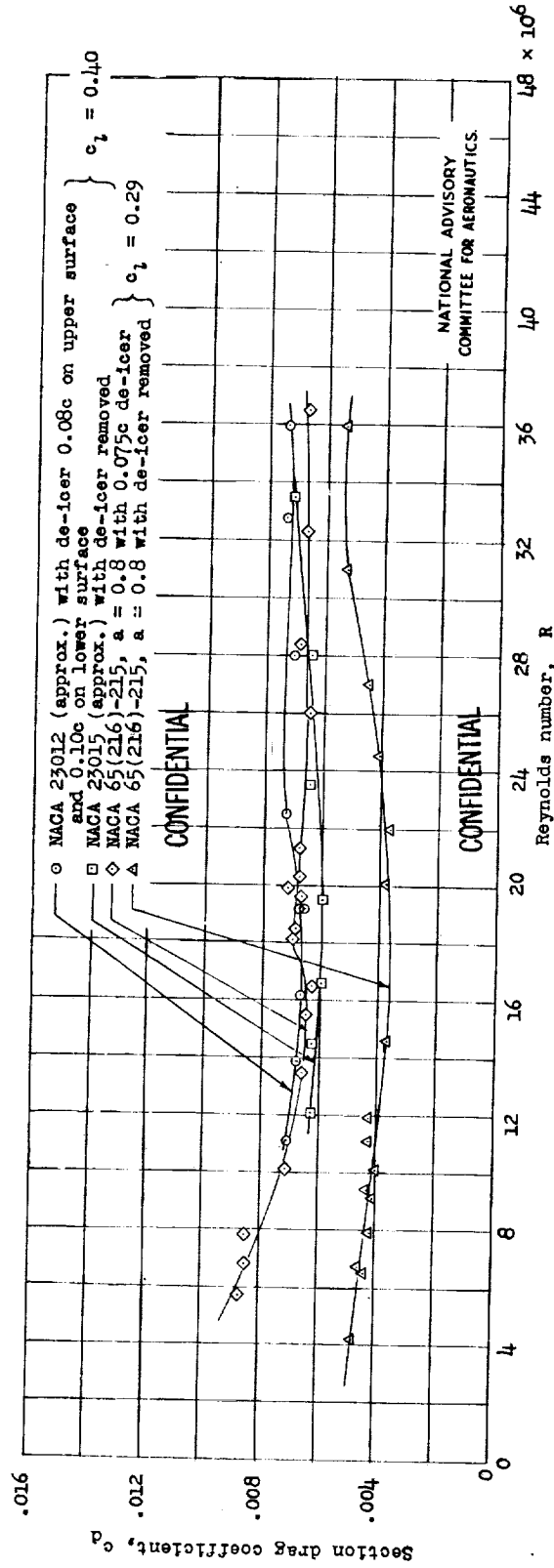
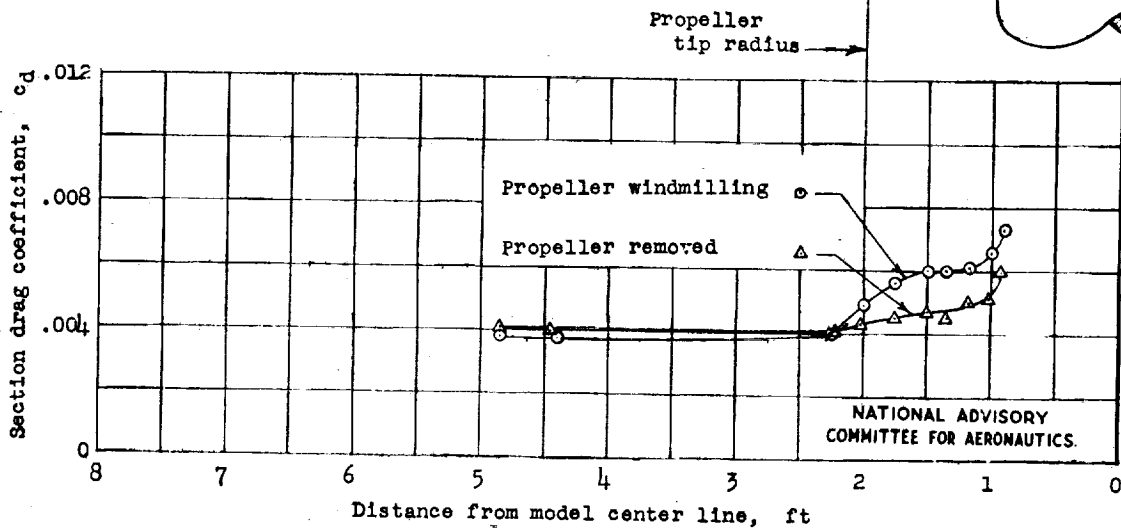
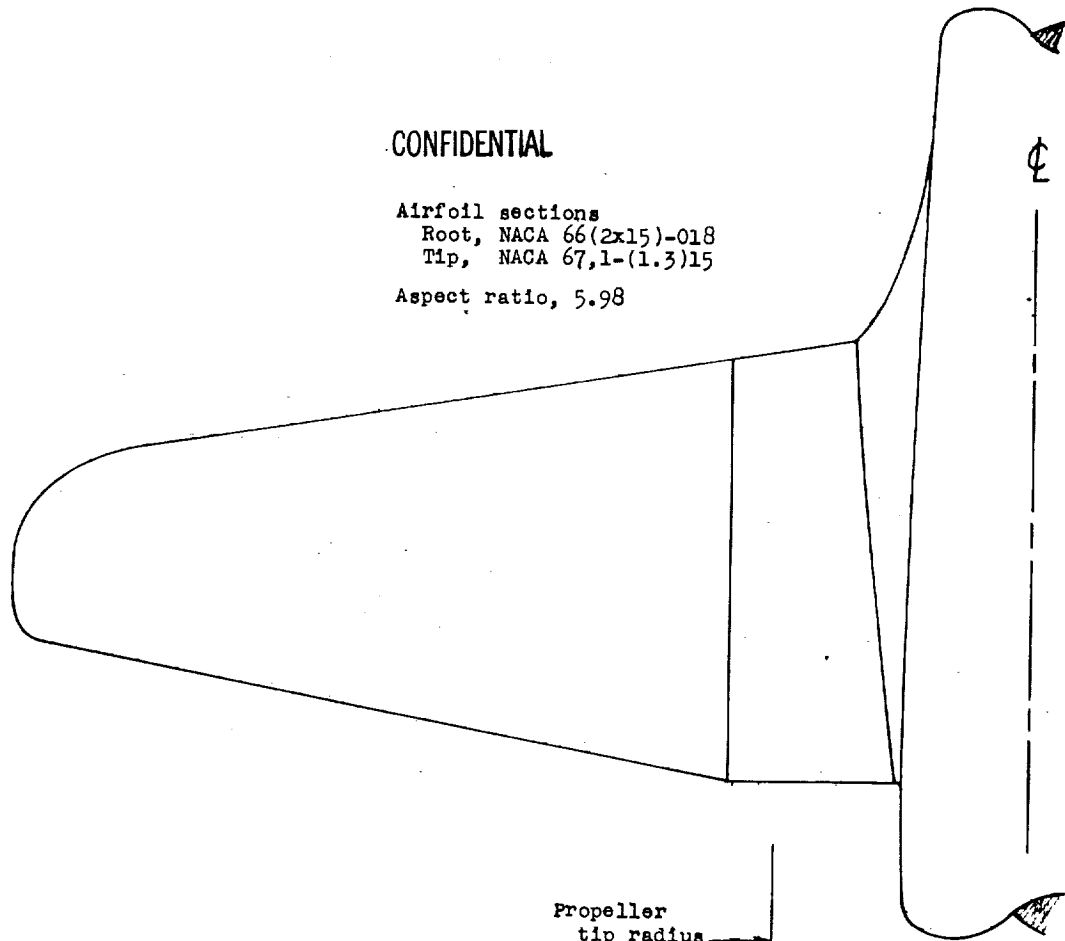


Figure 34.- Effect of de-icers on the drag of two practical-construction airfoil sections with relatively smooth surfaces.



CONFIDENTIAL

Airfoil sections
 Root, NACA 66(2x15)-018
 Tip, NACA 67,1-(1.3)15
 Aspect ratio, 5.98



CONFIDENTIAL

Figure 35.- The effect of propeller operation on section drag coefficient of a fighter-type airplane, from tests of a model, in the Langley 19-foot pressure tunnel; $C_L = 0.10$; $R, 3.7 \times 10^6$.



CONFIDENTIAL

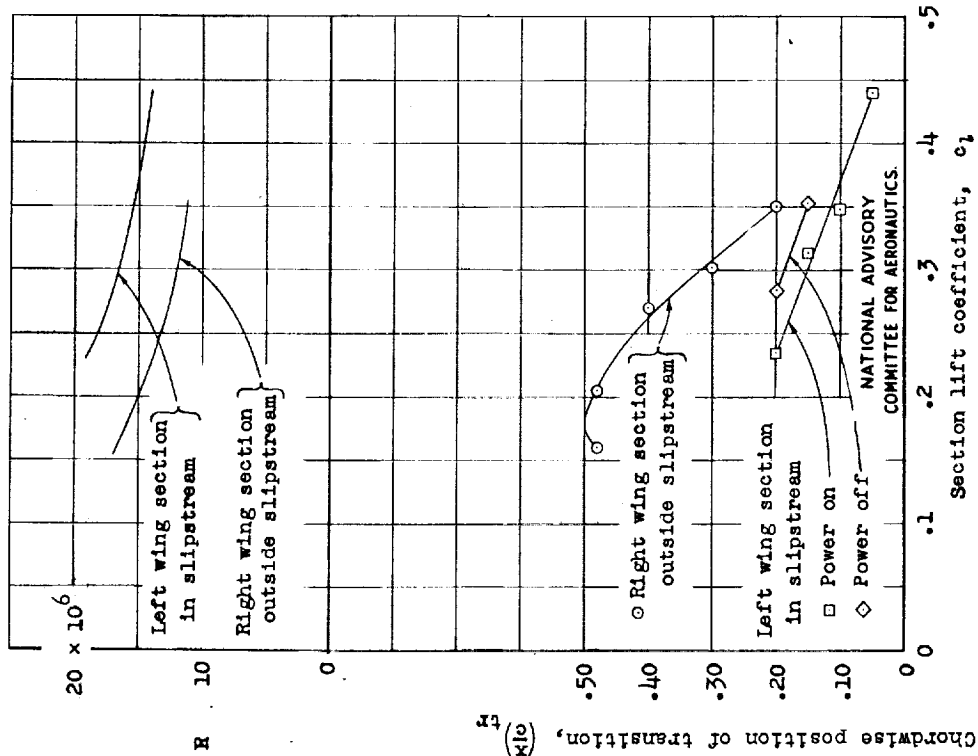


Figure 36.- Flight measurements of transition on an MACA 66-series wing within and outside the slipstream.

CONFIDENTIAL

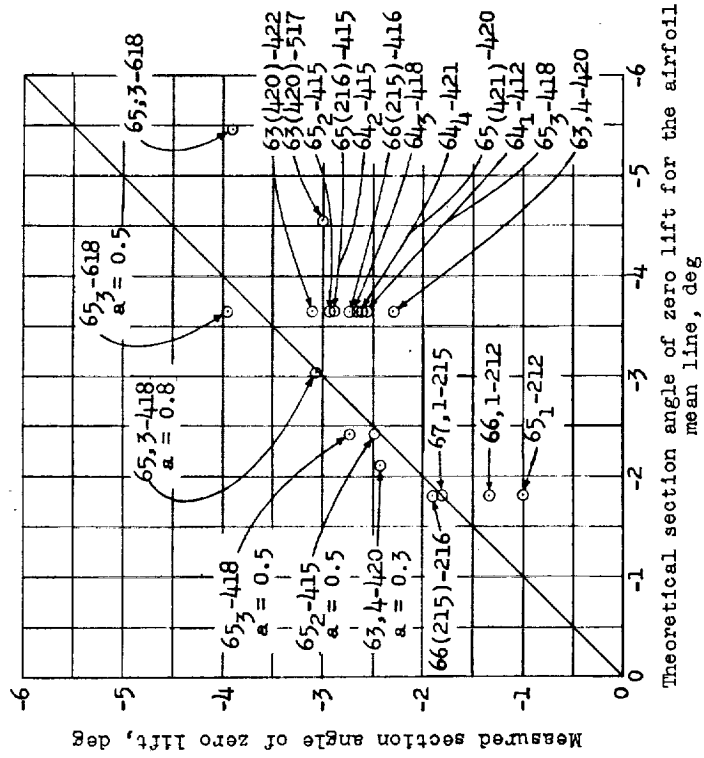
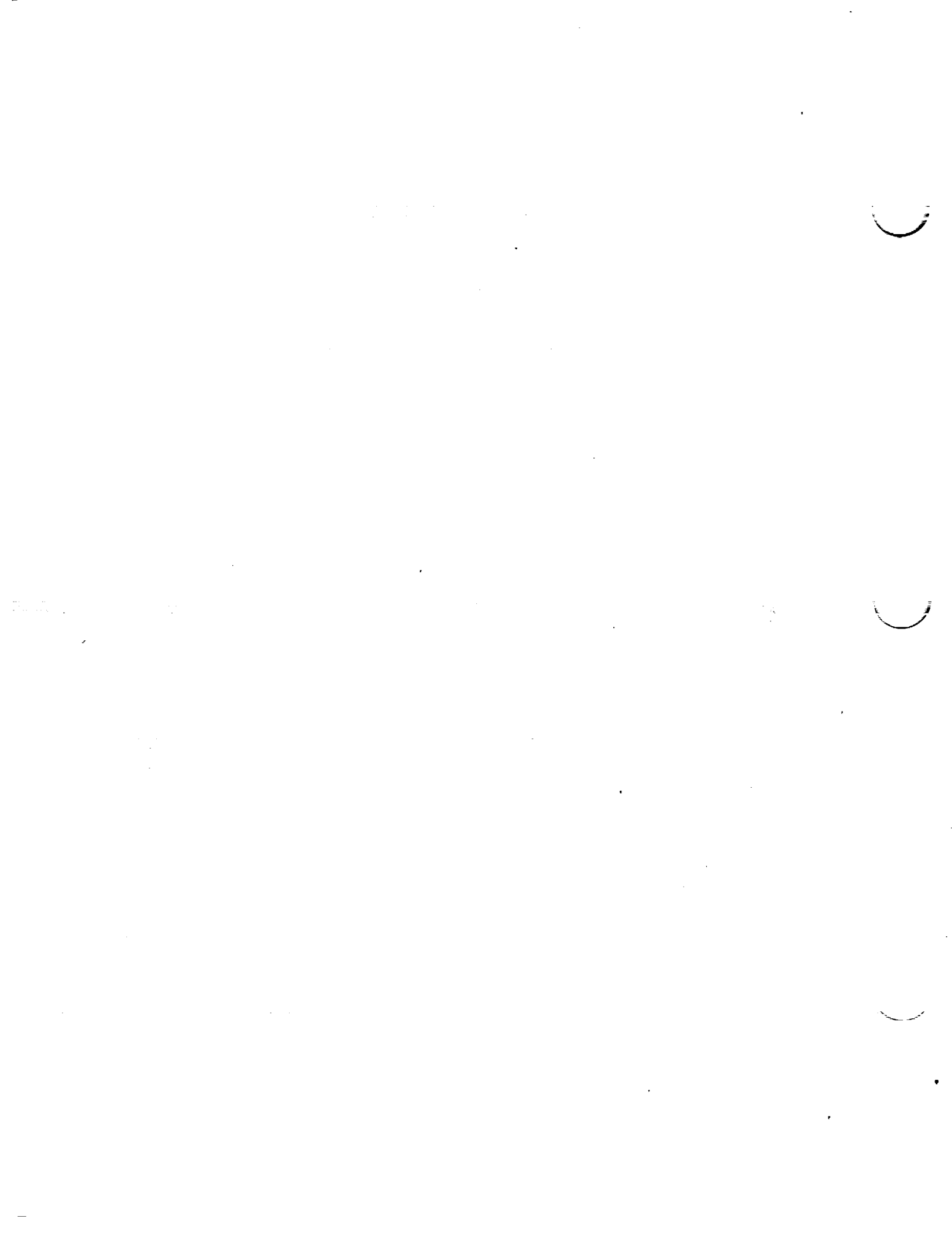


Figure 37.- Comparison of theoretical and measured section angles of zero lift for some MACA 6-series airfoils.

CONFIDENTIAL



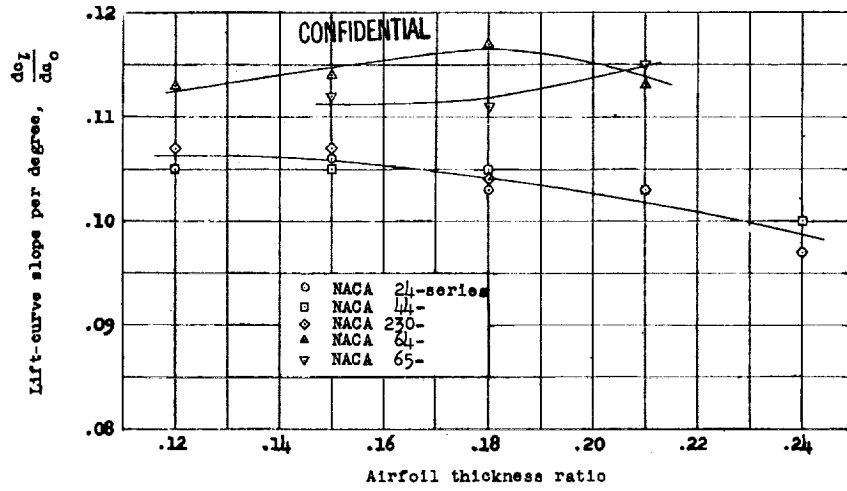


Figure 38.- Variation of lift-curve slope with thickness at a Reynolds number of 9×10^6 for the NACA 24-, 44-, and 230-series airfoil sections together with the NACA 64- and 65-series airfoil sections cambered for a design lift coefficient of 0.4.

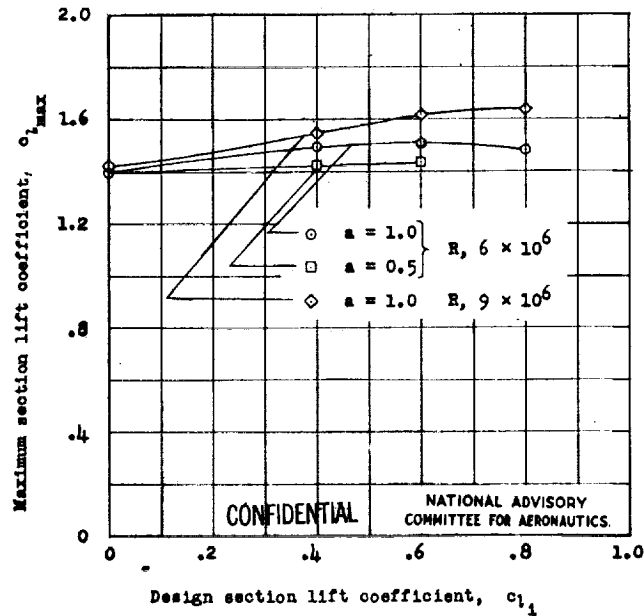


Figure 39.- Variation of maximum lift coefficient with amount of camber of some NACA 65-series airfoils of 18-percent thickness from tests in the Langley two-dimensional low-turbulence pressure tunnel.



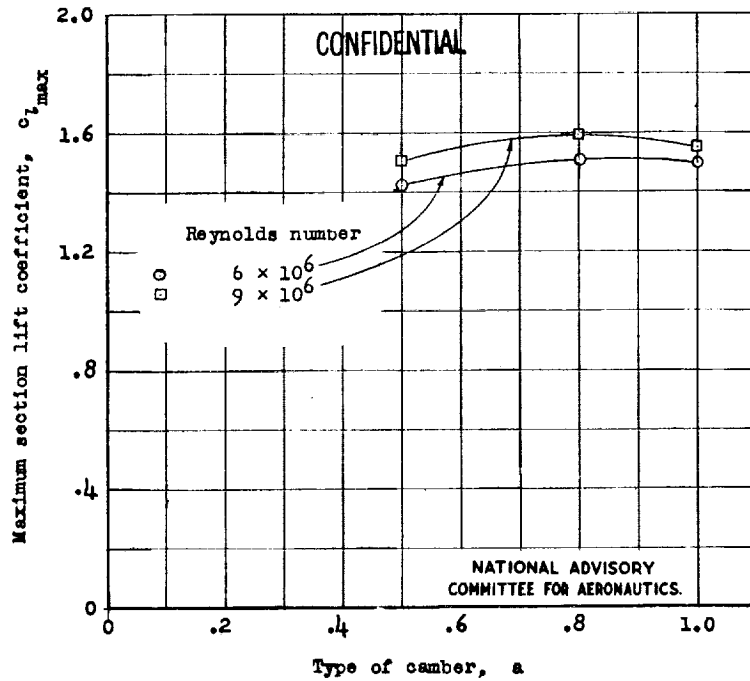


Figure 40.- Variation of maximum lift coefficient with type of camber for some NACA 65₃-418 airfoil sections from tests in the Langley two-dimensional low-turbulence pressure tunnel.

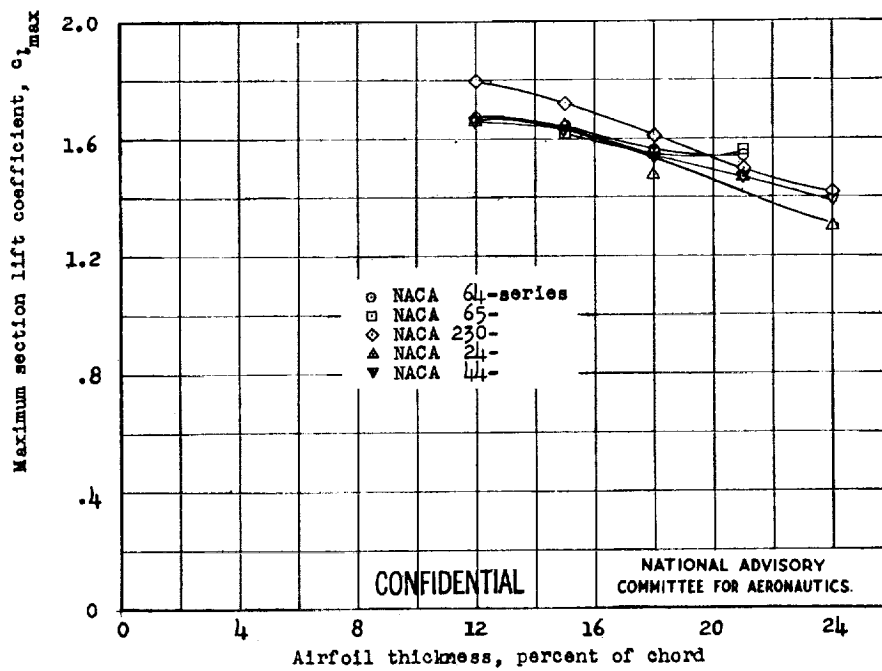
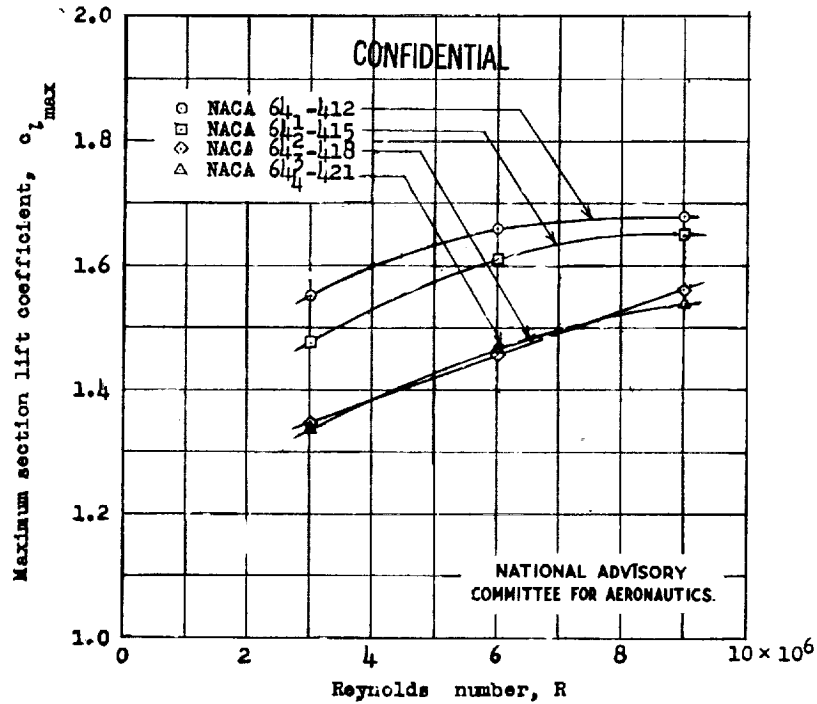
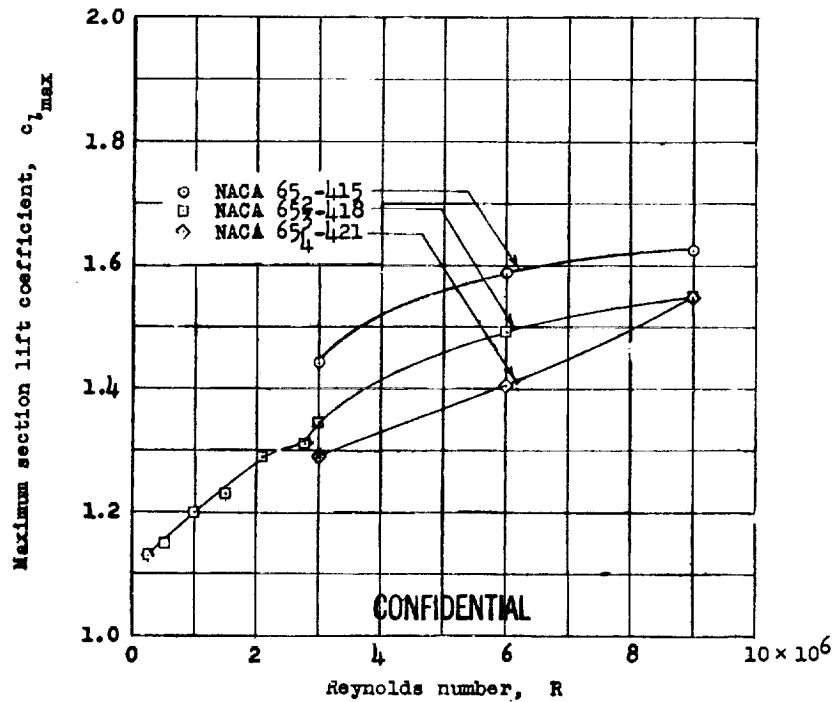


Figure 41.- Variation of maximum lift coefficient with thickness ratio for some NACA airfoils; $R, 9 \times 10^6$; all NACA 6-series airfoils cambered for $c_{l_1} = 0.4$, with mean line of type $a = 1.0$.





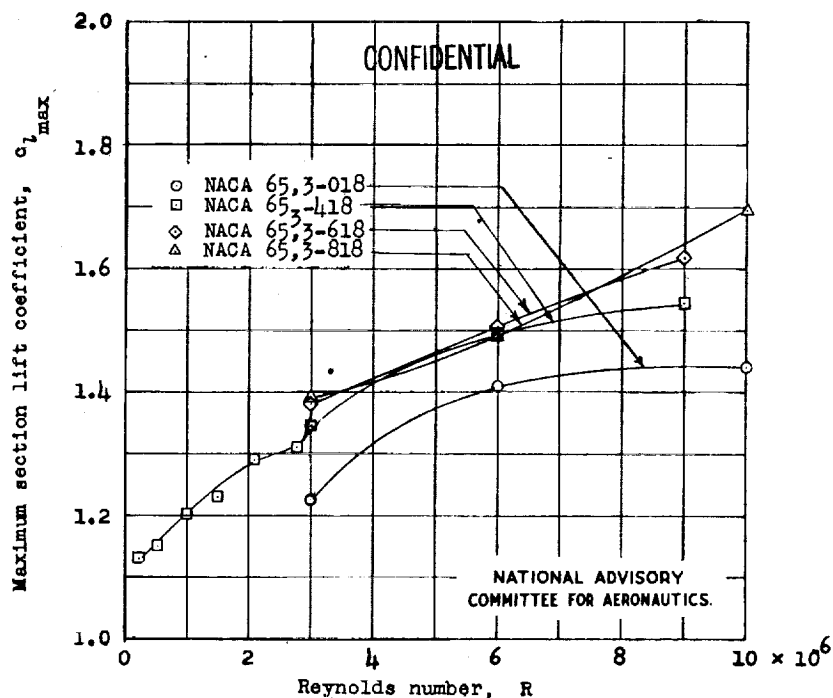
(a) Effect of thickness, 64-series cambered for a design lift coefficient of 0.4 .



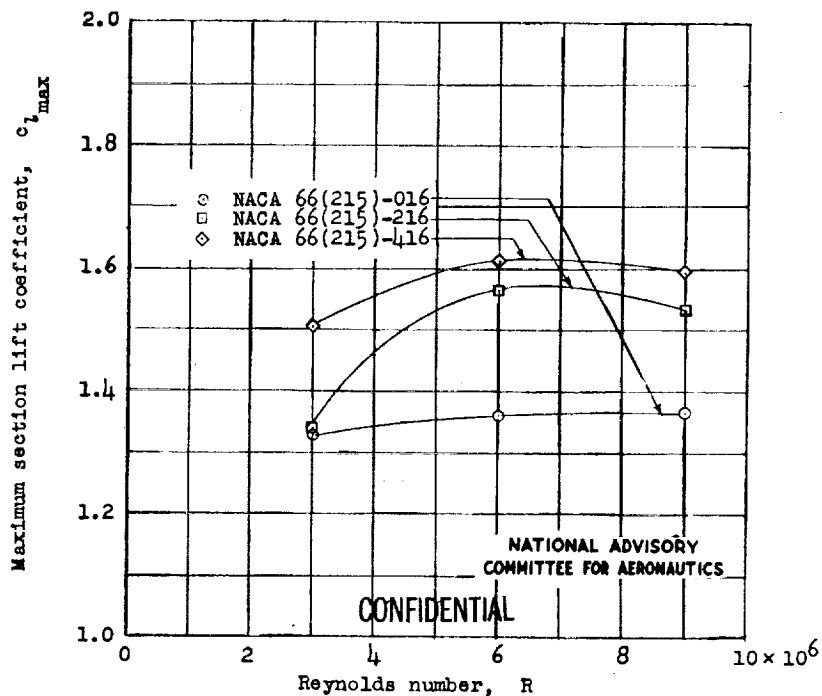
(b) Effect of thickness, 65-series cambered for a design lift coefficient of 0.4 .

Figure 42.- Scale effect on the maximum lift coefficient of selected NACA 6-series airfoil sections.





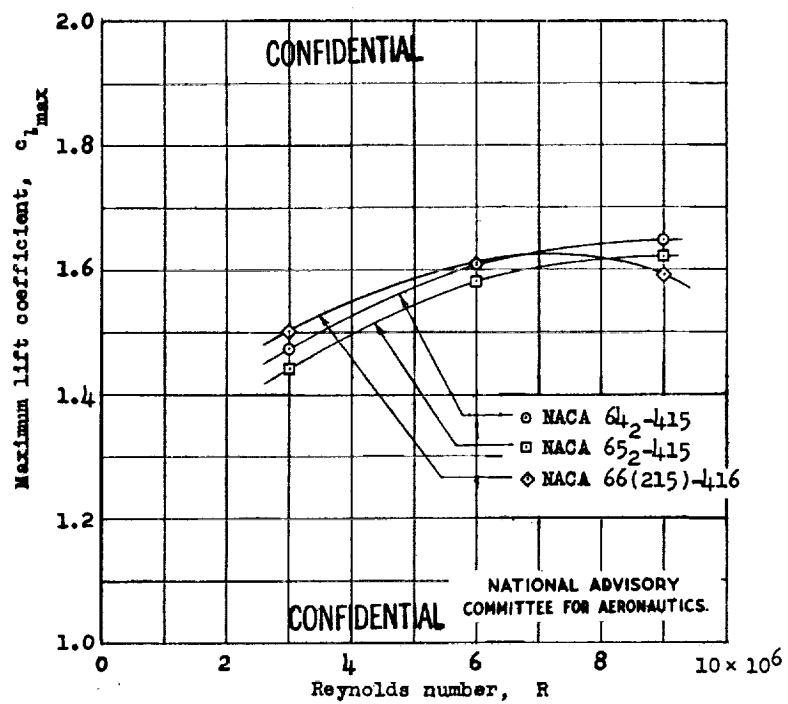
(c) Effect of camber, 65-series.



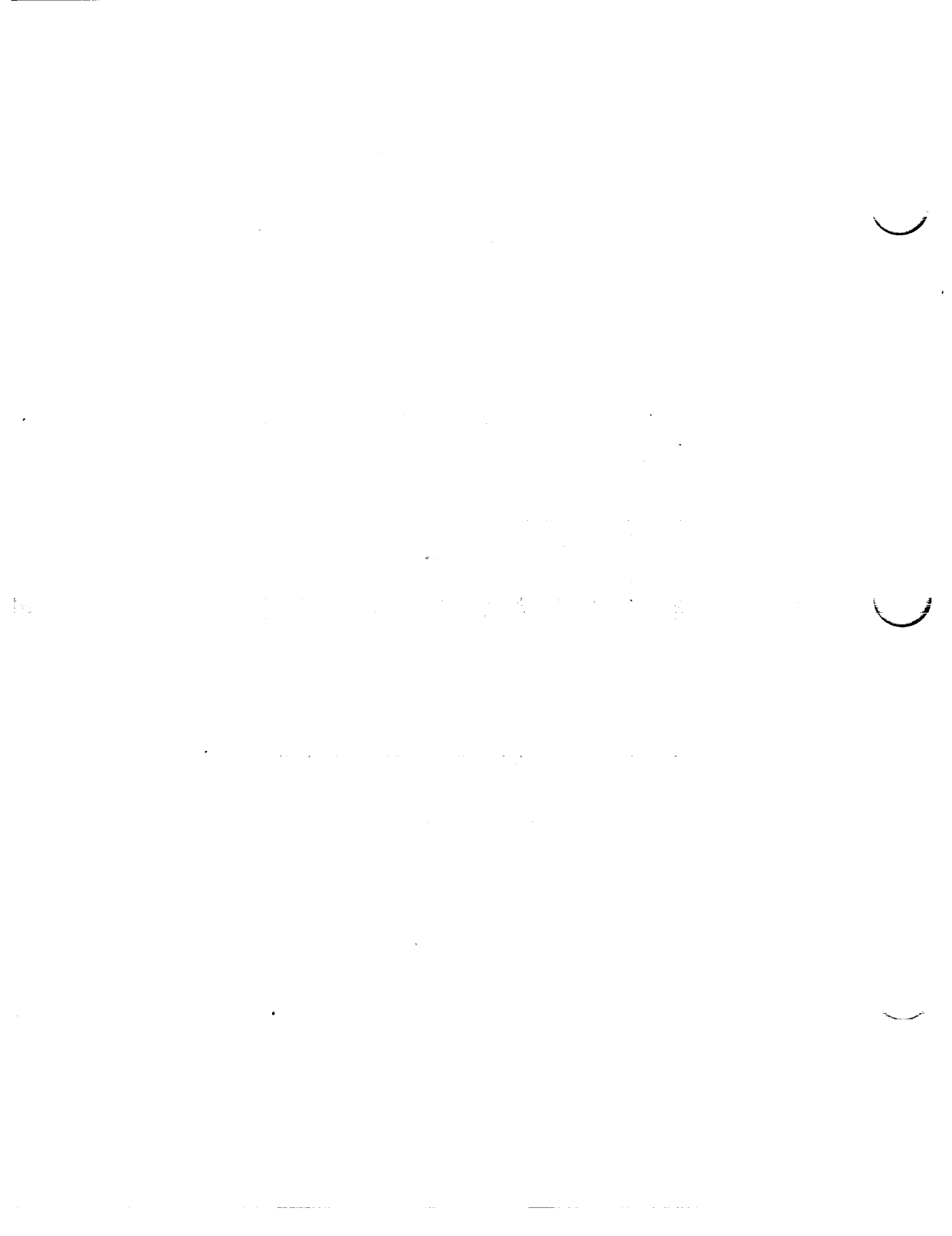
(d) Effect of camber, 66-series.

Figure 42.- Continued.





(e) Effect of position of minimum pressure.
 Figure 42.- Concluded.



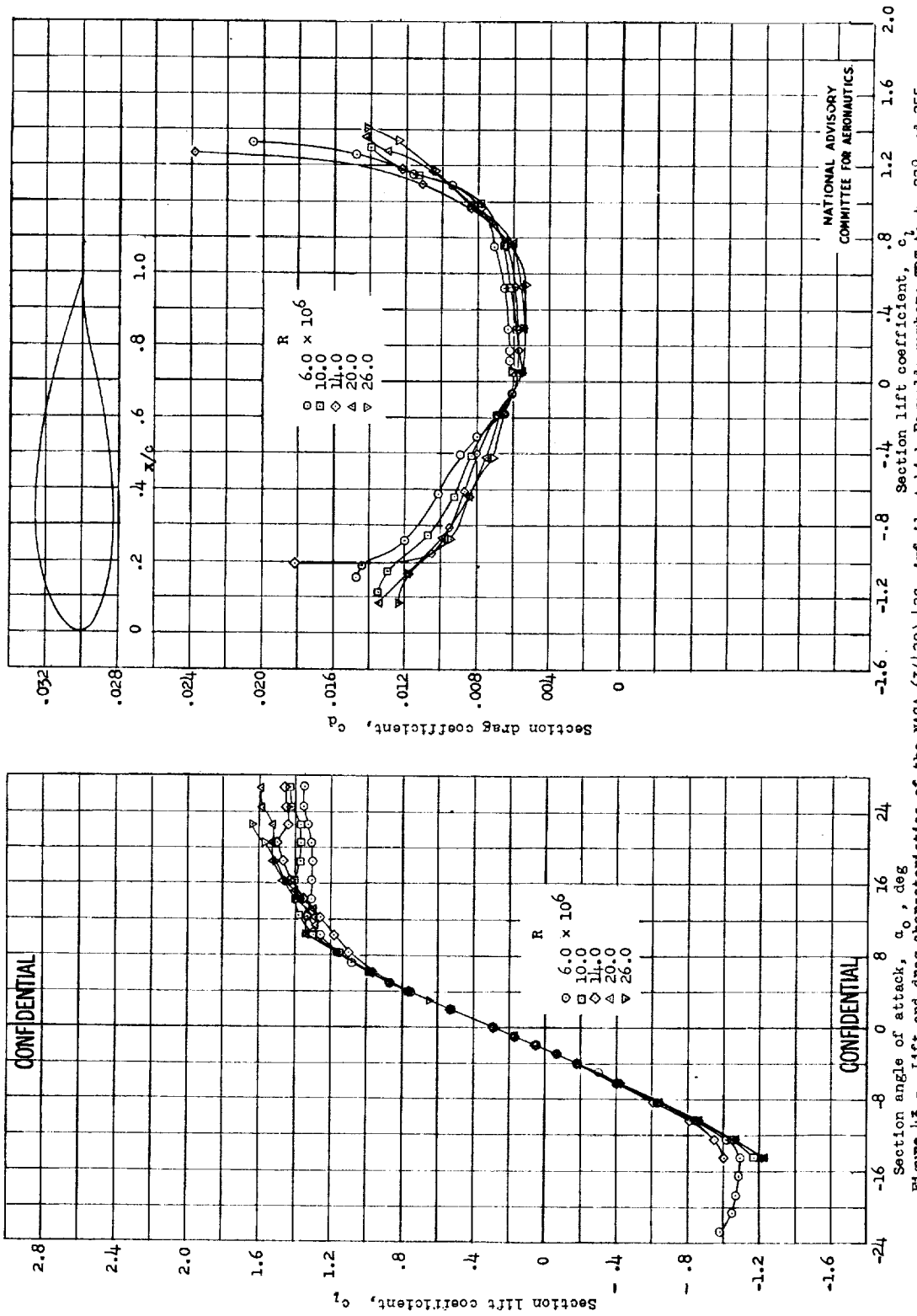
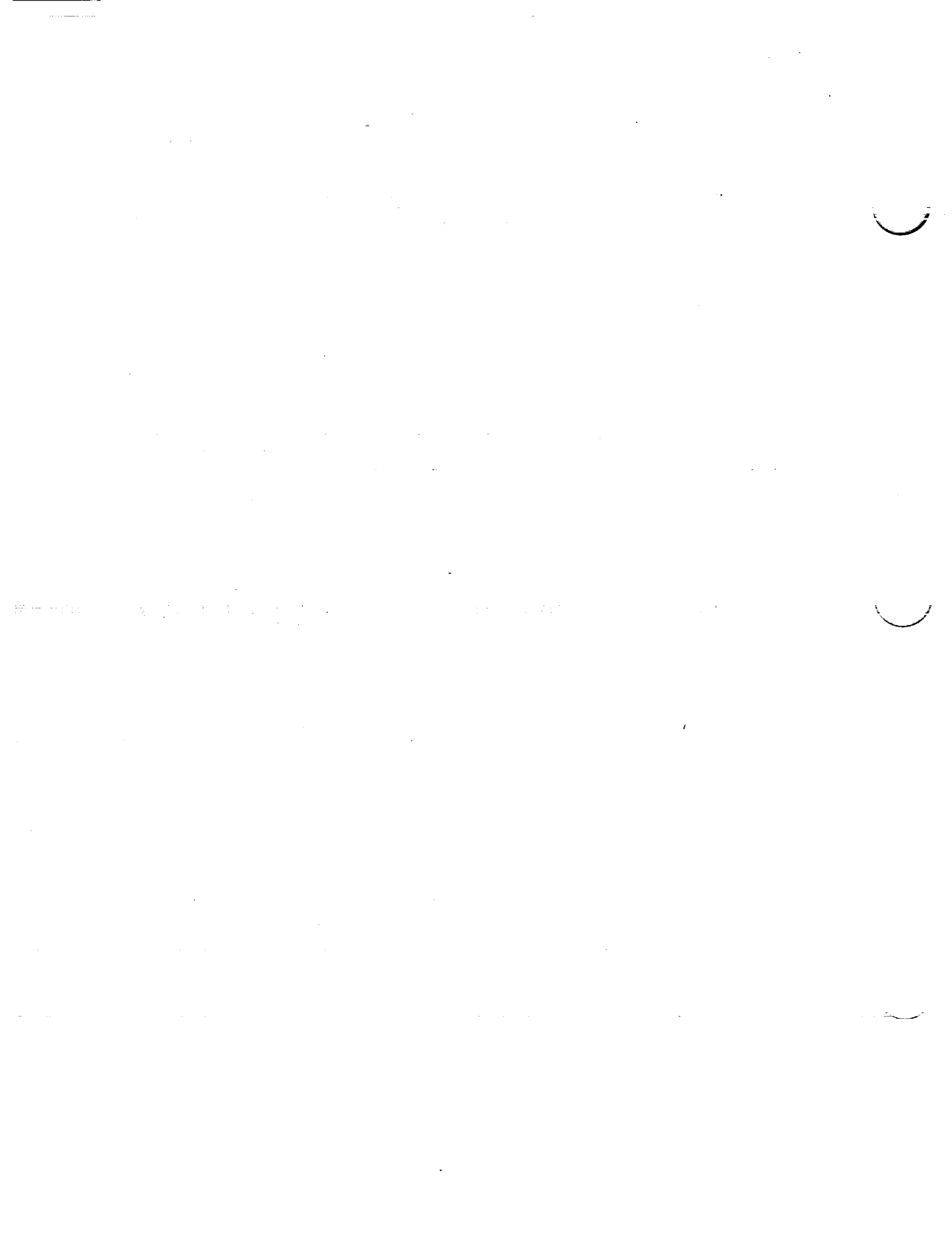


Figure 43.- Lift and drag characteristics of the NACA 63(120)-422 airfoil at high Reynolds number; DFR tests 228 and 255.

NATIONAL ADVISORY
COMMITTEE FOR AERONAUTICS.



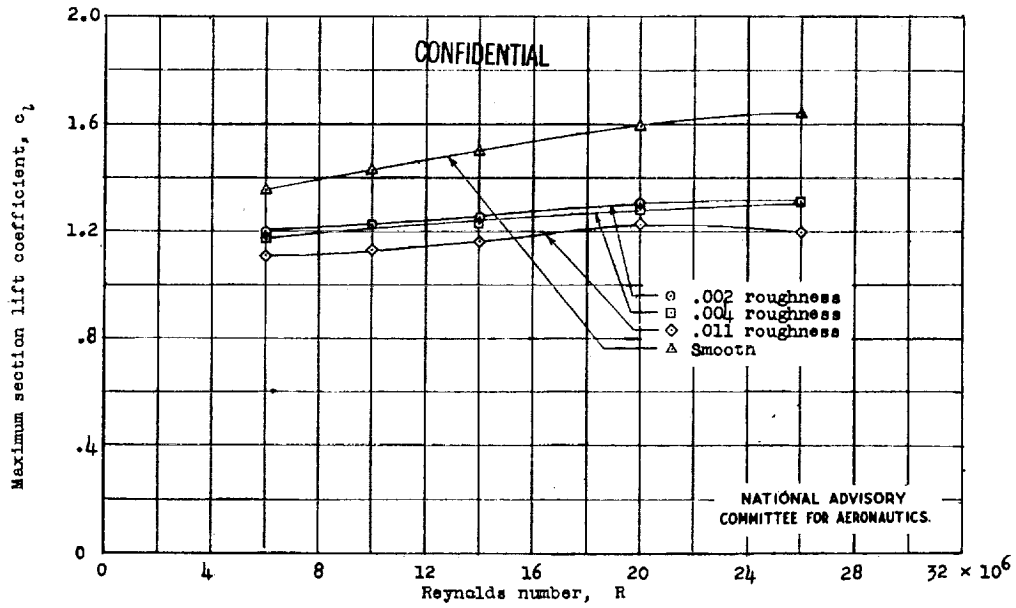


Figure 44.- Effects of Reynolds number on maximum section lift coefficient c_l of the NACA 63(420)-422 airfoil with roughened and smooth leading edge.

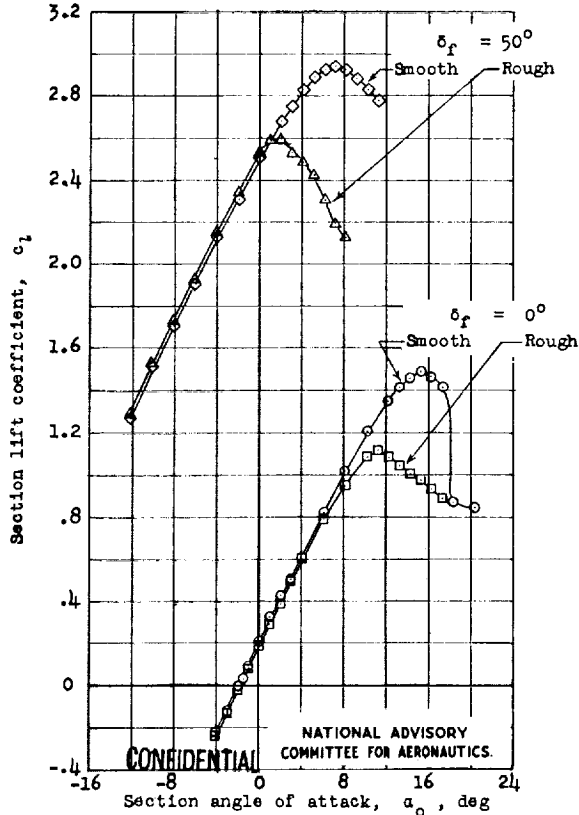


Figure 45.- Effect of standard roughness at the leading edge on the maximum lift coefficient of the NACA 66(215)-214 (approx.) airfoil section with a flap; $R, 6 \times 10^6$.



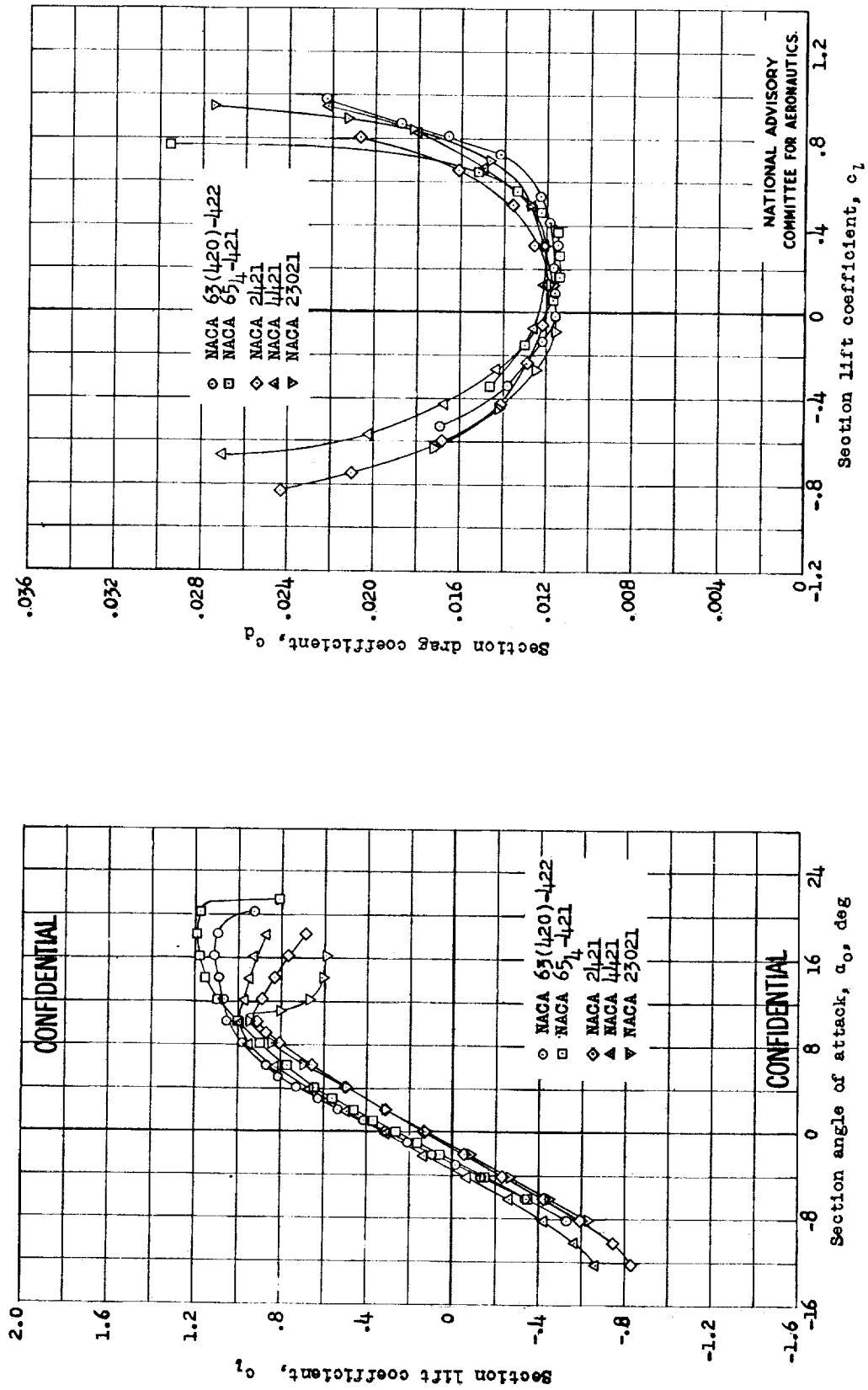
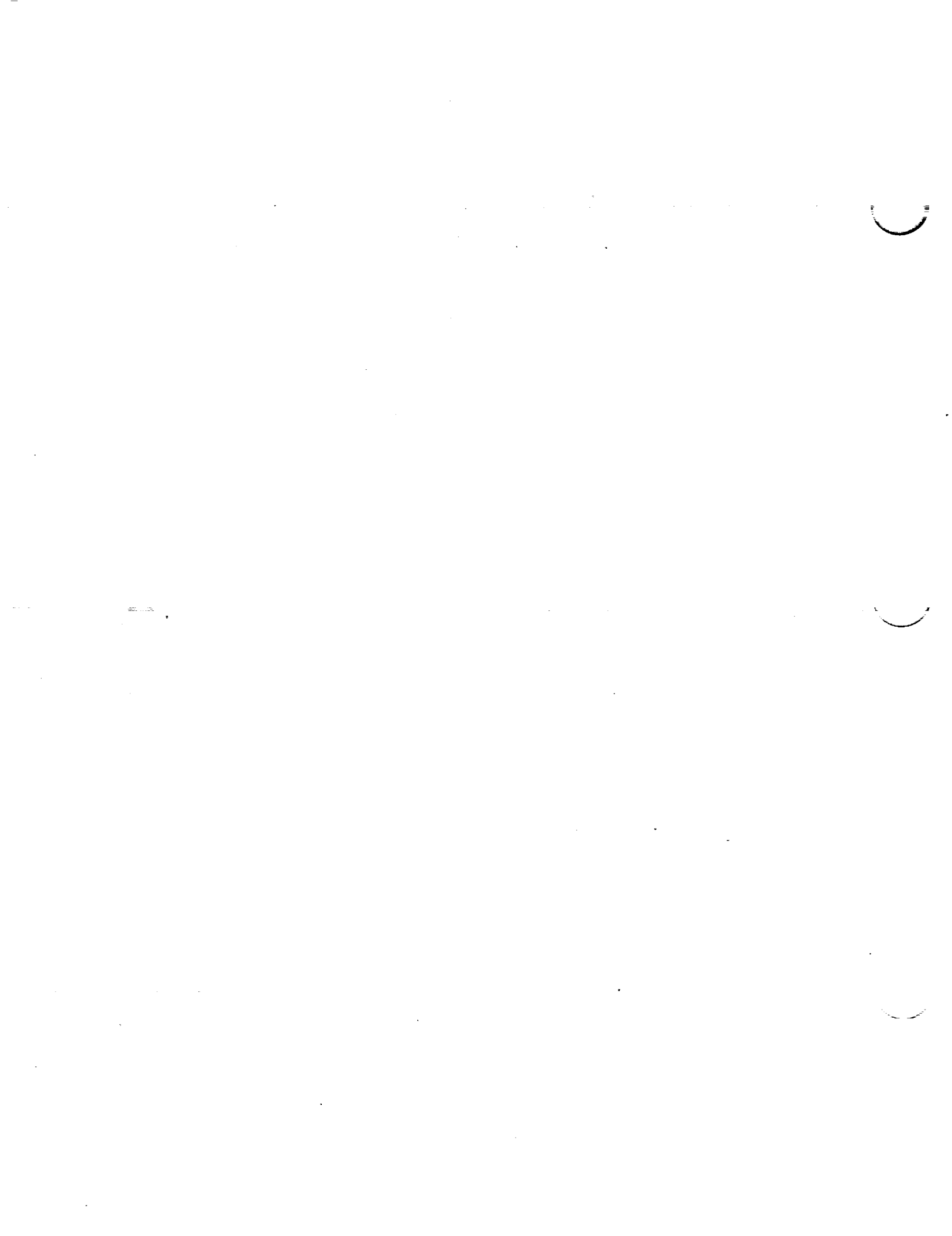


Figure 46.- Comparison of lift and drag characteristics of some thick NACA airfoils with standard roughness on the leading edge; $R_e, 6 \times 10^6$.



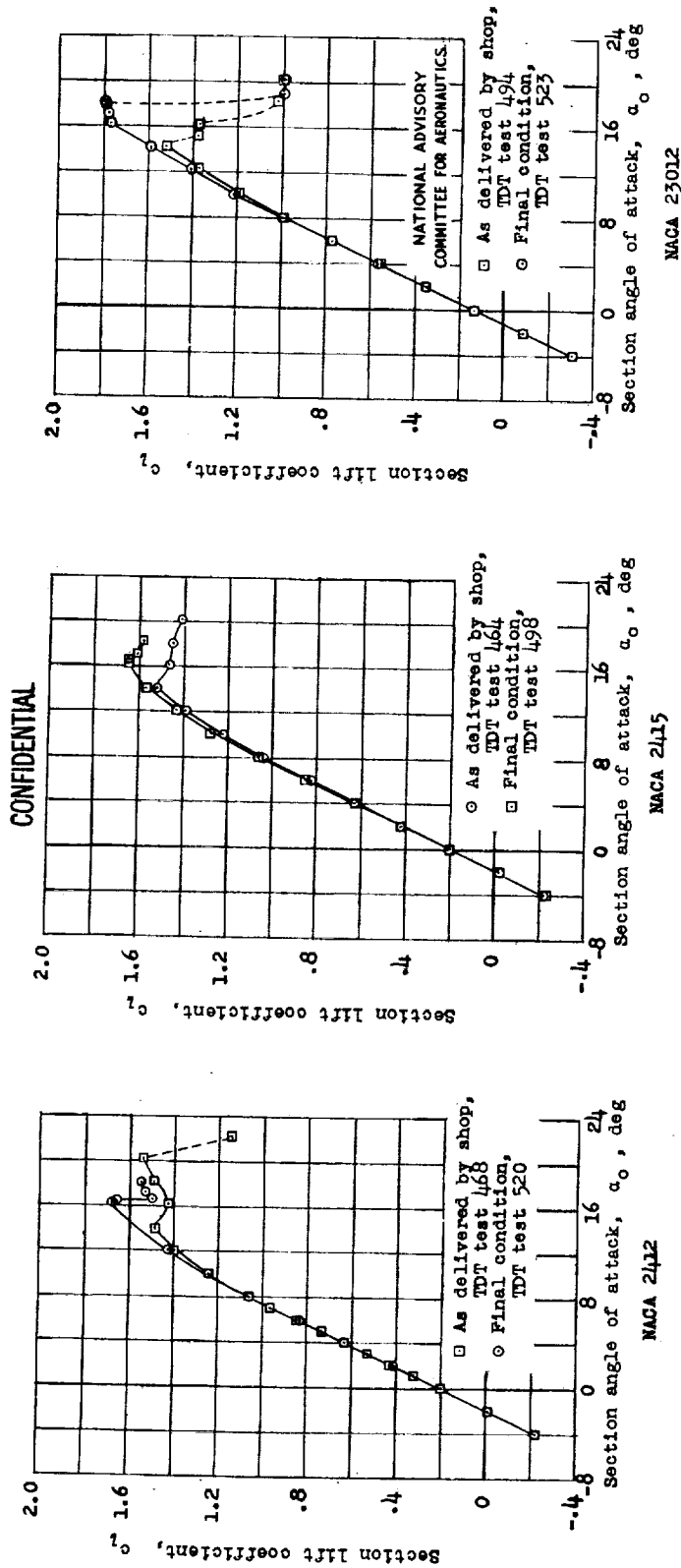
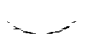


Figure 47.- Lift characteristics of the NACA 23012, 2412, and 2415 airfoil sections as affected by normal model inaccuracies; $R, 9 \times 10^6$ (approx.).



CONFIDENTIAL

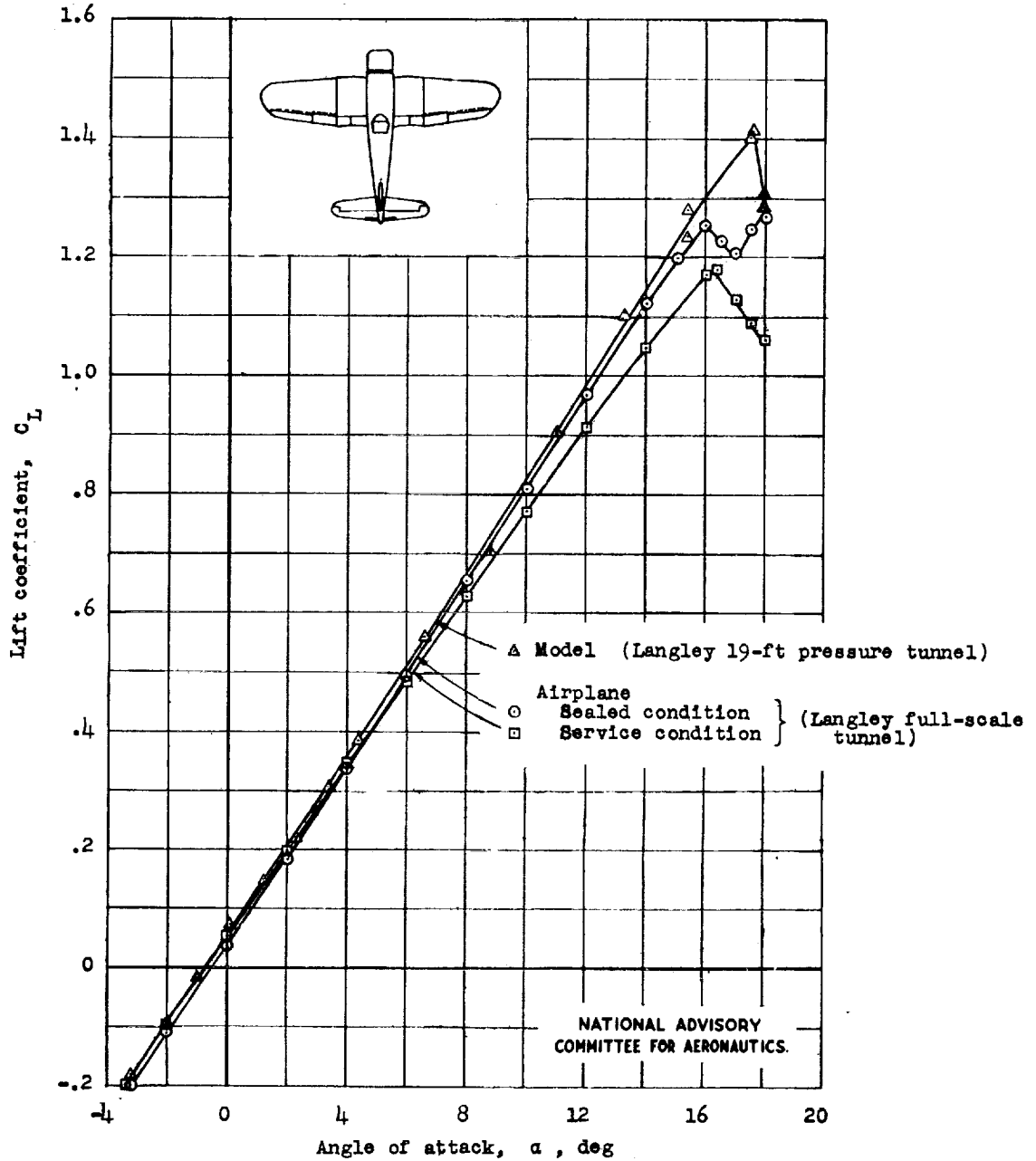


Figure 48.- The effects of surface conditions on the lift characteristics of a fighter-type airplane; $R, 2.8 \times 10^6$.

CONFIDENTIAL



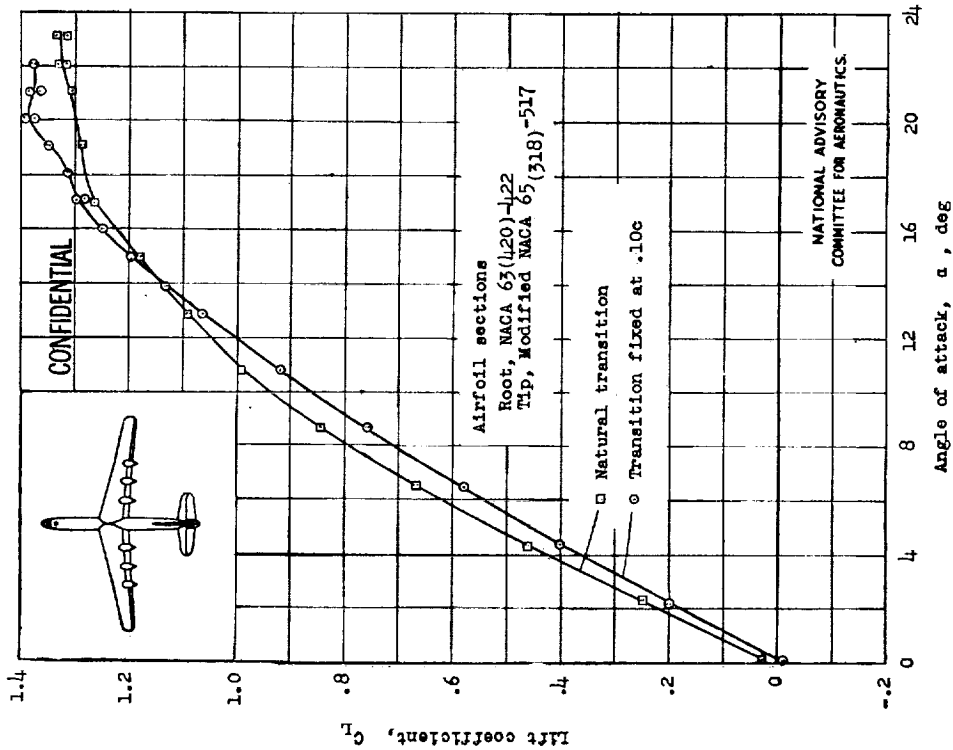


Figure 50.- The effect on the lift characteristics of fixing the transition on a model in the Langley 19-foot pressure tunnel; R , 2.7×10^6 . (Model with NACA airfoil sections.)

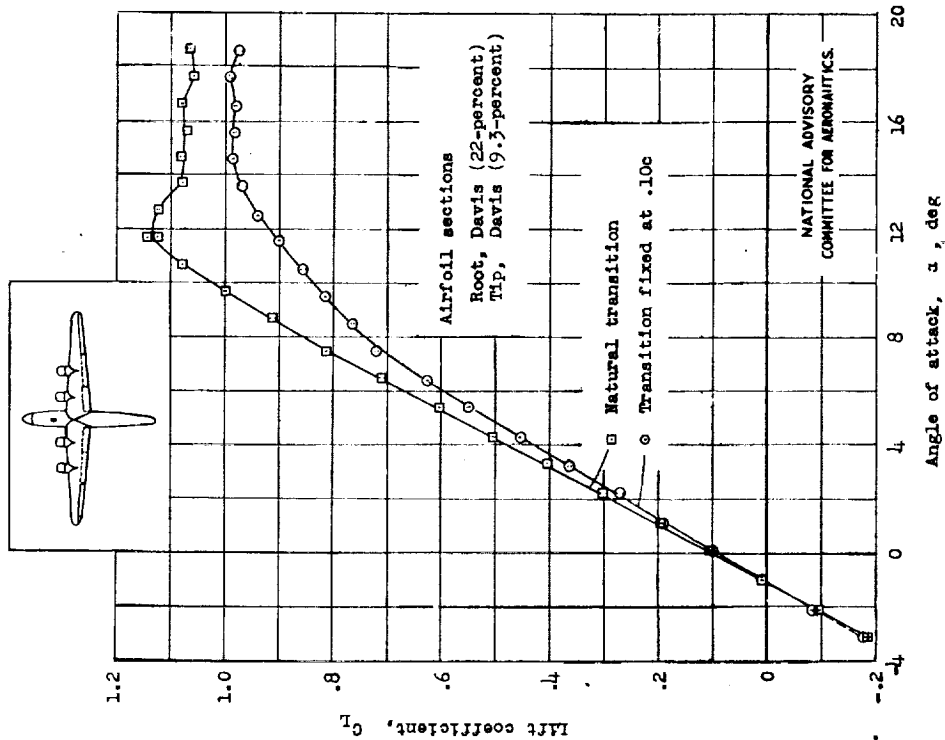


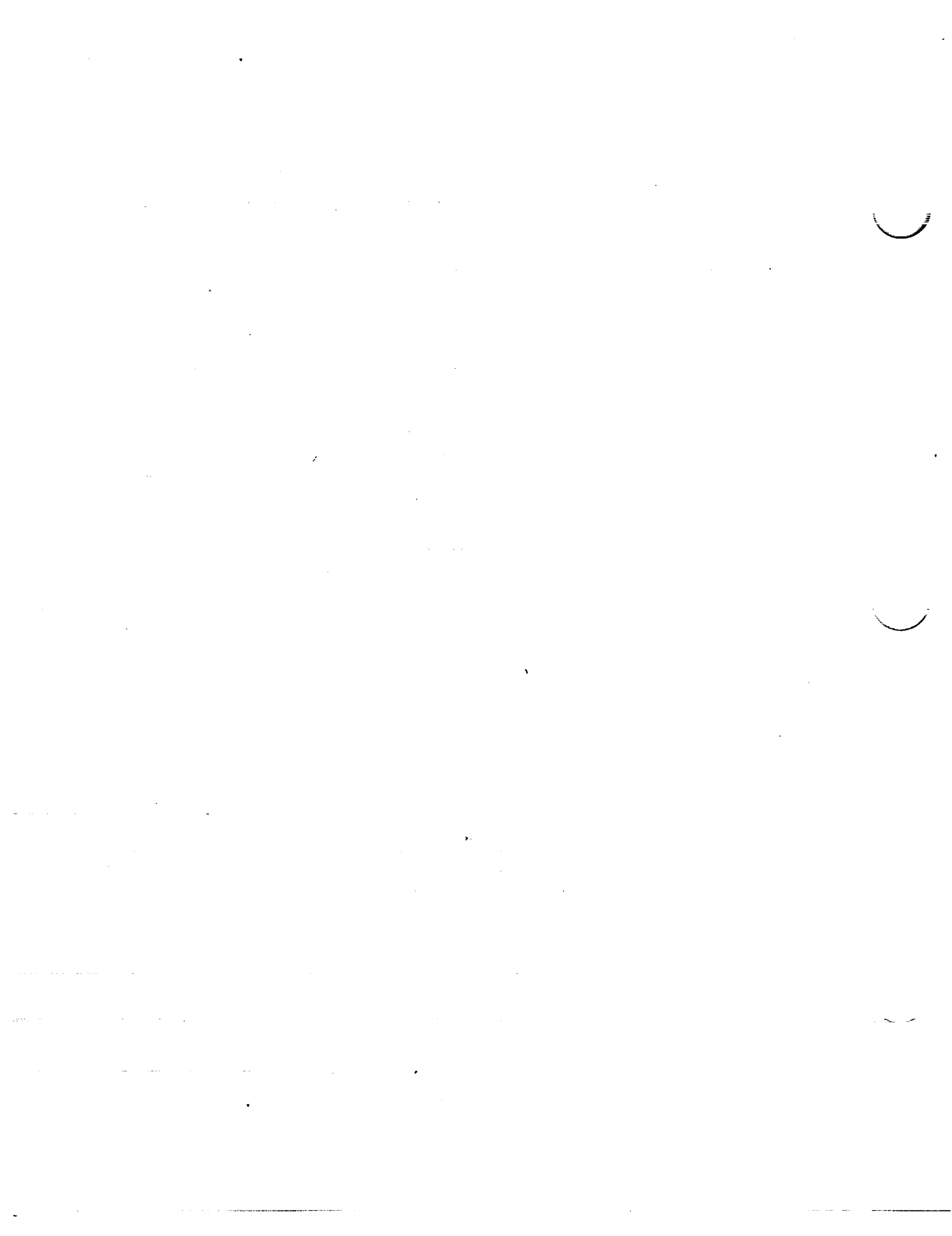
Figure 49.- The effect on the lift characteristics of fixing the transition on a model in the Langley 19-foot pressure tunnel; R , 2.7×10^6 . (Model with Davis airfoil sections.)

CONFIDENTIAL

CONFIDENTIAL

CONFIDENTIAL

CONFIDENTIAL



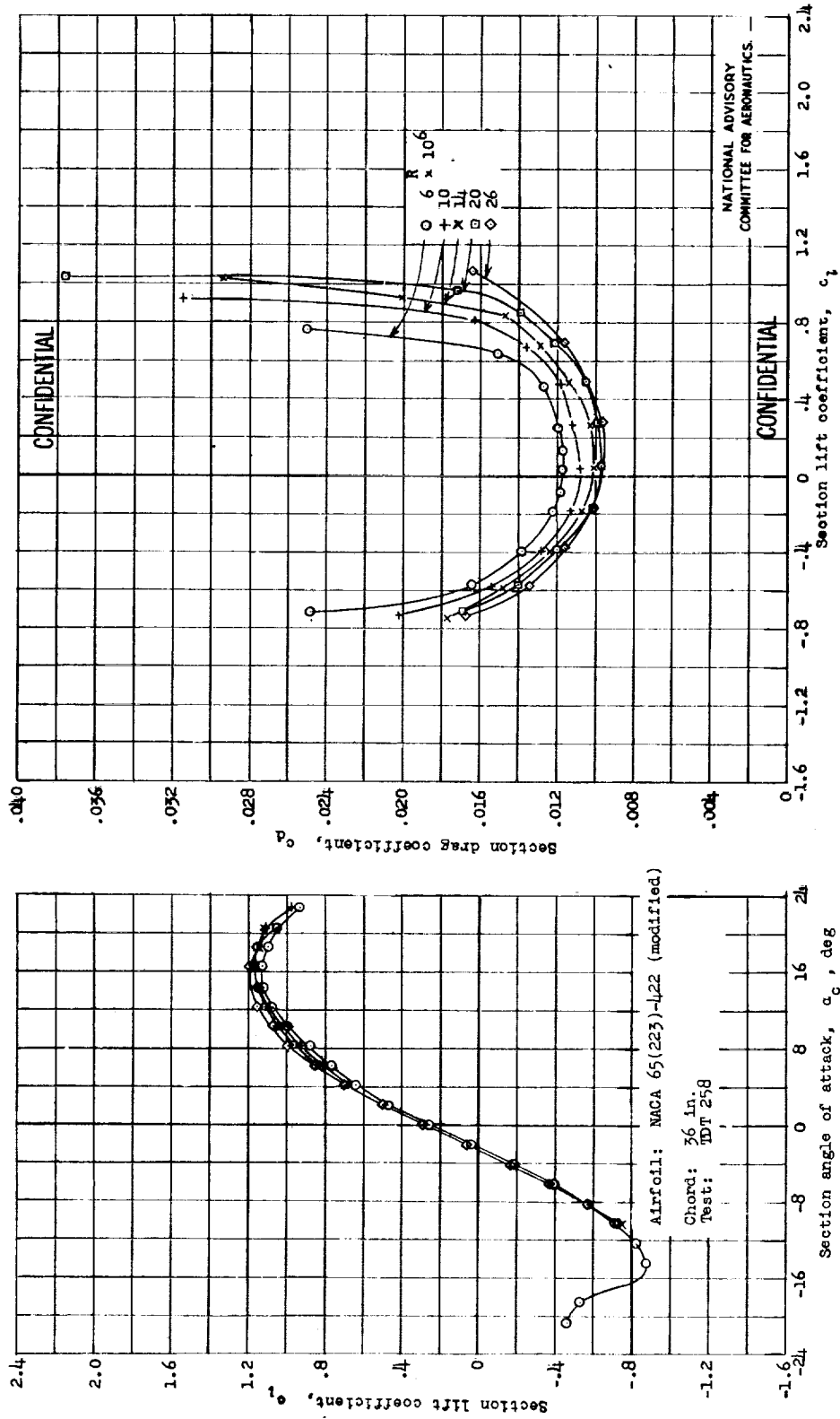
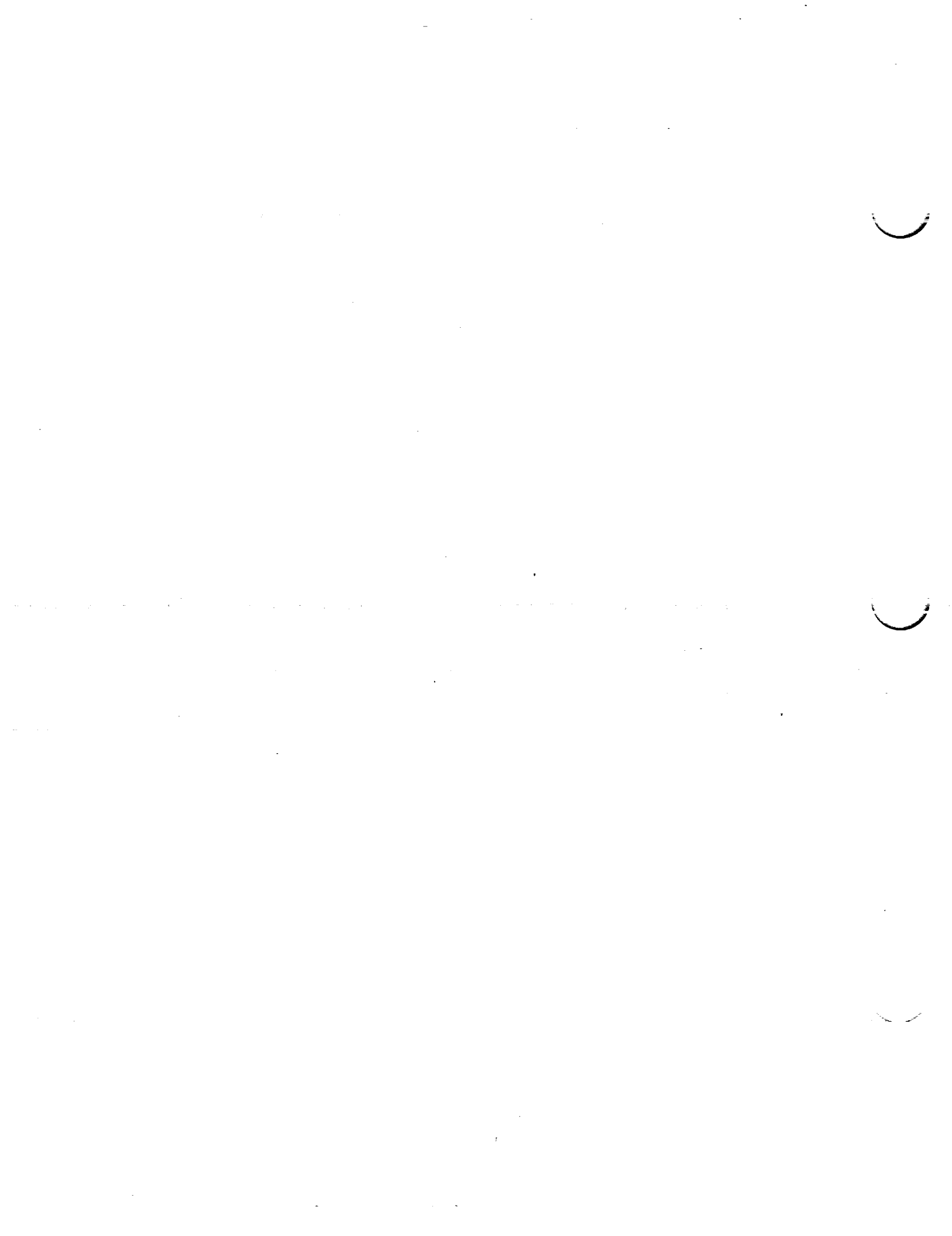


Figure 51.- Lift and drag characteristics of an MACA 65(223)-422 (modified) airfoil with standard roughness applied to the leading edge.



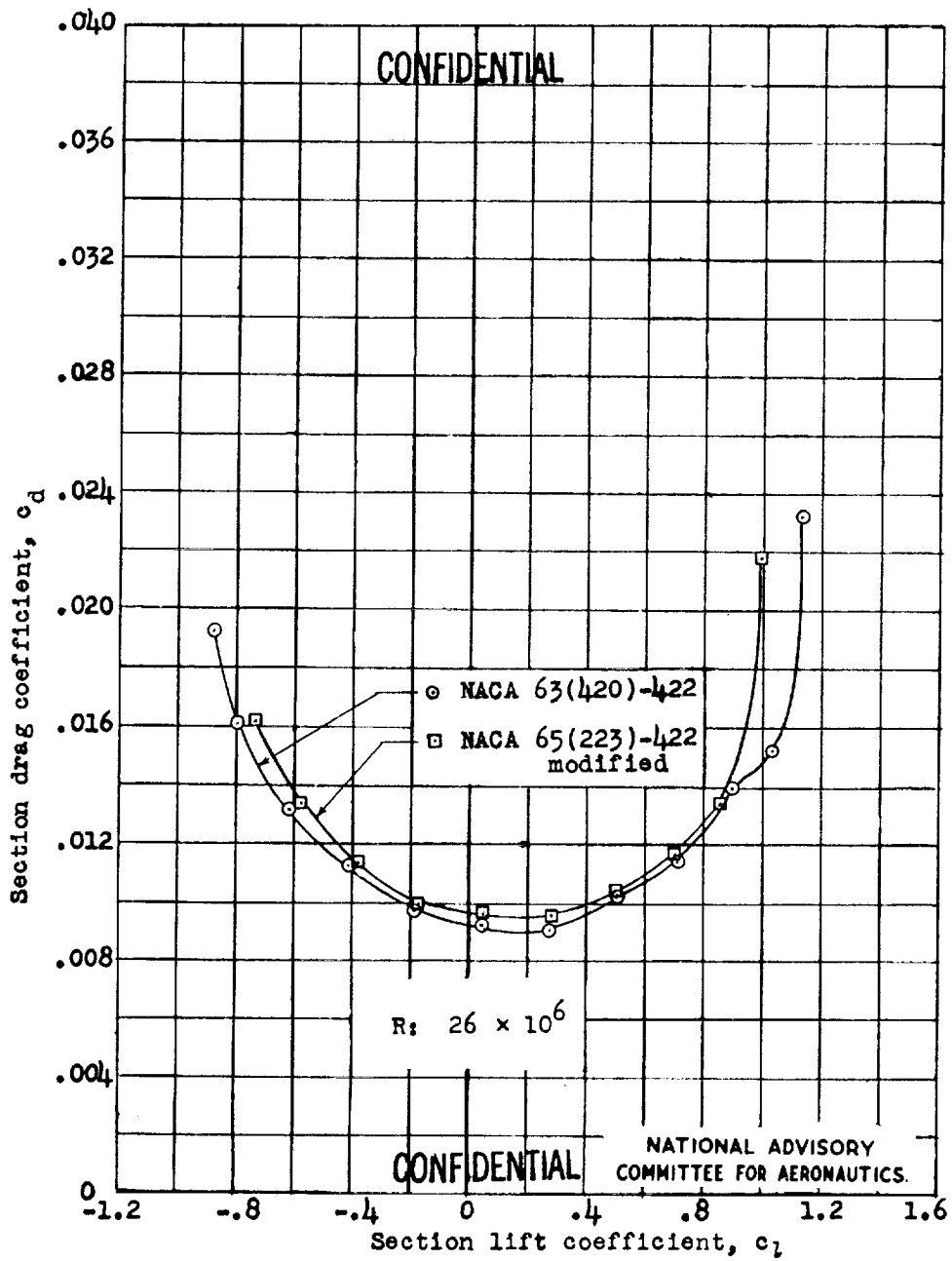


Figure 52.- Drag characteristics of two airfoils with standard roughness on the leading edge.

1. The first part of the document discusses the importance of maintaining accurate records of all transactions.



2. The second part of the document details the various methods used to collect and analyze data.



3. The final part of the document concludes with a summary of the findings and recommendations.



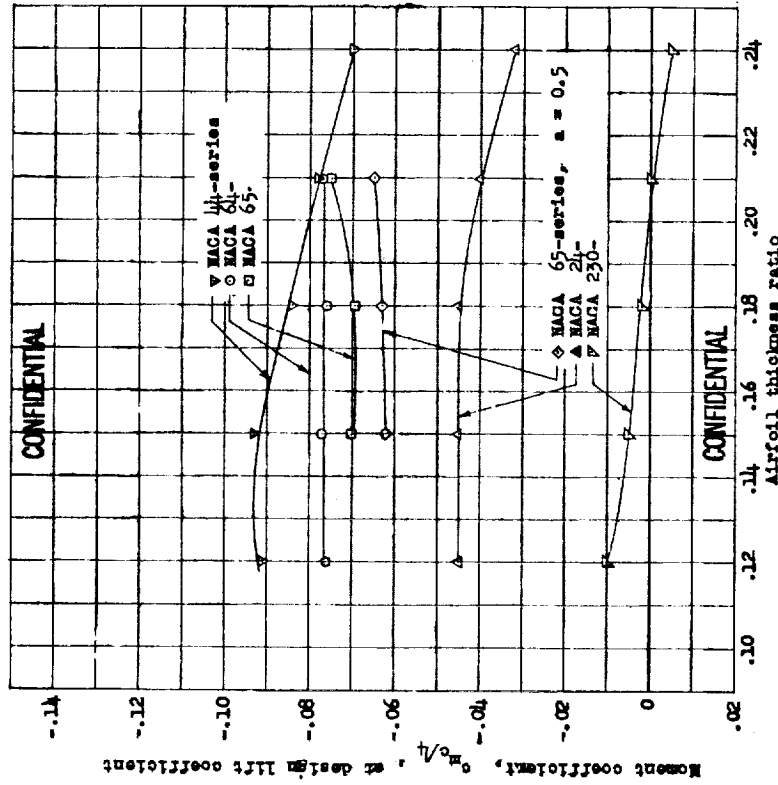


Figure 54.- Variation of pitching-moment coefficient at design lift coefficient with airfoil thickness ratio for some NACA airfoils. NACA 6-series airfoils cambered for a design lift coefficient of $c_{l,1} = 0.4$.

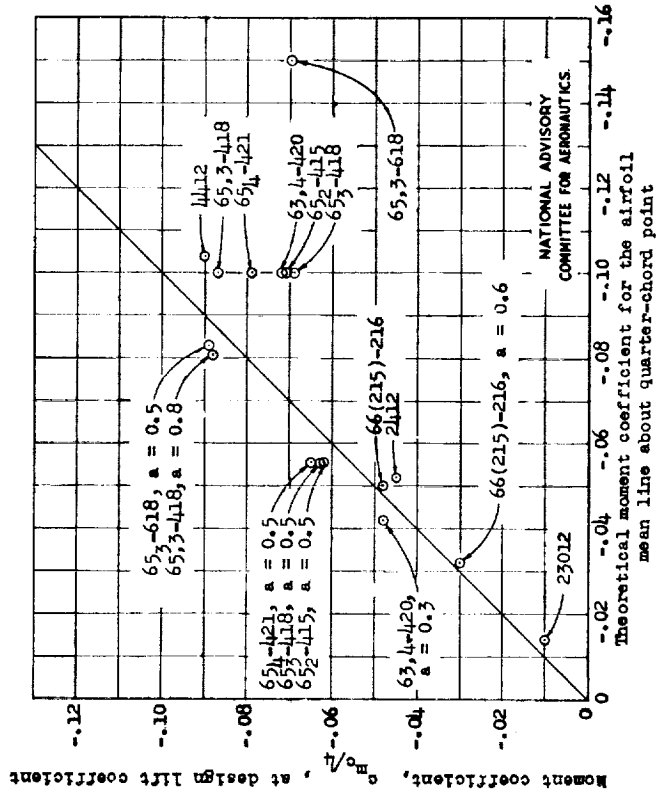
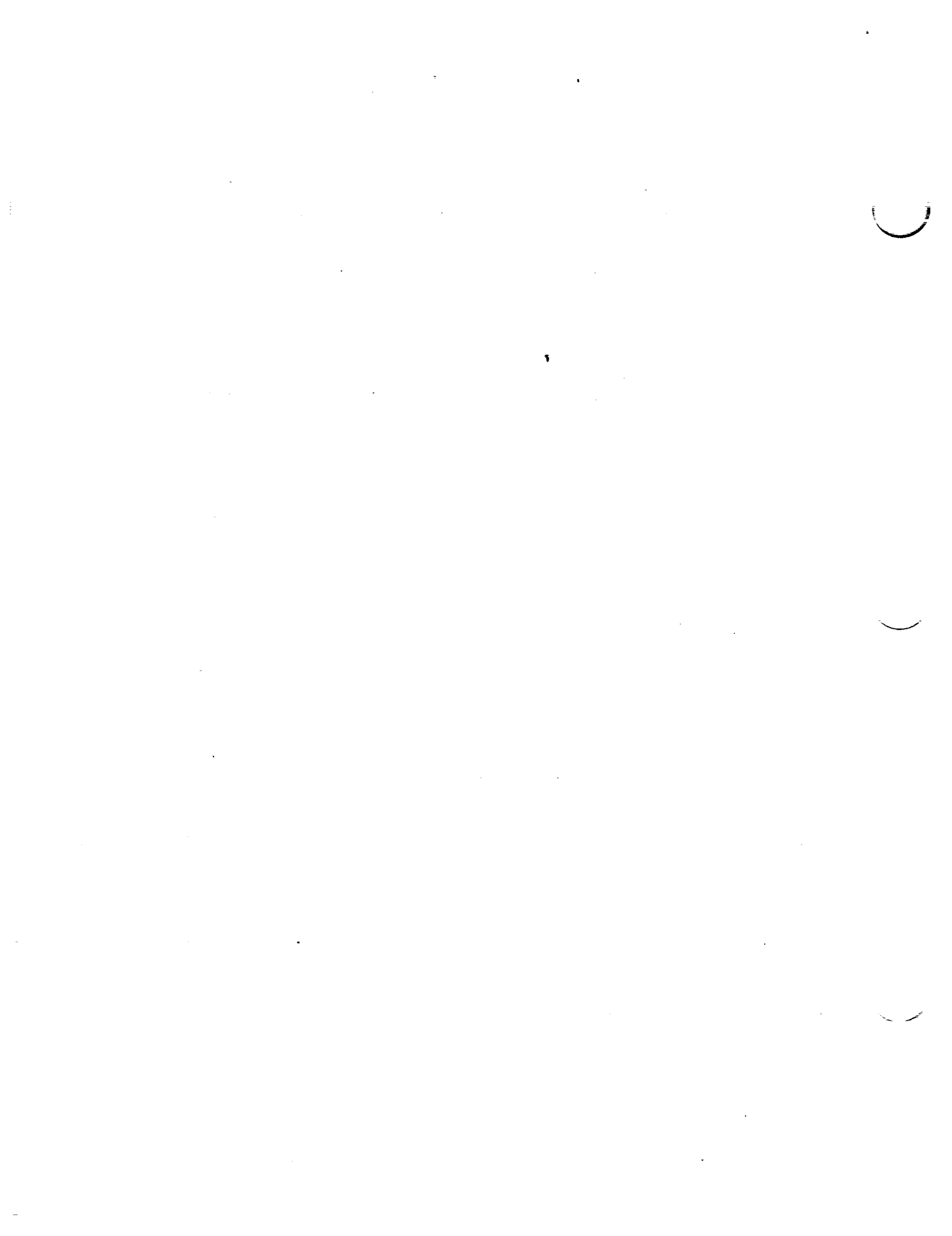


Figure 53.- Comparison of theoretical and measured pitching-moment coefficients for some NACA airfoils.



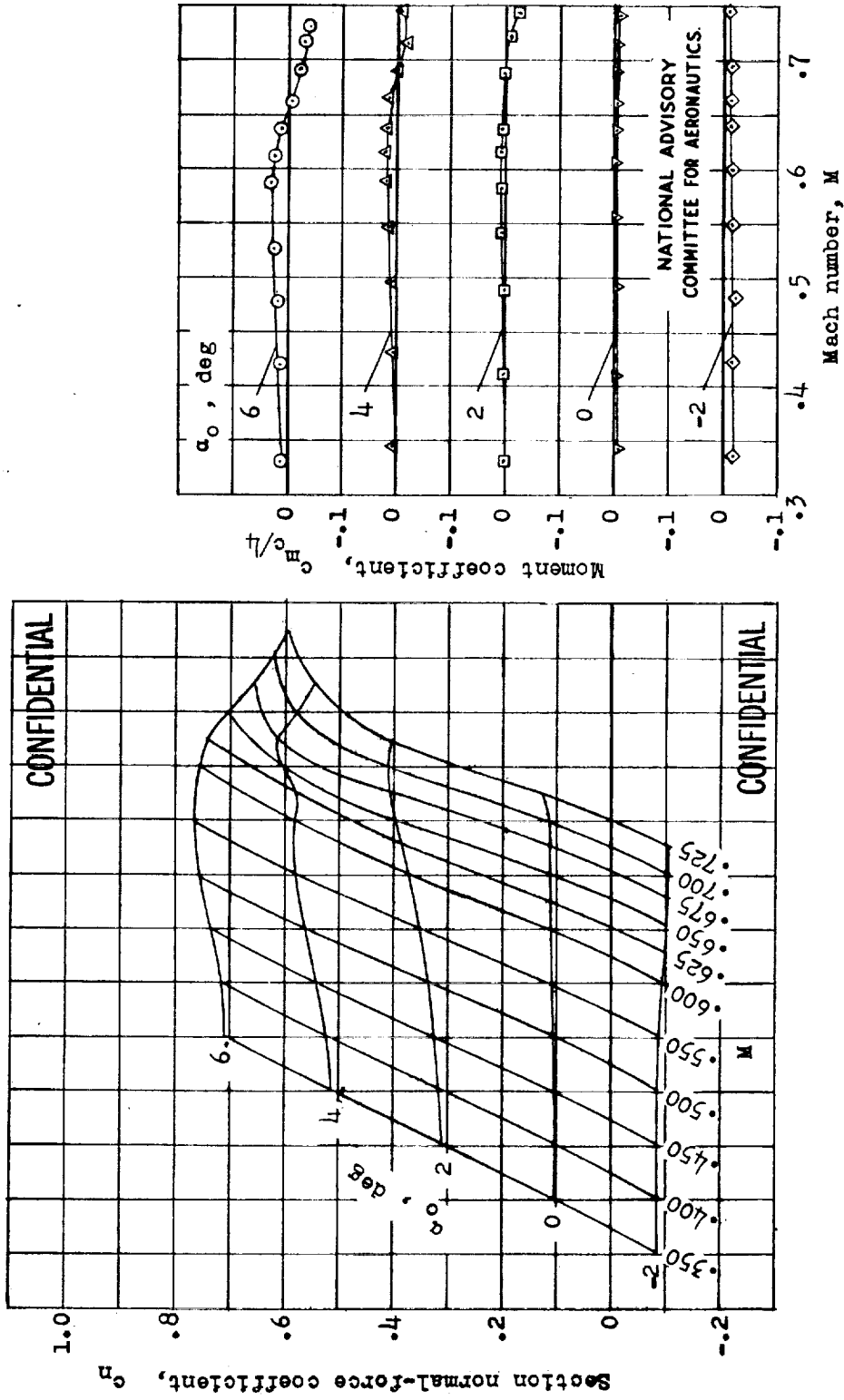
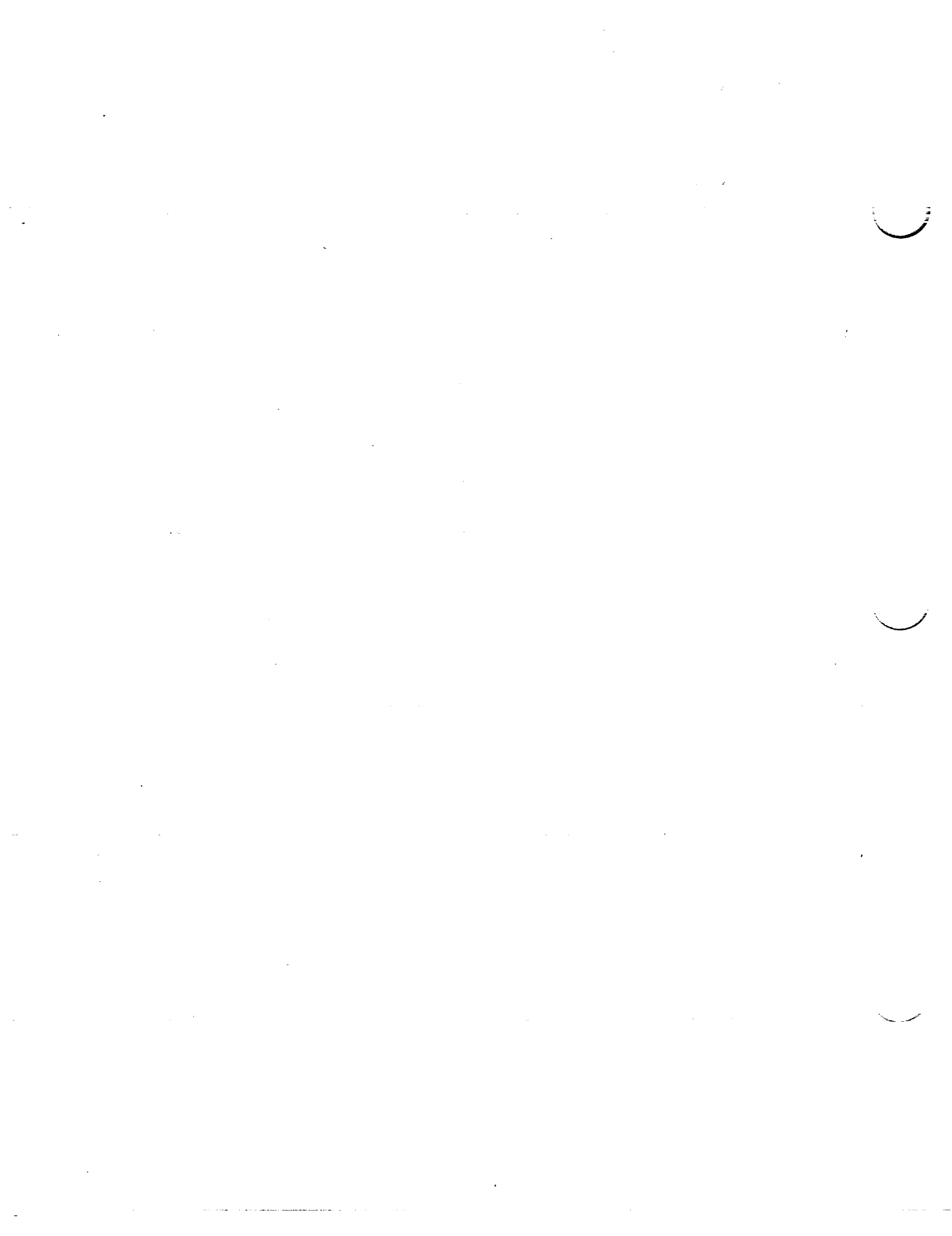
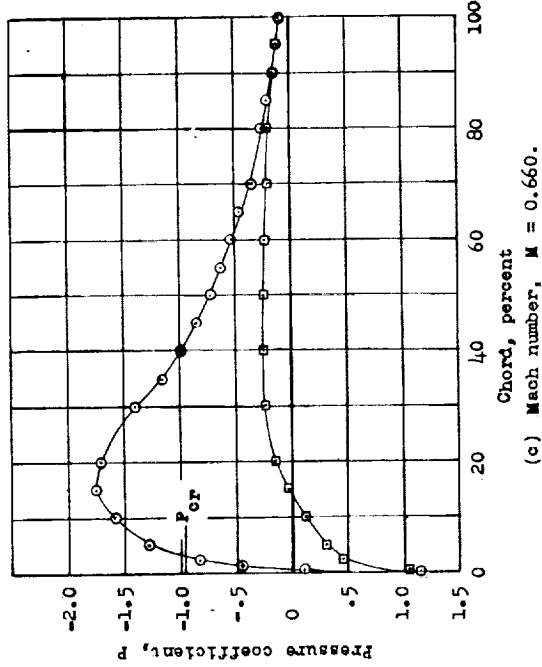


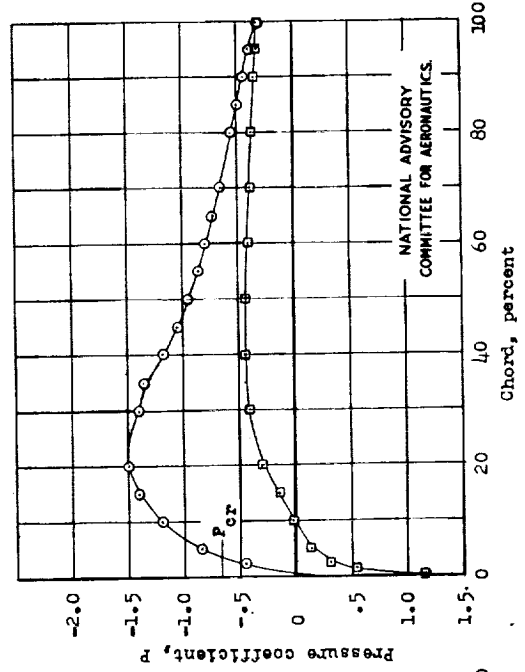
Figure 55.- Variation with Mach number and angle of attack of the section normal-force coefficient and the quarter-chord moment coefficient obtained from the section normal-force distribution for the IACA 23015 airfoil section. Data taken in the Langley rectangular high-speed tunnel.

NATIONAL ADVISORY
COMMITTEE FOR AERONAUTICS.

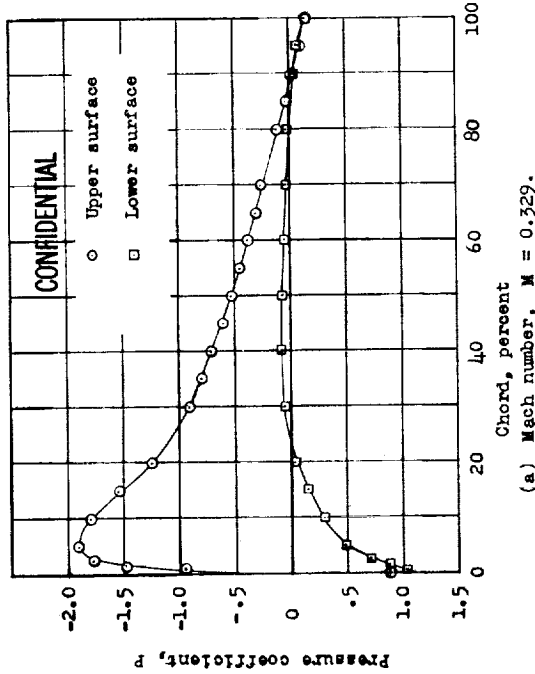




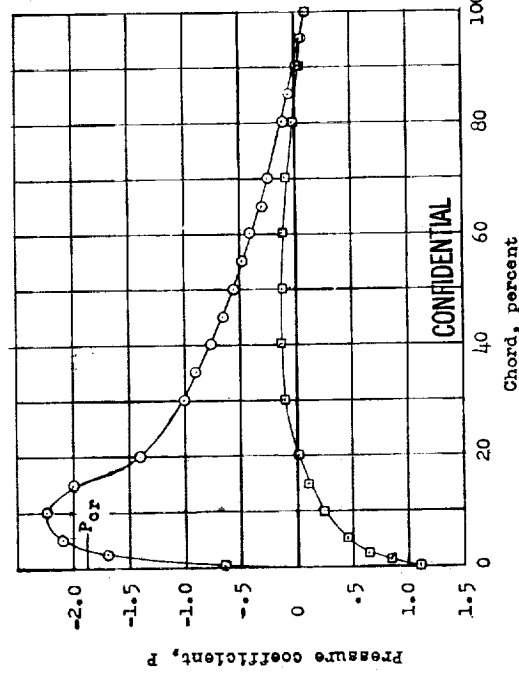
(c) Mach number, $M = 0.660$.



(d) Mach number, $M = 0.730$.



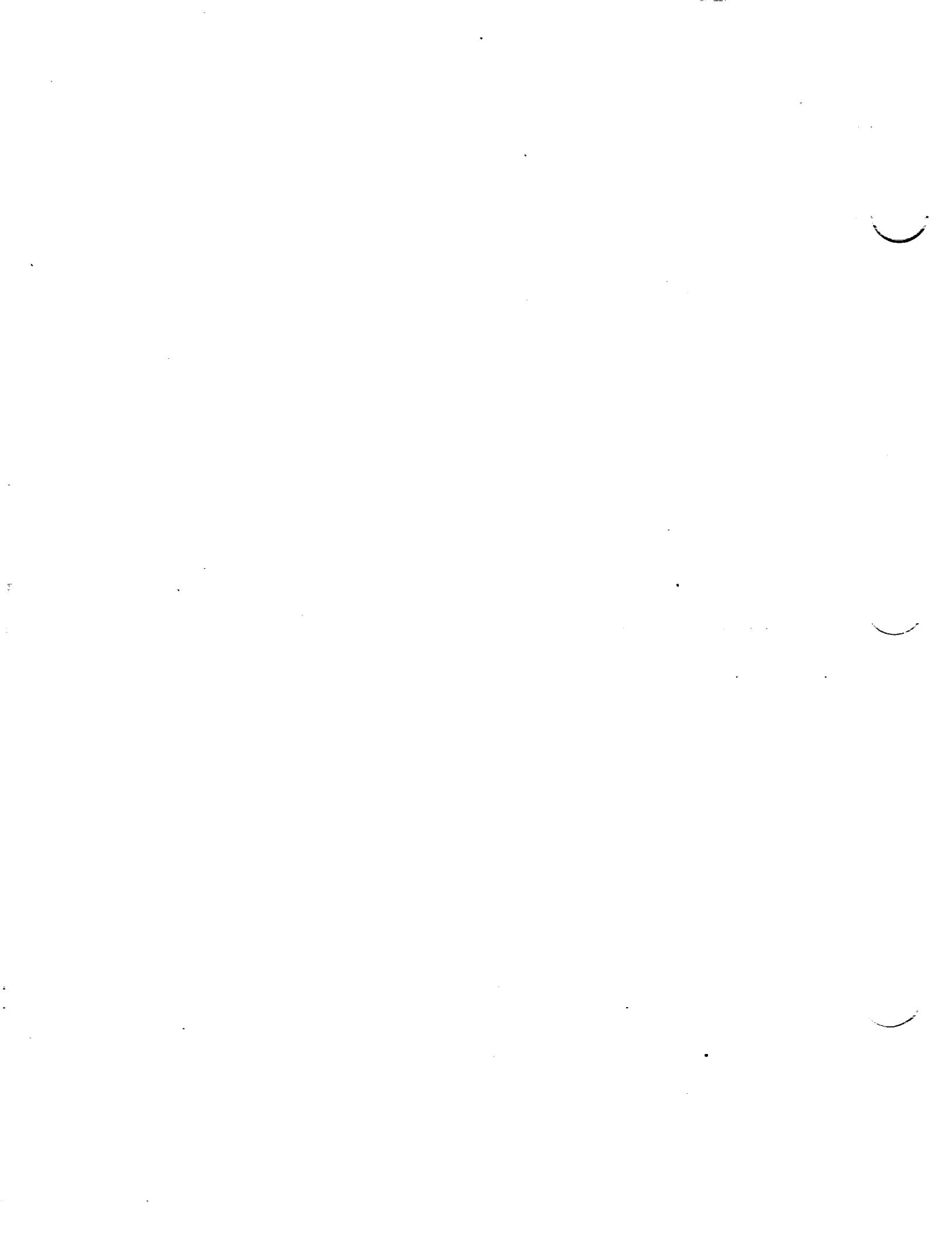
(a) Mach number, $M = 0.529$.



(b) Mach number, $M = 0.525$.

Figure 56.- Pressure distributions for the NACA 23015 airfoil section with constant angle of attack of 6° and varying Mach number. Data taken in the Langley rectangular high-speed tunnel.

NATIONAL ADVISORY
COMMITTEE FOR AERONAUTICS.



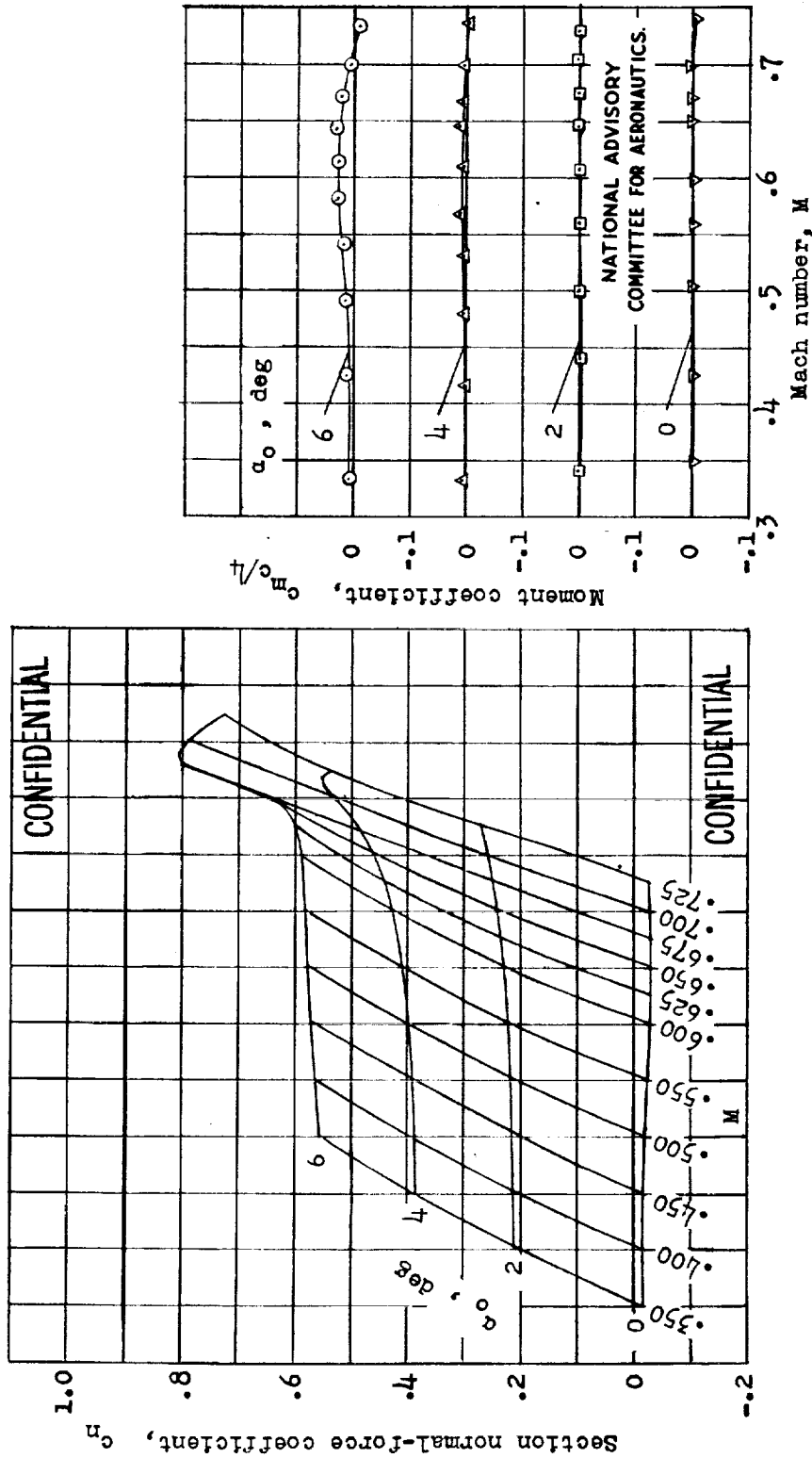
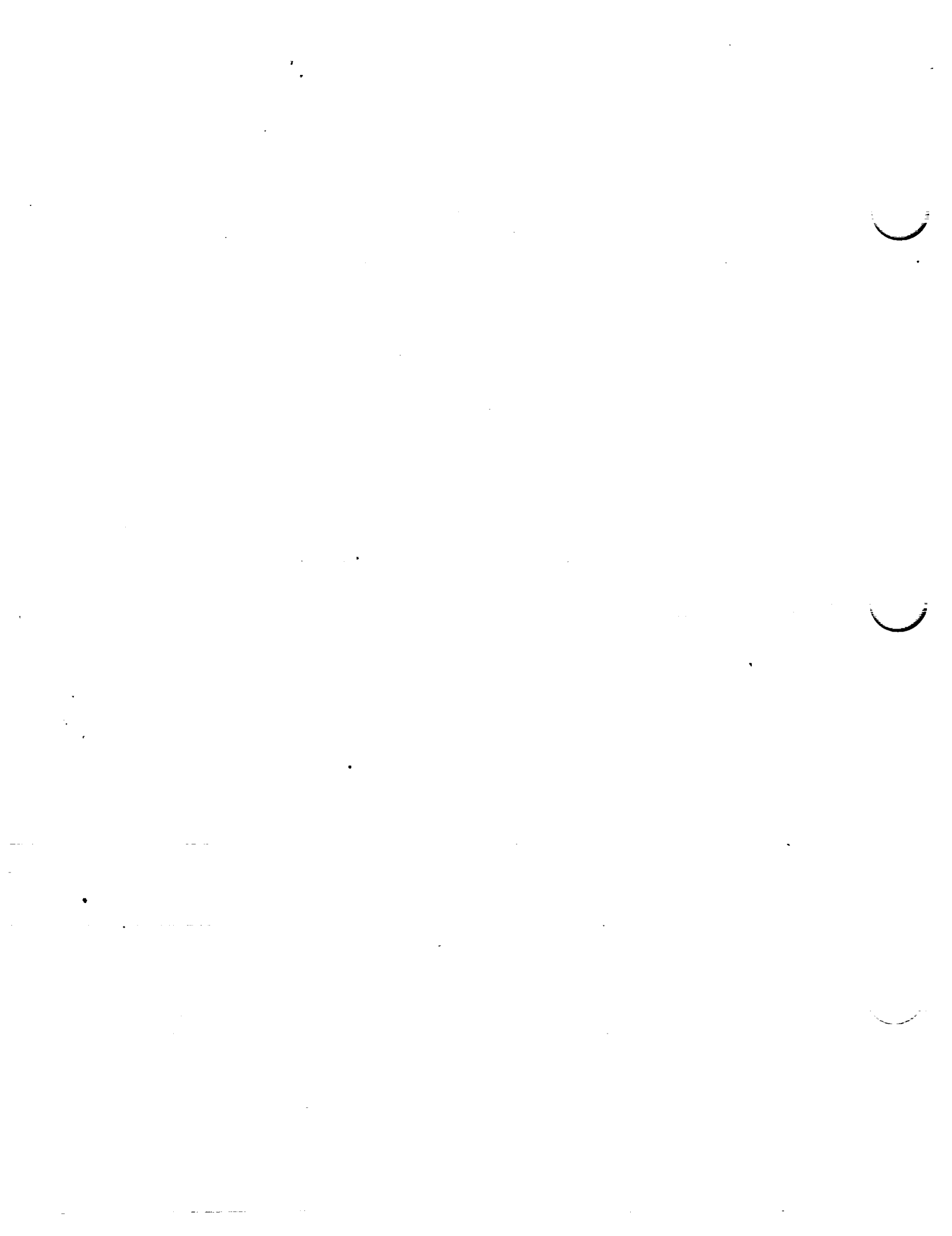


Figure 57.- Variation with Mach number and angle of attack of the section normal-force coefficient and the quarter-chord moment coefficient obtained from the section normal-force distribution for the NACA 66,2-015 airfoil section. Data taken in the Langley rectangular high-speed tunnel.



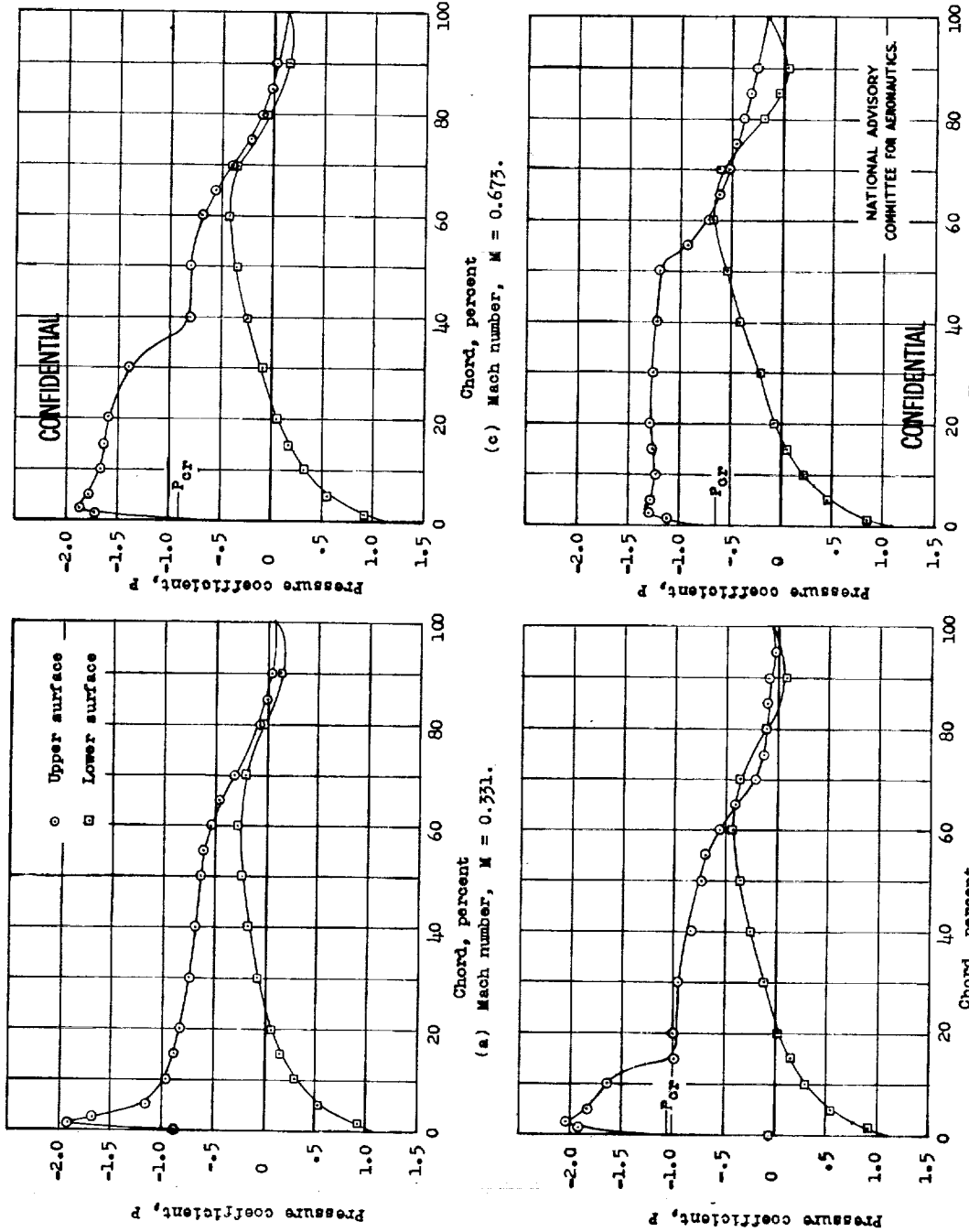


Figure 58.- Pressure distributions for the NACA 66,2-015 airfoil section with constant angle of attack of 6° and varying Mach number. Data taken in the Langley rectangular high-speed tunnel.

CONFIDENTIAL

CONFIDENTIAL

NATIONAL ADVISORY
COMMITTEE FOR AERONAUTICS.



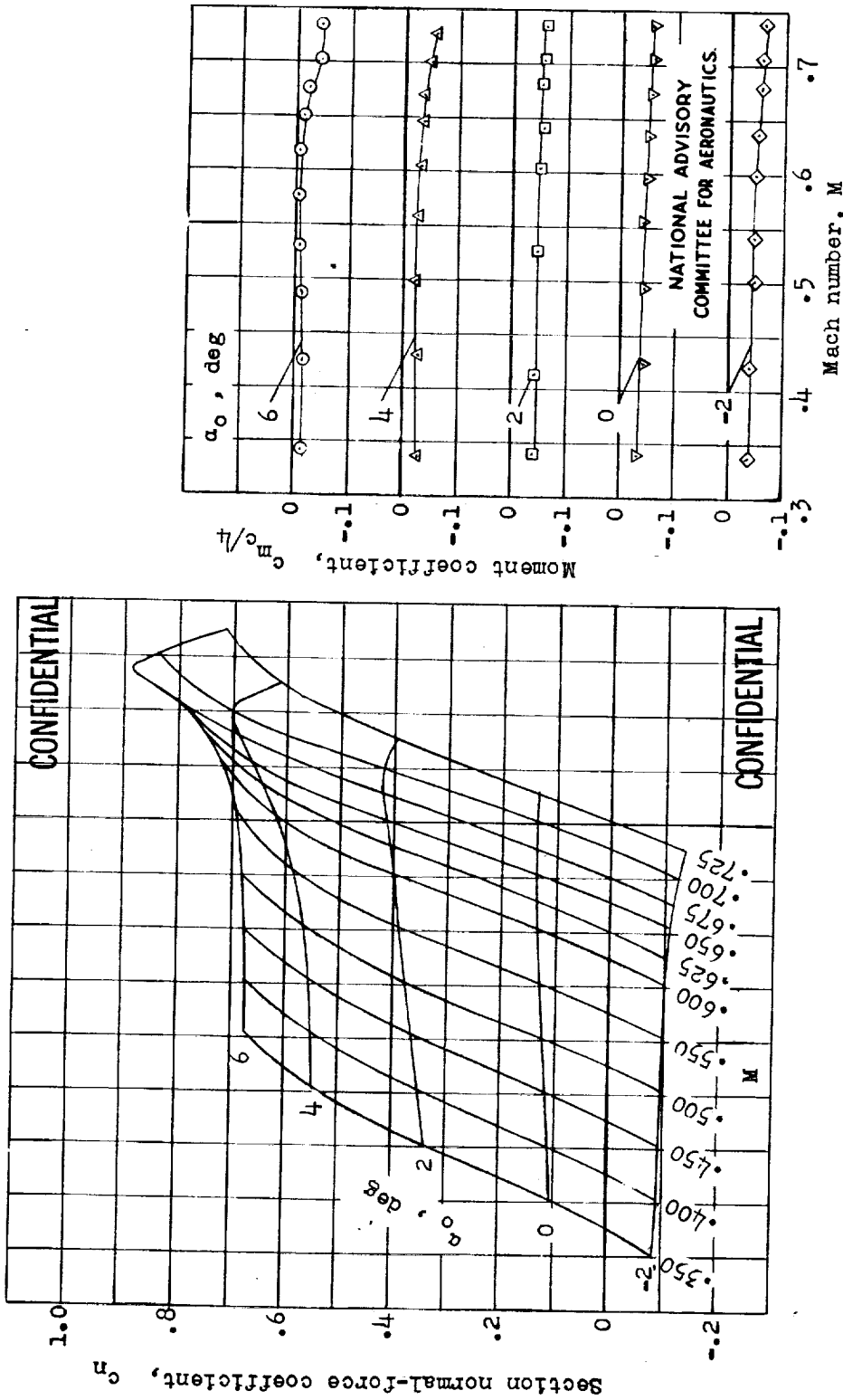
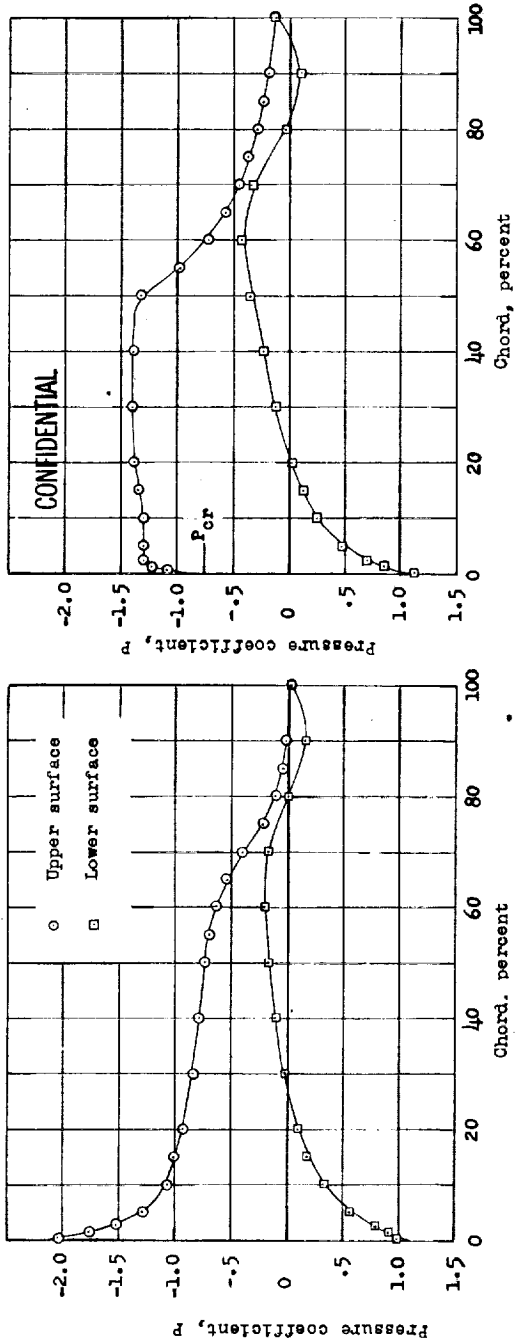
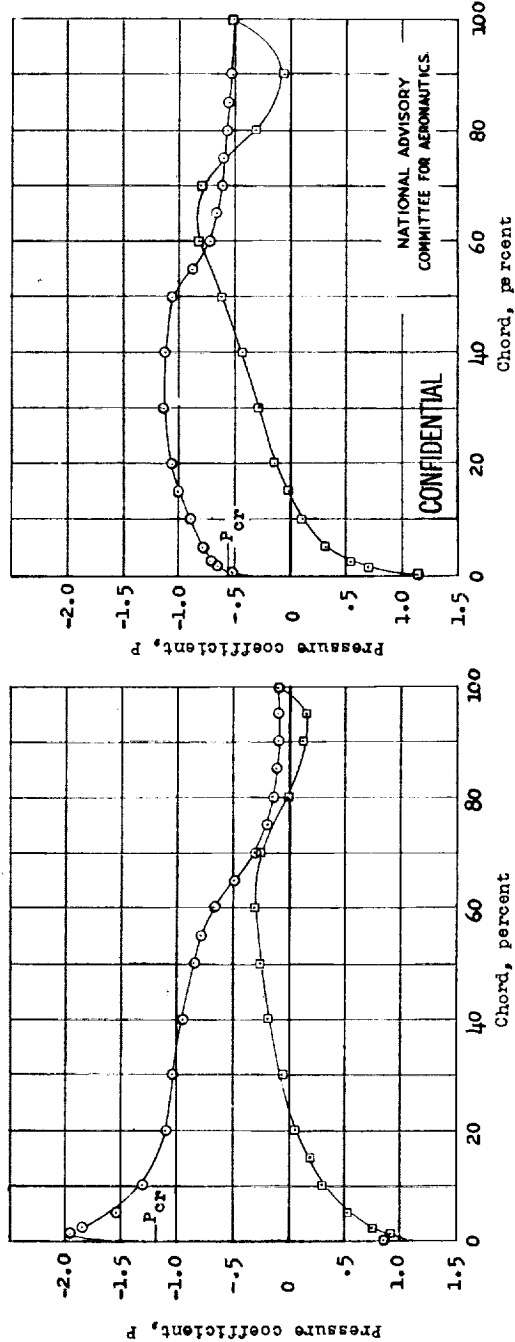


Figure 59.- Variation with Mach number and angle of attack of the section normal-force coefficient and the quarter-chord moment coefficient obtained from the section normal-force distribution for the NACA 66,2-215 airfoil section. Data taken in the Langley rectangular high-speed tunnel.





(c) Mach number, $M = 0.703$.



(d) Mach number, $M = 0.759$.

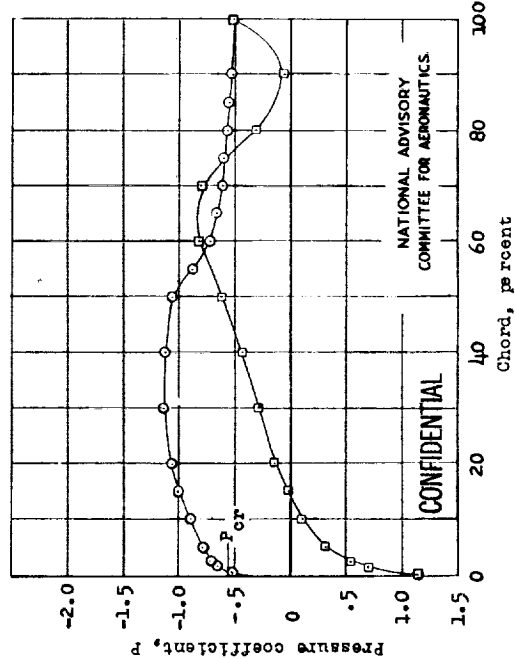
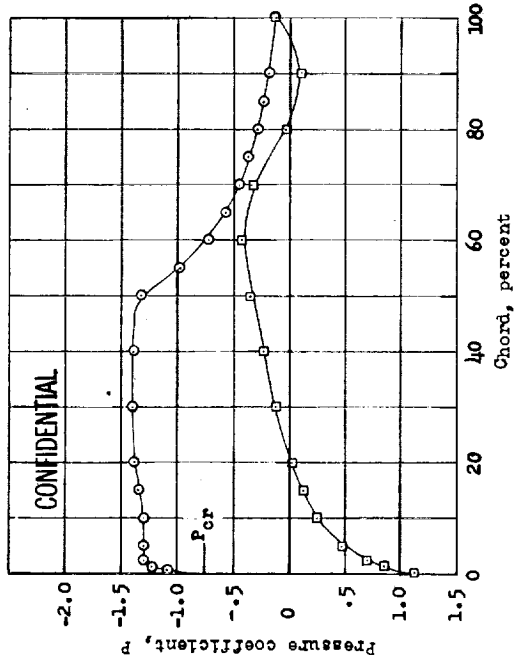
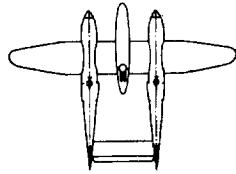


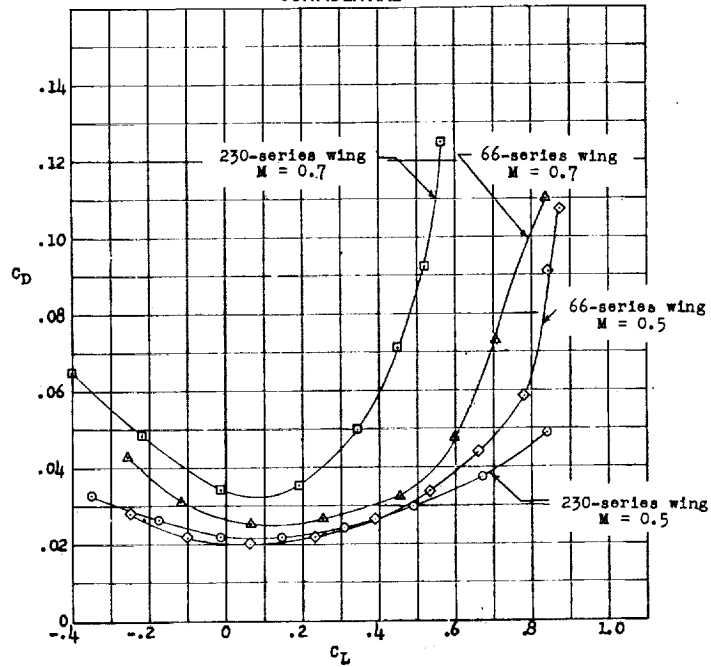
Figure 60.- Pressure distributions for the NACA 66,2-215 airfoil section with constant angle of attack of 6° and varying Mach number. Data taken in the Langley rectangular high-speed tunnel.



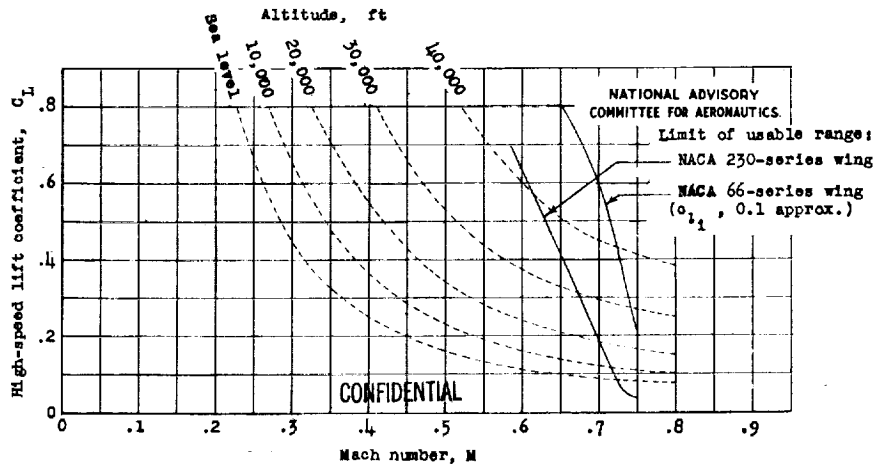


Wing	M
○ NACA 230-series	0.5
◇ NACA 66-	.5
□ NACA 230-	.7
△ NACA 66-	.7

CONFIDENTIAL



(a) Comparison of drag coefficients for complete model equipped with NACA 230-series wing and with NACA 66-series wing. Root thickness ratio of both wings, 0.16.



(b) Limits of usable range of lift coefficients at various Mach numbers and lift coefficients required for level flight at various altitudes with a wing loading of 60.5 pounds per square foot.

Figure 61.- Data obtained in the Ames 16-foot wind tunnel from tests of a complete model of a high-speed fighter-type airplane with two alternate wings.



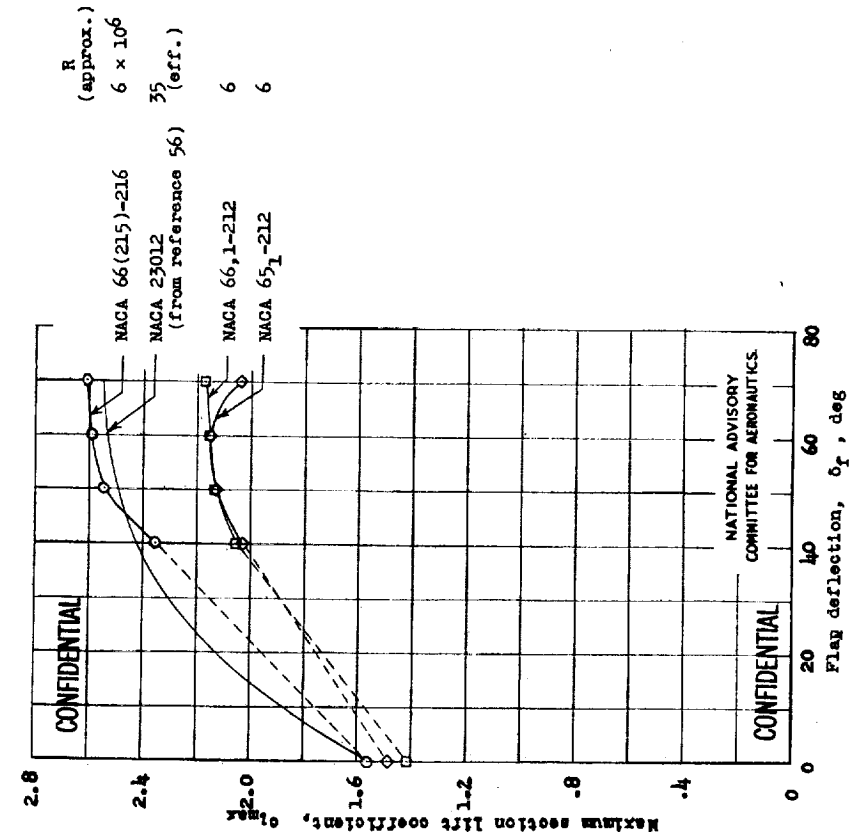


Figure 63.- Maximum lift coefficients for some NACA airfoils fitted with 0.20-airfoil-chord split flaps.

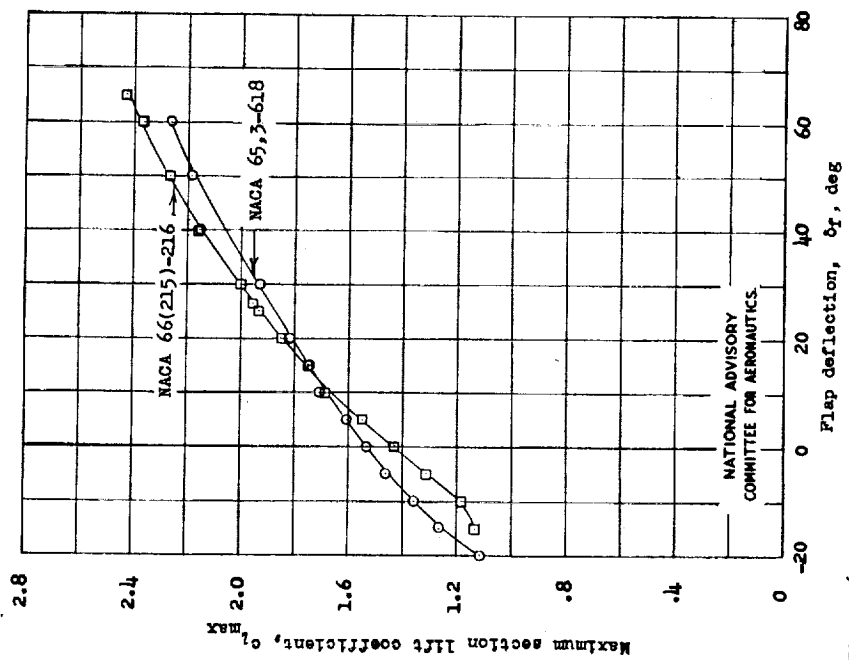
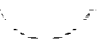
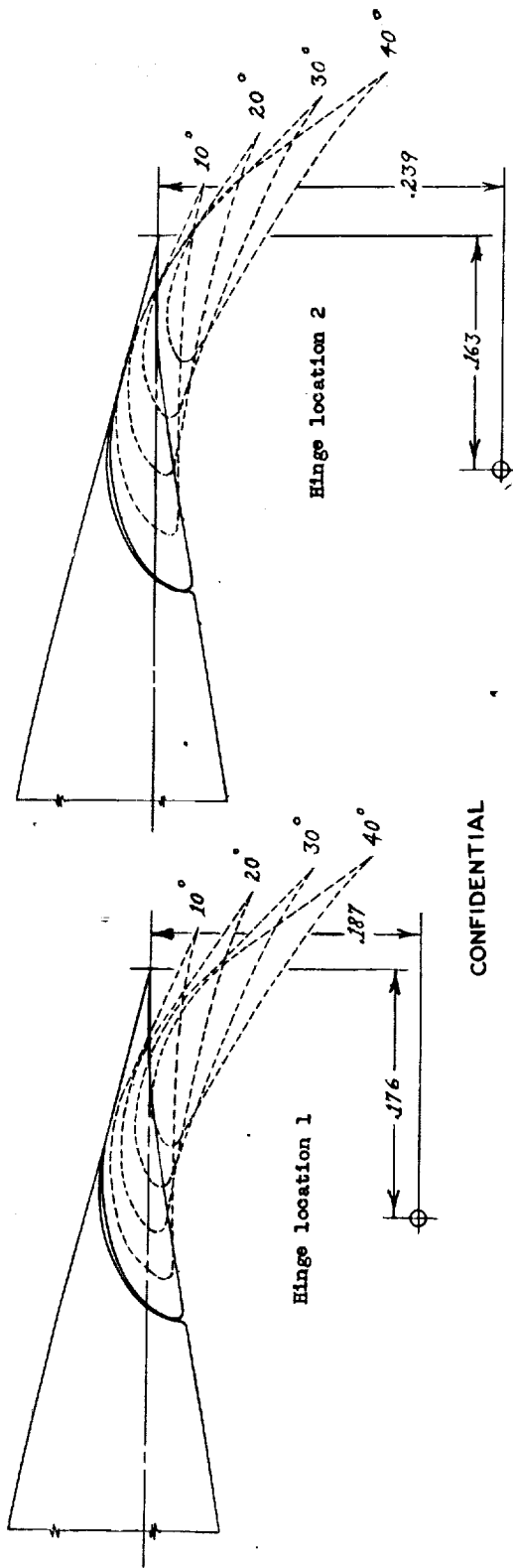
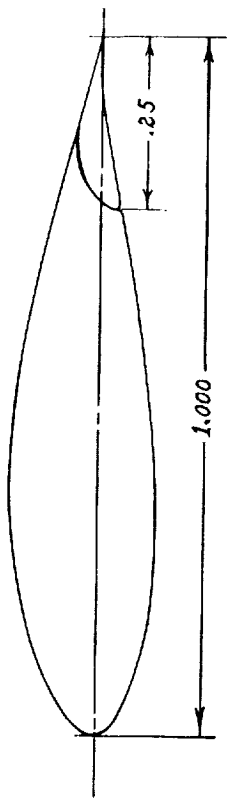


Figure 62.- Maximum lift coefficients for the NACA 65,3-618 and NACA 66(215)-216 airfoils fitted with 0.20-airfoil-chord plain flaps; R, 6×10^6 .



CONFIDENTIAL

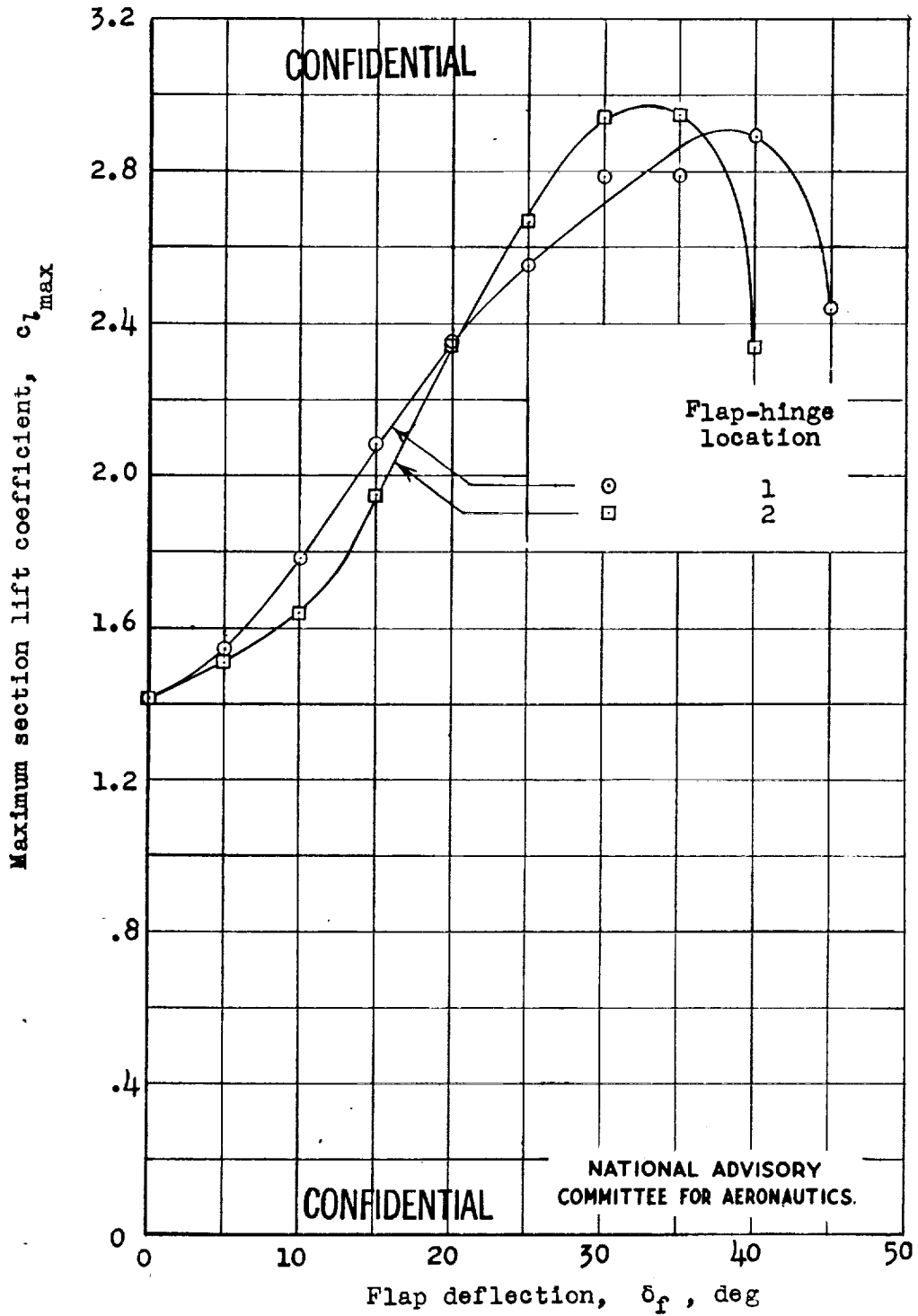


CONFIDENTIAL

(a) Flap configuration.
Figure 64.- Flap configuration and maximum lift coefficients for the NACA 63,4-420 airfoil with a 0.25-airfoil-chord hinged slotted flap; $R, 6 \times 10^6$.

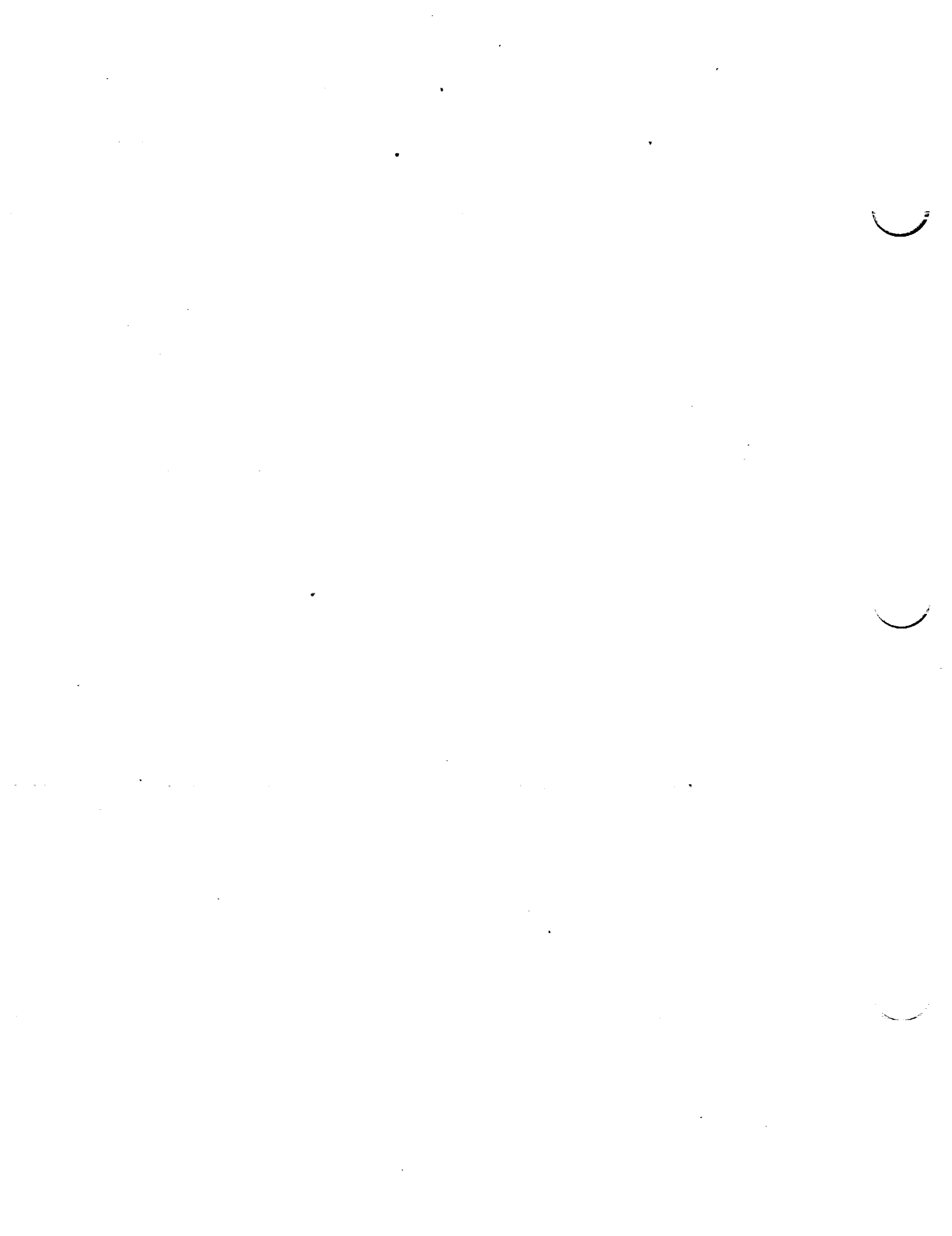
NATIONAL ADVISORY
COMMITTEE FOR AERONAUTICS

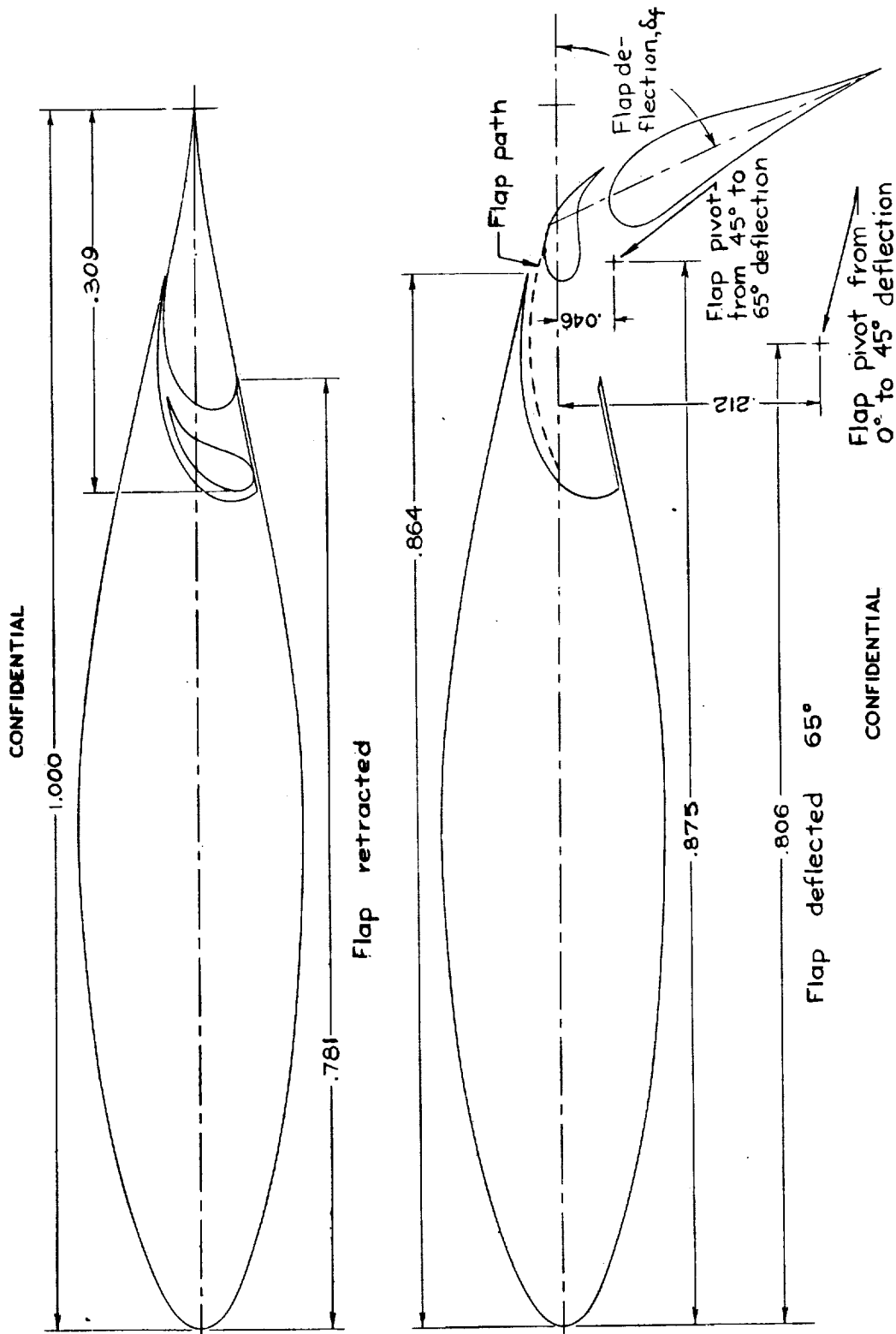




(b) Maximum lift characteristics.

Figure 64.- Concluded.





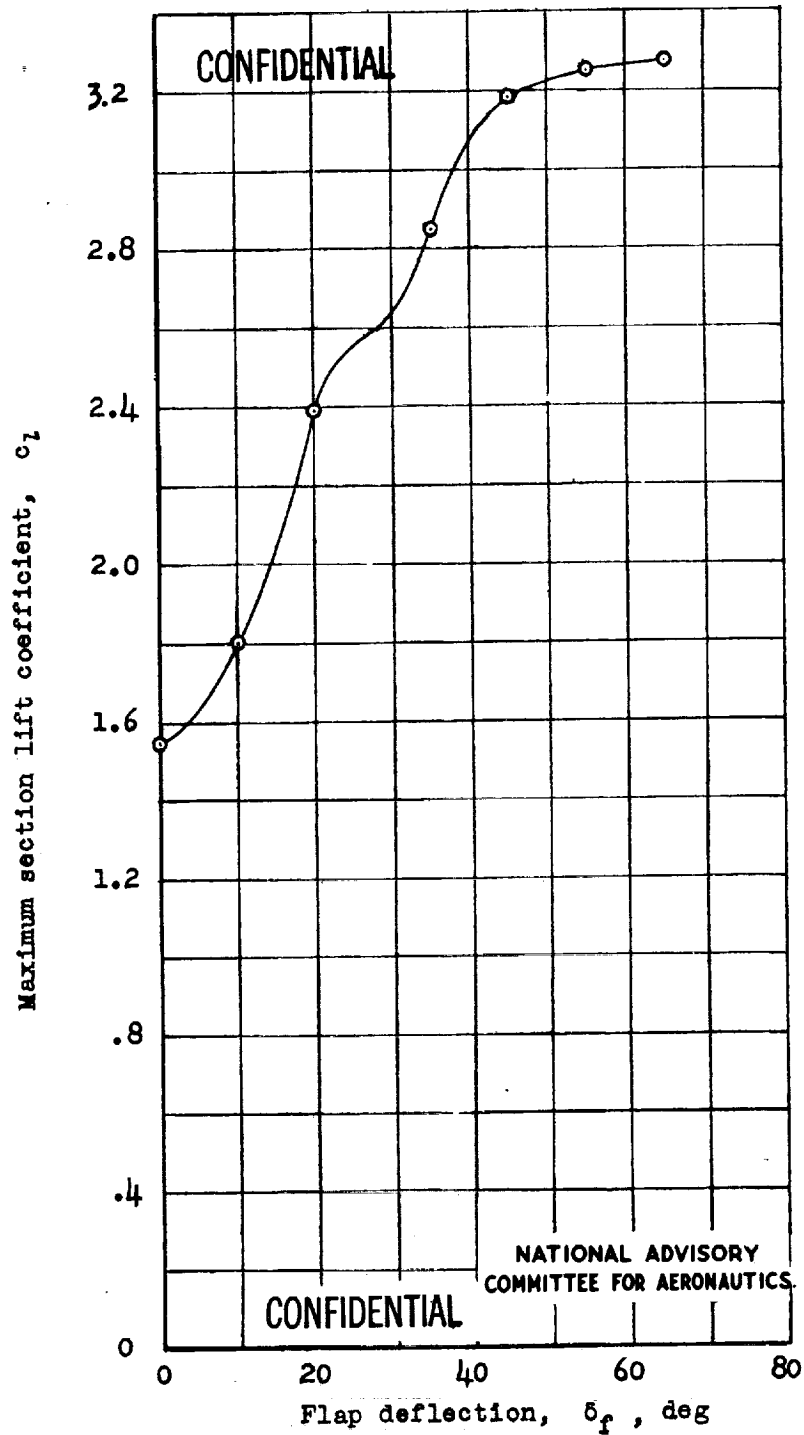
NATIONAL ADVISORY
COMMITTEE FOR AERONAUTICS.

(a) Flap configuration.
Figure 65.- Flap configuration and maximum lift coefficients for the NACA 65₃-118 airfoil with a double slotted flap; $R, 6 \times 10^6$.

CONFIDENTIAL

CONFIDENTIAL





(b) Maximum lift characteristics.

Figure 65.- Concluded.



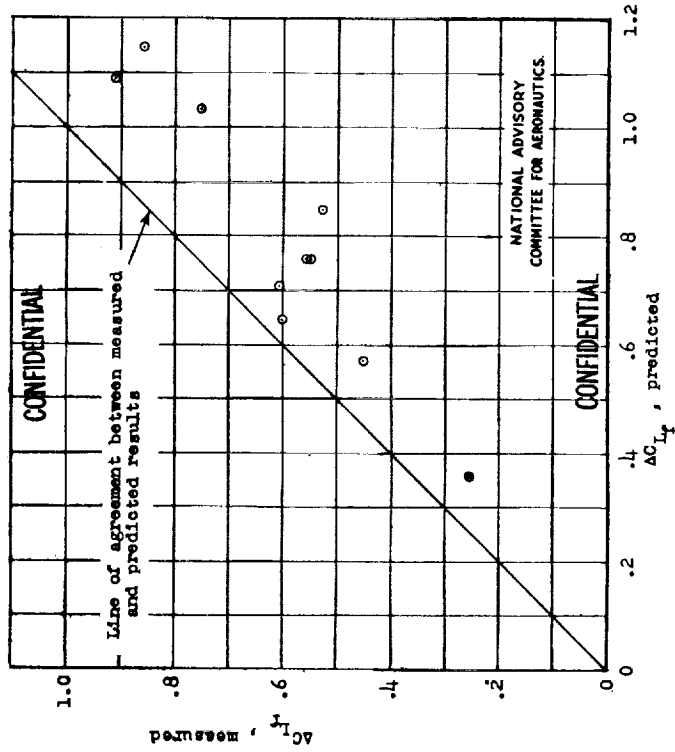


Figure 67.- Comparison between measured values of the increments in lift coefficients due to flap deflection and values predicted from two-dimensional data. Slotted flap.

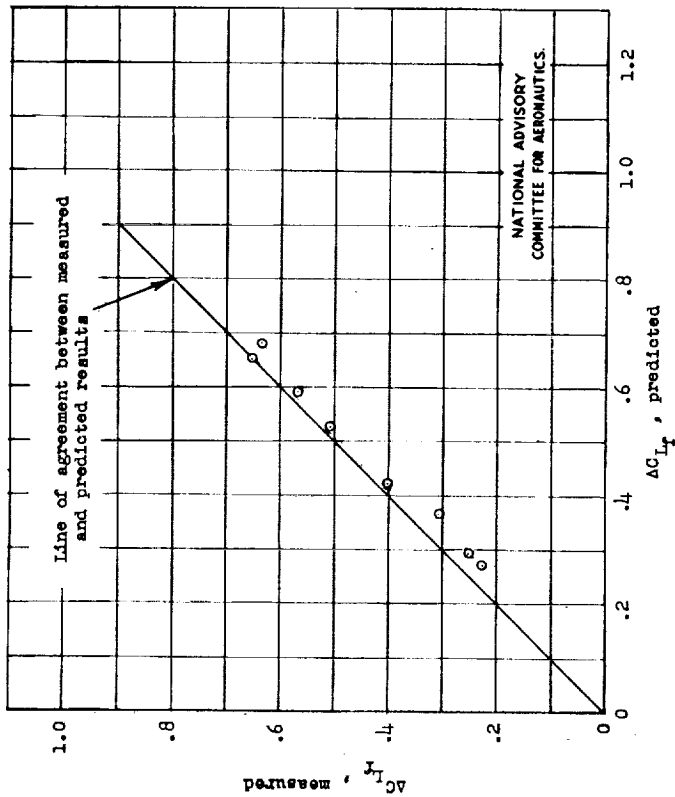


Figure 66.- Comparison between measured values of the increments in lift coefficients due to flap deflection and values predicted from two-dimensional data. Split flap.

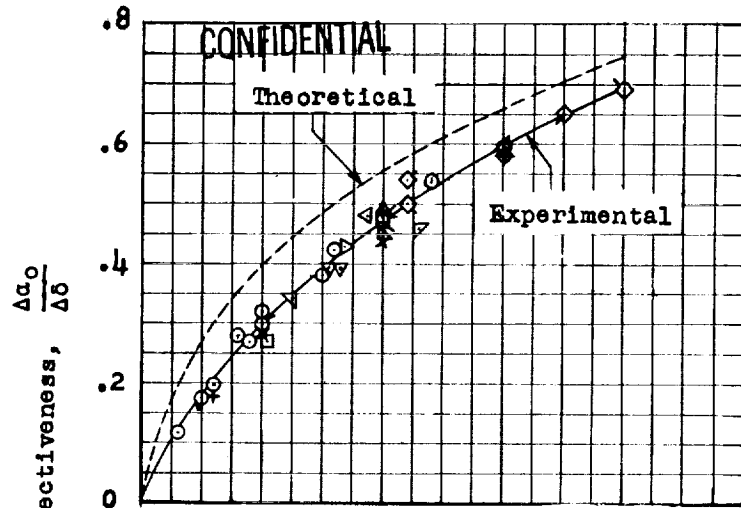
CONFIDENTIAL

TABLE III.- SUPPLEMENTARY INFORMATION REGARDING TESTS
OF TWO-DIMENSIONAL MODELS

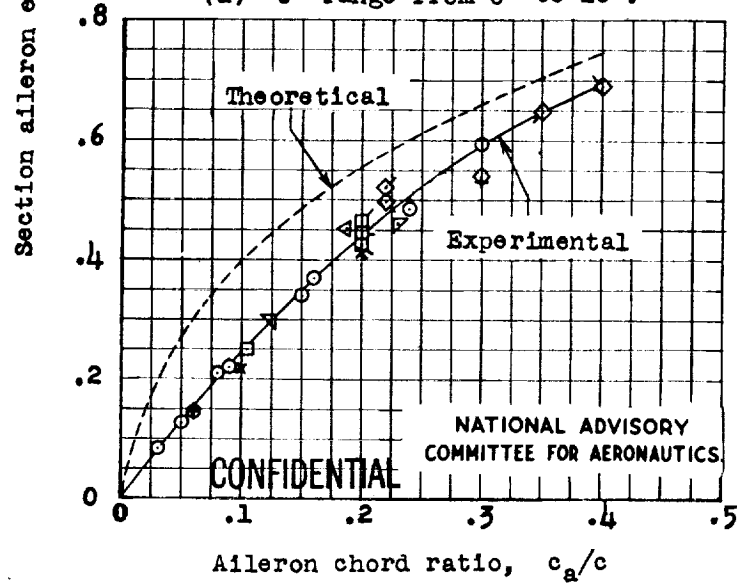
Model		Basic airfoil	Type of flap	Air-flow characteristics			Reference
Designation	Symbol			T	M	R	
1	○	NACA 0009	Plain	1.93	0.08	----	62 to 66
2	+	NACA 0015	Plain	1.93	0.10	1.4×10^6	67
3	×	NACA 23012	Plain	1.60	0.11	2.2×10^6	68, 59
4	□	NACA 66(2x15)-009	Plain, straight contour	1.93	0.10	1.4×10^6	-----
5	◇	NACA 66-009	Plain	1.93	0.11	1.4×10^6	69
6	△	NACA 63,4-4(7.8) approx.	Internally balanced	Approach- ing 1.00	0.17	2.5×10^6	70
7	▽	NACA 66(2x15)-216, m = 0.6	Internally balanced	Approach- ing 1.00	0.18	5.3×10^6	70
8	▷	NACA 66(2x15)-116, m = 0.6	Internally balanced	Approach- ing 1.00	0.14	6.0×10^6	70
9	◁	NACA 64,2-(1.4)(3.5)	Plain	Approach- ing 1.00	----	13.0×10^6	-----
10	▽	NACA 65,2-318 approx.	Internally balanced	Approach- ing 1.00	0.14	6.0×10^6	70
11	▾	NACA 63(420)-521 approx,	Internally balanced	Approach- ing 1.00	----	8.0×10^6	-----
12	▵	NACA 66(215)-216 m = 0.6	Internally balanced	Approach- ing 1.00	0.20 to 0.48	2.8×10^6 to 6.8×10^6	71
13	◀	NACA 66(215)-014	Plain	1.93	0.09	1.2×10^6	72
14	○	NACA 66(215)-216 m = 0.6	Plain	Approach- ing 1.00	----	6.0×10^6	53
15	◻	NACA 65 ₂ -415	Plain	Approach- ing 1.00	0.13	6.0×10^6	73
16	◻	NACA 65 ₃ -418	Plain	Approach- ing 1.00	0.13	6.0×10^6	73
17	◻	NACA 65 ₄ -421	Plain	Approach- ing 1.00	0.13	6.0×10^6	73
18	◇	NACA 65(112)-213	Internally balanced	Approach- ing 1.00	0.14	8.0×10^6	-----
19	◇	NACA 745A317 approx.	Internally balanced	Approach- ing 1.00	0.13	6.0×10^6	-----
20	◇	NACA 64,3-013 approx.	Internally balanced	Approach- ing 1.00	0.13	6.0×10^6	-----
21	◇	NACA 64,3-1(15.5) approx.	Internally balanced	Approach- ing 1.00	0.13	6.0×10^6	-----

CONFIDENTIAL

NATIONAL ADVISORY
COMMITTEE FOR AERONAUTICS

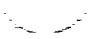


(a) δ range from 0° to 10° .



(b) δ range from 0° to 20° .

Figure 68.- Variation of section aileron effectiveness with aileron chord ratio for true-airfoil-contour ailerons without exposed overhang balance on a number of airfoil sections; gaps sealed; $c_l = 0$.
 (Symbols designating different airfoil sections are identified in table III.)



•

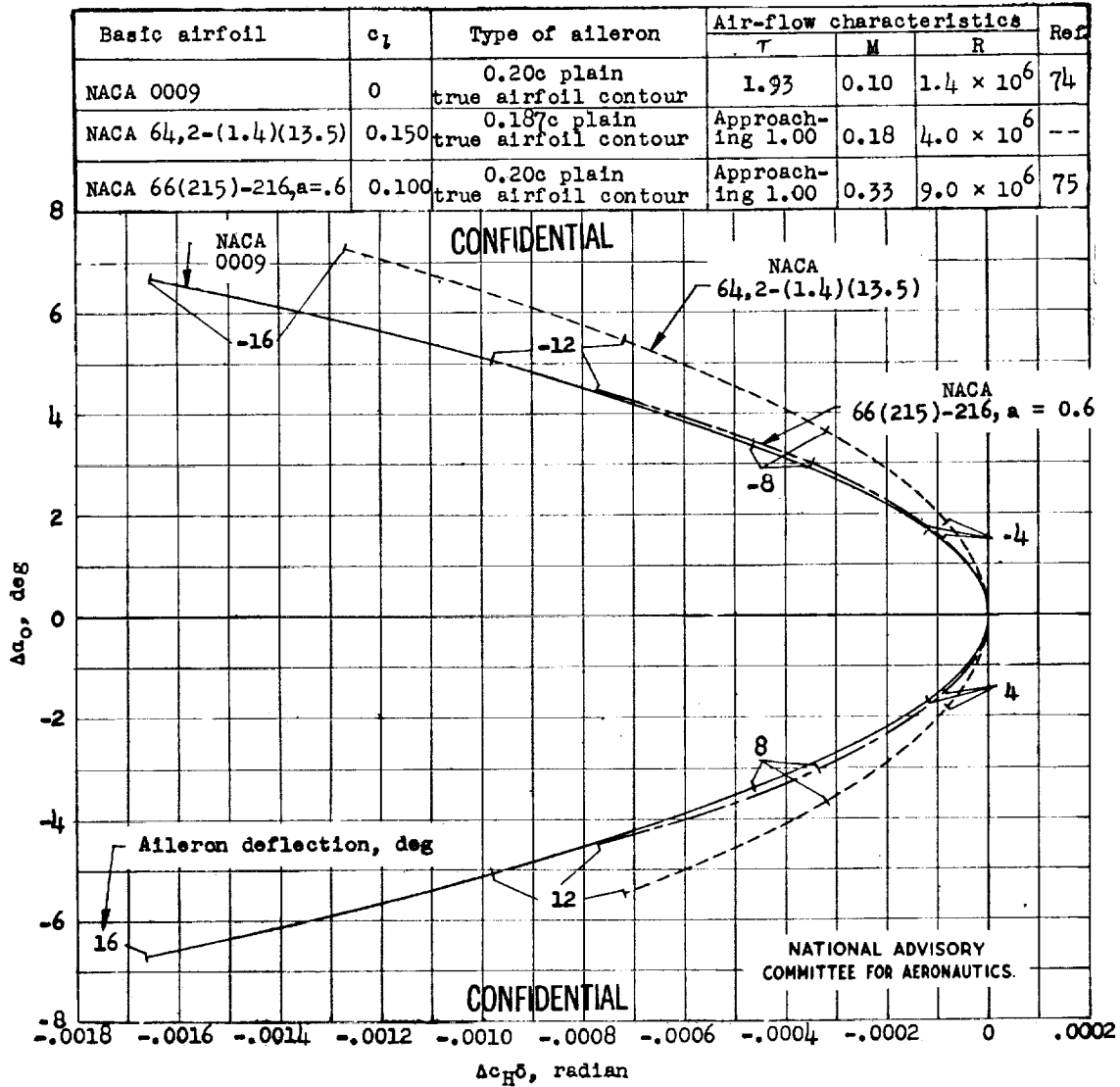


Figure 69.- Variation of the hinge-moment parameter $\Delta c_{H\delta}$ with the equivalent change in section angle of attack required to maintain a constant section lift coefficient for deflection of the aileron on the NACA 0009, NACA 64,2-(1.4)(13.5), and NACA 66(215)-216, a = 0.6 airfoil sections; gaps sealed.



CONFIDENTIAL

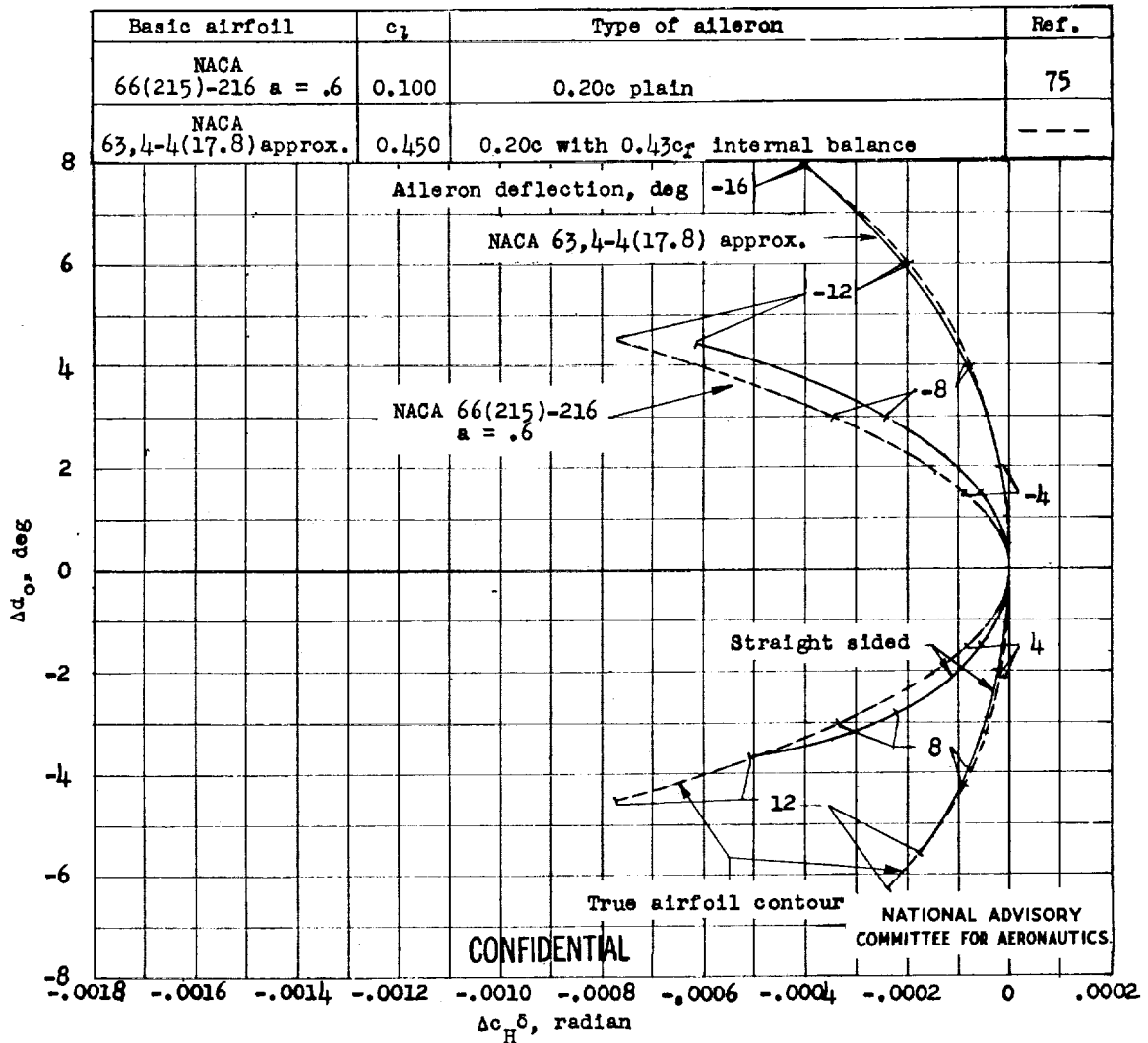


Figure 70.- Variation of the hinge-moment parameter $\Delta c_H \delta$ with the equivalent change in section angle of attack required to maintain a constant section lift coefficient for deflection of true-airfoil-contour and straight-sided ailerons on the NACA 66(215)-216, $\alpha = 0.6$, and the NACA 63,4-4(17.8) (approx.) airfoil sections; gaps sealed.



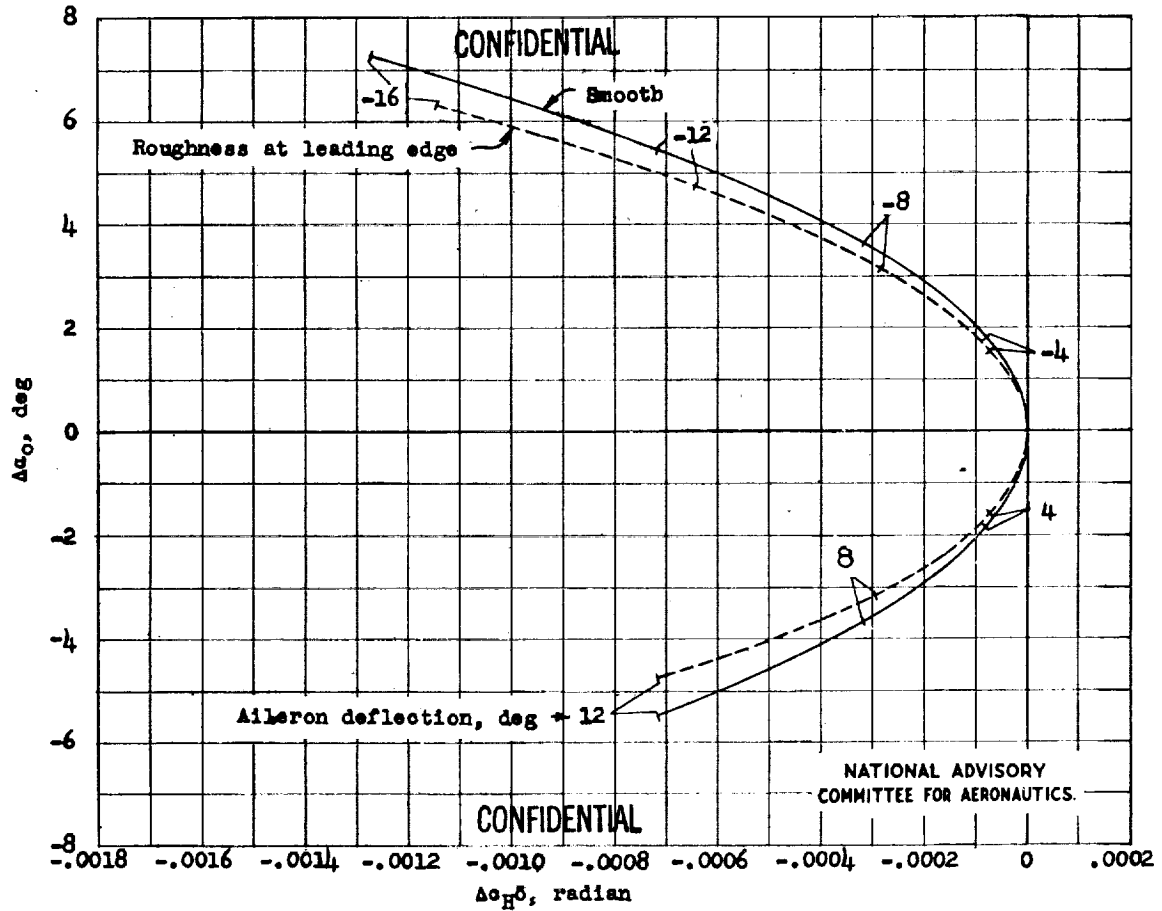
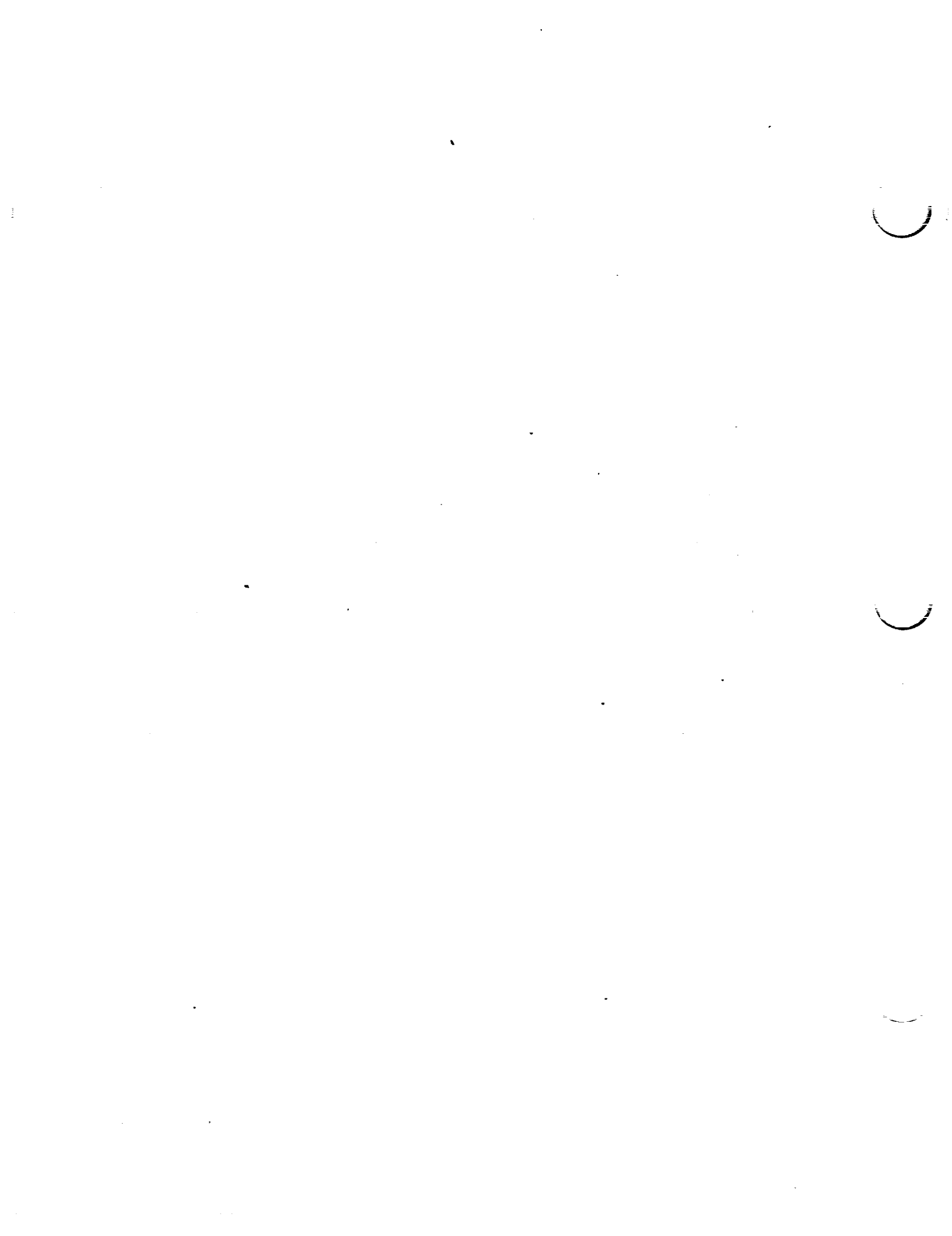


Figure 71.- Variation of the hinge-moment parameter $\Delta c_{H\delta}$ with the equivalent change in section angle of attack required to maintain a constant section lift coefficient for deflection of the aileron on the NACA 64,2-(1.4)(13.5) airfoil section smooth and with roughness at the leading edge of the airfoil. (For description of aileron, see fig. 69.)



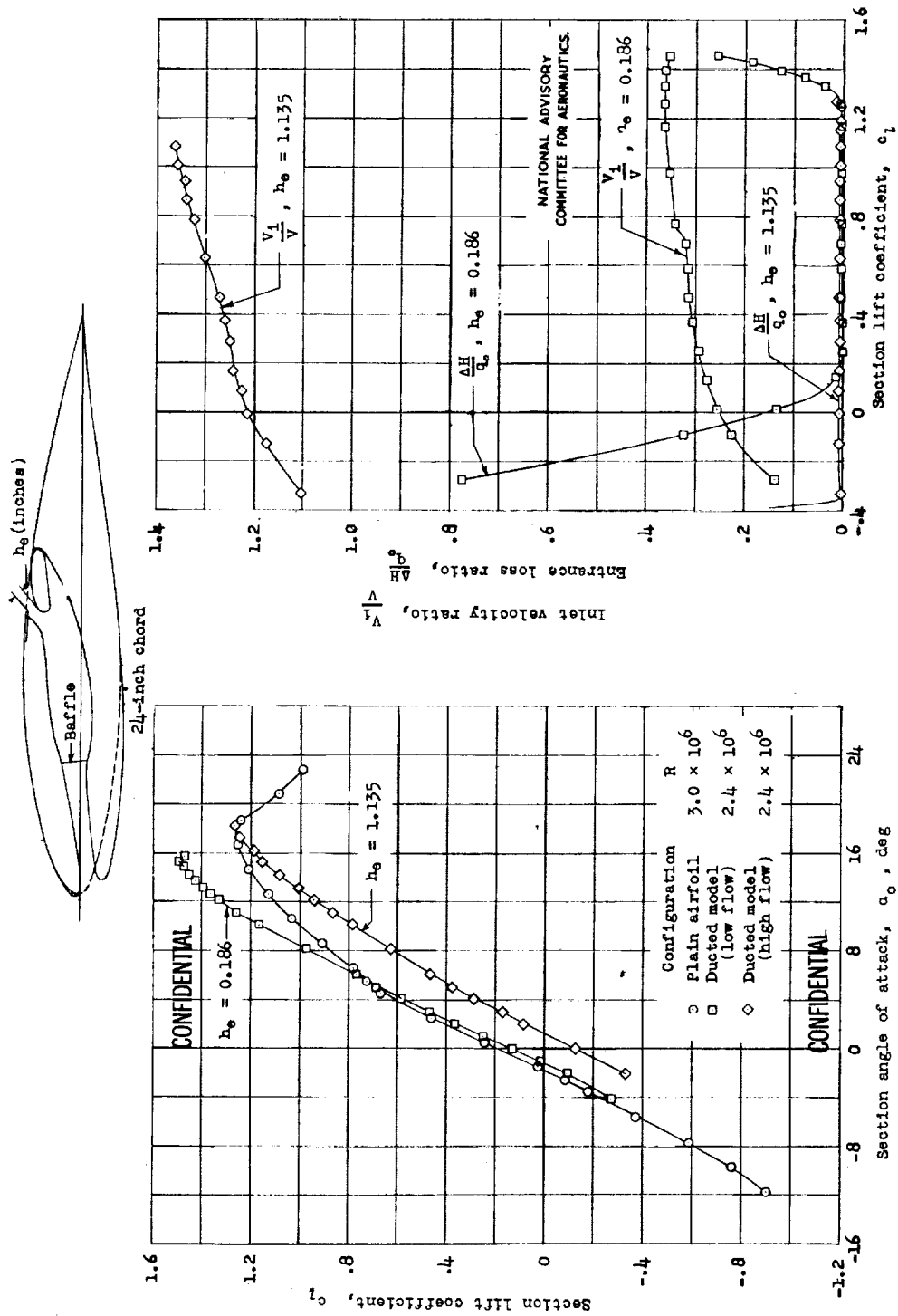


Figure 72.- Lift and flow characteristics of an NACA 7-series type airfoil section with leading-edge air intake.



CONFIDENTIAL

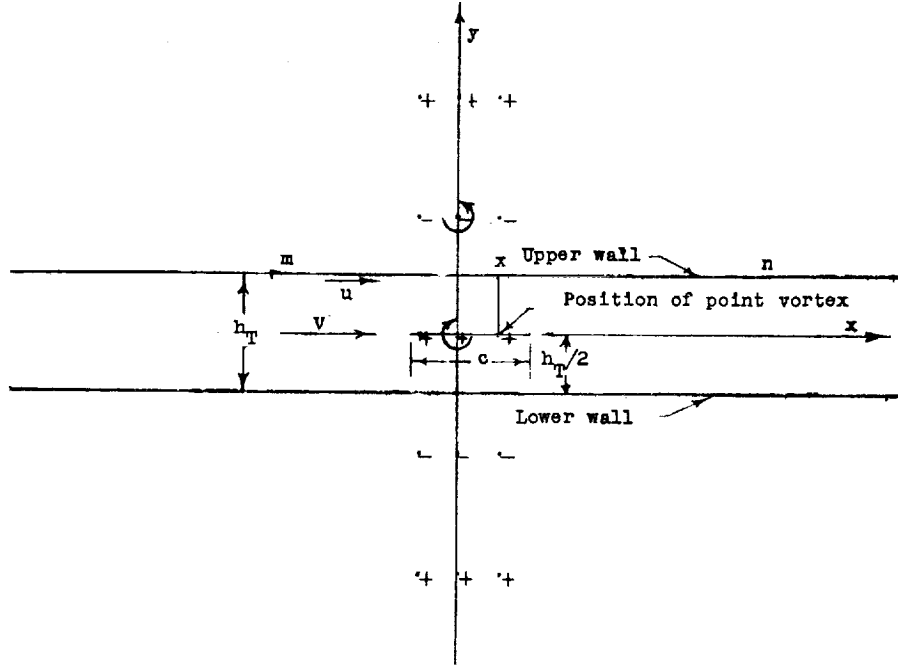
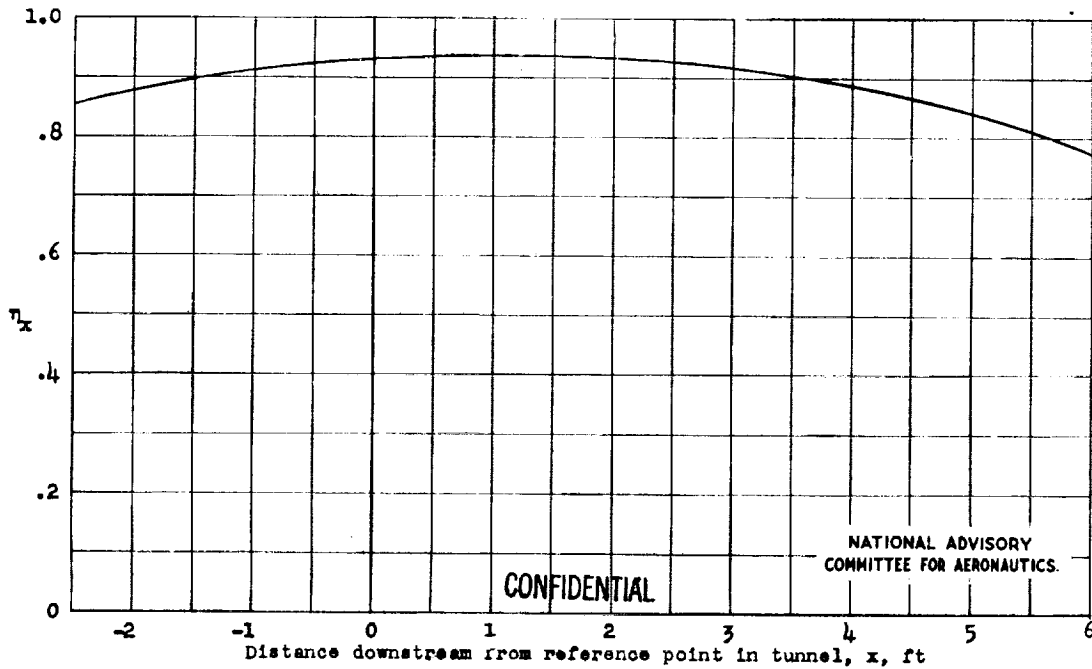


Figure 73.- Image system for calculation of η -factor in the Langley two-dimensional low-turbulence tunnels.



CONFIDENTIAL

NATIONAL ADVISORY COMMITTEE FOR AERONAUTICS.

Figure 74.- Lift efficiency factor η_x for a point vortex situated at various positions along the center line of the tunnel.



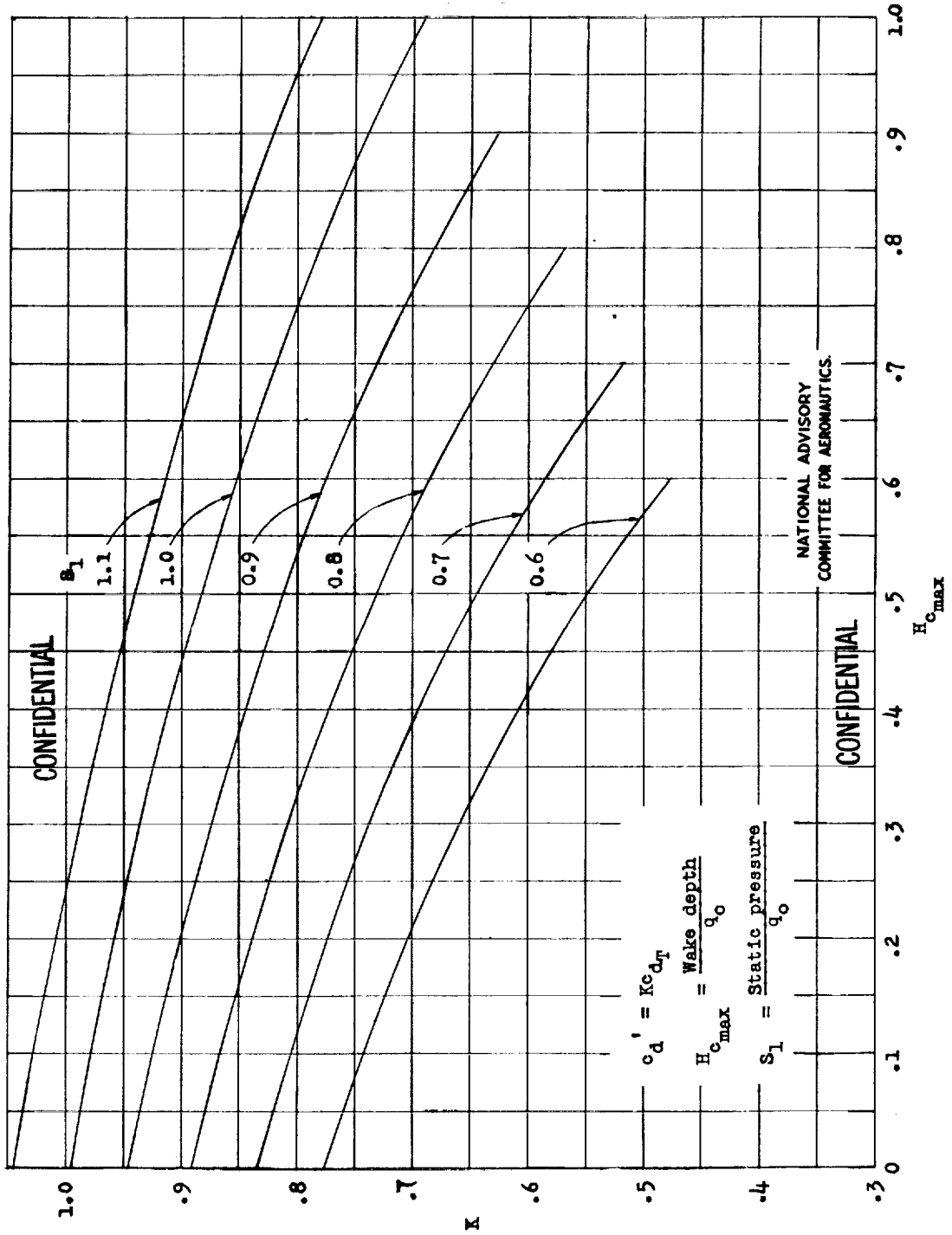


Figure 75.- Plot of K as a function of $H_{c_{max}}$ with S_1 as a parameter.



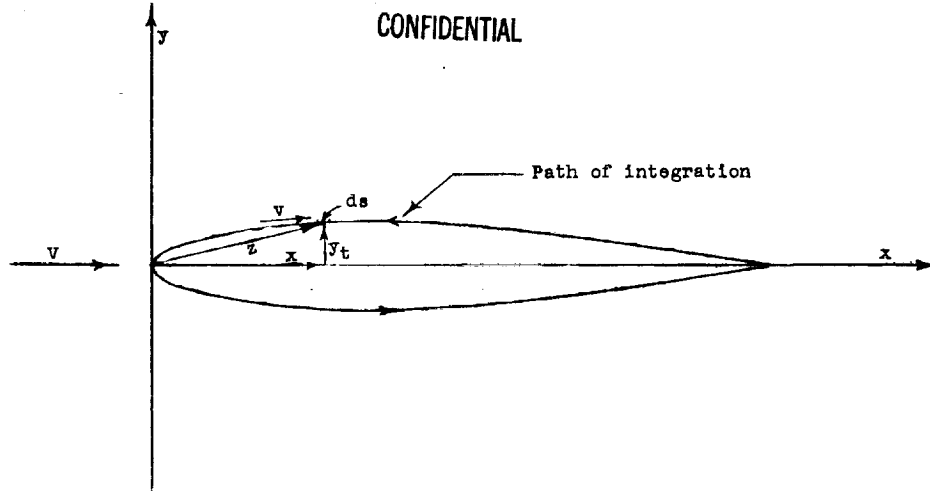


Figure 76.- Sketch for derivation of Λ -factor.

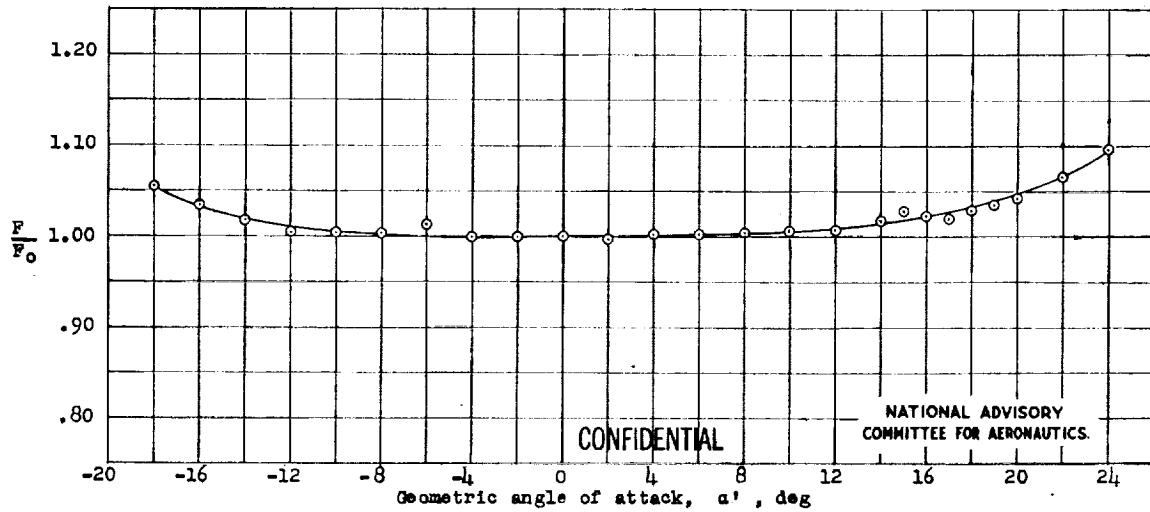


Figure 77.- Additional blocking factor at the tunnel walls plotted against angle of attack for the NACA 64₂-418 airfoil.



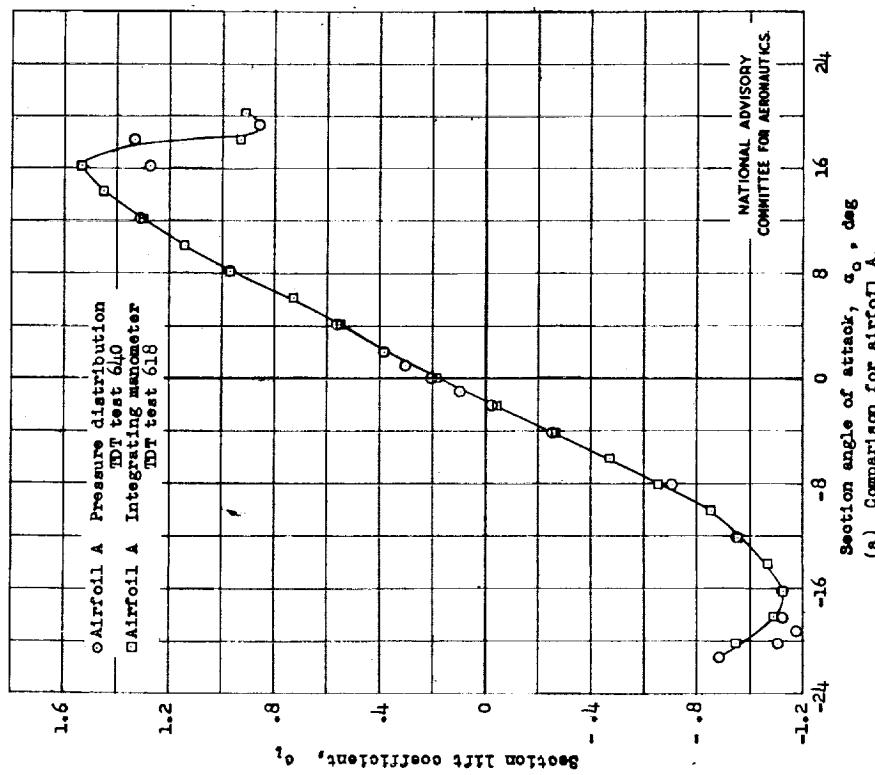
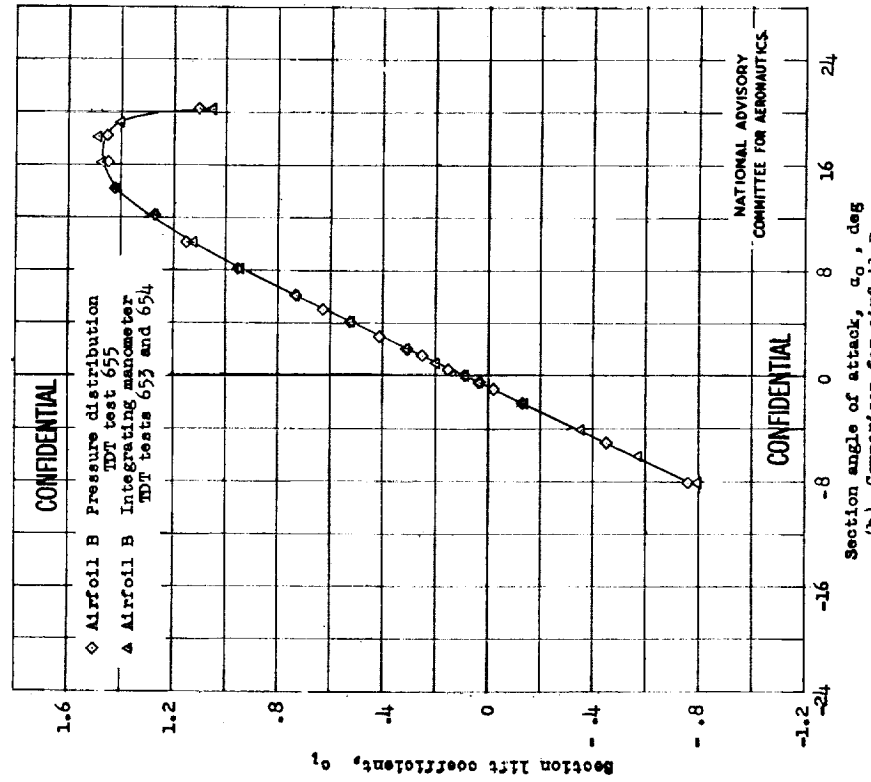


Figure 78.- Comparison between lifts obtained from pressure-distribution measurements and lifts obtained from reactions on the floor and ceiling of the tunnel.



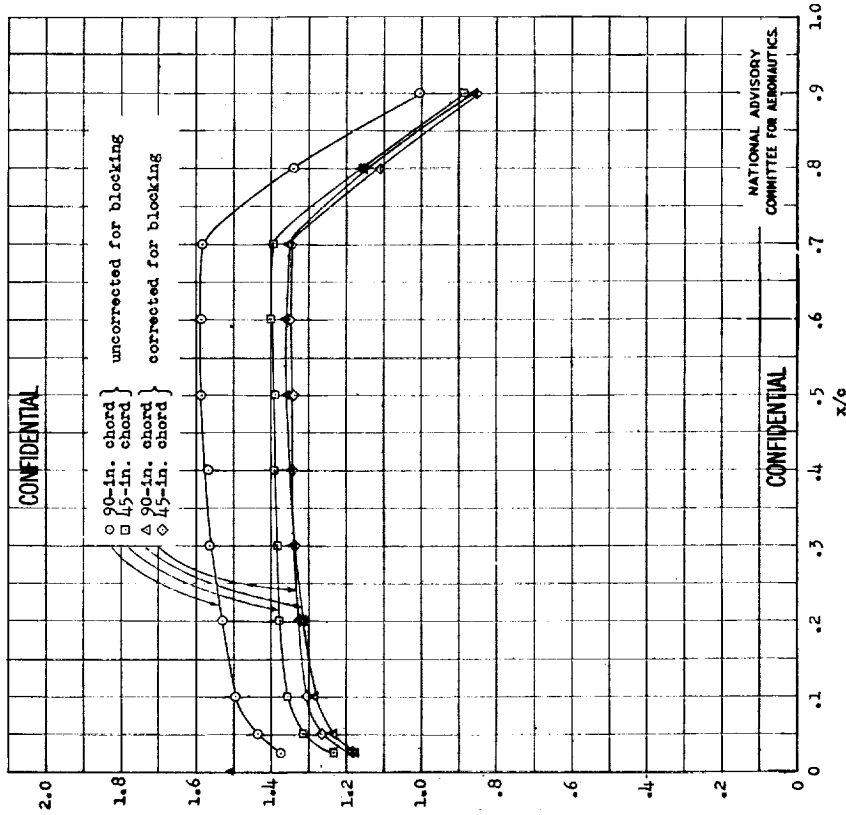


Figure 80.- Comparison between corrected and uncorrected pressure distributions for two chord sizes of a symmetrical MACA 6-series airfoil of 15-percent thickness. $c_o = 0$.

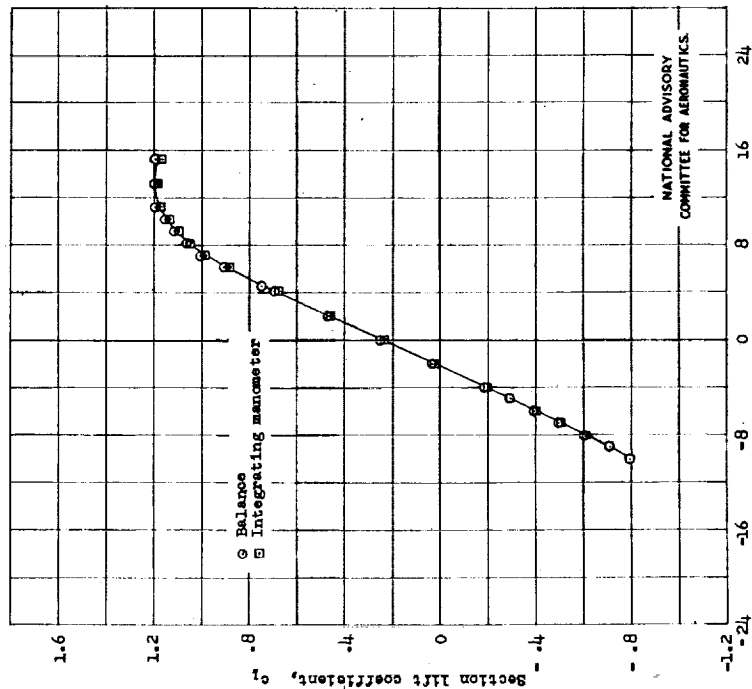
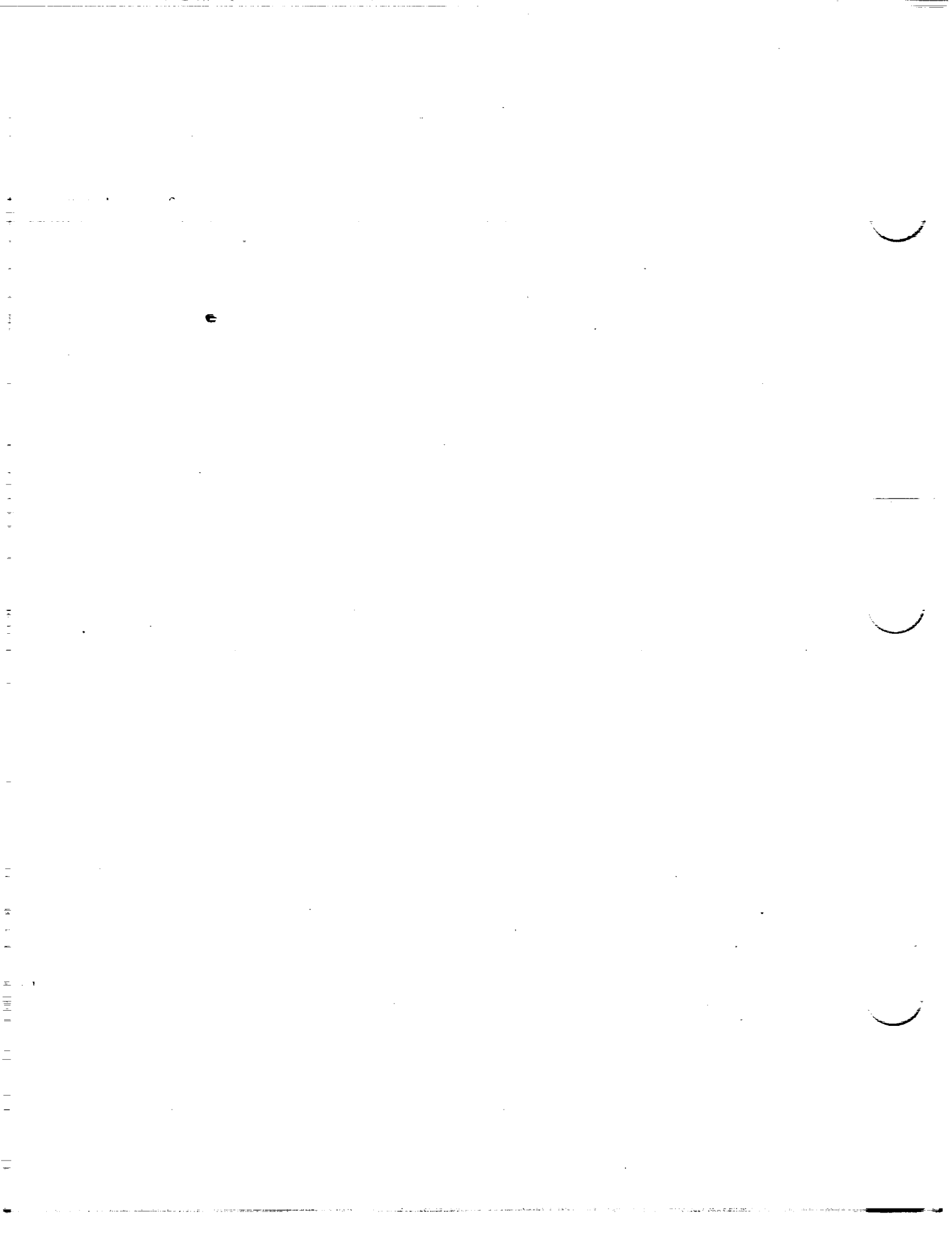


Figure 79.- Comparison between balance measurements and lifts obtained from reactions on the floor and ceiling of the tunnel.



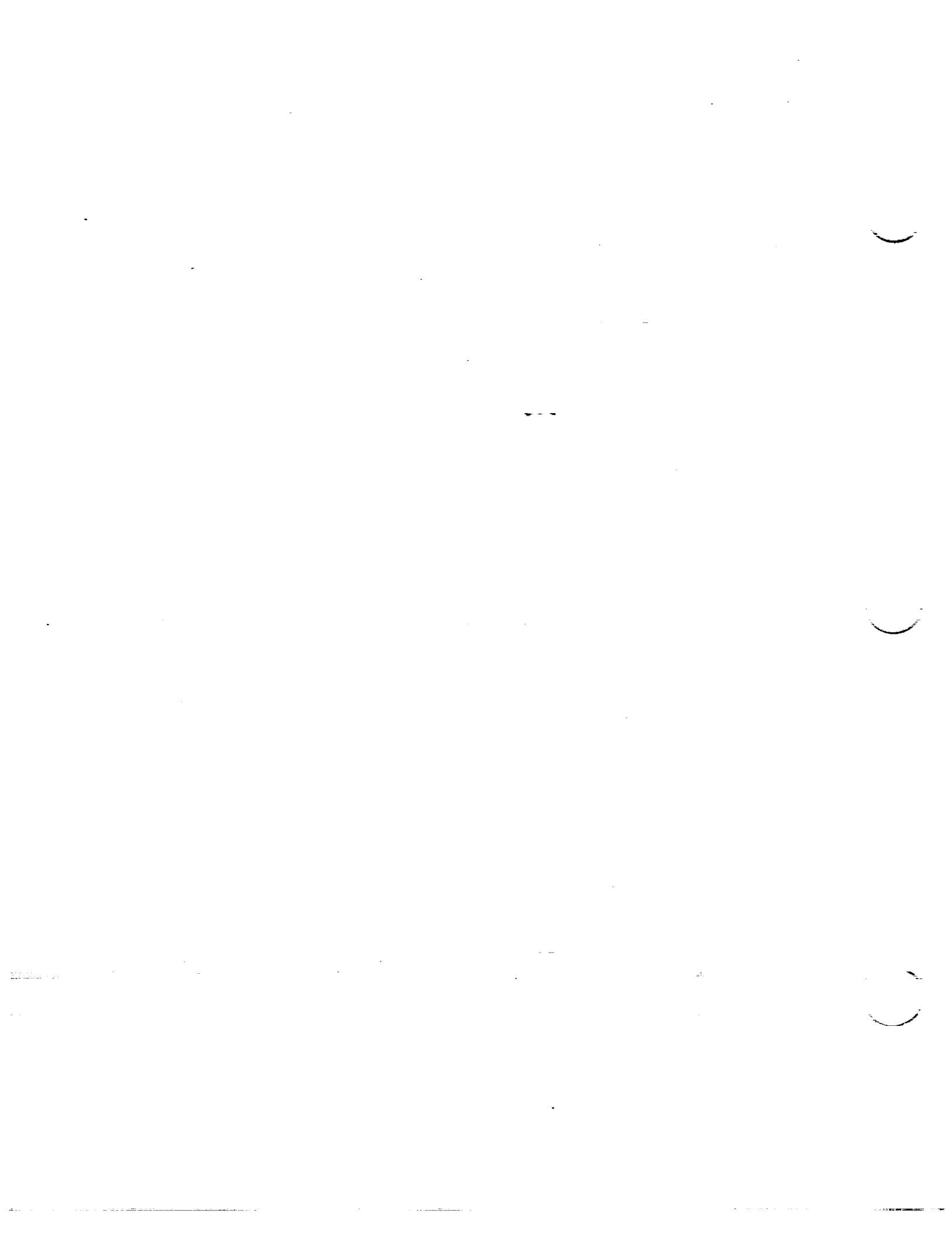
SUPPLEMENTARY DATA

I - BASIC THICKNESS FORMS

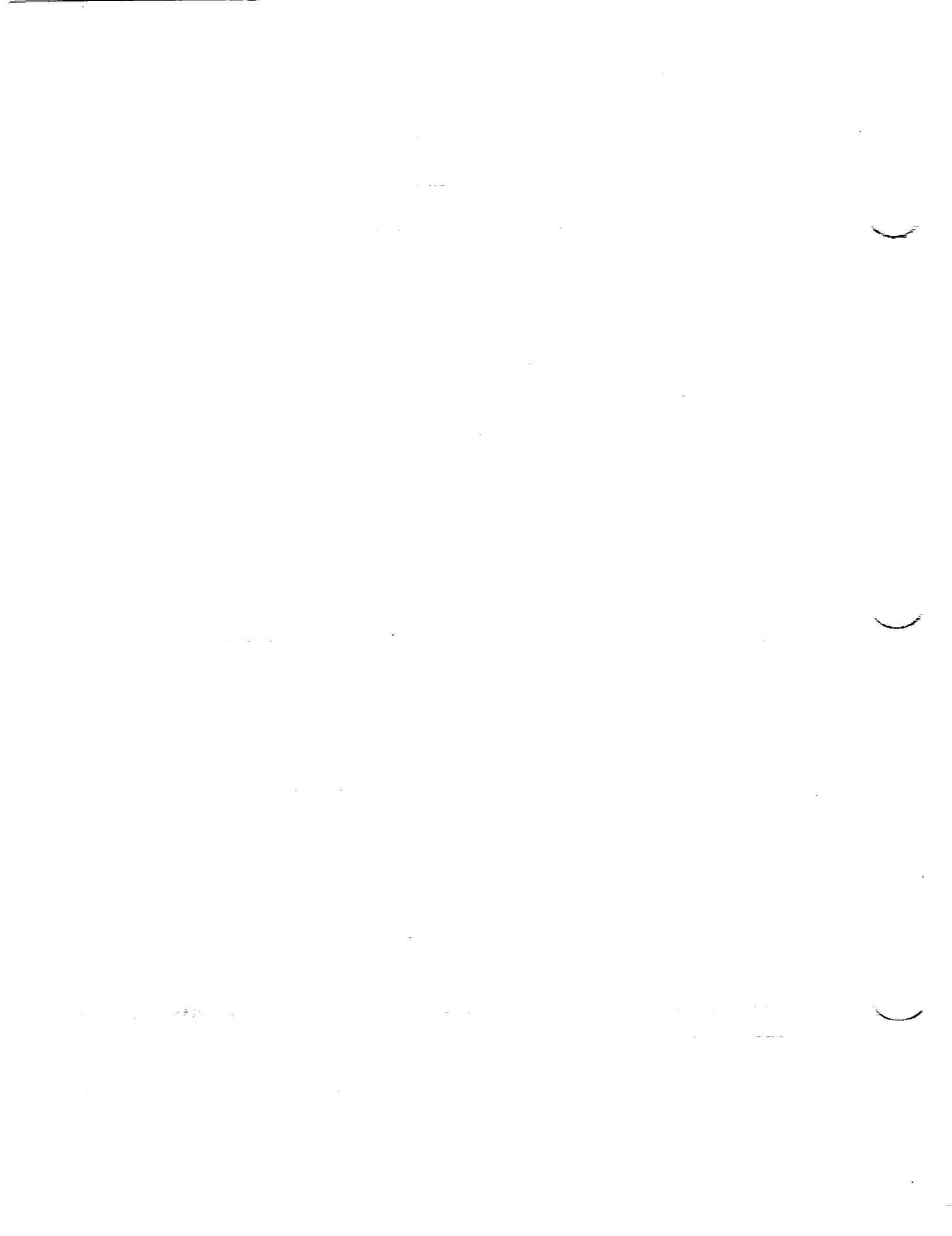


I - BASIC THICKNESS FORMS

NACA 0006 basic thickness form	S4
NACA 0008 basic thickness form	S4a
NACA 0009 basic thickness form	S5
NACA 0010 basic thickness form	S5a
NACA 0012 basic thickness form	S6
NACA 0015 basic thickness form	S7
NACA 0018 basic thickness form	S8
NACA 0021 basic thickness form	S9
NACA 0024 basic thickness form	S10
NACA 16-006 basic thickness form	S11
NACA 16-009 basic thickness form	S12
NACA 16-012 basic thickness form	S13
NACA 16-015 basic thickness form	S14
NACA 16-018 basic thickness form	S15
NACA 16-021 basic thickness form	S16
NACA 63,4-020 basic thickness form	S17
NACA 64,2-015 basic thickness form	S18
NACA 64 ₁ -006 basic thickness form	S18a
NACA 64 ₁ -008 basic thickness form	S18b
NACA 64 ₁ -009 basic thickness form	S18c
NACA 64 ₁ -010 basic thickness form	S18d
NACA 64 ₁ -012 basic thickness form	S19



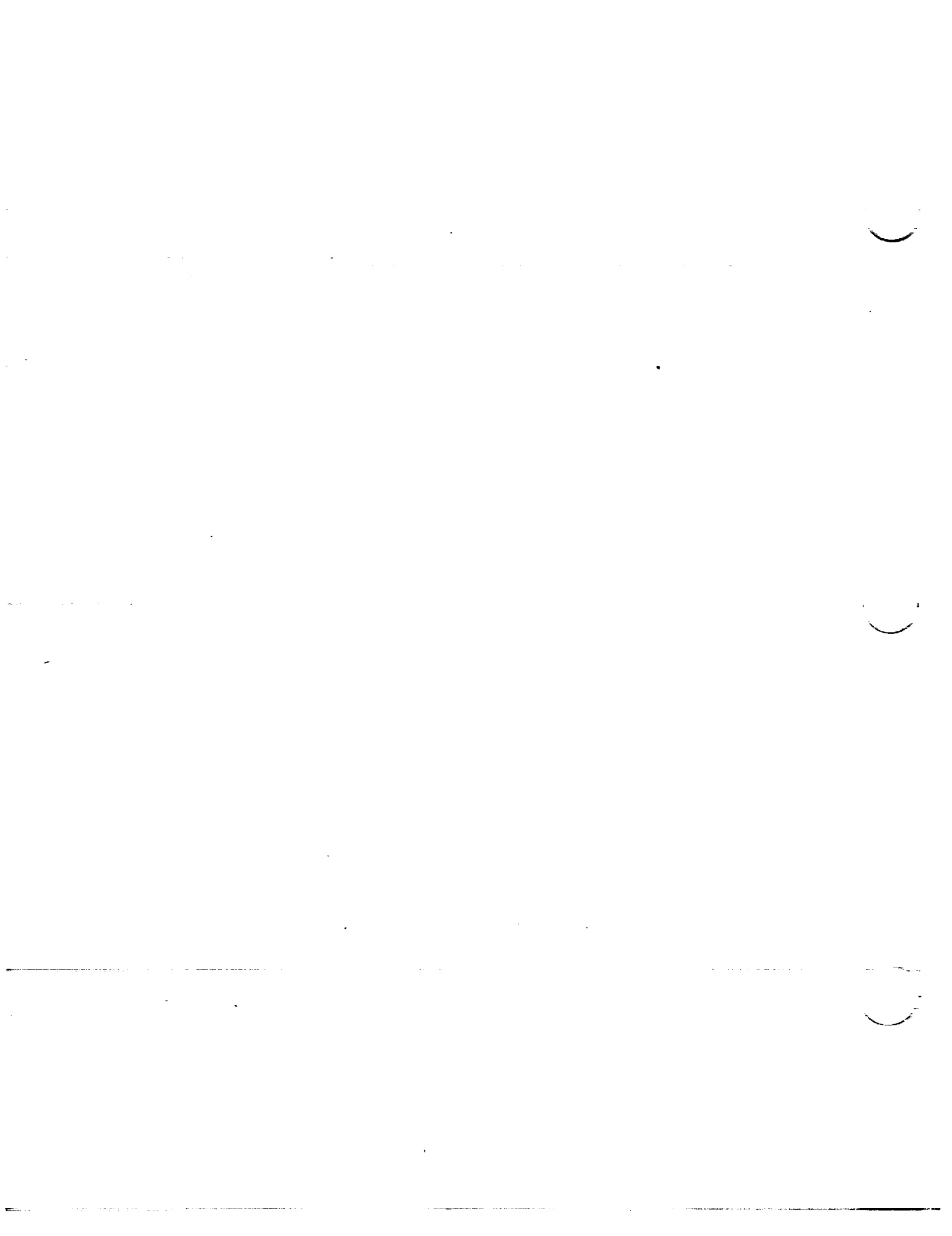
NACA 64₂-015 basic thickness form S20
NACA 64₃-018 basic thickness form S21
NACA 64₄-021 basic thickness form S22
NACA 65,2-016 basic thickness form S23
NACA 65,2-023 basic thickness form S24
NACA 65,3-018 basic thickness form S25
NACA 65₁-006 basic thickness form S25a
NACA 65₁-008 basic thickness form S25b
NACA 65₁-009 basic thickness form S25c
NACA 65₁-010 basic thickness form S26
NACA 65₁-012 basic thickness form S27
NACA 65₂-015 basic thickness form S28
NACA 65₃-018 basic thickness form S29
NACA 65₄-021 basic thickness form S30
NACA 66,1-012 basic thickness form S31
NACA 66,2-015 basic thickness form S32
NACA 66,2-018 basic thickness form S33
NACA 66₁-006 basic thickness form S33a
NACA 66₁-008 basic thickness form S33b
NACA 66₁-009 basic thickness form S33c
NACA 66₁-010 basic thickness form S33d
NACA 66₁-012 basic thickness form S34
NACA 66₂-015 basic thickness form S35
NACA 66₃-018 basic thickness form S36



NACA ACR No. L5C05 CONFIDENTIAL

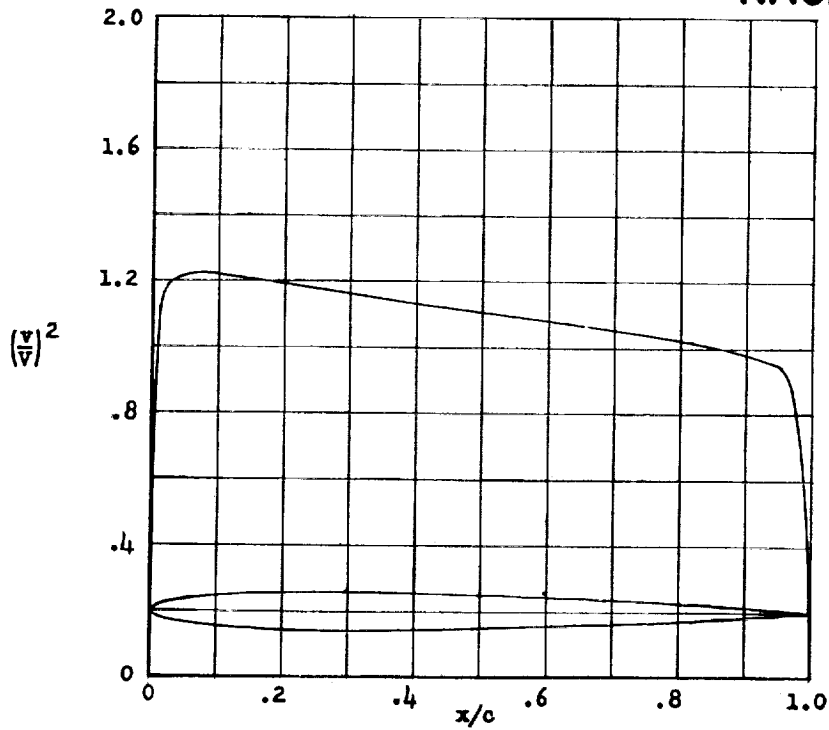
COPY NO. 119
S3a
April 2, 1945

NACA 66 ₄ -021 basic thickness form	S37
NACA 67,1-015 basic thickness form	S38
NACA 747A015 basic thickness form	S39



CONFIDENTIAL

NACA 0006



(percent \bar{x} c)	(percent \bar{y} c)	$(v/v)^2$	v/v	$\Delta v_a/v$
0	0	0	0	3.992
.5	-----	.880	.938	2.015
1.25	.947	1.117	1.057	1.364
2.5	1.307	1.186	1.089	.984
5.0	1.777	1.217	1.103	.696
7.5	2.100	1.225	1.107	.562
10	2.341	1.212	1.101	.478
15	2.673	1.206	1.098	.378
20	2.869	1.190	1.091	.316
25	2.971	1.179	1.086	.272
30	3.001	1.162	1.078	.239
40	2.902	1.136	1.066	.189
50	2.647	1.109	1.053	.152
60	2.282	1.086	1.042	.123
70	1.832	1.057	1.028	.097
80	1.312	1.026	1.013	.073
90	.724	.980	.990	.047
95	.403	.949	.974	.032
100	.063	0	0	0

L. E. radius: 0.40 percent c

NACA 0006 basic thickness form

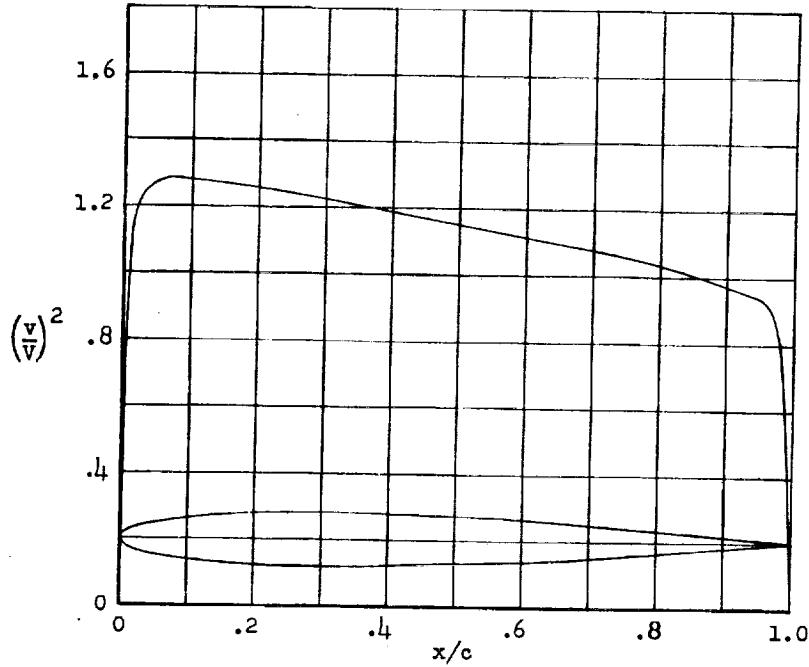
CONFIDENTIAL

NATIONAL ADVISORY
COMMITTEE FOR AERONAUTICS.



CONFIDENTIAL

NACA 0008



x (percent c)	y (percent c)	$(v/V)^2$	v/V	$\Delta v_a/V$
0	0	0	0	2.900
.5	-----	.792	.890	1.795
1.25	1.263	1.103	1.050	1.310
2.5	1.743	1.221	1.105	.971
5.0	2.369	1.272	1.128	.694
7.5	2.800	1.284	1.133	.561
10	3.121	1.277	1.130	.479
15	3.564	1.272	1.128	.379
20	3.825	1.259	1.122	.318
25	3.961	1.241	1.114	.273
30	4.001	1.223	1.106	.236
40	3.869	1.186	1.089	.188
50	3.529	1.149	1.072	.152
60	3.043	1.111	1.054	.121
70	2.443	1.080	1.039	.096
80	1.749	1.034	1.017	.071
90	.965	.968	.984	.047
95	.537	.939	.969	.031
100	0	-----	-----	0

L.E. radius: 0.70 percent c

NACA 0008 basic thickness form

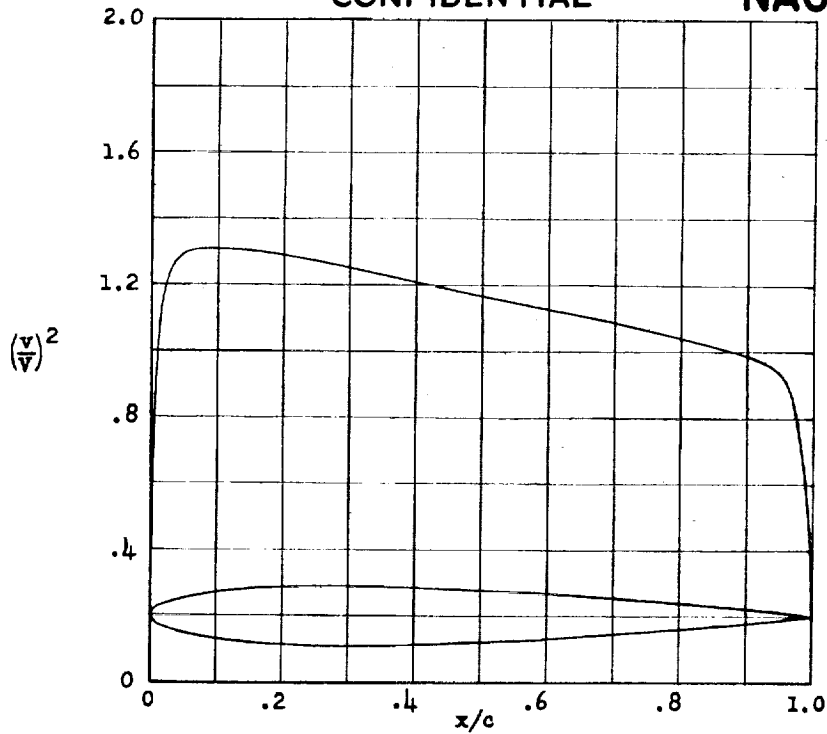
CONFIDENTIAL

NATIONAL ADVISORY
COMMITTEE FOR AERONAUTICS



CONFIDENTIAL

NACA 0009



(percent \bar{x})	(percent \bar{y})	$(v/V)^2$	v/V	$\Delta v_a/V$
0	0	0	0	.595
.5	-----	.750	.866	1.700
1.25	1.420	1.083	1.041	1.283
2.5	1.961	1.229	1.109	.963
5.0	2.666	1.299	1.140	.692
7.5	3.150	1.310	1.145	.560
10	3.512	1.309	1.144	.479
15	4.009	1.304	1.142	.380
20	4.303	1.293	1.137	.318
25	4.456	1.275	1.129	.273
30	4.501	1.252	1.119	.239
40	4.352	1.209	1.100	.188
50	3.971	1.170	1.082	.151
60	3.423	1.126	1.061	.120
70	2.748	1.087	1.043	.095
80	1.967	1.037	1.018	.070
90	1.086	.984	.992	.046
95	.605	.933	.966	.030
100	.095	0	0	0

U. E. radius: 0.89 percent c

NACA 0009 basic thickness form

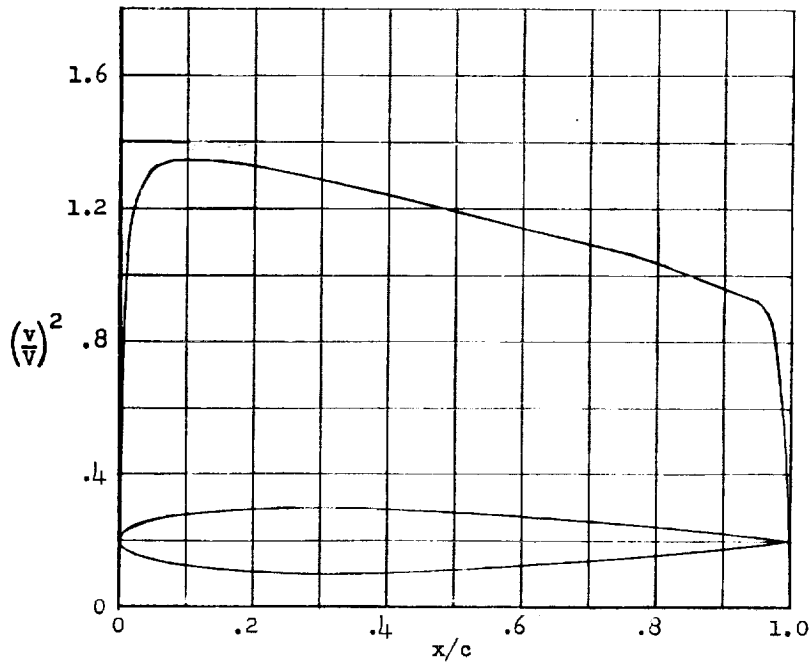
CONFIDENTIAL

NATIONAL ADVISORY
COMMITTEE FOR AERONAUTICS.



CONFIDENTIAL

NACA 0010



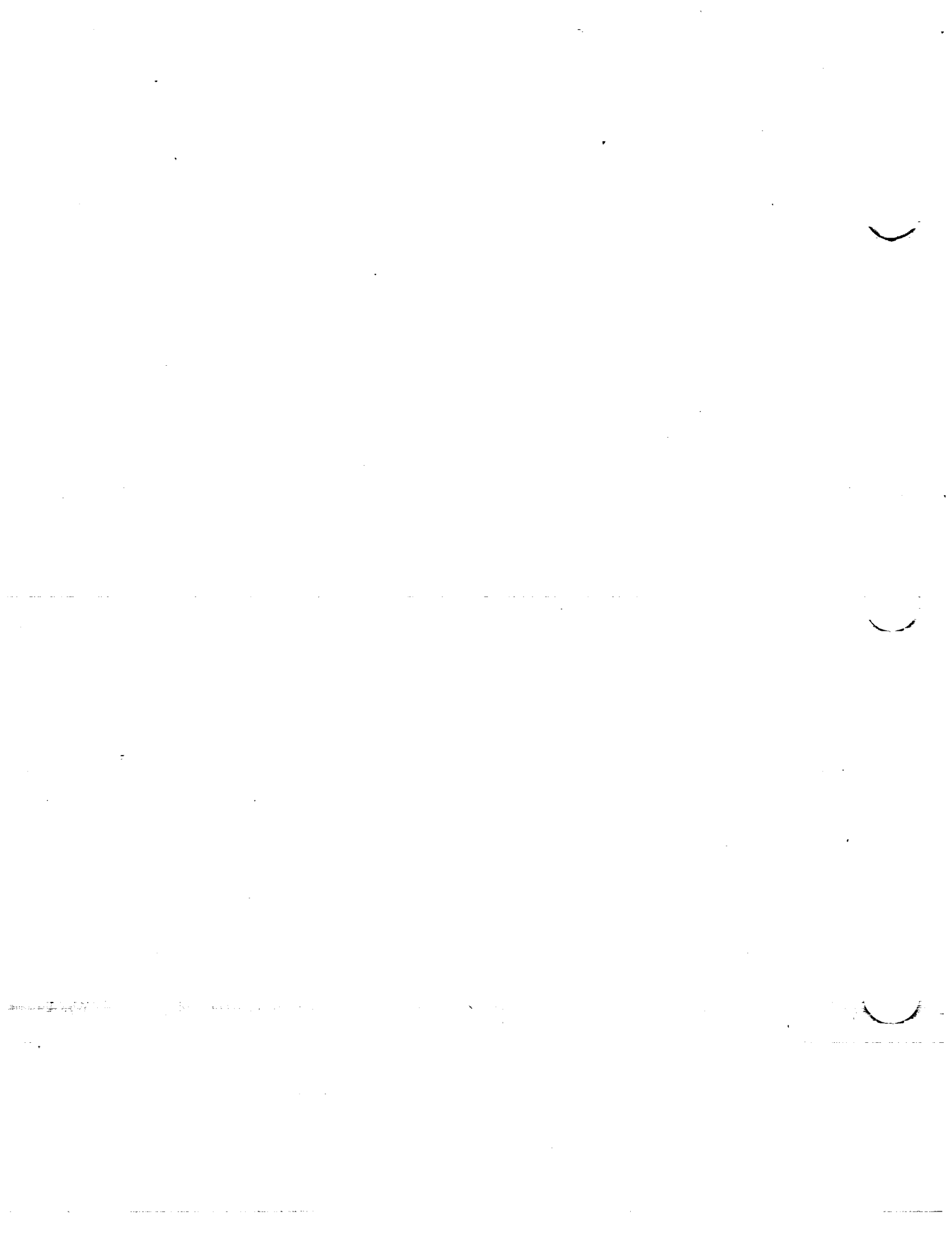
x (percent c)	y (percent c)	$(v/v)^2$	v/v	$\Delta v_a/V$
0	0	0	0	2.372
.5	-----	.712	.844	1.618
1.25	1.578	1.061	1.030	1.255
2.5	2.178	1.237	1.112	.955
5.0	2.962	1.325	1.151	.690
7.5	3.500	1.341	1.158	.559
10	3.902	1.341	1.158	.479
15	4.455	1.341	1.158	.380
20	4.782	1.329	1.153	.318
25	4.952	1.309	1.144	.273
30	5.002	1.284	1.133	.239
40	4.837	1.237	1.112	.188
50	4.412	1.190	1.091	.150
60	3.803	1.138	1.067	.119
70	3.053	1.094	1.046	.094
80	2.187	1.040	1.020	.069
90	1.207	.960	.980	.045
95	.672	.925	.962	.030
100	0	-----	-----	0

L.E. radius: 1.10 percent c

NACA 0010 basic thickness form

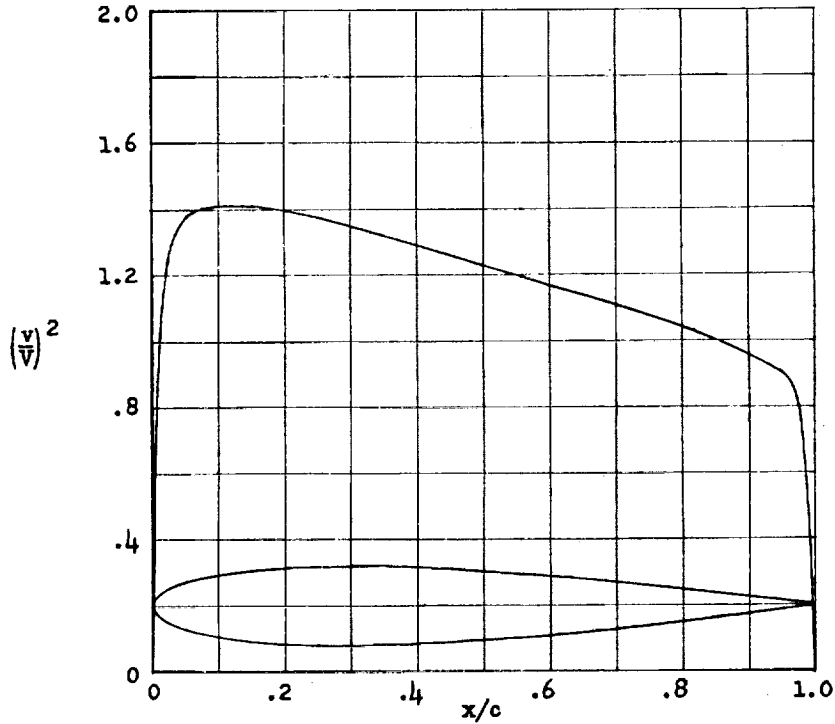
CONFIDENTIAL

NATIONAL ADVISORY
COMMITTEE FOR AERONAUTICS



CONFIDENTIAL

NACA 0012



(percent \bar{x} c)	(percent \bar{y} c)	$(v/V)^2$	v/V	$\Delta v_a/V$
0	0	0	0	1.988
.5	-----	.640	.800	1.475
1.25	1.894	1.010	1.005	1.199
2.5	2.615	1.241	1.114	.934
5.0	3.555	1.378	1.174	.685
7.5	4.200	1.402	1.184	.558
10	4.683	1.411	1.188	.479
15	5.345	1.411	1.188	.381
20	5.737	1.399	1.183	.319
25	5.941	1.378	1.174	.273
30	6.002	1.350	1.162	.239
40	5.803	1.288	1.135	.187
50	5.294	1.228	1.108	.149
60	4.563	1.166	1.080	.118
70	3.664	1.109	1.053	.092
80	2.623	1.044	1.022	.068
90	1.448	.956	.978	.044
95	.807	.906	.952	.029
100	.126	0	0	0

L. E. radius: 1.58 percent c

NACA 0012 basic thickness form

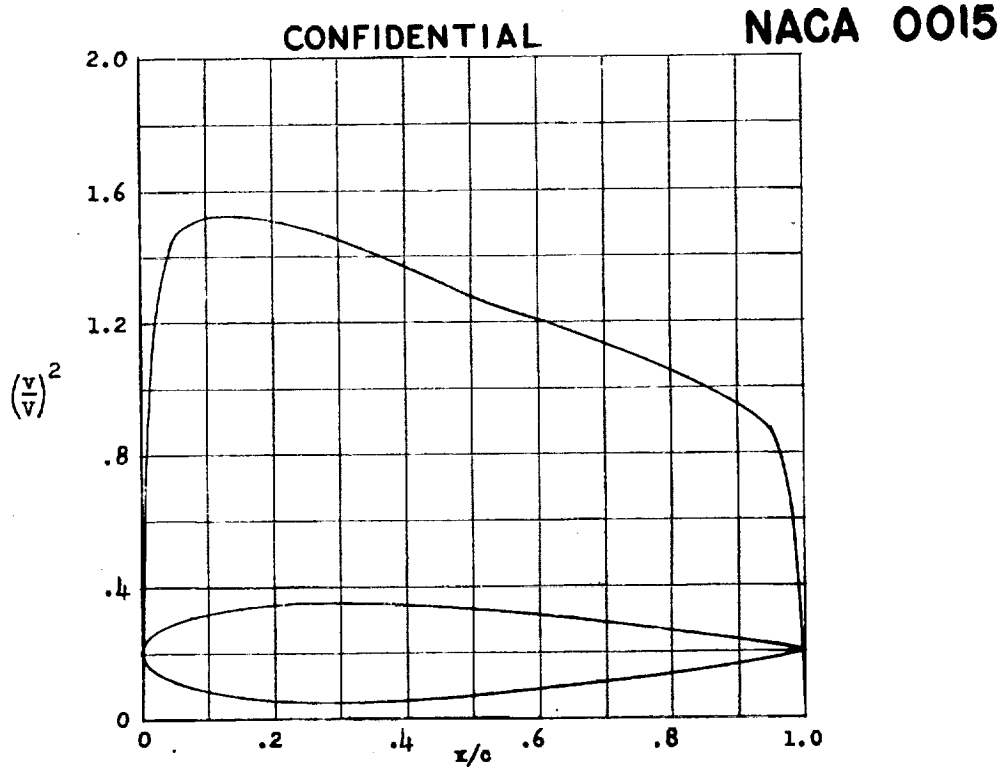
CONFIDENTIAL

NATIONAL ADVISORY
COMMITTEE FOR AERONAUTICS

1944-1945

1946-1947





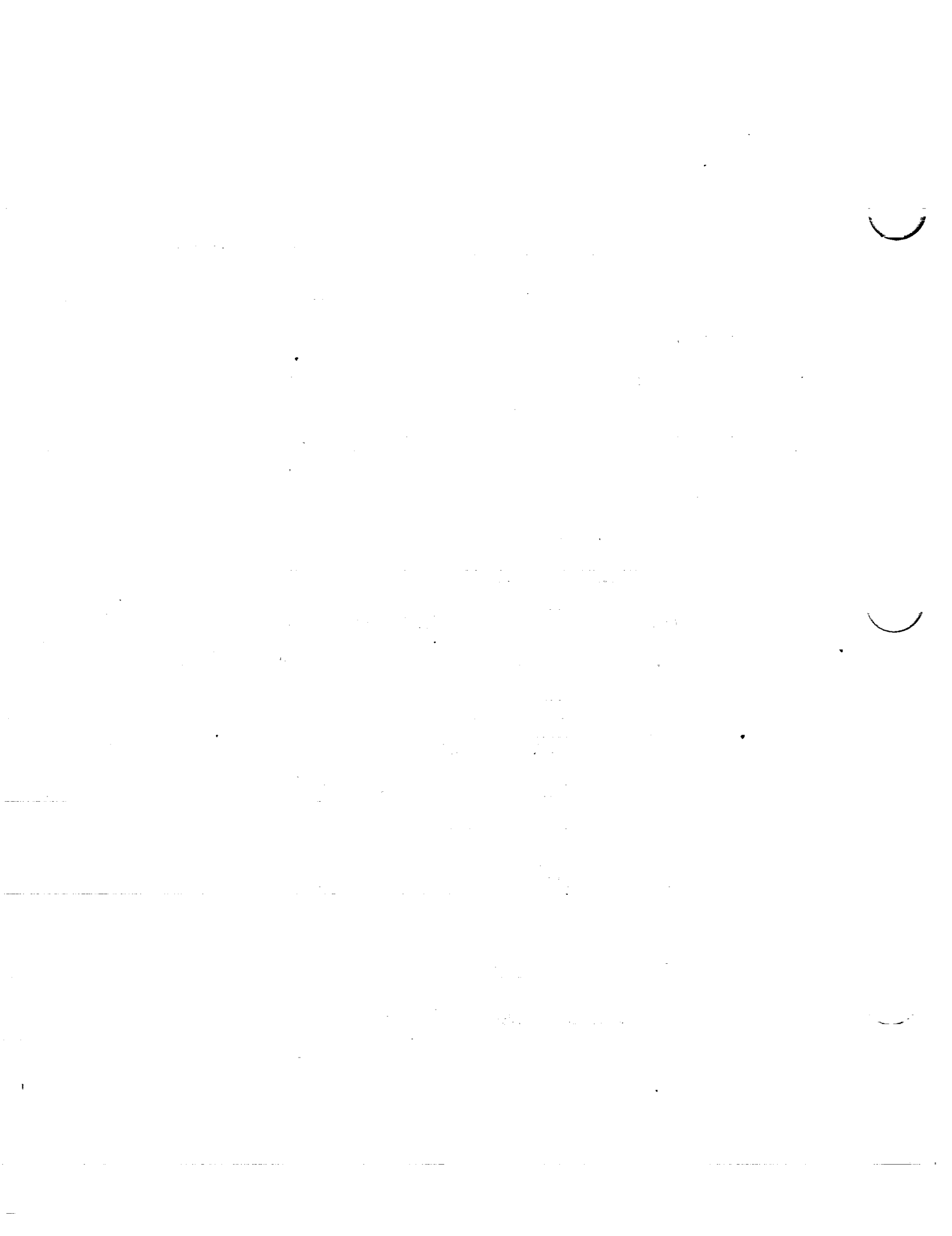
(percent x/c)	(percent y/c)	$(v/V)^2$	v/V	$\Delta v_a/V$
0	0	0	0	1.600
.5	-----	.546	.739	1.312
1.25	2.367	.933	.966	1.112
2.5	3.268	1.237	1.112	.900
5.0	4.443	1.450	1.204	.675
7.5	5.250	1.498	1.224	.557
10	5.853	1.520	1.233	.479
15	6.682	1.520	1.233	.381
20	7.172	1.510	1.229	.320
25	7.427	1.484	1.218	.274
30	7.502	1.450	1.204	.239
40	7.254	1.369	1.170	.185
50	6.617	1.279	1.131	.146
60	5.704	1.206	1.098	.115
70	4.580	1.132	1.064	.090
80	3.279	1.049	1.024	.065
90	1.810	.945	.972	.041
95	1.008	.872	.934	.027
100	.158	0	0	0

L. B. radius: 2.48 percent c

NACA 0015 basic thickness form

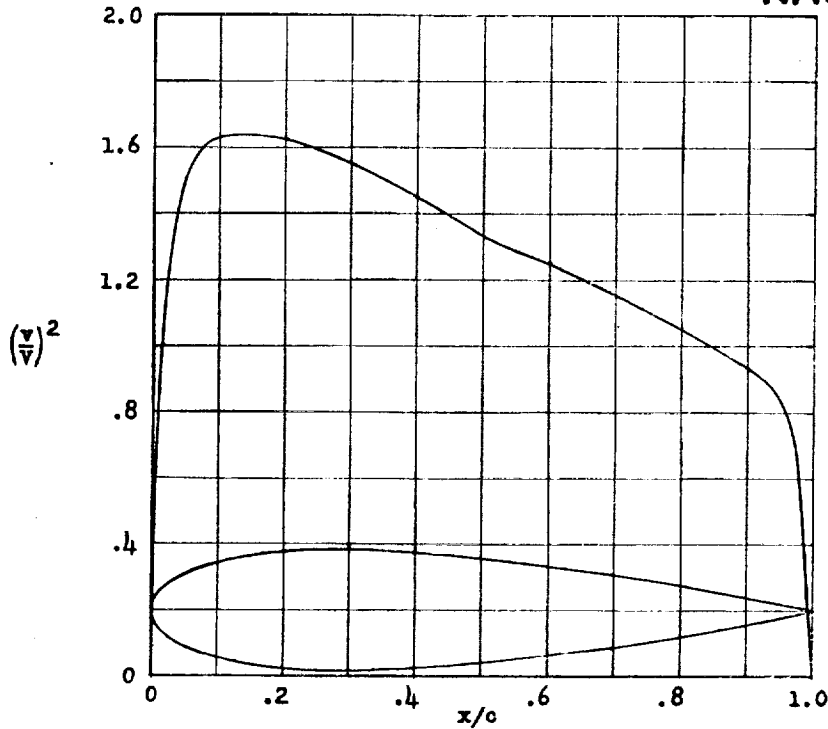
CONFIDENTIAL

NATIONAL ADVISORY
COMMITTEE FOR AERONAUTICS.



CONFIDENTIAL

NACA 0018



x (percent c)	y (percent c)	$(v/V)^2$	v/V	$\Delta v_a/V$
0	0	0	0	1.342
.5	-----	.465	.682	1.178
1.25	2.841	.857	.926	1.028
2.5	3.922	1.217	1.103	.861
5.0	5.332	1.507	1.228	.662
7.5	6.300	1.598	1.264	.555
10	7.024	1.628	1.276	.479
15	8.018	1.633	1.278	.381
20	8.606	1.625	1.275	.320
25	8.912	1.592	1.262	.274
30	9.003	1.556	1.247	.238
40	8.705	1.453	1.205	.184
50	7.941	1.331	1.154	.144
60	6.845	1.246	1.116	.113
70	5.496	1.153	1.074	.087
80	3.935	1.051	1.025	.063
90	2.172	.933	.966	.039
95	1.210	.836	.914	.025
100	.189	0	0	0

L. E. radius: 3.56 percent c

NACA 0018 basic thickness form

CONFIDENTIAL

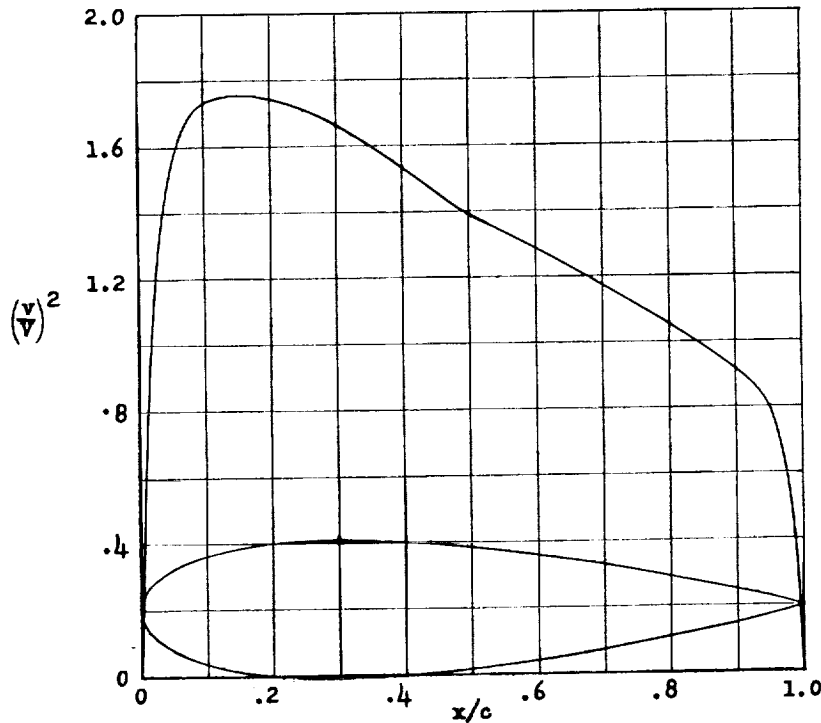
NATIONAL ADVISORY
COMMITTEE FOR AERONAUTICS.

8100



CONFIDENTIAL

NACA 0021



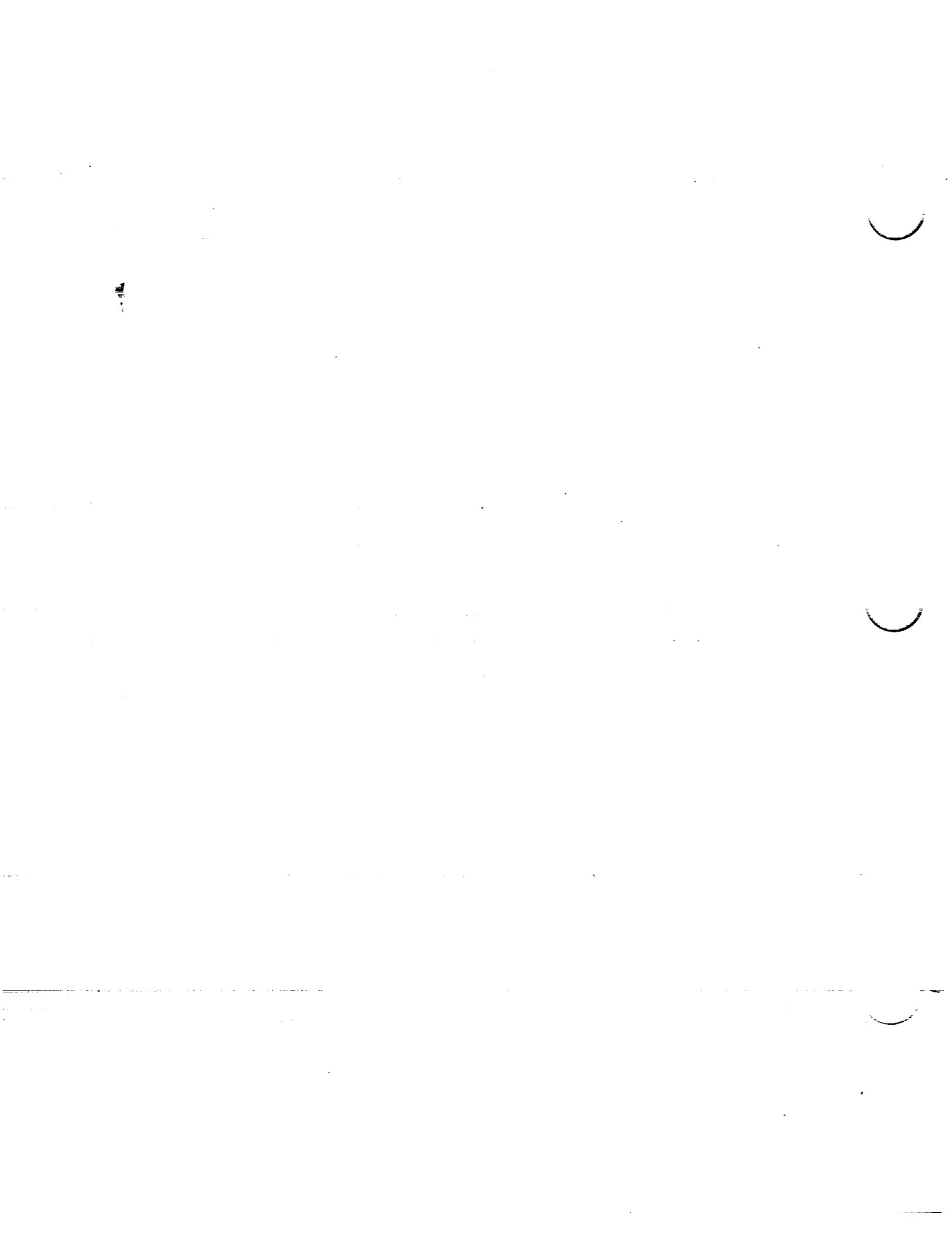
(percent \bar{x} c)	(percent \bar{y} c)	$(v/v)^2$	v/v	$\Delta v_u/v$
0	0	0	0	1.167
.5	-----	.397	.630	1.065
1.25	3.315	.787	.887	.946
2.5	4.576	1.182	1.087	.818
5	6.221	1.543	1.242	.648
7.5	7.350	1.682	1.297	.550
10	8.195	1.734	1.317	.478
15	9.354	1.756	1.325	.381
20	10.040	1.742	1.320	.320
25	10.397	1.706	1.306	.274
30	10.504	1.664	1.290	.238
40	10.156	1.538	1.240	.183
50	9.265	1.388	1.178	.142
60	7.986	1.284	1.133	.111
70	6.412	1.177	1.085	.084
80	4.591	1.055	1.027	.061
90	2.534	.916	.957	.037
95	1.412	.801	.895	.023
100	.221	0	0	0

L. E. radius: 4.85 percent c

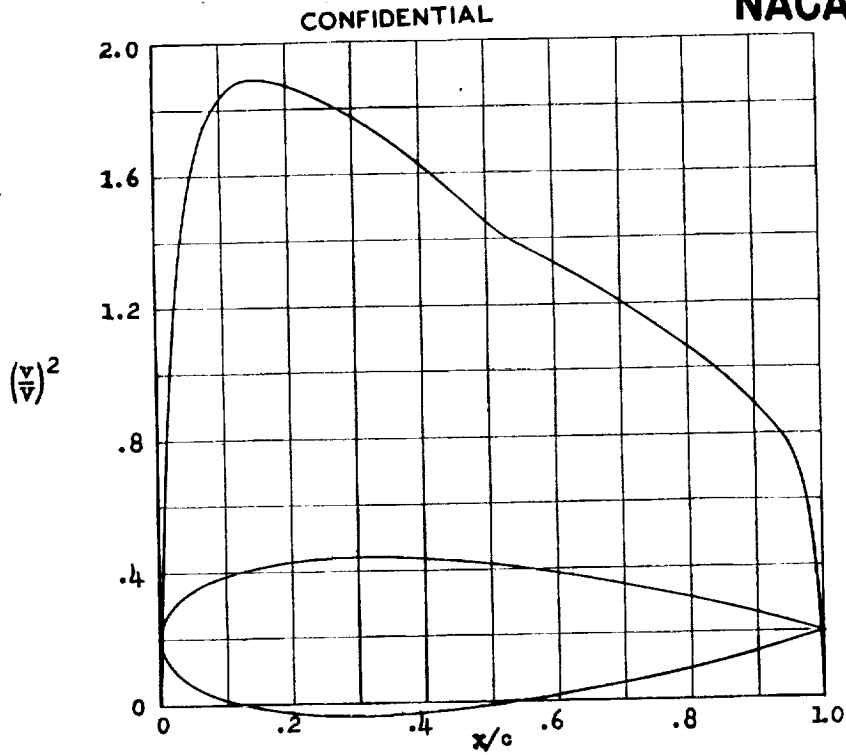
NACA 0021 basic thickness form

CONFIDENTIAL

NATIONAL ADVISORY
COMMITTEE FOR AERONAUTICS.



NACA 0024



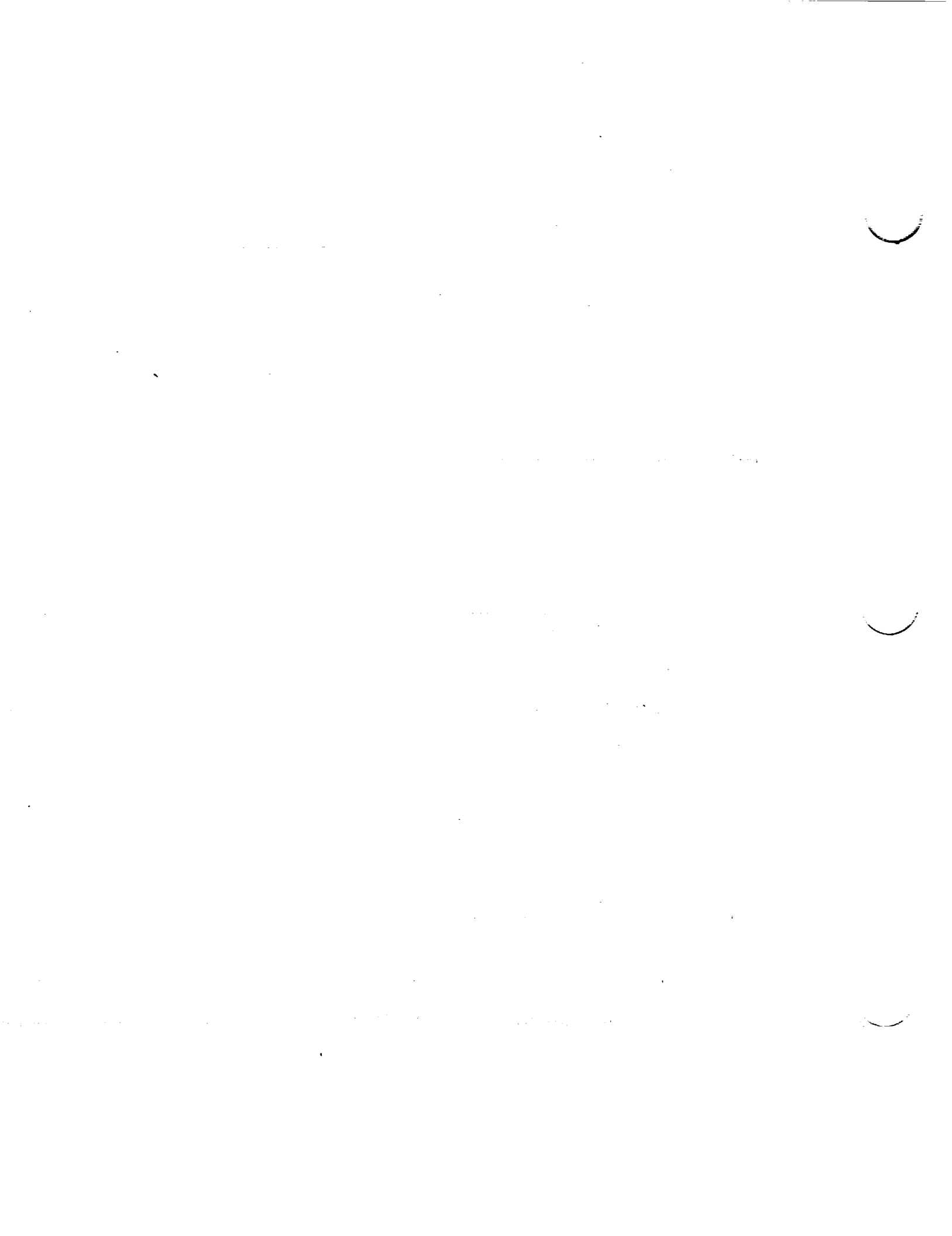
\bar{x} (percent c)	\bar{y} (percent c)	$(v/V)^2$	v/V	$\Delta v_a/V$
0	0	0	0	1.050
.5	-----	.335	.579	.964
1.25	3.788	.719	.848	.870
2.5	5.229	1.130	1.063	.771
5.0	7.109	1.548	1.244	.632
7.5	8.400	1.748	1.322	.542
10	9.365	1.833	1.354	.476
15	10.691	1.888	1.374	.383
20	11.475	1.871	1.368	.321
25	11.883	1.822	1.350	.274
30	12.004	1.777	1.333	.238
40	11.607	1.631	1.277	.181
50	10.588	1.450	1.204	.140
60	9.127	1.325	1.151	.109
70	7.328	1.203	1.097	.082
80	5.247	1.065	1.032	.059
90	2.896	.891	.944	.035
95	1.613	.773	.879	.022
100	.252	0	0	0

L. E. radius: 6.33 percent c

NACA 0024 basic thickness form

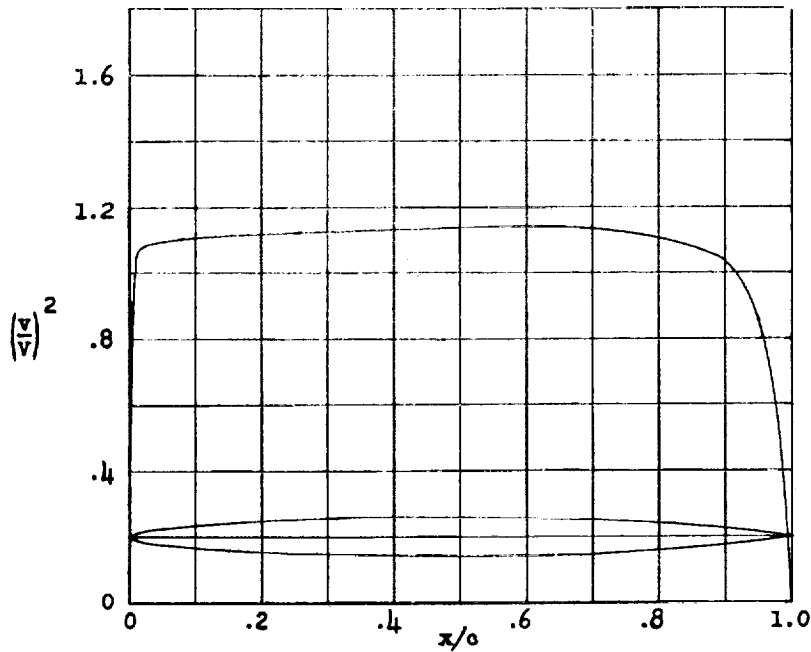
CONFIDENTIAL

NATIONAL ADVISORY
COMMITTEE FOR AERONAUTICS.



CONFIDENTIAL

NACA 16-006



x (percent c)	y (percent c)	(v/v) ²	v/v	Δv _a /V
0	0	0	0	5.471
1.25	.646	1.059	1.029	1.376
2.5	.903	1.085	1.042	.980
5.0	1.255	1.097	1.047	.689
7.5	1.516	1.105	1.051	.557
10	1.729	1.108	1.053	.476
15	2.067	1.112	1.055	.379
20	2.332	1.116	1.057	.319
30	2.709	1.123	1.060	.244
40	2.927	1.132	1.064	.196
50	3.000	1.137	1.066	.160
60	2.917	1.141	1.068	.130
70	2.635	1.132	1.064	.104
80	2.095	1.104	1.051	.077
90	1.259	1.035	1.017	.049
95	.707	.962	.981	.032
100	.060	0	0	0

L. B. radius: 0.176 percent c

NACA 16-006 basic thickness form

CONFIDENTIAL

NATIONAL ADVISORY
COMMITTEE FOR AERONAUTICS.

300-8 27 10

.....

.....

.....

.....

.....

.....

.....

.....

.....

.....

.....

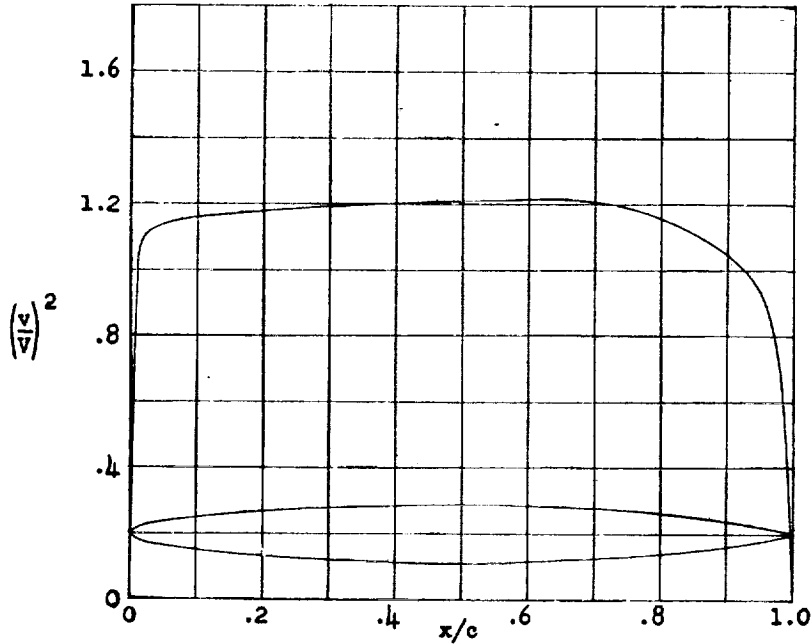
.....

.....

.....

CONFIDENTIAL

NACA 16-009



x (percent c)	y (percent c)	$(v/V)^2$	v/V	$\Delta v_a/V$
0	0	0	0	5.644
1.25	.969	1.042	1.021	1.330
2.5	1.354	1.109	1.053	.964
5.0	1.882	1.139	1.067	.684
7.5	2.274	1.152	1.073	.554
10	2.593	1.158	1.076	.475
15	3.101	1.168	1.081	.378
20	3.498	1.177	1.085	.319
30	4.063	1.190	1.091	.245
40	4.391	1.202	1.096	.197
50	4.500	1.211	1.100	.160
60	4.376	1.214	1.106	.131
70	3.952	1.206	1.099	.103
80	3.149	1.156	1.075	.076
90	1.888	1.043	1.022	.047
95	1.061	.939	.969	.030
100	.090	0	0	0

L. E. radius: 0.396 percent c

NACA 16-009 basic thickness form

CONFIDENTIAL

NATIONAL ADVISORY
COMMITTEE FOR AERONAUTICS.

1947

1948

1949

1950

1951

1952

1953

1954

1955

1956

1957

1958

1959

1960

1961

1962

1963

1964

1965

1966

1967

1968

1969

1970

1971

1972

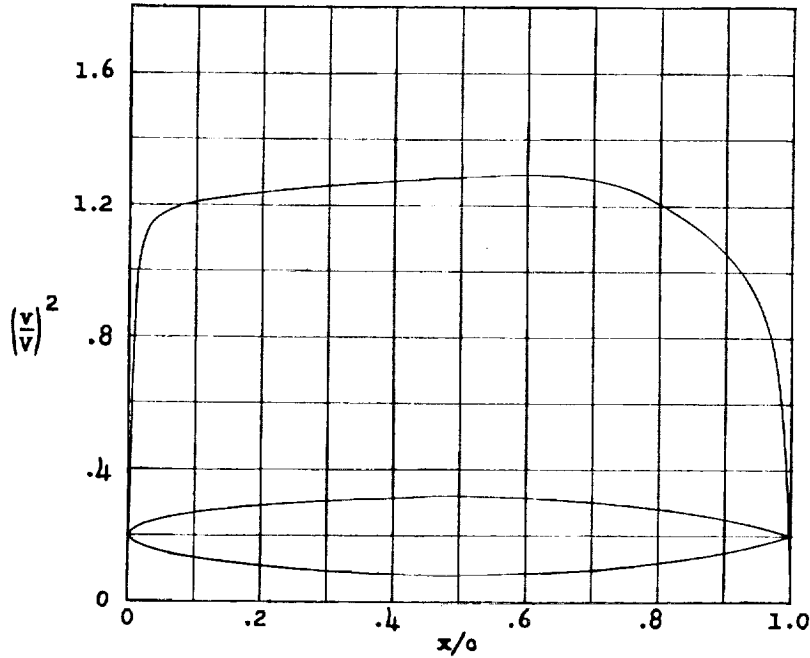
1973

1974

1975

CONFIDENTIAL

NACA 16-012



x (percent c)	y (percent c)	$(v/v)^2$	v/V	$\Delta v_a/V$
0	0	0	0	2.624
1.25	1.292	1.002	1.001	1.268
2.5	1.805	1.109	1.053	.942
5.0	2.509	1.173	1.083	.677
7.5	3.032	1.197	1.094	.551
10	3.457	1.208	1.099	.473
15	4.135	1.223	1.106	.378
20	4.664	1.237	1.112	.319
30	5.417	1.257	1.121	.245
40	5.855	1.271	1.128	.197
50	6.000	1.286	1.134	.161
60	5.835	1.293	1.137	.131
70	5.269	1.275	1.129	.102
80	4.199	1.203	1.097	.075
90	2.517	1.051	1.025	.045
95	1.415	.908	.953	.027
100	.120	0	0	0

L. E. radius: 0.703 percent c

NACA 16-012 basic thickness form

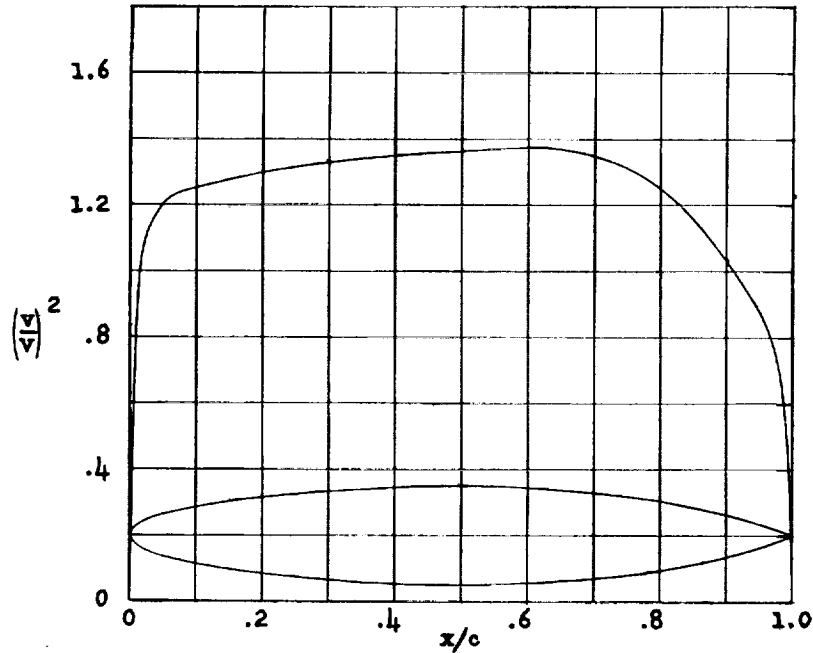
CONFIDENTIAL

NATIONAL ADVISORY
COMMITTEE FOR AERONAUTICS.



CONFIDENTIAL

NACA 16-015



\bar{x} (percent c)	\bar{y} (percent c)	$(v/v)^2$	v/V	$\Delta v_a/V$
0	0	0	0	2.041
1.25	1.615	.956	.978	1.209
2.5	2.257	1.105	1.051	.916
5.0	3.137	1.200	1.095	.668
7.5	3.790	1.239	1.113	.547
10	4.322	1.256	1.121	.471
15	5.168	1.278	1.130	.377
20	5.830	1.297	1.139	.318
30	6.772	1.327	1.152	.245
40	7.318	1.349	1.161	.197
50	7.500	1.364	1.168	.161
60	7.293	1.374	1.172	.131
70	6.587	1.348	1.161	.102
80	5.248	1.254	1.120	.074
90	3.147	1.053	1.026	.043
95	1.768	.875	.935	.025
100	.150	0	0	0

L. E. radius: 1.100 percent c

NACA 16-015 basic thickness form

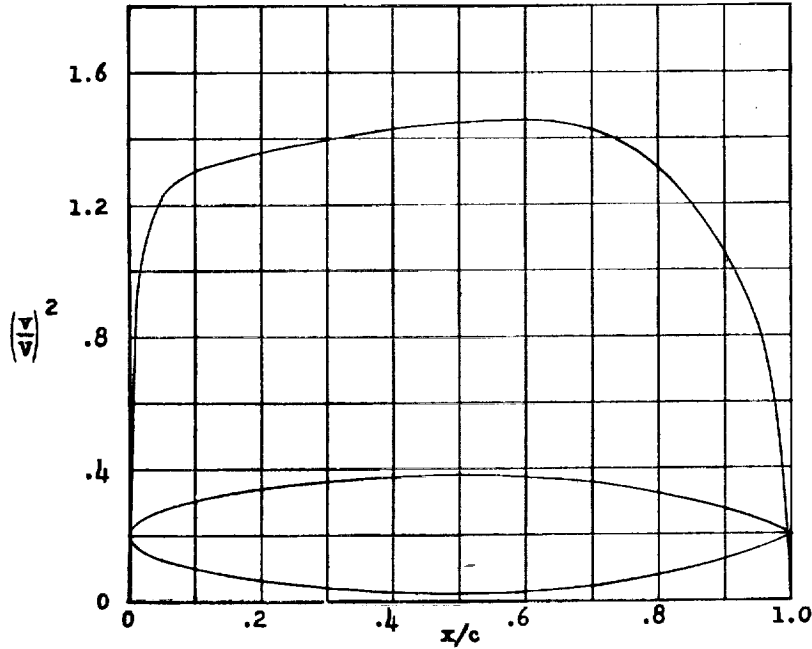
CONFIDENTIAL

NATIONAL ADVISORY
COMMITTEE FOR AERONAUTICS.



CONFIDENTIAL

NACA 16-018



x (percent c)	y (percent c)	$(v/v)^2$	v/v	$\Delta v_a/V$
0	0	0	0	1.744
1.25	1.938	.903	.950	1.140
2.5	2.708	1.092	1.045	.883
5.0	3.764	1.217	1.103	.657
7.5	4.548	1.271	1.128	.541
10	5.186	1.302	1.141	.468
15	6.202	1.332	1.154	.376
20	6.996	1.357	1.165	.318
30	8.126	1.399	1.183	.245
40	8.782	1.426	1.194	.198
50	9.000	1.447	1.203	.162
60	8.752	1.452	1.205	.131
70	7.904	1.421	1.192	.102
80	6.298	1.306	1.143	.073
90	3.776	1.051	1.025	.042
95	2.122	.837	.915	.024
100	.180	0	0	0

L. E. radius: 1.584 percent c

NACA 16-018 basic thickness form

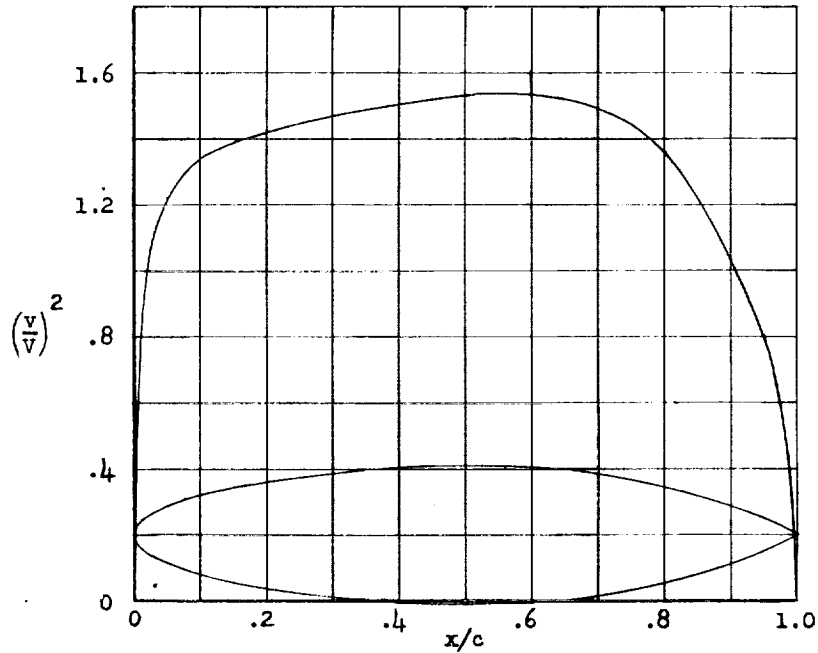
CONFIDENTIAL

NATIONAL ADVISORY
COMMITTEE FOR AERONAUTICS.



CONFIDENTIAL

NACA 16-021



x (percent c)	y (percent c)	$(v/V)^2$	v/V	$\Delta v_a/V$
0	0	0	0	1.574
1.25	2.261	.826	.909	1.069
2.5	3.159	1.062	1.031	.828
5.0	4.391	1.221	1.105	.640
7.5	5.306	1.295	1.138	.534
10	6.050	1.342	1.159	.463
15	7.236	1.391	1.179	.374
20	8.162	1.419	1.191	.317
30	9.480	1.474	1.214	.245
40	10.246	1.506	1.227	.198
50	10.500	1.535	1.239	.162
60	10.211	1.556	1.239	.131
70	9.221	1.495	1.223	.102
80	7.348	1.361	1.166	.072
90	4.405	1.039	1.019	.041
95	2.476	.801	.895	.023
100	.210	0	0	0

L. E. radius: 2.156 percent c

NACA 16-021 basic thickness form

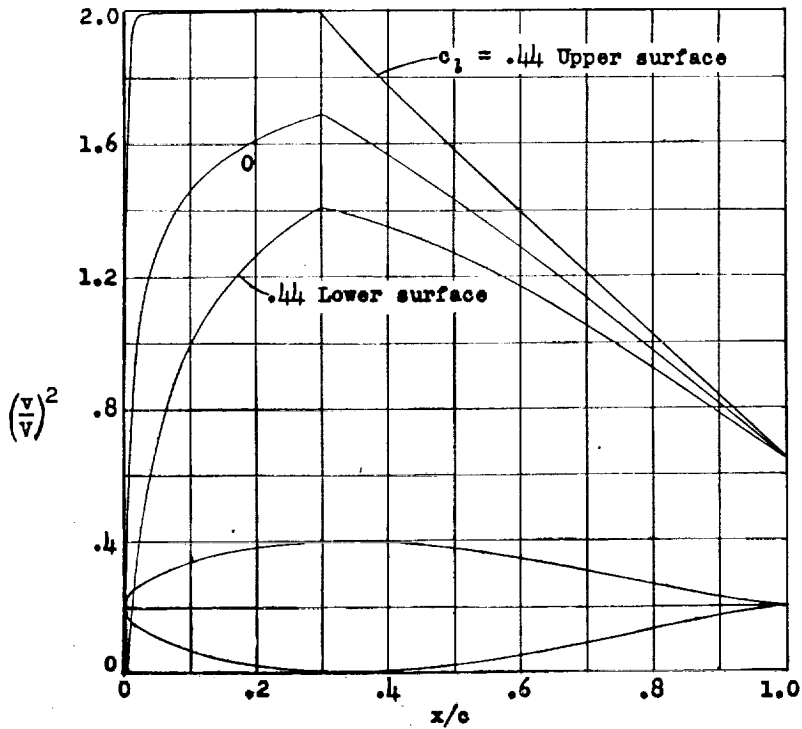
CONFIDENTIAL

NATIONAL ADVISORY
COMMITTEE FOR AERONAUTICS.



CONFIDENTIAL

NACA 63,4-020



x (percent c)	y (percent c)	(v/v) ²	v/v	Δv _a /v
0	0	0	0	1.395
.5	1.714	.444	.666	1.280
.75	2.081	.605	.778	1.201
1.25	2.638	.820	.906	1.072
2.5	3.606	1.080	1.039	.846
5.0	4.947	1.277	1.130	.645
7.5	5.964	1.383	1.176	.543
10	6.800	1.456	1.207	.475
15	8.090	1.551	1.245	.386
20	9.006	1.614	1.270	.330
25	9.630	1.659	1.288	.289
30	9.955	1.689	1.300	.257
35	9.978	1.630	1.277	.219
40	9.765	1.567	1.252	.192
45	9.366	1.500	1.225	.169
50	8.819	1.433	1.197	.148
55	8.143	1.362	1.167	.128
60	7.351	1.288	1.135	.112
65	6.464	1.213	1.101	.097
70	5.496	1.137	1.066	.084
75	4.466	1.059	1.029	.071
80	3.401	.978	.989	.059
85	2.342	.896	.947	.046
90	1.348	.811	.901	.036
95	.501	.728	.853	.023
100	0	.651	.807	0

L. E. radius: 3.16 percent c

NACA 63,4-020 basic thickness form

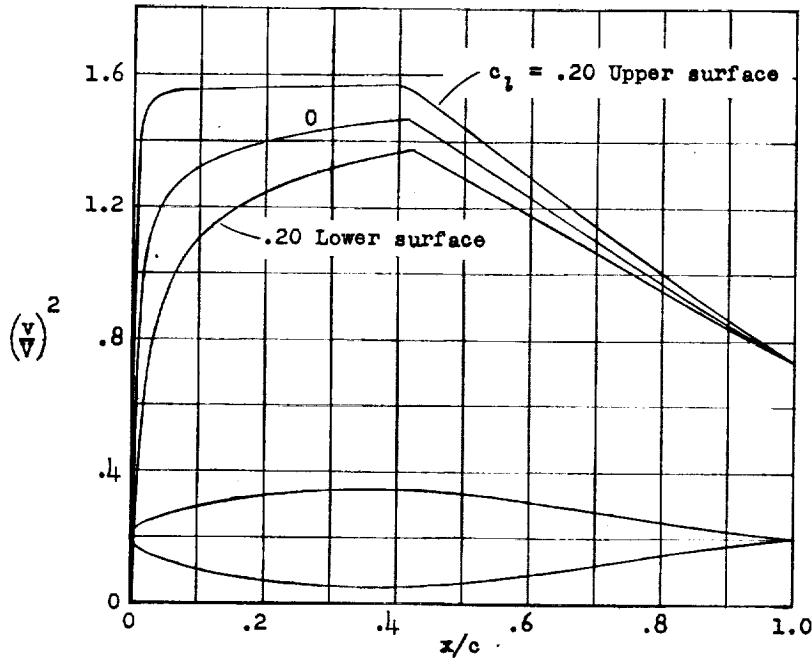
CONFIDENTIAL

NATIONAL ADVISORY
COMMITTEE FOR AERONAUTICS.



CONFIDENTIAL

NACA 64,2-015



x (percent c)	y (percent c)	$(v/V)^2$	v/V	$\Delta v_a/V$
0	0	0	0	1.930
.5	1.216	.710	.843	1.500
.75	1.453	.825	.908	1.359
1.25	1.829	.962	.981	1.161
2.5	2.538	1.122	1.059	.911
5.0	3.514	1.234	1.111	.678
7.5	4.243	1.288	1.135	.553
10	4.838	1.323	1.150	.477
15	5.781	1.371	1.171	.383
20	6.464	1.401	1.184	.325
25	6.967	1.422	1.192	.285
30	7.307	1.441	1.200	.253
35	7.481	1.458	1.207	.227
40	7.480	1.471	1.213	.202
45	7.268	1.432	1.197	.175
50	6.850	1.366	1.169	.156
55	6.311	1.299	1.140	.137
60	5.670	1.234	1.111	.122
65	4.944	1.168	1.081	.102
70	4.158	1.102	1.050	.086
75	3.338	1.039	1.019	.080
80	2.506	.973	.986	.071
85	1.698	.910	.954	.056
90	.961	.849	.921	.039
95	.351	.791	.889	.027
100	0	.739	.860	0

L. E. radius: 1.65 percent c

NACA 64,2-015 basic thickness form

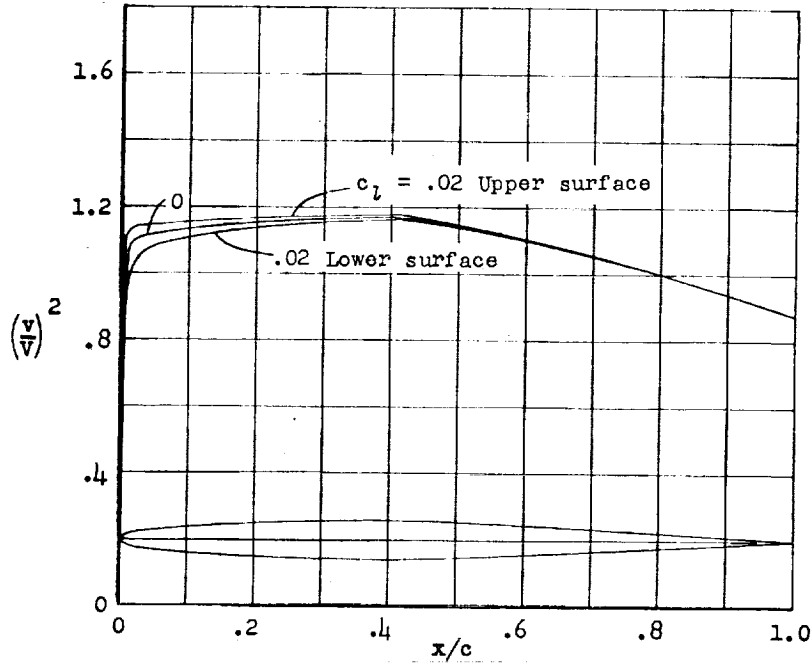
CONFIDENTIAL

NATIONAL ADVISORY
COMMITTEE FOR AERONAUTICS.



NACA 64₁-006

CONFIDENTIAL



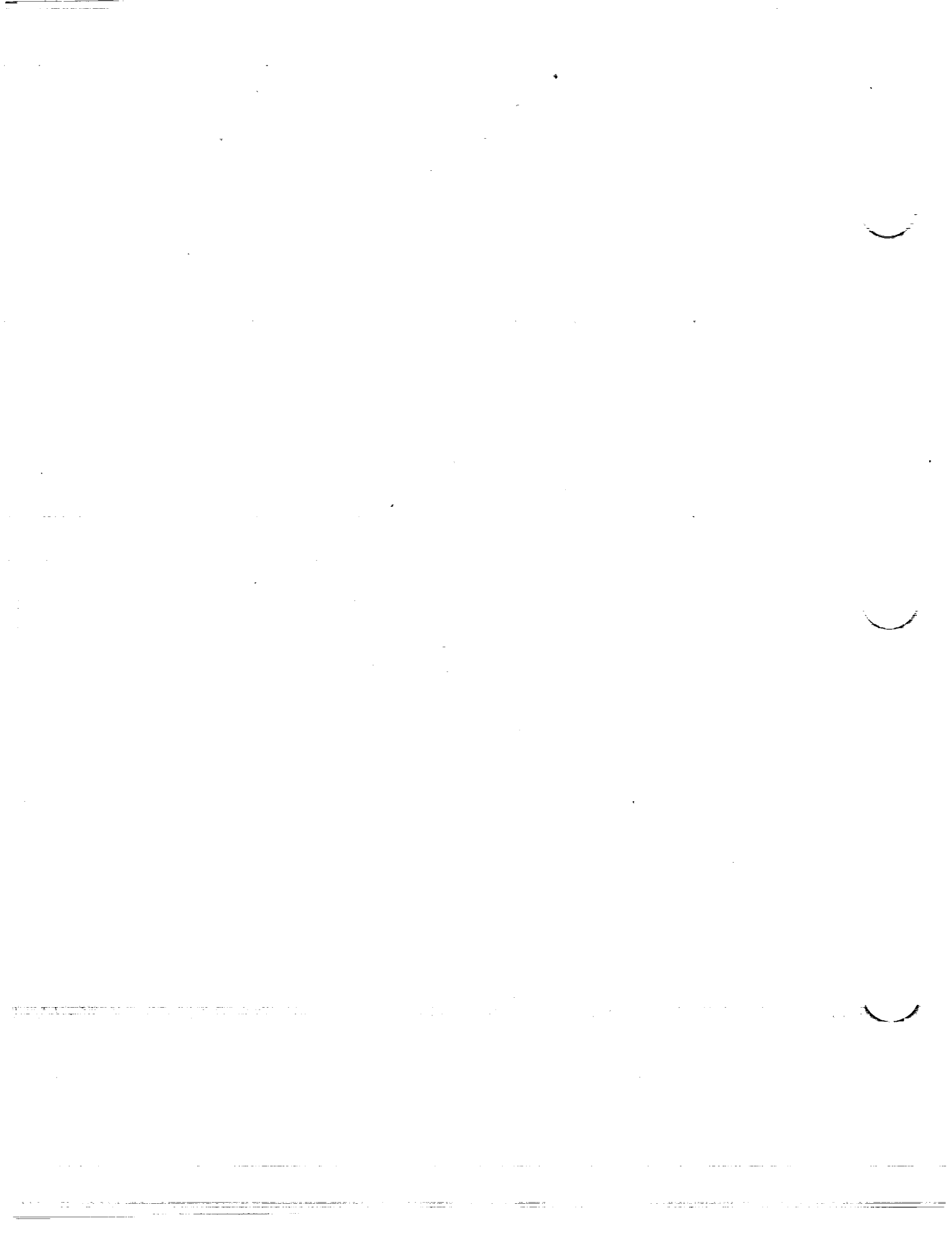
x (percent c)	y (percent c)	$(v/v)^2$	v/v	$\Delta v_a/V$
0	0	0	0	4.623
.5	.494	.995	.997	2.175
.75	.596	1.058	1.029	1.780
1.25	.754	1.085	1.042	1.418
2.5	1.024	1.108	1.053	.982
5.0	1.405	1.119	1.058	.692
7.5	1.692	1.128	1.062	.560
10	1.928	1.134	1.065	.483
15	2.298	1.146	1.071	.385
20	2.572	1.154	1.074	.321
25	2.772	1.160	1.077	.279
30	2.907	1.164	1.079	.246
35	2.981	1.168	1.081	.220
40	2.995	1.171	1.082	.198
45	2.919	1.160	1.077	.178
50	2.775	1.143	1.069	.158
55	2.575	1.124	1.060	.142
60	2.331	1.102	1.050	.126
65	2.050	1.079	1.039	.112
70	1.740	1.054	1.027	.098
75	1.412	1.028	1.014	.085
80	1.072	1.000	1.000	.072
85	.737	.970	.985	.060
90	.423	.939	.969	.047
95	.157	.908	.953	.031
100	0	.876	.936	0

L.E. radius: 0.256 percent c

NACA 64₁-006 basic thickness form

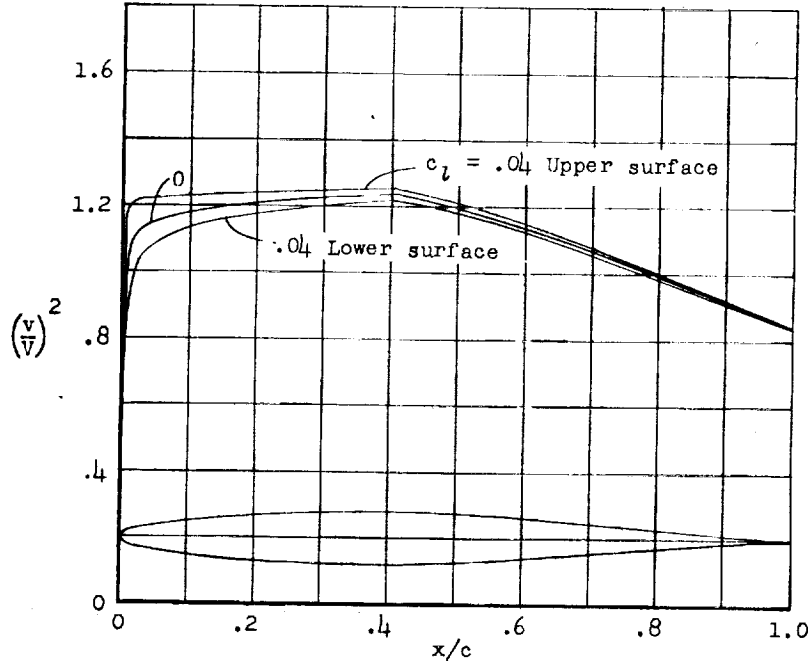
CONFIDENTIAL

NATIONAL ADVISORY
COMMITTEE FOR AERONAUTICS



CONFIDENTIAL

NACA 64₁-008



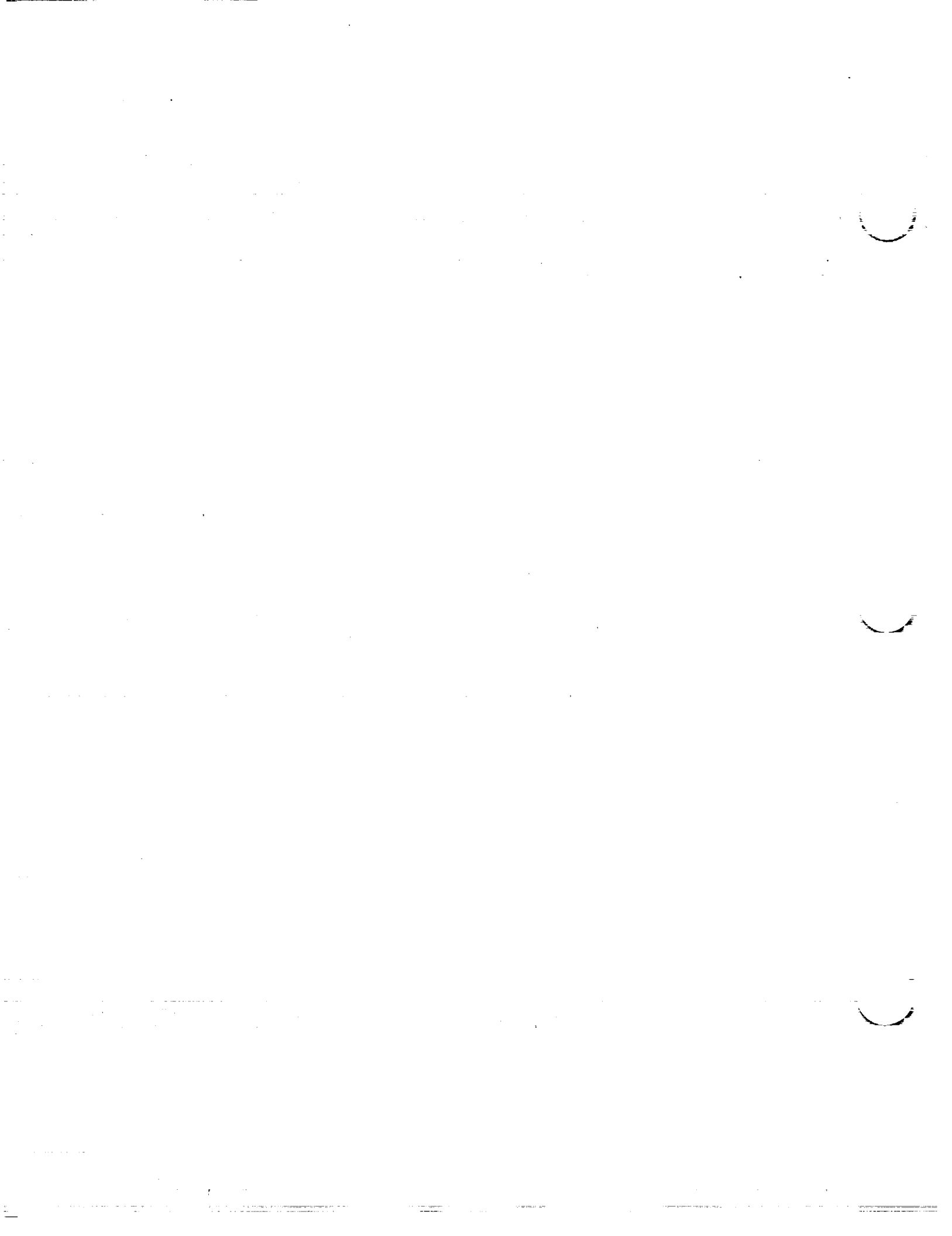
x (percent c)	y (percent c)	(v/v) ²	v/v	Δv _a /V
0	0	0	0	3.544
.5	.658	.912	.955	1.994
.75	.794	1.016	1.008	1.686
1.25	1.005	1.084	1.041	1.367
2.5	1.365	1.127	1.062	.969
5.0	1.875	1.152	1.073	.688
7.5	2.259	1.167	1.080	.560
10	2.574	1.179	1.086	.480
15	3.069	1.195	1.093	.385
20	3.437	1.208	1.099	.323
25	3.704	1.217	1.103	.279
30	3.884	1.225	1.107	.246
35	3.979	1.230	1.109	.220
40	3.992	1.235	1.111	.198
45	3.983	1.220	1.105	.176
50	3.684	1.191	1.091	.158
55	3.411	1.163	1.078	.141
60	3.081	1.133	1.064	.125
65	2.704	1.102	1.050	.110
70	2.291	1.069	1.034	.096
75	1.854	1.033	1.016	.083
80	1.404	.995	.997	.071
85	.961	.957	.978	.059
90	.550	.918	.958	.046
95	.206	.878	.937	.031
100	0	.839	.915	0

L.E. radius: 0.155 percent c

NACA 64₁-008 basic thickness form

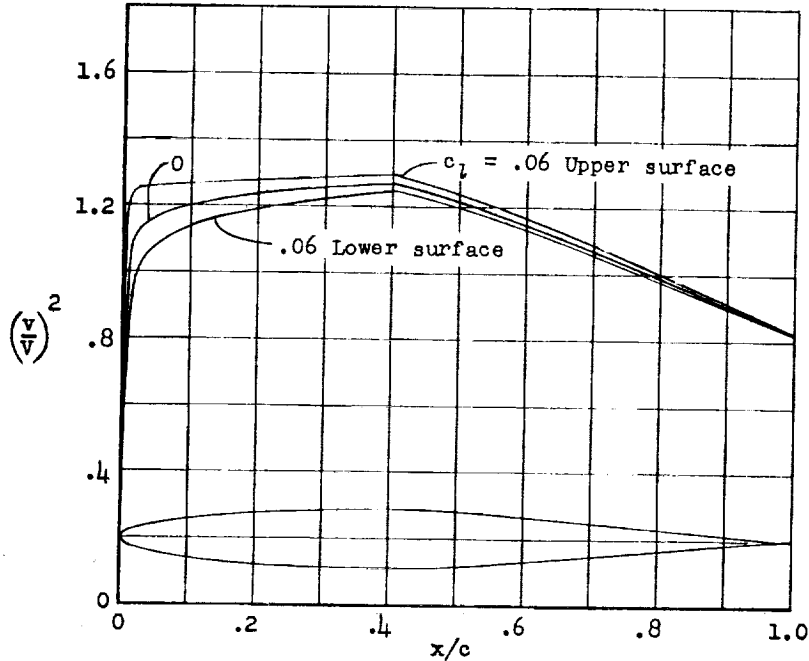
CONFIDENTIAL

NATIONAL ADVISORY
COMMITTEE FOR AERONAUTICS



CONFIDENTIAL

NACA 64₁-009



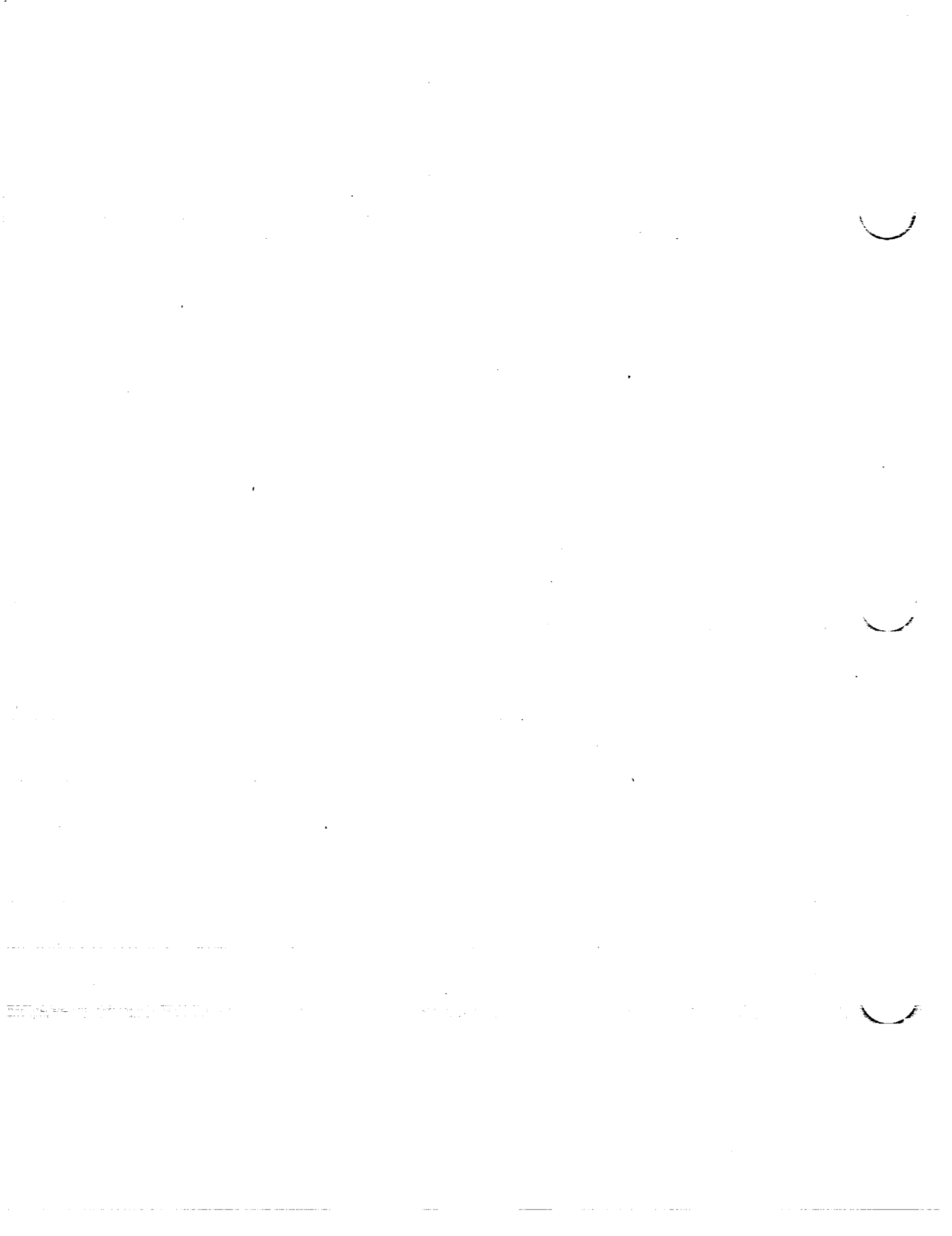
x (percent c)	y (percent c)	(v/v) ²	v/v	Δv _R /V
0	0	0	0	3.130
.5	.739	.872	.934	1.905
.75	.892	.990	.995	1.637
1.25	1.128	1.075	1.037	1.340
2.5	1.533	1.131	1.063	.963
5.0	2.109	1.166	1.080	.686
7.5	2.543	1.186	1.089	.560
10	2.898	1.200	1.095	.479
15	3.455	1.221	1.105	.383
20	3.868	1.236	1.112	.323
25	4.170	1.246	1.116	.281
30	4.373	1.255	1.120	.248
35	4.479	1.262	1.123	.221
40	4.490	1.267	1.126	.198
45	4.364	1.246	1.116	.176
50	4.136	1.217	1.103	.158
55	3.826	1.183	1.088	.140
60	3.452	1.149	1.072	.125
65	3.026	1.112	1.055	.109
70	2.561	1.073	1.036	.095
75	2.069	1.033	1.016	.082
80	1.564	.992	.996	.070
85	1.069	.950	.975	.057
90	.611	.907	.952	.044
95	.227	.865	.930	.030
100	0	.822	.907	0

L.E. radius: 0.579 percent c

NACA 64₁-009 basic thickness form

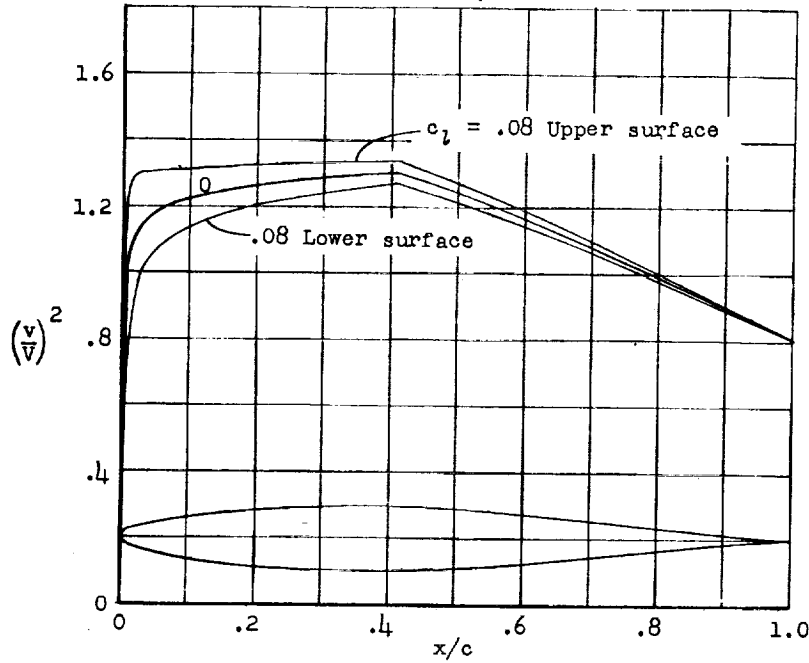
CONFIDENTIAL

NATIONAL ADVISORY
COMMITTEE FOR AERONAUTICS.



CONFIDENTIAL

NACA 64₁-010



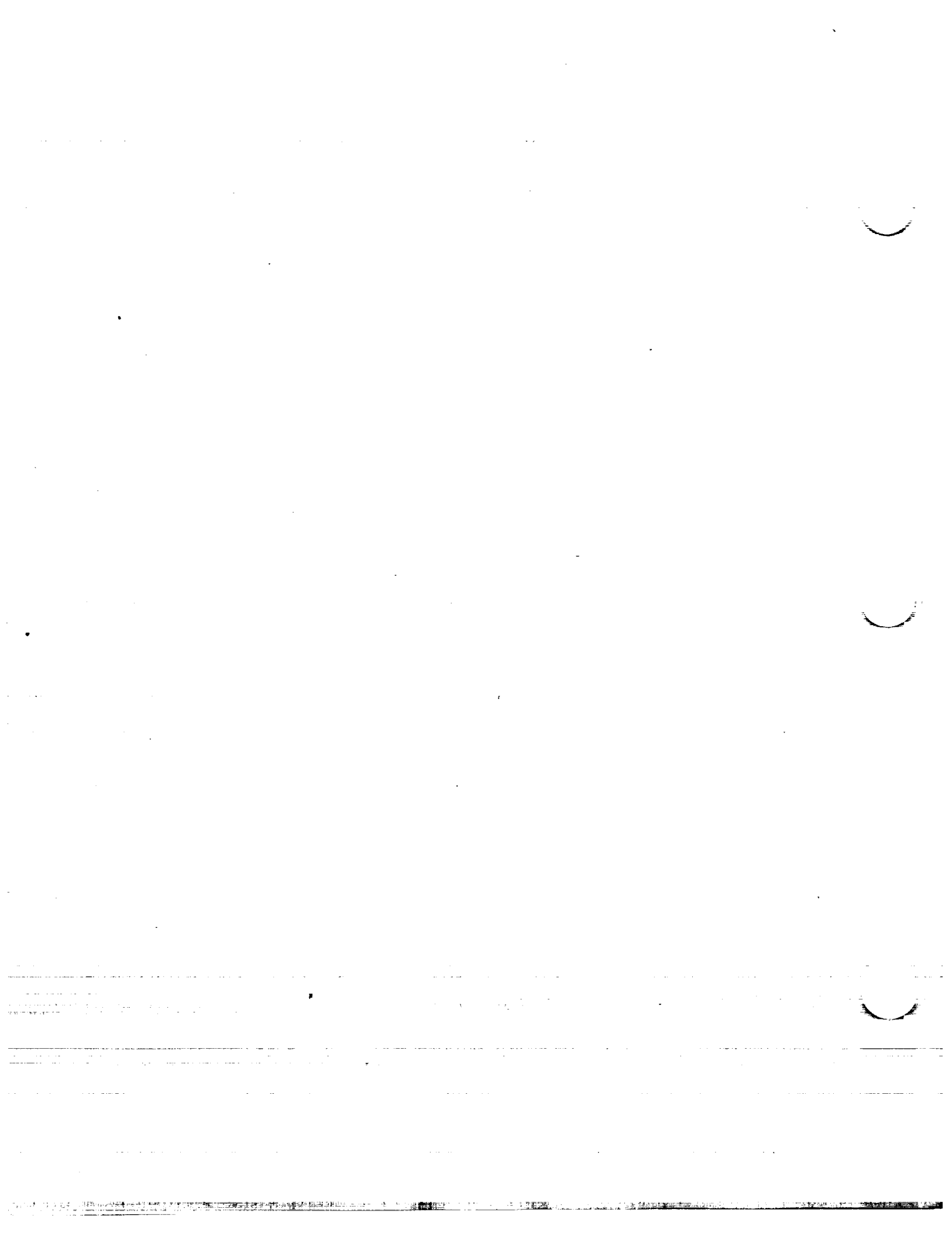
\bar{x} (percent c)	\bar{y} (percent c)	$(v/V)^2$	v/V	$\Delta v_a/V$
0	0	0	0	2.815
.5	.820	.834	.913	1.817
.75	.989	.962	.981	1.586
1.25	1.250	1.061	1.030	1.313
2.5	1.701	1.130	1.063	.957
5	2.343	1.181	1.087	.684
7.5	2.826	1.206	1.098	.559
10	3.221	1.221	1.105	.480
15	3.842	1.245	1.116	.386
20	4.302	1.262	1.123	.325
25	4.639	1.275	1.129	.280
30	4.864	1.286	1.134	.246
35	4.980	1.295	1.138	.220
40	4.988	1.300	1.140	.199
45	4.843	1.279	1.131	.176
50	4.586	1.241	1.114	.158
55	4.238	1.201	1.096	.139
60	3.820	1.161	1.077	.124
65	3.345	1.120	1.058	.109
70	2.827	1.080	1.039	.095
75	2.281	1.036	1.018	.081
80	1.722	.990	.995	.069
85	1.176	.944	.972	.057
90	.671	.900	.949	.044
95	.248	.850	.922	.030
100	0	.805	.897	0

L.E. radius: 0.720 percent c

NACA 64₁-010 basic thickness form

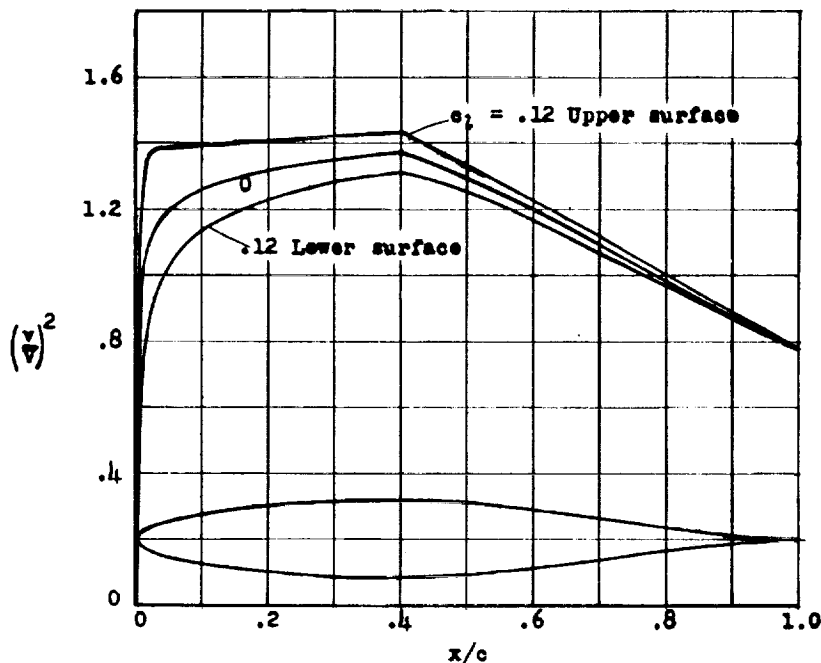
NATIONAL ADVISORY
COMMITTEE FOR AERONAUTICS

CONFIDENTIAL



NACA 64₁-012

CONFIDENTIAL



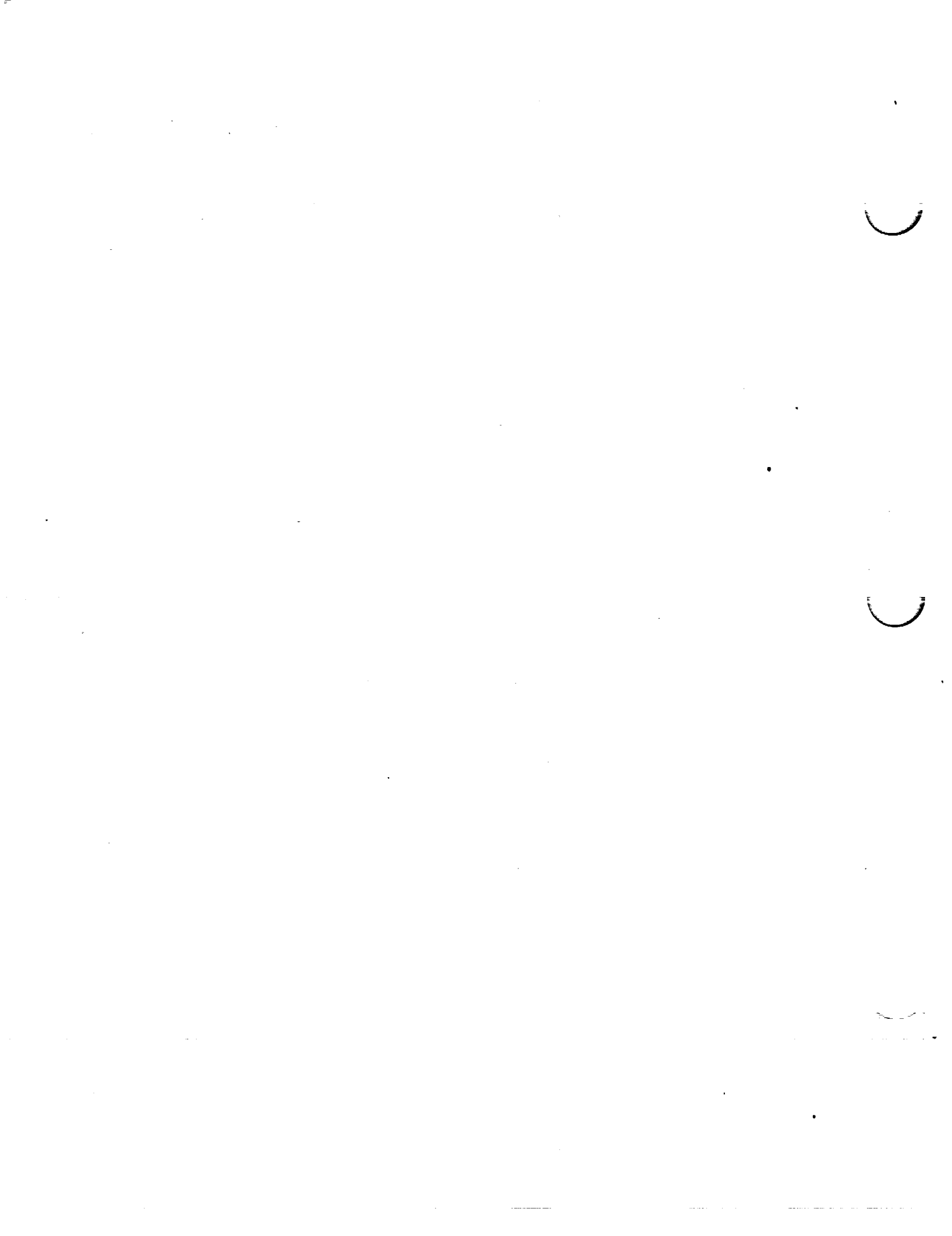
x (percent c)	y (percent c)	$(v/v)^2$	v/v	$\Delta v_e/v$
0	0	0	0	2.379
.5	.978	.750	.866	1.663
.75	1.179	.885	.941	1.508
1.25	1.490	1.020	1.010	1.271
2.5	2.035	1.129	1.063	.943
5.0	2.810	1.204	1.097	.685
7.5	3.394	1.240	1.114	.559
10	3.871	1.264	1.124	.482
15	4.620	1.296	1.139	.388
20	5.173	1.320	1.149	.328
25	5.576	1.338	1.156	.281
30	5.844	1.351	1.162	.247
35	5.978	1.362	1.167	.221
40	5.981	1.372	1.171	.199
45	5.798	1.335	1.156	.177
50	5.480	1.289	1.136	.158
55	5.056	1.243	1.115	.138
60	4.548	1.195	1.093	.122
65	3.974	1.144	1.070	.103
70	3.350	1.091	1.044	.088
75	2.695	1.037	1.018	.074
80	2.029	.981	.990	.063
85	1.382	.928	.963	.052
90	.786	.874	.935	.045
95	.288	.825	.908	.028
100	0	.775	.880	0

L. E. radius: 1.040 percent c

NACA 64₁-012 basic thickness form

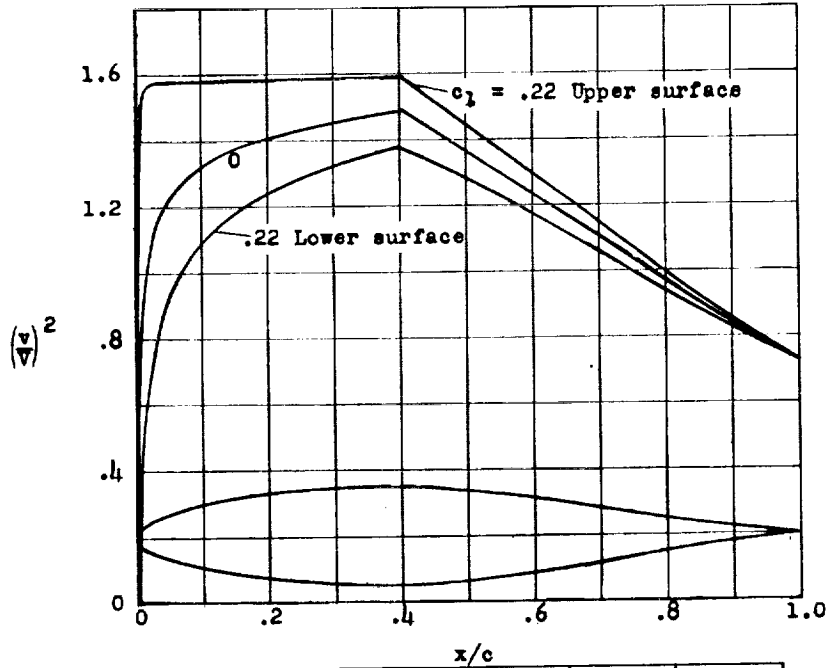
CONFIDENTIAL

NATIONAL ADVISORY
COMMITTEE FOR AERONAUTICS.



NACA 64₂-015

CONFIDENTIAL



\bar{x} (percent c)	\bar{y} (percent c)	$(v/v)^2$	v/v	$\Delta v_a/v$
0	0	0	0	1.939
.5	1.208	.670	.819	1.476
.75	1.456	.762	.873	1.354
1.25	1.842	.896	.947	1.188
2.5	2.528	1.113	1.055	.916
5.0	3.504	1.231	1.109	.670
7.5	4.240	1.284	1.133	.559
10	4.842	1.323	1.150	.482
15	5.785	1.375	1.172	.389
20	6.480	1.410	1.187	.326
25	6.985	1.434	1.198	.285
30	7.319	1.454	1.206	.250
35	7.482	1.470	1.213	.225
40	7.473	1.485	1.218	.202
45	7.224	1.426	1.195	.179
50	6.810	1.365	1.168	.158
55	6.266	1.300	1.140	.135
60	5.620	1.233	1.110	.121
65	4.895	1.167	1.080	.105
70	4.113	1.101	1.049	.090
75	3.296	1.033	1.016	.078
80	2.472	.967	.983	.065
85	1.677	.902	.950	.054
90	.950	.841	.917	.041
95	.546	.785	.886	.031
100	0	.730	.855	0

L. E. radius: 1.590 percent c

NACA 64₂-015 basic thickness form

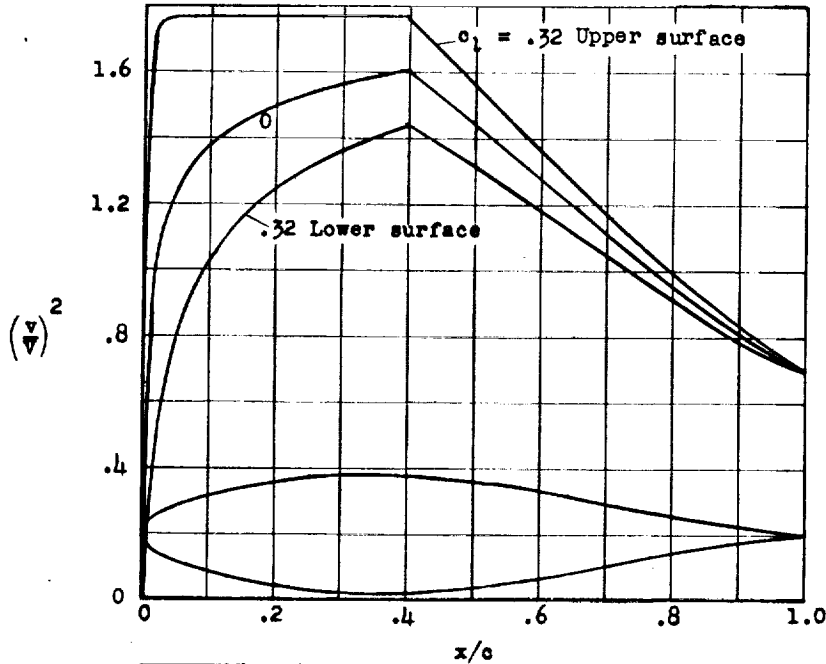
CONFIDENTIAL

NATIONAL ADVISORY
COMMITTEE FOR AERONAUTICS.



NACA 64₃-018

CONFIDENTIAL



x (percent c)	y (percent c)	$(v/V)^2$	v/V	$\Delta v_e/V$
0	0	0	0	1.646
.5	1.428	.546	.739	1.360
.75	1.720	.705	.840	1.269
1.25	2.177	.862	.920	1.128
2.5	3.005	1.079	1.039	.904
5.0	4.186	1.244	1.115	.669
7.5	5.076	1.327	1.152	.558
10	5.803	1.380	1.175	.486
15	6.942	1.450	1.204	.391
20	7.782	1.497	1.224	.331
25	8.391	1.535	1.239	.288
30	8.789	1.562	1.250	.255
35	8.979	1.585	1.259	.228
40	8.952	1.600	1.265	.200
45	8.630	1.518	1.232	.177
50	8.114	1.436	1.198	.154
55	7.445	1.354	1.164	.134
60	6.658	1.272	1.128	.117
65	5.782	1.190	1.091	.102
70	4.842	1.109	1.053	.088
75	3.866	1.028	1.014	.074
80	2.888	.952	.976	.063
85	1.951	.879	.937	.051
90	1.101	.812	.901	.039
95	.400	.747	.864	.027
100	0	.695	.834	0

L. E. radius: 2.208 percent c

NACA 64₃-018 basic thickness form

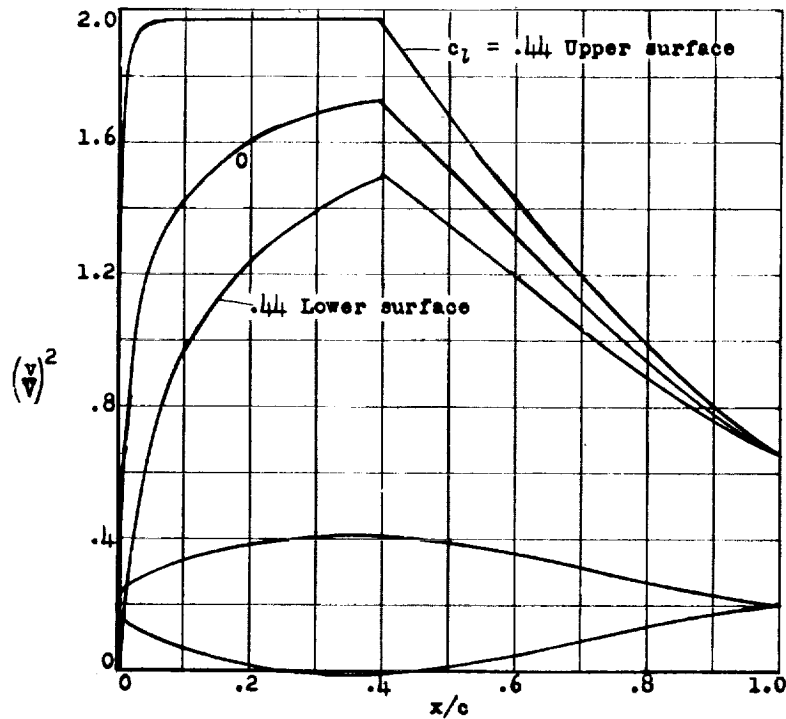
CONFIDENTIAL

NATIONAL ADVISORY
COMMITTEE FOR AERONAUTICS.



NACA 64₄-021

CONFIDENTIAL



x (percent c)	y (percent c)	(v/v) ²	v/v	Δv _a /v
0	0	0	0	1.458
.5	1.646	.462	.680	1.274
.75	1.985	.603	.776	1.203
1.25	2.517	.759	.871	1.084
2.5	3.485	1.010	1.005	.878
5.0	4.871	1.248	1.117	.665
7.5	5.915	1.358	1.165	.557
10	6.769	1.431	1.196	.486
15	8.108	1.527	1.236	.395
20	9.095	1.593	1.262	.335
25	9.807	1.654	1.281	.293
30	10.269	1.681	1.297	.259
35	10.481	1.712	1.308	.232
40	10.431	1.709	1.307	.202
45	10.030	1.607	1.268	.178
50	9.404	1.507	1.228	.155
55	8.607	1.406	1.186	.134
60	7.678	1.307	1.143	.116
65	6.649	1.209	1.099	.099
70	5.549	1.112	1.055	.084
75	4.416	1.020	1.010	.071
80	3.287	.932	.965	.059
85	2.213	.851	.923	.047
90	1.245	.778	.882	.036
95	.449	.711	.844	.022
100	0	.653	.808	0

L. E. radius: 2.884 percent c

NACA 64₄-021 basic thickness form

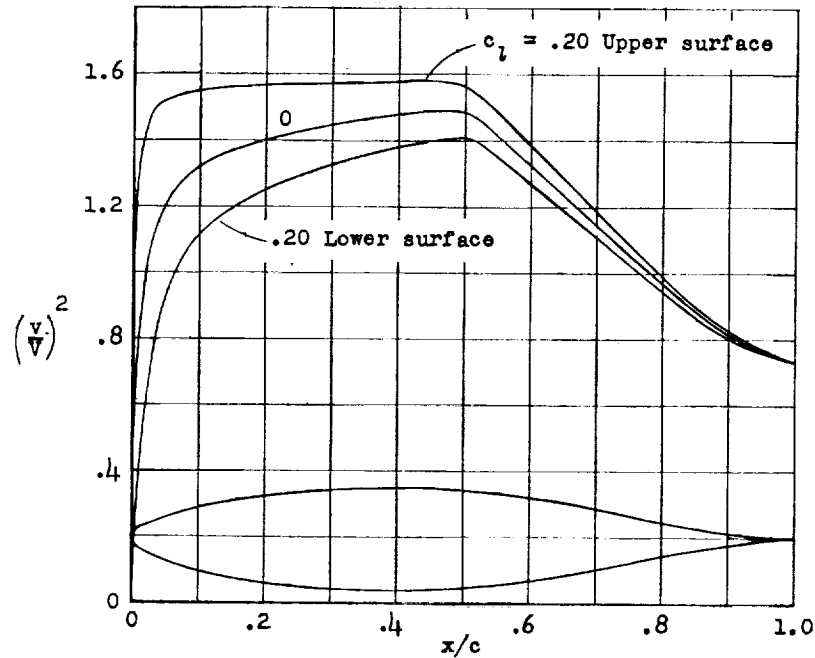
CONFIDENTIAL

NATIONAL ADVISORY
COMMITTEE FOR AERONAUTICS.



CONFIDENTIAL

NACA 65,2-016



x (percent c)	y (percent c)	(v/V) ²	v/V	Δv _a /V
0	0	0	0	1.950
.5	1.202	.560	.748	1.650
.75	1.423	.690	.831	1.500
1.25	1.796	.842	.918	1.275
2.5	2.507	1.068	1.033	.920
5.0	3.543	1.217	1.103	.680
7.5	4.316	1.287	1.134	.545
10	4.954	1.328	1.152	.480
15	5.958	1.379	1.174	.390
20	6.701	1.409	1.187	.325
25	7.252	1.433	1.197	.285
30	7.645	1.453	1.205	.255
35	7.892	1.469	1.212	.225
40	7.995	1.484	1.218	.200
45	7.938	1.497	1.224	.180
50	7.672	1.491	1.221	.160
55	7.184	1.421	1.192	.140
60	6.495	1.328	1.152	.125
65	5.647	1.235	1.111	.110
70	4.713	1.147	1.071	.095
75	3.738	1.056	1.028	.080
80	2.759	.970	.985	.066
85	1.817	.886	.941	.050
90	.982	.816	.903	.040
95	.340	.769	.877	.025
100	0	.733	.856	0

L. E. radius: 1.704 percent c

NACA 65,2-016 basic thickness form

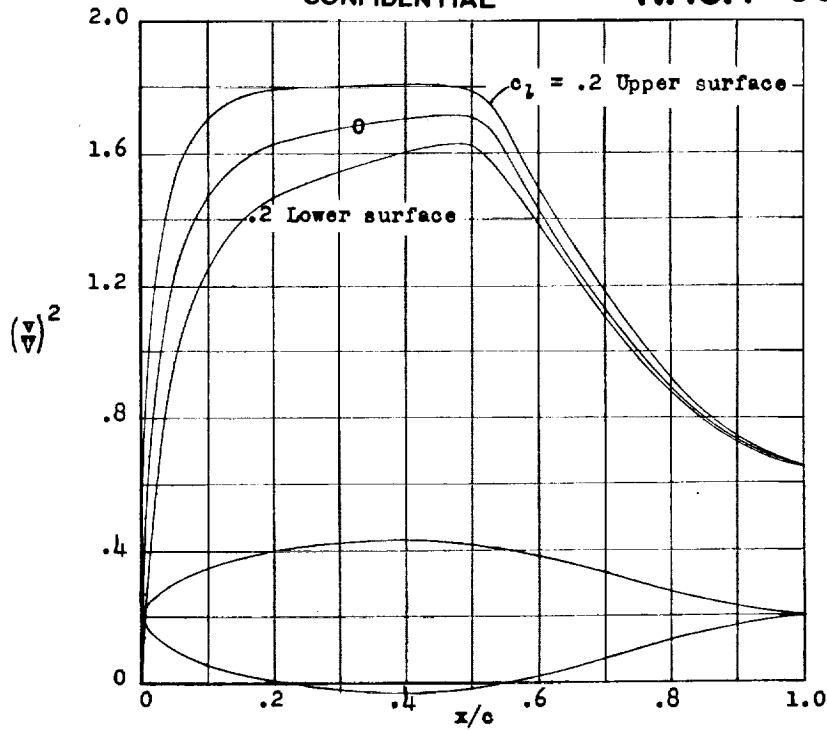
CONFIDENTIAL

NATIONAL ADVISORY
COMMITTEE FOR AERONAUTICS.



CONFIDENTIAL

NACA 65,2-023



(percent c)	(percent c)	$(v/v)^2$	v/v	$\Delta v_a/v$
0	0	0	0	1.414
.5	1.664	.400	.632	1.161
.75	2.040	.500	.707	1.084
1.25	2.628	.682	.826	.967
2.5	3.715	.943	.971	.811
5.0	5.300	1.232	1.110	.633
7.5	6.478	1.375	1.173	.539
10	7.433	1.467	1.211	.479
15	8.889	1.577	1.256	.380
20	9.917	1.628	1.276	.324
25	10.648	1.655	1.286	.281
30	11.142	1.677	1.295	.247
35	11.423	1.694	1.302	.220
40	11.499	1.708	1.307	.198
45	11.361	1.716	1.310	.178
50	10.949	1.712	1.308	.161
55	10.179	1.606	1.267	.147
60	9.108	1.428	1.195	.110
65	7.848	1.274	1.129	.096
70	6.461	1.135	1.065	.093
75	5.015	1.003	1.001	.080
80	3.618	.893	.945	.053
85	2.345	.803	.896	.035
90	1.258	.732	.856	.022
95	.439	.682	.826	.018
100	0	.651	.807	0

L. E. radius: 2.955 percent c

NACA 65,2-023 basic thickness form

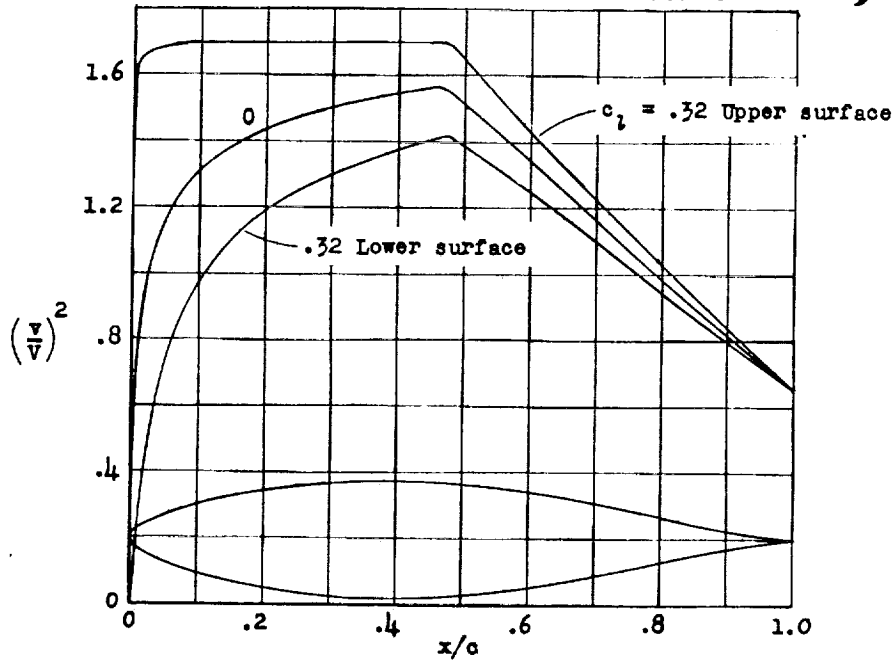
CONFIDENTIAL

NATIONAL ADVISORY
COMMITTEE FOR AERONAUTICS.



CONFIDENTIAL

NACA 65,3-018



x (percent c)	y (percent c)	$(v/v)^2$	v/v	$\Delta v_a/V$
0	0	0	0	1.750
.5	1.324	.650	.806	1.387
.75	1.599	.750	.866	1.268
1.25	2.004	.872	.934	1.108
2.5	2.728	1.020	1.010	.890
5.0	3.831	1.179	1.086	.677
7.5	4.701	1.263	1.124	.568
10	5.424	1.320	1.149	.489
15	6.568	1.393	1.180	.395
20	7.434	1.439	1.200	.334
25	8.093	1.473	1.214	.292
30	8.568	1.502	1.226	.260
35	8.868	1.526	1.235	.232
40	8.990	1.546	1.243	.209
45	8.916	1.562	1.250	.186
50	8.593	1.513	1.230	.165
55	8.045	1.433	1.197	.142
60	7.317	1.348	1.161	.123
65	6.450	1.258	1.122	.107
70	5.486	1.169	1.081	.093
75	4.456	1.079	1.039	.080
80	3.390	.992	.996	.066
85	2.325	.905	.951	.054
90	1.524	.818	.904	.040
95	.492	.738	.859	.024
100	0	.658	.811	0

L. E. radius: 1.92 percent c

NACA 65,3-018 basic thickness form

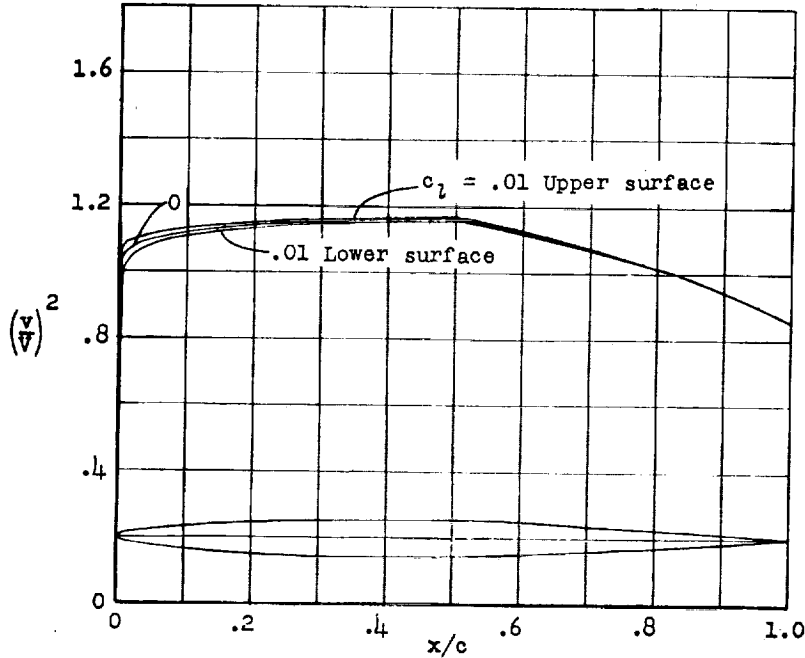
CONFIDENTIAL

NATIONAL ADVISORY
COMMITTEE FOR AERONAUTICS.



CONFIDENTIAL

NACA 65₁-006



x (percent c)	y (percent c)	(v/v) ²	v/v	Δv _a /V
0	0	0	0	4.815
.5	.476	1.044	1.022	2.110
.75	.574	1.055	1.027	1.780
1.25	.717	1.063	1.031	1.390
2.5	.956	1.081	1.040	.965
5.0	1.310	1.100	1.049	.695
7.5	1.589	1.112	1.055	.560
10	1.824	1.120	1.058	.474
15	2.197	1.134	1.065	.381
20	2.482	1.143	1.069	.322
25	2.697	1.149	1.072	.281
30	2.852	1.155	1.075	.247
35	2.952	1.159	1.077	.220
40	2.998	1.163	1.078	.198
45	2.983	1.166	1.080	.178
50	2.900	1.165	1.079	.160
55	2.741	1.145	1.070	.144
60	2.518	1.124	1.060	.128
65	2.246	1.100	1.049	.114
70	1.935	1.073	1.036	.100
75	1.594	1.044	1.022	.086
80	1.233	1.013	1.006	.074
85	.865	.981	.990	.060
90	.510	.944	.972	.046
95	.195	.902	.950	.031
100	0	.858	.926	0

L.E. radius: 0.240 percent c

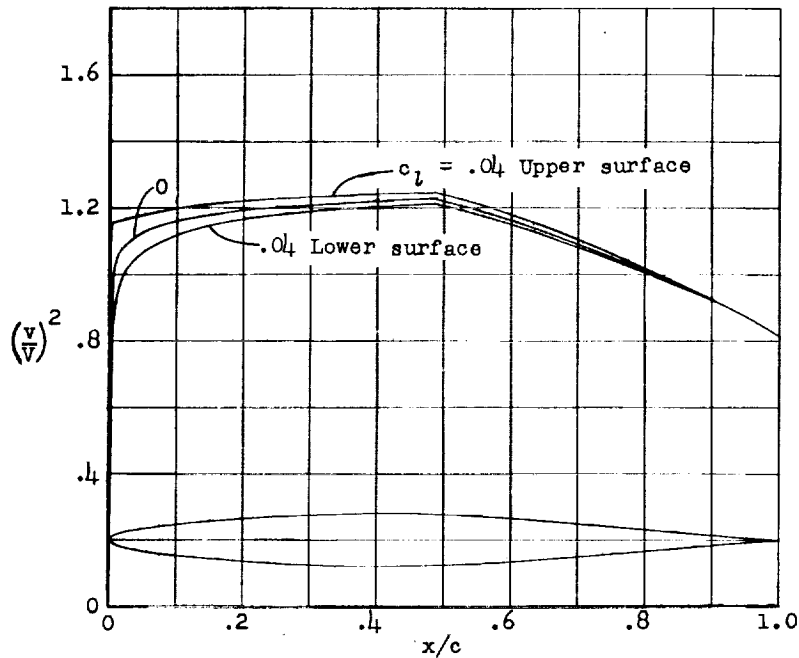
NACA 65₁-006 basic thickness form

CONFIDENTIAL



NACA 65₁-008

CONFIDENTIAL



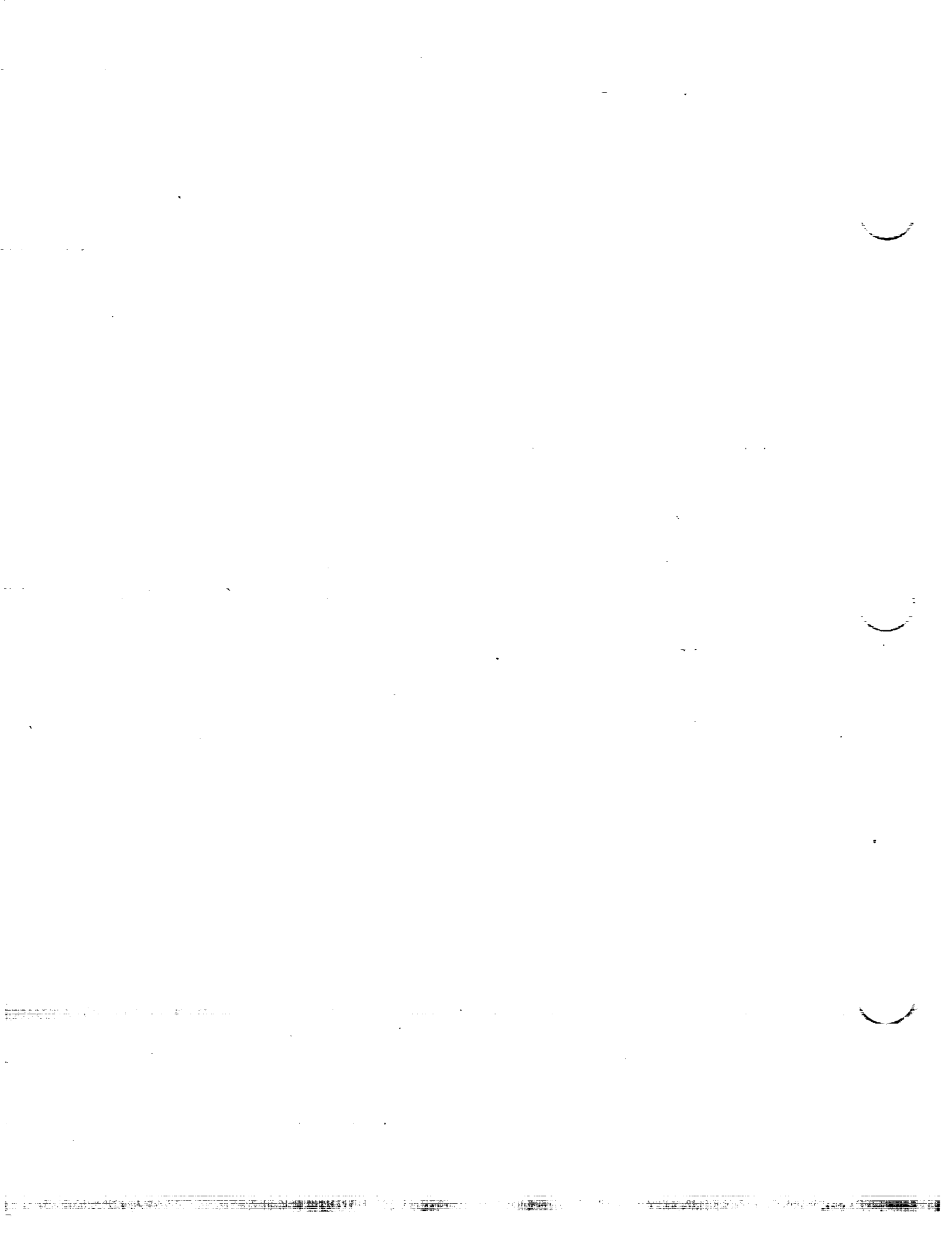
x (percent c)	y (percent c)	(v/v) ²	v/v	Δv _a /V
0	0	0	0	3.695
.5	.627	.978	.989	2.010
.75	.756	1.010	1.005	1.696
1.25	.945	1.043	1.021	1.340
2.5	1.267	1.086	1.042	.956
5.0	1.745	1.125	1.061	.689
7.5	2.118	1.145	1.070	.560
10	2.432	1.158	1.076	.477
15	2.931	1.178	1.085	.382
20	3.312	1.192	1.092	.323
25	3.599	1.203	1.097	.281
30	3.805	1.210	1.100	.248
35	3.938	1.217	1.103	.221
40	3.998	1.222	1.105	.199
45	3.974	1.226	1.107	.178
50	3.857	1.222	1.105	.160
55	3.638	1.193	1.092	.145
60	3.337	1.163	1.078	.128
65	2.971	1.130	1.063	.113
70	2.553	1.094	1.046	.098
75	2.096	1.055	1.027	.084
80	1.617	1.014	1.007	.072
85	1.131	.971	.985	.059
90	.664	.923	.961	.044
95	.252	.873	.934	.031
100	0	.817	.904	0

L.E. radius: 0.434

NACA 65₁-008 basic thickness form

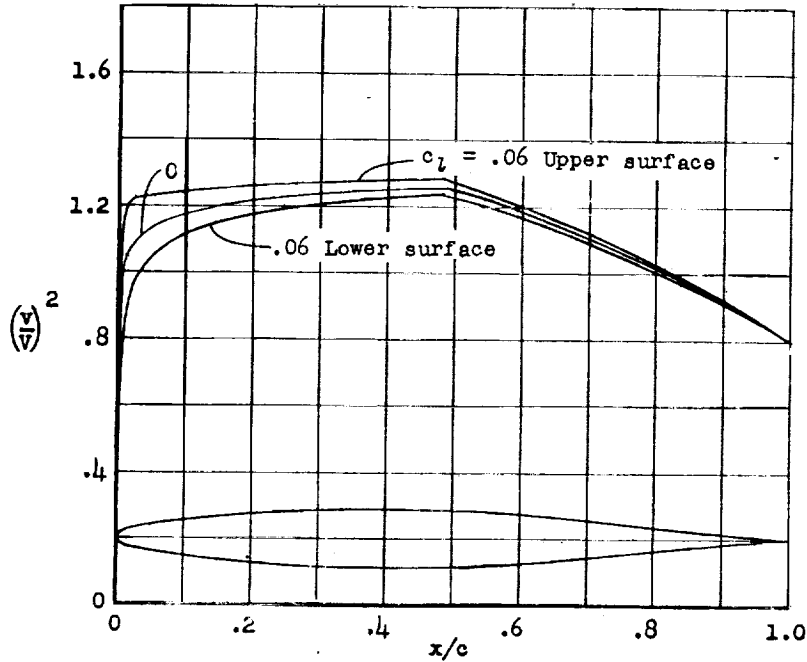
NATIONAL ADVISORY
COMMITTEE FOR AERONAUTICS.

CONFIDENTIAL



NACA 65₁-009

CONFIDENTIAL



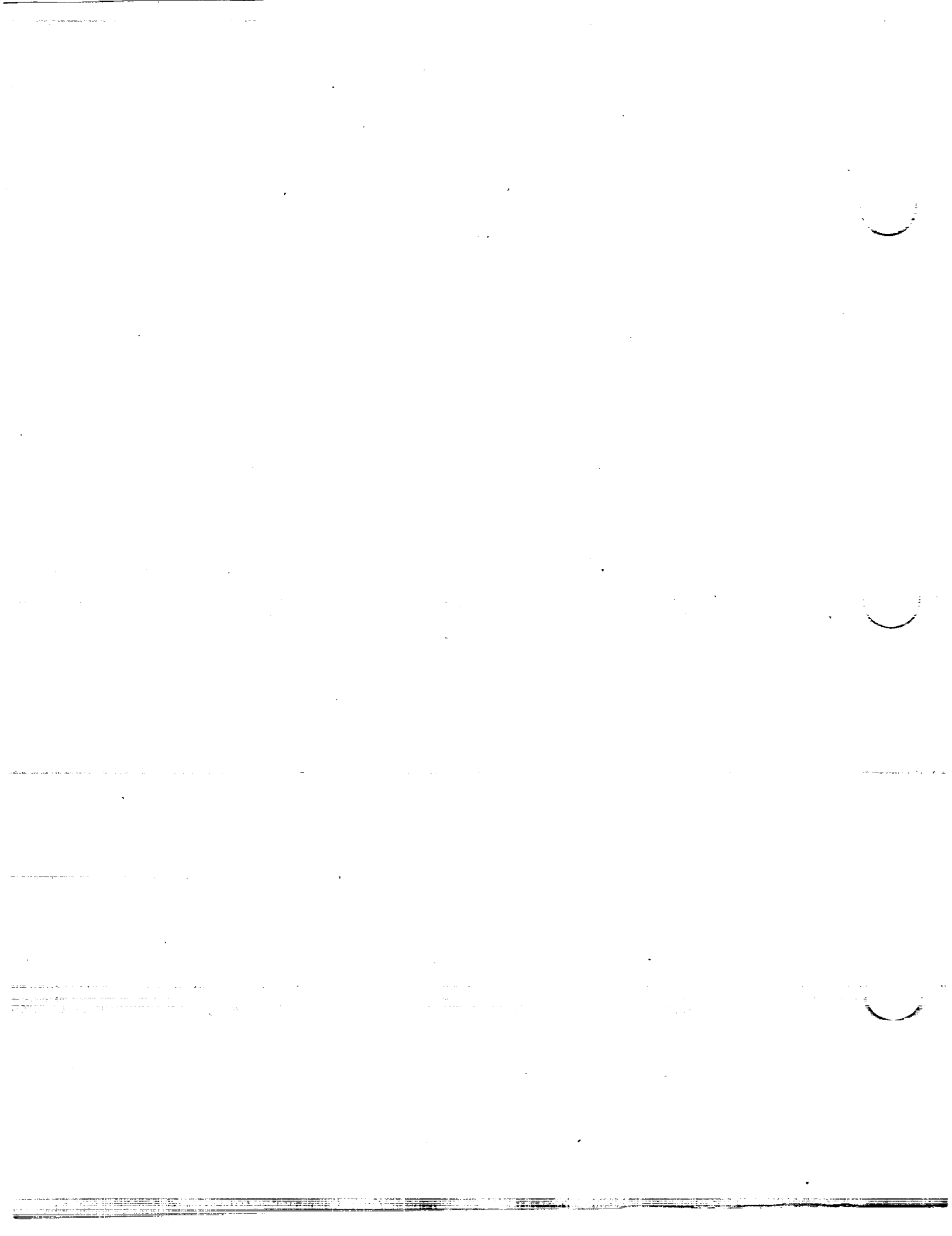
x (percent c)	y (percent c)	$(v/v)^2$	v/v	$\Delta v_a/v$
0	0	0	0	3.270
.5	.700	.945	.972	1.962
.75	.845	.985	.992	1.655
1.25	1.058	1.077	1.018	1.315
2.5	1.421	1.089	1.044	.950
5.0	1.961	1.134	1.065	.687
7.5	2.383	1.159	1.077	.560
10	2.736	1.177	1.085	.477
15	3.299	1.200	1.095	.382
20	3.727	1.216	1.103	.323
25	4.050	1.229	1.109	.280
30	4.282	1.233	1.113	.248
35	4.431	1.246	1.116	.220
40	4.496	1.252	1.119	.198
45	4.469	1.258	1.122	.178
50	4.336	1.250	1.118	.160
55	4.086	1.220	1.105	.144
60	3.743	1.185	1.089	.128
65	3.328	1.145	1.070	.111
70	2.856	1.103	1.050	.097
75	2.342	1.059	1.029	.084
80	1.805	1.013	1.006	.071
85	1.260	.963	.981	.059
90	.738	.912	.955	.044
95	.280	.856	.925	.030
100	0	.797	.893	0

L.E. radius: 0.552 percent c

NACA 65₁-009 basic thickness form

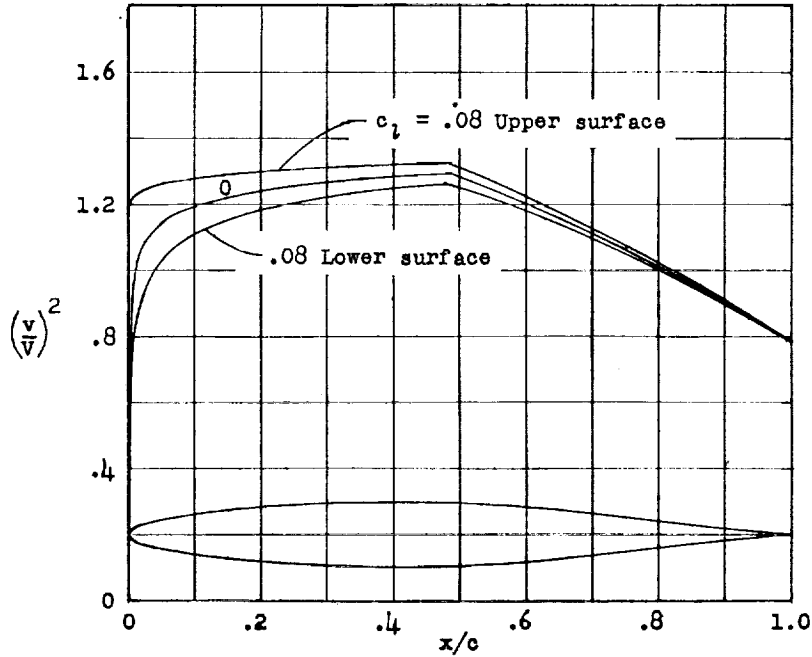
CONFIDENTIAL

NATIONAL ADVISORY
COMMITTEE FOR AERONAUTICS



NACA 65₁-010

CONFIDENTIAL



x (percent c)	y (percent c)	(v/V) ²	v/V	Δv _R /V
0	0	0	0	2.967
.5	.772	.911	.954	1.911
.75	.932	.960	.980	1.614
1.25	1.169	1.025	1.012	1.292
2.5	1.574	1.085	1.042	.932
5.0	2.177	1.143	1.069	.679
7.5	2.647	1.177	1.085	.558
10	3.040	1.197	1.094	.480
15	3.666	1.224	1.106	.383
20	4.143	1.242	1.114	.321
25	4.503	1.257	1.121	.280
30	4.760	1.268	1.126	.248
35	4.924	1.277	1.130	.222
40	4.996	1.284	1.133	.199
45	4.963	1.290	1.136	.179
50	4.812	1.284	1.133	.160
55	4.530	1.244	1.115	.141
60	4.146	1.202	1.096	.126
65	3.682	1.158	1.076	.110
70	3.156	1.112	1.055	.097
75	2.584	1.062	1.031	.082
80	1.987	1.011	1.005	.070
85	1.385	.958	.979	.058
90	.810	.903	.950	.045
95	.306	.844	.919	.030
100	0	.781	.884	0

L.E. radius: 0.687 percent c

NACA 65₁-010 basic thickness form

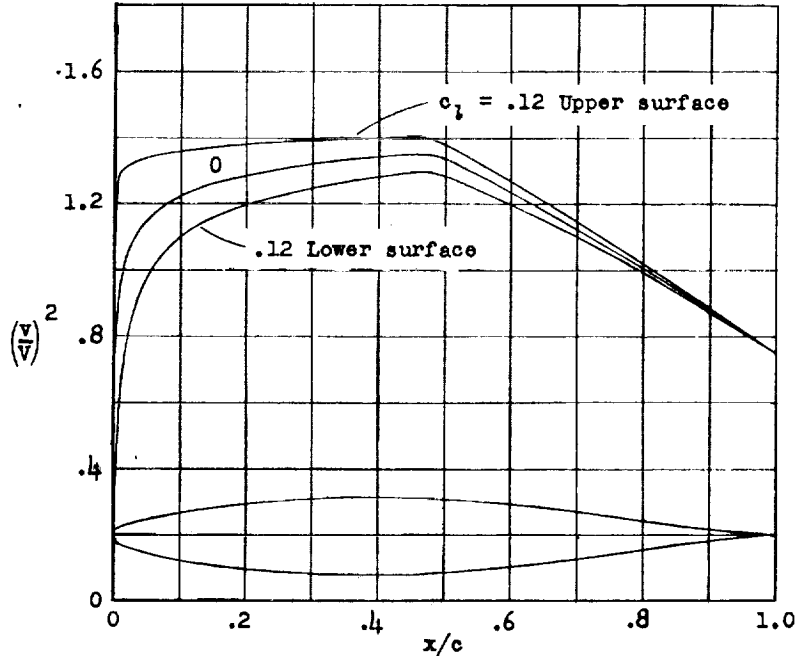
CONFIDENTIAL

NATIONAL ADVISORY
COMMITTEE FOR AERONAUTICS.



NACA 65₁-012

CONFIDENTIAL



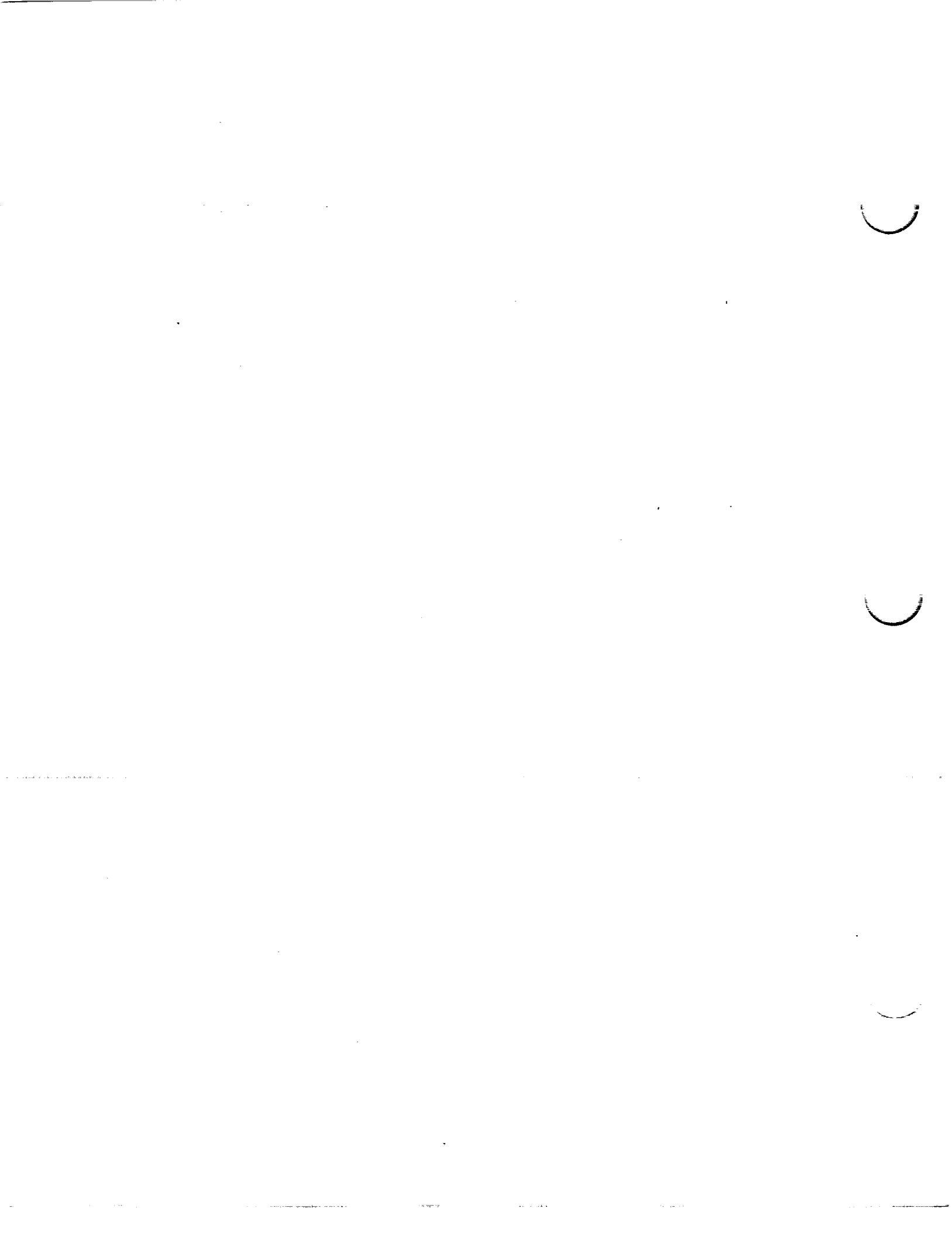
x (percent c)	y (percent c)	(v/V) ²	v/V	Δv _a /V
0	0	0	0	2.444
.5	.923	.848	.921	1.776
.75	1.109	.935	.967	1.465
1.25	1.387	1.000	1.000	1.200
2.5	1.875	1.082	1.040	.931
5.0	2.606	1.162	1.078	.702
7.5	3.172	1.201	1.096	.568
10	3.647	1.232	1.110	.480
15	4.402	1.268	1.126	.389
20	4.975	1.295	1.138	.326
25	5.406	1.316	1.147	.282
30	5.716	1.332	1.154	.251
35	5.912	1.343	1.159	.223
40	5.997	1.350	1.162	.201
45	5.949	1.357	1.165	.188
50	5.757	1.343	1.159	.169
55	5.412	1.295	1.138	.145
60	4.943	1.243	1.115	.127
65	4.381	1.188	1.090	.111
70	3.743	1.134	1.065	.094
75	3.059	1.073	1.036	.074
80	2.345	1.010	1.005	.062
85	1.630	.949	.974	.049
90	.947	.884	.940	.038
95	.356	.819	.905	.025
100	0	.748	.865	0

L. B. radius: 1.000 percent c

NACA 65₁-012 basic thickness form

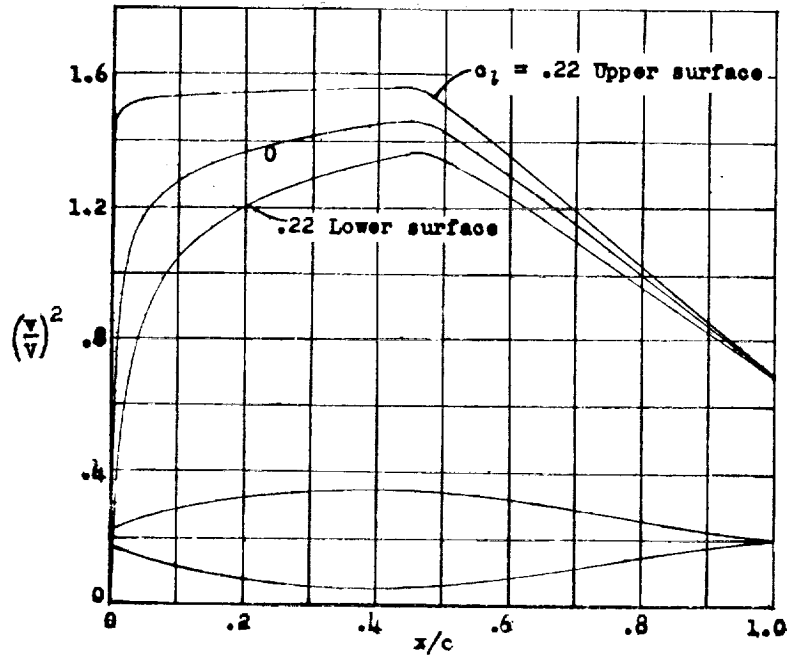
CONFIDENTIAL

NATIONAL ADVISORY
COMMITTEE FOR AERONAUTICS.



NACA 65₂-015

CONFIDENTIAL



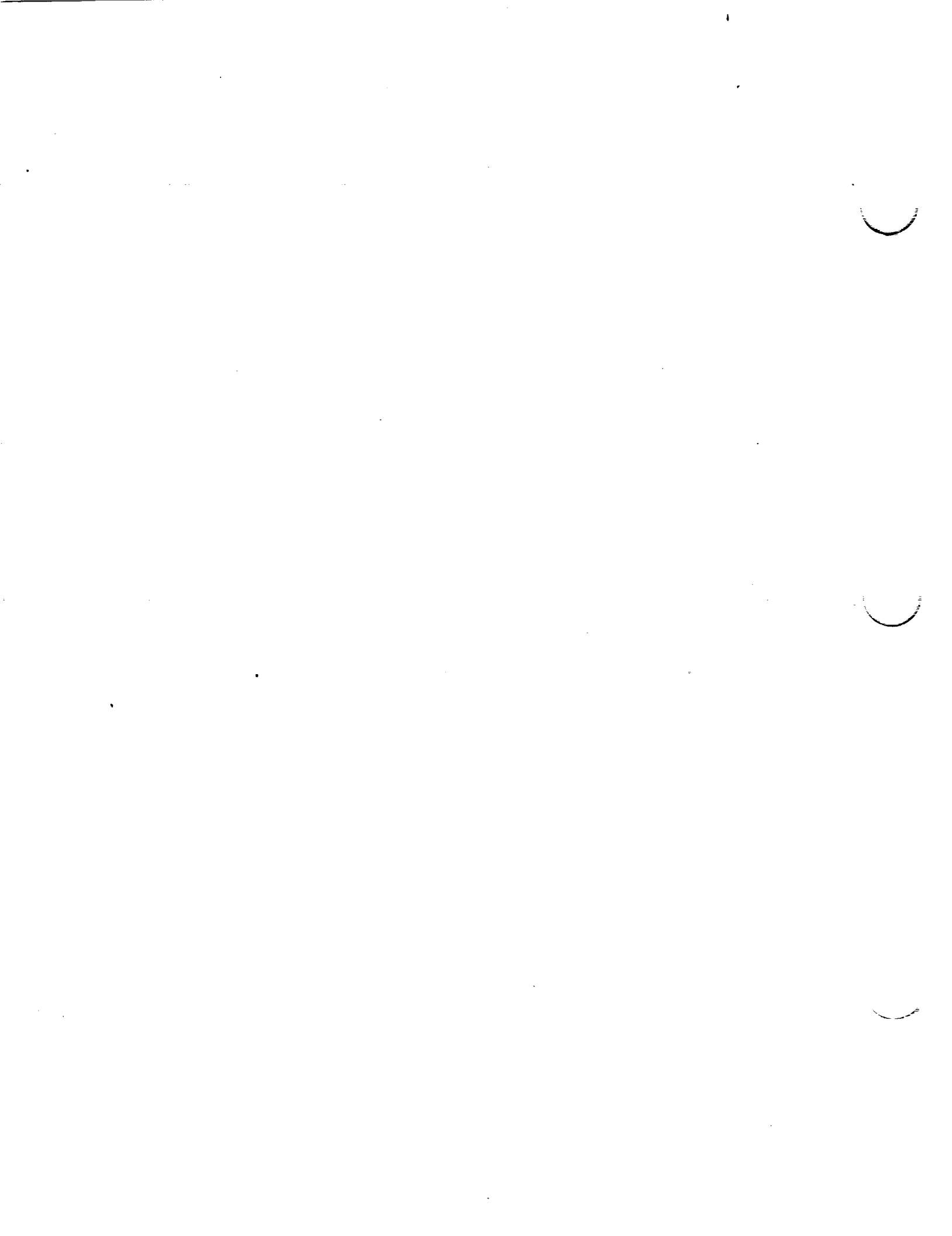
\bar{x} (percent c)	\bar{y} (percent c)	$(v/v)^2$	v/v	$\Delta v_a/v$
0	0	0	0	2.038
.5	1.124	.654	.809	1.729
.75	1.356	.817	.904	1.390
1.25	1.702	.939	.969	1.156
2.5	2.324	1.063	1.031	.920
5.0	3.245	1.184	1.088	.682
7.5	3.959	1.241	1.114	.563
10	4.555	1.281	1.132	.487
15	5.504	1.336	1.156	.393
20	6.223	1.374	1.172	.334
25	6.764	1.397	1.182	.290
30	7.152	1.418	1.191	.255
35	7.396	1.438	1.199	.227
40	7.498	1.452	1.205	.203
45	7.427	1.464	1.210	.184
50	7.168	1.433	1.197	.160
55	6.720	1.369	1.170	.143
60	6.118	1.297	1.139	.127
65	5.403	1.228	1.108	.109
70	4.600	1.151	1.073	.096
75	3.744	1.077	1.038	.078
80	2.858	1.002	1.001	.068
85	1.977	.924	.961	.052
90	1.144	.846	.920	.038
95	.428	.773	.879	.026
100	0	.697	.835	0

L. E. radius: 1.505 percent c

NACA 65₂-015 basic thickness form

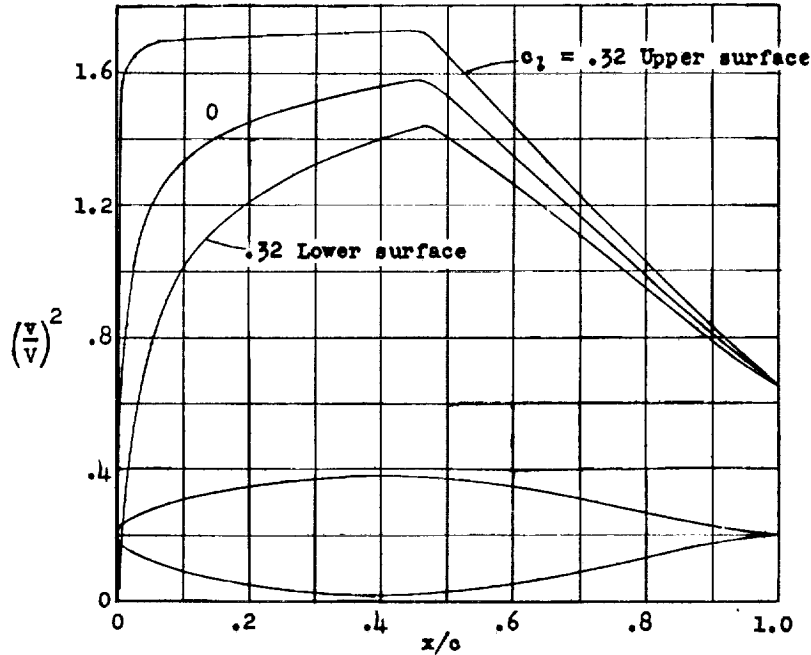
CONFIDENTIAL

NATIONAL ADVISORY
COMMITTEE FOR AERONAUTICS.



NACA 65₃-018

CONFIDENTIAL



(percent c_x)	(percent c_y)	$(v/v)^2$	v/v	$\Delta v_a/v$
0	0	0	0	1.746
.5	1.337	.625	.791	1.437
.75	1.608	.702	.838	1.302
1.25	2.014	.817	.904	1.123
2.5	2.751	1.020	1.010	.858
5.0	3.866	1.192	1.092	.650
7.5	4.733	1.275	1.129	.542
10	5.457	1.329	1.153	.474
15	6.606	1.402	1.184	.385
20	7.476	1.452	1.205	.327
25	8.129	1.488	1.220	.285
30	8.595	1.515	1.231	.251
35	8.886	1.539	1.241	.225
40	8.999	1.561	1.249	.203
45	8.901	1.578	1.256	.182
50	8.568	1.526	1.235	.157
55	8.008	1.440	1.200	.137
60	7.267	1.353	1.163	.118
65	6.395	1.262	1.123	.104
70	5.426	1.170	1.082	.087
75	4.396	1.076	1.037	.074
80	3.338	.985	.992	.062
85	2.295	.896	.947	.050
90	1.319	.813	.902	.039
95	.490	.730	.854	.026
100	0	.657	.811	0

L. E. radius: 1.96 percent c

NACA 65₃-018 basic thickness form

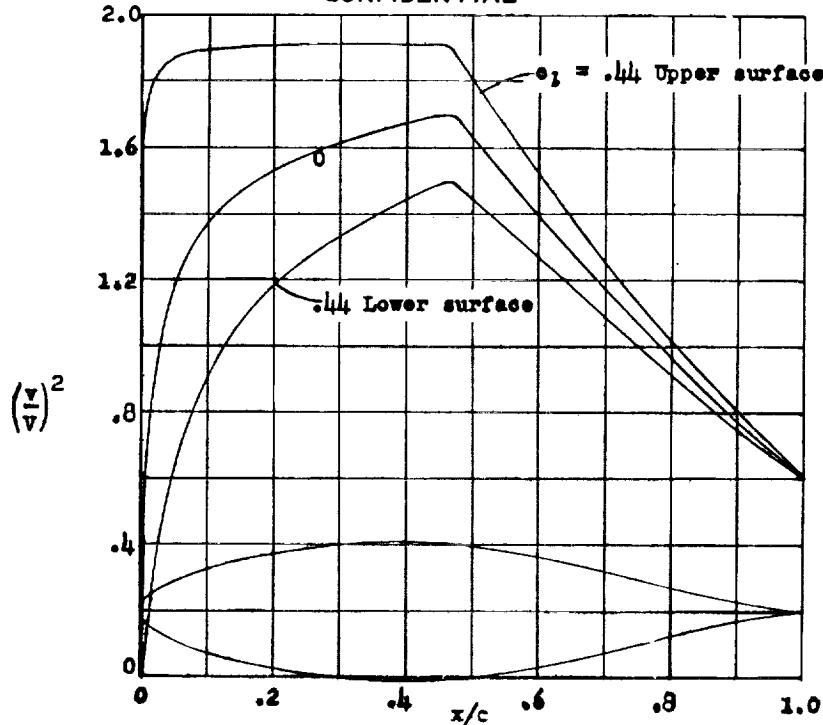
CONFIDENTIAL

NATIONAL ADVISORY
COMMITTEE FOR AERONAUTICS.



NACA 65₄-021

CONFIDENTIAL



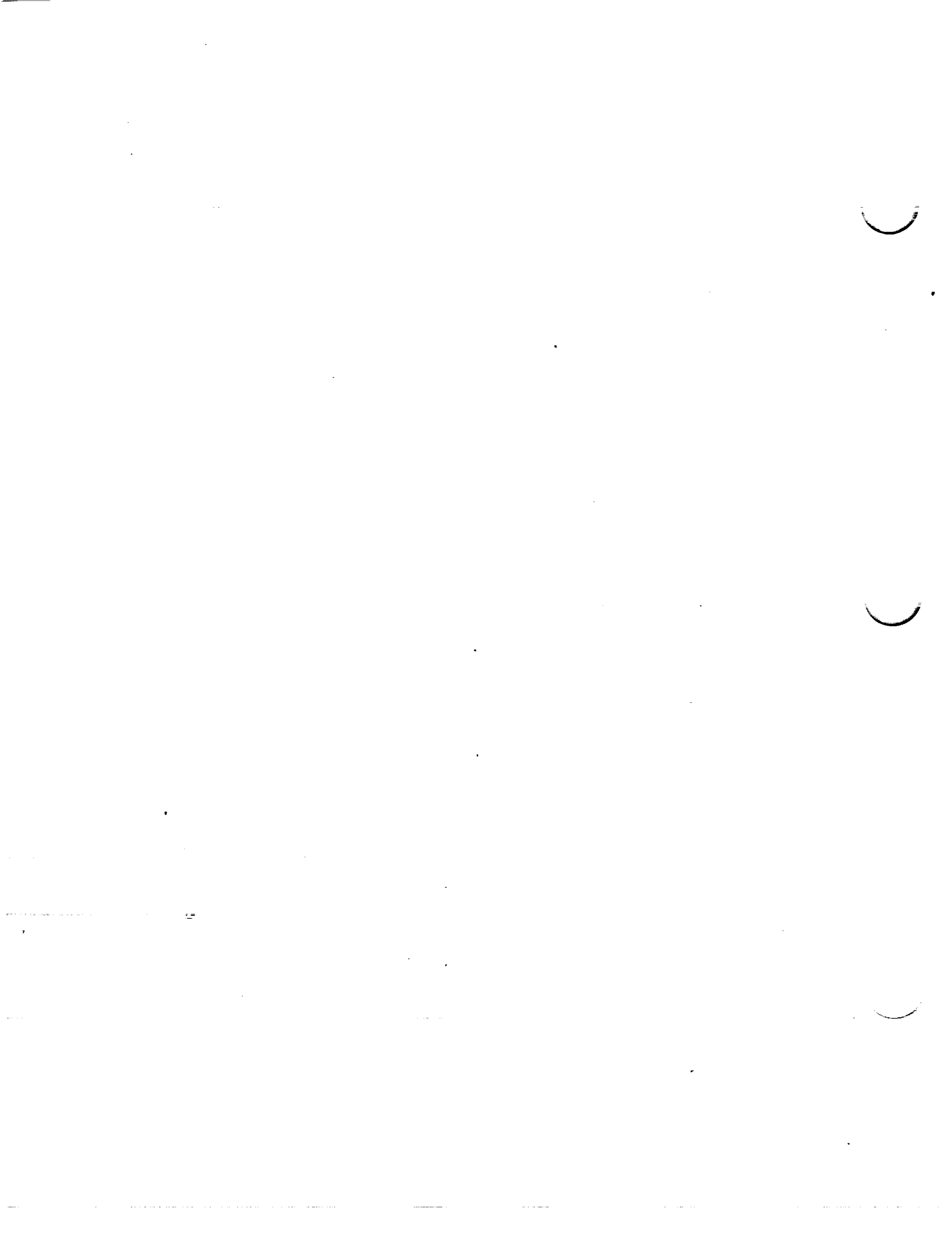
\bar{x} (percent c)	\bar{y} (percent c)	$(v/V)^2$	v/V	$\Delta v_a/V$
0	0	0	0	1.531
.5	1.522	.514	.717	1.333
.75	1.838	.607	.779	1.215
1.25	2.301	.740	.860	1.062
2.5	3.154	.960	.980	.838
5.0	4.472	1.186	1.089	.649
7.5	5.498	1.293	1.137	.544
10	6.352	1.371	1.171	.478
15	7.700	1.469	1.212	.388
20	8.720	1.533	1.238	.330
25	9.487	1.580	1.257	.289
30	10.036	1.621	1.273	.255
35	10.375	1.654	1.286	.229
40	10.499	1.680	1.296	.206
45	10.366	1.700	1.304	.184
50	9.952	1.633	1.278	.158
55	9.277	1.508	1.228	.139
60	8.390	1.397	1.182	.120
65	7.360	1.286	1.134	.101
70	6.224	1.177	1.085	.087
75	5.024	1.073	1.036	.073
80	3.800	.970	.985	.058
85	2.598	.872	.934	.047
90	1.484	.778	.882	.035
95	.546	.694	.833	.020
100	0	.616	.785	0

L. E. radius: 2.50 percent c

NACA 65₄-021 basic thickness form

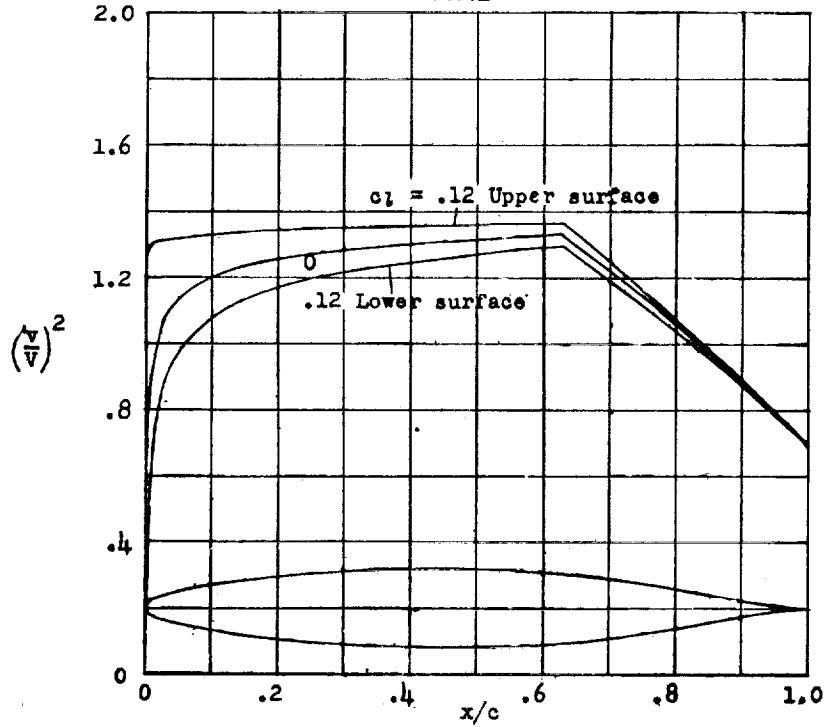
CONFIDENTIAL

NATIONAL ADVISORY
COMMITTEE FOR AERONAUTICS.



CONFIDENTIAL

NACA 66,1-012



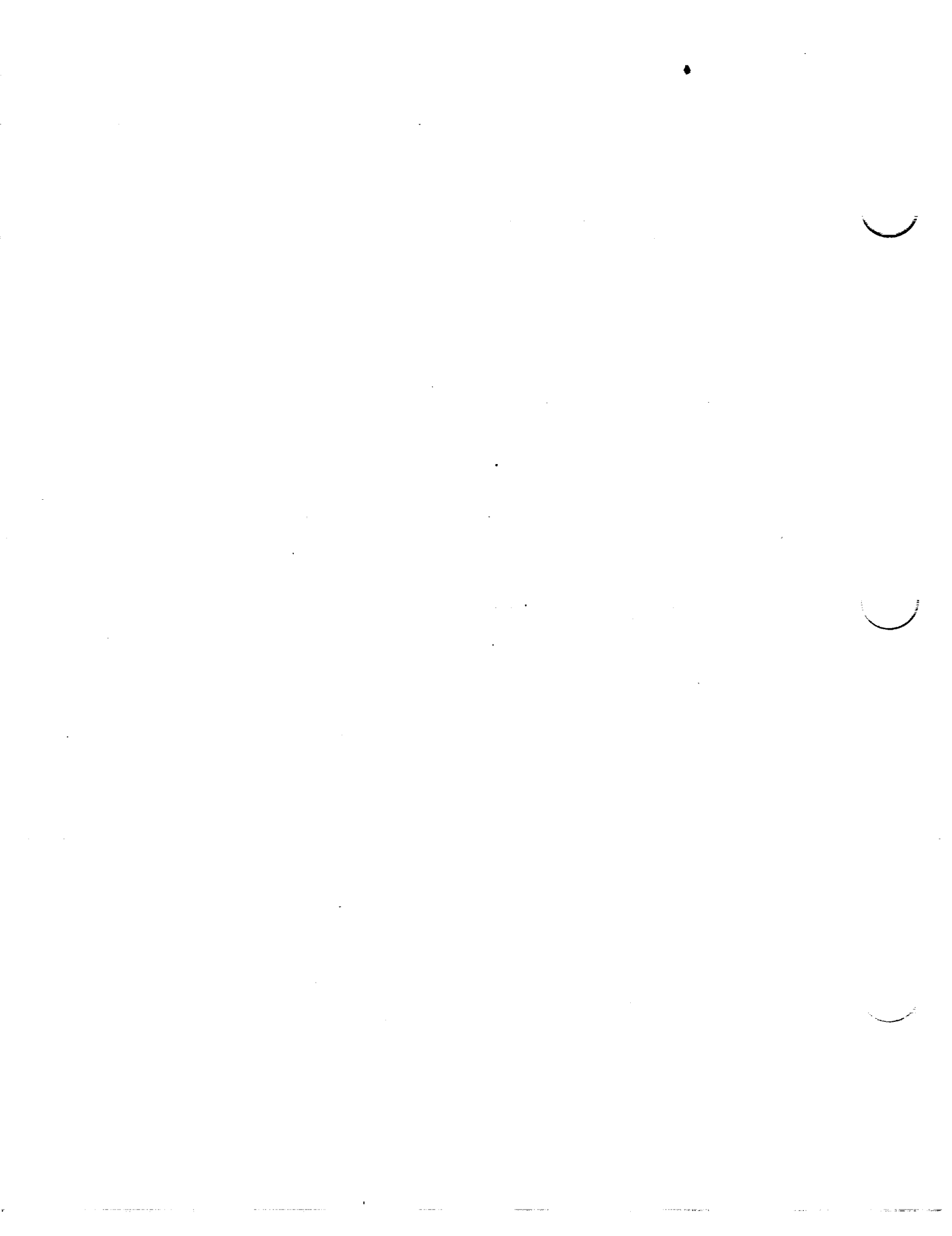
\bar{x} (percent c)	\bar{y} (percent c)	$(v/V)^2$	v/V	$\Delta v_a/V$
0	0	0	0	2.555
.5	.900	.854	.924	1.780
.75	1.083	.902	.950	1.540
1.25	1.343	.964	.982	1.247
2.5	1.803	1.069	1.034	.925
5.0	2.484	1.138	1.067	.673
7.5	3.019	1.175	1.084	.552
10	3.482	1.201	1.096	.474
15	4.214	1.237	1.112	.381
20	4.779	1.257	1.121	.319
25	5.218	1.272	1.128	.280
30	5.550	1.284	1.133	.248
35	5.786	1.293	1.137	.220
40	5.934	1.302	1.141	.195
45	5.998	1.309	1.144	.176
50	5.972	1.313	1.146	.161
55	5.844	1.320	1.149	.144
60	5.594	1.327	1.152	.130
65	5.165	1.297	1.139	.117
70	4.535	1.221	1.105	.099
75	3.789	1.143	1.069	.083
80	2.964	1.061	1.030	.069
85	2.098	.974	.987	.053
90	1.244	.885	.941	.041
95	.477	.792	.890	.028
100	0	.701	.837	0

L. E. radius: 0.893 percent c

NACA 66,1-012 basic thickness form

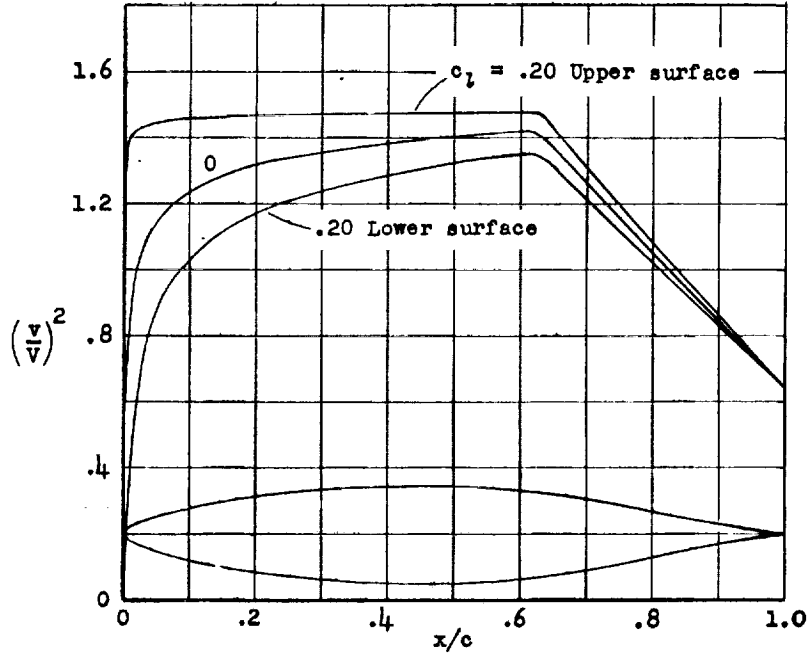
CONFIDENTIAL

NATIONAL ADVISORY
COMMITTEE FOR AERONAUTICS.



CONFIDENTIAL

NACA 66,2-015



x (percent c)	y (percent c)	$(v/v)^2$	v/v	$\Delta v_a/v$
0	0	0	0	.2.085
.5	1.110	.700	.837	1.703
.75	1.329	.870	.933	1.382
1.25	1.645	.940	.970	1.156
2.5	2.229	1.048	1.024	.898
5.0	3.086	1.154	1.074	.656
7.5	3.757	1.210	1.100	.547
10	4.337	1.244	1.115	.473
15	5.255	1.290	1.136	.382
20	5.964	1.323	1.150	.323
25	6.516	1.342	1.158	.283
30	6.933	1.359	1.166	.248
35	7.230	1.374	1.172	.222
40	7.415	1.387	1.178	.199
45	7.495	1.397	1.182	.179
50	7.460	1.407	1.186	.161
55	7.294	1.415	1.190	.145
60	6.961	1.421	1.192	.131
65	6.405	1.372	1.171	.122
70	5.597	1.267	1.126	.102
75	4.652	1.162	1.078	.080
80	3.616	1.057	1.028	.066
85	2.545	.953	.976	.050
90	1.488	.848	.921	.037
95	.560	.743	.862	.025
100	0	.640	.800	0

L. E. radius; 1.384 percent c

NACA 66,2-015 basic thickness form

CONFIDENTIAL

NATIONAL ADVISORY
COMMITTEE FOR AERONAUTICS

100-100-100

100-100-100

Year	1950	1951	1952	1953	1954	1955	1956	1957	1958	1959	1960
...

Year	1961	1962	1963	1964	1965	1966	1967	1968	1969	1970
...

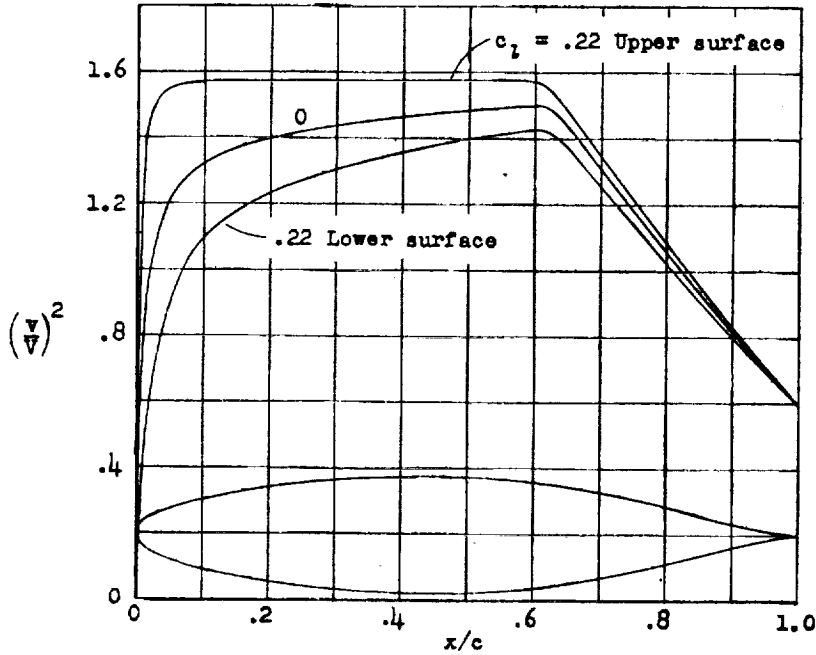
...

...

...

NACA 66,2-018

CONFIDENTIAL



x (percent c)	y (percent c)	(v/v) ²	v/v	Δv _a /V
0	0	0	0	1.659
.5	1.438	.590	.768	1.317
.75	1.730	.740	.860	1.209
1.25	2.180	.918	.958	1.091
2.5	2.938	1.084	1.041	.867
5.0	3.984	1.217	1.103	.665
7.5	4.804	1.285	1.134	.544
10	5.486	1.325	1.151	.469
15	6.541	1.373	1.172	.379
20	7.342	1.401	1.184	.323
25	7.957	1.422	1.192	.282
30	8.419	1.440	1.200	.251
35	8.741	1.456	1.207	.224
40	8.933	1.468	1.212	.201
45	8.998	1.478	1.216	.181
50	8.934	1.488	1.220	.162
55	8.719	1.497	1.224	.146
60	8.316	1.502	1.226	.134
65	7.629	1.442	1.201	.102
70	6.657	1.314	1.146	.089
75	5.523	1.185	1.089	.078
80	4.296	1.059	1.029	.064
85	3.027	.936	.967	.052
90	1.789	.817	.904	.041
95	.672	.700	.837	.027
100	0	.594	.771	0

L. E. radius: 2.30 percent c

NACA 66,2-018 basic thickness form

CONFIDENTIAL

NATIONAL ADVISORY
COMMITTEE FOR AERONAUTICS.

The first part of the report discusses the overall situation in the country, including the political and economic context. It highlights the challenges faced by the government and the population, particularly in terms of poverty and social inequality. The report also mentions the role of the international community in providing assistance and support.

The second part of the report provides a detailed analysis of the economic situation. It examines the growth rate, inflation, and the balance of payments. The report notes that the economy has experienced significant fluctuations over the period, with a notable decline in growth and an increase in inflation. The balance of payments has also shown a deficit, which is a concern for the government.

The third part of the report focuses on the social and human development indicators. It discusses the progress made in areas such as education, health, and housing. While there has been some improvement in these areas, the report also points out that there is still a long way to go, particularly in terms of access to quality education and healthcare for all citizens.

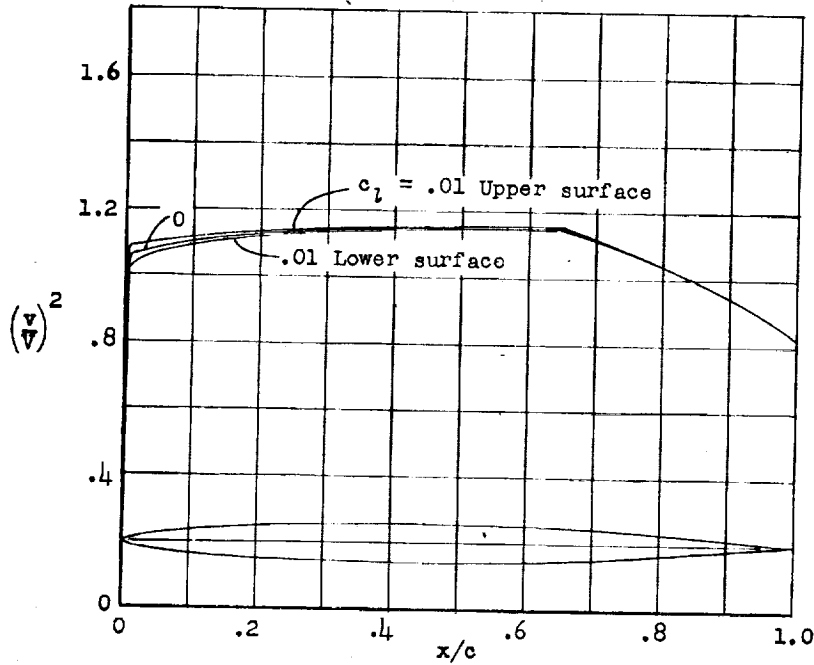
The fourth part of the report discusses the political and governance issues. It examines the role of the government, the judiciary, and the media. The report notes that there have been some challenges in terms of transparency and accountability, but it also mentions the efforts being made to improve the governance framework.

The fifth part of the report provides a summary of the findings and recommendations. It emphasizes the need for a comprehensive reform program that addresses the economic, social, and political challenges. The report also calls for increased international cooperation and support to help the country overcome its current difficulties.

Year	Indicator	Value
1998	GDP Growth	4.5%
1999	GDP Growth	3.2%
2000	GDP Growth	2.8%
2001	GDP Growth	1.5%
2002	GDP Growth	2.1%
2003	GDP Growth	3.5%
2004	GDP Growth	5.2%
2005	GDP Growth	6.8%
2006	GDP Growth	8.1%
2007	GDP Growth	9.5%
2008	GDP Growth	11.2%
2009	GDP Growth	13.5%
2010	GDP Growth	15.8%
2011	GDP Growth	17.2%
2012	GDP Growth	18.5%
2013	GDP Growth	19.8%
2014	GDP Growth	21.1%
2015	GDP Growth	22.5%
2016	GDP Growth	23.8%
2017	GDP Growth	25.1%
2018	GDP Growth	26.5%
2019	GDP Growth	27.8%
2020	GDP Growth	29.1%
2021	GDP Growth	30.5%
2022	GDP Growth	31.8%
2023	GDP Growth	33.1%
2024	GDP Growth	34.5%
2025	GDP Growth	35.8%
2026	GDP Growth	37.1%
2027	GDP Growth	38.5%
2028	GDP Growth	39.8%
2029	GDP Growth	41.1%
2030	GDP Growth	42.5%
2031	GDP Growth	43.8%
2032	GDP Growth	45.1%
2033	GDP Growth	46.5%
2034	GDP Growth	47.8%
2035	GDP Growth	49.1%
2036	GDP Growth	50.5%
2037	GDP Growth	51.8%
2038	GDP Growth	53.1%
2039	GDP Growth	54.5%
2040	GDP Growth	55.8%
2041	GDP Growth	57.1%
2042	GDP Growth	58.5%
2043	GDP Growth	59.8%
2044	GDP Growth	61.1%
2045	GDP Growth	62.5%
2046	GDP Growth	63.8%
2047	GDP Growth	65.1%
2048	GDP Growth	66.5%
2049	GDP Growth	67.8%
2050	GDP Growth	69.1%
2051	GDP Growth	70.5%
2052	GDP Growth	71.8%
2053	GDP Growth	73.1%
2054	GDP Growth	74.5%
2055	GDP Growth	75.8%
2056	GDP Growth	77.1%
2057	GDP Growth	78.5%
2058	GDP Growth	79.8%
2059	GDP Growth	81.1%
2060	GDP Growth	82.5%
2061	GDP Growth	83.8%
2062	GDP Growth	85.1%
2063	GDP Growth	86.5%
2064	GDP Growth	87.8%
2065	GDP Growth	89.1%
2066	GDP Growth	90.5%
2067	GDP Growth	91.8%
2068	GDP Growth	93.1%
2069	GDP Growth	94.5%
2070	GDP Growth	95.8%
2071	GDP Growth	97.1%
2072	GDP Growth	98.5%
2073	GDP Growth	99.8%
2074	GDP Growth	101.1%
2075	GDP Growth	102.5%
2076	GDP Growth	103.8%
2077	GDP Growth	105.1%
2078	GDP Growth	106.5%
2079	GDP Growth	107.8%
2080	GDP Growth	109.1%
2081	GDP Growth	110.5%
2082	GDP Growth	111.8%
2083	GDP Growth	113.1%
2084	GDP Growth	114.5%
2085	GDP Growth	115.8%
2086	GDP Growth	117.1%
2087	GDP Growth	118.5%
2088	GDP Growth	119.8%
2089	GDP Growth	121.1%
2090	GDP Growth	122.5%
2091	GDP Growth	123.8%
2092	GDP Growth	125.1%
2093	GDP Growth	126.5%
2094	GDP Growth	127.8%
2095	GDP Growth	129.1%
2096	GDP Growth	130.5%
2097	GDP Growth	131.8%
2098	GDP Growth	133.1%
2099	GDP Growth	134.5%
2100	GDP Growth	135.8%

Source: Ministry of Planning, National Bureau of Statistics, and International Monetary Fund.

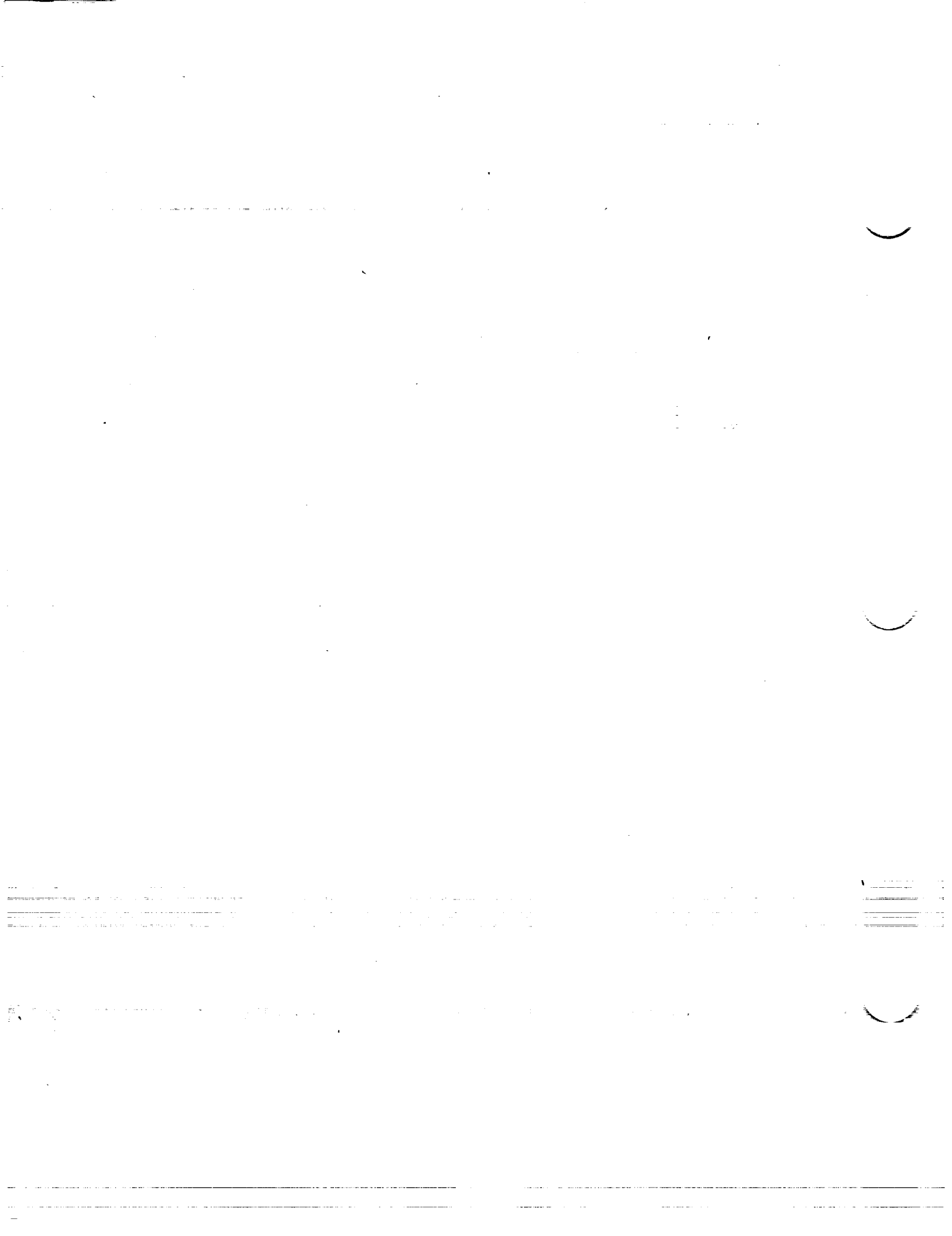
CONFIDENTIAL **NACA 66₁-006**



x (percent c)	y (percent c)	(v/V) ²	v/V	Δv _a /V
0	0	0	0	4.941
.5	.461	1.052	1.026	2.500
.75	.554	1.057	1.028	2.020
1.25	.693	1.062	1.031	1.500
2.5	.918	1.071	1.035	.967
5.0	1.257	1.086	1.042	.695
7.5	1.524	1.098	1.048	.554
10	1.752	1.107	1.052	.474
15	2.119	1.119	1.058	.379
20	2.401	1.128	1.062	.320
25	2.618	1.133	1.064	.278
30	2.782	1.138	1.067	.245
35	2.899	1.142	1.069	.219
40	2.971	1.145	1.070	.197
45	3.000	1.148	1.071	.178
50	2.985	1.151	1.073	.161
55	2.925	1.153	1.074	.145
60	2.815	1.155	1.075	.130
65	2.611	1.154	1.074	.116
70	2.316	1.118	1.057	.102
75	1.953	1.081	1.040	.089
80	1.543	1.040	1.020	.075
85	1.107	.996	.998	.061
90	.665	.948	.974	.047
95	.262	.890	.943	.030
100	0	.822	.907	0

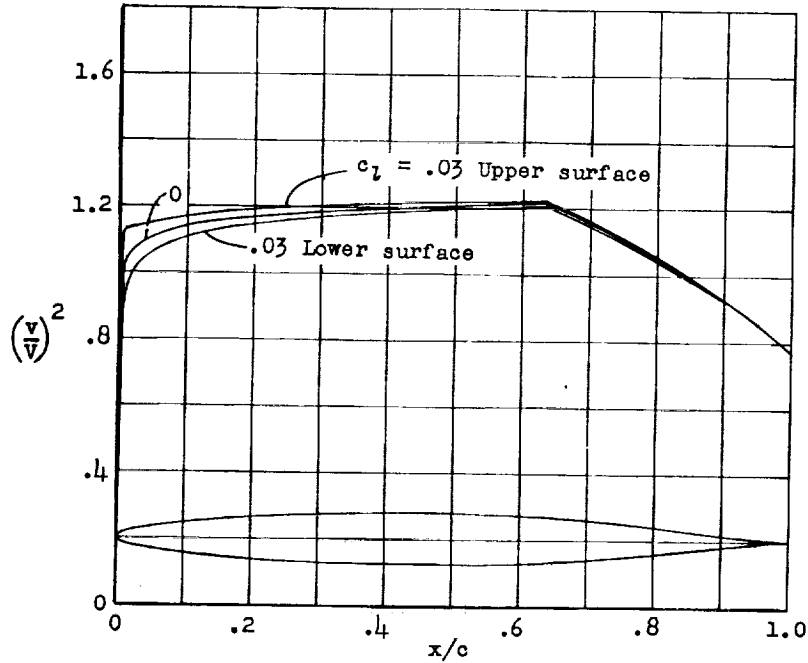
L.E. radius: 0.223 percent c

NACA 66₁-006 basic thickness form



CONFIDENTIAL

NACA 66₁-008



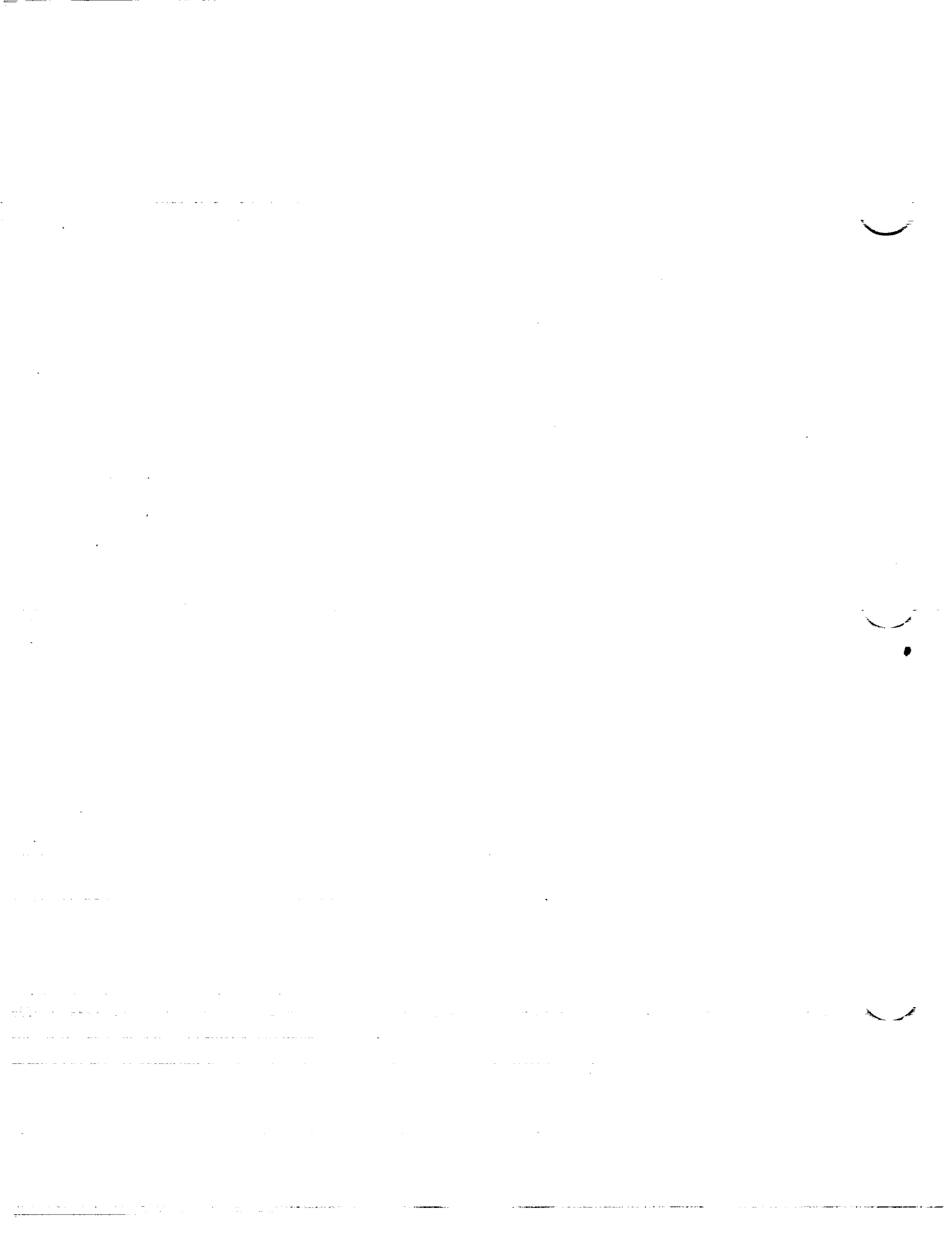
x (percent c)	y (percent c)	(v/v) ²	v/v	Δv _a /V
0	0	0	0	3.794
.5	.610	.968	.984	2.220
.75	.735	1.023	1.011	1.825
1.25	.919	1.046	1.023	1.388
2.5	1.219	1.078	1.038	.949
5.0	1.673	1.107	1.052	.689
7.5	2.031	1.128	1.062	.552
10	2.335	1.141	1.068	.474
15	2.826	1.158	1.076	.379
20	3.201	1.171	1.082	.321
25	3.490	1.178	1.085	.278
30	3.709	1.186	1.089	.246
35	3.865	1.191	1.091	.220
40	3.962	1.196	1.094	.198
45	4.000	1.201	1.096	.178
50	3.978	1.205	1.098	.161
55	3.896	1.208	1.099	.145
60	3.740	1.213	1.101	.130
65	3.459	1.202	1.096	.115
70	3.062	1.156	1.075	.101
75	2.574	1.103	1.050	.087
80	2.027	1.048	1.024	.073
85	1.447	.989	.994	.058
90	.864	.926	.962	.045
95	.338	.855	.925	.029
100	0	.768	.876	0

L.E. radius: 0.411

NACA 66₁-008 basic thickness form

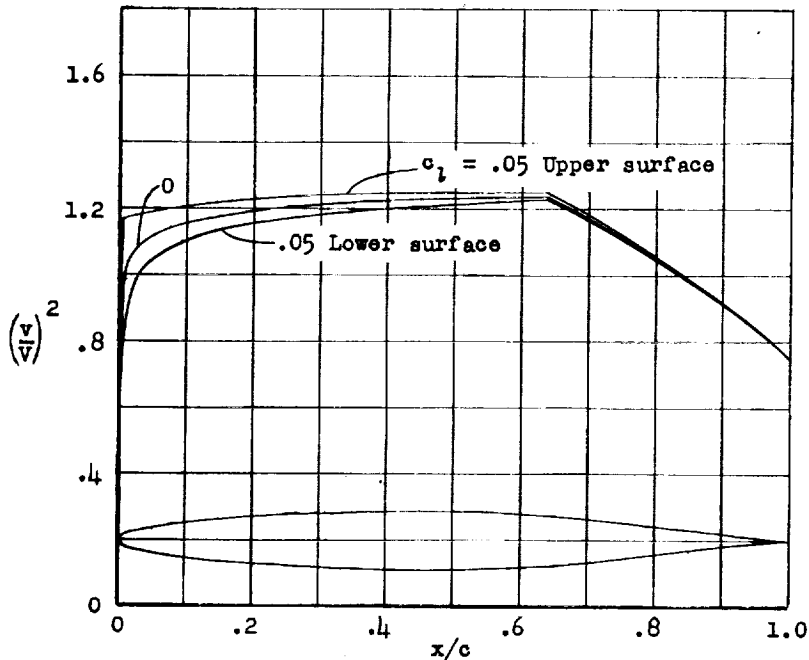
CONFIDENTIAL

NATIONAL ADVISORY
COMMITTEE FOR AERONAUTICS



CONFIDENTIAL

NACA 66₁-009



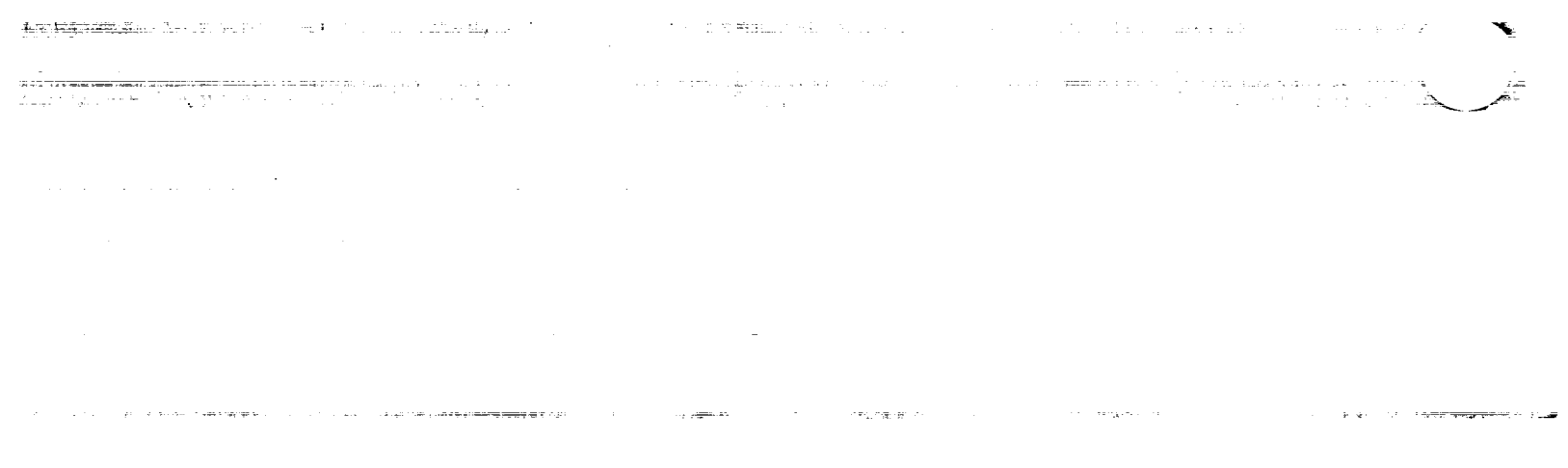
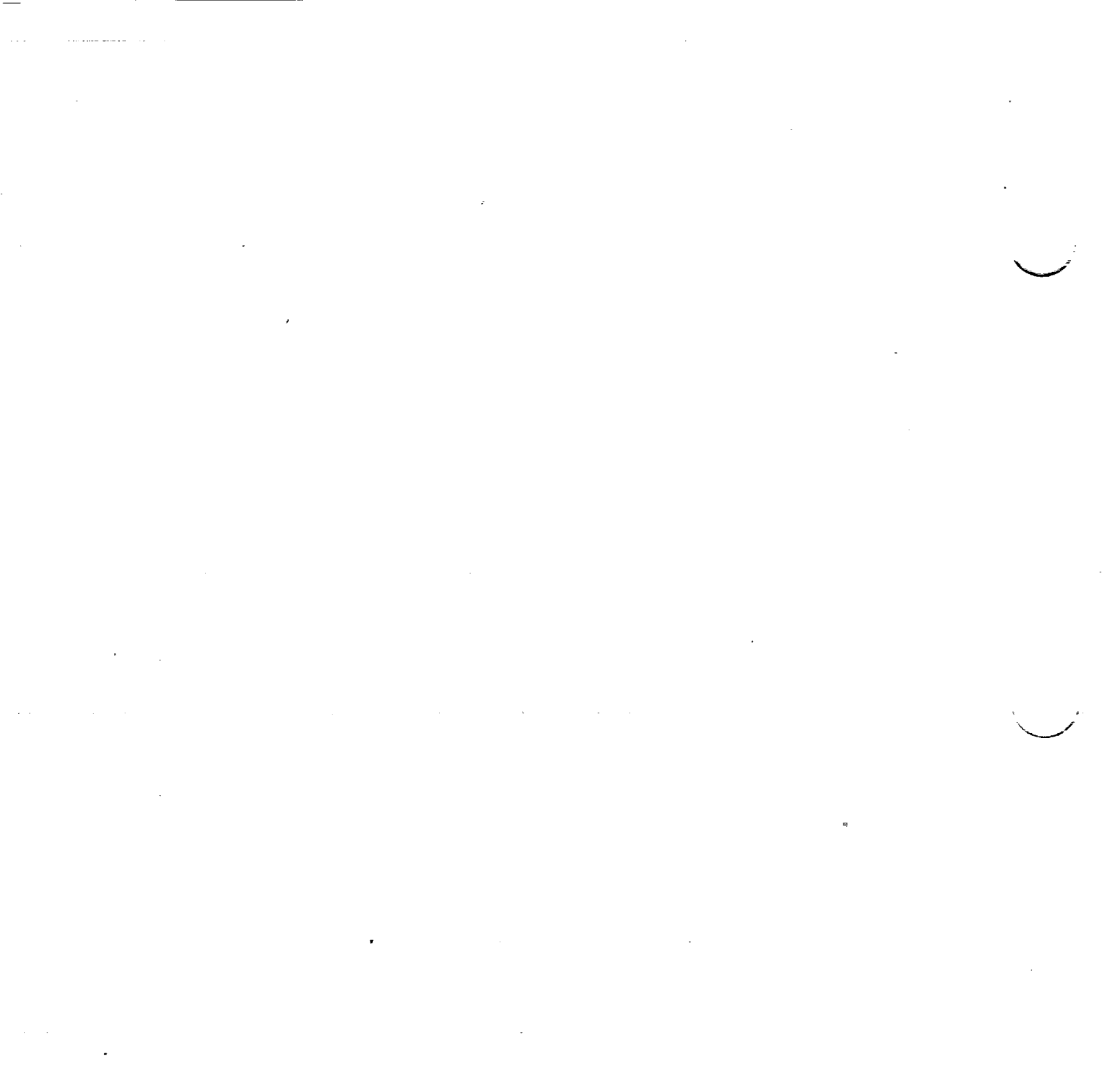
x (percent c)	y (percent c)	(v/v) ²	v/v	Δv _a /V
0	0	0	0	3.352
.5	.687	.930	.964	2.100
.75	.824	.999	.999	1.750
1.25	1.030	1.036	1.018	1.340
2.5	1.368	1.079	1.039	.940
5.0	1.880	1.119	1.058	.686
7.5	2.283	1.142	1.069	.552
10	2.626	1.159	1.077	.473
15	3.178	1.178	1.085	.379
20	3.601	1.190	1.091	.323
25	3.927	1.201	1.096	.280
30	4.173	1.210	1.100	.246
35	4.348	1.217	1.103	.220
40	4.457	1.221	1.105	.197
45	4.499	1.228	1.108	.178
50	4.475	1.232	1.110	.161
55	4.381	1.237	1.112	.145
60	4.204	1.240	1.114	.130
65	3.882	1.230	1.109	.116
70	3.428	1.172	1.083	.100
75	2.877	1.113	1.055	.085
80	2.263	1.050	1.025	.071
85	1.611	.985	.992	.057
90	.961	.915	.957	.043
95	.374	.839	.916	.028
100	0	.747	.864	0

L.E. radius: 0.530 percent c

NACA 66₁-009 basic thickness form

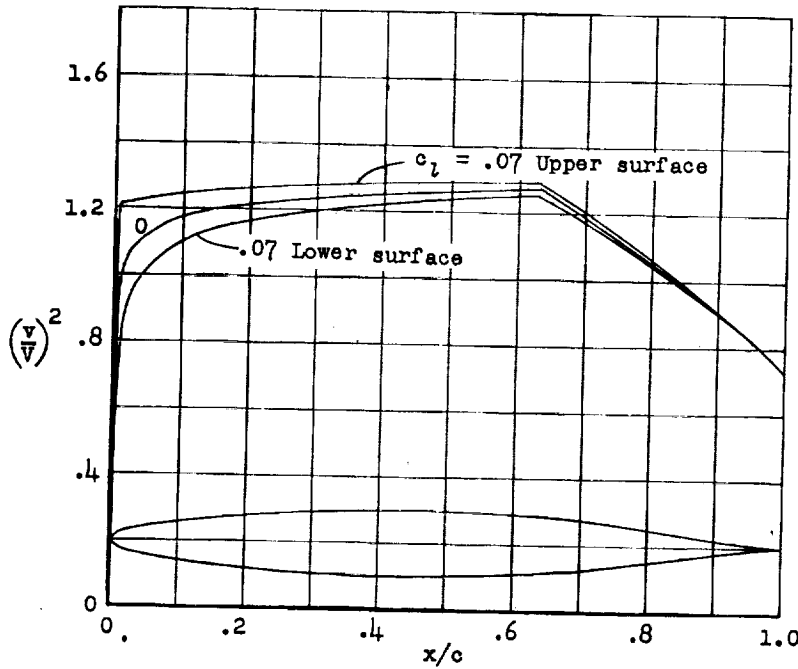
CONFIDENTIAL

NATIONAL ADVISORY
COMMITTEE FOR AERONAUTICS



CONFIDENTIAL

NACA 66₁-010



x (percent c)	y (percent c)	(v/v) ²	v/v	Δv _a /v
0	0	0	0	3.002
.5	.759	.896	.947	2.012
.75	.913	.972	.986	1.686
1.25	1.141	1.023	1.011	1.296
2.5	1.516	1.078	1.038	.931
5.0	2.087	1.125	1.061	.682
7.5	2.536	1.154	1.074	.551
10	2.917	1.174	1.084	.473
15	3.530	1.198	1.095	.379
20	4.001	1.215	1.102	.322
25	4.363	1.226	1.107	.279
30	4.636	1.236	1.112	.246
35	4.832	1.243	1.115	.220
40	4.953	1.249	1.118	.198
45	5.000	1.255	1.120	.178
50	4.971	1.261	1.123	.161
55	4.865	1.265	1.125	.146
60	4.665	1.270	1.127	.130
65	4.302	1.250	1.118	.114
70	3.787	1.190	1.091	.099
75	3.176	1.121	1.059	.085
80	2.494	1.052	1.026	.070
85	1.773	.979	.989	.056
90	1.054	.904	.951	.043
95	.408	.821	.906	.027
100	0	.729	.854	0

L.E. radius: 0.662

NACA 66₁-010 basic thickness form

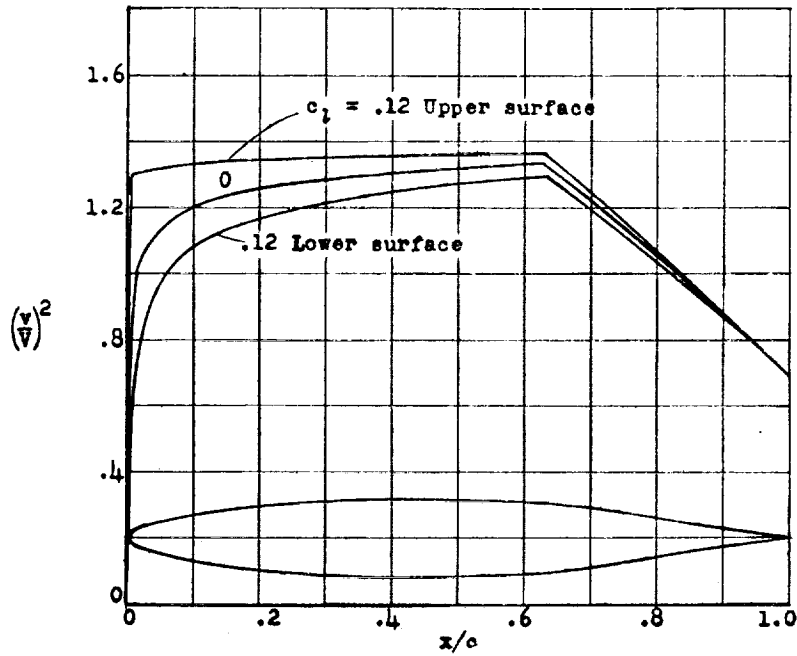
CONFIDENTIAL

NATIONAL ADVISORY
COMMITTEE FOR AERONAUTICS



NACA 66₁-012

CONFIDENTIAL



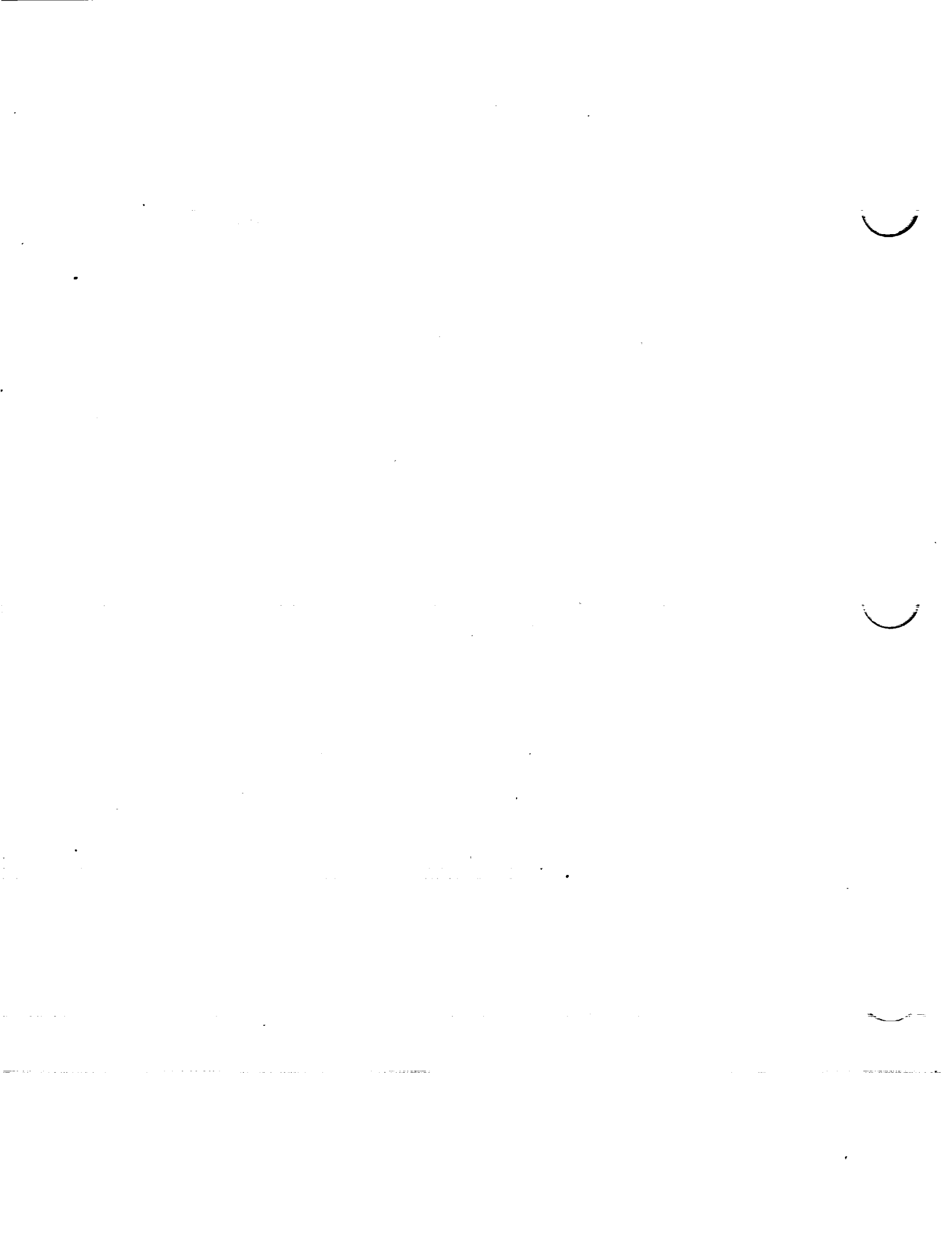
\bar{x} (percent c)	\bar{y} (percent c)	$(v/V)^2$	v/V	$\Delta v_a/V$
0	0	0	0	2.569
.5	.906	.800	.894	1.847
.75	1.087	.915	.957	1.575
1.25	1.358	.980	.990	1.237
2.5	1.808	1.073	1.036	.913
5	2.496	1.138	1.067	.674
7.5	3.037	1.177	1.085	.549
10	3.496	1.204	1.097	.473
15	4.234	1.237	1.112	.380
20	4.801	1.259	1.122	.323
25	5.238	1.275	1.129	.280
30	5.568	1.287	1.134	.246
35	5.803	1.297	1.139	.221
40	5.947	1.303	1.142	.197
45	6.000	1.311	1.145	.176
50	5.965	1.318	1.148	.162
55	5.836	1.323	1.150	.147
60	5.588	1.331	1.154	.132
65	5.139	1.302	1.141	.113
70	4.515	1.221	1.105	.098
75	3.767	1.139	1.067	.084
80	2.944	1.053	1.026	.069
85	2.083	.968	.984	.053
90	1.234	.879	.938	.040
95	.474	.788	.888	.031
100	0	.687	.829	0

L. E. radius: 0.952 percent c

NACA 66₁-012 basic thickness form

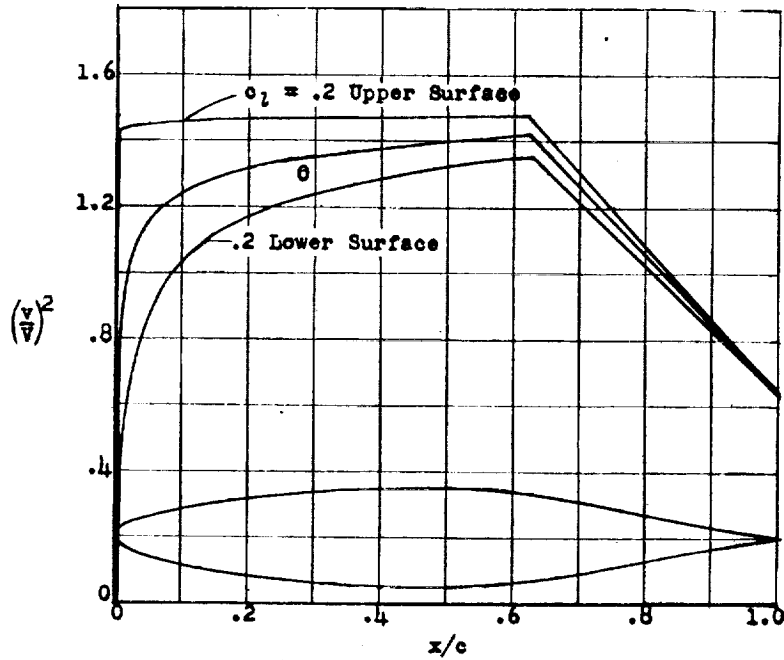
CONFIDENTIAL

NATIONAL ADVISORY
COMMITTEE FOR AERONAUTICS.



NACA 66₂-015

CONFIDENTIAL



x (percent c)	y (percent c)	$(v/V)^2$	v/V	$\Delta v_n/V$
0	0	0	0	2.139
.5	1.122	.760	.872	1.652
.75	1.343	.840	.916	1.431
1.25	1.675	.929	.964	1.172
2.5	2.235	1.055	1.027	.895
5	3.100	1.163	1.078	.663
7.5	3.781	1.208	1.099	.547
10	4.358	1.242	1.114	.473
15	5.286	1.288	1.134	.381
20	5.995	1.317	1.148	.322
25	6.543	1.340	1.158	.280
30	6.956	1.356	1.164	.248
35	7.250	1.370	1.170	.222
40	7.430	1.380	1.175	.200
45	7.495	1.391	1.179	.180
50	7.450	1.401	1.184	.163
55	7.283	1.411	1.188	.146
60	6.959	1.420	1.192	.131
65	6.372	1.367	1.169	.113
70	5.576	1.260	1.122	.096
75	4.632	1.156	1.075	.080
80	3.598	1.053	1.026	.065
85	2.530	.949	.974	.051
90	1.489	.847	.920	.039
95	.566	.744	.863	.025
100	0	.639	.799	0

L. E. radius: 1.435 percent c

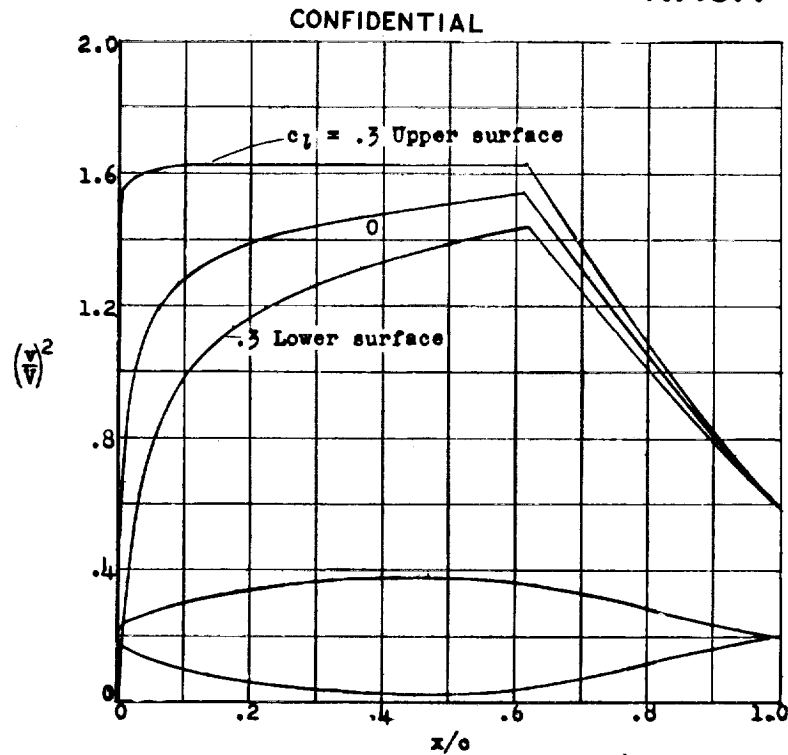
NACA 66₂-015 basic thickness form

CONFIDENTIAL

NATIONAL ADVISORY
COMMITTEE FOR AERONAUTICS.



NACA 66₃-018



x (percent c)	y (percent c)	(v/v) ²	v/v	Δv ₉₀ /V
0	0	0	0	1.773
.5	1.323	.650	.806	1.456
.75	1.571	.735	.857	1.312
1.25	1.952	.850	.897	1.121
2.5	2.646	1.005	1.002	.858
5	3.690	1.154	1.074	.649
7.5	4.513	1.234	1.111	.545
10	5.210	1.285	1.134	.472
15	6.333	1.350	1.162	.381
20	7.188	1.393	1.180	.323
25	7.848	1.423	1.193	.282
30	8.346	1.445	1.202	.250
35	8.701	1.464	1.210	.223
40	8.918	1.481	1.217	.201
45	8.998	1.496	1.223	.181
50	8.942	1.509	1.228	.163
55	8.733	1.522	1.234	.147
60	8.323	1.534	1.238	.131
65	7.580	1.438	1.199	.114
70	6.597	1.302	1.141	.095
75	5.451	1.172	1.083	.077
80	4.206	1.045	1.022	.061
85	2.934	.922	.950	.048
90	1.714	.803	.896	.037
95	.646	.692	.832	.022
100	0	.587	.766	0

L. E. radius: 1.955 percent c

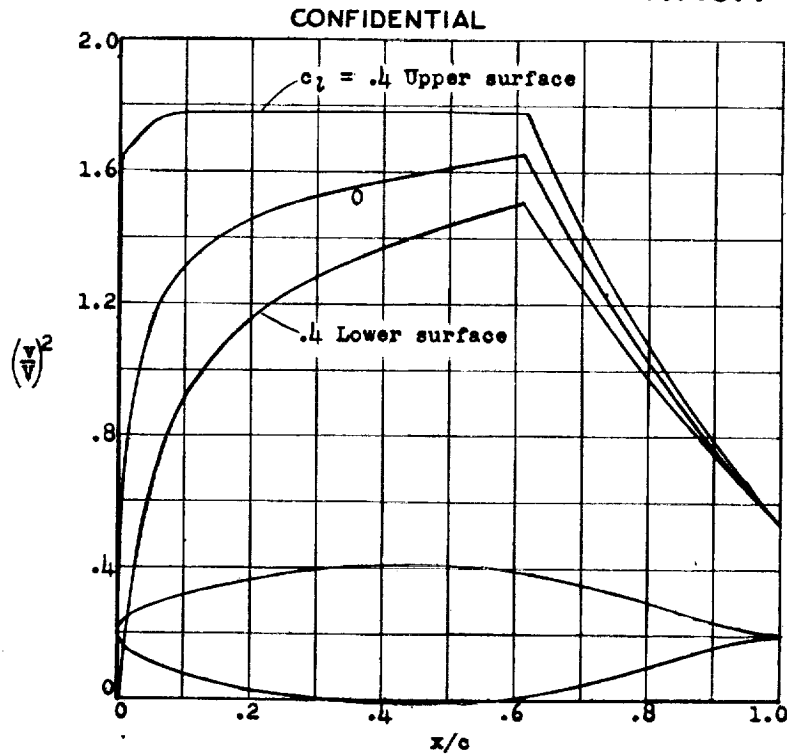
NACA 66₃-018 basic thickness form

CONFIDENTIAL

NATIONAL ADVISORY
COMMITTEE FOR AERONAUTICS.



NACA 66₄-021



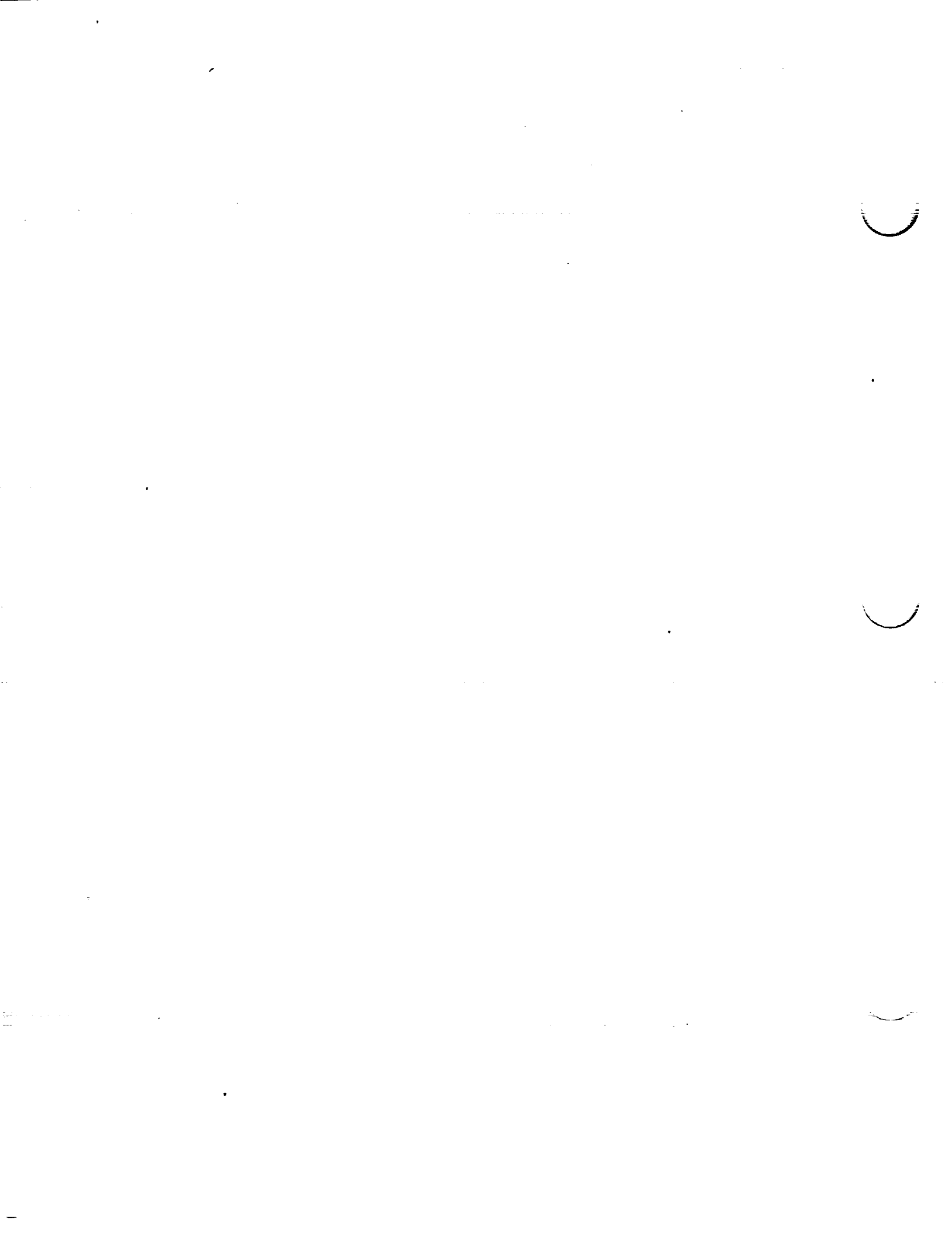
(percent x/c)	(percent y/c)	$(v/v)^2$	v/v	$\Delta v_a/v$
0	0	0	0	1.547
.5	1.525	.580	.761	1.314
.75	1.804	.635	.797	1.218
1.25	2.240	.755	.869	1.054
2.5	3.045	.952	.976	.828
5	4.269	1.143	1.069	.635
7.5	5.233	1.246	1.116	.542
10	6.052	1.318	1.148	.472
15	7.369	1.405	1.185	.381
20	8.376	1.459	1.208	.324
25	9.153	1.499	1.224	.283
30	9.738	1.528	1.236	.251
35	10.154	1.551	1.245	.224
40	10.407	1.574	1.255	.202
45	10.500	1.594	1.263	.183
50	10.434	1.611	1.269	.165
55	10.186	1.629	1.276	.148
60	9.692	1.648	1.284	.132
65	8.793	1.508	1.228	.114
70	7.610	1.335	1.155	.093
75	6.251	1.176	1.084	.073
80	4.796	1.031	1.015	.058
85	3.324	.891	.944	.046
90	1.924	.763	.873	.034
95	.717	.648	.805	.020
100	0	.539	.734	0

L. E. radius: 2.550 percent c

NACA 66₄-021 basic thickness form

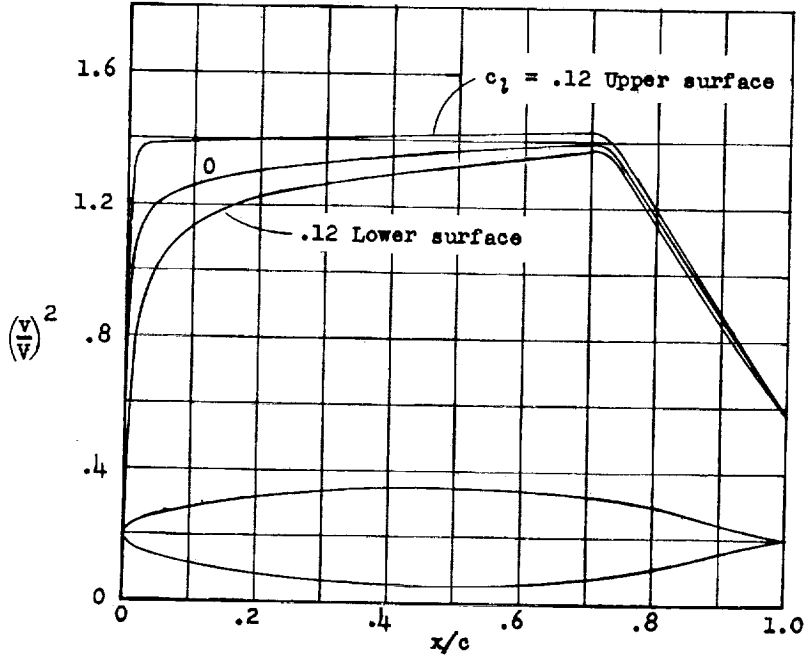
CONFIDENTIAL

NATIONAL ADVISORY
COMMITTEE FOR AERONAUTICS



CONFIDENTIAL

NACA 67,1-015



x (percent c)	y (percent c)	$(v/V)^2$	v/V	$\Delta v_a/V$
0	0	0	0	2.042
.5	1.167	.650	.806	1.560
.75	1.394	.970	.985	1.370
1.25	1.764	1.059	1.029	1.152
2.5	2.395	1.140	1.068	.906
5.0	3.245	1.209	1.100	.667
7.5	3.900	1.239	1.113	.548
10	4.433	1.259	1.122	.470
15	5.283	1.285	1.134	.370
20	5.940	1.304	1.142	.312
25	6.454	1.318	1.148	.276
30	6.854	1.330	1.153	.248
35	7.155	1.341	1.158	.221
40	7.359	1.351	1.162	.201
45	7.475	1.360	1.166	.180
50	7.497	1.368	1.170	.160
55	7.421	1.375	1.173	.142
60	7.231	1.381	1.175	.124
65	6.905	1.388	1.178	.111
70	6.402	1.390	1.179	.108
75	5.621	1.321	1.149	.094
80	4.540	1.176	1.084	.071
85	3.327	1.018	1.009	.060
90	2.021	.864	.930	.045
95	.788	.712	.844	.025
100	0	.570	.755	0

L. E. radius: 1.523 percent c

NACA 67,1-015 basic thickness form

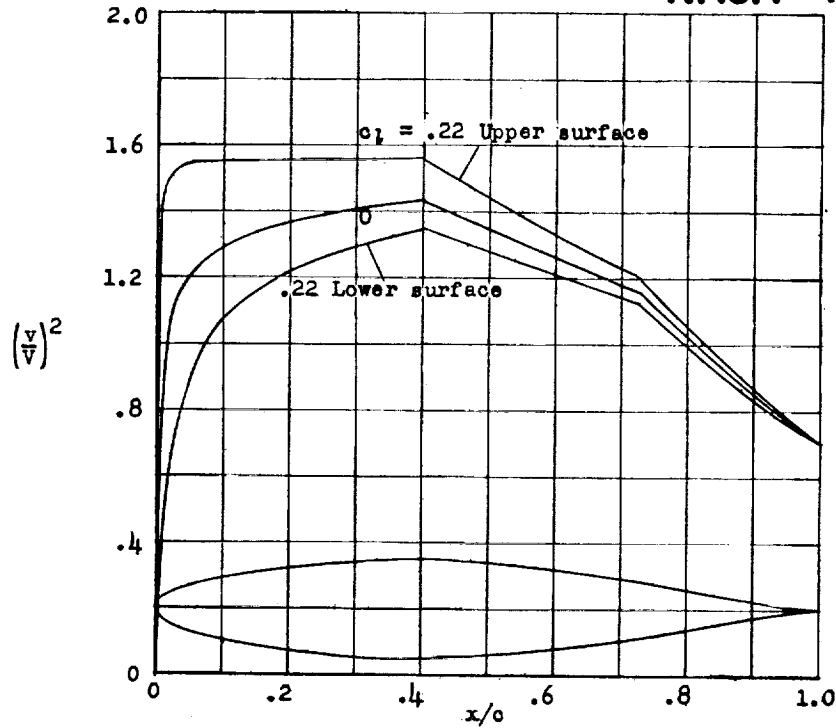
CONFIDENTIAL

NATIONAL ADVISORY
COMMITTEE FOR AERONAUTICS



CONFIDENTIAL

NACA 747A015



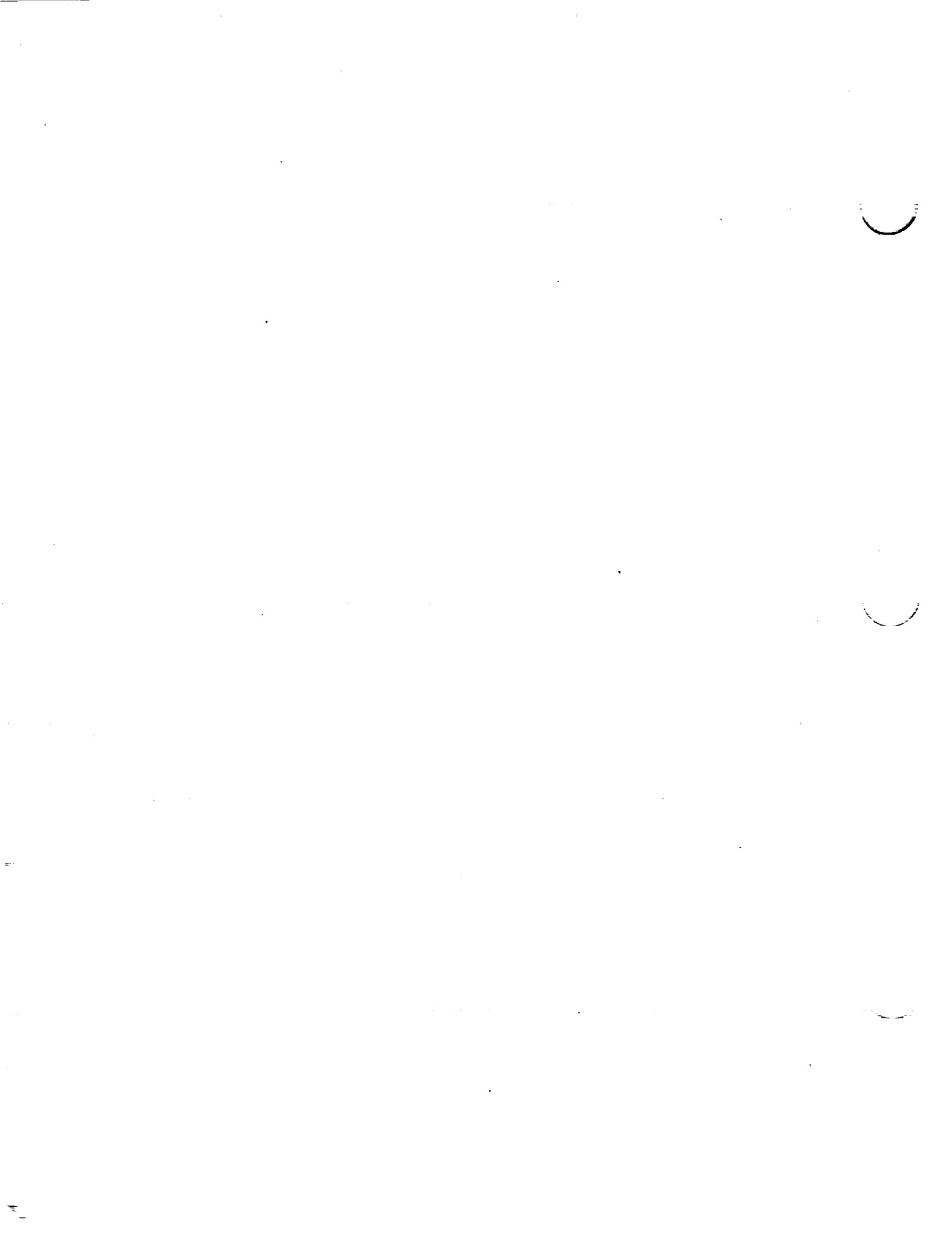
(percent \bar{x} c)	(percent \bar{y} c)	$(v/v)^2$	v/v	$\Delta v_a/v$
0	0	0	0	2.028
.5	1.199	.660	.812	1.680
.75	1.435	.799	.894	1.560
1.25	1.801	.942	.971	1.325
2.5	2.462	1.100	1.049	.990
5	3.419	1.201	1.096	.695
7.5	4.143	1.259	1.122	.551
10	4.743	1.295	1.138	.465
15	5.684	1.339	1.156	.383
20	6.384	1.369	1.170	.324
25	6.898	1.390	1.179	.283
30	7.253	1.409	1.187	.252
35	7.454	1.423	1.193	.224
40	7.494	1.435	1.198	.199
45	7.316	1.391	1.179	.176
50	7.003	1.348	1.161	.156
55	6.584	1.306	1.143	.138
60	6.064	1.265	1.125	.122
65	5.449	1.221	1.105	.108
70	4.738	1.178	1.085	.093
75	3.921	1.115	1.056	.079
80	3.020	1.027	1.013	.065
85	2.086	.938	.969	.052
90	1.193	.852	.923	.040
95	.443	.774	.880	.028
100	0	.703	.838	.018

L. E. radius: 1.544 percent c

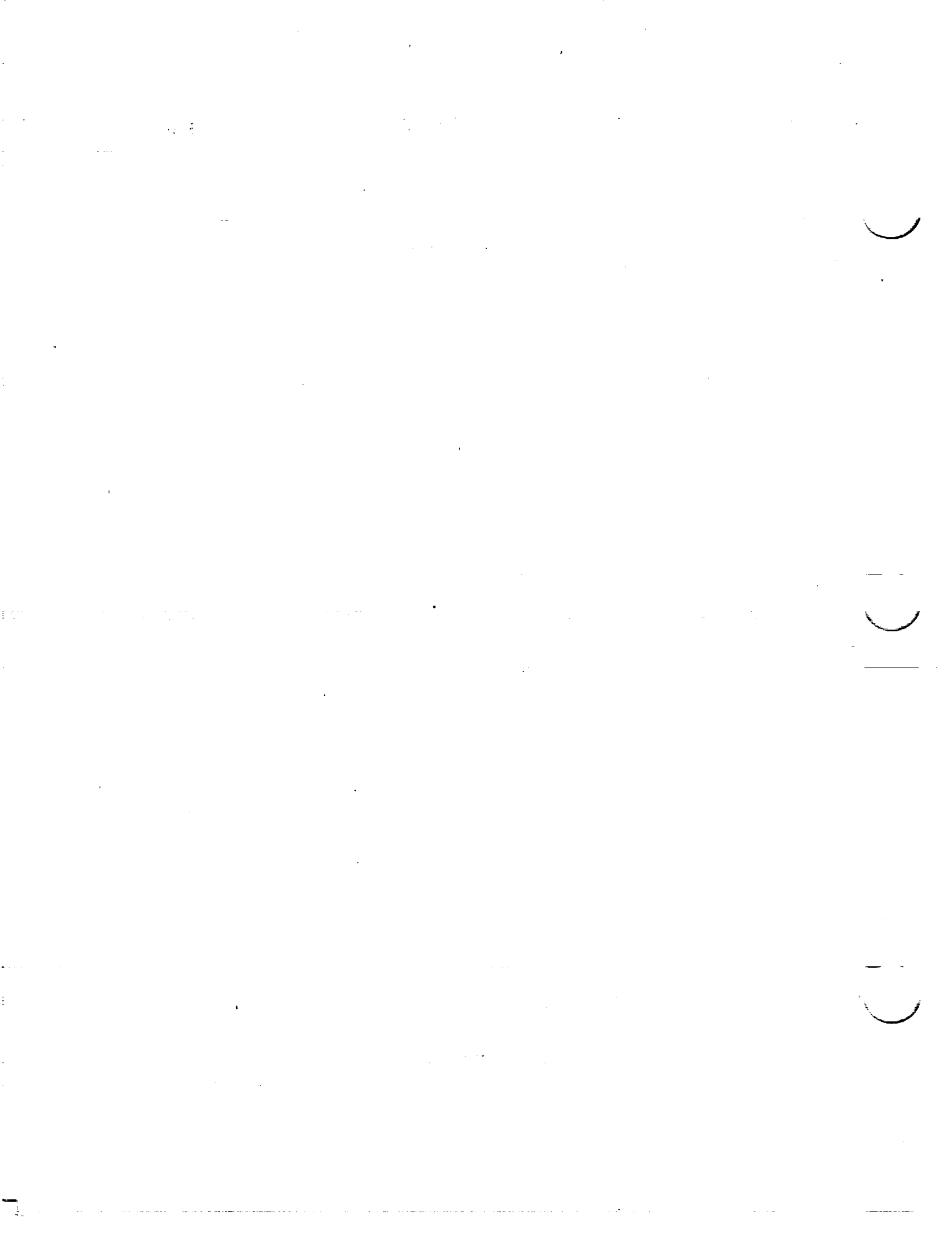
NACA 747A015 basic thickness form

CONFIDENTIAL

NATIONAL ADVISORY
COMMITTEE FOR AERONAUTICS.



II - MEAN LINES



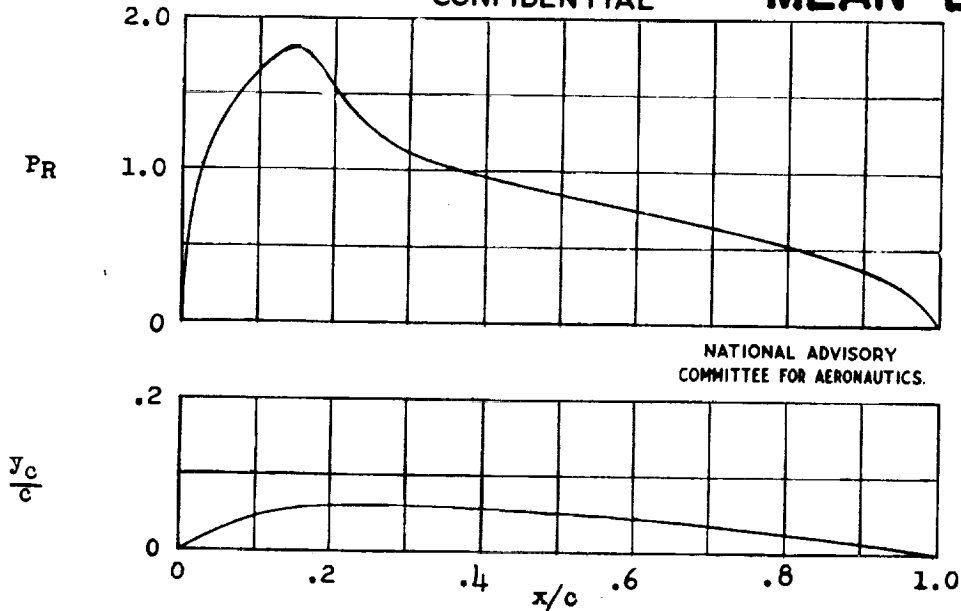
II - MEAN LINES

Data for NACA mean line 62	s42
Data for NACA mean line 63	s43
Data for NACA mean line 64	s44
Data for NACA mean line 65	s45
Data for NACA mean line 66	s46
Data for NACA mean line 67	s47
Data for NACA mean line 210	s48
Data for NACA mean line 220	s49
Data for NACA mean line 230	s50
Data for NACA mean line 240	s51
Data for NACA mean line 250	s52
Data for NACA mean line $a = 0$	s53
Data for NACA mean line $a = 0.1$	s54
Data for NACA mean line $a = 0.2$	s55
Data for NACA mean line $a = 0.3$	s56
Data for NACA mean line $a = 0.4$	s57
Data for NACA mean line $a = 0.5$	s58
Data for NACA mean line $a = 0.6$	s59
Data for NACA mean line $a = 0.7$	s60
Data for NACA mean line $a = 0.8$	s61
Data for NACA mean line $a = 0.9$	s62
Data for NACA mean line $a = 1.0$	s63



NACA 62 MEAN LINE

CONFIDENTIAL



NATIONAL ADVISORY
COMMITTEE FOR AERONAUTICS.

$c_{l1} = 0.90$ $\alpha_1 = 2.81^\circ$ $c_{mc/4} = -0.113$				
x (percent c)	y_c (percent c)	dy_c/dx	PR	$\Delta v/V = PR/4$
0	0	0.60000	0	0
1.25	.726	.56250	.682	.171
2.5	1.406	.52500	1.031	.258
5.0	2.625	.45000	1.314	.328
7.5	3.656	.37500	1.503	.376
10	4.500	.30000	1.651	.413
15	5.625	.15000	1.802	.451
20	6.000	0	1.530	.383
25	5.977	-.00938	1.273	.318
30	5.906	-.01875	1.113	.279
40	5.625	-.03750	.951	.238
50	5.156	-.05625	.843	.211
60	4.500	-.07500	.741	.185
70	3.656	-.09375	.635	.159
80	2.625	-.11250	.525	.131
90	1.406	-.13125	.377	.094
95	.727	-.14062	.261	.065
100	0	-.15000	0	0

Data for NACA mean line 62

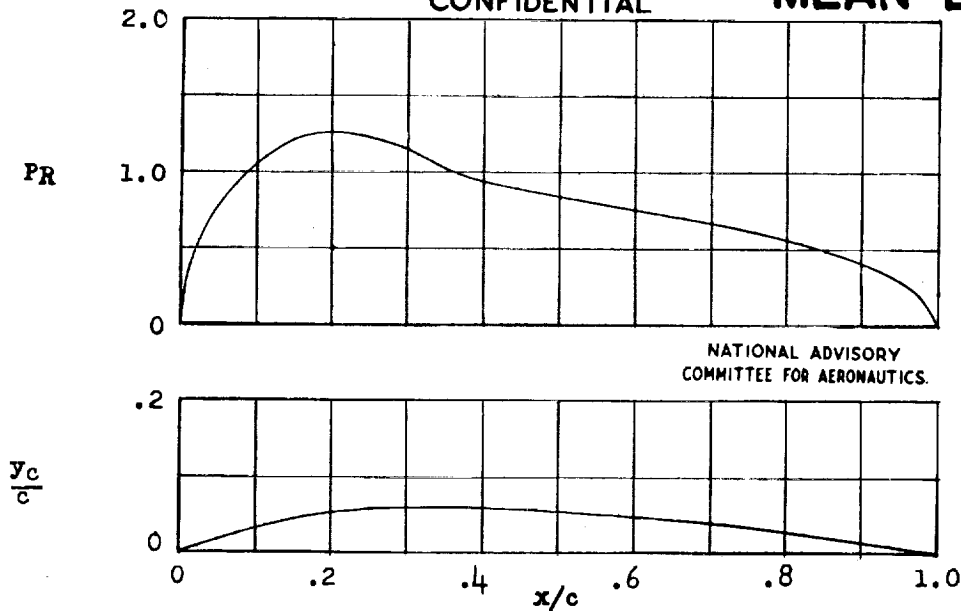
CONFIDENTIAL

12.50



NACA 63 MEAN LINE

CONFIDENTIAL

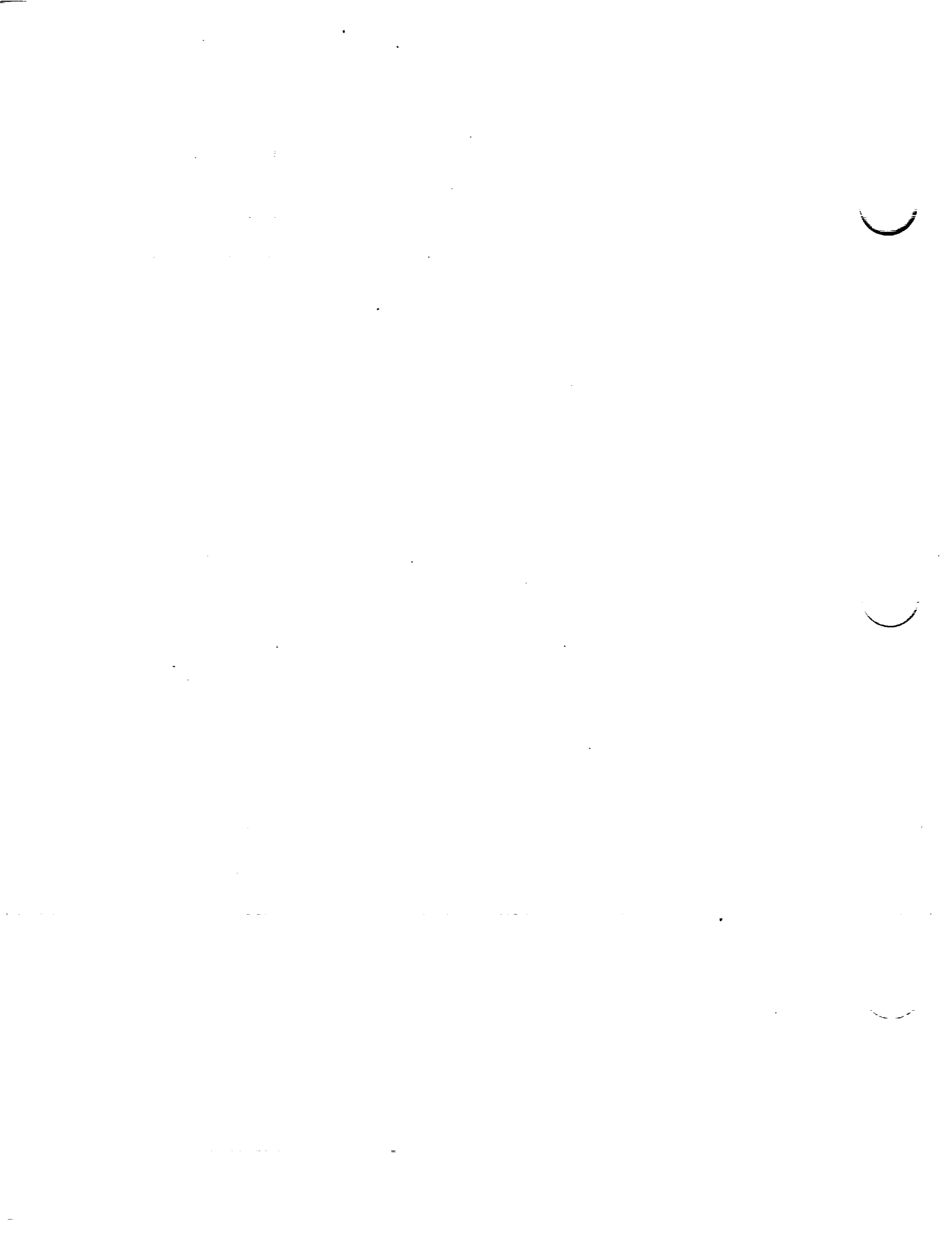


NATIONAL ADVISORY
COMMITTEE FOR AERONAUTICS.

$c_{l1} = 0.80 \quad a_1 = 1.60^\circ \quad c_{m_c}/l_4 = -0.134$				
x	y _c	dy _c /dx	P _R	Δv/V = P _R /4
(percent c)	(percent c)			
0	0	0.40000	0	0
1.25	.489	.38333	.389	.097
2.5	.958	.36667	.553	.138
5.0	1.833	.33333	.788	.197
7.5	2.625	.30000	.940	.235
10	3.333	.26667	1.066	.267
15	4.500	.20000	1.220	.305
20	5.333	.13333	1.259	.315
25	5.833	.06667	1.233	.308
30	6.000	0	1.160	.290
40	5.878	-.02449	.949	.237
50	5.510	-.04898	.850	.213
60	4.898	-.07347	.762	.191
70	4.041	-.09796	.673	.168
80	2.939	-.12245	.560	.140
90	1.592	-.14694	.406	.102
95	.827	-.15918	.291	.073
100	0	-.17143	0	0

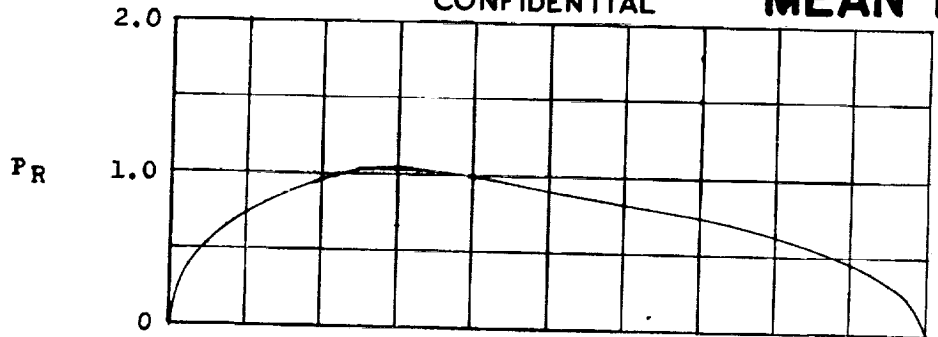
Data for NACA mean line 63

CONFIDENTIAL

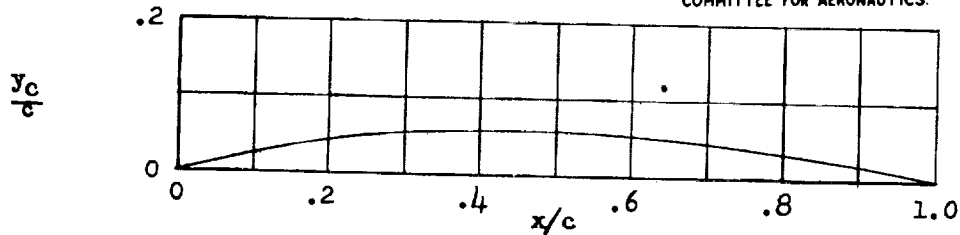


NACA 64 MEAN LINE

CONFIDENTIAL



NATIONAL ADVISORY
COMMITTEE FOR AERONAUTICS.

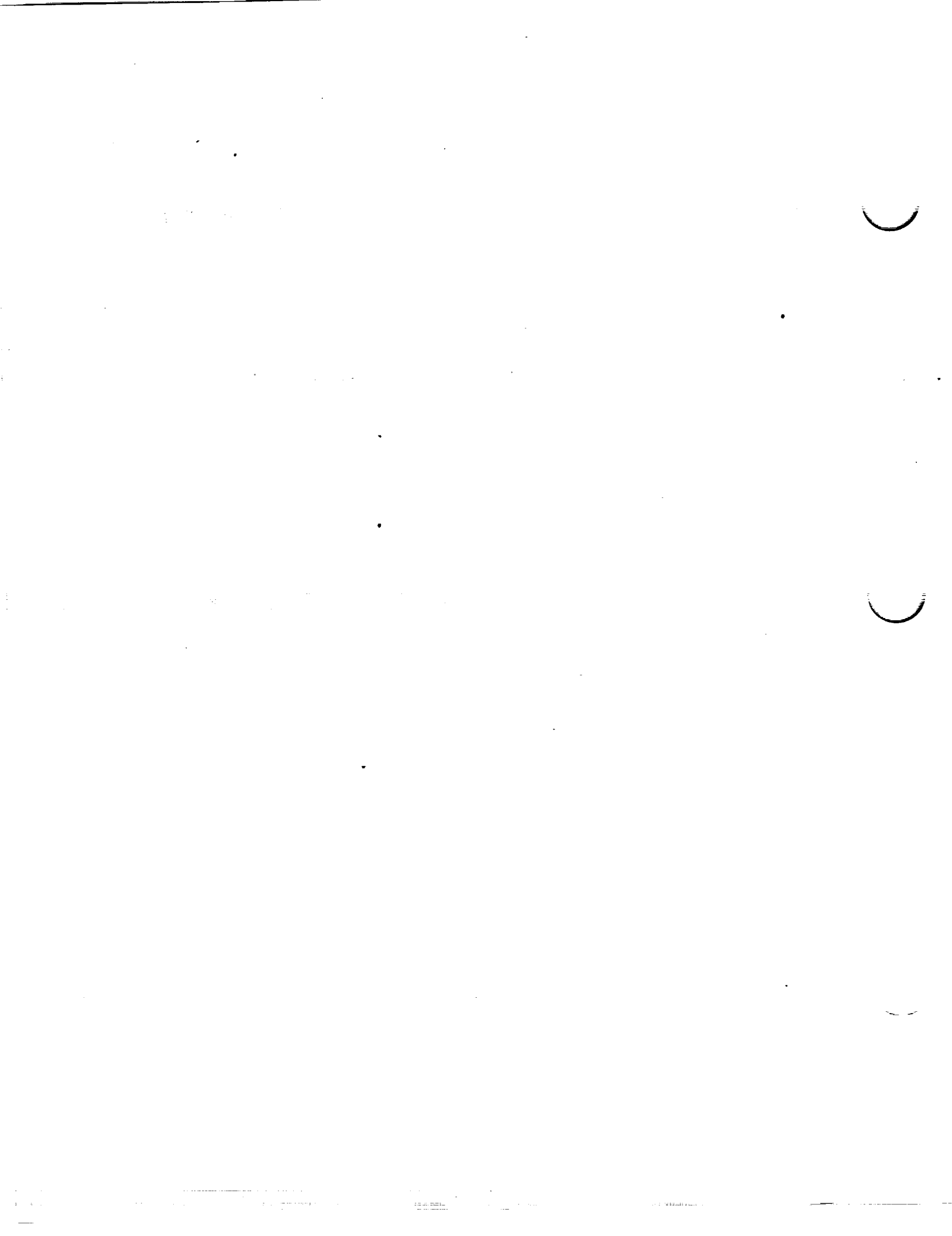


$cl_1 = 0.76$ $\alpha_1 = 0.74^\circ$ $c_{mc}/4 = -0.157$

x (percent c)	y_c (percent c)	dy_c/dx	P_R	$\Delta v/V = P_R/4$
0	0	0.30000	0	0
1.25	.369	.29062	.257	.064
2.5	.726	.28125	.391	.098
5.0	1.406	.26250	.546	.137
7.5	2.039	.24375	.668	.167
10	2.625	.22500	.748	.187
15	3.656	.18750	.871	.218
20	4.500	.15000	.966	.242
25	5.156	.11250	1.030	.258
30	5.625	.07500	1.040	.260
40	6.000	0	.999	.250
50	5.833	-.03333	.910	.228
60	5.333	-.06667	.827	.207
70	4.500	-.10000	.750	.188
80	3.333	-.13333	.635	.159
90	1.833	-.16667	.466	.117
95	.958	-.18333	.334	.084
100	0	-.20000	0	0

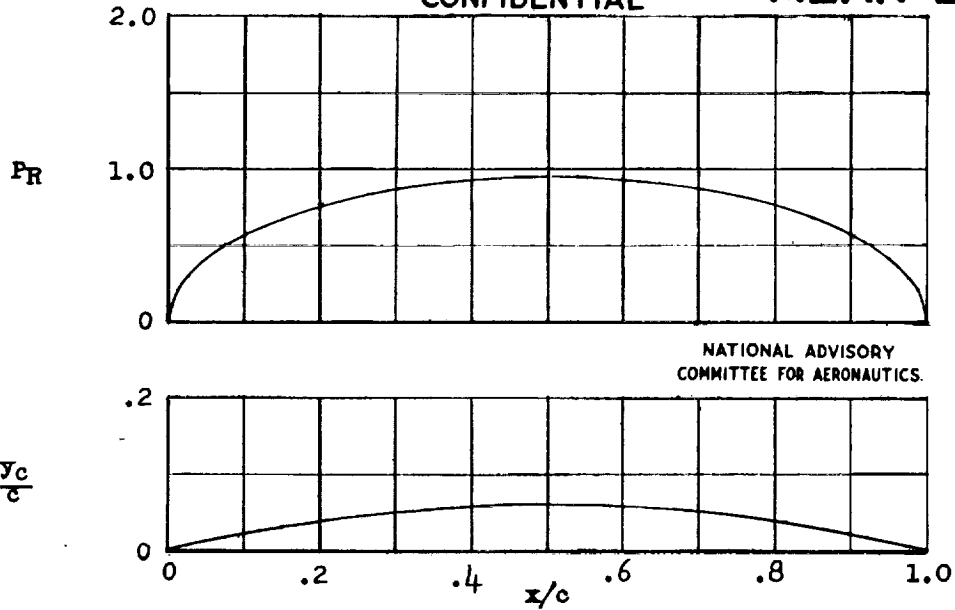
Data for NACA mean line 64

CONFIDENTIAL



NACA 65 MEAN LINE

CONFIDENTIAL



NATIONAL ADVISORY
COMMITTEE FOR AERONAUTICS.

$c_{l1} = 0.75$ $\alpha_1 = 0^\circ$ $c_{mc}/4 = -0.187$				
x (percent c)	y_c (percent c)	dy_c/dx	P_R	$\Delta v/v = P_R/4$
0	0	0.24000	0	0
1.25	.296	.23400	.205	.051
2.5	.585	.22800	.294	.074
5.0	1.140	.21600	.413	.103
7.5	1.665	.20400	.502	.126
10	2.160	.19200	.571	.143
15	3.060	.16800	.679	.170
20	3.840	.14400	.760	.190
25	4.500	.12000	.824	.206
30	5.040	.09600	.872	.218
40	5.760	.04800	.932	.233
50	6.000	0	.951	.238
60	5.760	-.04800	.932	.233
70	5.040	-.09600	.872	.218
80	3.840	-.14400	.760	.190
90	2.160	-.19200	.571	.143
95	1.140	-.21600	.413	.103
100	0	-.24000	0	0

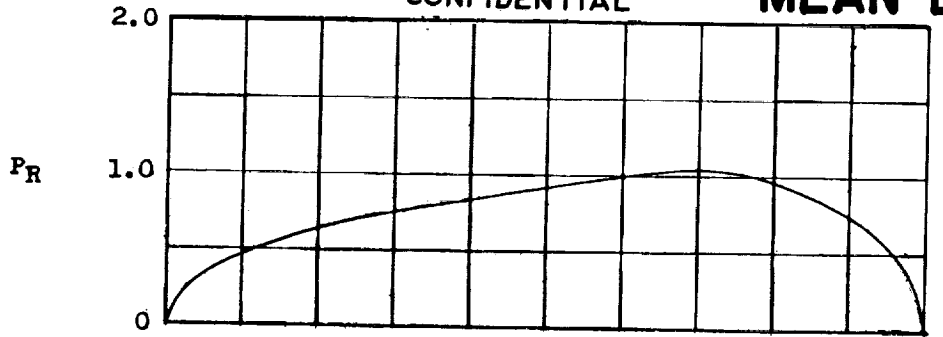
Data for NACA mean line 65

CONFIDENTIAL

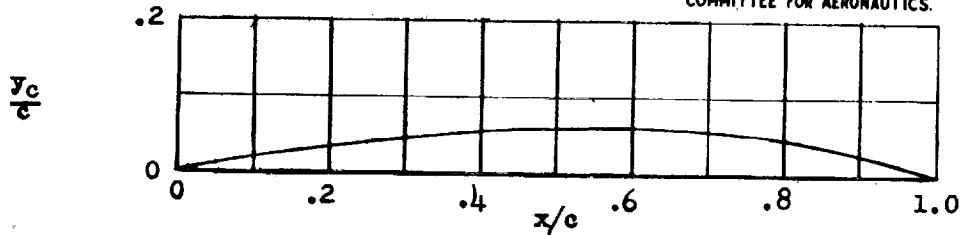


NACA 66 MEAN LINE

CONFIDENTIAL



NATIONAL ADVISORY
COMMITTEE FOR AERONAUTICS.

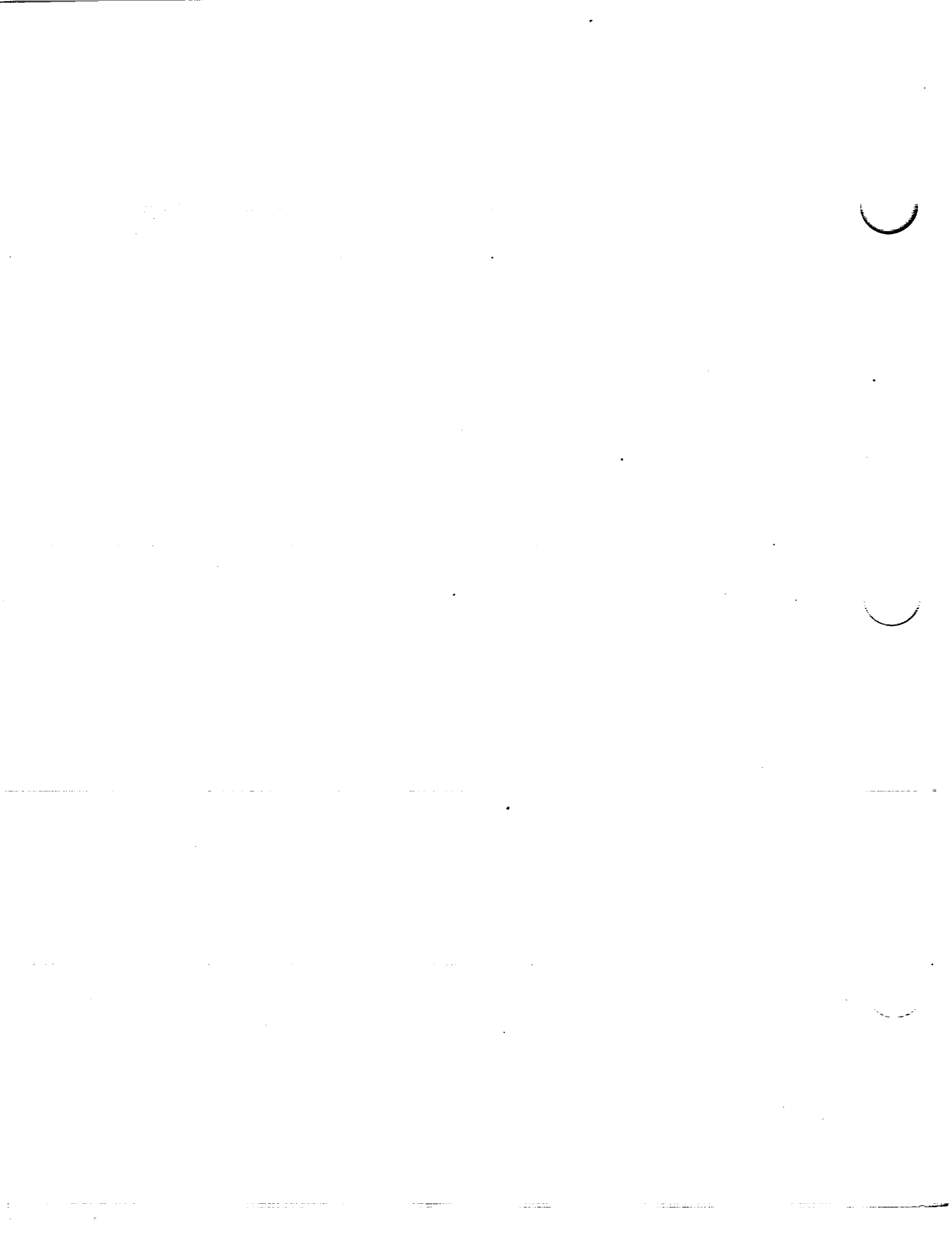


$\alpha_1 = 0.76$ $\alpha_1 = -0.74^\circ$ $c_{mc}/4 = -0.222$

x (percent c)	y_c (percent c)	dy_c/dx	P_R	$\Delta v/V = P_R/4$
0	0	0.20000	0	0
1.25	.247	.19583	.135	.034
2.5	.490	.19167	.244	.061
5.0	.958	.18333	.334	.084
7.5	1.406	.17500	.408	.102
10	1.833	.16667	.466	.117
15	2.625	.15000	.557	.139
20	3.333	.13333	.635	.159
25	3.958	.11667	.700	.175
30	4.500	.10000	.750	.188
40	5.333	.06667	.827	.207
50	5.833	.03333	.910	.228
60	6.000	0	.999	.250
70	5.625	-.07500	1.040	.260
80	4.500	-.15000	.966	.242
90	2.625	-.22500	.748	.187
95	1.406	-.26250	.546	.137
100	0	-.30000	0	0

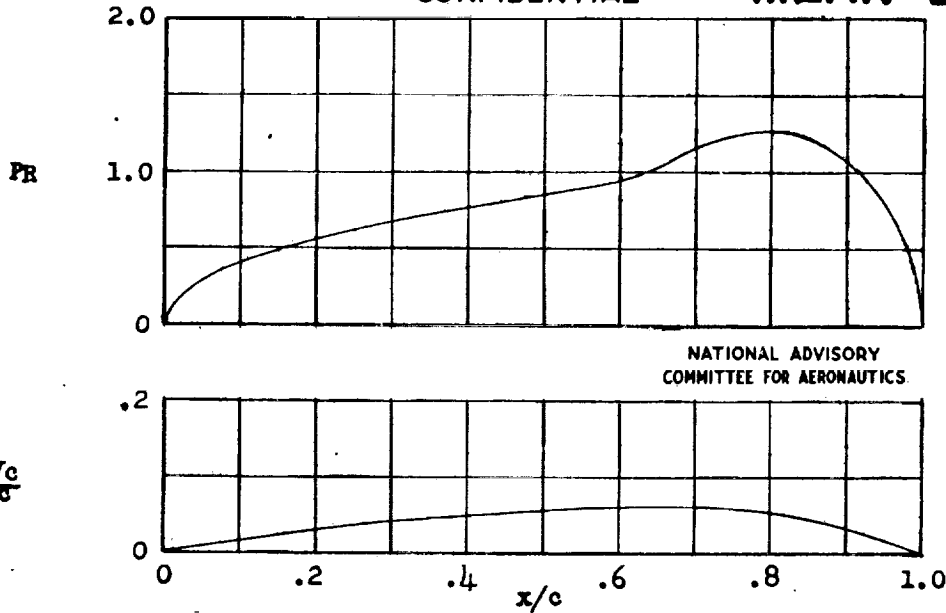
Data for NACA mean line 66

CONFIDENTIAL



NACA 67 MEAN LINE

CONFIDENTIAL



NATIONAL ADVISORY
COMMITTEE FOR AERONAUTICS

$c_{l_1} = 0.80 \quad \alpha_1 = -1.60^\circ \quad c_{m_c/4} = -0.266$				
x	y_c	dy_c/dx	P_R	$\Delta v/v = P_R/4$
(percent c)	(percent c)			
0	0	0.17113	0	0
1.25	.212	.16837	.137	.034
2.5	.421	.16531	.195	.049
5	.827	.15918	.291	.073
7.5	1.217	.15306	.356	.089
10	1.592	.14694	.406	.102
15	2.296	.13469	.483	.121
20	2.939	.12245	.560	.140
25	3.520	.11020	.616	.154
30	4.041	.09796	.673	.168
40	4.898	.07347	.762	.191
50	5.510	.04898	.850	.213
60	5.878	.02449	.949	.237
70	6.000	0	1.160	.290
80	5.333	-.13333	1.259	.315
90	3.333	-.26667	1.066	.267
95	1.833	-.33333	.788	.197
100	0	-.40000	0	0

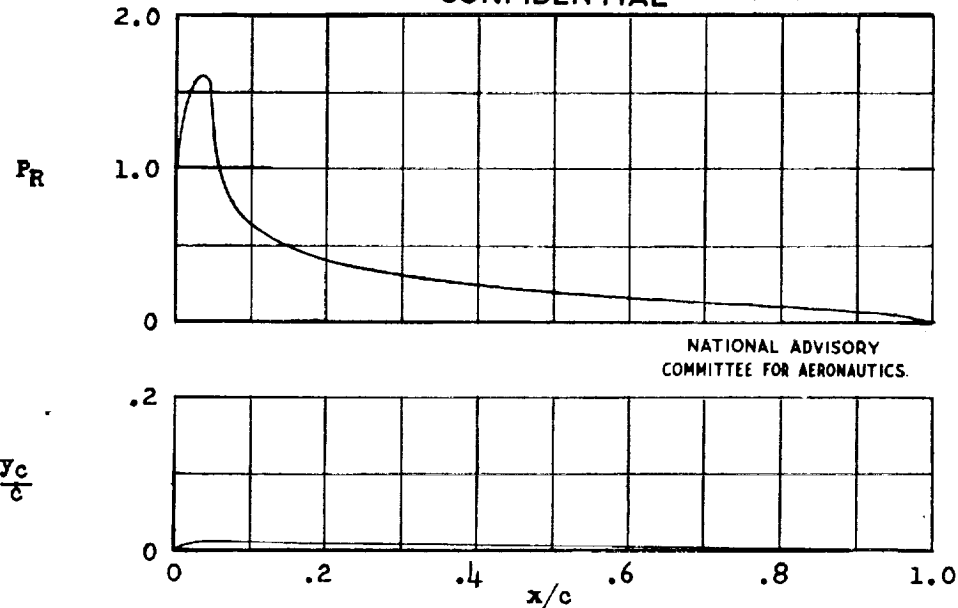
Data for NACA mean line 67

CONFIDENTIAL



NACA 210 MEAN LINE

CONFIDENTIAL

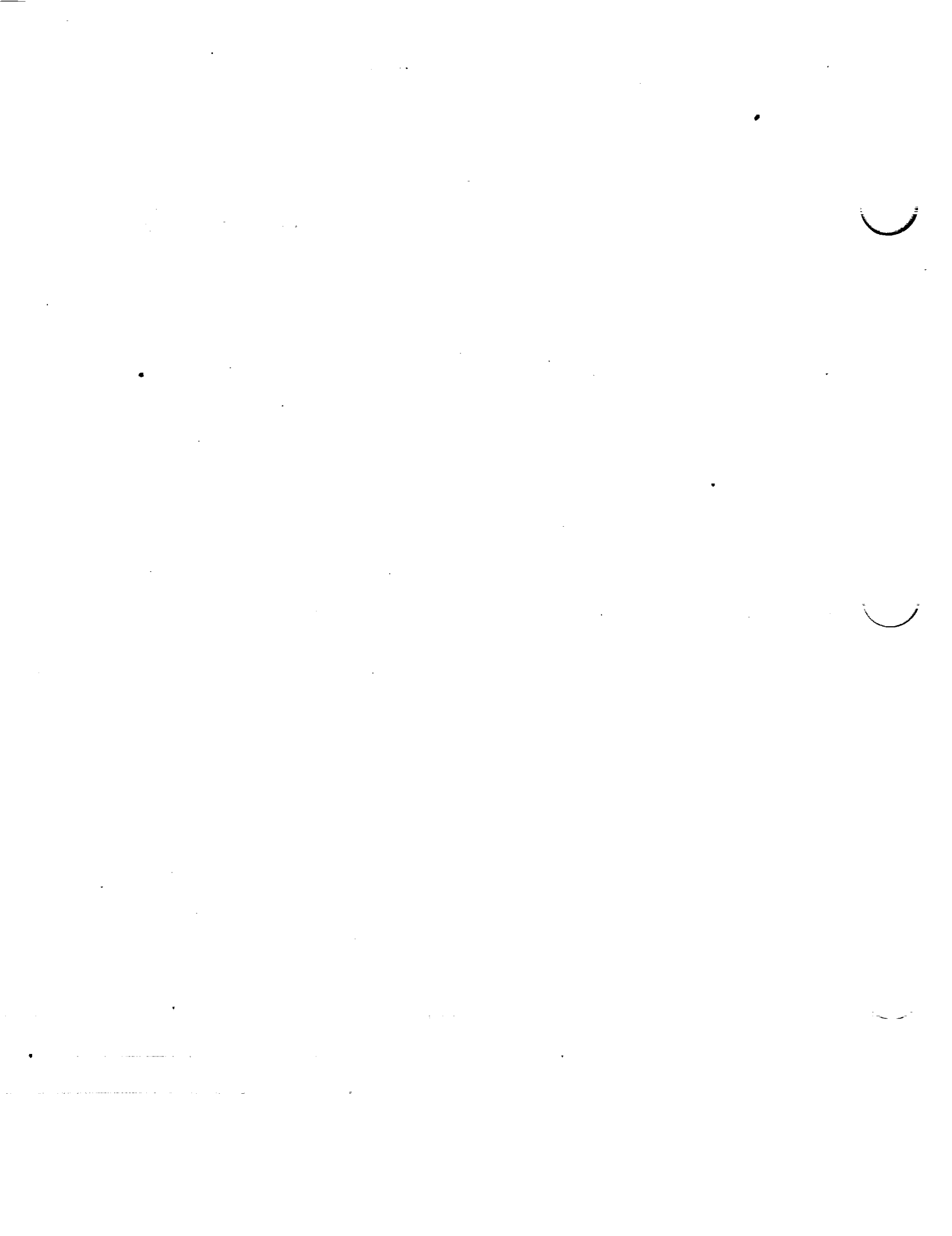


NATIONAL ADVISORY
COMMITTEE FOR AERONAUTICS.

$c_{l_1} = 0.30$ $\alpha_1 = 2.09^\circ$ $c_{m_c/4} = -0.006$				
x (percent c)	yc (percent c)	dy _c /dx	P _R	$\Delta v/v = P_R/4$
0	0	0.59613	0	0
1.25	.596	.36236	1.381	.345
2.5	.928	.18504	1.565	.391
5.0	1.114	-.00018	1.221	.305
7.5	1.087	-.01175	.781	.195
10	1.058		.626	.156
15	.999		.489	.122
20	.940		.408	.102
25	.881		.348	.087
30	.823		.302	.075
40	.705		.242	.061
50	.588		.198	.049
60	.470		.160	.040
70	.353		.128	.032
80	.235	.098	.025	
90	.118	.065	.016	
95	.059	.044	.011	
100	0	0	0	

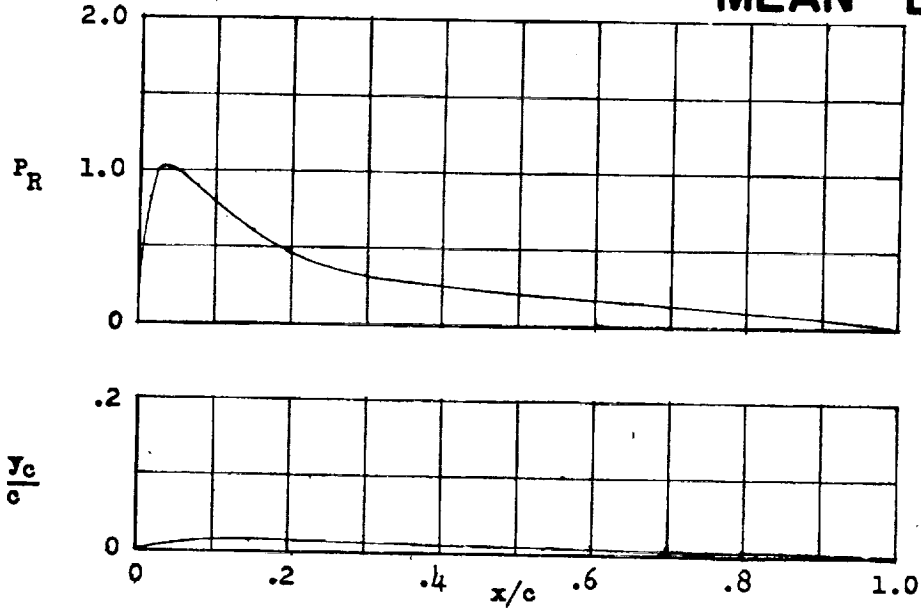
Data for NACA mean line 210

CONFIDENTIAL



CONFIDENTIAL

**NACA 220
MEAN LINE**



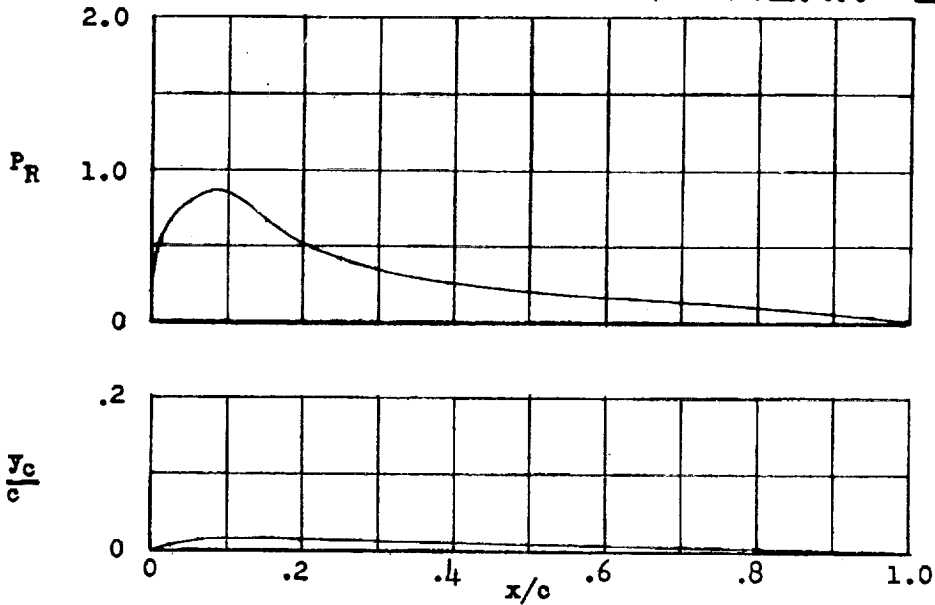
$c_{l1} = 0.30$ $\alpha_1 = 1.86^\circ$ $c_{m_{c/4}} = -0.010$				
x (percent c)	y_c (percent c)	dy_c/dx	P_R	$\Delta v/v = P_R/4$
0	0	0.39270	0	0
1.25	.442	.31541	.822	.206
2.5	.793	.24618	1.003	.251
5.0	1.257	.13192	.988	.247
7.5	1.479	.04994	.900	.225
10	1.535	.00024	.801	.200
15	1.463		.615	.154
20	1.377		.465	.116
25	1.291		.378	.095
30	1.205		.326	.082
40	1.033		.253	.063
50	.861	.01722	.205	.051
60	.689		.169	.042
70	.516		.135	.034
80	.344		.100	.025
90	.172		.064	.016
95	.086		.040	.010
100	0		0	0

Data for NACA mean line 220



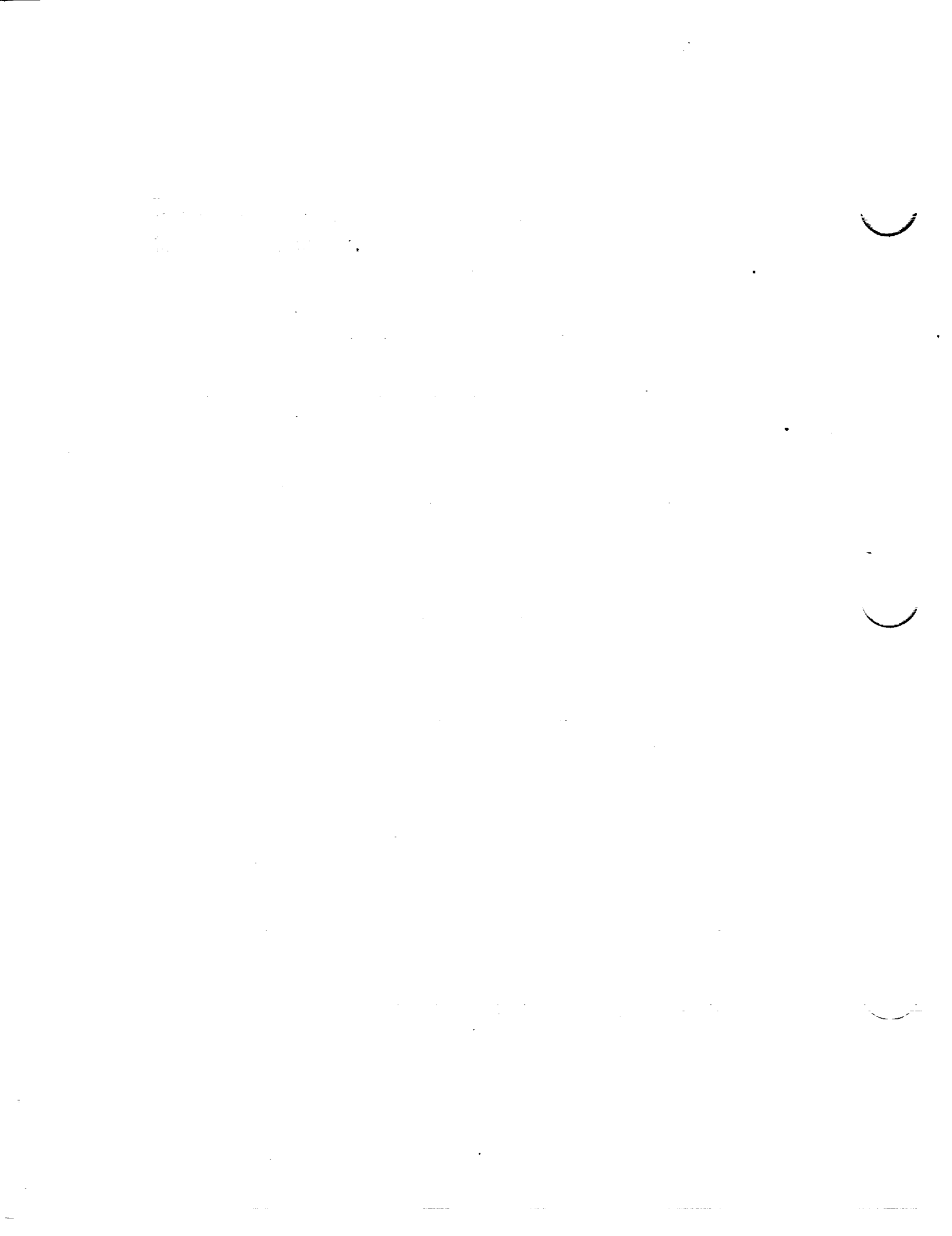
NACA 230 MEAN LINE

CONFIDENTIAL



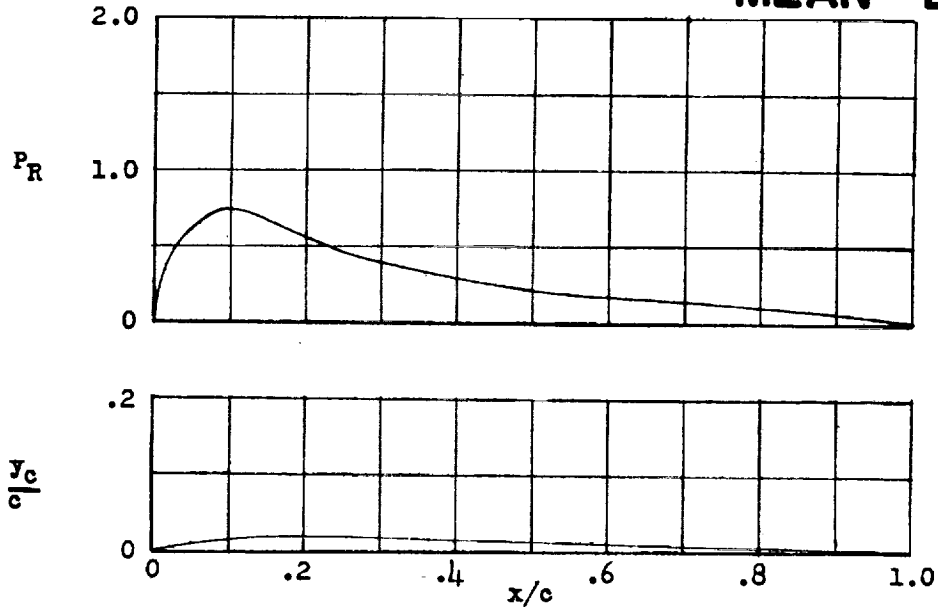
$c_{l_1} = 0.30$ $\alpha_1 = 1.65^\circ$ $c_{m_c/4} = -0.014$				
x (percent c)	y _c (percent c)	dy _c /dx	P _R	Δv/V = P _R /4
0	0	0.30508	0	0
1.25	.357	.26594	.528	.132
2.5	.666	.22929	.673	.168
5.0	1.155	.16347	.791	.198
7.5	1.492	.10762	.853	.213
10	1.701	.06174	.859	.215
15	1.838	-.00009	.678	.170
20	1.767	-.02203	.519	.130
25	1.656		.419	.105
30	1.546		.361	.090
40	1.325		.274	.069
50	1.104		.217	.054
60	.883	-.02208	.177	.044
70	.662		.144	.036
80	.442		.105	.026
90	.221		.069	.017
95	.110		.042	.011
100	0		0	0

Data for NACA mean line 230



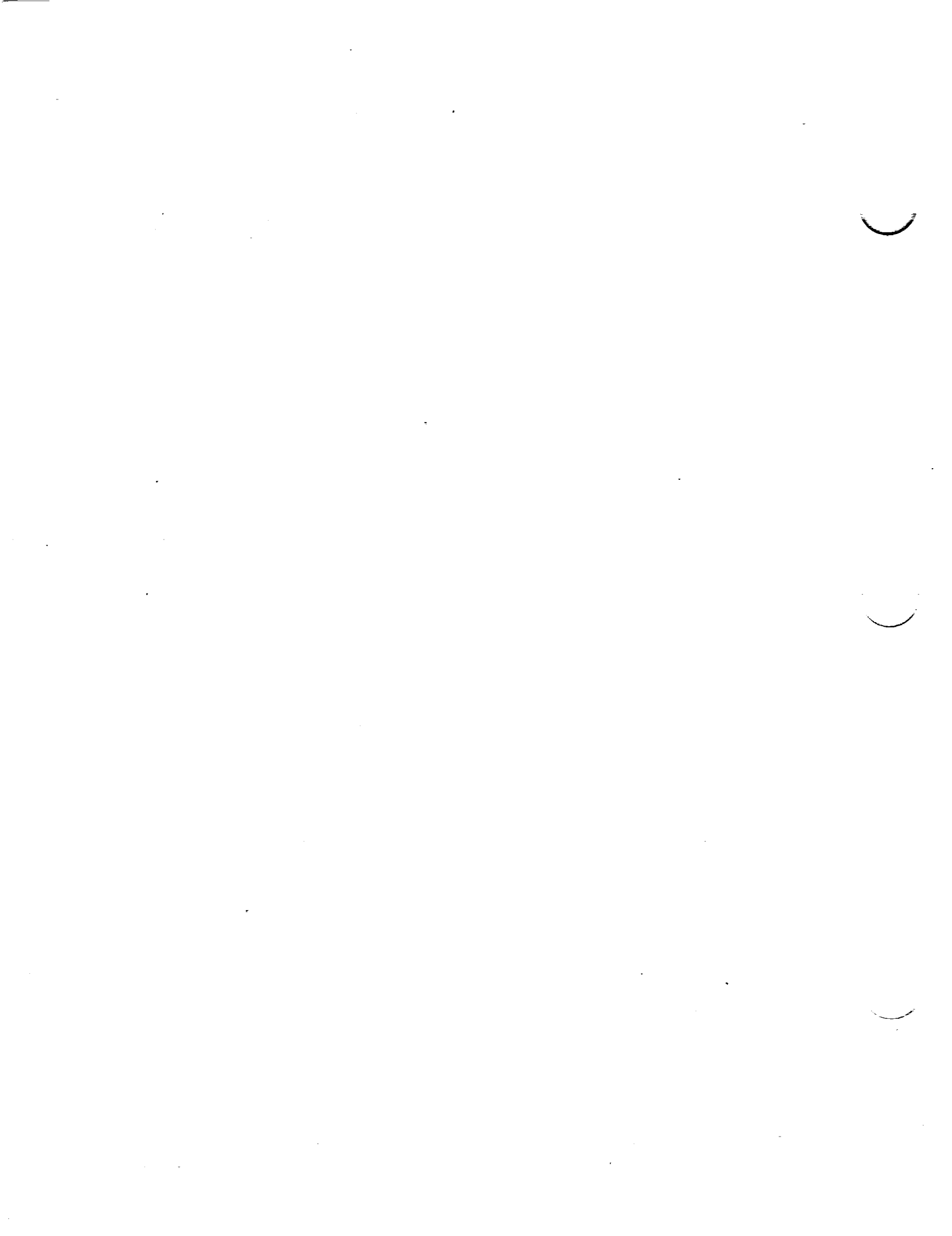
CONFIDENTIAL

**NACA 240
MEAN LINE**

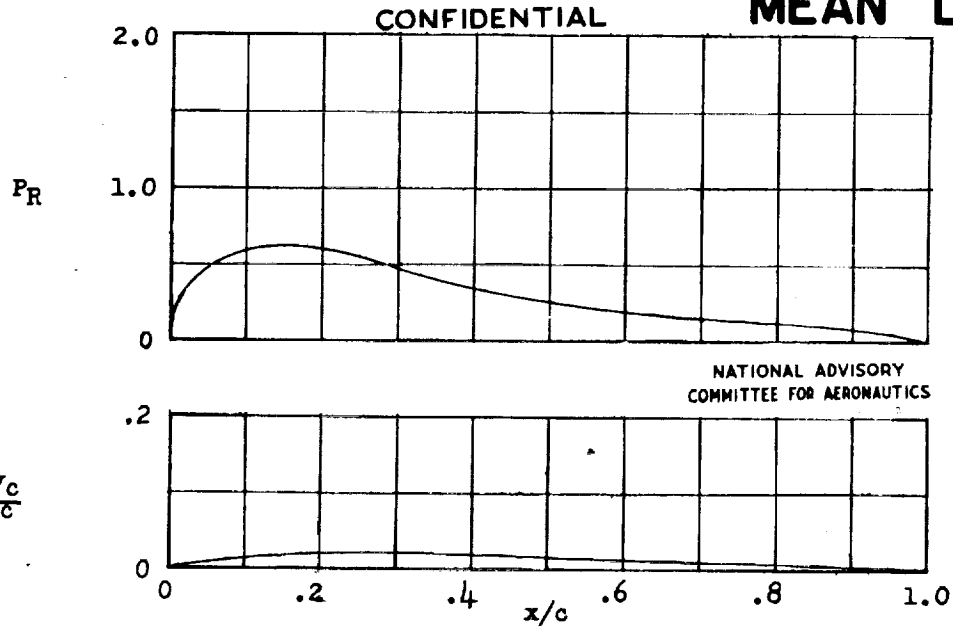


$c_{l_1} = 0.30$ $\alpha_1 = 1.45^\circ$ $c_{m_c/4} = -0.019$				
x (percent c)	y_c (percent c)	dy_c/dx	P_R	$\Delta v/V = P_R/4$
0	0	0.25233	0	0
1.25	.301	.22877	.377	.094
2.5	.572	.20625	.491	.123
5.0	1.035	.16432	.625	.156
7.5	1.397	.12653	.718	.180
10	1.671	.09290	.750	.188
15	1.991	.03810	.677	.169
20	2.079	-.00010	.566	.142
25	2.018	-.02169	.477	.119
30	1.890		.410	.103
40	1.620		.304	.076
50	1.350		.234	.059
60	1.080	-.02700	.186	.047
70	.810		.150	.038
80	.540		.110	.028
90	.270		.071	.018
95	.135		.047	.012
100	0		0	0

Data for NACA mean line 240



NACA 250 MEAN LINE



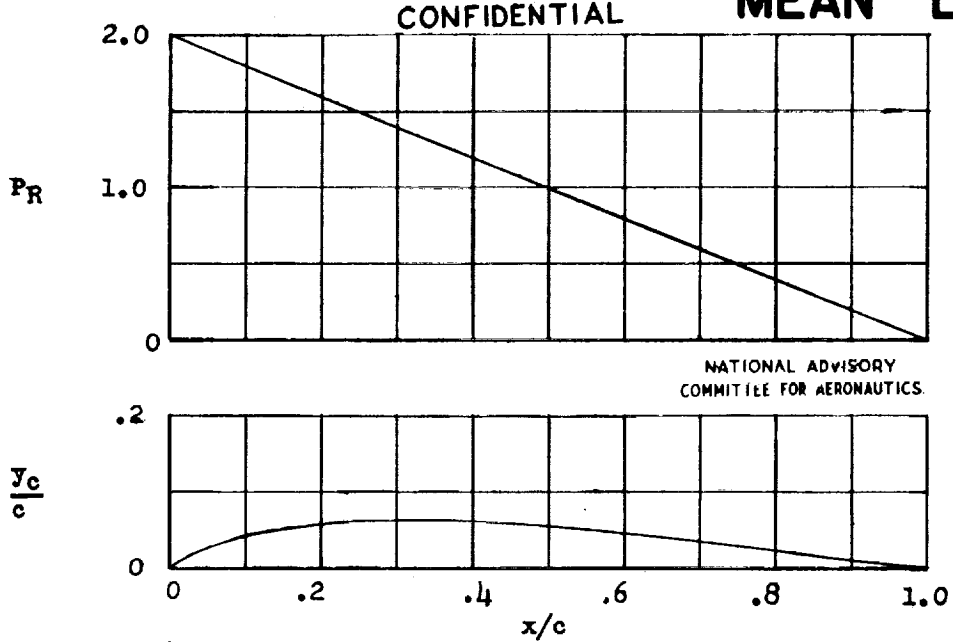
$c_{l1} = 0.30 \quad \alpha_1 = 1.26^\circ \quad c_{mc}/4 = -0.026$				
x (percent c)	y_c (percent c)	dy_c/dx	P_R	$\Delta v/v = P_R/4$
0	0	0.21472	0	0
1.25	.258	.19920	.281	.070
2.5	.498	.18416	.369	.092
5.0	.922	.15562	.477	.119
7.5	1.277	.12909	.552	.138
10	1.570	.10458	.592	.148
15	1.982	.06162	.624	.156
20	2.199	.02674	.610	.153
25	2.263	-.00007	.547	.137
30	2.212	-.01880	.470	.117
40	1.931	} -.03218	.346	.087
50	1.609		.255	.064
60	1.287		.197	.049
70	.965		.154	.038
80	.644		.119	.030
90	.322		.076	.019
95	.161		.051	.013
100	0	0	0	

Data for NACA mean line 250

CONFIDENTIAL



**NACA $\alpha=0$
MEAN LINE**

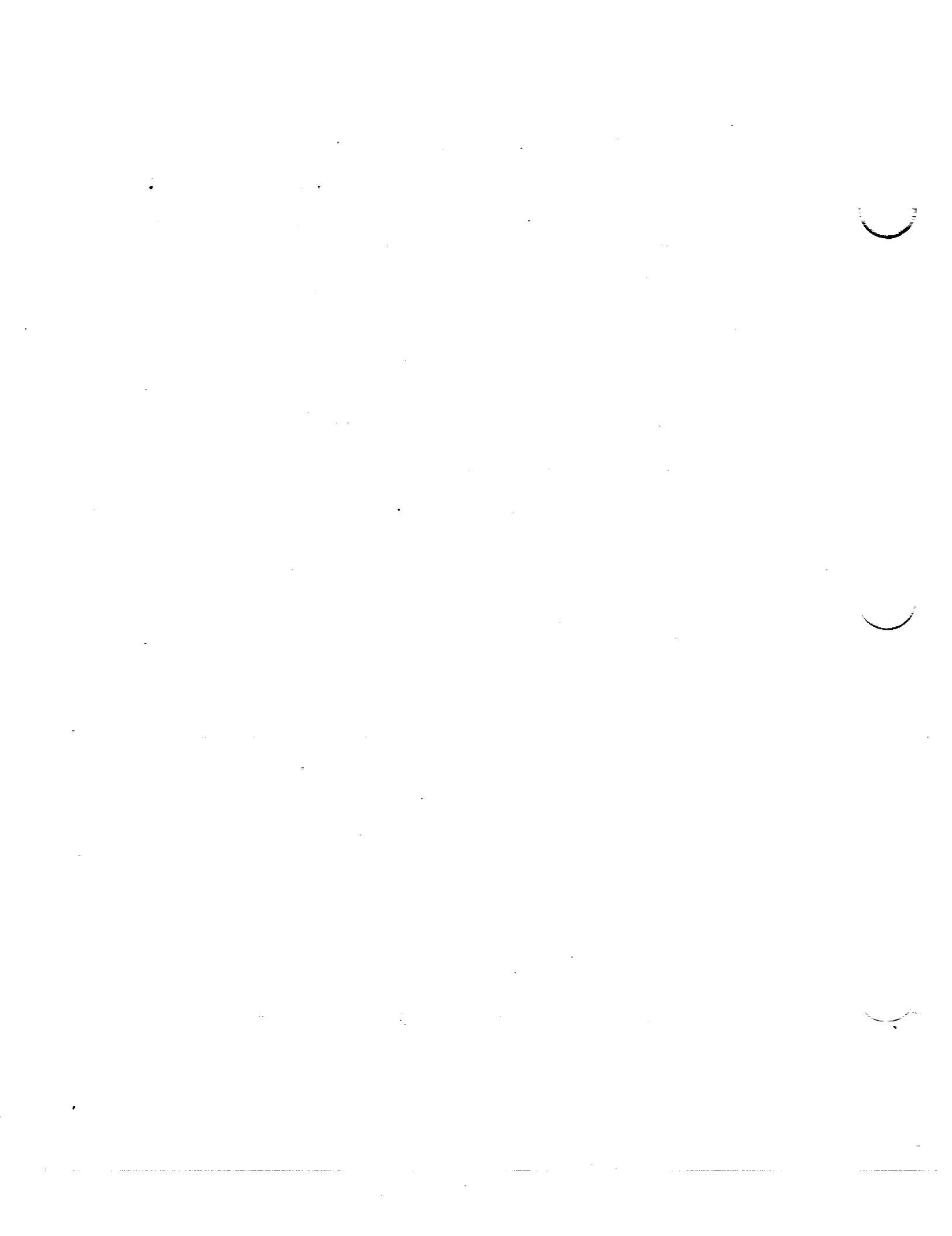


$c_{l1} = 1.0$ $\alpha_1 = 4.90^\circ$ $c_{m c/4} = -0.083$

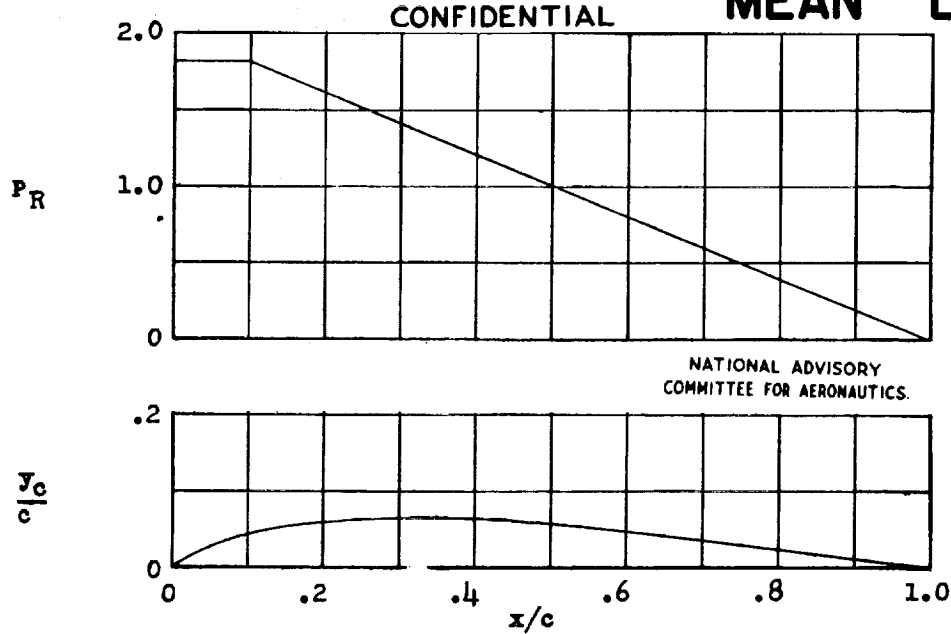
x (percent c)	y_c (percent c)	dy_c/dx	P_R	$\Delta v/V = P_R/4$
0	0	-----	-----	-----
.5	0.460	0.75867	1.990	0.498
.75	.641	.69212	1.985	.496
1.25	.964	.60715	1.975	.494
2.5	1.641	.48892	1.950	.488
5.0	2.693	.36561	1.900	.475
7.5	3.507	.29028	1.850	.463
10	4.161	.23515	1.800	.450
15	5.124	.15508	1.700	.425
20	5.747	.09693	1.600	.400
25	6.114	.05156	1.500	.375
30	6.277	.01482	1.400	.350
35	6.273	-.01554	1.300	.325
40	6.130	-.04086	1.200	.300
45	5.871	-.06201	1.100	.275
50	5.516	-.07958	1.000	.250
55	5.081	-.09395	.900	.225
60	4.581	-.10539	.800	.200
65	4.032	-.11406	.700	.175
70	3.445	-.12003	.600	.150
75	2.836	-.12329	.500	.125
80	2.217	-.12371	.400	.100
85	1.604	-.12099	.300	.075
90	1.013	-.11455	.200	.050
95	.467	-.10301	.100	.025
100	0	-.07953	0	0

CONFIDENTIAL

Data for NACA mean line $\alpha = 0$

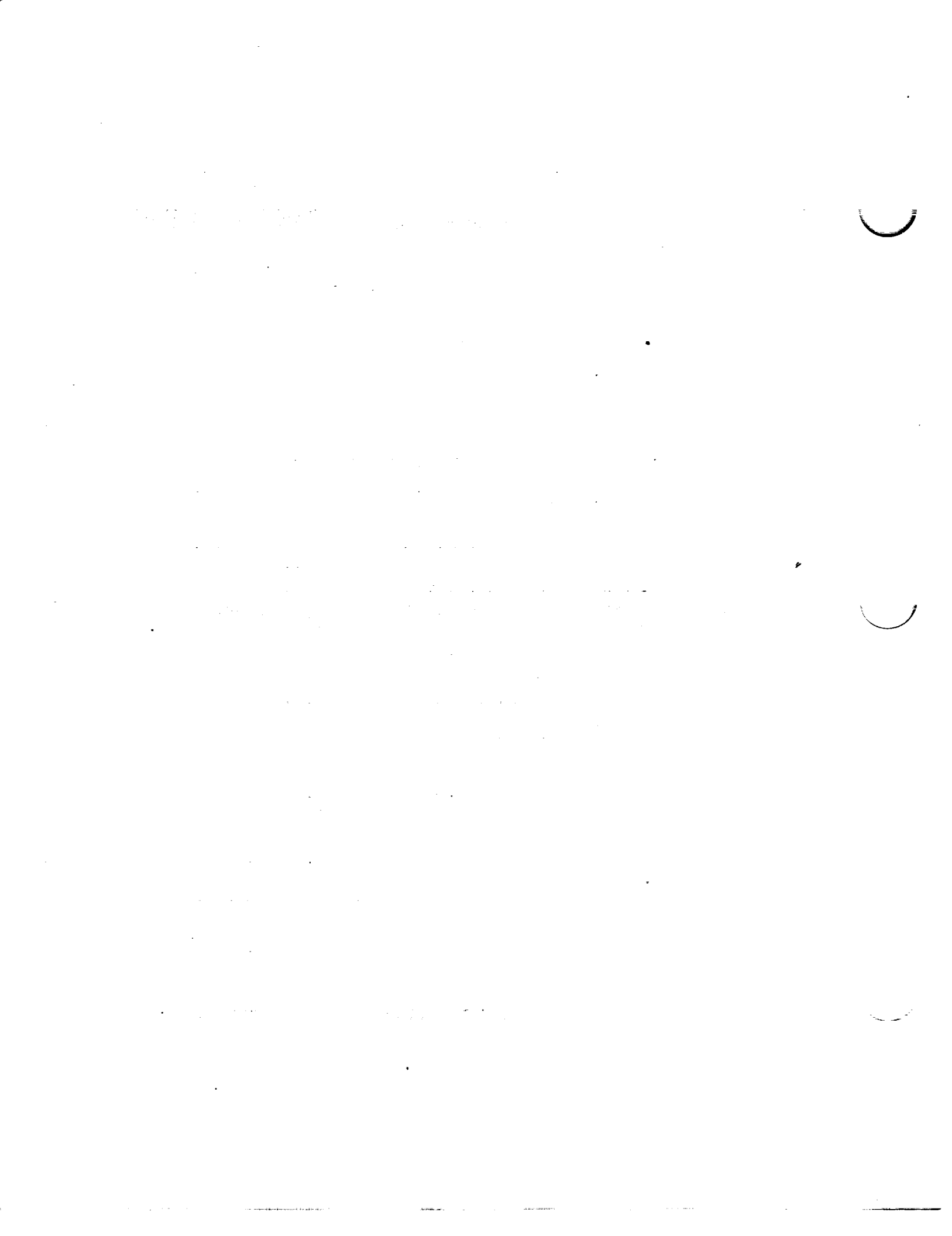


**NACA $\alpha = 0.1$
MEAN LINE**

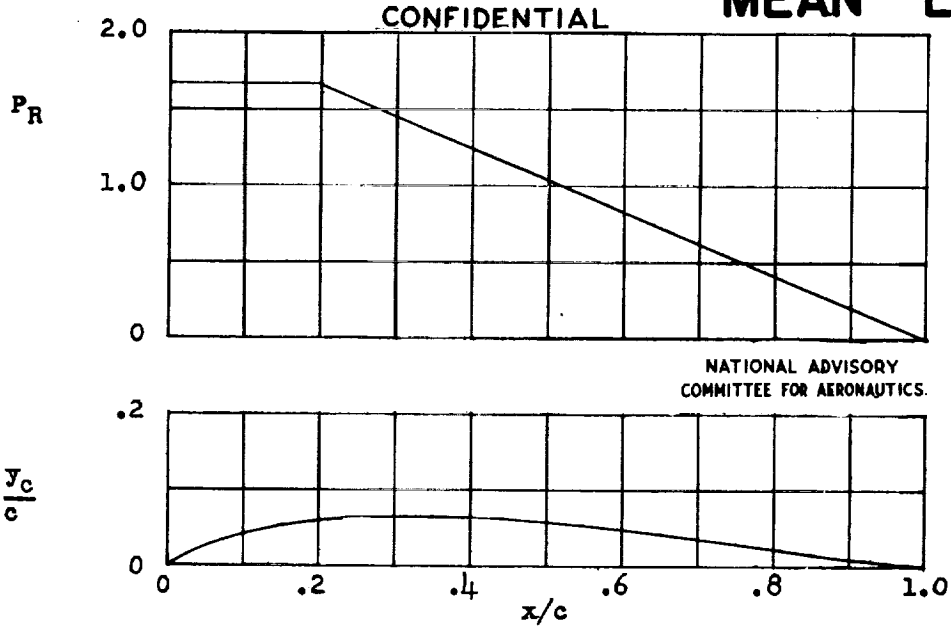


$c_{l1} = 1.0$ $\alpha_1 = 4.78^\circ$ $c_{m,c/4} = -0.086$				
x (percent c)	y_c (percent c)	dy_c/dx	P_R	$\Delta v/v = P_R/4$
0	0	0.73441	-----	-----
.5	0.440	.67479	1.818	0.455
.75	.616	.59896		
1.25	.933	.49366		
2.5	1.608	.38235		
5.0	2.689	.31067		
7.5	3.551	.25057		
10	4.253	.16087	1.717	.429
15	5.261	.09981	1.616	.404
20	5.905	.05281	1.515	.379
25	6.282	.01498	1.414	.354
30	6.449	-.01617	1.313	.328
35	6.443	-.04210	1.212	.303
40	6.296	-.06373	1.111	.278
45	6.029	-.08168	1.010	.253
50	5.664	-.09637	.909	.227
55	5.218	-.10806	.808	.202
60	4.706	-.11694	.707	.177
65	4.142	-.12307	.606	.152
70	3.541	-.12644	.505	.126
75	2.916	-.12693	.404	.101
80	2.281	-.12425	.303	.076
85	1.652	-.11781	.202	.050
90	1.045	-.10620	.101	.025
95	.482	-.08258	0	0
100	0			

CONFIDENTIAL
Data for NACA mean line $\alpha = 0.1$



**NACA $\alpha = 0.2$
MEAN LINE**

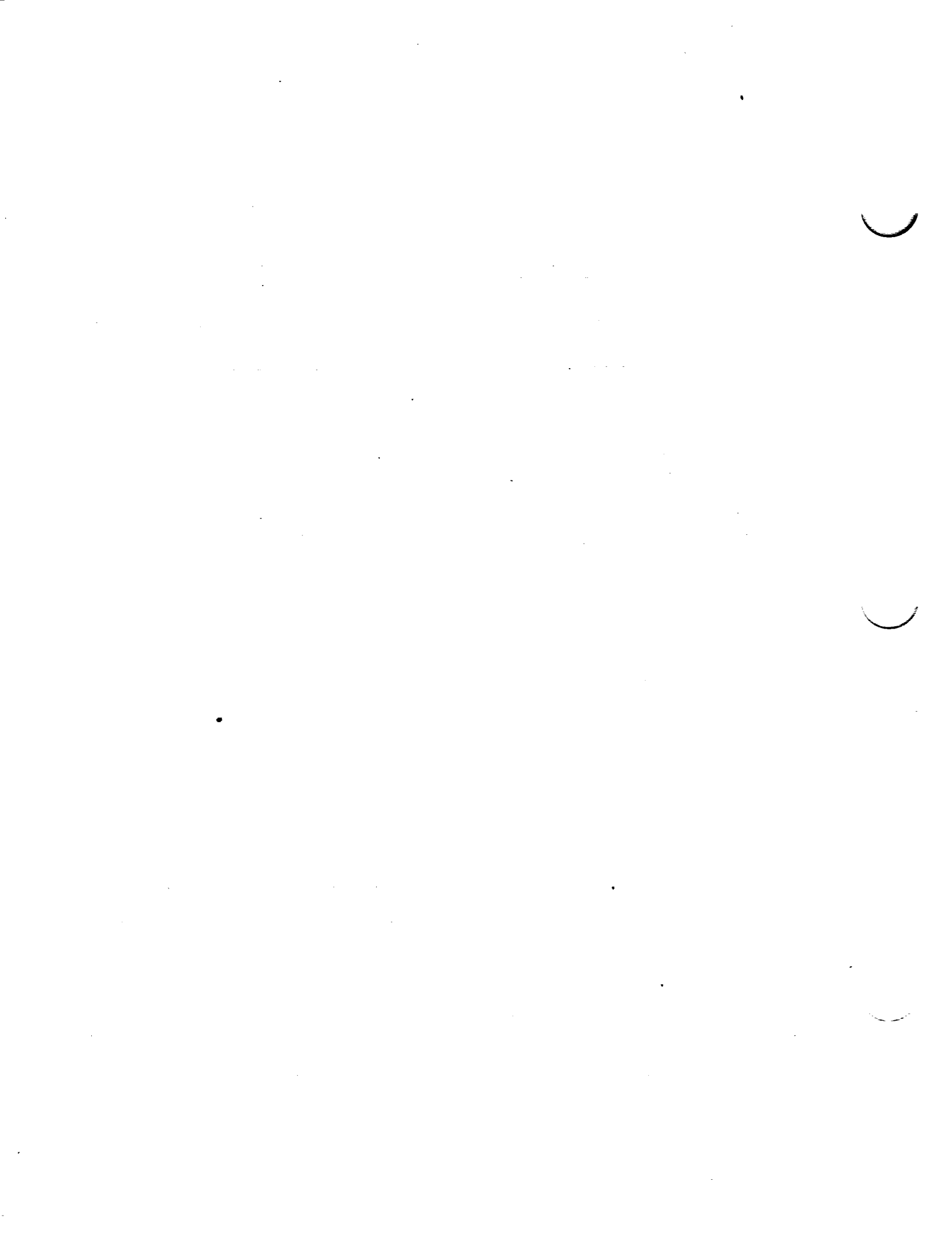


$c_{l1} = 1.0$ $\alpha_1 = 4.36^\circ$ $c_{mc}/4 = -0.094$

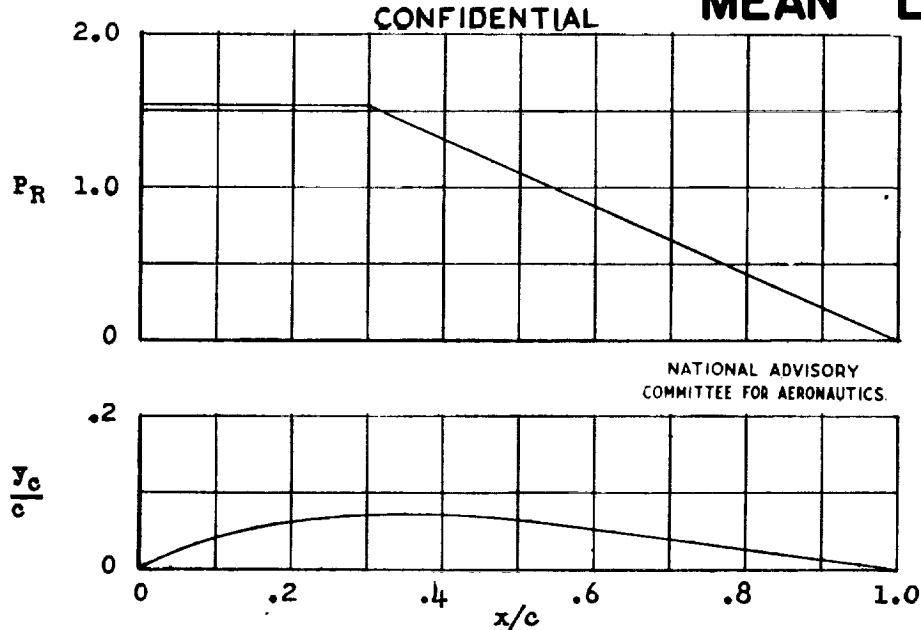
x (percent c)	y_c (percent c)	dy_c/dx	P_R	$\Delta v/v = P_R/4$
0	0	-----	-----	-----
.5	0.414	0.69492	1.667	0.417
.75	.581	.64047		
1.25	.882	.57135		
2.5	1.530	.47592		
5.0	2.583	.37661		
7.5	3.443	.31487		
10	4.169	.26803		
15	5.317	.19373		
20	6.117	.12405		
25	6.572	.06345	1.563	.391
30	6.777	.02030	1.459	.365
35	6.789	-.01418	1.355	.339
40	6.646	-.04246	1.250	.313
45	6.373	-.06588	1.146	.287
50	5.994	-.08522	1.042	.260
55	5.527	-.10101	.938	.234
60	4.989	-.11359	.834	.208
65	4.396	-.12317	.729	.182
70	3.762	-.12985	.625	.156
75	3.102	-.13363	.521	.130
80	2.431	-.13440	.417	.104
85	1.764	-.13186	.313	.078
90	1.119	-.12541	.208	.052
95	.518	-.11361	.104	.026
100	0	-.08941	0	0

CONFIDENTIAL

Data for NACA mean line $\alpha = 0.2$



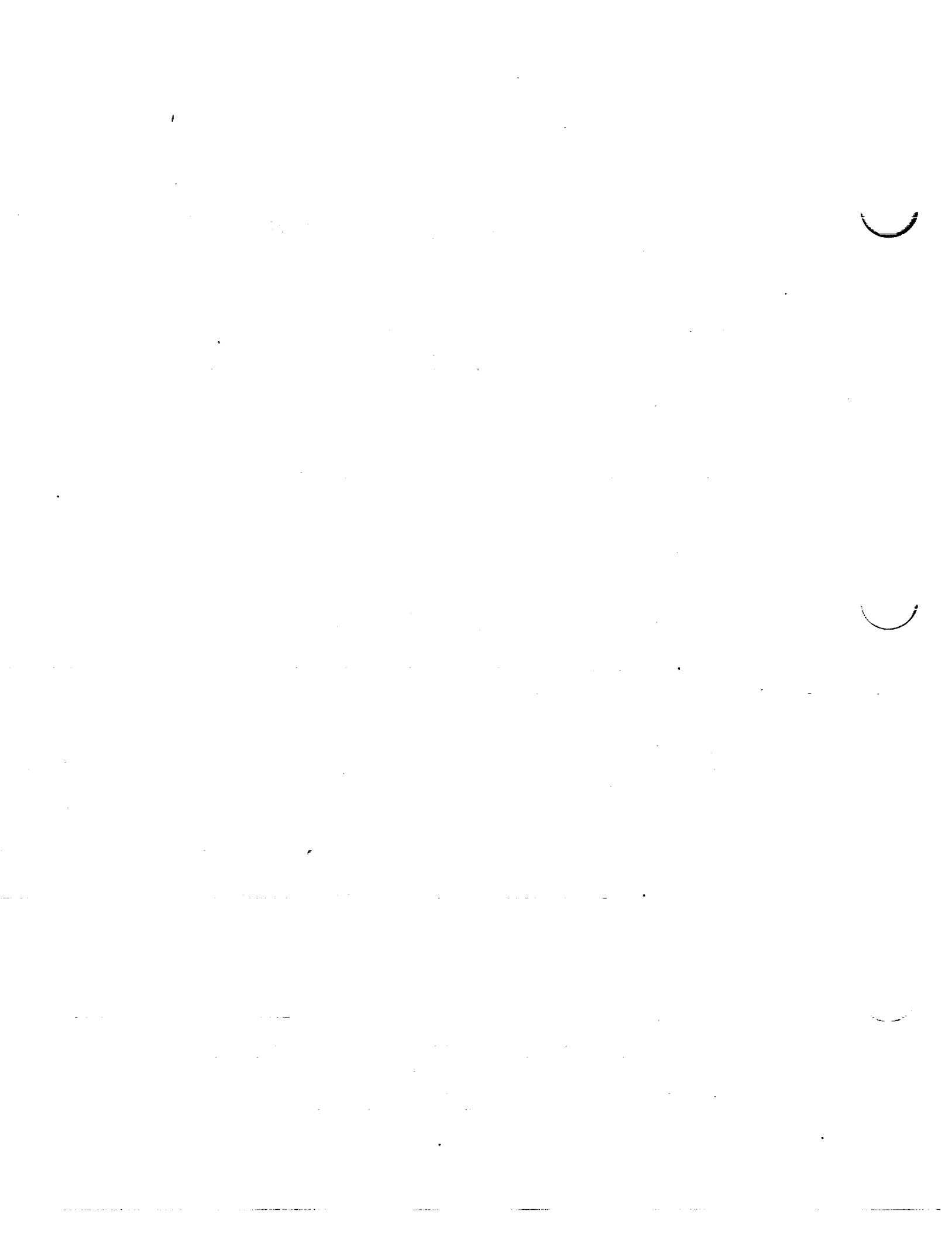
**NACA $\alpha = 0.3$
MEAN LINE**



$c_{l_1} = 1.0$		$\alpha_1 = 3.97^\circ$		$c_{m_{c/4}} = -0.106$				
x (percent c)	y_c (percent c)	dy_c/dx	P_R	$\Delta v/V = P_R/4$				
0	0	-----	-----	-----				
.5	.390	0.65540	1.538	0.385				
.75	.545	.60525						
1.25	.835	.54160						
2.5	1.450	.45405						
5.0	2.455	.36350						
7.5	3.295	.30785						
10	4.010	.26625						
15	5.170	.20250	1.429	.357				
20	6.050	.15070						
25	6.685	.10280						
30	7.070	.04835						
35	7.175	-.00205						
40	7.075	-.03710						
45	6.815	-.06495						
50	6.435	-.08745						
55	5.950	-.10570						
60	5.385	-.12015						
65	4.755	-.13120	.879	.220				
70	4.080	-.13900						
75	3.370	-.14365						
80	2.645	-.14500						
85	1.925	-.14280						
90	1.225	-.13640						
95	.570	-.12430						
100	0	-.09905				0	0	

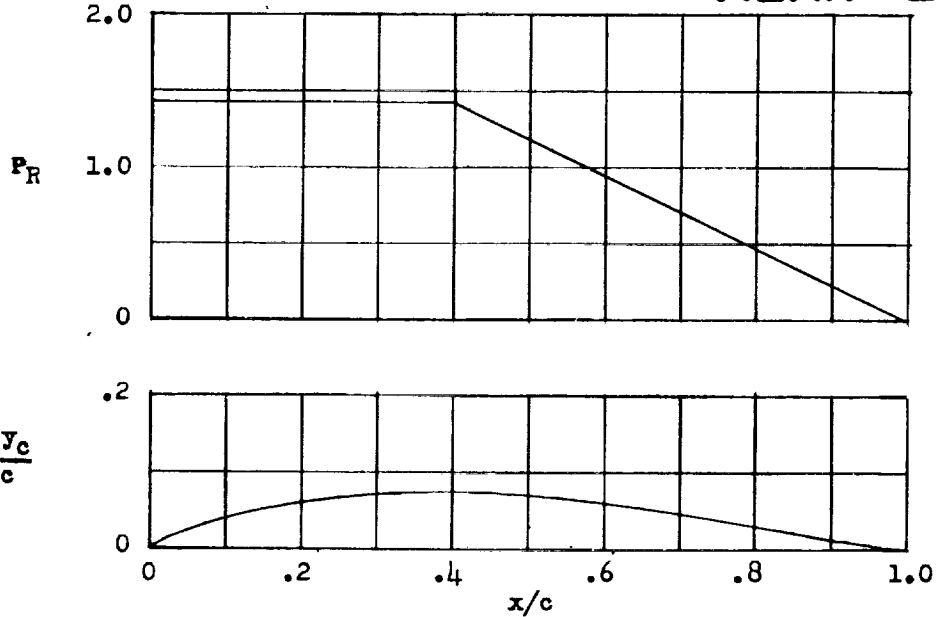
Data for NACA mean line $\alpha = 0.3$

CONFIDENTIAL



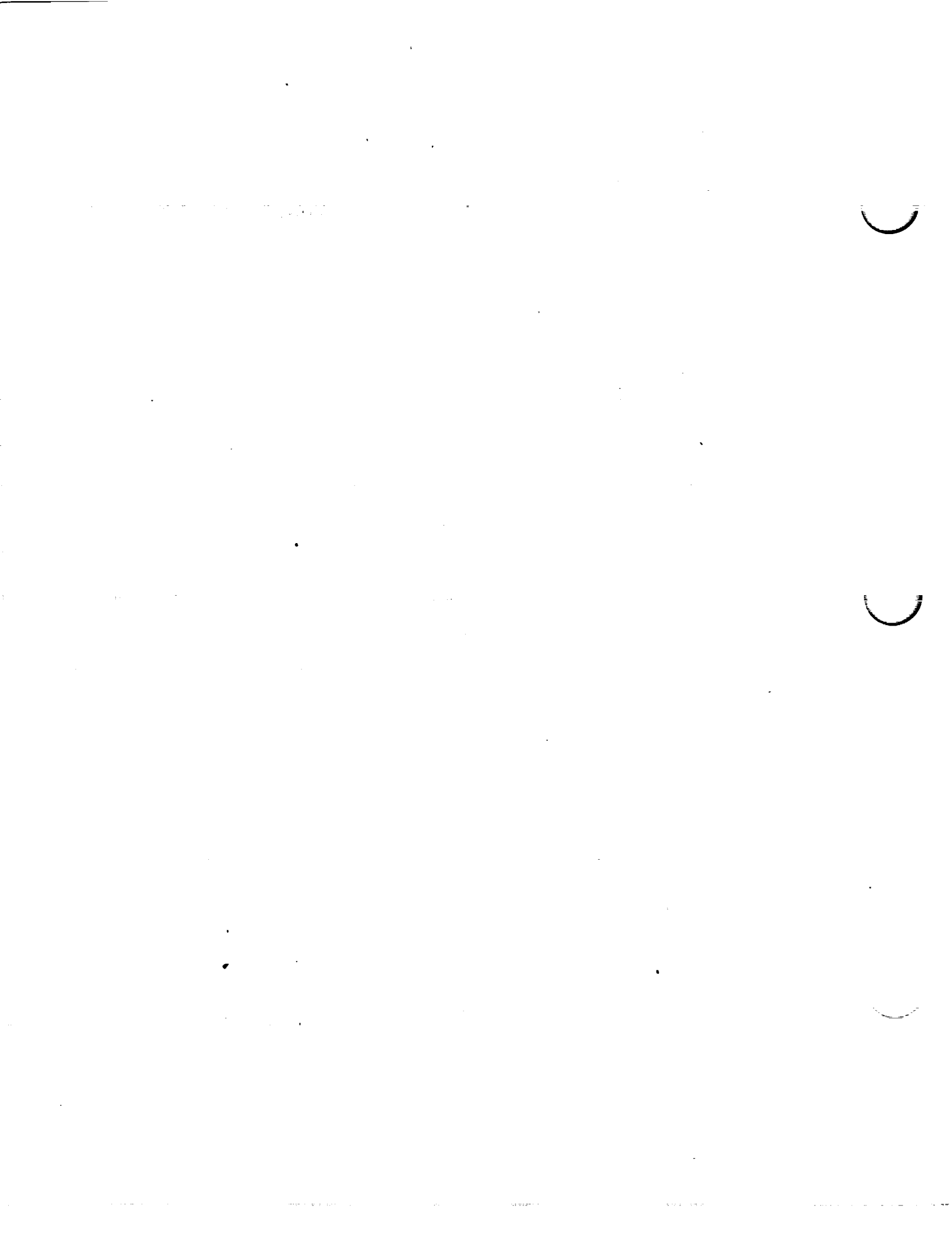
**NACA $\alpha = 0.4$
MEAN LINE**

CONFIDENTIAL



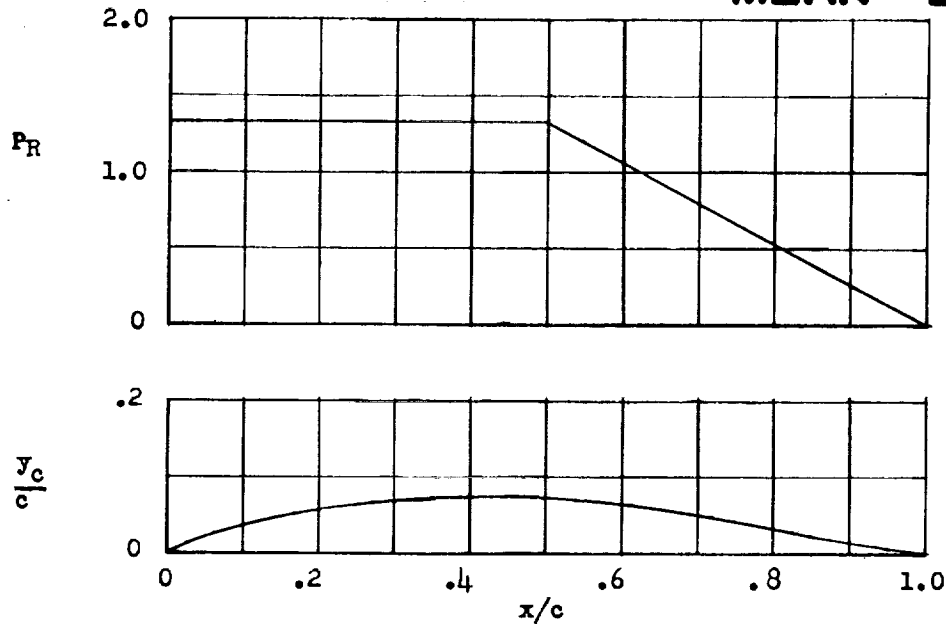
$c_{l_1} = 1.0$ $\alpha_1 = 3.47^\circ$ $c_{m_c/4} = -0.121$						
x (percent c)	y_c (percent c)	dy_c/dx	P_R	$\Delta v/v = P_R/4$		
0	0	-----	-----	-----		
.5	.365	0.61755	1.429	0.357		
.75	.515	.57105				
1.25	.785	.51210				
2.5	1.365	.43105				
5.0	2.330	.34760				
7.5	3.135	.29670				
10	3.825	.25890				
15	4.270	.20185				
20	5.860	.15680				
25	6.545	.11730				
30	7.035	.07985	1.310	.327		
35	7.340	.04135				
40	7.440	-.00725				
45	7.275	-.05325				
50	6.930	-.08385				
55	6.450	-.10735				
60	5.860	-.12570				
65	5.200	-.13965				
70	4.475	-.14965				
75	3.705	-.15590			.190	.298
80	2.920	-.15840				
85	2.130	-.15685				
90	1.360	-.15065				
95	.635	-.13820				
100	0	-.11140				
			0	0		

Data for NACA mean line $\alpha = 0.4$



**NACA $\alpha = 0.5$
MEAN LINE**

CONFIDENTIAL



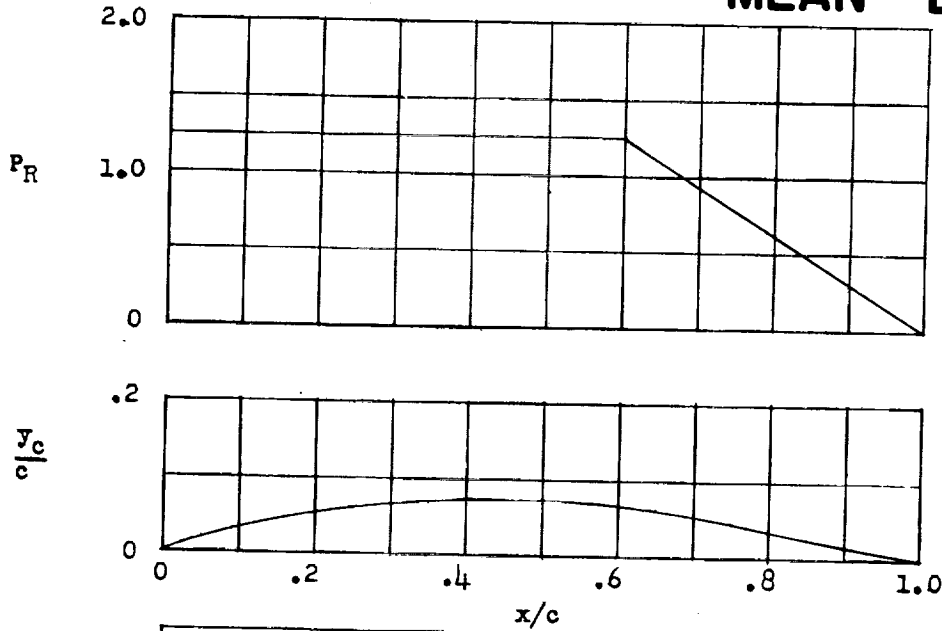
$c_{l1} = 1.0$ $\alpha_1 = 3.04^\circ$ $c_{m_{c/4}} = -0.139$				
x (percent a)	y _c (percent c)	dy _c /dx	P _R	$\Delta v/V = P_R/4$
0	0	-----	-----	-----
.5	.345	0.58195	1.333	0.333
.75	.485	.53855		
1.25	.735	.48360		
2.5	1.295	.40815		
5.0	2.205	.33070		
7.5	2.970	.28365		
10	3.630	.24890		
15	4.740	.19690		
20	5.620	.15650		
25	6.310	.12180		
30	6.840	.09000		
35	7.215	.05930		
40	7.430	.02800		
45	7.490	-.00630		
50	7.350	-.05305		
55	6.965	-.09765		
60	6.405	-.12550		
65	5.725	-.14570		
70	4.955	-.16015		
75	4.130	-.16960		
80	3.285	-.17435		
85	2.395	-.17415		
90	1.535	-.16850		
95	.720	-.15565		
100	0	-.12660		
		0	0	0

Data for NACA mean line $\alpha = 0.5$



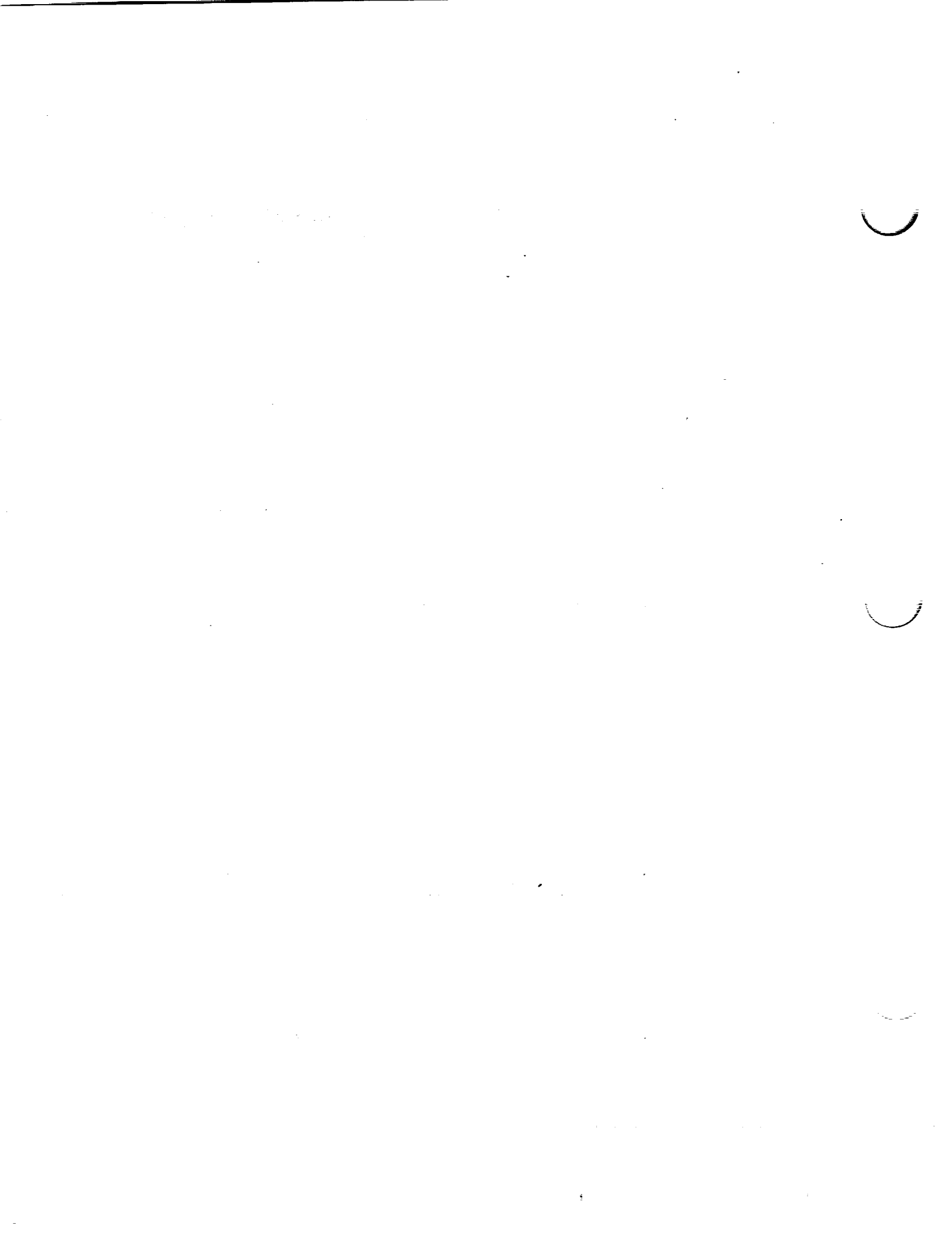
**NACA $\alpha = 0.6$
MEAN LINE**

CONFIDENTIAL



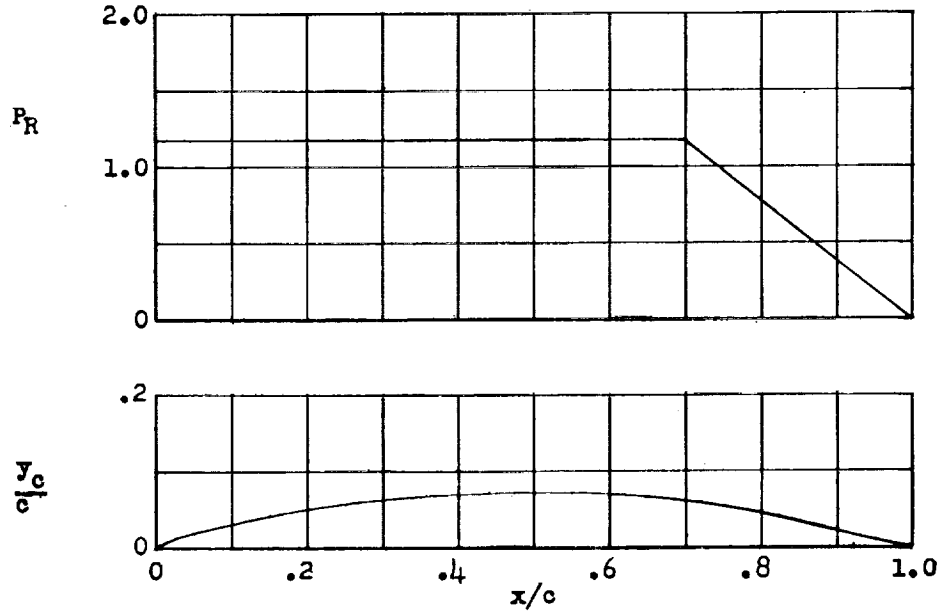
$c_{l1} = 1.0$ $\alpha_1 = 2.58^\circ$ $c_{mC/4} = -0.158$				
x (percent c)	y_c (percent c)	$\frac{dy_c}{dx}$	P_R	$\Delta v/V = P_R/4$
0	0	-----	-----	-----
.5	.325	0.54825	1.250	0.312
.75	.455	.50760		
1.25	.695	.45615		
2.5	1.220	.38555		
5.0	2.080	.31325		
7.5	2.805	.26950		
10	3.435	.23730		
15	4.495	.18935		
20	5.345	.15250		
25	6.035	.12125		
30	6.570	.09310		
35	6.965	.06660		
40	7.235	.04060		
45	7.370	.01405		
50	7.370	-.01135		
55	7.220	-.04700		
60	6.880	-.09470		
65	6.275	-.14015		
70	5.505	-.16595		
75	4.630	-.18270		
80	3.695	-.19225		
85	2.720	-.19515		
90	1.755	-.19095		
95	.825	-.17790		
100	0	-.14550		
		0	1.094	.273
			.938	.234
			.781	.195
			.625	.156
			.469	.117
			.312	.078
			.156	.039
			0	0

Data for NACA mean line $\alpha = 0.6$

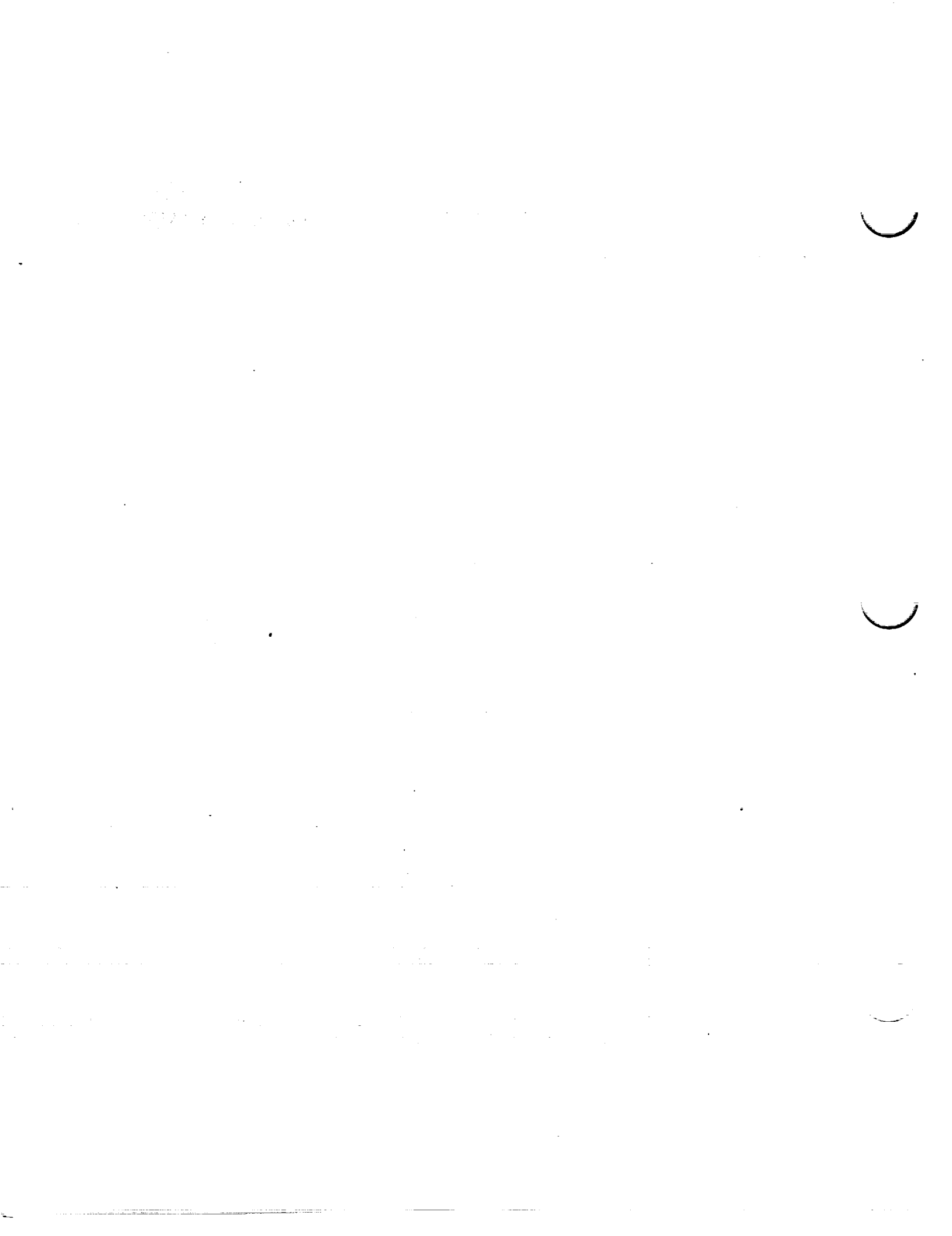


**NACA $\alpha=0.7$
MEAN LINE**

CONFIDENTIAL

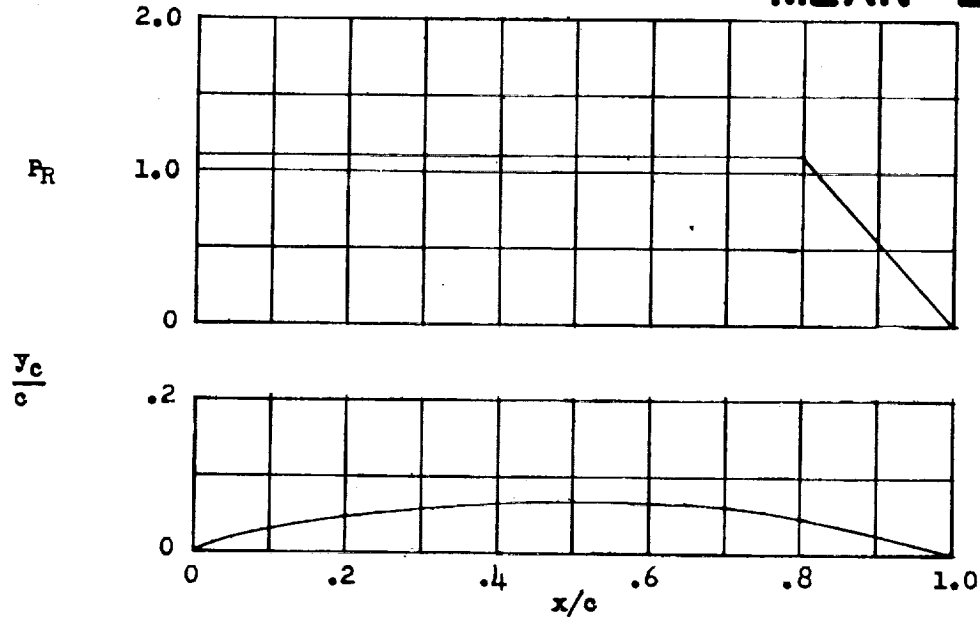


$c_{l_1} = 1.0$		$\alpha_1 = 2.09^\circ$		$c_{m_c/4} = -0.179$	
x (percent c)	y_c (percent c)	dy_c/dx	P_R	$\Delta v/V = P_R/4$	
0	0	-----	-----	-----	
.5	.305	0.51620	1.176	0.294	
.75	.425	.47795			
1.25	.655	.42960			
2.5	1.160	.36325			
5.0	1.955	.29545			
7.5	2.645	.25450			
10	3.240	.22445			
15	4.245	.17995			
20	5.060	.14595			
25	5.715	.11740			
30	6.240	.09200			
35	6.635	.06840			
40	6.925	.04570			
45	7.095	.02315			
50	7.155	0			
55	7.090	-.02455	.980	.245	
60	6.900	-.05185			
65	6.565	-.08475			
70	6.030	-.13650			
75	5.205	-.18510			
80	4.215	-.20855			
85	3.140	-.21955	.784	.196	
90	2.035	-.21960	.588	.147	
95	.965	-.20725	.392	.098	
100	0	-.16985	.196	.049	
			0	0	



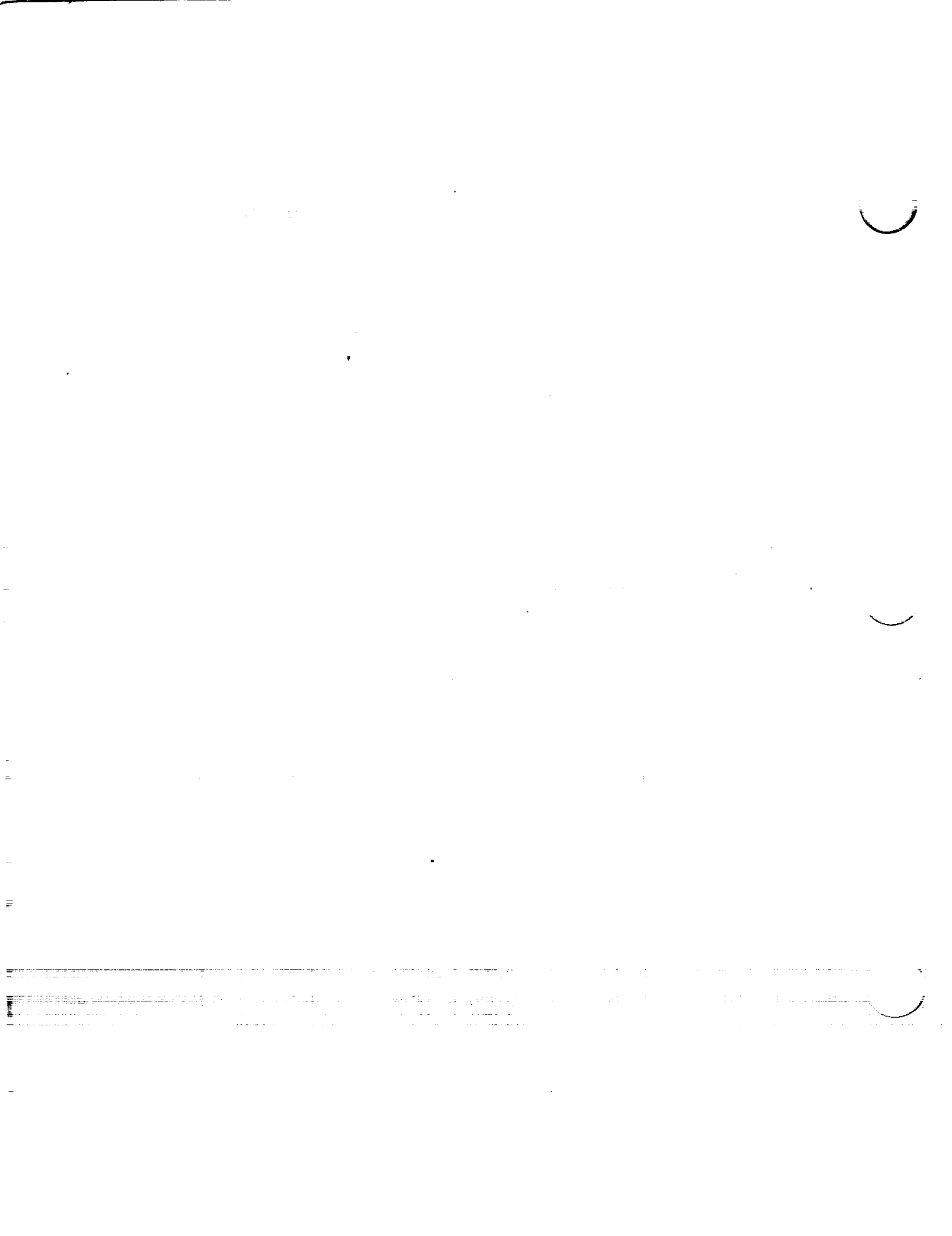
CONFIDENTIAL

**NACA $\alpha = 0.8$
MEAN LINE**



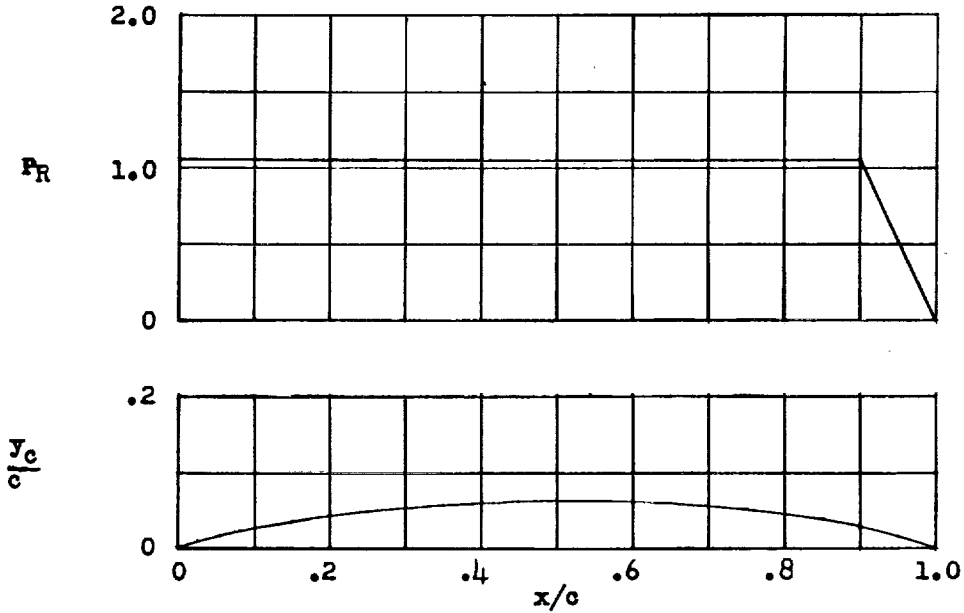
$c_{l_1} = 1.0$ $\alpha_1 = 1.54^\circ$ $c_{m_c/4} = -0.202$				
x (percent c)	yc (percent c)	dy _c /dx	P _R	$\Delta v/V = P_R/4$
0	0	-----	-----	-----
.5	.290	0.48540	1.111	0.278
.75	.405	.41930		
1.25	.615	.40365		
2.5	1.075	.34115		
5.0	1.835	.27730		
7.5	2.480	.23875		
10	3.030	.21080		
15	3.990	.16880		
20	4.740	.13740		
25	5.370	.11100		
30	5.865	.08765		
35	6.260	.06630		
40	6.530	.04590		
45	6.715	.01910		
50	6.785	.00620		
55	6.765	-.01430		
60	6.645	-.03605		
65	6.420	-.06005		
70	6.040	-.08780		
75	5.500	-.12300		
80	4.770	-.18405		
85	3.760	-.23920		
90	2.430	-.25595		
95	1.100	-.24905		
100	0	-.20380		
			0	0

Data for NACA mean line $\alpha = 0.8$



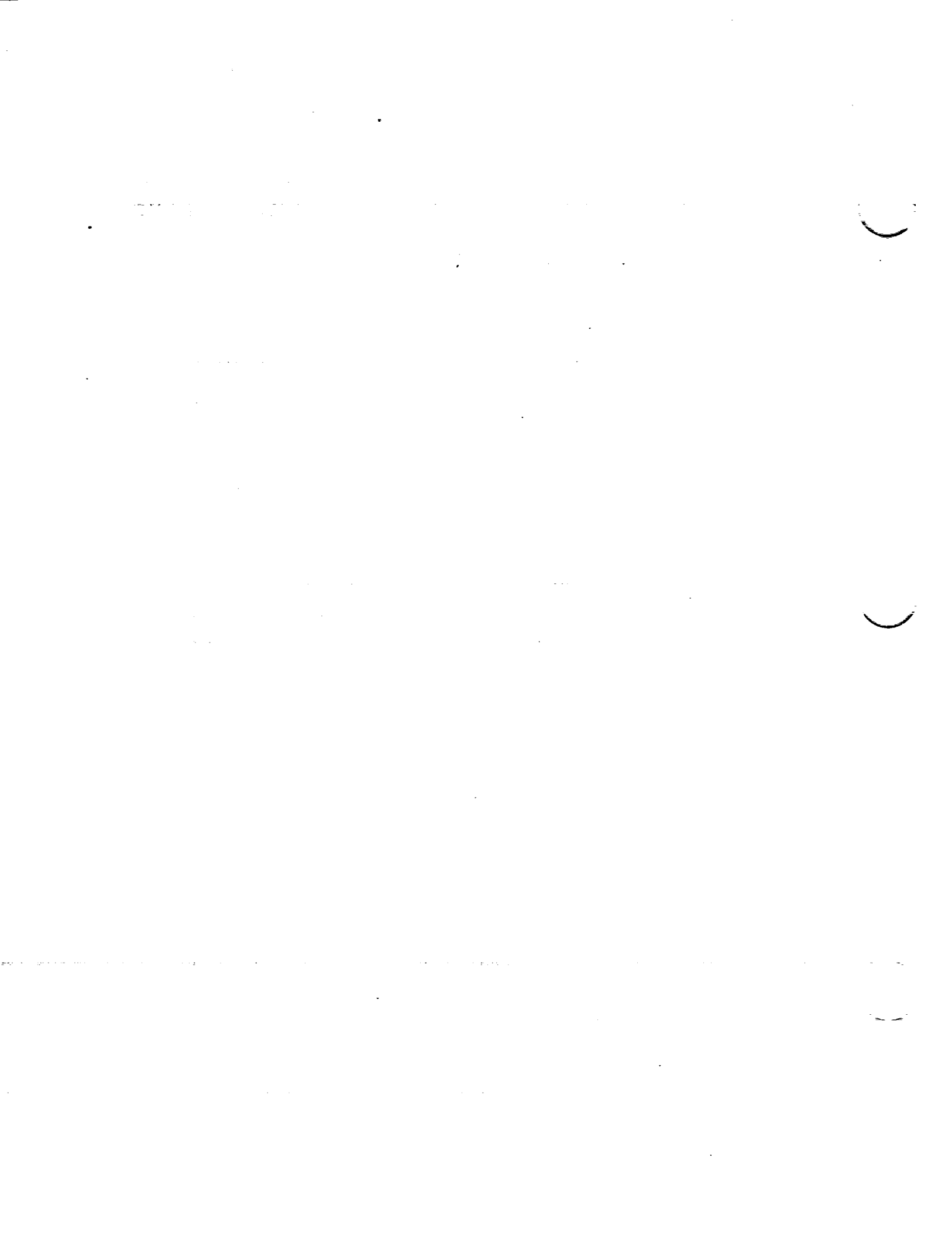
**NACA $\alpha=0.9$
MEAN LINE**

CONFIDENTIAL



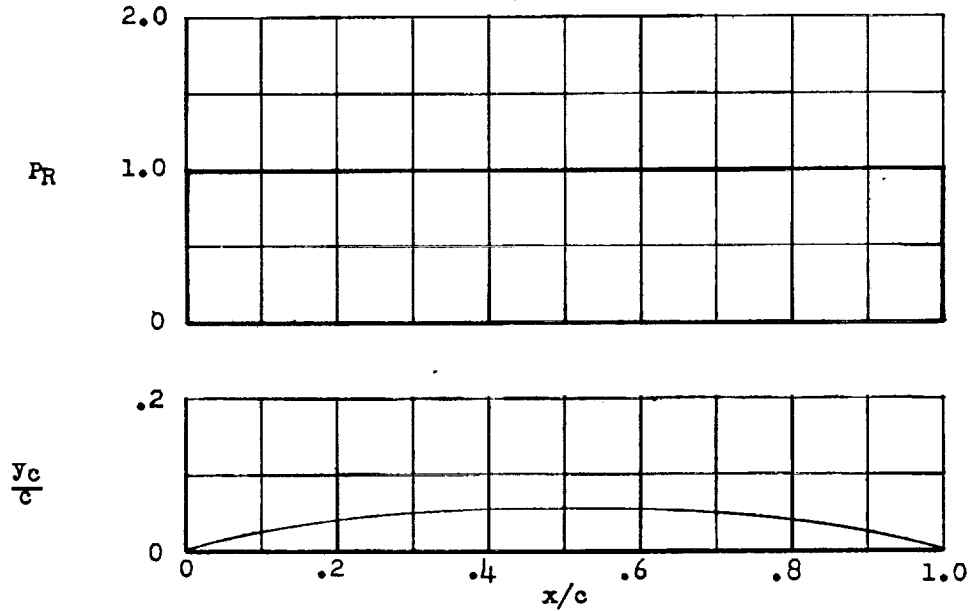
$c_{l\alpha} = 1.0$ $\alpha_1 = 0.91^\circ$ $c_{m_{c/4}} = -0.225$				
x (percent c)	y_c (percent c)	dy_c/dx	P_R	$\Delta v/V = P_R/4$
0	0	-----	-----	-----
.5	.269	0.45482	1.053	0.263
.75	.379	.42064		
1.25	.575	.37730		
2.5	1.010	.31810		
5.0	1.720	.25775		
7.5	2.320	.22145		
10	2.840	.19490		
15	3.705	.15590		
20	4.410	.12640		
25	4.980	.10190		
30	5.430	.08045		
35	5.785	.06080		
40	6.045	.04230		
45	6.212	.02447		
50	6.290	.00675		
55	6.279	-.01111		
60	6.175	-.02970		
65	5.981	-.04937		
70	5.680	-.07105		
75	5.265	-.09582		
80	4.710	-.12605		
85	3.985	-.16725		
90	2.980	-.25200		
95	1.495	-.31460		
100	0	-.26085	0	0

Data for NACA mean line $\alpha = 0.9$



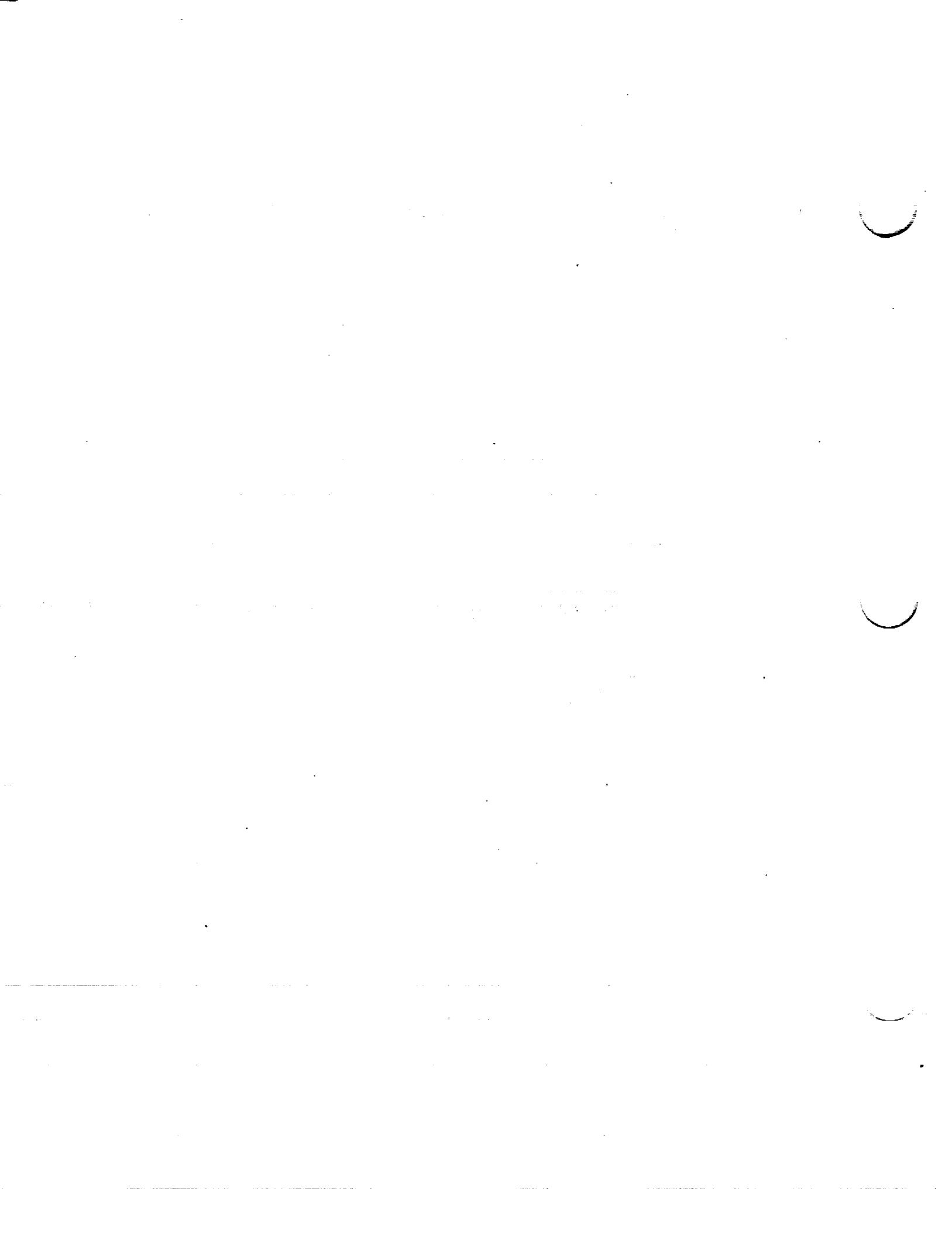
**NACA $a=1.0$
MEAN LINE**

CONFIDENTIAL



$c_{l_1} = 1.0$ $\alpha_1 = 0^\circ$ $c_{m_c}/4 = -0.250$				
x (percent c)	y_c (percent c)	dy_c/dx	P_R	$\Delta v/V = P_R/4$
0	0	-----	-----	-----
.5	.250	0.42120	} 1.000	0.250
.75	.350	.38875		
1.25	.535	.34770		
2.5	.930	.29155		
5.0	1.580	.23430		
7.5	2.120	.19995		
10	2.585	.17485		
15	3.365	.13805		
20	3.980	.11030		
25	4.475	.08745		
30	4.860	.06745		
35	5.150	.04925		
40	5.355	.03225		
45	5.475	.01595		
50	5.515	0		
55	5.475	-.01595		
60	5.355	-.03225		
65	5.150	-.04925		
70	4.860	-.06745		
75	4.475	-.08745		
80	3.980	-.11030		
85	3.365	-.13805		
90	2.585	-.17485		
95	1.580	-.23430		
100	0	-----	-----	-----

Data for NACA mean line $a = 1.0$



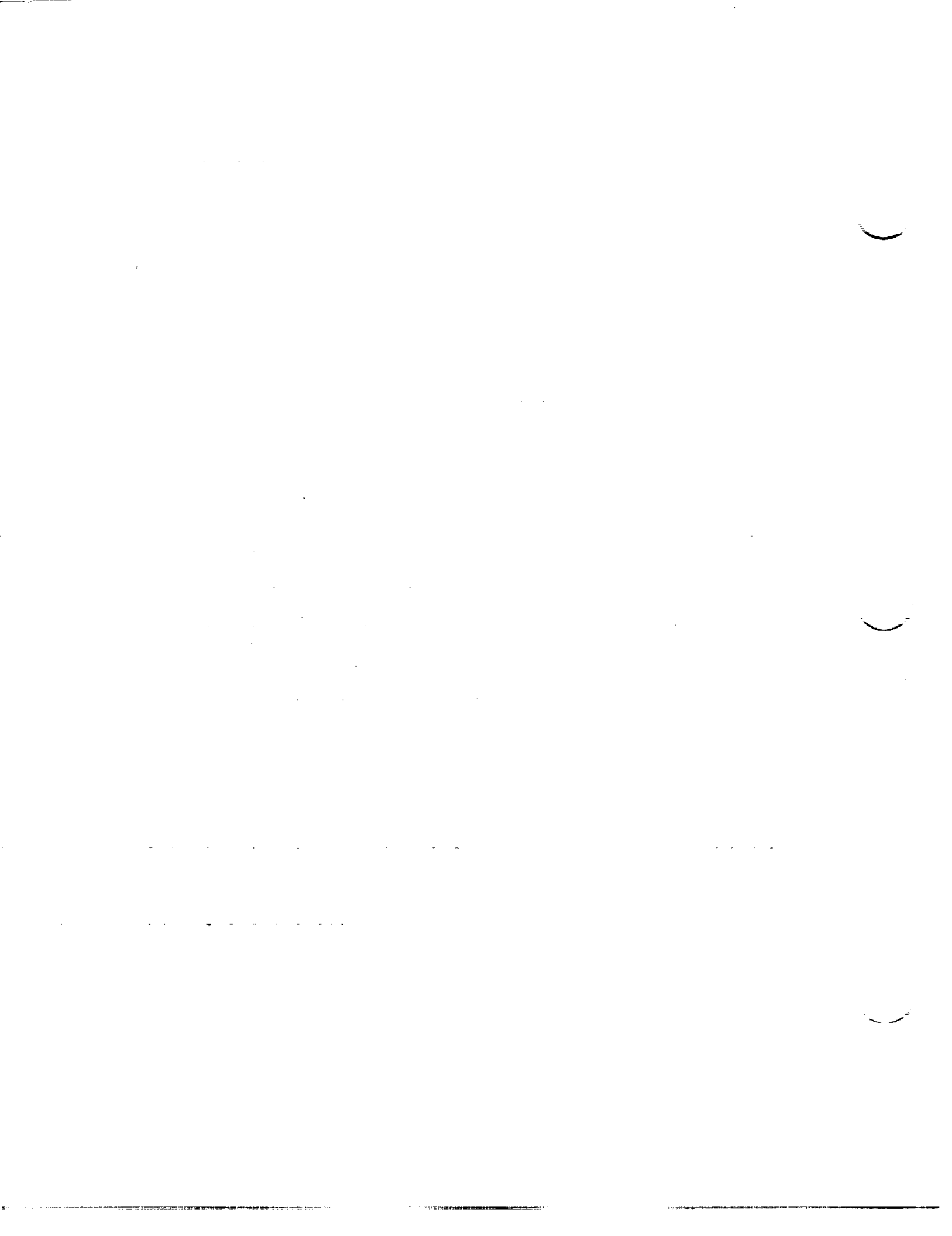
III - AIRFOIL ORDINATES

CONFIDENTIAL



III - AIRFOIL ORDINATES

NACA 0006	S66a
NACA 0009	S66a
NACA 1408	S66b
NACA 1410	S66b
NACA 1412	S66b
NACA 2412	S67
NACA 2415	S67
NACA 2418	S67
NACA 2421	S67
NACA 2424	S68
NACA 4412	S68
NACA 4415	S68
NACA 4418	S68
NACA 4421	S69
NACA 4424	S69
NACA 23012	S69
NACA 23015	S69
NACA 23018	S70
NACA 23021	S70
NACA 23024	S70
NACA 63,4-420	S70
NACA 63,4-420, $\alpha = 0.3$	S71
NACA 63(420)-422	S71



NACA 63(420)-517	S71
NACA 64 ₁ -006	S71a
NACA 64 ₁ -009	S71a
NACA 64 ₁ -012	S71a
NACA 64 ₁ -108	S71b
NACA 64 ₁ -110	S71b
NACA 64 ₁ -112	S71b
NACA 64 ₁ -206	S71c
NACA 64 ₁ -209	S71c
NACA 64 ₁ -212	S71c
NACA 64 ₁ -412	S71c
NACA 64 ₂ -415	S72
NACA 64 ₃ -418	S72
NACA 64 ₄ -421	S72
NACA 65(216)-415, a = 0.5	S72
NACA 65,3-018	S73
NACA 65,3-418, a = 0.8	S73
NACA 65,3-618	S73
NACA 65 ₁ -006	S73a
NACA 65 ₁ -009	S73a
NACA 65 ₁ -012	S73a
NACA 65 ₁ -206	S73a
NACA 65 ₁ -209	S73b
NACA 65 ₁ -210	S73b

THE UNIVERSITY OF CHICAGO

PHYSICS DEPARTMENT

PHYSICS 435

LECTURE 1

1.1. THE CLASSICAL LIMIT

1.2. QUANTIZATION

1.3. THE HEISENBERG UNCERTAINTY PRINCIPLE

1.4. THE SCHRODINGER EQUATION

1.5. THE WAVEFUNCTION

1.6. THE ENERGY EIGENFUNCTIONS

1.7. THE TUNNELING EFFECT

1.8. THE CLASSICAL LIMIT

1.9. THE QUANTUM MECHANICS

1.10. THE QUANTUM MECHANICS

1.11. THE QUANTUM MECHANICS

NACA ACR No. L5C05	CONFIDENTIAL	
NACA 65 ₁ -212		S73b
NACA 65 ₁ -410		S73b
NACA 65 ₁ -412		S74
NACA 65 ₂ -415		S74
NACA 65 ₂ -415, a = 0.5		S74
NACA 65 ₃ -418		S74
NACA 65 ₃ -418, a = 0.5		S75
NACA 65 ₃ -618, a = 0.5		S75
NACA 65 ₄ -421		S75
NACA 65 ₄ -421, a = 0.5		S75
NACA 65(421)-420		S76
NACA 66,1-212		S76
NACA 66(215)-016		S76
NACA 66(215)-216		S76
NACA 66(215)-216, a = 0.6		S77
NACA 66(215)-416		S77
NACA 66 ₁ -006		S77
NACA 66 ₁ -009		S77
NACA 66 ₁ -012		S77a
NACA 66 ₁ -206		S77a
NACA 66 ₁ -209		S77a
NACA 66 ₁ -212		S77a

1. The first part of the document discusses the importance of maintaining accurate records of all transactions.

2. It is essential to ensure that all entries are dated and clearly describe the nature of the transaction.

3. Regularly reconciling the accounts helps to identify any discrepancies or errors early on.

4. Keeping receipts and supporting documents for all transactions provides a clear audit trail.

5. It is also important to review the records periodically to ensure they are up-to-date and accurate.

6. Maintaining organized records can save time and reduce the risk of financial loss.

7. Proper record-keeping is a key component of sound financial management.

8. By following these guidelines, you can ensure the integrity and accuracy of your financial records.

9. Consistent record-keeping is vital for making informed financial decisions.

10. Finally, always double-check your entries to avoid any mistakes or omissions.

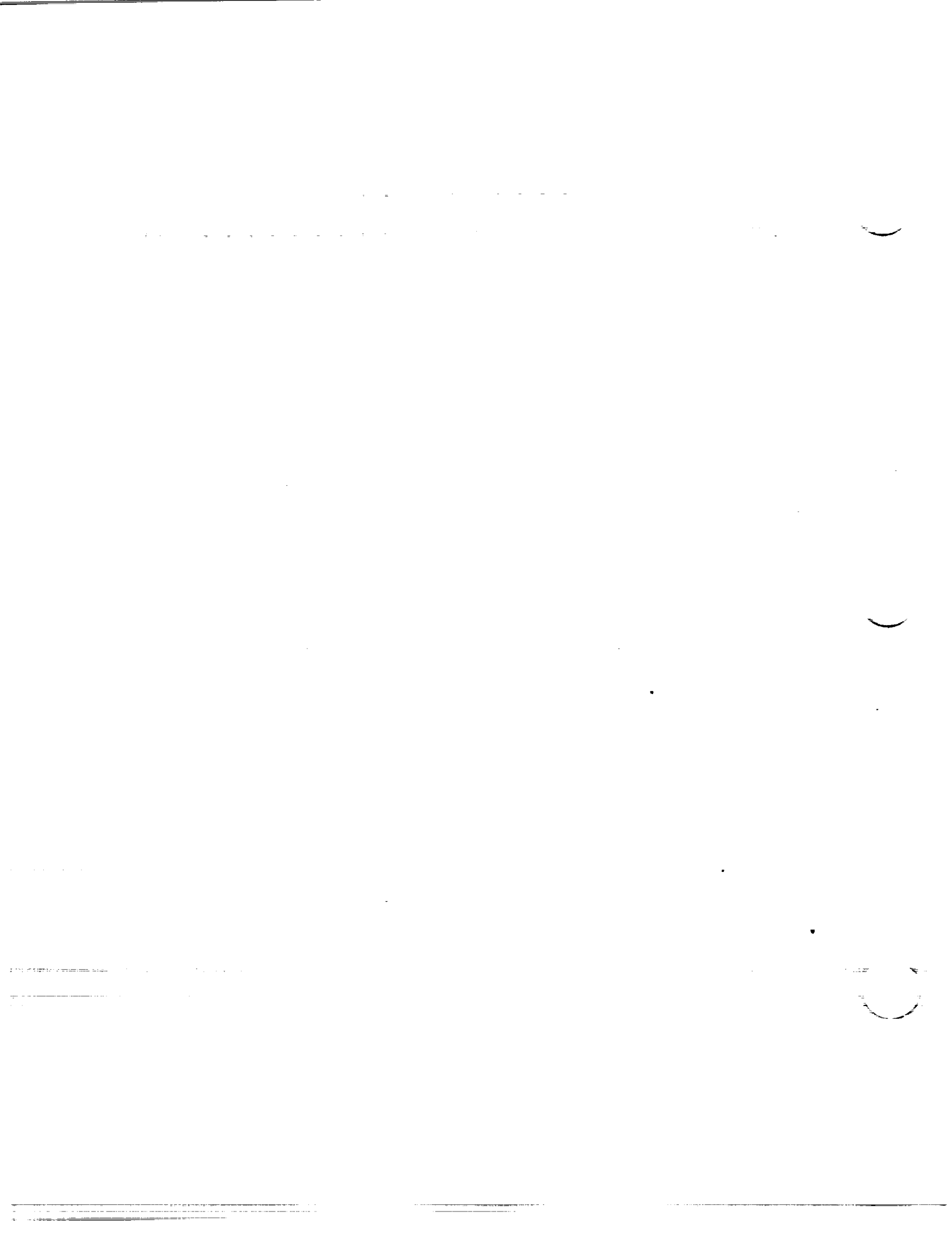
11. These steps will help you maintain a clear and accurate record of your financial activities.

12. Remember, good record-keeping is the foundation of successful financial planning.

NACA ACR No. L5005 CONFIDENTIAL

COPY NO. 119
S66
April 2, 1945

NACA 67,1-215 S78
NACA 747A315 S78
NACA 747A415 S78



CONFIDENTIAL

NACA 0006

[Stations and ordinates given in percent of airfoil chord]

Upper Surface		Lower Surface	
Station	Ordinate	Station	Ordinate
0	0	0	0
1.25	.95	1.25	-.95
2.5	1.31	2.5	-1.31
5.0	1.78	5.0	-1.78
7.5	2.10	7.5	-2.10
10	2.34	10	-2.34
15	2.67	15	-2.67
20	2.87	20	-2.87
25	2.97	25	-2.97
30	3.00	30	-3.00
40	2.90	40	-2.90
50	2.65	50	-2.65
60	2.28	60	-2.28
70	1.83	70	-1.83
80	1.31	80	-1.31
90	.72	90	-.72
95	.40	95	-.40
100	(.06)	100	(-.06)
100	0	100	0

L.E. radius: 0.40

NACA 0009

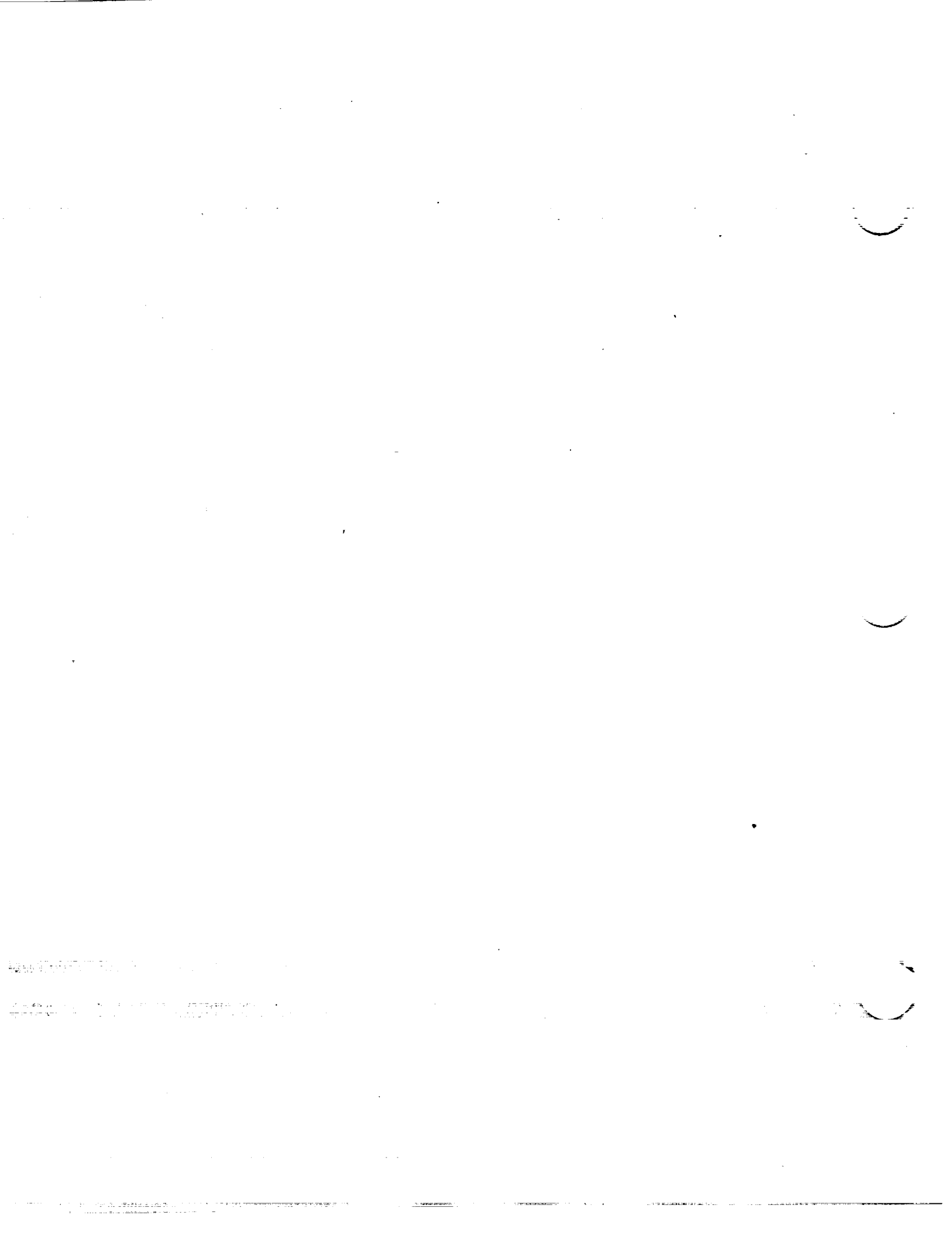
[Stations and ordinates given in percent of airfoil chord]

Upper Surface		Lower Surface	
Station	Ordinate	Station	Ordinate
0	0	0	0
1.25	1.42	1.25	-1.42
2.5	1.96	2.5	-1.96
5.0	2.67	5.0	-2.67
7.5	3.15	7.5	-3.15
10	3.51	10	-3.51
15	4.01	15	-4.01
20	4.30	20	-4.30
25	4.46	25	-4.46
30	4.50	30	-4.50
40	4.35	40	-4.35
50	3.97	50	-3.97
60	3.42	60	-3.42
70	2.75	70	-2.75
80	1.97	80	-1.97
90	1.09	90	-1.09
95	.60	95	-.60
100	(.10)	100	(-.10)
100	0	100	0

L.E. radius: 0.89

CONFIDENTIAL

NATIONAL ADVISORY
COMMITTEE FOR AERONAUTICS



CONFIDENTIAL

NACA 1408

[Stations and ordinates given in percent of airfoil chord]

Upper Surface		Lower Surface	
Station	Ordinate	Station	Ordinate
0	0	0	0
1.189	1.324	1.311	-1.200
2.418	1.862	2.582	-1.620
4.896	2.602	5.104	-2.134
7.386	3.138	7.614	-2.458
9.883	3.558	10.117	-2.682
14.889	4.171	15.111	-2.953
19.904	4.574	20.096	-3.074
24.926	4.819	25.074	-3.101
29.950	4.939	30.050	-3.063
40.000	4.869	40.000	-2.869
50.020	4.502	49.980	-2.556
60.034	3.931	59.966	-2.153
70.041	3.193	69.959	-1.693
80.039	2.305	79.961	-1.193
90.027	1.271	89.973	-.659
95.016	.698	94.984	-.378
100.000	.084	100.000	-.084

L.E. radius: 0.70
Slope of radius through L.E.: 0.05

NACA 1410

[Stations and ordinates given in percent of airfoil chord]

Upper Surface		Lower Surface	
Station	Ordinate	Station	Ordinate
0	0	0	0
1.174	1.639	1.326	-1.515
2.398	2.297	2.602	-2.055
4.870	3.194	5.130	-2.726
7.358	3.837	7.642	-3.157
9.861	4.338	10.146	-3.462
14.861	5.062	15.139	-3.844
19.880	5.531	20.120	-4.031
24.907	5.809	25.093	-4.091
29.937	5.940	30.063	-4.064
40.000	5.836	40.000	-3.836
50.025	5.385	49.975	-3.459
60.042	4.692	59.958	-2.914
70.051	3.804	69.949	-2.304
80.049	2.741	79.951	-1.629
90.034	1.513	89.966	-.901
95.021	.832	94.979	-.512
100.000	.105	100.000	-.105

L.E. radius: 1.10
Slope of radius through L.E.: 0.05

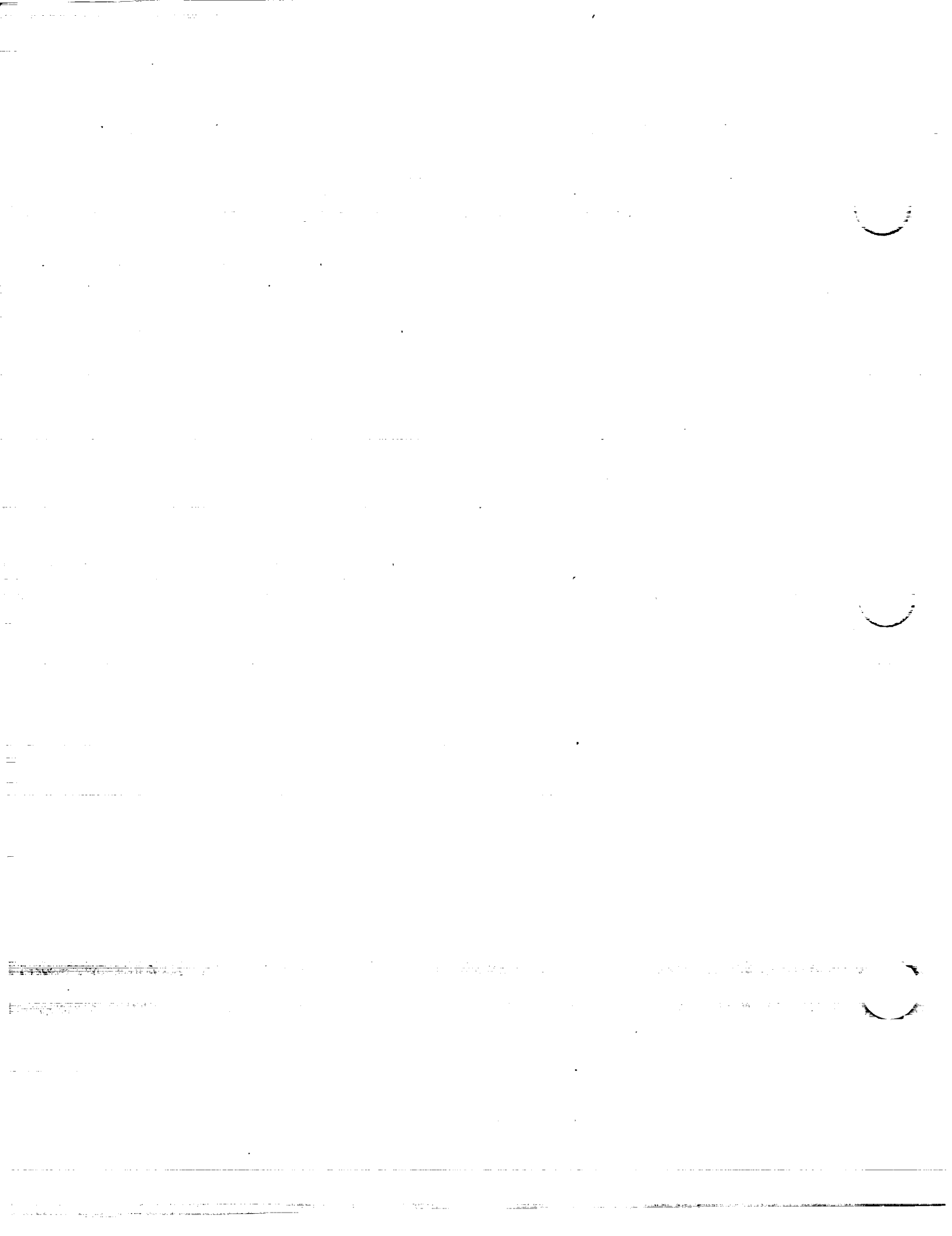
NACA 1412

[Stations and ordinates given in percent of airfoil chord]

Upper Surface		Lower Surface	
Station	Ordinate	Station	Ordinate
0	0	0	0
1.158	1.954	1.342	-1.830
2.378	2.733	2.622	-2.491
4.845	3.786	5.155	-3.318
7.330	4.537	7.670	-3.857
9.824	5.118	10.176	-4.242
14.823	5.953	15.167	-4.733
19.857	6.486	20.143	-5.086
24.889	6.799	25.111	-5.081
29.925	6.940	30.075	-5.064
40.000	6.803	40.000	-4.803
50.029	6.267	49.971	-4.321
60.051	5.453	59.949	-3.675
70.061	4.413	69.939	-2.913
80.058	3.178	79.942	-2.066
90.040	1.753	89.960	-1.141
95.025	.966	94.975	-.646
100.000	.126	100.000	-.126

L.E. radius: 1.58
Slope of radius through L.E.: 0.05

CONFIDENTIAL



NACA 2412

CONFIDENTIAL

NACA 2415

[Stations and ordinates given in percent of airfoil chord]

[Stations and ordinates given in percent of airfoil chord]

Upper Surface		Lower Surface	
Station	Ordinate	Station	Ordinate
0	-----	0	0
1.25	2.15	1.25	-1.65
2.5	2.99	2.5	-2.27
5.0	4.15	5.0	-3.01
7.5	4.98	7.5	-3.46
10	5.63	10	-3.75
15	6.61	15	-4.10
20	7.26	20	-4.23
25	7.67	25	-4.22
30	7.88	30	-4.12
40	7.80	40	-3.80
50	7.21	50	-3.34
60	6.36	60	-2.76
70	5.18	70	-2.11
80	3.75	80	-1.50
90	2.08	90	-0.82
95	1.11	95	-0.48
100	(.13)	100	(-.13)
100	-----	100	0

L. E. radius: 1.58
Slope of radius through L.E.: 0.10

Upper Surface		Lower Surface	
Station	Ordinate	Station	Ordinate
0	-----	0	0
1.25	2.71	1.25	-2.06
2.5	3.71	2.5	-2.86
5.0	5.07	5.0	-3.84
7.5	6.06	7.5	-4.47
10	6.83	10	-4.90
15	7.97	15	-5.42
20	8.70	20	-5.66
25	9.17	25	-5.70
30	9.38	30	-5.52
40	8.25	40	-5.25
50	6.57	50	-4.67
60	4.50	60	-3.90
70	2.10	70	-3.05
80	0.41	80	-2.15
90	2.45	90	-1.17
95	1.31	95	-0.68
100	(.16)	100	(-.16)
100	-----	100	0

L. E. radius: 2.48
Slope of radius through L.E.: 0.10

NATIONAL ADVISORY
COMMITTEE FOR AERONAUTICS.

NACA 2418

NACA 2421

[Stations and ordinates given in percent of airfoil chord]

[Stations and ordinates given in percent of airfoil chord]

Upper Surface		Lower Surface	
Station	Ordinate	Station	Ordinate
0	-----	0	0
1.25	3.28	1.25	-2.45
2.5	4.45	2.5	-3.44
5.0	6.03	5.0	-4.68
7.5	7.17	7.5	-5.48
10	8.05	10	-6.03
15	9.34	15	-6.74
20	10.15	20	-7.09
25	10.65	25	-7.18
30	10.88	30	-7.12
40	10.71	40	-6.71
50	9.89	50	-5.99
60	8.65	60	-5.04
70	7.02	70	-3.97
80	5.08	80	-2.80
90	2.81	90	-1.53
95	1.55	95	-0.87
100	(.19)	100	(-.19)
100	-----	100	0

L. E. radius: 3.56
Slope of radius through L. E.: 0.10

Upper Surface		Lower Surface	
Station	Ordinate	Station	Ordinate
0	-----	0	0
1.25	3.87	1.25	-2.82
2.5	5.21	2.5	-4.02
5.0	7.00	5.0	-5.51
7.5	8.29	7.5	-6.48
10	9.28	10	-7.18
15	10.70	15	-8.05
20	11.59	20	-8.52
25	12.15	25	-8.67
30	12.38	30	-8.62
40	12.16	40	-8.16
50	11.22	50	-7.31
60	9.79	60	-6.17
70	7.94	70	-4.87
80	5.74	80	-3.44
90	3.18	90	-1.88
95	1.76	95	-1.06
100	(.22)	100	(-.22)
100	-----	100	0

L. E. radius: 4.85
Slope of radius through L. E.: 0.10

CONFIDENTIAL



NACA 2424 CONFIDENTIAL **NACA 4412**

[Stations and ordinates given in percent of airfoil chord]

Upper Surface		Lower Surface	
Station	Ordinate	Station	Ordinate
0	0	0	0
.885	3.892	1.615	-3.646
2.012	5.449	2.988	-4.965
4.380	7.552	5.620	-6.614
6.820	9.052	8.180	-7.692
9.300	10.215	10.700	-8.465
14.333	11.888	15.667	-9.450
19.427	12.952	20.573	-9.959
24.555	13.555	25.445	-10.155
29.700	13.874	30.300	-10.124
40.000	13.606	40.000	-9.606
50.118	12.532	49.882	-8.644
60.203	10.903	59.797	-7.317
70.244	8.824	69.756	-5.824
80.233	6.352	79.767	-4.130
90.161	3.502	89.839	-2.280
95.098	1.930	94.902	-1.292
100.000	-----	100.000	0

L. E. radius; 6.33
Slope of radius through L. E.: 0.10

[Stations and ordinates given in percent of airfoil chord]

Upper Surface		Lower Surface	
Station	Ordinate	Station	Ordinate
0	0	0	0
1.25	2.44	1.25	-1.43
2.5	3.39	2.5	-1.95
5.0	4.73	5.0	-2.49
7.5	5.76	7.5	-2.74
10	6.59	10	-2.86
15	7.89	15	-2.88
20	8.80	20	-2.74
25	9.41	25	-2.50
30	9.76	30	-2.26
40	9.80	40	-1.80
50	9.19	50	-1.40
60	8.14	60	-1.00
70	6.69	70	-.65
80	4.89	80	-.39
90	2.71	90	-.22
95	1.47	95	-.16
100	(.13)	100	(-.13)
100	-----	100	0

L. E. radius; 1.58
Slope of radius through L. E.: 0.20

NATIONAL ADVISORY COMMITTEE FOR AERONAUTICS.

NACA 4415 CONFIDENTIAL **NACA 4418**

[Stations and ordinates given in percent of airfoil chord]

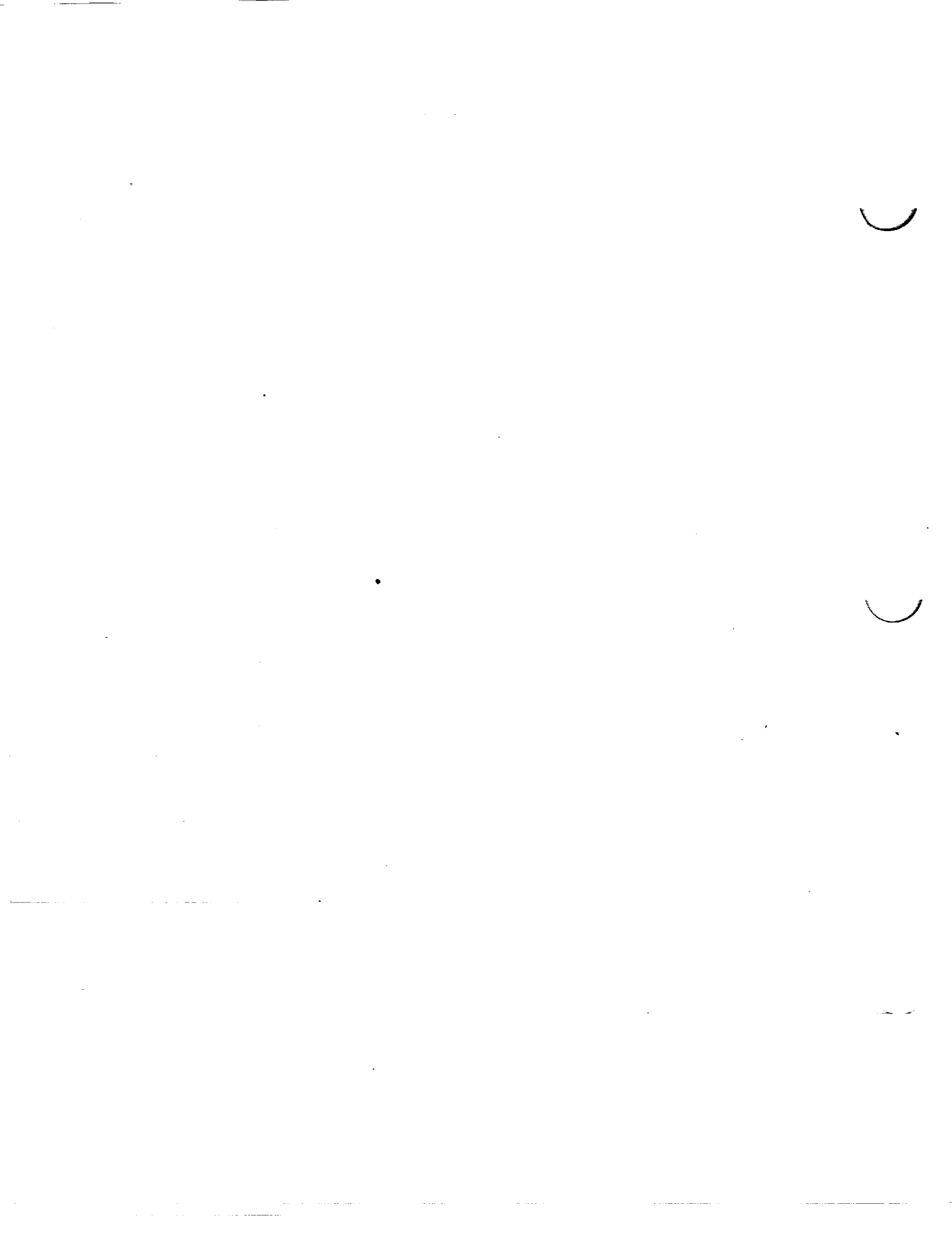
Upper Surface		Lower Surface	
Station	Ordinate	Station	Ordinate
0	-----	0	0
1.25	3.07	1.25	-1.79
2.5	4.17	2.5	-2.48
5.0	5.74	5.0	-3.27
7.5	6.91	7.5	-3.71
10	7.84	10	-3.98
15	9.27	15	-4.18
20	10.25	20	-4.15
25	10.92	25	-3.98
30	11.25	30	-3.75
40	11.25	40	-3.25
50	10.53	50	-2.72
60	9.30	60	-2.14
70	7.63	70	-1.55
80	5.55	80	-1.03
90	3.08	90	-.57
95	1.67	95	-.38
100	(.16)	100	(-.16)
100	-----	100	0

L. E. radius; 2.48
Slope of radius through L. E.: 0.20

[Stations and ordinates given in percent of airfoil chord]

Upper Surface		Lower Surface	
Station	Ordinate	Station	Ordinate
0	-----	0	0
1.25	3.76	1.25	-2.11
2.5	5.00	2.5	-2.99
5.0	6.75	5.0	-4.06
7.5	8.06	7.5	-4.67
10	9.11	10	-5.06
15	10.66	15	-5.49
20	11.72	20	-5.56
25	12.40	25	-5.49
30	12.76	30	-5.26
40	12.70	40	-4.70
50	11.85	50	-4.02
60	10.44	60	-3.24
70	8.55	70	-2.42
80	6.22	80	-1.67
90	3.46	90	-.93
95	1.89	95	-.55
100	(.19)	100	(-.19)
100	-----	100	0

L. E. radius; 3.56
Slope of radius through L. E.: 0.20



NACA 4421

CONFIDENTIAL

NACA 4424

[Stations and ordinates given
in percent of airfoil chord]

Upper Surface		Lower Surface	
Station	Ordinate	Station	Ordinate
0	-----	0	0
1.25	4.45	1.25	-2.42
2.5	5.84	2.5	-3.48
5.0	7.82	5.0	-4.78
7.5	9.24	7.5	-5.62
10	10.35	10	-6.15
15	12.04	15	-6.75
20	13.17	20	-6.98
25	13.88	25	-6.92
30	14.27	30	-6.76
40	14.16	40	-6.16
50	13.18	50	-5.34
60	11.60	60	-4.40
70	9.50	70	-3.35
80	6.91	80	-2.31
90	3.85	90	-1.27
95	2.11	95	-.74
100	(.22)	100	(-.22)
100	-----	100	0

L. E. radius: 4.85
Slope of radius through L. E.: 0.20

[Stations and ordinates given
in percent of airfoil chord]

Upper Surface		Lower Surface	
Station	Ordinate	Station	Ordinate
0	0	0	0
.530	3.964	1.970	-3.472
1.536	5.624	3.464	-4.643
3.775	7.942	6.225	-6.066
6.153	9.651	8.847	-6.931
8.611	11.012	11.389	-7.512
13.674	13.045	16.326	-8.169
18.858	14.416	21.142	-8.416
24.111	15.287	25.889	-8.411
29.401	15.738	30.599	-8.238
40.000	15.606	40.000	-7.606
50.235	14.474	49.765	-6.698
60.405	12.674	59.592	-5.562
70.487	10.312	69.513	-4.312
80.464	7.447	79.536	-3.003
90.320	4.099	89.680	-1.655
95.196	2.240	94.804	-.964
100.000	-----	100.000	0

L. E. radius: 6.33
Slope of radius through L. E.: 0.20

NATIONAL ADVISORY
COMMITTEE FOR AERONAUTICS

NACA 23012

NACA 23015

[Stations and ordinates given
in percent of airfoil chord]

Upper Surface		Lower Surface	
Station	Ordinate	Station	Ordinate
0	-----	0	0
1.25	2.67	1.25	-1.23
2.5	3.61	2.5	-1.71
5.0	4.91	5.0	-2.26
7.5	5.80	7.5	-2.61
10	6.43	10	-2.92
15	7.19	15	-3.50
20	7.50	20	-3.97
25	7.60	25	-4.28
30	7.55	30	-4.46
40	7.14	40	-4.48
50	6.41	50	-4.17
60	5.47	60	-3.67
70	4.36	70	-3.00
80	3.08	80	-2.16
90	1.68	90	-1.23
95	.92	95	-.70
100	(.13)	100	(-.13)
100	-----	100	0

L. E. radius: 1.58
Slope of radius through L. E.: 0.305

[Stations and ordinates given
in percent of airfoil chord]

Upper Surface		Lower Surface	
Station	Ordinate	Station	Ordinate
0	-----	0	0
1.25	3.34	1.25	-1.54
2.5	4.44	2.5	-2.25
5.0	5.89	5.0	-3.04
7.5	6.90	7.5	-3.61
10	7.64	10	-4.09
15	8.22	15	-4.84
20	8.92	20	-5.41
25	9.08	25	-5.78
30	9.05	30	-5.96
40	8.59	40	-5.92
50	7.74	50	-5.50
60	6.61	60	-4.81
70	5.25	70	-4.01
80	3.73	80	-3.03
90	2.04	90	-1.99
95	1.12	95	-.90
100	(.16)	100	(-.16)
100	-----	100	0

L. E. radius: 2.48
Slope of radius through L. E.: 0.305

CONFIDENTIAL



CONFIDENTIAL

NACA 23018

Stations and ordinates given in percent of airfoil chord

Upper Surface		Lower Surface	
Station	Ordinate	Station	Ordinate
0		0	0
1.25	4.09	1.25	-1.85
2.5	5.29	2.5	-2.71
5.0	6.92	5.0	-3.90
7.5	8.01	7.5	-4.60
10	8.83	10	-5.22
15	9.86	15	-6.18
20	10.36	20	-6.86
25	10.56	25	-7.27
30	10.55	30	-7.47
40	10.04	40	-7.37
50	9.05	50	-6.51
60	7.78	60	-5.24
70	6.18	70	-3.82
80	4.40	80	-2.48
90	2.39	90	-1.94
95	1.52	95	-1.09
100	(.19)	100	(-.19)
100		100	0

L. E. radius: 3.56
Slope of radius through L. E.: 0.305

NACA 23021

Stations and ordinates given in percent of airfoil chord

Upper Surface		Lower Surface	
Station	Ordinate	Station	Ordinate
0		0	0
1.25	4.87	1.25	-2.08
2.5	6.14	2.5	-3.14
5.0	7.93	5.0	-4.52
7.5	9.13	7.5	-5.55
10	10.03	10	-6.42
15	11.19	15	-7.41
20	11.80	20	-8.38
25	12.05	25	-8.76
30	12.06	30	-8.95
40	11.49	40	-8.89
50	10.40	50	-8.14
60	8.90	60	-7.07
70	7.09	70	-5.72
80	5.05	80	-4.15
90	2.78	90	-2.30
95	1.53	95	-1.56
100	(.22)	100	(-.22)
100		100	0

L. E. radius: 4.85
Slope of radius through L. E.: 0.305

NATIONAL ADVISORY COMMITTEE FOR AERONAUTICS.

NACA 23024

Stations and ordinates given in percent of airfoil chord

Upper Surface		Lower Surface	
Station	Ordinate	Station	ordinate
0		0	0
.277	4.017	2.223	-3.303
1.331	5.764	3.669	-4.432
3.853	8.172	6.147	-5.862
6.661	9.844	8.399	-6.860
9.423	11.049	10.577	-7.647
15.001	12.528	11.999	-8.852
20.253	13.237	19.747	-9.703
25.262	13.555	24.738	-10.223
30.265	13.546	29.735	-10.454
40.256	12.928	39.744	-10.278
50.235	11.690	49.766	-9.482
60.202	10.008	59.798	-8.242
70.162	7.988	69.858	-6.664
80.116	5.687	79.864	-4.903
90.064	3.115	89.936	-2.673
95.036	1.724	94.964	-1.504
100		100	0

L. E. radius: 6.33
Slope of radius through L.E.: 0.305

NACA 63,4-420

Stations and ordinates given in percent of airfoil chord

Upper Surface		Lower Surface	
Station	Ordinate	Station	Ordinate
0		0	0
.215	1.790	.785	-1.590
.430	2.196	1.070	-1.916
.887	2.827	1.613	-2.399
2.082	3.954	2.918	-3.210
4.538	5.557	5.462	-4.293
7.024	6.793	7.976	-5.097
9.526	7.817	10.474	-5.749
14.554	9.424	15.446	-6.732
19.603	10.589	20.397	-7.405
24.663	11.414	25.357	-7.834
29.732	11.895	30.268	-8.007
34.809	12.056	35.197	-7.916
39.874	11.906	40.126	-7.622
44.940	11.556	45.060	-7.176
50.000	11.025	50.000	-6.613
55.052	10.333	54.948	-5.943
60.095	9.492	59.905	-5.208
65.127	8.523	64.873	-4.403
70.148	7.438	69.852	-3.550
75.156	6.253	74.841	-2.673
80.150	4.990	79.850	-1.806
85.129	3.684	84.871	-.992
90.094	2.379	89.906	-.311
95.047	1.131	94.953	.133
100		100	0

L. E. radius: 3.16
Slope of radius through L. E.: 0.168

CONFIDENTIAL



NACA 63,4-420
a = 0.3

[Stations and ordinates given in percent of airfoil chord]

Upper Surface		Lower Surface	
Station	Ordinate	Station	Ordinate
0	0	0	0
.065	1.814	.935	-1.502
.260	2.241	1.240	-1.805
.691	2.912	1.809	-2.244
1.856	4.128	3.144	-2.968
4.288	5.878	5.712	-3.914
6.771	7.237	8.229	-4.601
9.280	8.366	10.720	-5.158
14.347	10.132	15.653	-5.996
19.458	11.410	20.542	-6.570
24.604	12.296	25.396	-6.948
29.808	12.781	30.192	-7.125
35.008	12.848	34.992	-7.108
40.145	12.594	39.855	-6.924
45.213	12.089	44.757	-6.637
50.308	11.388	49.692	-6.240
55.344	10.516	54.656	-5.756
60.353	9.497	59.647	-5.189
65.359	8.357	64.661	-4.553
70.365	7.120	69.695	-3.856
75.256	5.807	74.744	-3.111
80.197	4.453	79.803	-2.337
85.134	3.108	84.866	-1.568
90.073	1.836	89.927	-0.856
95.025	.728	94.975	-0.272
100.000	0	100.000	0

L.E. radius: 3.16
Slope of radius through L.E.: 0.262

CONFIDENTIAL

NACA 63(420)-422

[Stations and ordinates given in percent of airfoil chord]

Upper Surface		Lower Surface	
Station	Ordinate	Station	Ordinate
0	0	0	0
.187	1.959	.813	-1.759
.398	2.402	1.102	-2.122
.850	3.088	1.650	-2.660
2.041	4.312	2.959	-3.568
4.492	6.050	5.508	-4.786
6.977	7.387	8.023	-5.691
9.478	8.496	10.522	-6.428
14.509	10.231	15.491	-7.539
19.563	11.489	20.437	-8.305
24.630	12.377	25.370	-8.797
29.705	12.890	30.295	-9.002
34.784	13.034	35.216	-8.914
39.861	12.883	40.139	-8.599
44.934	12.493	45.066	-8.113
50.000	11.907	50.000	-7.495
55.057	11.147	54.943	-6.767
60.104	10.227	59.896	-5.943
65.140	9.169	64.860	-5.049
70.163	7.988	69.837	-4.100
75.172	6.700	74.828	-3.120
80.165	5.329	79.835	-2.115
85.142	3.918	84.858	-1.226
90.103	2.513	89.897	-0.445
95.051	1.181	94.949	-0.083
100.000	0	100.000	0

L.E. radius: 3.82
Slope of radius through L.E.: 0.168

NACA 63(420)-517

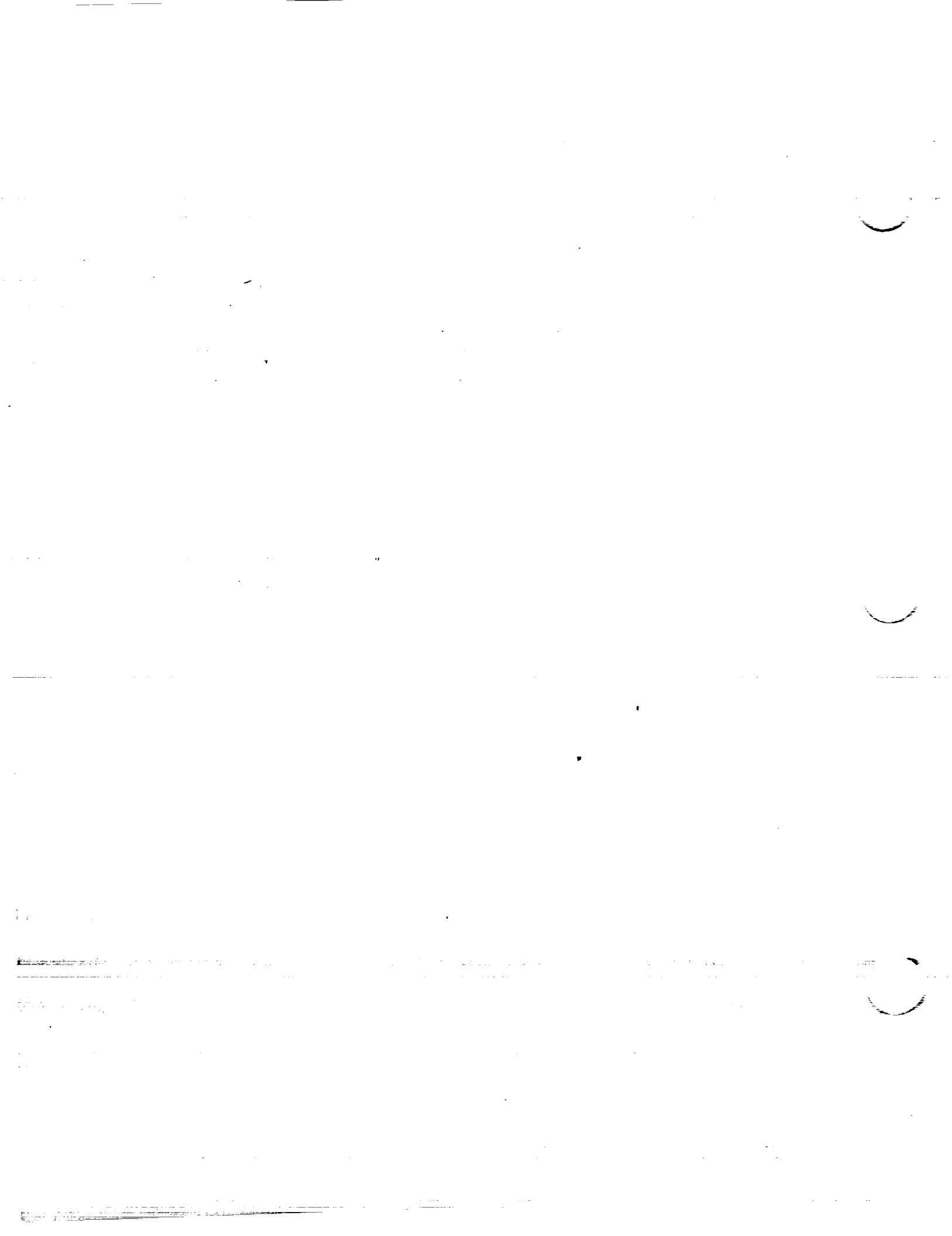
[Stations and ordinates given in percent of airfoil chord]

Upper Surface		Lower Surface	
Station	Ordinate	Station	Ordinate
0	0	0	0
.200	1.551	.800	-1.301
.412	1.912	1.088	-1.562
.866	2.477	1.634	-1.941
2.058	3.498	2.942	-2.568
4.511	4.966	5.489	-3.386
6.996	6.104	8.004	-3.984
9.497	7.050	10.503	-4.466
14.527	8.542	15.473	-5.178
19.578	9.633	20.422	-5.653
24.642	10.416	25.358	-5.940
29.715	10.887	30.285	-6.027
34.791	11.053	35.209	-5.903
39.866	10.977	40.134	-5.621
44.936	10.699	45.064	-5.223
50.000	10.254	50.000	-4.738
55.055	9.660	54.945	-4.184
60.101	8.925	59.899	-3.569
65.135	8.067	64.865	-2.917
70.157	7.099	69.843	-2.239
75.166	6.030	74.834	-1.554
80.159	4.877	79.841	-0.897
85.137	3.668	84.863	-0.304
90.100	2.434	89.900	.150
95.050	1.213	94.950	.367
100.000	0	100.000	0

L.E. radius: 2.283
Slope of radius through L.E.: 0.211

CONFIDENTIAL

NATIONAL ADVISORY
COMMITTEE FOR AERONAUTICS



CONFIDENTIAL

NACA 64₁-006

[Stations and ordinates given in percent of airfoil chord]

Upper Surface		Lower Surface	
Station	Ordinate	Station	Ordinate
0	0	0	0
.50	.494	.50	-.494
.75	.596	.75	-.596
1.25	.754	1.25	-.754
2.5	1.024	2.5	-1.024
5.0	1.405	5.0	-1.405
7.5	1.692	7.5	-1.692
10	1.928	10	-1.928
15	2.298	15	-2.298
20	2.572	20	-2.572
25	2.772	25	-2.772
30	2.907	30	-2.907
35	2.981	35	-2.981
40	2.995	40	-2.995
45	2.919	45	-2.919
50	2.775	50	-2.775
55	2.575	55	-2.575
60	2.331	60	-2.331
65	2.050	65	-2.050
70	1.740	70	-1.740
75	1.412	75	-1.412
80	1.072	80	-1.072
85	.737	85	-.737
90	.423	90	-.423
95	.157	95	-.157
100	0	100	0

L.E. radius: 0.256

NACA 64₁-009

[Stations and ordinates given in percent of airfoil chord]

Upper Surface		Lower Surface	
Station	Ordinate	Station	Ordinate
0	0	0	0
.50	.739	.50	-.739
.75	.892	.75	-.892
1.25	1.128	1.25	-1.128
2.5	1.533	2.5	-1.533
5.0	2.109	5.0	-2.109
7.5	2.543	7.5	-2.543
10	2.898	10	-2.898
15	3.455	15	-3.455
20	3.868	20	-3.868
25	4.170	25	-4.170
30	4.373	30	-4.373
35	4.479	35	-4.479
40	4.490	40	-4.490
45	4.364	45	-4.364
50	4.136	50	-4.136
55	3.826	55	-3.826
60	3.452	60	-3.452
65	3.026	65	-3.026
70	2.561	70	-2.561
75	2.069	75	-2.069
80	1.564	80	-1.564
85	1.069	85	-1.069
90	.611	90	-.611
95	.227	95	-.227
100	0	100	0

L.E. radius: 0.579

NACA 64₁-012

[Stations and ordinates given in percent of airfoil chord]

Upper Surface		Lower Surface	
Station	Ordinate	Station	Ordinate
0	0	0	0
.5	.978	.5	-.978
.75	1.179	.75	-1.179
1.25	1.490	1.25	-1.490
2.5	2.035	2.5	-2.035
5.0	2.810	5.0	-2.810
7.5	3.394	7.5	-3.394
10	3.871	10	-3.871
15	4.620	15	-4.620
20	5.173	20	-5.173
25	5.576	25	-5.576
30	5.844	30	-5.844
35	5.978	35	-5.978
40	5.981	40	-5.981
45	5.798	45	-5.798
50	5.480	50	-5.480
55	5.056	55	-5.056
60	4.548	60	-4.548
65	3.974	65	-3.974
70	3.350	70	-3.350
75	2.695	75	-2.695
80	2.029	80	-2.029
85	1.382	85	-1.382
90	.786	90	-.786
95	.288	95	-.288
100	0	100	0

L.E. radius: 1.040

NATIONAL ADVISORY
COMMITTEE FOR AERONAUTICS

CONFIDENTIAL



NACA 64₁-108

CONFIDENTIAL

NACA 64₁-110

[Stations and ordinates given in percent of airfoil chord]

[Stations and ordinates given in percent of airfoil chord]

Upper Surface		Lower Surface	
Station	Ordinate	Station	Ordinate
0	0	0	0
.472	.682	.528	-.632
.719	.828	.781	-.758
1.215	1.058	1.285	-.950
2.460	1.457	2.540	-1.271
4.956	2.032	5.044	-1.716
7.452	2.471	7.545	-2.047
9.952	2.832	10.045	-2.316
14.958	3.405	15.042	-2.733
19.962	3.825	20.038	-3.039
24.968	4.152	25.032	-3.256
29.974	4.370	30.026	-3.398
34.980	4.494	35.020	-3.464
39.987	4.528	40.013	-3.456
44.994	4.431	45.006	-3.335
50.000	4.236	50.000	-3.132
55.005	3.959	54.995	-2.863
60.010	3.617	59.990	-2.515
65.013	3.219	64.987	-2.189
70.015	2.777	69.985	-1.805
75.016	2.302	74.984	-1.406
80.015	1.802	79.985	-1.006
85.013	1.297	84.987	-.625
90.010	.808	89.990	-.292
95.005	.364	94.995	-.048
100.000	0	100.000	0

L.E. radius: 0.455
Slope of radius through L.E.: 0.042

Upper Surface		Lower Surface	
Station	Ordinate	Station	Ordinate
0	0	0	0
.465	.814	.535	-.794
.712	1.023	.788	-.953
1.207	1.303	1.293	-1.155
2.450	1.793	2.550	-1.607
4.945	2.500	5.055	-2.184
7.443	3.037	7.557	-2.613
9.944	3.479	10.056	-2.963
14.947	4.178	15.053	-3.506
19.953	4.700	20.047	-3.904
24.959	5.087	25.041	-4.191
29.967	5.350	30.033	-4.378
34.975	5.495	35.025	-4.465
39.984	5.524	40.016	-4.452
44.992	5.391	45.008	-4.295
50.000	5.138	50.000	-4.034
55.007	4.786	54.993	-3.690
60.012	4.356	59.988	-3.284
65.016	3.860	64.984	-2.830
70.019	3.313	69.981	-2.341
75.020	2.729	74.980	-1.833
80.019	2.120	79.981	-1.324
85.016	1.512	84.984	-.810
90.012	.929	89.988	-.413
95.006	.406	94.994	-.090
100.000	0	100.000	0

L.E. radius: 0.720
Slope of radius through L.E.: 0.042

NACA 64₁-112

[Stations and ordinates given in percent of airfoil chord]

Upper Surface		Lower Surface	
Station	Ordinate	Station	Ordinate
0	0	0	0
.459	1.002	.541	-.952
.704	1.213	.796	-1.143
1.198	1.543	1.302	-1.435
2.441	2.127	2.559	-1.941
4.934	2.967	5.066	-2.651
7.432	3.605	7.568	-3.181
9.932	4.128	10.068	-3.612
14.936	4.956	15.064	-4.284
19.943	5.571	20.057	-4.775
24.951	6.024	25.049	-5.128
29.961	6.330	30.039	-5.358
34.971	6.493	35.029	-5.463
39.981	6.517	40.019	-5.445
44.991	6.346	45.009	-5.250
50.000	6.032	50.000	-4.928
55.008	5.604	54.992	-4.508
60.015	5.084	59.985	-4.012
65.020	4.489	64.980	-3.459
70.023	3.836	69.977	-2.864
75.024	3.143	74.976	-2.247
80.022	2.427	79.978	-1.631
85.019	1.718	84.981	-1.046
90.014	1.044	89.986	-.528
95.007	.446	94.993	-.130
100.000	0	100.000	0

L.E. radius: 1.040
Slope of radius through L.E.: 0.042

100
100

100
100

100
100



NACA 64₁-206

CONFIDENTIAL

NACA 64₁-209

[Stations and ordinates given in percent of airfoil chord]

Upper Surface		Lower Surface	
Station	Ordinate	Station	Ordinate
0	0	0	0
.459	.542	.541	-.442
.704	.661	.736	-.721
1.198	.859	1.302	-.845
2.440	1.208	2.560	-.836
4.934	1.719	5.066	-1.087
7.432	2.115	7.568	-1.267
9.933	2.444	10.067	-1.410
14.937	2.970	15.063	-1.624
19.943	3.567	20.057	-1.775
24.952	3.667	25.048	-1.877
29.961	3.879	30.039	-1.935
34.971	4.011	35.029	-1.951
39.981	4.066	40.019	-1.924
44.991	4.014	45.009	-1.824
50.000	3.878	50.000	-1.672
55.008	3.670	54.992	-1.480
60.015	3.402	59.985	-1.260
65.020	3.080	64.980	-1.020
70.023	2.712	69.977	-.768
75.025	2.307	74.975	-.517
80.024	1.868	79.976	-.276
85.020	1.410	84.980	-.064
90.015	.940	89.985	.094
95.007	.473	94.993	.159
100.000	0	100.000	0

L.E. radius; 0.256
Slope of radius through L.E.; 0.084

[Stations and ordinates given in percent of airfoil chord]

Upper Surface		Lower Surface	
Station	Ordinate	Station	Ordinate
0	0	0	0
.438	.786	.562	-.686
.680	.959	.820	-.819
1.172	1.232	1.328	-1.018
2.411	1.716	2.589	-1.734
4.901	2.423	5.099	-1.791
7.398	2.965	7.602	-2.117
9.899	3.413	10.101	-2.379
14.905	4.127	15.095	-2.781
19.915	4.663	20.085	-3.071
24.927	5.064	25.073	-3.274
29.941	5.345	30.059	-3.401
34.956	5.509	35.044	-3.449
39.971	5.561	40.029	-3.419
44.986	5.459	45.014	-3.269
50.000	5.239	50.000	-3.033
55.012	4.921	54.988	-2.731
60.022	4.523	59.978	-2.381
65.030	4.056	64.970	-1.996
70.035	3.533	69.965	-1.589
75.036	2.964	74.964	-1.174
80.035	2.360	79.965	-.768
85.030	1.742	84.970	-.396
90.021	1.128	89.979	-.064
95.011	.543	94.989	.089
100.000	0	100.000	0

L.E. radius; 0.579
Slope of radius through L.E.; 0.084

NACA 64₁-212

[Stations and ordinates given in percent of airfoil chord]

Upper Surface		Lower Surface	
Station	Ordinate	Station	Ordinate
0	0	0	0
.418	1.025	.582	-.925
.659	1.245	.841	-1.105
1.147	1.593	1.353	-1.379
2.382	2.218	2.618	-1.846
4.868	3.123	5.132	-2.491
7.364	3.815	7.636	-2.967
9.865	4.386	10.135	-3.352
14.872	5.291	15.128	-3.945
19.886	5.968	20.114	-4.376
24.903	6.470	25.097	-4.680
29.921	6.815	30.079	-4.871
34.941	7.008	35.059	-4.948
39.961	7.052	40.039	-4.910
44.982	6.893	45.018	-4.703
50.000	6.583	50.000	-4.377
55.016	6.151	54.984	-3.961
60.029	5.619	59.971	-3.477
65.039	5.004	64.961	-2.944
70.045	4.322	69.955	-2.378
75.047	3.590	74.953	-1.800
80.045	2.825	79.953	-1.233
85.038	2.054	84.962	-.708
90.027	1.303	89.973	-.269
95.013	.604	94.987	.028
100.000	0	100.000	0

L.E. radius; 1.040
Slope of radius through L.E.; 0.084

NACA 64₁-412

[Stations and ordinates given in percent of airfoil chord]

Upper Surface		Lower Surface	
Station	Ordinate	Station	Ordinate
0	0	0	0
.338	1.064	.662	-.864
.569	1.305	.931	-1.025
1.045	1.690	1.455	-1.262
2.264	2.393	2.736	-1.649
4.738	3.430	5.262	-2.166
7.229	4.231	7.771	-2.533
9.730	4.896	10.270	-2.828
14.745	5.959	15.255	-3.267
19.772	6.760	20.228	-3.576
24.805	7.363	25.195	-3.783
29.842	7.786	30.158	-3.898
34.882	8.037	35.118	-3.917
39.923	8.123	40.077	-3.859
44.963	7.988	45.037	-3.608
50.000	7.686	50.000	-3.274
55.032	7.246	54.968	-2.866
60.059	6.690	59.941	-2.406
65.078	6.033	64.922	-1.913
70.090	5.293	69.910	-1.405
75.094	4.483	74.906	-.903
80.089	3.619	79.911	-.435
85.076	2.722	84.924	-.038
90.055	1.818	89.945	.250
95.027	.919	94.973	.345
100.000	0	100.000	0

L.E. radius; 1.040
Slope of radius through L.E.; 0.168



DATE	DESCRIPTION	AMOUNT
1950-01-01
1950-01-15
1950-02-01
1950-02-15
1950-03-01
1950-03-15
1950-04-01
1950-04-15
1950-05-01
1950-05-15
1950-06-01
1950-06-15
1950-07-01
1950-07-15
1950-08-01
1950-08-15
1950-09-01
1950-09-15
1950-10-01
1950-10-15
1950-11-01
1950-11-15
1950-12-01
1950-12-15
1950-12-31

NACA 64₂-415

NACA 64₃-418

[Stations and ordinates given in percent of airfoil chord] CONFIDENTIAL

[Stations and ordinates given in percent of airfoil chord]

Upper Surface		Lower Surface	
Station	Ordinate	Station	Ordinate
0	0	0	0
.299	1.291	.701	-1.091
.526	1.579	.974	-1.299
.996	2.038	1.504	-1.610
2.207	2.883	2.793	-2.139
4.673	4.121	5.327	-2.857
7.162	5.073	7.838	-3.379
9.662	5.864	10.338	-3.796
14.681	7.122	15.319	-4.430
19.714	8.066	20.286	-4.882
24.756	8.771	25.244	-5.191
29.803	9.260	30.197	-5.372
34.853	9.541	35.147	-5.421
39.904	9.614	40.096	-5.350
44.954	9.414	45.046	-5.034
50.000	9.016	50.000	-4.604
55.040	8.456	54.960	-4.076
60.072	7.762	59.928	-3.478
65.096	6.954	64.904	-2.834
70.111	6.055	69.889	-2.167
75.115	5.084	74.885	-1.504
80.109	4.062	79.891	-.878
85.092	3.020	84.908	-.329
90.066	1.982	89.934	.086
95.032	.976	94.968	.288
100.000	0	100.000	0

L. E. radius: 1.590
Slope of radius through L. E.: 0.168

Upper Surface		Lower Surface	
Station	Ordinate	Station	Ordinate
0	0	0	0
.263	1.508	.737	-1.308
.486	1.840	1.014	-1.560
.950	2.370	1.550	-1.942
2.152	3.347	2.848	-2.613
4.609	4.800	5.391	-3.536
7.095	5.908	7.905	-4.212
9.595	6.823	10.405	-4.755
14.617	8.277	15.383	-5.585
19.657	9.366	20.343	-6.182
24.707	10.176	25.293	-6.596
29.763	10.730	30.237	-6.842
34.823	11.037	35.177	-6.917
39.885	11.093	40.115	-6.809
44.945	10.820	45.055	-6.440
50.000	10.320	50.000	-5.908
55.047	9.635	54.953	-5.255
60.086	8.799	59.914	-4.515
65.114	7.841	64.886	-3.721
70.131	6.784	69.869	-2.896
75.135	5.654	74.865	-2.074
80.127	4.477	79.873	-1.293
85.108	3.294	84.892	-.602
90.077	2.132	89.923	-.064
95.037	1.030	94.963	.234
100.000	0	100.000	0

L. E. radius: 2.208
Slope of radius through L. E.: 0.168

NATIONAL ADVISORY COMMITTEE FOR AERONAUTICS.

NACA 64₄-421

NACA 65(216)-415
a = 0.5

[Stations and ordinates given in percent of airfoil chord]

[Stations and ordinates given in percent of airfoil chord]

Upper Surface		Lower Surface	
Station	Ordinate	Station	Ordinate
0	0	0	0
.227	1.723	.773	-1.523
.445	2.101	1.055	-1.821
.903	2.707	1.597	-2.279
2.096	3.834	2.904	-3.090
4.545	5.482	5.455	-4.218
7.028	6.744	7.972	-5.048
9.528	7.786	10.472	-5.718
14.553	9.442	15.447	-6.750
19.599	10.678	20.401	-7.494
24.657	11.591	25.343	-8.011
29.723	12.209	30.277	-8.321
34.794	12.539	35.206	-8.419
39.865	12.572	40.135	-8.288
44.936	12.220	45.064	-7.840
50.000	11.610	50.000	-7.198
55.055	10.797	54.945	-6.417
60.099	9.819	59.901	-5.535
65.131	8.708	64.869	-4.588
70.150	7.491	69.850	-3.603
75.154	6.203	74.846	-2.623
80.145	4.876	79.855	-1.692
85.122	3.556	84.878	-.864
90.087	2.276	89.913	-.208
95.042	1.079	94.958	.185
100.000	0	100.000	0

L. E. radius: 2.884
Slope of radius through L. E.: 0.168

Upper Surface		Lower Surface	
Station	Ordinate	Station	Ordinate
0	0	0	0
.244	1.236	.756	-.960
.469	1.498	1.031	-1.110
.930	1.947	1.570	-1.359
2.121	2.837	2.879	-1.801
4.564	4.175	5.436	-2.411
7.044	5.208	7.956	-3.232
9.540	6.073	10.460	-3.169
14.561	7.465	15.439	-3.673
19.608	8.518	20.392	-4.022
24.669	9.315	25.331	-4.267
29.742	9.900	30.258	-4.428
34.825	10.279	35.175	-4.507
39.916	10.467	40.084	-4.523
45.019	10.438	44.981	-4.446
50.153	10.131	49.847	-4.251
55.263	9.512	54.737	-3.940
60.305	8.645	59.695	-3.521
65.308	7.575	64.692	-2.995
70.281	6.373	69.719	-2.409
75.237	5.152	74.763	-1.848
80.180	3.890	79.820	-1.278
85.117	2.639	84.883	-.723
90.062	1.533	89.938	-.305
95.020	.606	94.900	-.030
100.000	0	100.000	0

L. E. radius: 1.498
Slope of radius through L. E.: 0.233



NACA 65,3-018

[Stations and ordinates given in percent of airfoil chord]

Upper Surface		Lower Surface	
Station	Ordinate	Station	Ordinate
0	0	0	0
.5	1.324	.5	-1.324
.75	1.599	.75	-1.599
1.25	2.004	1.25	-2.004
2.5	2.728	2.5	-2.728
5.0	3.831	5.0	-3.831
7.5	4.701	7.5	-4.701
10	5.424	10	-5.424
15	6.568	15	-6.568
20	7.434	20	-7.434
25	8.093	25	-8.093
30	8.568	30	-8.568
35	8.868	35	-8.868
40	8.990	40	-8.990
45	8.916	45	-8.916
50	8.593	50	-8.593
55	8.045	55	-8.045
60	7.317	60	-7.317
65	6.450	65	-6.450
70	5.486	70	-5.486
75	4.456	75	-4.456
80	3.390	80	-3.390
85	2.325	85	-2.325
90	1.324	90	-1.324
95	.492	95	-.492
100	0	100	0

L.E. radius: 1.92

CONFIDENTIAL

NACA 65,3-418
a=0.8

[Stations and ordinates given in percent of airfoil chord]

Upper Surface		Lower Surface	
Station	Ordinate	Station	Ordinate
0	0	0	0
.248	1.416	.752	-1.194
.467	1.736	1.033	-1.412
.931	2.224	1.569	-1.732
2.131	3.133	2.869	-2.273
4.578	4.542	5.422	-3.074
7.053	5.672	7.947	-3.688
9.544	6.617	10.456	-4.193
11.558	8.149	15.442	-4.927
19.592	9.319	20.408	-5.527
24.641	10.233	25.359	-5.937
29.700	10.909	30.300	-6.217
34.765	11.369	35.235	-6.361
39.835	11.600	40.165	-6.376
44.932	11.602	45.068	-6.270
49.979	11.307	45.021	-5.879
55.046	10.751	54.954	-5.339
60.106	9.974	59.894	-4.658
65.155	9.016	64.845	-3.880
70.193	7.899	69.807	-3.067
75.219	6.651	74.781	-2.251
80.249	5.289	79.751	-1.473
85.221	3.818	84.779	-.810
90.135	2.289	89.865	-.345
95.049	.930	94.951	-.050
100.000	0	100.000	0

L.E. radius: 1.92
Slope of radius through L.E.: 0.194

NACA 65,3-618

[Stations and ordinates given in percent of airfoil chord]

Upper Surface		Lower Surface	
Station	Ordinate	Station	Ordinate
0	0	0	0
.176	1.434	.824	-1.134
.387	1.767	1.113	-1.347
.841	2.283	1.659	-1.641
2.030	3.245	2.970	-2.129
4.467	4.742	5.533	-2.846
6.940	5.940	8.060	-3.396
9.434	6.945	10.566	-3.843
11.458	8.565	15.542	-4.527
19.509	9.806	20.491	-5.030
24.576	10.767	25.421	-5.397
29.654	11.477	30.346	-5.645
34.738	11.954	35.262	-5.774
39.826	12.201	40.174	-5.775
44.915	12.201	45.085	-5.631
50.000	11.902	50.000	-5.281
55.077	11.330	54.923	-4.760
60.142	10.529	59.858	-4.103
65.191	9.537	64.809	-3.357
70.222	8.398	69.778	-2.566
75.233	7.135	74.767	-1.765
80.224	5.771	79.776	-.995
85.192	4.336	84.808	-.298
90.138	2.868	89.862	.234
95.068	1.435	94.932	.461
100.000	0	100.000	0

L.E. radius: 1.92
Slope of radius through L.E.: 0.253

NATIONAL ADVISORY
COMMITTEE FOR AERONAUTICS

CONFIDENTIAL



NACA 65-006

CONFIDENTIAL

NACA 65-009

[Stations and ordinates given in percent of airfoil chord]

[Stations and ordinates given in percent of airfoil chord]

Upper Surface		Lower Surface	
Station	Ordinate	Station	Ordinate
0	0	0	0
.5	.476	.5	-.476
.75	.714	.75	-.714
1.25	.717	1.25	-.717
2.5	.956	2.5	-.956
5.0	1.310	5.0	-1.310
7.5	1.589	7.5	-1.589
10	1.824	10	-1.824
15	2.197	15	-2.197
20	2.482	20	-2.482
25	2.697	25	-2.697
30	2.852	30	-2.852
35	2.952	35	-2.952
40	2.998	40	-2.998
45	2.983	45	-2.983
50	2.900	50	-2.900
55	2.741	55	-2.741
60	2.518	60	-2.518
65	2.246	65	-2.246
70	1.935	70	-1.935
75	1.594	75	-1.594
80	1.233	80	-1.233
85	.865	85	-.865
90	.510	90	-.510
95	-.195	95	-.195
100	0	100	0

L.E. radius: 0.240

Upper Surface		Lower Surface	
Station	Ordinate	Station	Ordinate
0	0	0	0
.5	.700	.5	-.700
.75	.845	.75	-.845
1.25	1.058	1.25	-1.058
2.5	1.421	2.5	-1.421
5.0	1.961	5.0	-1.961
7.5	2.383	7.5	-2.383
10	2.736	10	-2.736
15	3.299	15	-3.299
20	3.727	20	-3.727
25	4.050	25	-4.050
30	4.282	30	-4.282
35	4.431	35	-4.431
40	4.496	40	-4.496
45	4.469	45	-4.469
50	4.336	50	-4.336
55	4.086	55	-4.086
60	3.743	60	-3.743
65	3.328	65	-3.328
70	2.856	70	-2.856
75	2.342	75	-2.342
80	1.805	80	-1.805
85	1.260	85	-1.260
90	.738	90	-.738
95	.280	95	-.280
100	0	100	0

L.E. radius: 0.552

NACA 65-012

[Stations and ordinates given in percent of airfoil chord]

NACA 65-206

[Stations and ordinates given in percent of airfoil chord]

Upper Surface		Lower Surface	
Station	Ordinate	Station	Ordinate
0	0	0	0
.5	.923	.5	-.923
.75	1.109	.75	-1.109
1.25	1.387	1.25	-1.387
2.5	1.875	2.5	-1.875
5.0	2.606	5.0	-2.606
7.5	3.172	7.5	-3.172
10	3.647	10	-3.647
15	4.402	15	-4.402
20	4.975	20	-4.975
25	5.406	25	-5.406
30	5.716	30	-5.716
35	5.912	35	-5.912
40	5.997	40	-5.997
45	5.949	45	-5.949
50	5.757	50	-5.757
55	5.412	55	-5.412
60	4.943	60	-4.943
65	4.381	65	-4.381
70	3.743	70	-3.743
75	3.059	75	-3.059
80	2.345	80	-2.345
85	1.630	85	-1.630
90	.947	90	-.947
95	.356	95	-.356
100	0	100	0

L.E. radius: 1.000

Upper Surface		Lower Surface	
Station	Ordinate	Station	Ordinate
0	0	0	0
.460	.524	.540	-.424
.706	.642	.794	-.502
1.200	.822	1.300	-.608
2.444	1.140	2.556	-.768
4.939	1.625	5.061	-.993
7.437	2.012	7.563	-1.164
9.936	2.340	10.064	-1.306
14.939	2.869	15.061	-1.523
19.945	3.277	20.055	-1.685
24.953	3.592	25.047	-1.802
29.962	3.824	30.038	-1.880
34.971	3.982	35.029	-1.922
39.981	4.069	40.019	-1.927
44.990	4.078	45.010	-1.888
50.000	4.003	50.000	-1.797
55.009	3.838	54.991	-1.701
60.016	3.589	59.984	-1.646
65.022	3.276	64.978	-1.447
70.026	2.907	69.974	-.963
75.028	2.489	74.972	-.699
80.027	2.029	79.973	-.437
85.024	1.538	84.976	-.192
90.018	1.027	89.982	.007
95.009	.511	94.991	.121
100.000	0	100.000	0

L.E. radius: 0.240
Slope of radius through L.E.: 0.084

CONFIDENTIAL

NATIONAL ADVISORY
COMMITTEE FOR AERONAUTICS



CONFIDENTIAL

NACA 65₁-209

[Stations and ordinates given in percent of airfoil chord]

Upper Surface		Lower Surface	
Station	Ordinate	Station	Ordinate
0	0	0	0
.441	.748	.559	-.648
.684	.912	.816	-.772
1.177	1.162	1.323	-.948
2.417	1.605	2.583	-1.233
4.908	2.275	5.092	-1.643
7.405	2.805	7.595	-1.957
9.904	3.251	10.096	-2.217
14.909	3.971	15.091	-2.625
19.918	4.522	20.082	-2.930
24.929	4.944	25.071	-3.154
29.942	5.254	30.058	-3.310
34.956	5.461	35.044	-3.401
39.971	5.567	40.029	-3.425
44.986	5.564	45.014	-3.374
50.000	5.439	50.000	-3.233
55.013	5.181	54.987	-2.991
60.024	4.814	59.976	-2.672
65.033	4.358	64.967	-2.298
70.039	3.828	69.961	-1.884
75.041	3.237	74.959	-1.447
80.040	2.601	79.960	-1.009
85.035	1.933	84.965	-.587
90.026	1.257	89.974	-.227
95.013	.596	94.987	-.036
100.000	0	100.000	0

L.E. radius; 0.552
Slope of radius through L.E.: 0.08425

NACA 65₁-210

[Stations and ordinates given in percent of airfoil chord]

Upper Surface		Lower Surface	
Station	Ordinate	Station	Ordinate
0	0	0	0
.435	.819	.565	-.719
.678	.999	.822	-.859
1.169	1.273	1.331	-1.059
2.408	1.757	2.592	-1.385
4.898	2.491	5.102	-1.859
7.394	3.069	7.606	-2.221
9.894	3.555	10.106	-2.521
14.899	4.338	15.101	-2.992
19.909	4.938	20.091	-3.346
24.921	5.397	25.079	-3.607
29.936	5.732	30.064	-3.788
34.951	5.954	35.049	-3.894
39.968	6.067	40.032	-3.925
44.984	6.058	45.016	-3.868
50.000	5.915	50.000	-3.709
55.014	5.625	54.986	-3.435
60.027	5.217	59.973	-3.075
65.036	4.712	64.964	-2.652
70.043	4.128	69.957	-2.184
75.045	3.479	74.955	-1.689
80.044	2.783	79.956	-1.191
85.038	2.057	84.962	-.711
90.028	1.327	89.972	-.293
95.014	.622	94.986	-.010
100.000	0	100.000	0

L.E. radius; 0.687
Slope of radius through L.E.: 0.084

NACA 65₁-212

[Stations and ordinates given in percent of airfoil chord]

Upper Surface		Lower Surface	
Station	Ordinate	Station	Ordinate
0	0	0	0
.423	.970	.577	-.870
.664	1.176	.836	-1.036
1.154	1.491	1.346	-1.277
2.391	2.058	2.609	-1.686
4.878	2.919	5.122	-2.287
7.373	3.593	7.627	-2.745
9.873	4.162	10.127	-3.128
14.879	5.073	15.121	-3.727
19.890	5.770	20.110	-4.178
24.906	6.300	25.094	-4.510
29.923	6.687	30.077	-4.743
34.942	6.942	35.053	-4.882
39.961	7.068	40.029	-4.926
44.981	7.044	45.019	-4.854
50.000	6.860	50.000	-4.654
55.017	6.507	54.983	-4.317
60.032	6.014	59.968	-3.872
65.043	5.411	64.957	-3.351
70.050	4.715	69.950	-2.771
75.053	3.954	74.947	-2.164
80.052	3.140	79.948	-1.548
85.045	2.302	84.955	-.956
90.033	1.463	89.967	-.429
95.017	.672	94.983	-.040
100.000	0	100.000	0

L.E. radius; 1.000
Slope of radius through L.E.: 0.084

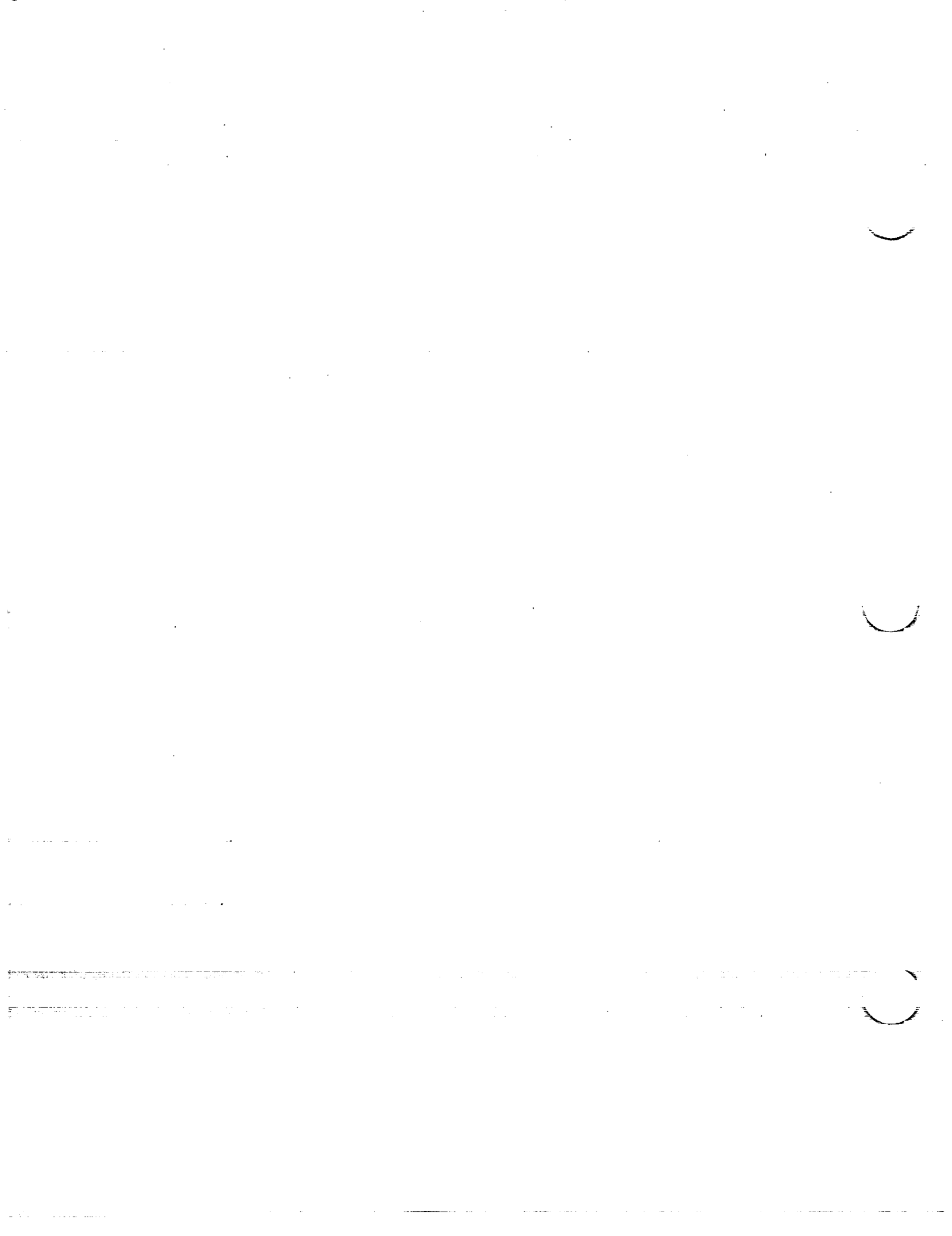
NACA 65₁-410

[Stations and ordinates given in percent of airfoil chord]

Upper Surface		Lower Surface	
Station	Ordinate	Station	Ordinate
0	0	0	0
.372	.861	.628	-.661
.607	1.061	.893	-.781
1.089	1.372	1.411	-.944
2.318	1.935	2.682	-1.191
4.797	2.800	5.203	-1.536
7.289	3.487	7.711	-1.791
9.788	4.067	10.212	-1.999
14.798	5.006	15.202	-2.314
19.817	5.731	20.183	-2.547
24.843	6.290	25.157	-2.710
29.872	6.702	30.128	-2.814
34.903	6.983	35.097	-2.863
39.936	7.138	40.064	-2.854
44.968	7.153	45.032	-2.773
50.000	7.018	50.000	-2.606
55.029	6.720	54.971	-2.340
60.053	6.288	59.947	-2.004
65.073	5.741	64.927	-1.621
70.085	5.099	69.915	-1.211
75.096	4.372	74.910	-.792
80.088	3.577	79.912	-.393
85.076	2.729	84.924	-.037
90.057	1.842	89.943	.226
95.029	.937	94.971	.327
100.000	0	100.000	0

L.E. radius; 0.687
Slope of radius through L.E.: 0.168

CONFIDENTIAL



NACA 65₁-412

[Stations and ordinates given in percent of airfoil chord]

Upper Surface		Lower Surface	
Station	Ordinate	Station	Ordinate
0	0	0	0
.347	1.010	.653	-.810
.580	1.236	.920	-.956
1.059	1.588	1.441	-1.160
2.283	2.234	2.717	-1.490
4.757	3.227	5.243	-1.963
7.247	4.010	7.753	-2.314
9.746	4.672	10.254	-2.604
11.757	5.741	15.243	-3.049
19.781	6.562	20.219	-3.378
24.811	7.193	25.189	-3.613
29.846	7.658	30.154	-3.770
34.884	7.971	35.116	-3.851
39.923	8.139	40.077	-3.855
44.962	8.139	45.038	-3.759
50.000	7.963	50.000	-3.551
55.035	7.602	54.965	-3.222
60.064	7.085	59.936	-2.801
65.086	6.440	64.911	-2.320
70.101	5.686	69.899	-1.798
75.107	4.847	74.892	-1.267
80.103	3.927	79.897	-.751
85.090	2.974	84.910	-.282
90.066	1.979	89.934	.089
95.033	.986	94.967	.278
100.000	0	100.000	0

L.E. radius: 1.000
Slope of radius through L.E.: 0.168

CONFIDENTIAL

NACA 65₂-415

[Stations and ordinates given in percent of airfoil chord]

Upper Surface		Lower Surface	
Station	Ordinate	Station	Ordinate
0	0	0	0
.313	1.208	.687	-1.008
.542	1.480	.958	-1.200
1.016	1.900	1.484	-1.472
2.231	2.680	2.769	-1.936
4.697	3.863	5.303	-2.599
7.184	4.794	7.816	-3.098
9.682	5.578	10.318	-3.510
11.697	6.812	15.303	-4.150
19.726	7.809	20.274	-4.625
24.764	8.550	25.236	-4.970
29.807	9.093	30.193	-5.205
34.854	9.455	35.146	-5.335
39.903	9.639	40.097	-5.355
44.953	9.617	45.047	-5.237
50.000	9.374	50.000	-4.962
55.043	8.910	54.957	-4.530
60.075	8.260	59.921	-3.976
65.106	7.462	64.894	-3.342
70.124	6.542	69.876	-2.654
75.131	5.532	74.869	-1.952
80.126	4.447	79.874	-1.263
85.109	3.320	84.891	-.628
90.080	2.175	89.920	-.107
95.040	1.058	94.960	.206
100.000	0	100.000	0

L.E. radius: 1.505
Slope of radius through L.E.: 0.168

NACA 65₂-415 a = 0.5

[Stations and ordinates given in percent of airfoil chord]

Upper Surface		Lower Surface	
Station	Ordinate	Station	Ordinate
0	0	0	0
.245	1.233	.755	-.957
.464	1.520	1.036	-1.132
.927	1.965	1.373	-1.277
2.126	2.612	2.874	-1.776
4.574	4.099	5.426	-2.335
7.054	5.122	7.946	-2.746
9.549	5.985	10.451	-3.081
11.568	7.383	15.432	-3.591
19.611	8.459	20.389	-3.963
24.671	9.280	25.329	-4.232
29.743	9.883	30.257	-4.411
34.825	10.280	35.175	-4.508
39.916	10.470	40.084	-4.526
45.019	10.423	44.981	-4.431
50.152	10.106	49.848	-4.226
55.262	9.501	54.738	-3.929
60.307	8.672	59.693	-3.548
65.314	7.684	64.686	-3.104
70.294	6.573	69.706	-2.609
75.253	5.387	74.747	-2.083
80.199	4.157	79.801	-1.545
85.137	2.930	84.863	-1.011
90.077	1.755	89.923	-.527
95.027	.715	94.973	-.139
100.000	0	100.000	0

L.E. radius: 1.505
Slope of radius through L.E.: 0.233

NACA 65₃-418

[Stations and ordinates given in percent of airfoil chord]

Upper Surface		Lower Surface	
Station	Ordinate	Station	Ordinate
0	0	0	0
.278	1.418	.722	-1.218
.503	1.729	.997	-1.449
.973	2.209	1.527	-1.781
2.181	3.104	2.819	-2.360
4.639	4.481	5.361	-3.217
7.123	5.566	7.877	-3.870
9.619	6.478	10.381	-4.410
11.636	7.942	15.364	-5.250
19.671	9.061	20.329	-5.877
24.716	9.914	25.284	-6.334
29.768	10.536	30.232	-6.648
34.825	10.944	35.175	-6.824
39.884	11.140	40.116	-6.856
44.943	11.091	45.057	-6.711
50.000	10.774	50.000	-6.362
55.051	10.198	54.949	-5.818
60.094	9.408	59.906	-5.124
65.126	8.454	64.874	-4.334
70.146	7.368	69.854	-3.480
75.154	6.183	74.846	-2.603
80.147	4.927	79.853	-1.743
85.127	3.638	84.873	-.946
90.092	2.350	89.908	-.282
95.046	1.120	94.954	.144
100.000	0	100.000	0

L.E. radius: 1.96
Slope of radius through L.E.: 0.168

CONFIDENTIAL



NACA 65₃-418
a = 0.5

CONFIDENTIAL

[Stations and ordinates given in percent of airfoil chord]

Upper Surface		Lower Surface	
Station	Ordinate	Station	Ordinate
0	0	0	0
.197	1.440	.803	-1.164
.411	1.766	1.089	-1.378
.868	2.271	1.632	-1.683
2.057	3.233	2.943	-2.197
4.493	4.715	5.507	-2.951
6.966	5.891	8.034	-3.515
9.459	6.882	10.541	-3.978
14.481	8.482	15.519	-4.690
19.533	9.709	20.467	-5.213
24.604	10.643	25.396	-5.595
29.691	11.325	30.309	-5.853
34.789	11.770	35.211	-5.998
39.899	11.970	40.101	-6.026
45.022	11.897	44.978	-5.925
50.182	11.506	49.818	-5.626
55.313	10.788	54.697	-5.216
60.364	9.820	59.636	-4.696
65.372	8.674	64.628	-4.094
70.347	7.397	69.653	-3.433
75.298	6.038	74.702	-2.734
80.232	4.636	79.768	-2.024
85.159	3.247	84.841	-1.331
90.089	1.920	89.911	-0.702
95.030	.777	94.970	-0.201
100.000	0	100.000	0

L. E. radius; 1.96
Slope of radius through L. E.: 0.233

NACA 65₃-618
a = 0.5

[Stations and ordinates given in percent of airfoil chord]

Upper Surface		Lower Surface	
Station	Ordinate	Station	Ordinate
0	0	0	0
.059	1.469	.941	-1.055
.256	1.821	1.244	-1.239
.689	2.375	1.811	-1.493
1.346	3.449	3.154	-1.895
4.249	5.115	5.752	-2.469
6.706	6.448	8.294	-2.884
9.194	7.575	10.806	-3.219
14.225	9.404	15.775	-3.716
19.301	10.815	20.699	-4.071
24.407	11.893	25.593	-4.321
29.537	12.687	30.463	-4.479
34.684	13.209	35.316	-4.551
39.849	13.456	40.151	-4.540
45.034	13.395	44.966	-4.477
50.273	12.974	49.727	-4.274
55.468	12.173	54.532	-3.815
60.546	11.090	59.454	-3.140
65.557	9.806	64.443	-2.336
70.519	8.374	69.481	-1.428
75.445	6.851	74.555	-0.495
80.347	5.279	79.653	-1.361
85.239	3.720	84.761	-2.846
90.133	2.233	89.867	-3.391
95.046	.920	94.954	-0.056
100.000	0	100.000	0

L. E. radius; 1.96
Slope of radius through L. E.: 0.349

NATIONAL ADVISORY
COMMITTEE FOR AERONAUTICS.

NACA 65₄-421

[Stations and ordinates given in percent of airfoil chord]

Upper Surface		Lower Surface	
Station	Ordinate	Station	Ordinate
0	0	0	0
.247	1.601	.753	-1.401
.468	1.956	1.032	-1.676
.933	2.493	1.567	-2.065
2.155	3.505	2.865	-2.761
4.582	5.085	5.417	-3.821
7.062	6.329	7.938	-4.633
9.557	7.371	10.443	-5.303
14.575	9.034	15.425	-6.342
19.616	10.304	20.384	-7.120
24.668	11.271	25.332	-7.691
29.729	11.976	30.271	-8.088
34.796	12.433	35.204	-8.313
39.865	12.640	40.135	-8.356
44.934	12.556	45.066	-8.176
50.000	12.158	50.000	-7.746
55.059	11.467	54.941	-7.087
60.108	10.531	59.892	-6.247
65.145	9.419	64.855	-5.299
70.168	8.166	69.832	-4.278
75.176	6.811	74.824	-3.231
80.167	5.388	79.833	-2.204
85.143	3.940	84.857	-1.248
90.104	2.514	89.896	-0.446
95.051	1.176	94.949	0.088
100.000	0	100.000	0

L. E. radius; 2.50
Slope of radius through L. E.: 0.168

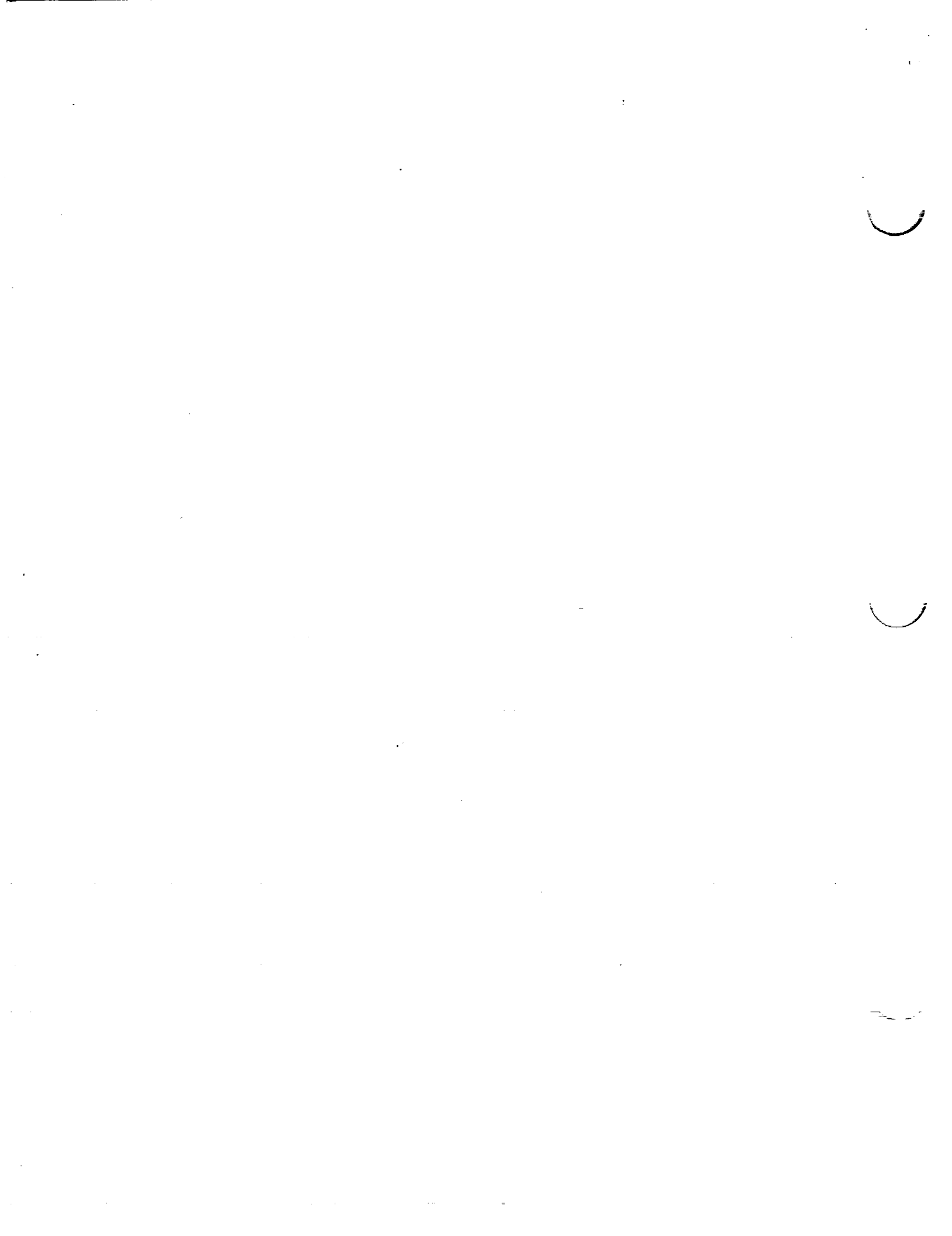
NACA 65₄-421
a = 0.5

[Stations and ordinates given in percent of airfoil chord]

Upper Surface		Lower Surface	
Station	Ordinate	Station	Ordinate
0	0	0	0
.155	1.620	.845	-1.344
.363	1.991	1.137	-1.603
.813	2.553	1.687	-1.963
1.992	3.631	3.008	-2.595
4.414	5.315	5.586	-3.551
6.880	6.651	8.120	-4.275
9.371	7.773	10.629	-4.869
14.395	9.572	15.605	-5.780
19.455	10.951	20.545	-6.455
24.538	12.000	25.462	-6.952
29.639	12.765	30.361	-7.293
34.754	13.258	35.246	-7.486
39.882	13.470	40.118	-7.526
45.026	13.362	44.974	-7.370
50.211	12.890	49.789	-7.010
55.362	12.056	54.638	-6.484
60.421	10.942	59.579	-5.818
65.428	9.637	64.572	-5.057
70.398	8.193	69.602	-4.229
75.340	6.664	74.660	-3.360
80.264	5.097	79.736	-2.485
85.181	3.550	84.819	-1.634
90.100	2.095	89.900	-0.867
95.034	.833	94.966	-0.257
100.000	0	100.000	0

L. E. radius; 2.50
Slope of radius through L. E.: 0.233

CONFIDENTIAL



CONFIDENTIAL

NACA 65(421)-420

[Stations and ordinates given in percent of airfoil chord]

Upper Surface		Lower Surface	
Station	Ordinate	Station	Ordinate
0	0	0	0
.258	1.537	.742	-1.337
.482	1.864	1.018	-1.554
.950	2.374	1.550	-1.974
2.152	3.358	2.848	-2.614
4.603	4.866	5.397	-3.602
7.083	6.066	7.917	-4.370
9.579	7.060	10.421	-4.992
14.596	8.665	15.404	-5.973
19.634	9.885	20.366	-6.701
24.684	10.815	25.316	-7.235
29.742	11.494	30.258	-7.606
34.805	11.939	35.195	-7.819
39.871	12.140	40.129	-7.856
44.937	12.056	45.063	-7.676
50.000	11.672	50.000	-7.260
55.056	11.015	54.944	-6.635
60.103	10.126	59.897	-5.842
65.138	9.060	64.862	-4.940
70.160	7.861	69.840	-3.973
75.167	6.563	74.833	-2.965
80.159	5.200	79.841	-2.016
85.136	3.813	84.864	-1.121
90.098	2.441	89.902	-.373
95.049	1.150	94.951	-.114
100.000	0	100.000	0

L. E. radius: 2.27
Slope of radius through L. E.: 0.168

NACA 66,1-212

[Stations and ordinates given in percent of airfoil chord]

Upper Surface		Lower Surface	
Station	Ordinate	Station	Ordinate
0	0	0	0
.424	.947	.576	-.847
.666	1.150	.834	-1.010
1.157	1.447	1.343	-1.233
2.395	1.986	2.605	-1.614
4.884	2.797	5.116	-2.165
7.379	3.441	7.621	-2.593
9.878	3.997	10.122	-2.963
14.884	4.885	15.116	-3.539
19.895	5.574	20.105	-3.982
24.906	6.112	25.091	-4.322
29.925	6.522	30.075	-4.578
34.943	6.816	35.057	-4.756
39.962	7.005	40.038	-4.863
44.981	7.093	45.019	-4.903
50.000	7.075	50.000	-4.869
55.019	6.939	54.981	-4.749
60.036	6.665	59.964	-4.523
65.051	6.195	64.949	-4.135
70.061	5.507	69.939	-3.563
75.066	4.683	74.934	-2.893
80.065	3.759	79.935	-2.167
85.058	2.770	84.942	-1.424
90.043	1.760	89.957	-.726
95.022	.792	94.978	-.160
100.000	0	100.000	0

L. E. radius: 0.893
Slope of radius through L. E.: 0.084

NATIONAL ADVISORY
COMMITTEE FOR AERONAUTICS

NACA 66(215)-016

[Stations and ordinates given in percent of airfoil chord]

Upper Surface		Lower Surface	
Station	Ordinate	Station	Ordinate
0	0	0	0
.5	1.184	.5	-1.184
1.25	1.418	1.25	-1.418
1.75	1.755	1.75	-1.755
2.5	2.378	2.5	-2.378
5.0	3.292	5.0	-3.292
7.5	4.007	7.5	-4.007
10	4.626	10	-4.626
15	5.605	15	-5.605
20	6.362	20	-6.362
25	6.950	25	-6.950
30	7.395	30	-7.395
35	7.706	35	-7.706
40	7.909	40	-7.909
45	7.997	45	-7.997
50	7.957	50	-7.957
55	7.780	55	-7.780
60	7.425	60	-7.425
65	6.832	65	-6.832
70	5.970	70	-5.970
75	4.966	75	-4.966
80	3.849	80	-3.849
85	2.723	85	-2.723
90	1.587	90	-1.587
95	.597	95	-.597
100	0	100	0

L. E. radius: 1.575

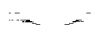
NACA 66(215)-216

[Stations and ordinates given in percent of airfoil chord]

Upper Surface		Lower Surface	
Station	Ordinate	Station	Ordinate
0	0	0	0
.401	1.230	.599	-1.130
.640	1.484	.860	-1.344
1.128	1.858	1.372	-1.644
2.362	2.560	2.638	-2.188
4.846	3.604	5.154	-2.972
7.340	4.428	7.660	-3.580
9.838	5.110	10.162	-4.106
14.845	6.276	15.155	-4.930
19.860	7.156	20.140	-5.564
24.879	7.844	25.121	-6.054
29.900	8.366	30.100	-6.422
34.924	8.736	35.076	-6.676
39.949	8.980	40.051	-6.838
44.974	9.092	45.026	-6.902
50.000	9.060	50.000	-6.854
55.025	8.875	54.975	-6.685
60.048	8.496	59.952	-6.354
65.067	7.862	64.933	-5.802
70.081	6.941	69.919	-5.097
75.087	5.860	74.913	-4.070
80.085	4.644	79.915	-3.052
85.075	3.395	84.925	-2.049
90.055	2.103	89.945	-1.069
95.028	.913	94.972	-.281
100.000	0	100.000	0

L. E. radius: 1.575
Slope of radius through L. E.: 0.084

CONFIDENTIAL



NACA 66(215)-216
 $\alpha = 0.6$

CONFIDENTIAL

NACA 66(215)-416

[Stations and ordinates given in percent of airfoil chord]

[Stations and ordinates given in percent of airfoil chord]

Upper Surface		Lower Surface	
Station	Ordinate	Station	Ordinate
0	0	0	0
.371	1.242	.629	-1.112
.607	1.501	.893	-1.319
1.091	1.886	1.409	-1.608
2.317	2.615	2.683	-2.127
4.794	3.701	5.206	-2.869
7.284	4.563	7.716	-3.441
9.781	5.308	10.219	-3.934
14.788	6.500	15.212	-4.702
19.806	7.428	20.194	-5.290
24.832	8.155	25.163	-5.741
29.862	8.708	30.138	-6.080
34.897	9.098	35.103	-6.312
39.936	9.356	40.064	-6.462
44.978	9.471	45.022	-6.523
50.023	9.431	49.977	-6.483
55.073	9.224	54.927	-6.336
60.141	8.800	59.859	-6.048
65.191	8.084	64.809	-5.574
70.198	7.068	69.802	-4.866
75.181	5.889	74.819	-4.037
80.148	4.585	79.852	-3.107
85.106	3.265	84.894	-2.177
90.061	1.937	89.939	-1.235
95.021	.762	94.979	-.432
100.000	0	100.000	0

L.E. radius: 1.575
Slope of radius through L.E.: 0.110

Upper Surface		Lower Surface	
Station	Ordinate	Station	Ordinate
0	0	0	0
.303	1.268	.697	-1.068
.532	1.541	.968	-1.261
1.008	1.952	1.492	-1.524
2.225	2.754	2.775	-1.990
4.693	3.910	5.307	-2.646
7.180	4.843	7.820	-3.147
9.677	5.649	10.323	-3.581
14.691	6.942	15.309	-4.250
19.720	7.948	20.280	-4.764
24.757	8.736	25.243	-5.156
29.801	9.336	30.199	-5.448
34.848	9.765	35.152	-5.645
39.898	10.050	40.102	-5.766
44.949	10.187	45.051	-5.807
50.000	10.163	50.000	-5.751
55.050	9.970	54.950	-5.590
60.096	9.566	59.901	-5.282
65.135	8.891	64.865	-4.771
70.161	7.912	69.839	-4.024
75.174	6.753	74.826	-3.173
80.170	5.437	79.830	-2.253
85.150	4.065	84.850	-1.373
90.111	2.617	89.889	-.549
95.056	1.226	94.944	-.038
100.000	0	100.000	0

L.E. radius: 1.575
Slope of radius through L.E.: 0.168

NACA 66-006

NACA 66-009

[Stations and ordinates given in percent of airfoil chord]

[Stations and ordinates given in percent of airfoil chord]

Upper Surface		Lower Surface	
Station	Ordinate	Station	Ordinate
0	0	0	0
.50	.461	.50	-.461
.75	.554	.75	-.554
1.25	.693	1.25	-.693
2.5	.918	2.5	-.918
5.0	1.257	5.0	-1.257
7.5	1.524	7.5	-1.524
10	1.752	10	-1.752
15	2.119	15	-2.119
20	2.401	20	-2.401
25	2.618	25	-2.618
30	2.782	30	-2.782
35	2.899	35	-2.899
40	2.971	40	-2.971
45	3.000	45	-3.000
50	2.985	50	-2.985
55	2.925	55	-2.925
60	2.815	60	-2.815
65	2.611	65	-2.611
70	2.316	70	-2.316
75	1.953	75	-1.953
80	1.543	80	-1.543
85	1.107	85	-1.107
90	.665	90	-.665
95	.262	95	-.262
100	0	100	0

L.E. radius: 0.223

Upper Surface		Lower Surface	
Station	Ordinate	Station	Ordinate
0	0	0	0
.50	.687	.50	-.687
.75	.824	.75	-.824
1.25	1.030	1.25	-1.030
2.5	1.368	2.5	-1.368
5.0	1.880	5.0	-1.880
7.5	2.283	7.5	-2.283
10	2.626	10	-2.626
15	3.178	15	-3.178
20	3.601	20	-3.601
25	3.927	25	-3.927
30	4.173	30	-4.173
35	4.348	35	-4.348
40	4.457	40	-4.457
45	4.499	45	-4.499
50	4.475	50	-4.475
55	4.381	55	-4.381
60	4.204	60	-4.204
65	3.882	65	-3.882
70	3.428	70	-3.428
75	2.877	75	-2.877
80	2.263	80	-2.263
85	1.611	85	-1.611
90	.961	90	-.961
95	.374	95	-.374
100	0	100	0

L.E. radius: 0.530

CONFIDENTIAL

NATIONAL ADVISORY
COMMITTEE FOR AERONAUTICS



NACA 66₁-012

CONFIDENTIAL

NACA 66₁-206

[Stations and ordinates given in percent of airfoil chord]

[Stations and ordinates given in percent of airfoil chord]

Upper Surface		Lower Surface	
Station	Ordinate	Station	Ordinate
0	0	0	0
.5	.906	.5	-.906
.75	1.087	.75	-1.087
1.25	1.358	1.25	-1.358
2.5	1.808	2.5	-1.808
5.0	2.496	5.0	-2.496
7.5	3.037	7.5	-3.037
10	3.496	10	-3.496
15	4.234	15	-4.234
20	4.801	20	-4.801
25	5.238	25	-5.238
30	5.568	30	-5.568
35	5.803	35	-5.803
40	5.947	40	-5.947
45	6.000	45	-6.000
50	5.965	50	-5.965
55	5.836	55	-5.836
60	5.588	60	-5.588
65	5.139	65	-5.139
70	4.515	70	-4.515
75	3.767	75	-3.767
80	2.944	80	-2.944
85	2.083	85	-2.083
90	1.234	90	-1.234
95	.474	95	-.474
100	0	100	0

L.E. radius: 0.952

Upper Surface		Lower Surface	
Station	Ordinate	Station	Ordinate
0	0	0	0
.461	.509	.539	-.409
.707	.622	.793	-.482
1.202	.798	1.298	-.584
2.117	1.102	2.555	-.730
4.911	1.572	5.059	-.940
7.439	1.947	7.561	-1.099
9.939	2.268	10.061	-1.234
11.912	2.791	15.058	-1.445
19.917	3.196	20.053	-1.604
24.954	3.513	25.046	-1.723
29.962	3.751	30.038	-1.810
34.971	3.929	35.029	-1.869
39.981	4.042	40.019	-1.900
44.990	4.095	45.010	-1.905
50.000	4.088	50.000	-1.882
55.009	4.020	54.991	-1.830
60.018	3.886	59.982	-1.764
65.026	3.641	64.974	-1.581
70.031	3.288	69.966	-1.341
75.034	2.848	74.966	-1.058
80.034	2.339	79.966	-.747
85.031	1.780	84.969	-.434
90.023	1.182	89.977	-.118
95.012	.578	94.988	.054
100.000	0	100.000	0

L.E. radius: 0.223
Slope of radius through L.E.: 0.084

NACA 66₁-209

[Stations and ordinates given in percent of airfoil chord]

Upper Surface		Lower Surface	
Station	Ordinate	Station	Ordinate
0	0	0	0
.442	.735	.558	-.635
.686	.892	.814	-.752
1.179	1.135	1.321	-.921
2.420	1.552	2.580	-1.180
4.912	2.194	5.088	-1.562
7.409	2.705	7.591	-1.857
9.908	3.141	10.092	-2.107
14.912	3.850	15.088	-2.504
19.921	4.396	20.079	-2.804
24.931	4.821	25.069	-3.031
29.941	5.145	30.056	-3.201
34.957	5.378	35.043	-3.318
39.971	5.528	40.029	-3.386
44.986	5.591	45.014	-3.404
50.000	5.578	50.000	-3.372
55.011	5.476	54.986	-3.286
60.027	5.275	59.973	-3.133
65.038	4.912	64.962	-2.852
70.046	4.400	69.954	-2.456
75.050	3.772	74.950	-1.982
80.050	3.058	79.950	-1.466
85.044	2.283	84.956	-.937
90.034	1.477	89.965	-.411
95.018	.690	94.982	-.058
100.000	0	100.000	0

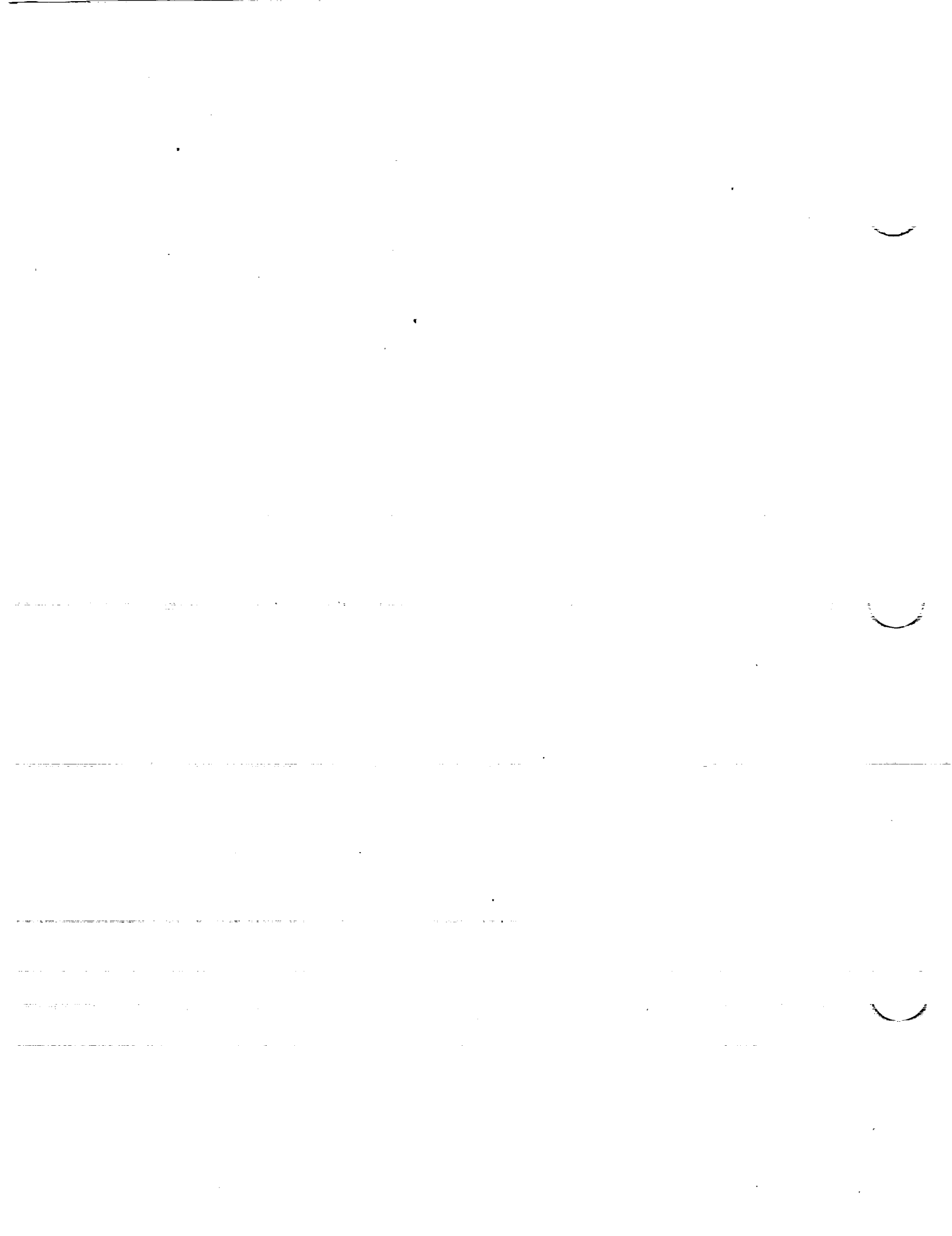
L.E. radius: 0.530
Slope of radius through L.E.: 0.084

NACA 66₁-212

[Stations and ordinates given in percent of airfoil chord]

Upper Surface		Lower Surface	
Station	Ordinate	Station	Ordinate
0	0	0	0
.421	.953	.576	-.853
.666	1.154	.834	-1.014
1.156	1.462	1.314	-1.248
2.395	1.991	2.605	-1.619
4.885	2.809	5.117	-2.177
7.379	3.459	7.621	-2.611
9.878	4.011	10.122	-2.977
14.885	4.905	15.117	-3.559
19.894	5.596	20.106	-4.004
24.908	6.132	25.092	-4.342
29.925	6.539	30.075	-4.595
34.943	6.833	35.057	-4.773
39.962	7.018	40.038	-4.876
44.981	7.095	45.019	-4.905
50.000	7.068	50.000	-4.862
55.019	6.931	54.981	-4.741
60.036	6.659	59.964	-4.517
65.051	6.169	64.949	-4.109
70.061	5.487	69.939	-3.513
75.066	4.661	74.934	-2.871
80.065	3.739	79.935	-2.147
85.057	2.755	84.943	-1.409
90.043	1.750	89.957	-.716
95.022	.789	94.978	-.157
100.000	0	100.000	0

L.E. radius: 0.952
Slope of radius through L.E.: 0.084



NACA 67,1-215

[Stations and ordinates given in percent of airfoil chord]

Upper Surface		Lower Surface	
Station	Ordinate	Station	Ordinate
0	0	0	0
.402	1.213	.598	-1.113
.642	1.460	.858	-1.320
1.128	1.867	1.372	-1.653
2.361	2.577	2.639	-2.205
4.848	3.557	5.152	-2.925
7.344	4.321	7.656	-3.473
9.845	4.947	10.155	-3.913
14.854	5.954	15.146	-4.608
19.869	6.735	20.131	-5.143
24.887	7.348	25.113	-5.558
29.906	7.825	30.092	-5.881
34.930	8.185	35.070	-6.125
39.953	8.430	40.047	-6.288
44.976	8.570	45.024	-6.380
50.000	8.600	50.000	-6.394
55.024	8.516	54.976	-6.326
60.047	8.302	59.953	-6.160
65.068	7.935	64.932	-5.875
70.086	7.373	69.914	-5.429
75.098	6.515	74.902	-4.725
80.100	5.335	79.900	-3.743
85.092	3.999	84.908	-2.653
90.071	2.537	89.929	-1.503
95.037	1.103	94.963	-.471
100.000	0	100.000	0

L.E. radius: 1.523
Slope of radius through L.E.: 0.084

CONFIDENTIAL

NACA 747A315

[Stations and ordinates given in percent of airfoil chord]

Upper Surface		Lower Surface	
Station	Ordinate	Station	Ordinate
0	0	0	0
.229	1.305	.771	-1.031
.446	1.599	1.051	-1.207
.911	2.065	1.589	-1.473
2.109	2.935	2.891	-1.927
4.564	4.264	5.436	-2.518
7.053	5.286	7.947	-2.952
9.558	6.140	10.442	-3.304
14.599	7.497	15.401	-3.843
19.668	8.503	20.332	-4.247
24.758	9.242	25.242	-4.546
29.867	9.731	30.133	-4.773
35.001	9.982	34.999	-4.926
40.200	9.962	39.800	-5.020
45.375	9.572	44.625	-5.040
50.447	8.964	49.553	-5.014
55.463	8.206	54.537	-4.930
60.435	7.324	59.565	-4.772
65.366	6.365	64.634	-4.509
70.241	5.354	69.759	-4.110
75.130	4.356	74.870	-3.502
80.073	3.295	79.927	-2.743
85.038	2.257	84.962	-1.915
90.016	1.289	89.984	-1.097
95.004	.481	94.996	-.405
100.000	0	100.000	0

L.E. radius: 1.544
Slope of radius through L.E.: 0.232

NACA 747A415

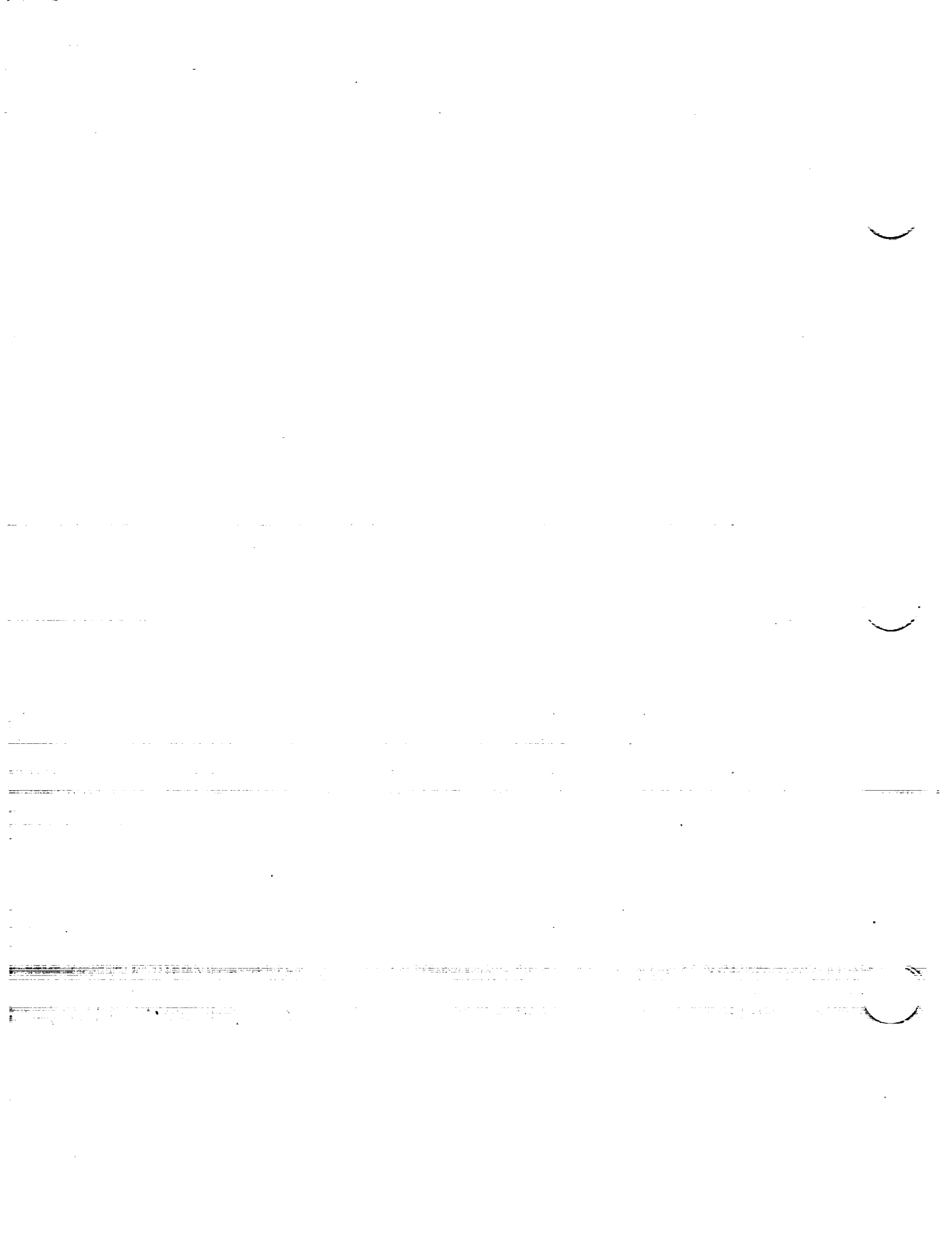
[Stations and ordinates given in percent of airfoil chord]

Upper Surface		Lower Surface	
Station	Ordinate	Station	Ordinate
0	0	0	0
.183	1.318	.817	-.994
.398	1.622	1.102	-1.160
.852	2.106	1.648	-1.406
2.041	3.016	2.959	-1.822
4.487	4.411	5.513	-2.349
6.972	5.488	8.028	-2.730
9.476	6.390	10.524	-3.038
14.521	7.827	15.479	-3.501
19.598	8.897	20.402	-3.845
24.698	9.687	25.302	-4.095
29.818	10.216	30.182	-4.286
34.964	10.497	35.036	-4.411
40.176	10.499	39.824	-4.485
45.364	10.121	44.636	-4.493
50.447	9.516	49.553	-4.462
55.474	8.753	54.526	-4.381
60.454	7.859	59.546	-4.235
65.393	6.878	64.607	-3.992
70.273	5.838	69.727	-3.622
75.164	4.783	74.836	-3.053
80.107	3.692	79.893	-2.344
85.066	2.592	84.934	-1.578
90.037	1.546	89.963	-.838
95.015	.639	94.985	-.247
100.000	0	100.000	0

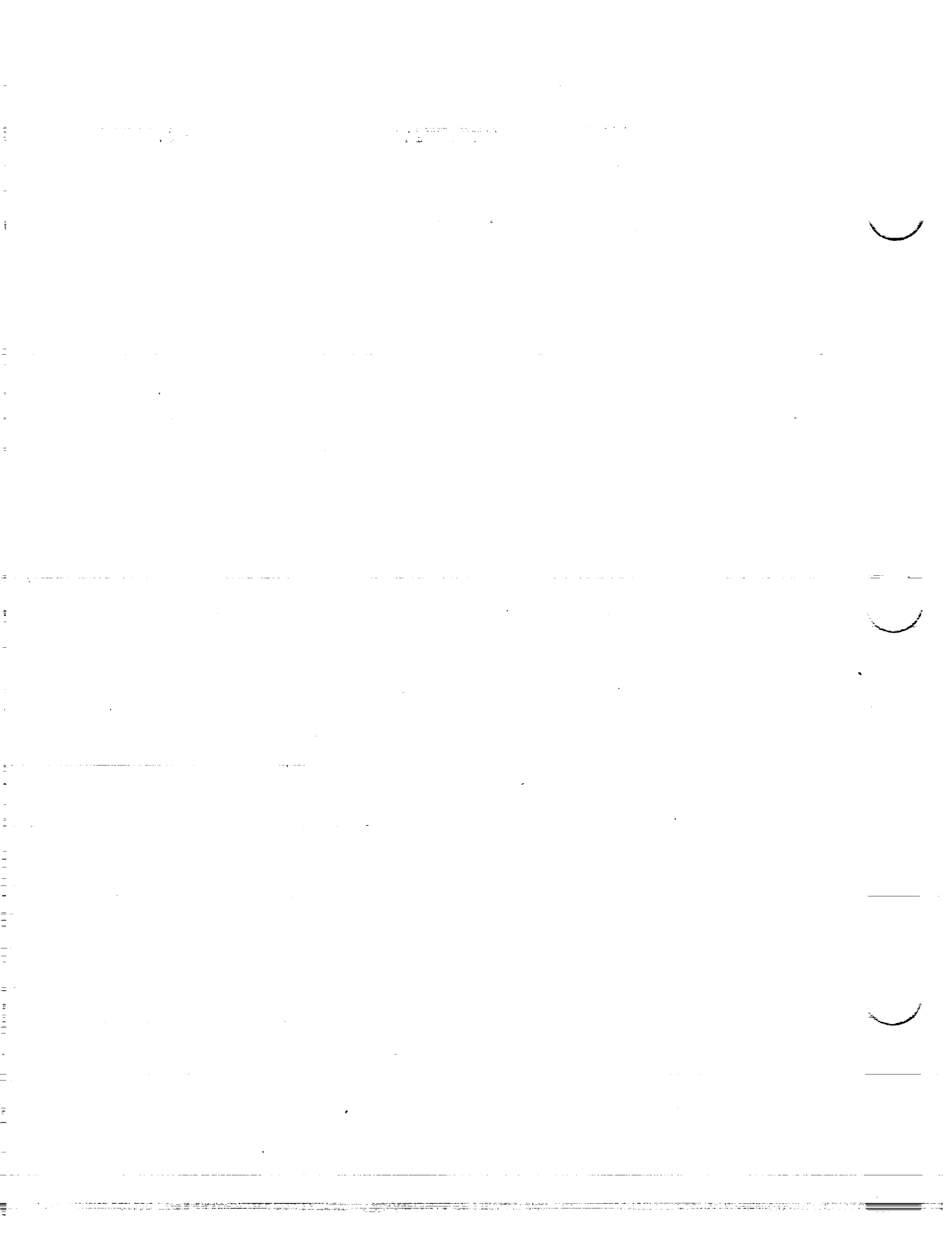
L.E. radius: 1.544
Slope of radius through L.E.: 0.274

NATIONAL ADVISORY
COMMITTEE FOR AERONAUTICS

CONFIDENTIAL



IV - PREDICTED CRITICAL MACH NUMBERS



IV - PREDICTED CRITICAL MACH NUMBERS

Critical Mach number chart	S83
Mach numbers corresponding to a wing loading of 30 pounds per square foot for level flight at various speeds and altitudes	S84
Mach numbers corresponding to a wing loading of 40 pounds per square foot for level flight at various speeds and altitudes	S85
Mach numbers corresponding to a wing loading of 50 pounds per square foot for level flight at various speeds and altitudes	S86
Mach numbers corresponding to a wing loading of 60 pounds per square foot for level flight at various speeds and altitudes	S87
Mach numbers corresponding to a wing loading of 70 pounds per square foot for level flight at various speeds and altitudes	S88
Mach numbers corresponding to a wing loading of 80 pounds per square foot for level flight at various speeds and altitudes	S89
Variation of critical Mach number with low-speed section lift coefficient for the NACA 0006, 0009, and 0012 airfoil sections	S89a
Variation of critical Mach number with low-speed section lift coefficient for several NACA 14-series airfoil sections of various thicknesses	S89b
Variation of critical Mach number with low-speed section lift coefficient for several NACA 24-series airfoil sections of various thicknesses	S90
Variation of critical Mach number with low-speed section lift coefficient for several NACA 44-series airfoil sections of various thicknesses	S91
Variation of critical Mach number with low-speed section lift coefficient for several NACA 230-series airfoil sections of various thicknesses	S92



- Variation of critical Mach number with low-speed section lift coefficient for several NACA 63-series airfoil sections of various thicknesses, cambered for various design lift coefficients S93
- Variation of critical Mach number with low-speed section lift coefficient for several NACA 64-series symmetrical airfoil sections of various thicknesses S94
- Variation of critical Mach number with low-speed section lift coefficient for several NACA 64-series airfoil sections of various thicknesses, cambered for a design lift coefficient of 0.1 S94a
- Variation of critical Mach number with low-speed section lift coefficient for several NACA 64-series airfoil sections of various thicknesses, cambered for a design lift coefficient of 0.2 . . . S95
- Variation of critical Mach number with low-speed section lift coefficient for several NACA 64-series airfoil sections of various thicknesses, cambered for a design lift coefficient of 0.4 . . S96
- Variation of critical Mach number with low-speed section lift coefficient for two NACA 64-series airfoil sections of different thicknesses, cambered for a design lift coefficient of 0.6 . . S97
- Variation of critical Mach number with low-speed section lift coefficient for several NACA 65-series symmetrical airfoil sections of various thicknesses S98
- Variation of critical Mach number with low-speed section lift coefficient for several NACA 65-series airfoil sections with a thickness ratio of 0.18 and cambered for various design lift coefficients . S99
- Variation of critical Mach number with low-speed section lift coefficient for several NACA 65-series airfoil sections of various thicknesses, cambered for a design lift coefficient of 0.2 S100
- Variation of critical Mach number with low-speed section lift coefficient for several NACA 65-series airfoil sections of various thicknesses, cambered for a design lift coefficient of 0.4 S101

...

...

...

...

...

...

...

...

...

...

...

...

...

...

...

...

...

...

...

...

...

...

- Variation of critical Mach number with low-speed section lift coefficient for several NACA 65-series airfoil sections with mean line of the type $a = 0.5$ and cambered for a design lift coefficient of 0.4 S102

- Variation of critical Mach number with low-speed section lift coefficient for two NACA 65-series airfoil sections of different thicknesses, cambered for a design lift coefficient of 0.6 . . . S103

- Variation of critical Mach number with low-speed section lift coefficient for two NACA 65-series airfoil sections with mean line of the type $a = 0.5$, with different thicknesses, and cambered for a design lift coefficient of 0.6 S104

- Variation of critical Mach number with low-speed section lift coefficient for several NACA 66-series symmetrical airfoil sections of various thicknesses S105

- Variation of critical Mach number with low-speed section lift coefficient for several NACA 66-series airfoil sections of various thicknesses, cambered for a design lift coefficient of 0.2 S106

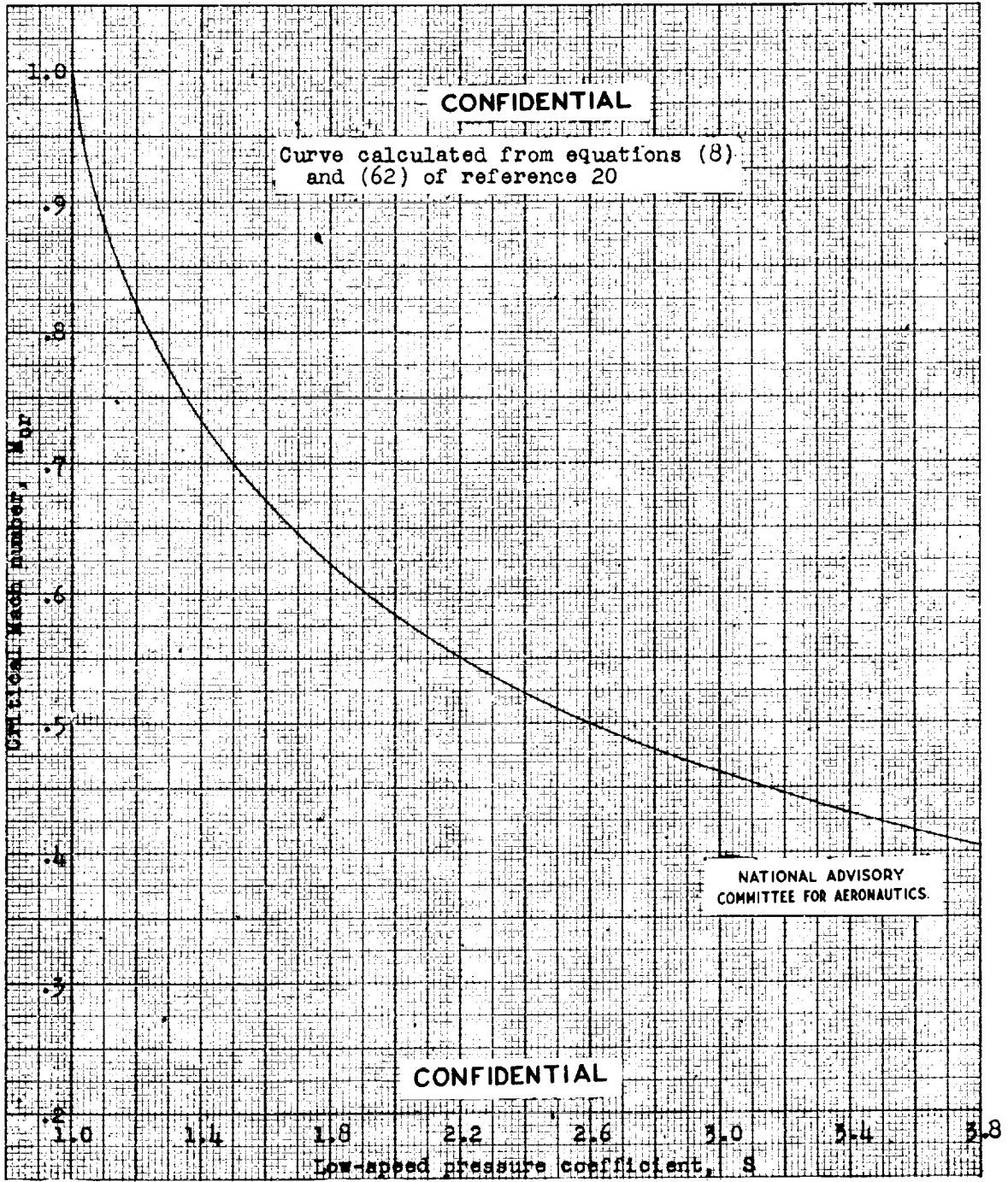
- Variation of critical Mach number with low-speed section lift coefficient for two NACA 66-series airfoil sections of different thicknesses, cambered for a design lift coefficient of 0.4 . . . S107

- Variation of critical Mach number with low-speed section lift coefficient for several NACA 66-series airfoil sections with a thickness ratio of 0.16 and cambered for various design lift coefficients. S108

- Variation of critical Mach number with low-speed section lift coefficient for several NACA 6-series airfoil sections with different positions of minimum pressure and various thicknesses, cambered for various design lift coefficients S109

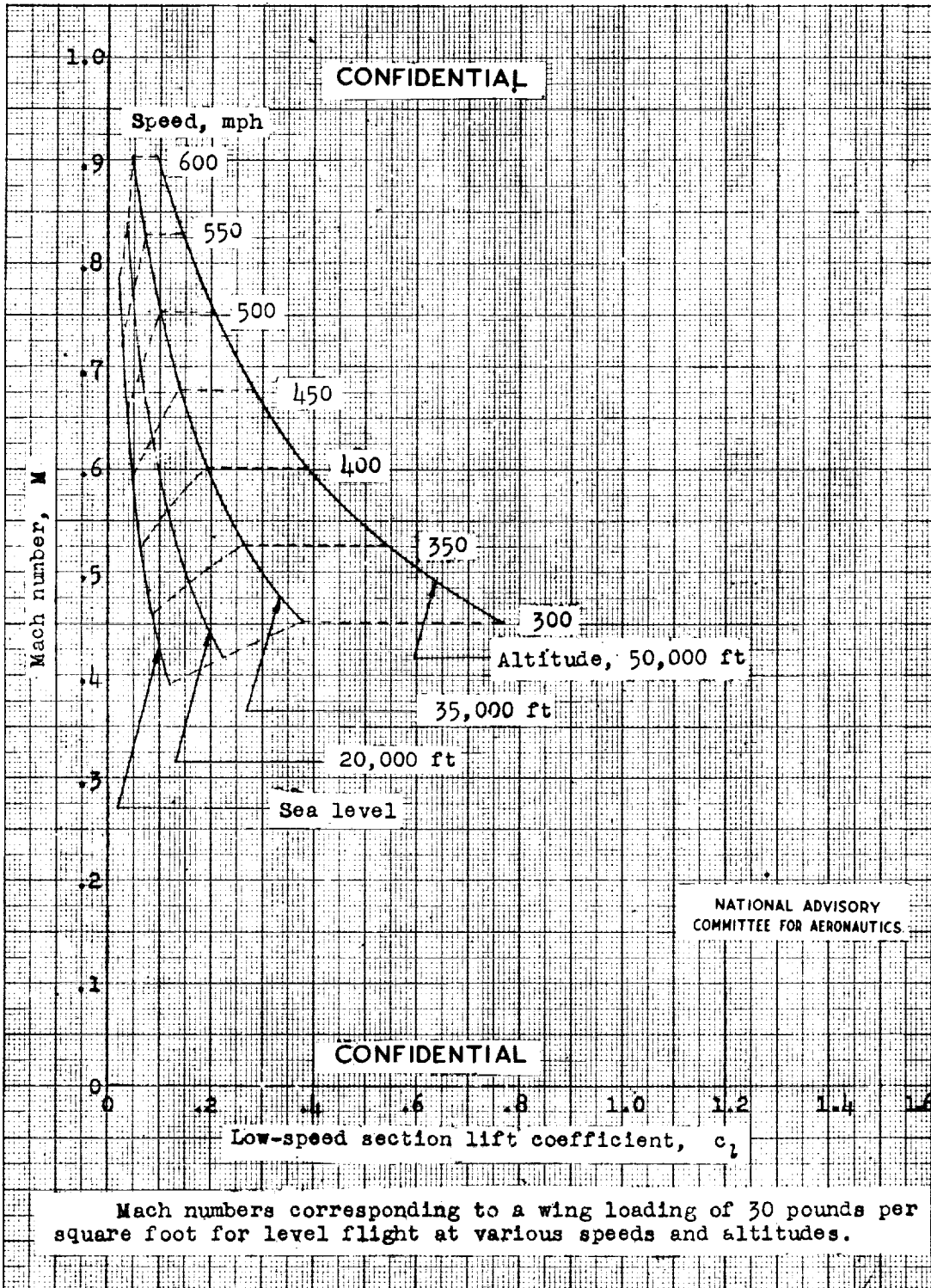
- Variation of critical Mach number with low-speed section lift coefficient for two NACA 7-series airfoil sections with a thickness ratio of 0.15 and cambered for different design lift coefficients S110



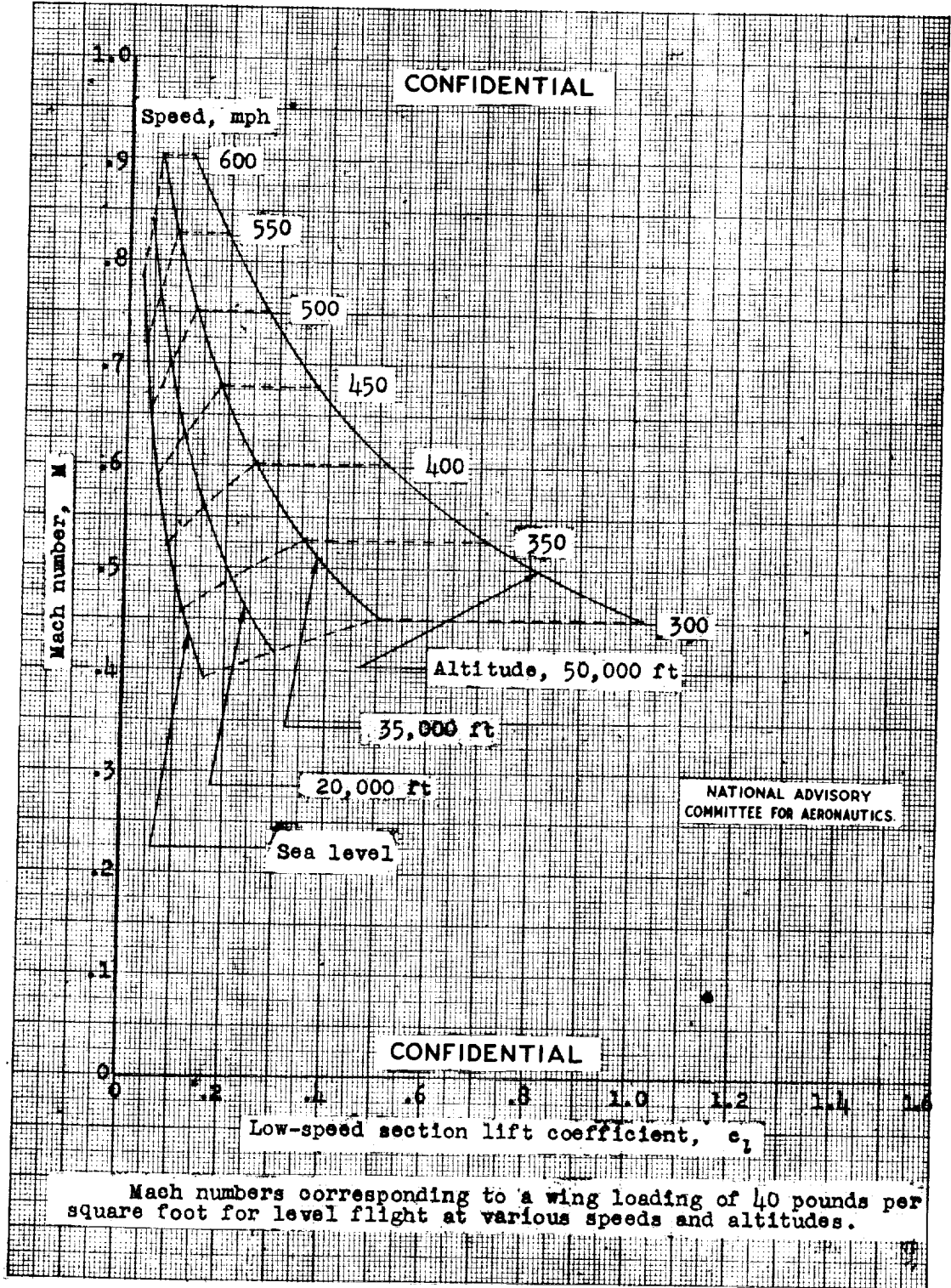


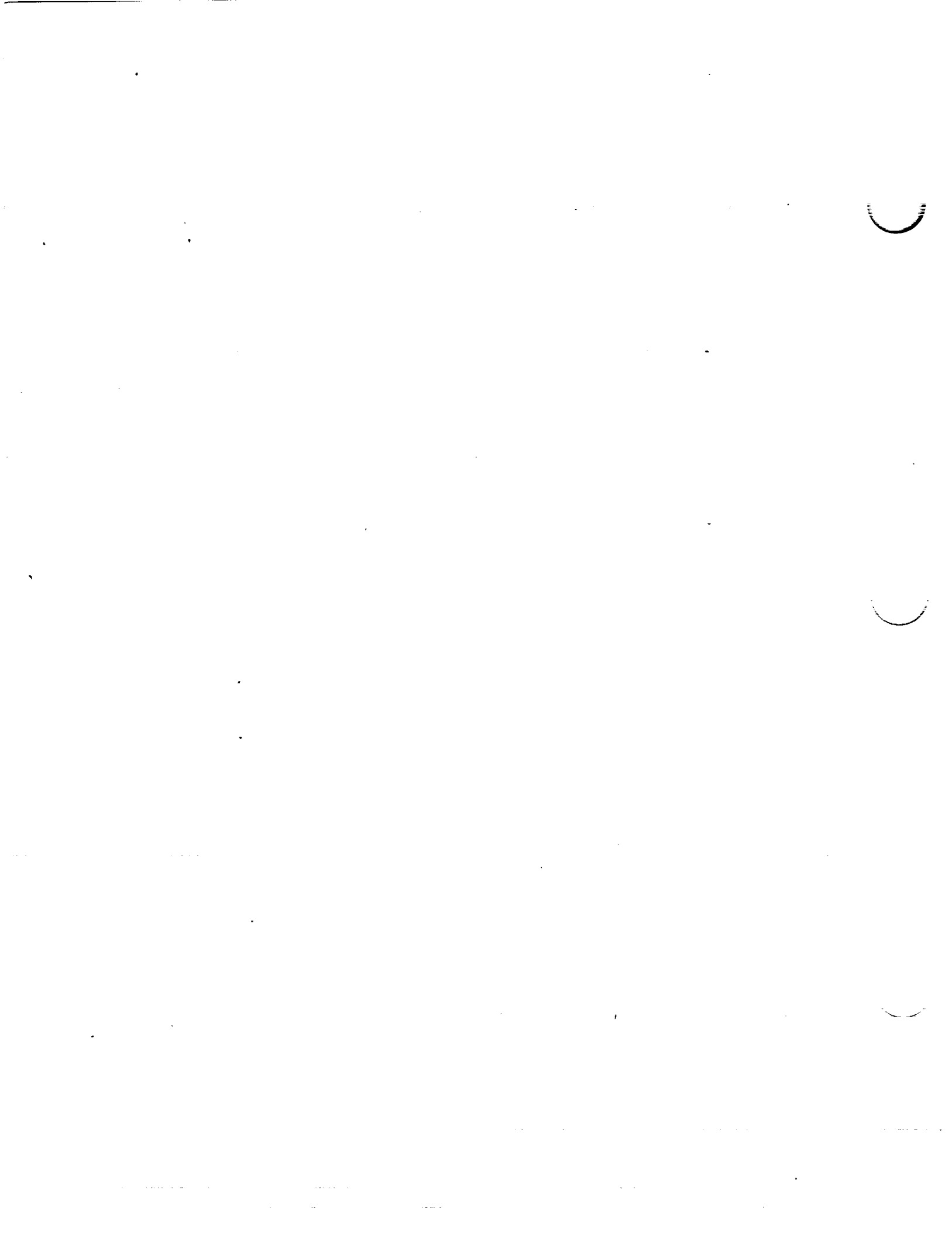
Critical Mach number chart

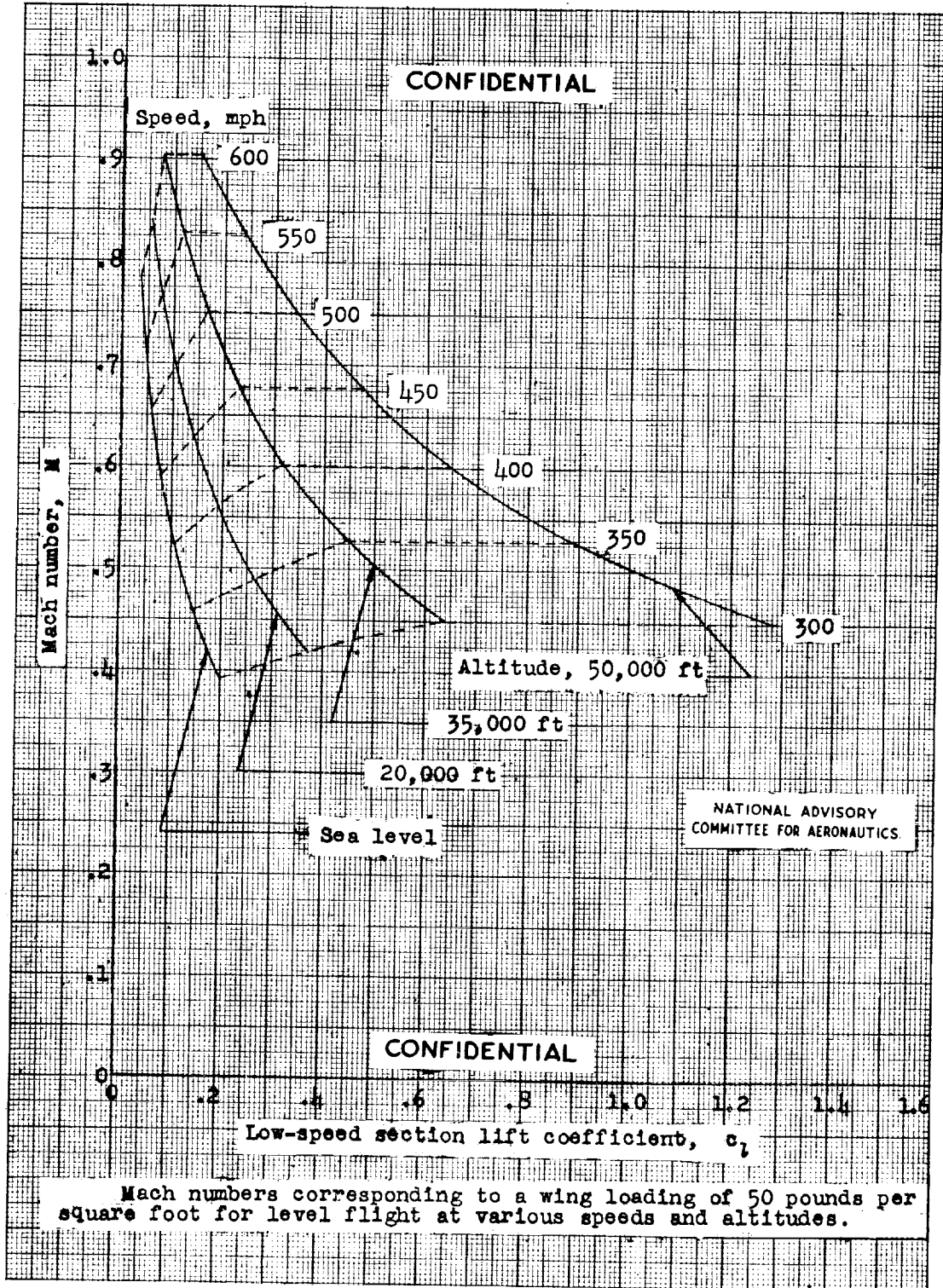




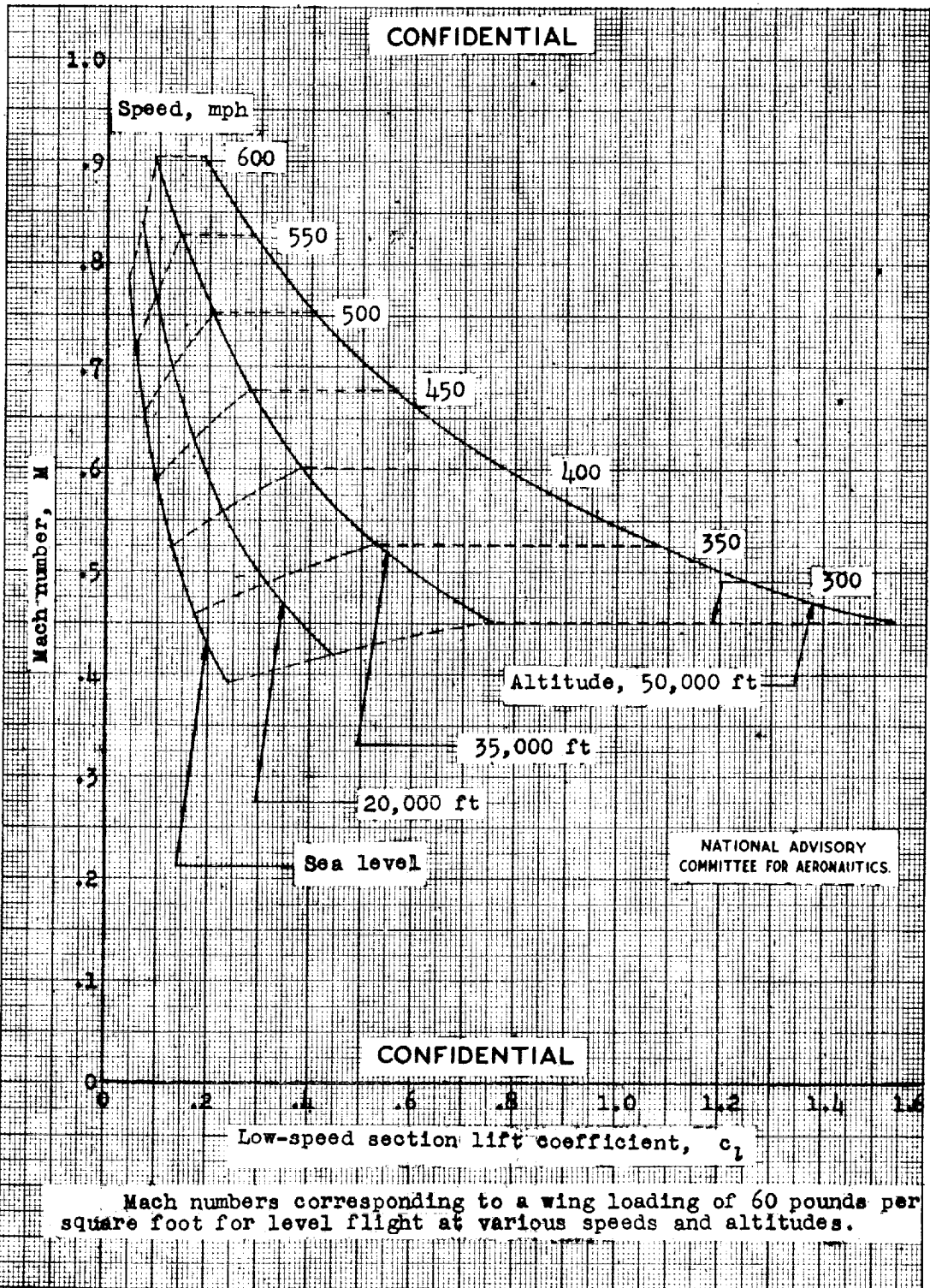




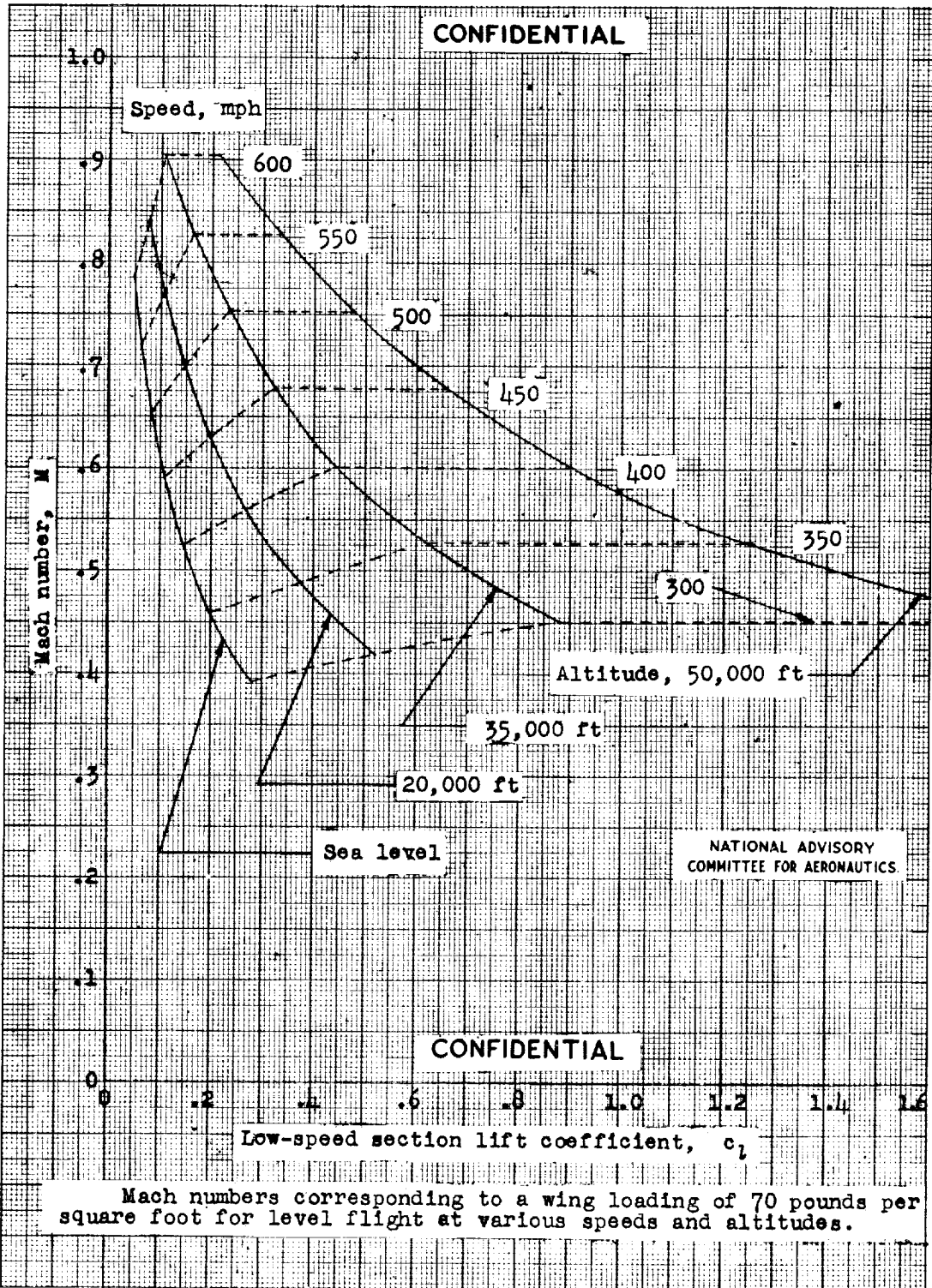




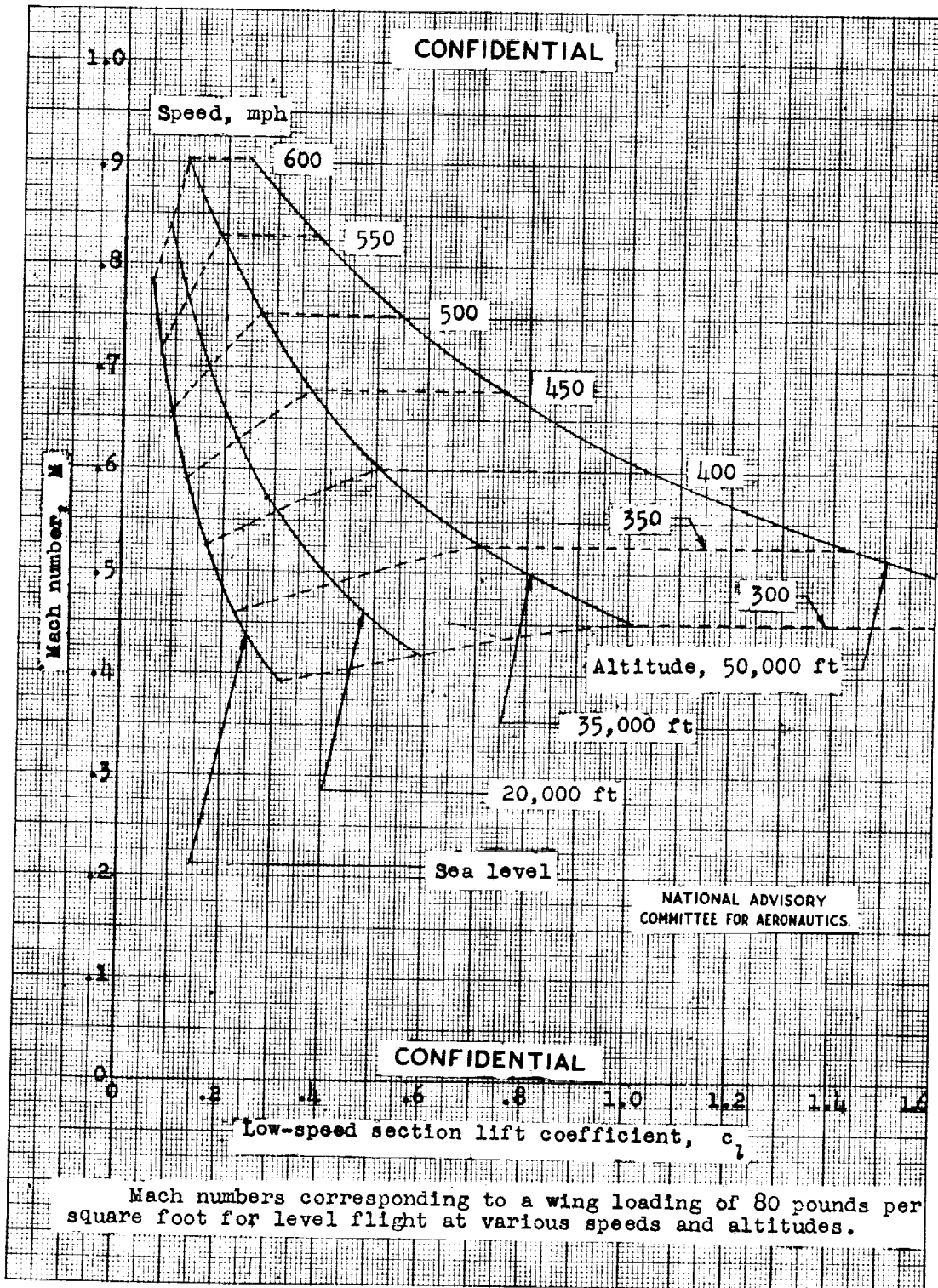




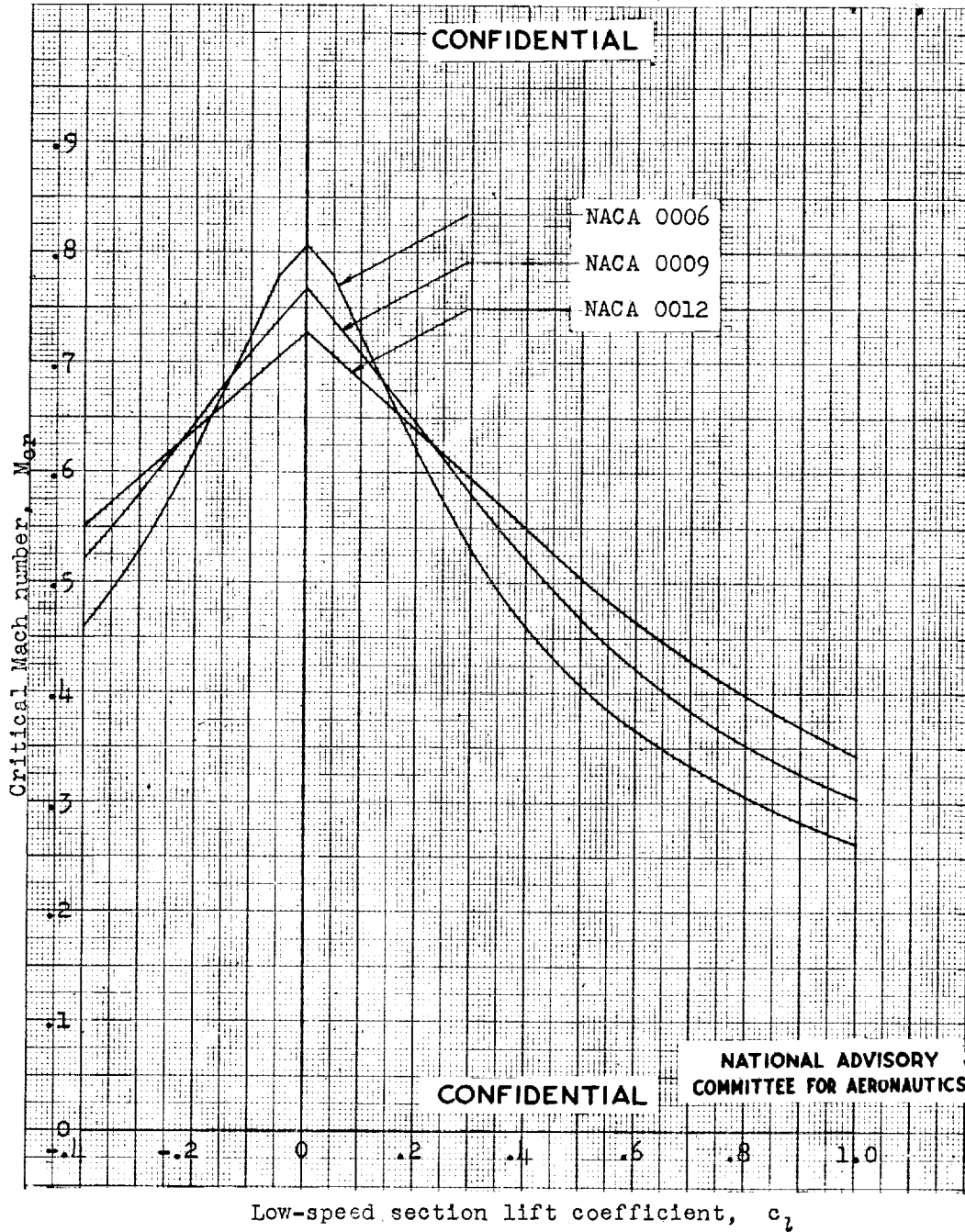




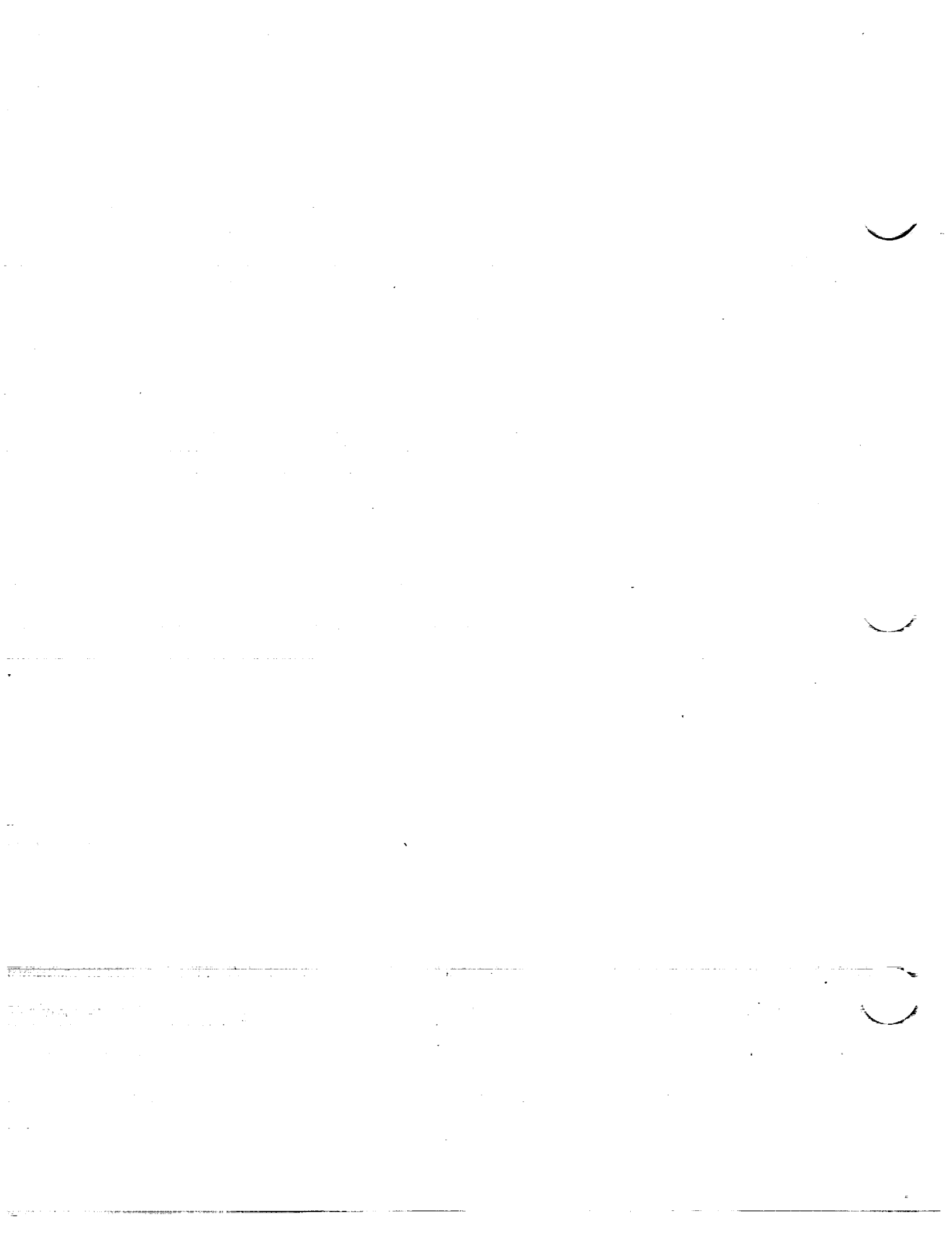


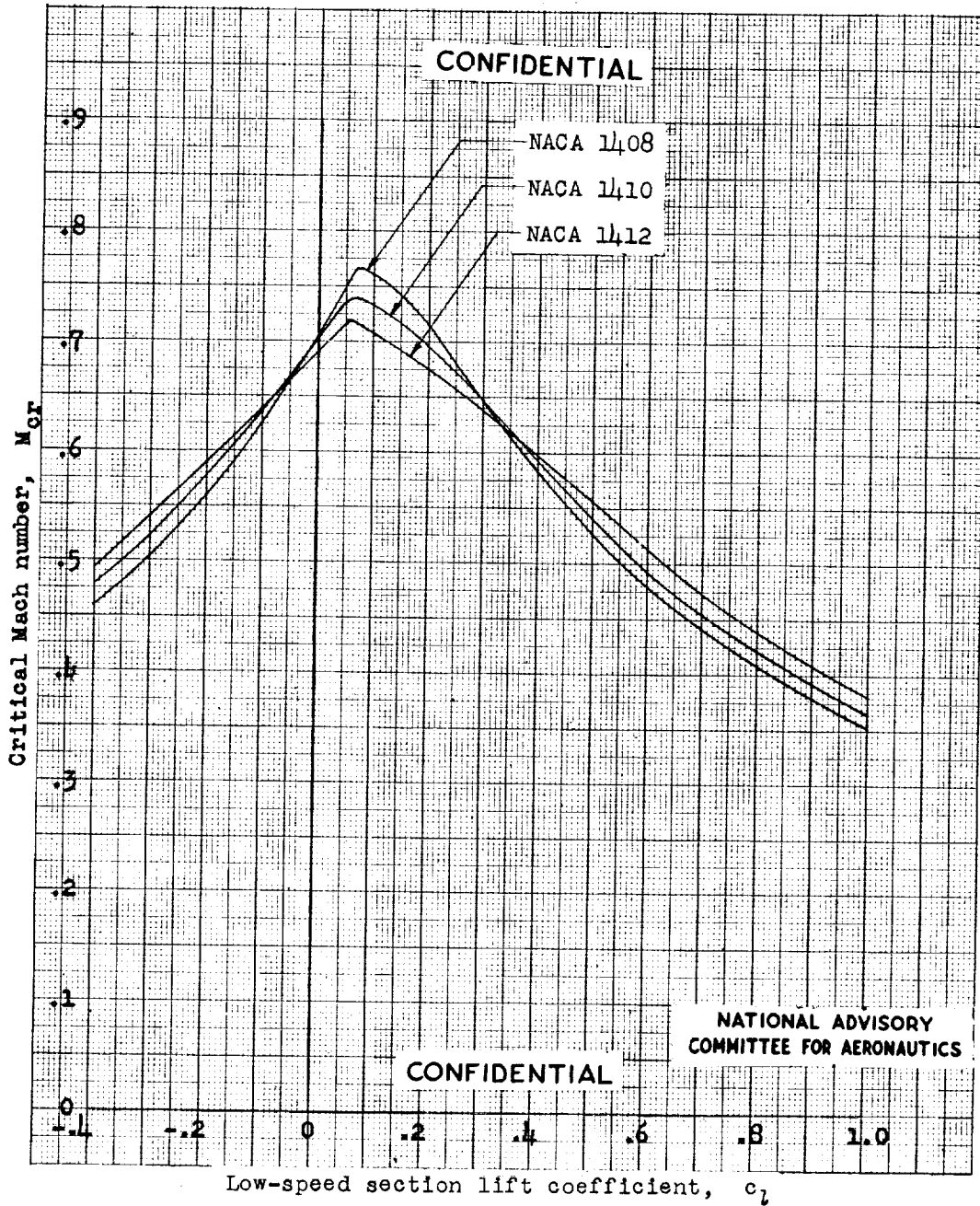






Variation of critical Mach number with low-speed section lift coefficient for the NACA 0006, 0009, and 0012 airfoil sections.





Variation of critical Mach number with low-speed section lift coefficient for several NACA 14-series airfoil sections of various thicknesses.

100

100

100

100

100

100

100

100

100

100

100

100

100

100

100

100

100

100

100

100

100

100

100

100

100

100

100

100

100

100

100

100

100

100

100

100

100

100

100

100

100

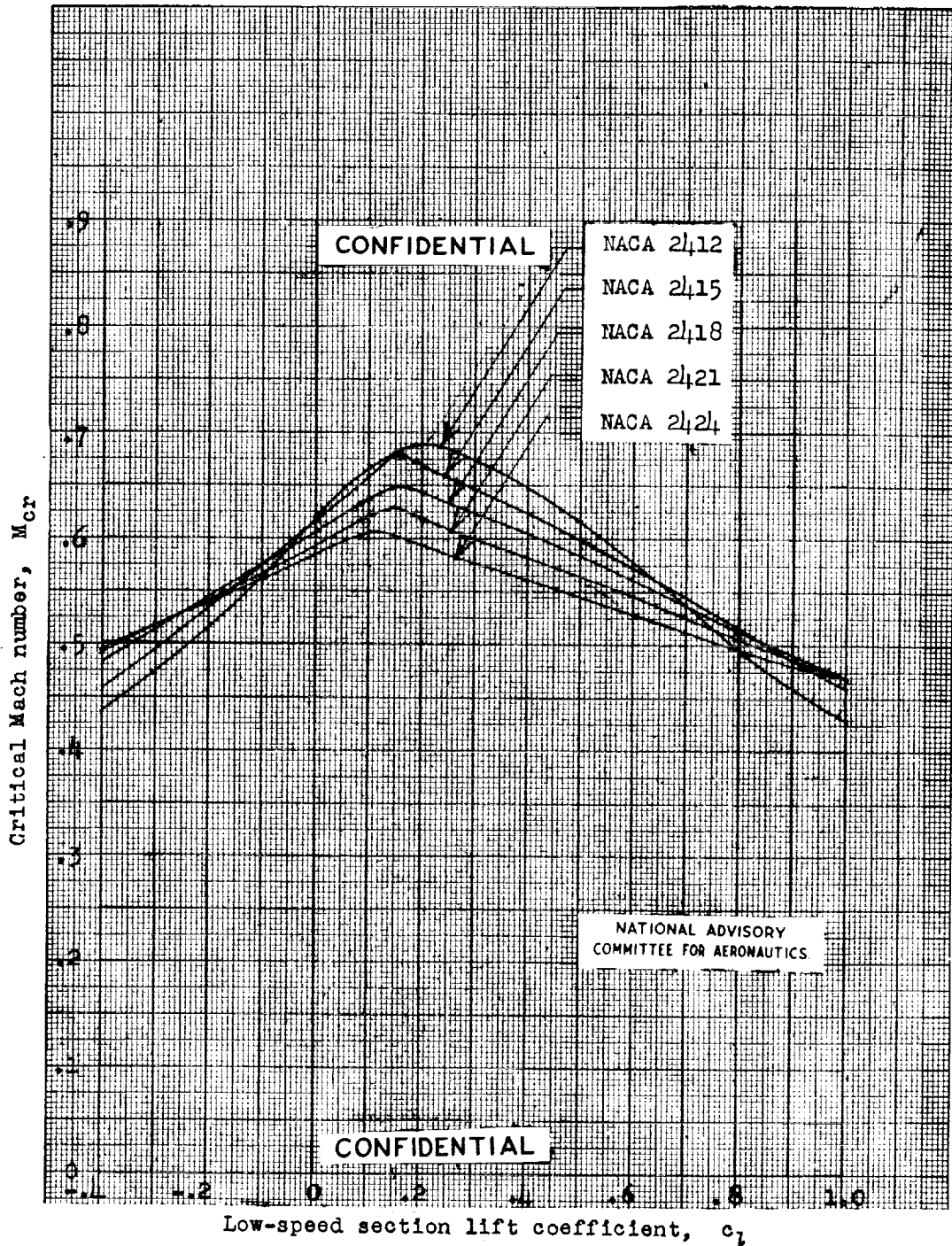
100

100

100

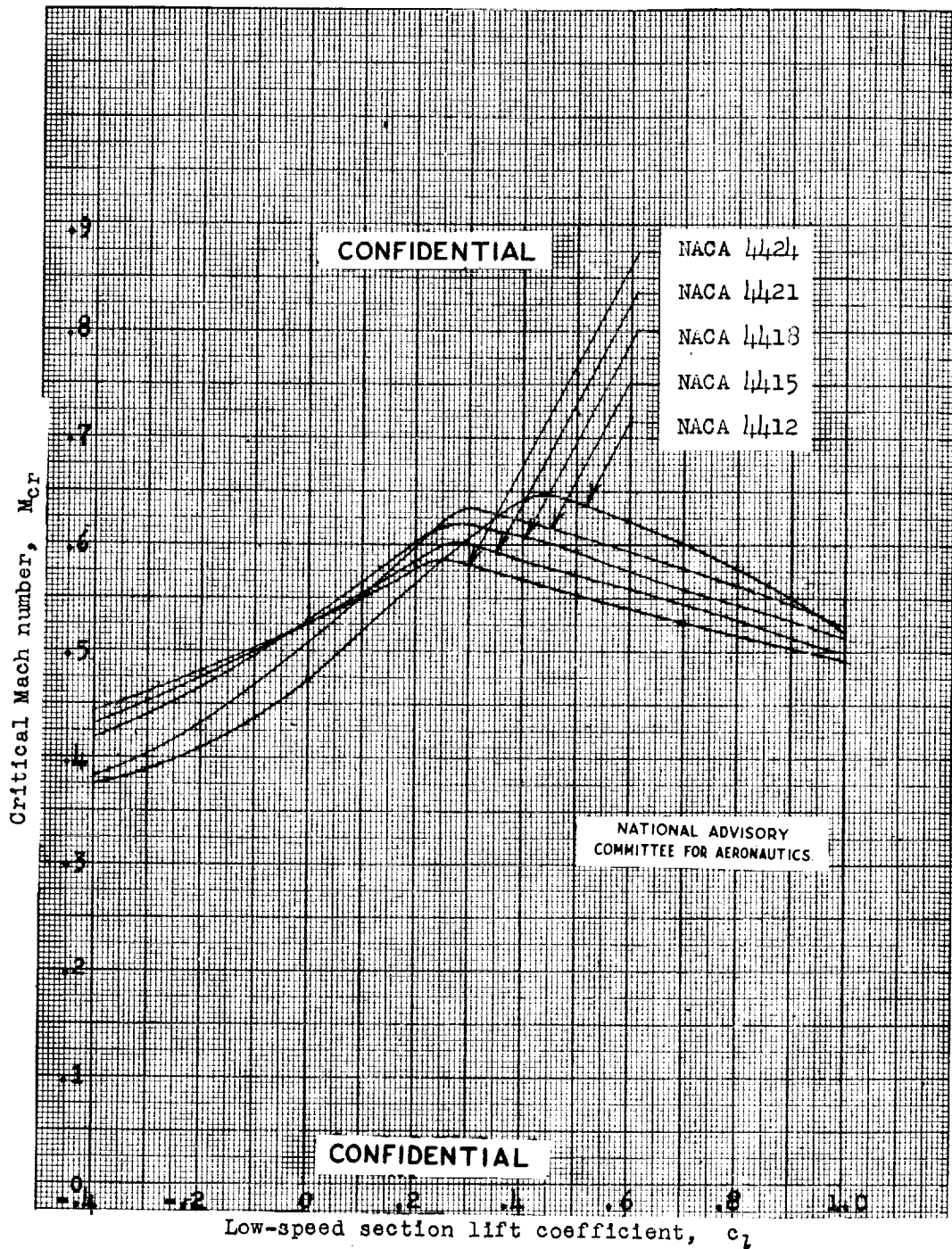
100





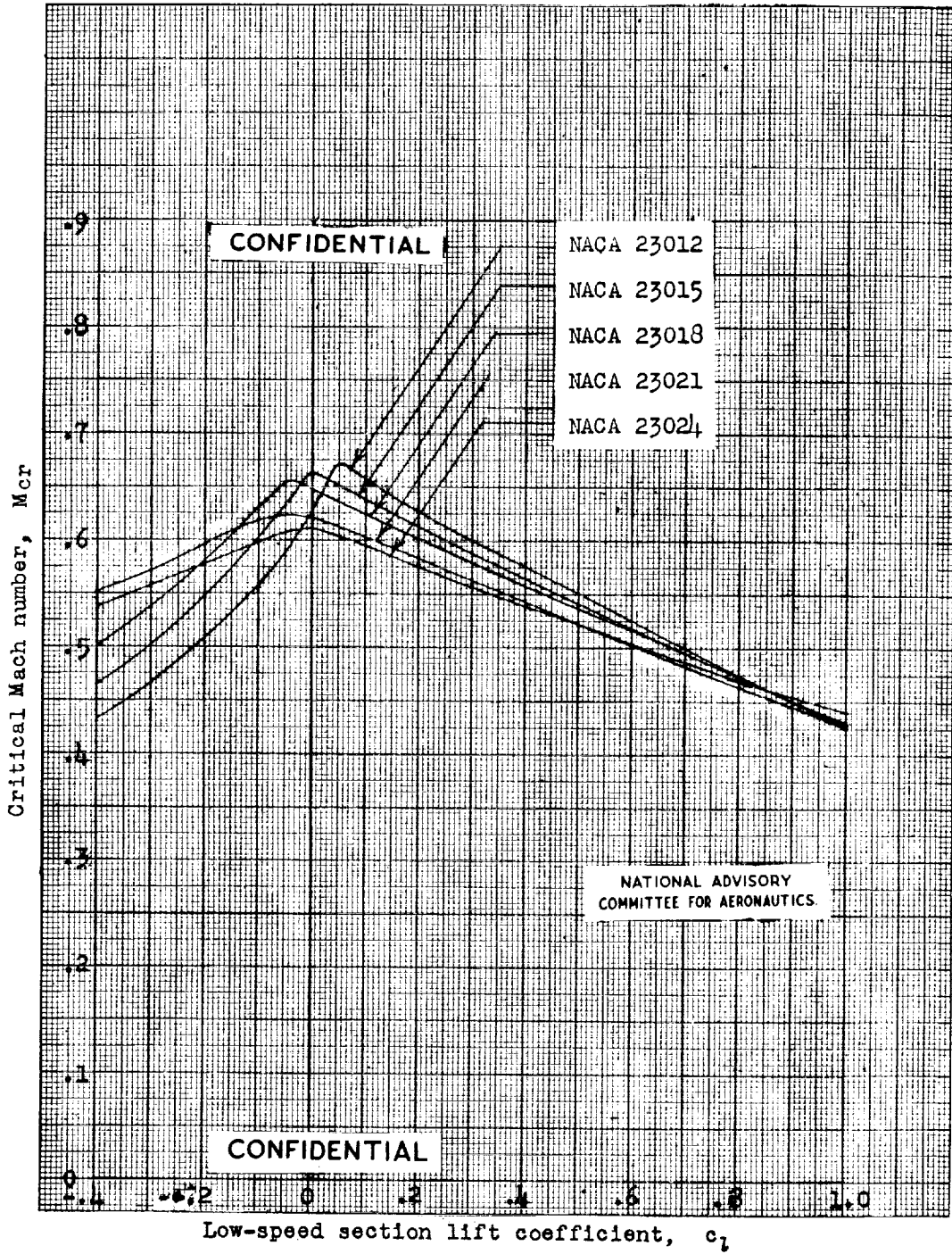
Variation of critical Mach number with low-speed section lift coefficient for several NACA 24-series airfoil sections of various thicknesses.





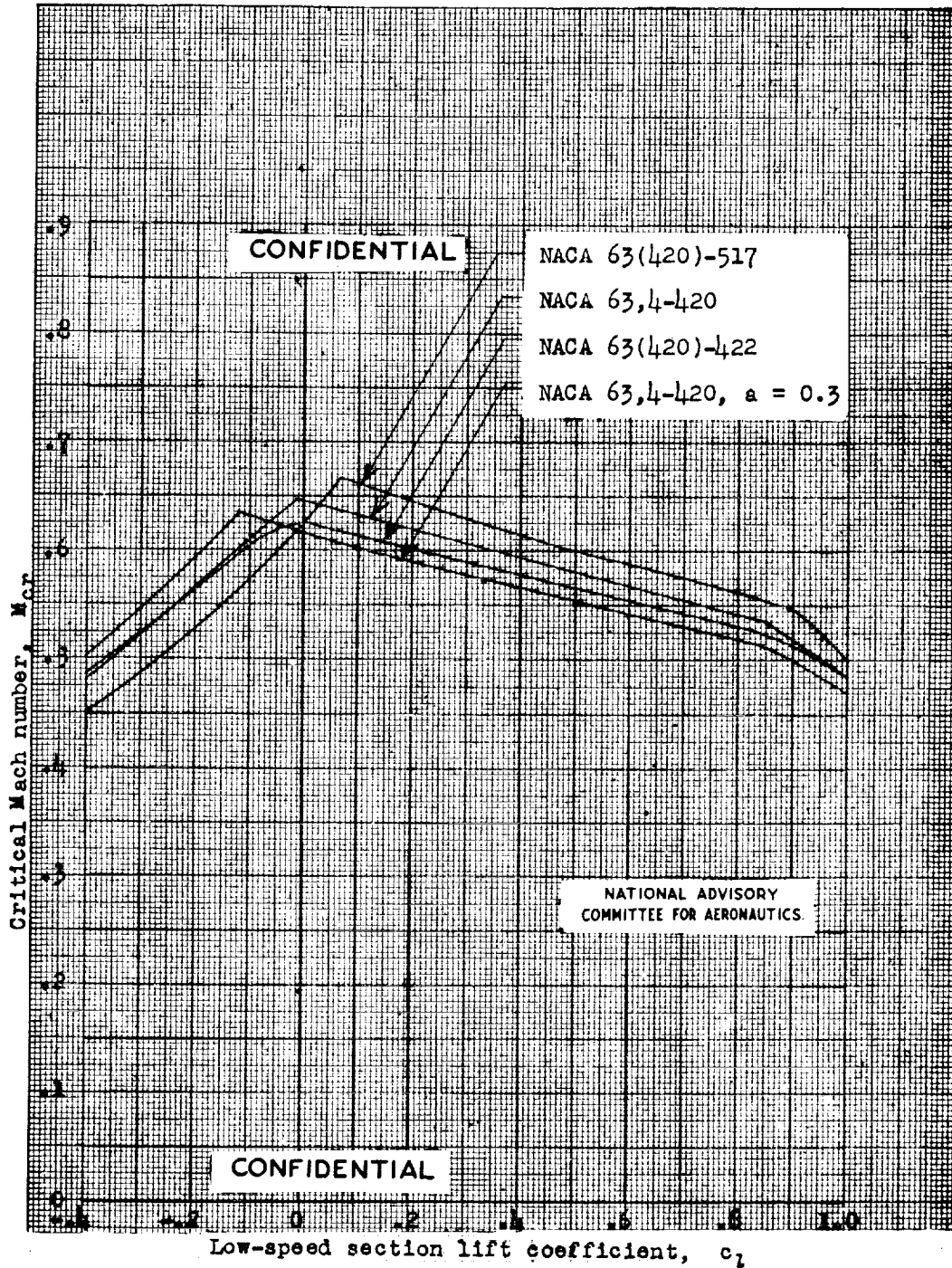
Variation of critical Mach number with low-speed section lift coefficient for several NACA 44-series airfoil sections of various thicknesses.



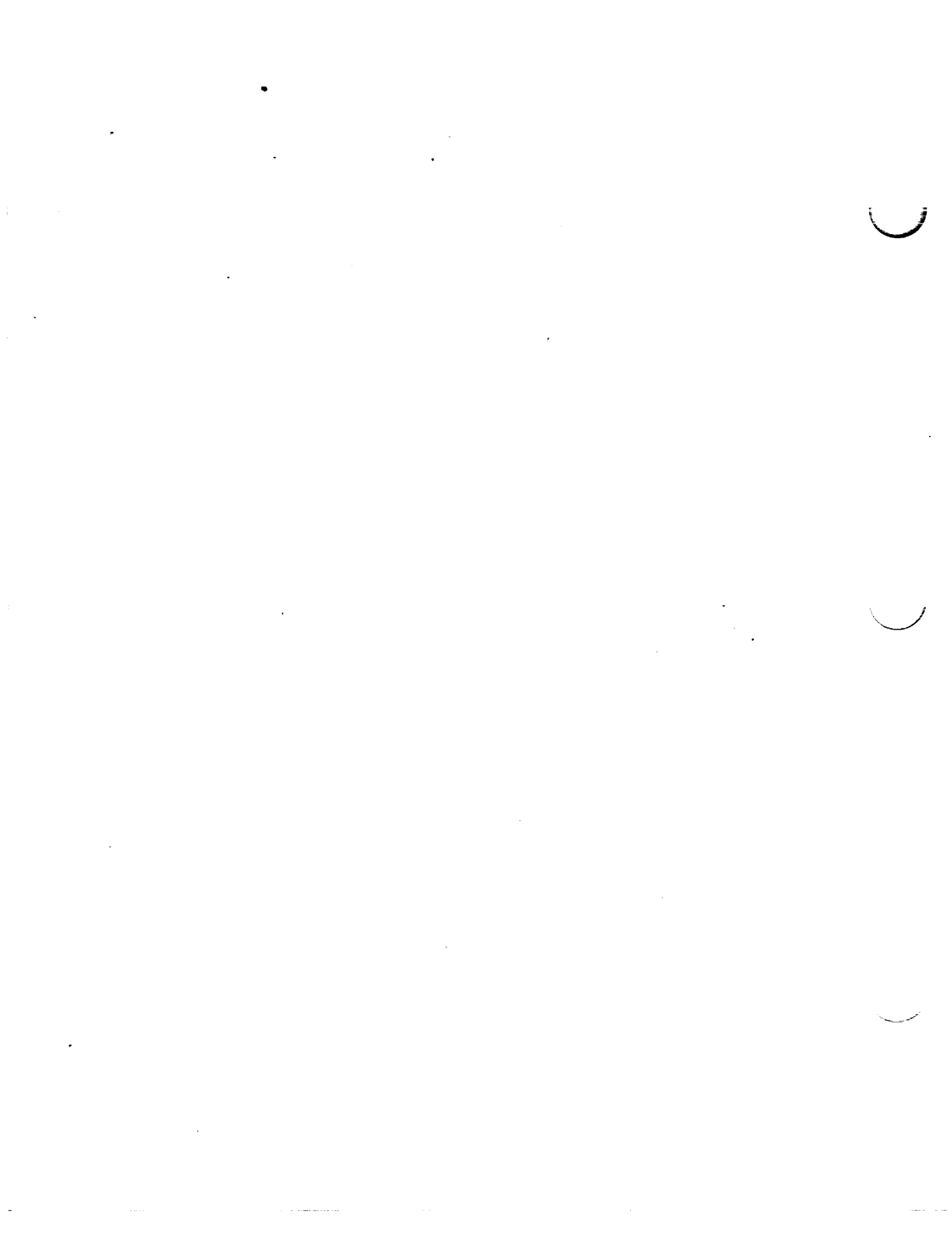


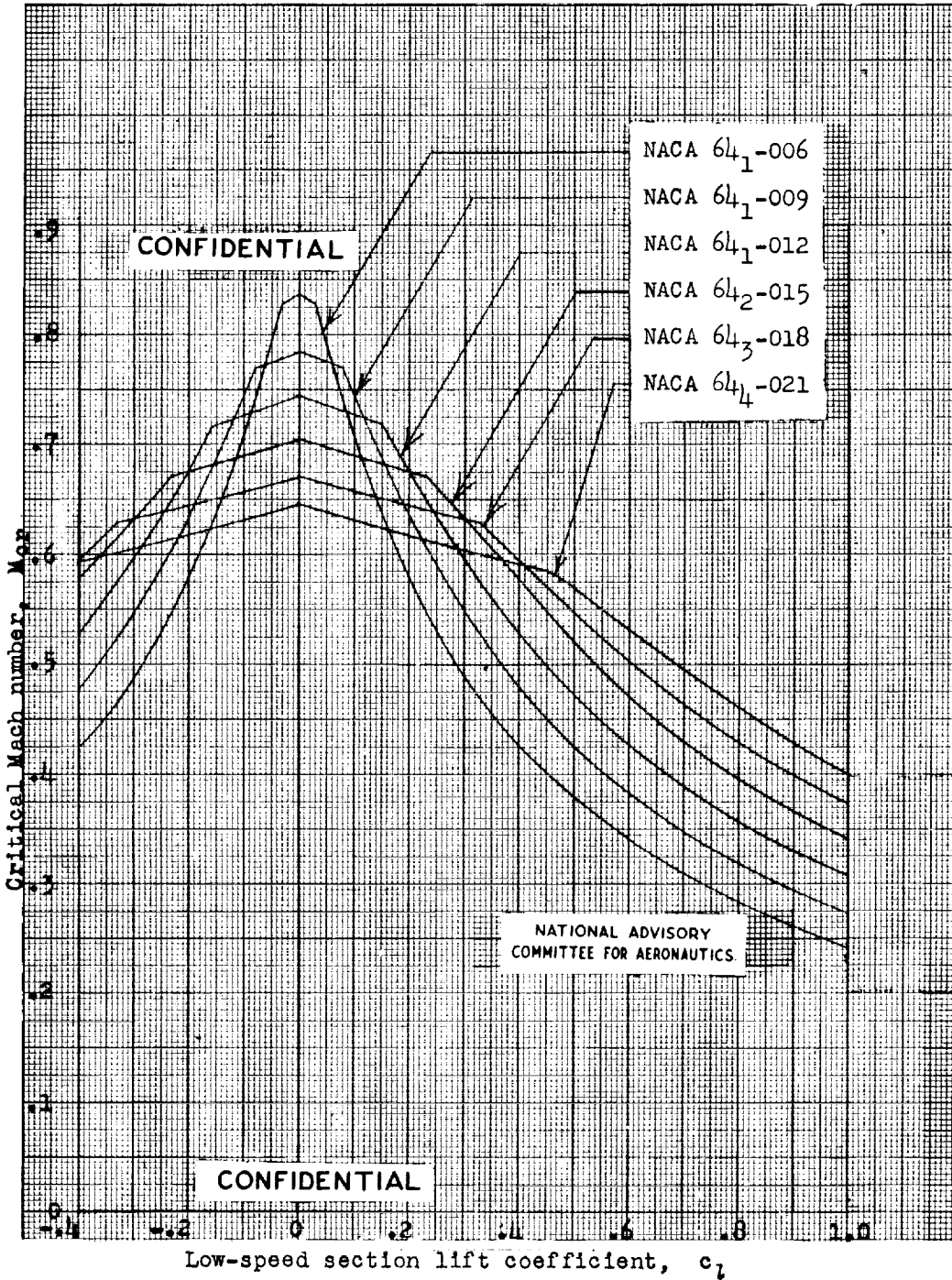
Variation of critical Mach number with low-speed section lift coefficient for several NACA 230-series airfoil sections of various thicknesses.





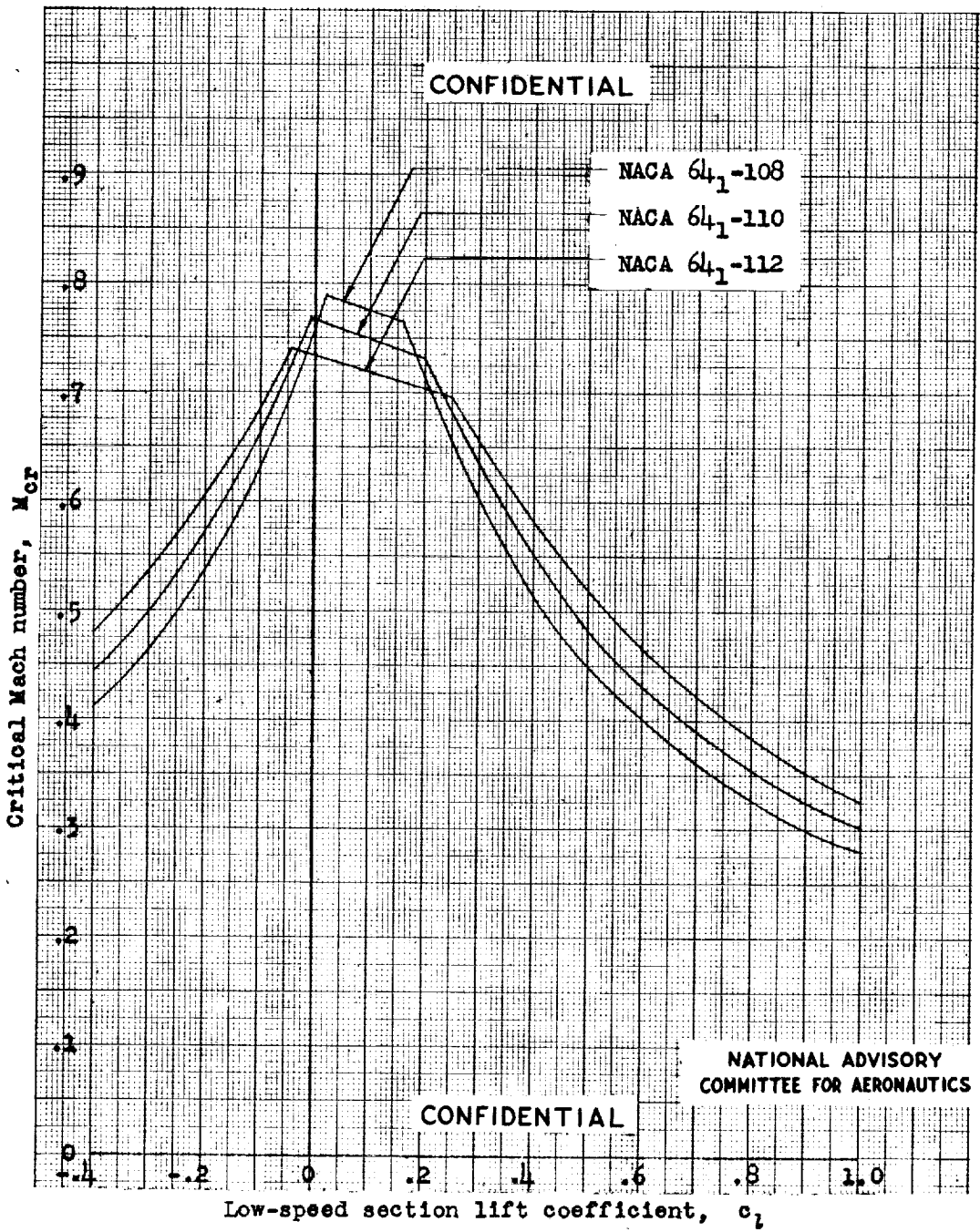
Variation of critical Mach number with low-speed section lift coefficient for several NACA 63-series airfoil sections of various thicknesses, cambered for various design lift coefficients.



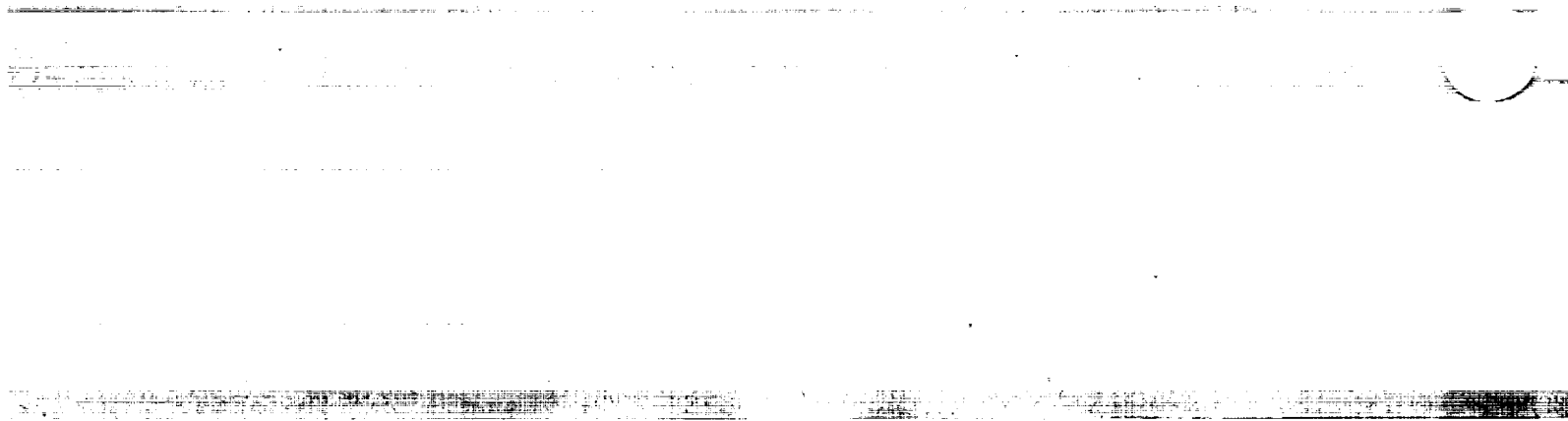


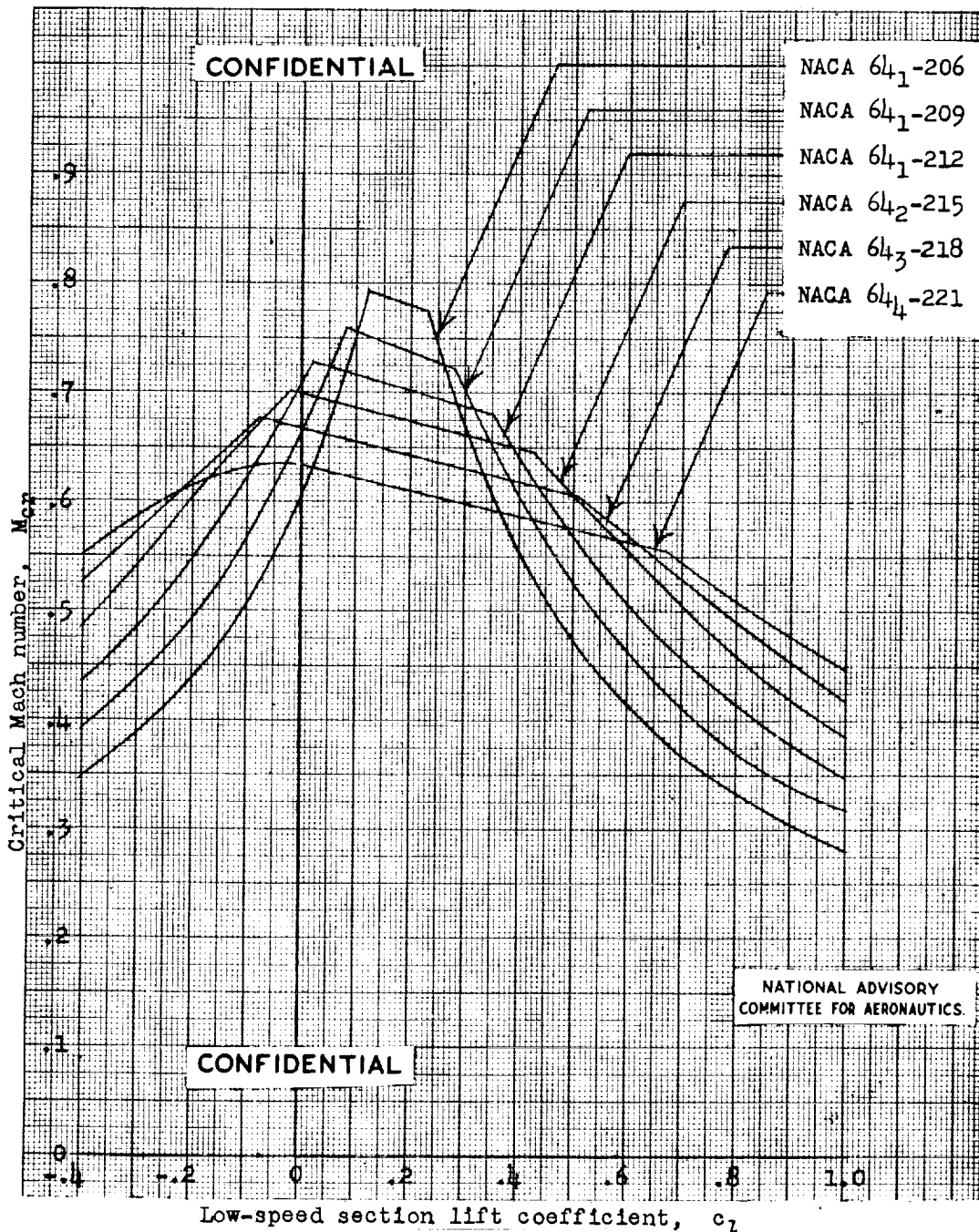
Variation of critical Mach number with low-speed section lift coefficient for several NACA 64-series symmetrical airfoil sections of various thicknesses.





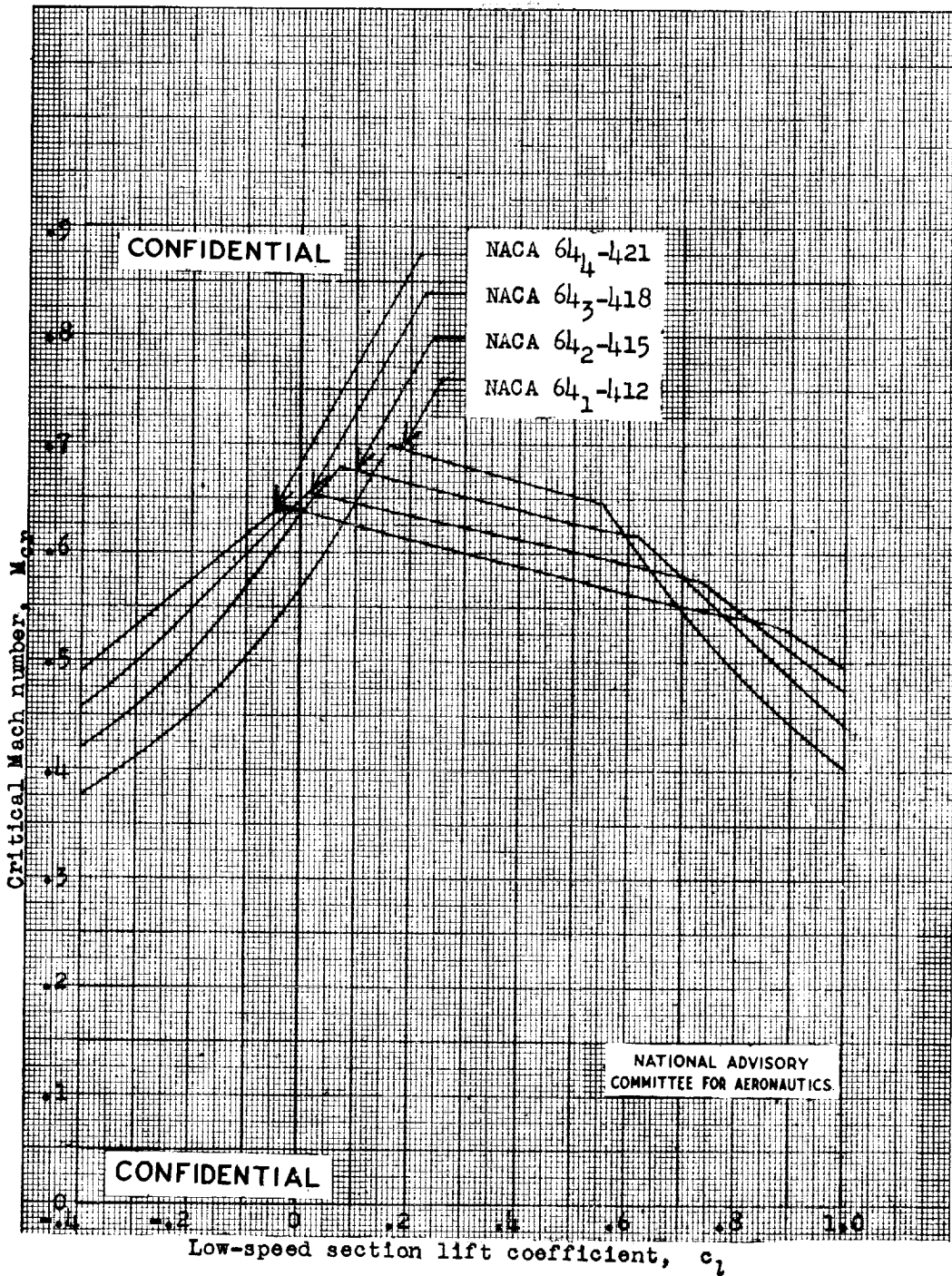
Variation of critical Mach number with low-speed section lift coefficient for several NACA 64-series airfoil sections of various thicknesses, cambered for a design lift coefficient of 0.1.





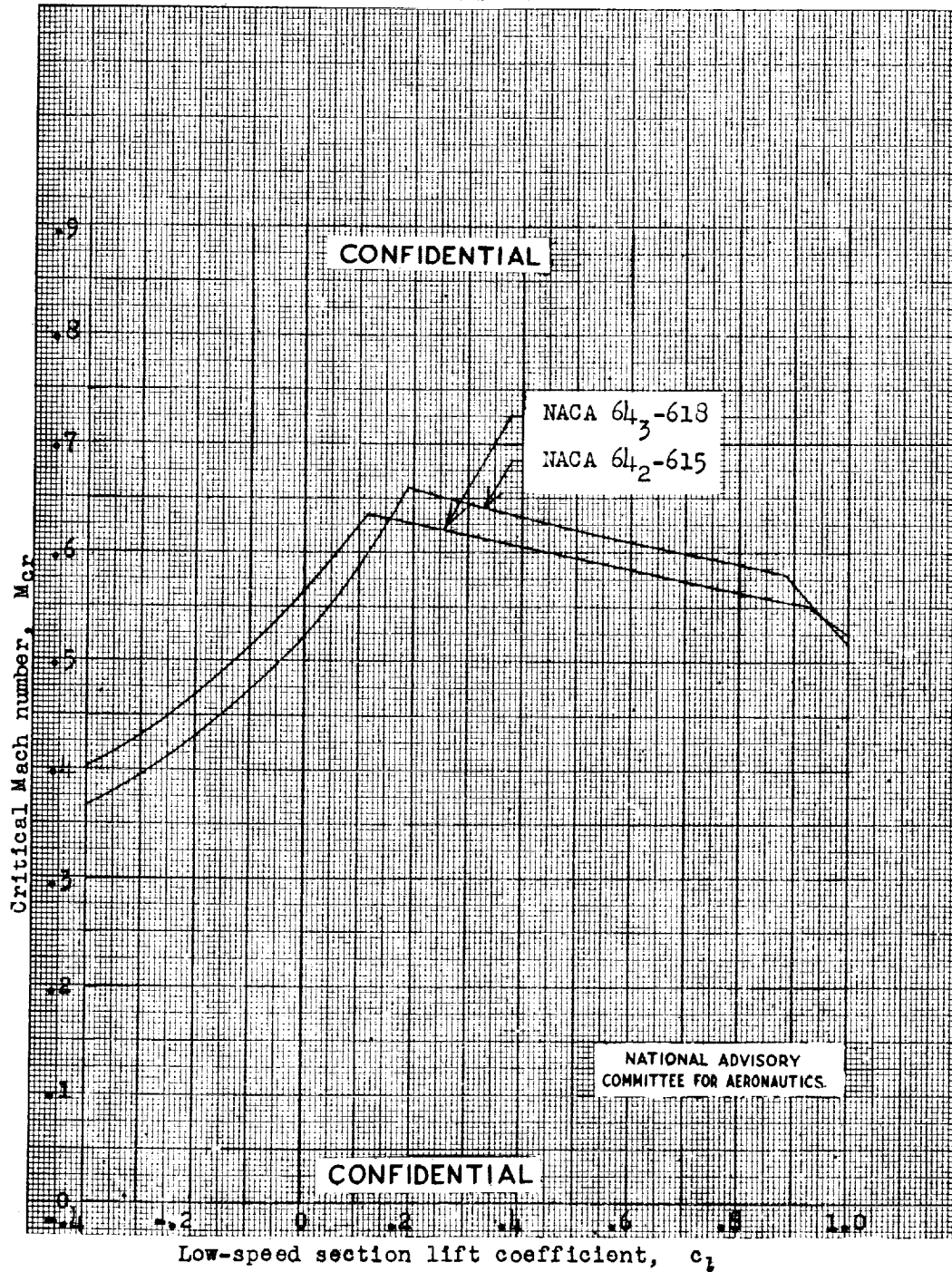
Variation of critical Mach number with low-speed section lift coefficient for several NACA 64-series airfoil sections of various thicknesses, cambered for a design lift coefficient of 0.2.





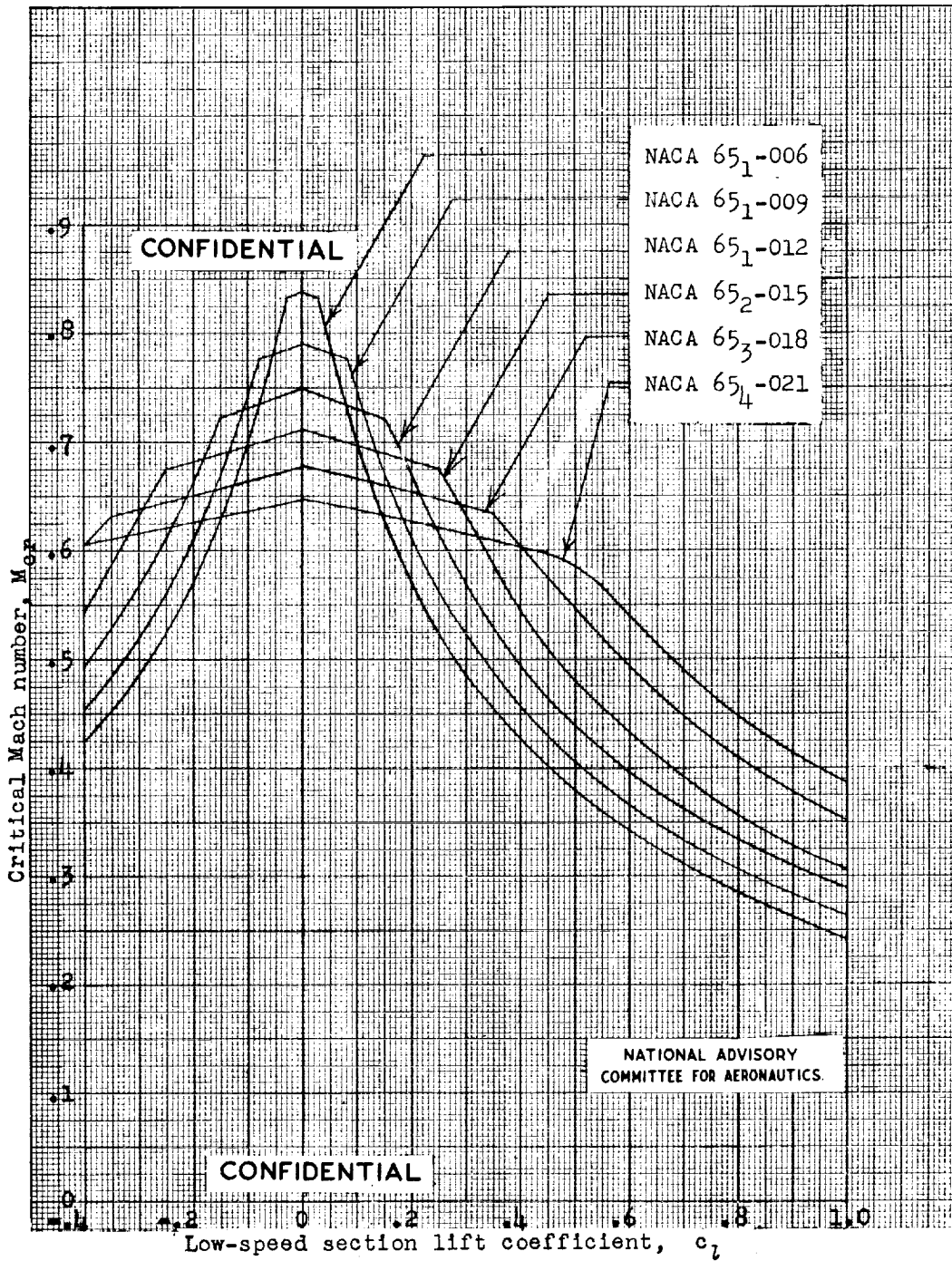
Variation of critical Mach number with low-speed section lift coefficient for several NACA 64-series airfoil sections of various thicknesses, cambered for a design lift coefficient of 0.4.



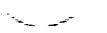


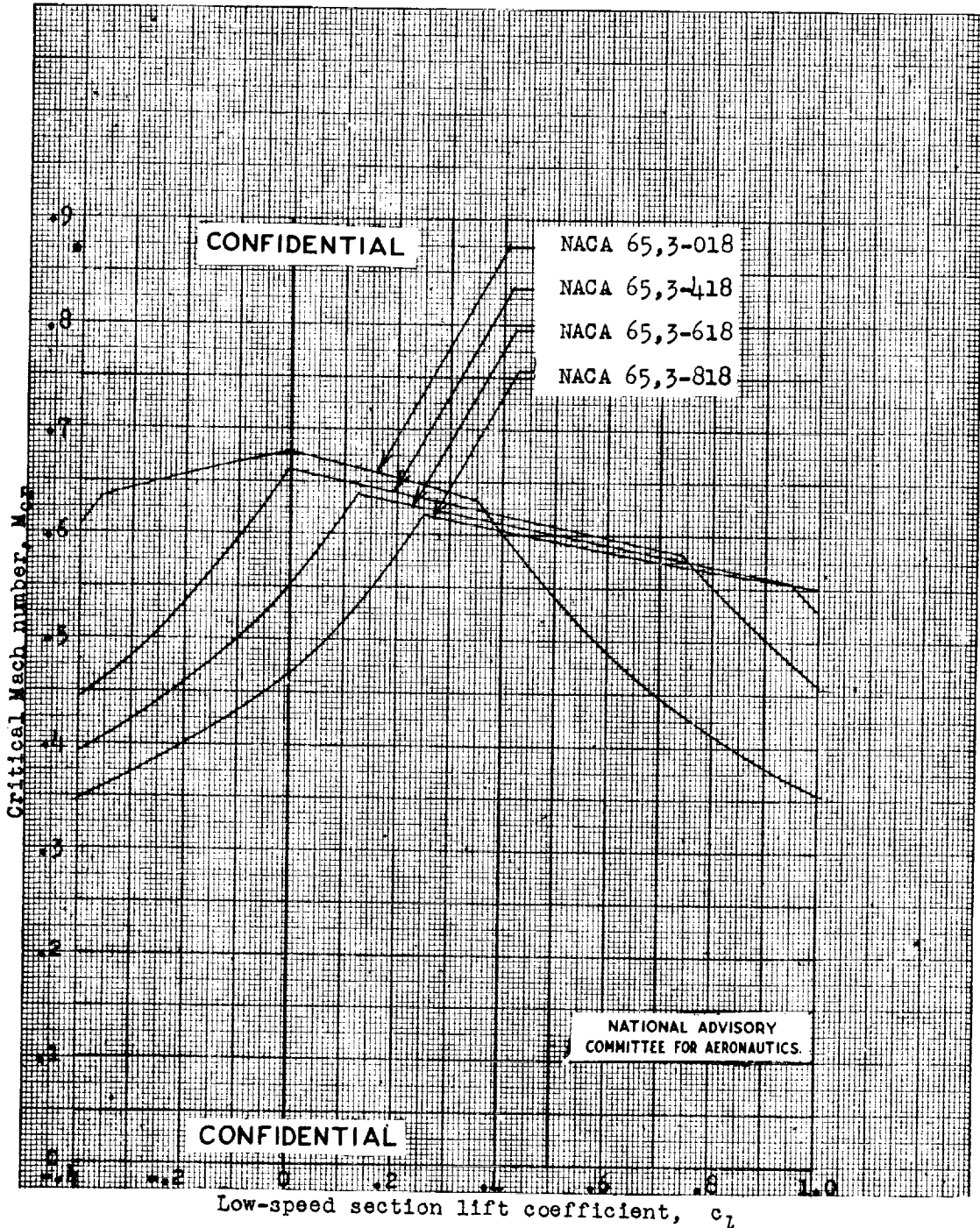
Variation of critical Mach number with low-speed section lift coefficient for two NACA 64-series airfoil sections of different thicknesses, cambered for a design lift coefficient of 0.6.





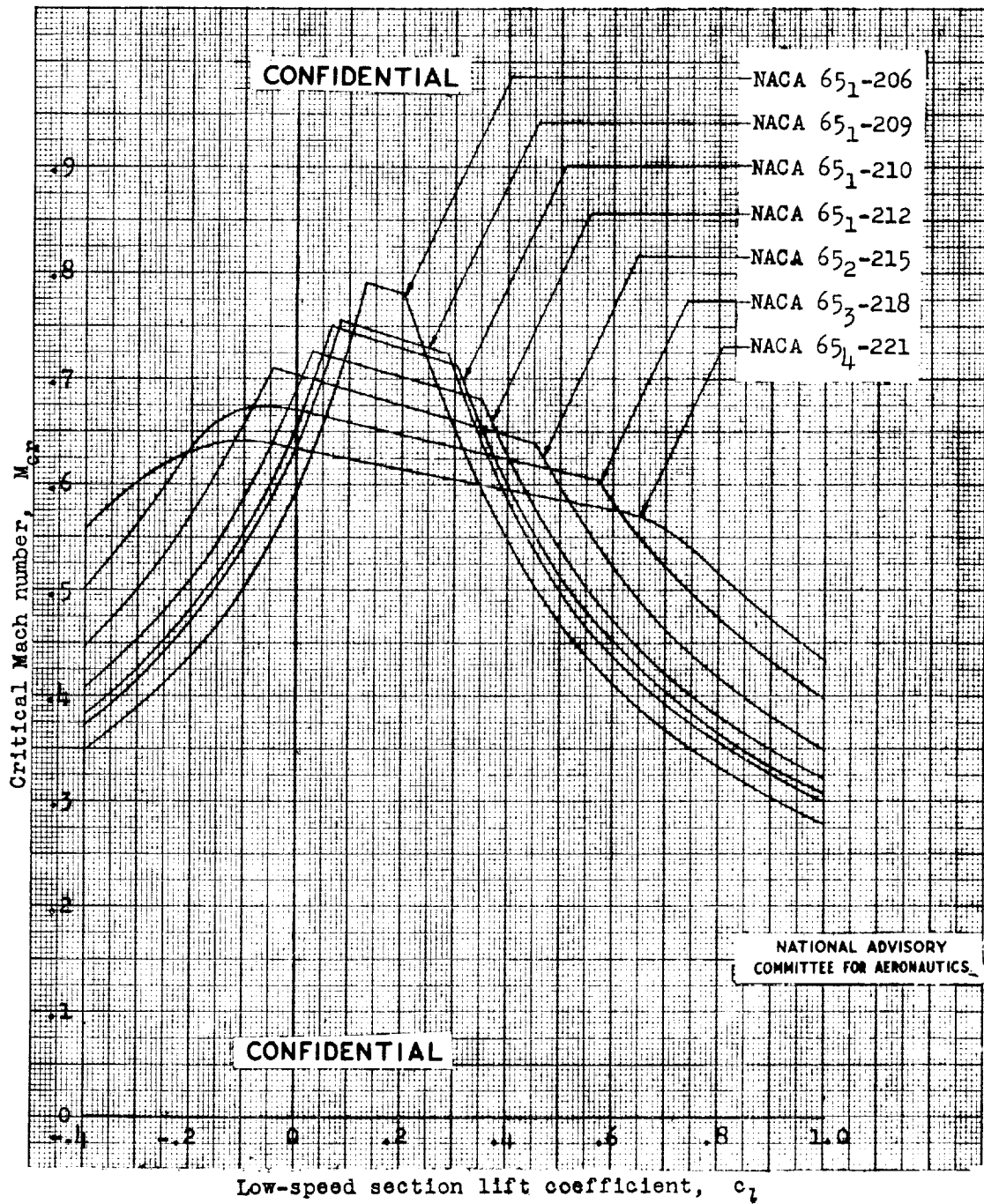
Variation of critical Mach number with low-speed section lift coefficient for several NACA 65-series symmetrical airfoil sections of various thicknesses.





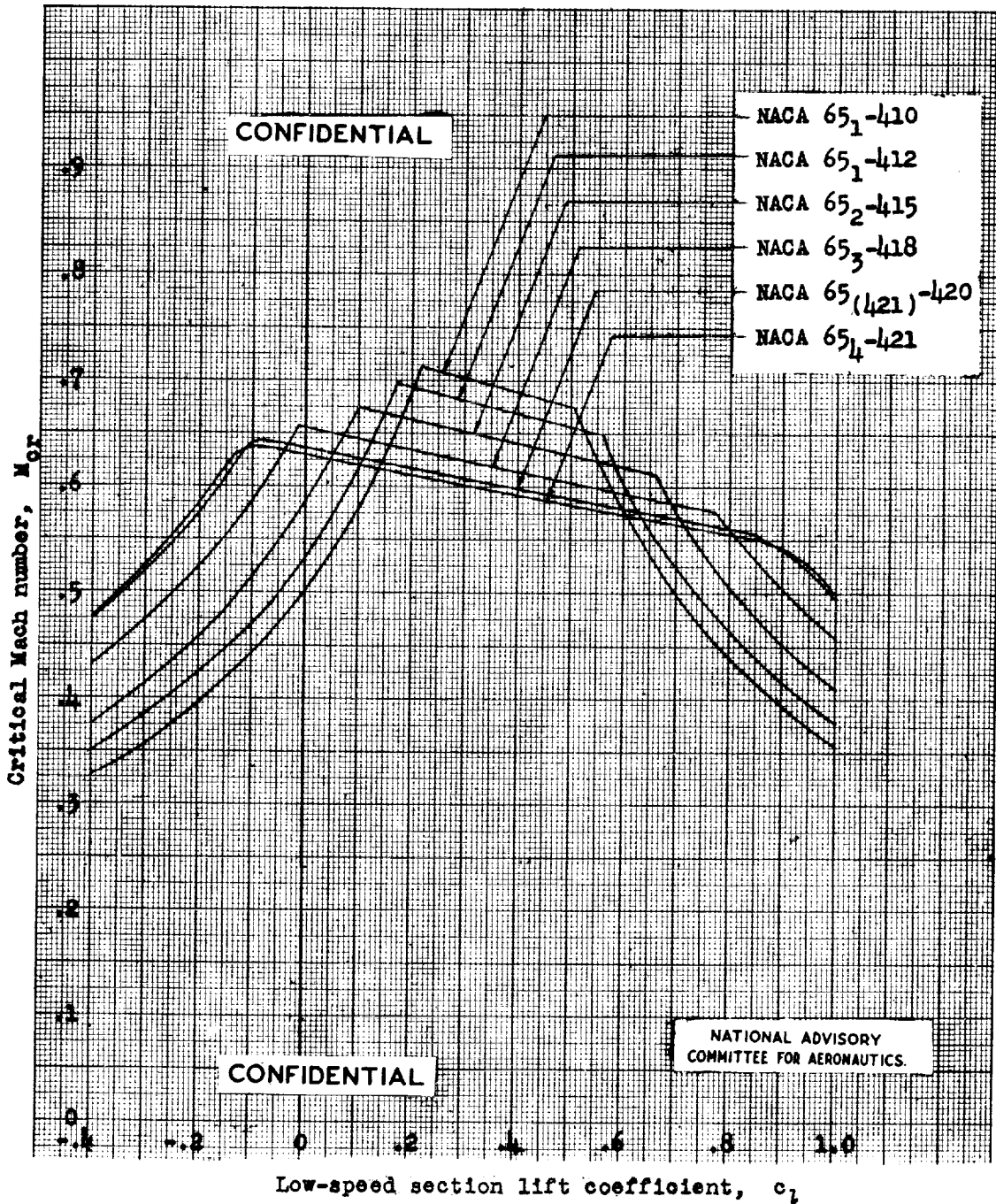
Variation of critical Mach number with low-speed section lift coefficient for several NACA 65-series airfoil sections with a thickness ratio of 0.18 and cambered for various design lift coefficients.



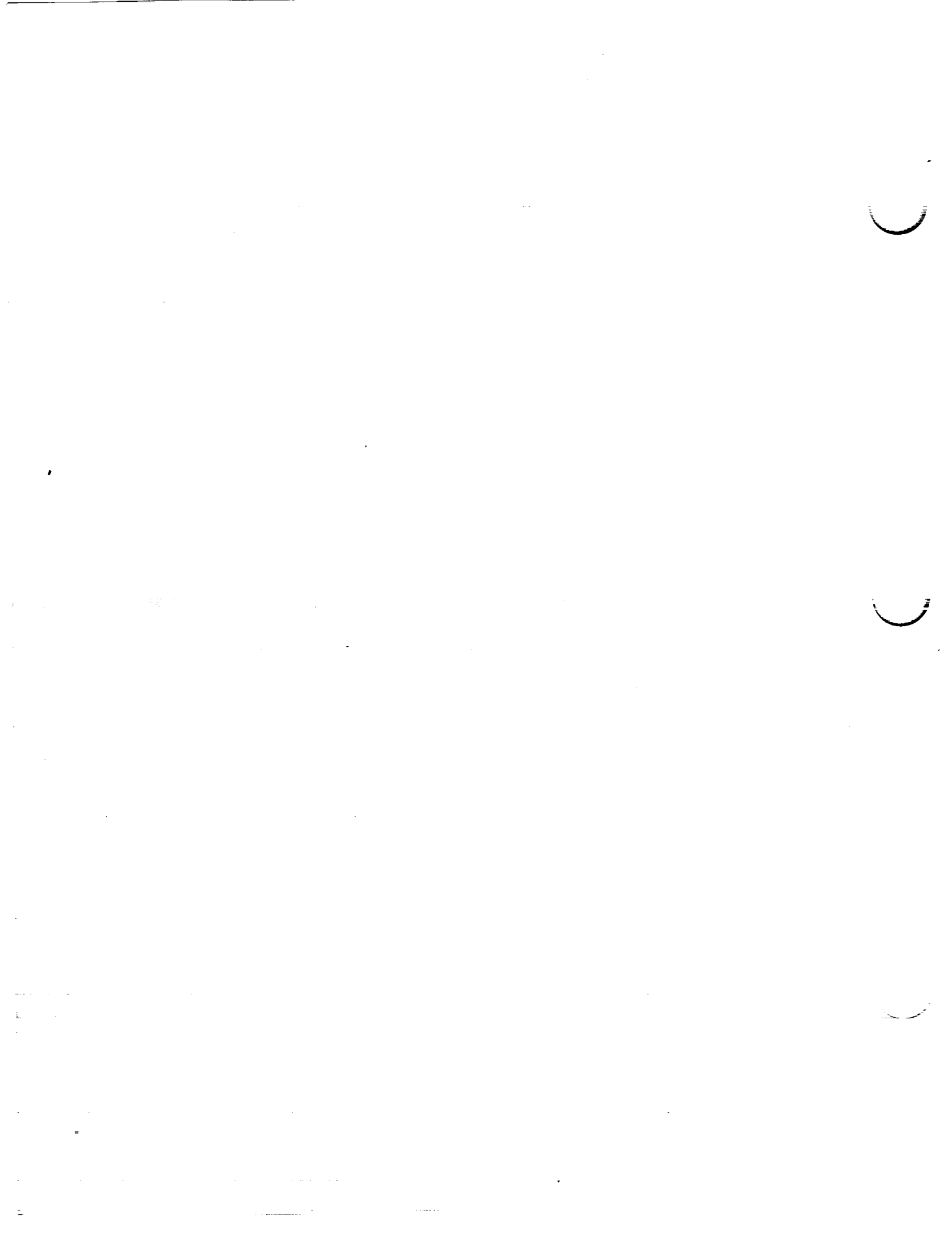


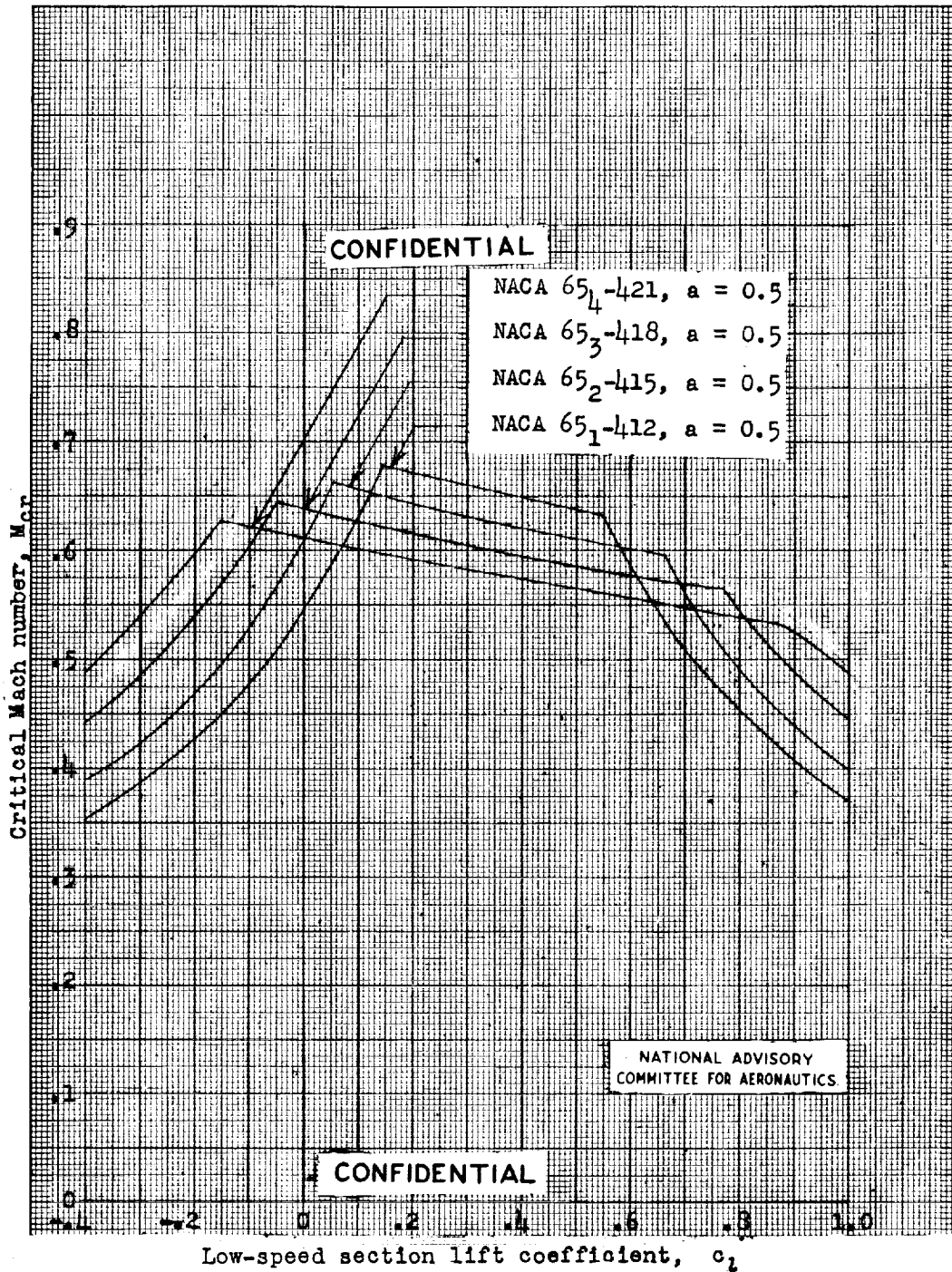
Variation of critical Mach number with low-speed section lift coefficient for several NACA 65-series airfoil sections of various thicknesses, cambered for a design lift coefficient of 0.2.





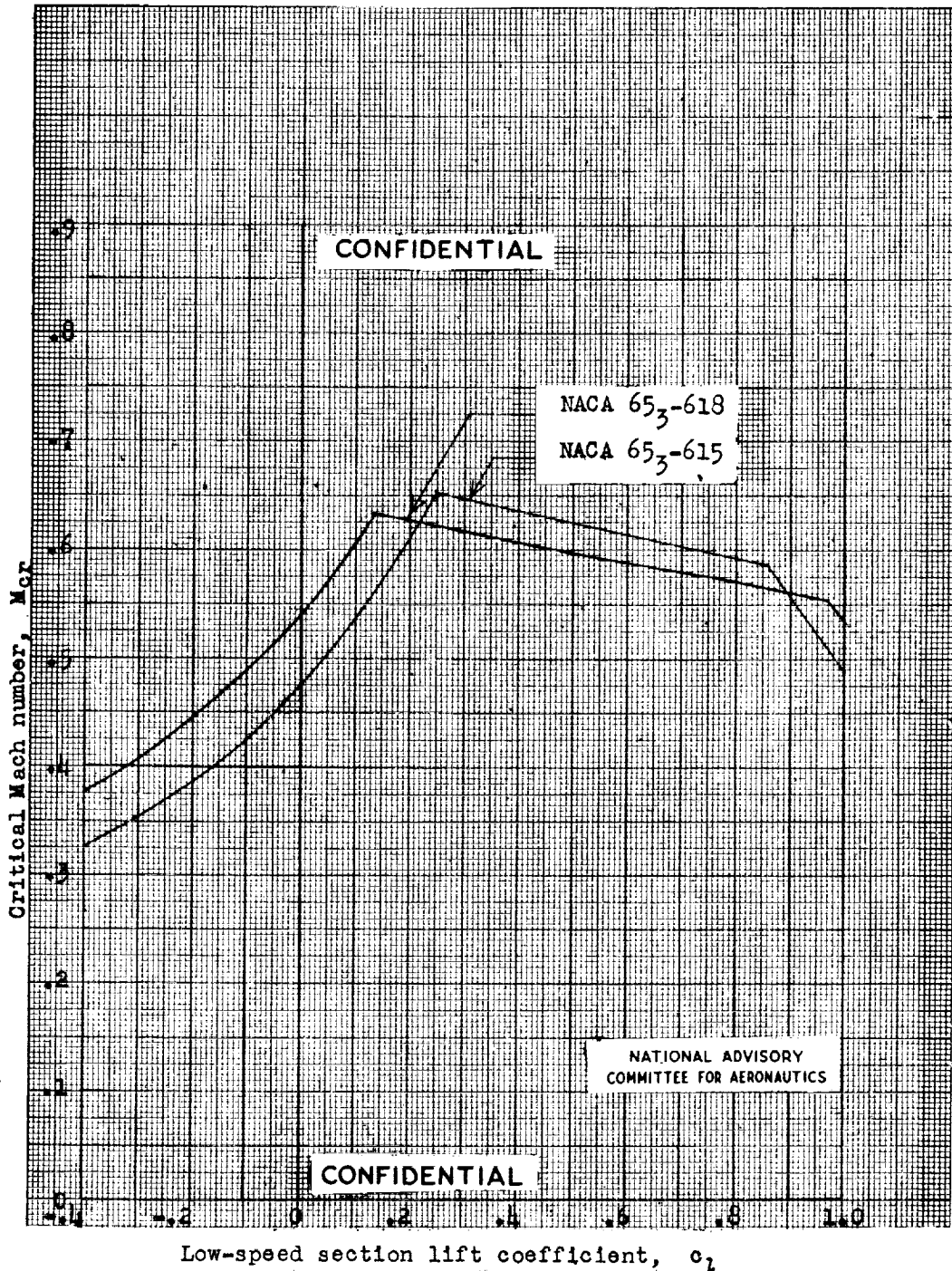
Variation of critical Mach number with low-speed section lift coefficient for several NACA 65-series airfoil sections of various thicknesses, cambered for a design lift coefficient of 0.4.





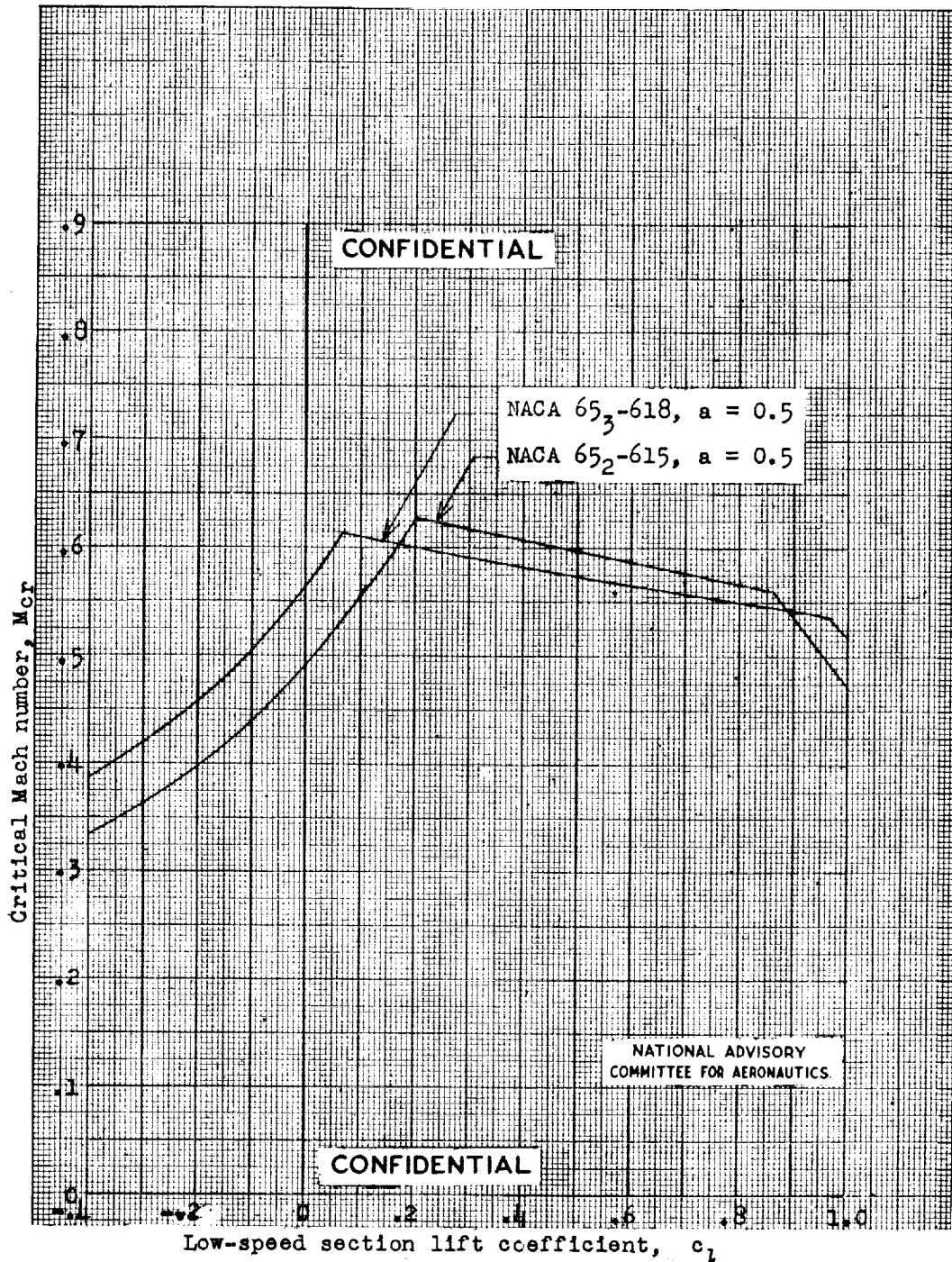
Variation of critical Mach number with low-speed section lift coefficient for several NACA 65-series airfoil sections with mean line of the type $a = 0.5$ and cambered for a design lift coefficient of 0.4.





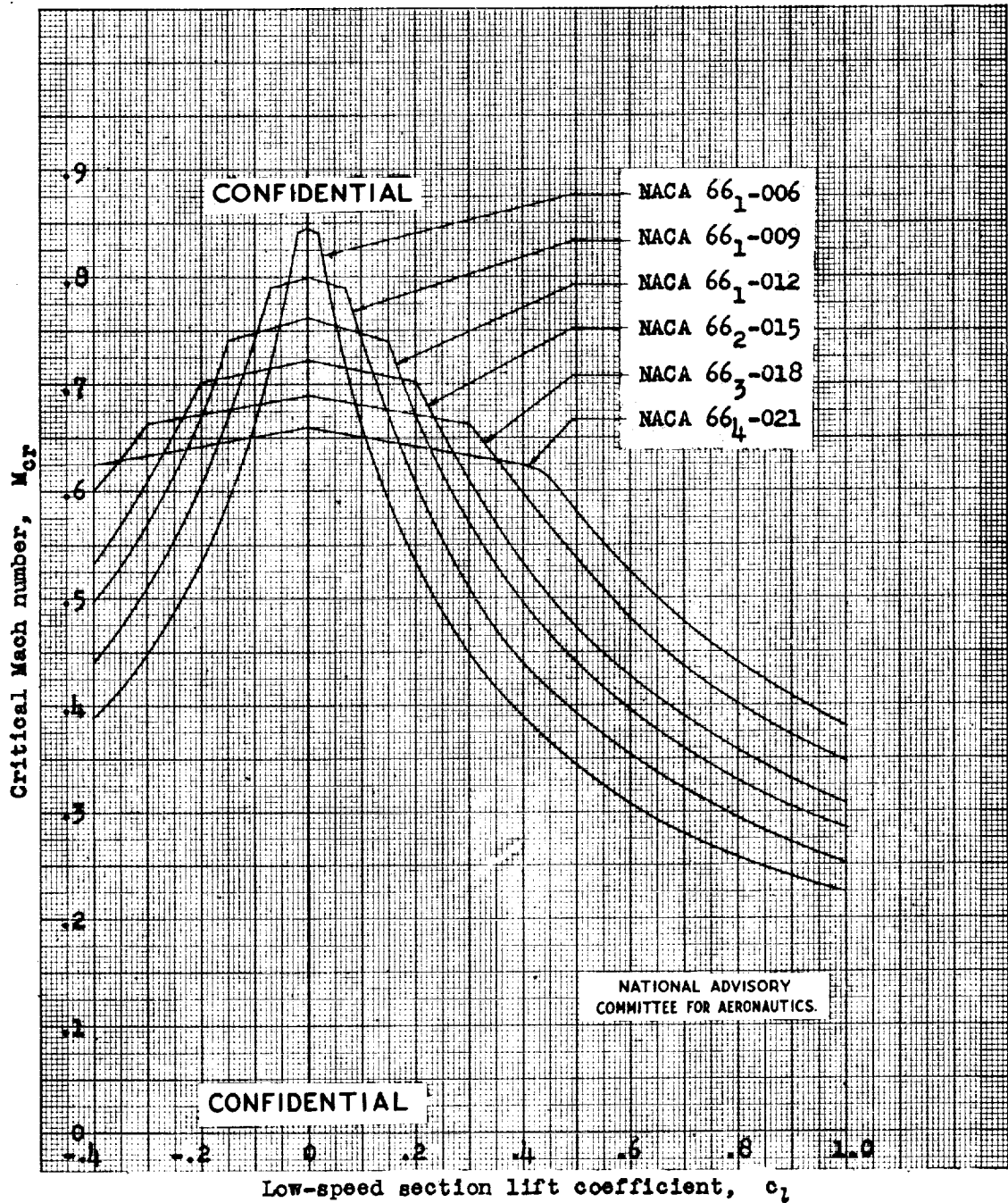
Variation of critical Mach number with low-speed section lift coefficient for two NACA 65-series airfoil sections of different thicknesses, cambered for a design lift coefficient of 0.6.



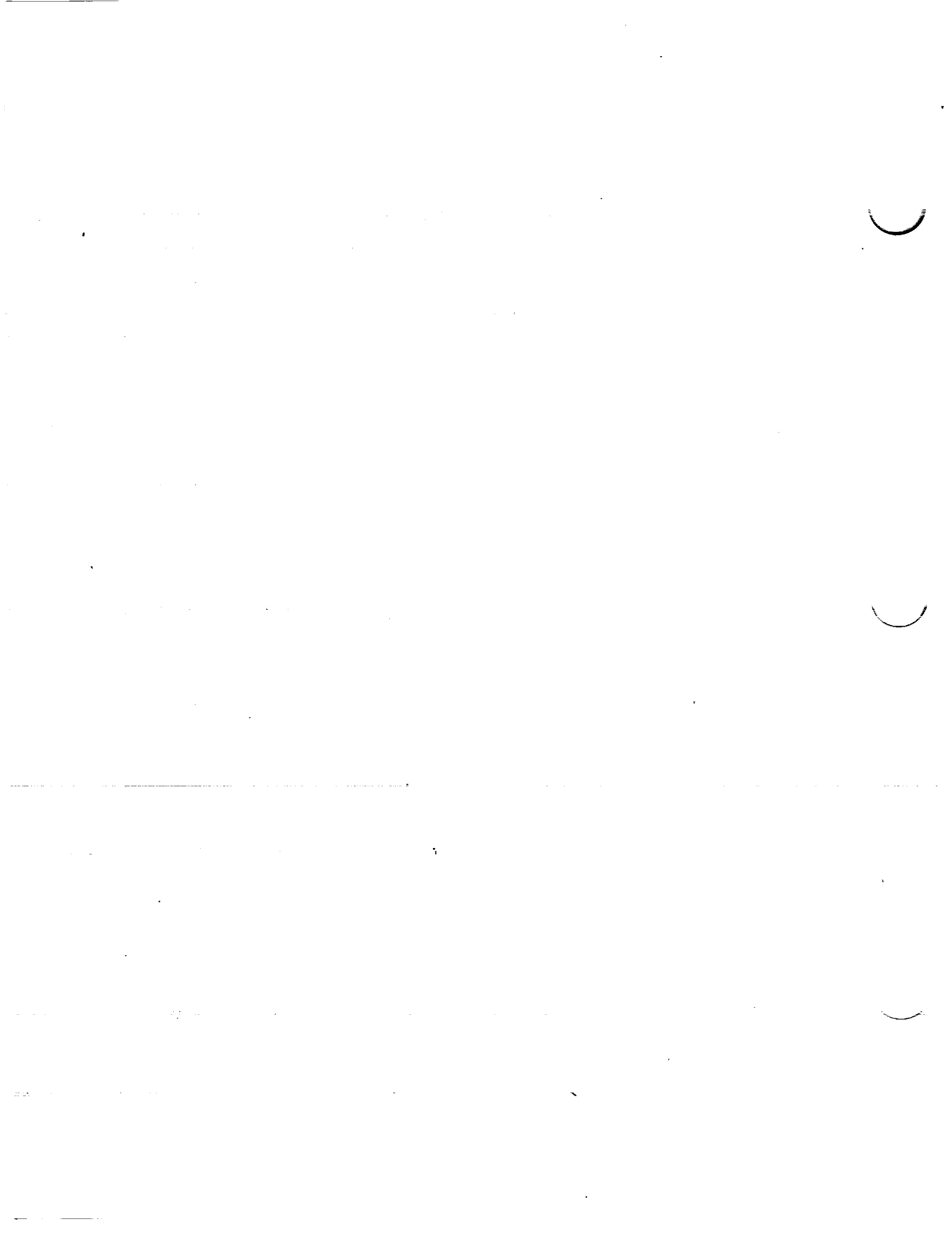


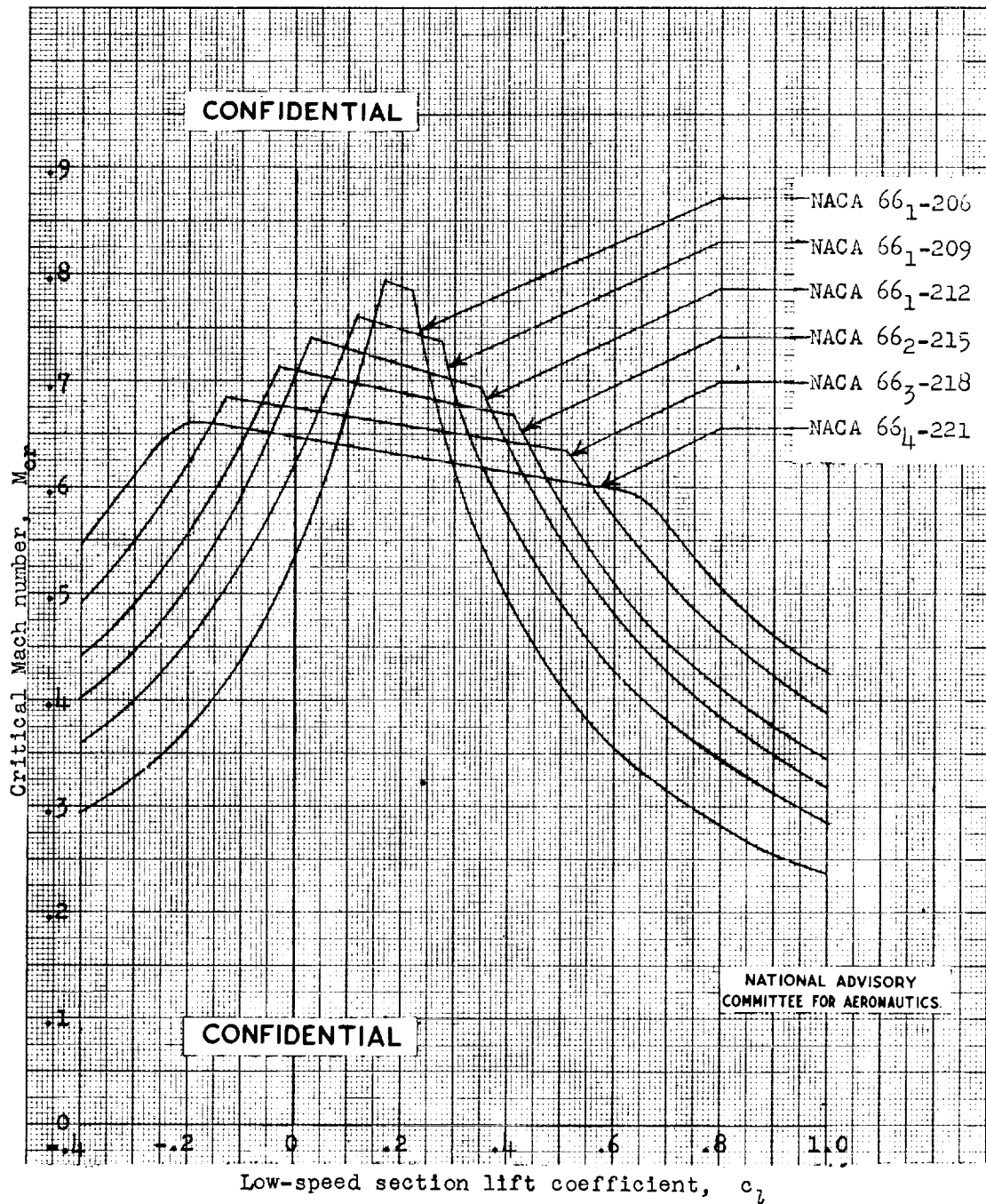
Variation of critical Mach number with low-speed section lift coefficient for two NACA 65-series airfoil sections with mean line of the type $a = 0.5$, with different thicknesses, and cambered for a design lift coefficient of 0.6.





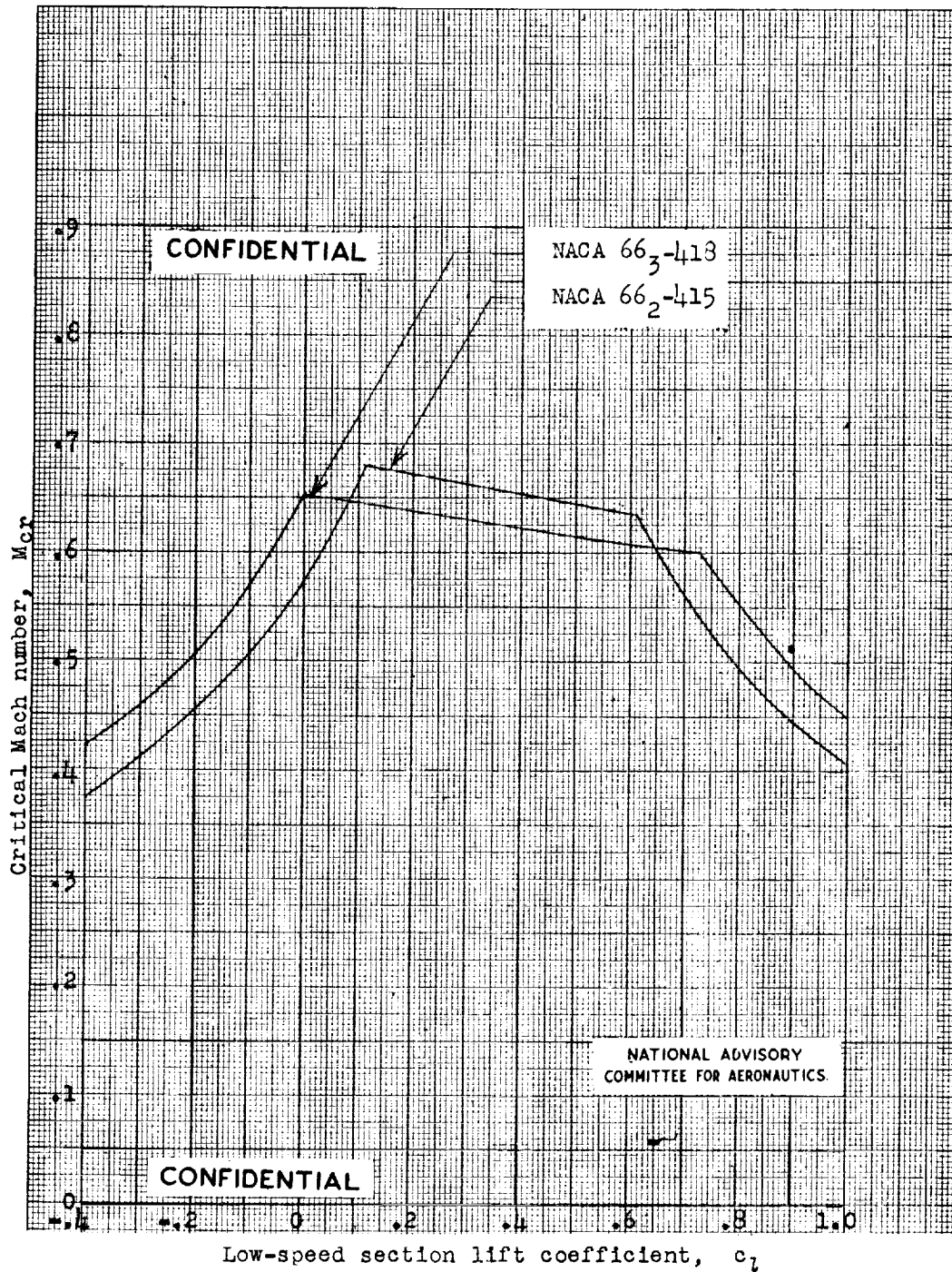
Variation of critical Mach number with low-speed section lift coefficient for several NACA 66-series symmetrical airfoil sections of various thicknesses.



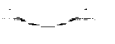


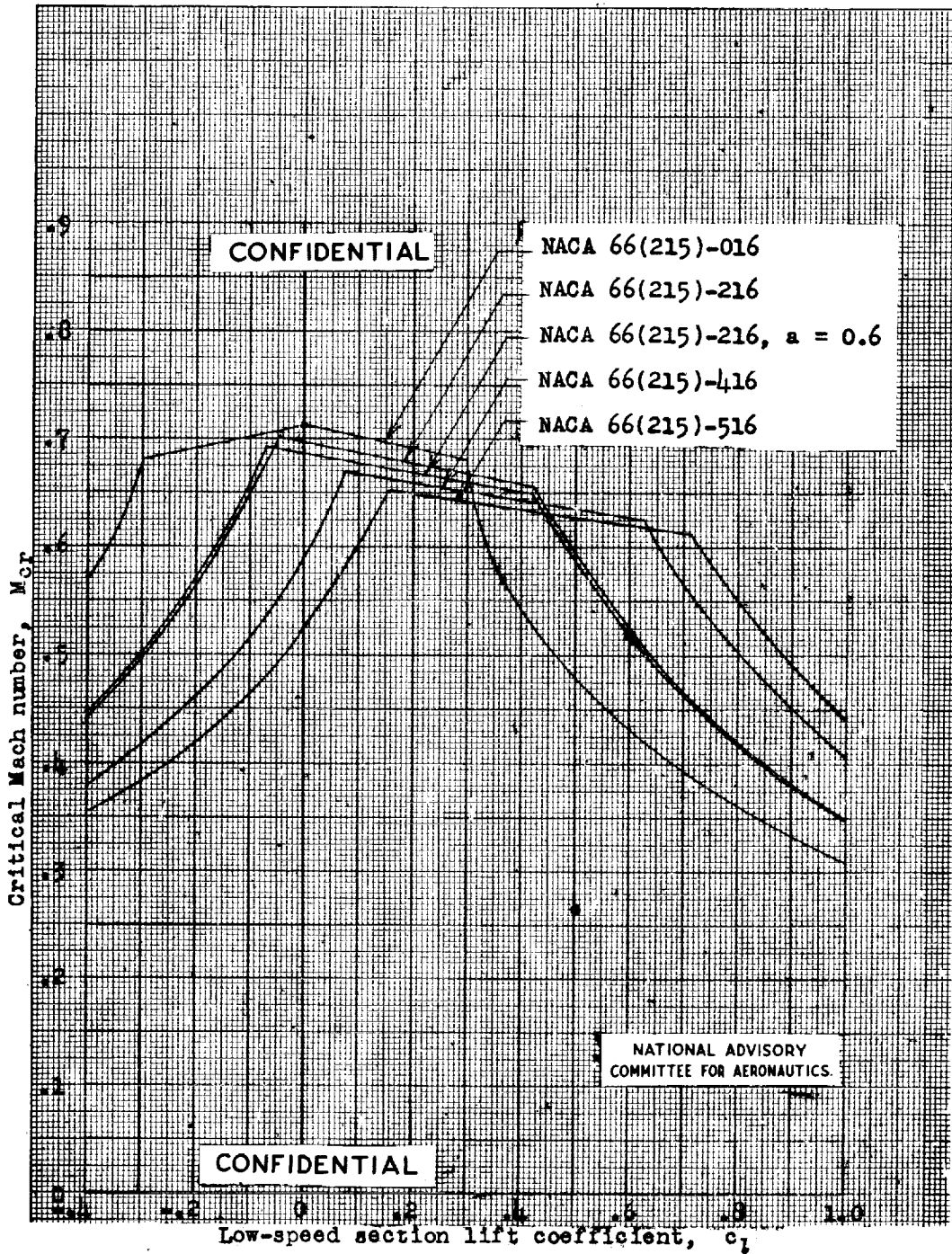
Variation of critical Mach number with low-speed section lift coefficient for several NACA 66-series airfoil sections of various thicknesses, cambered for a design lift coefficient of 0.2.





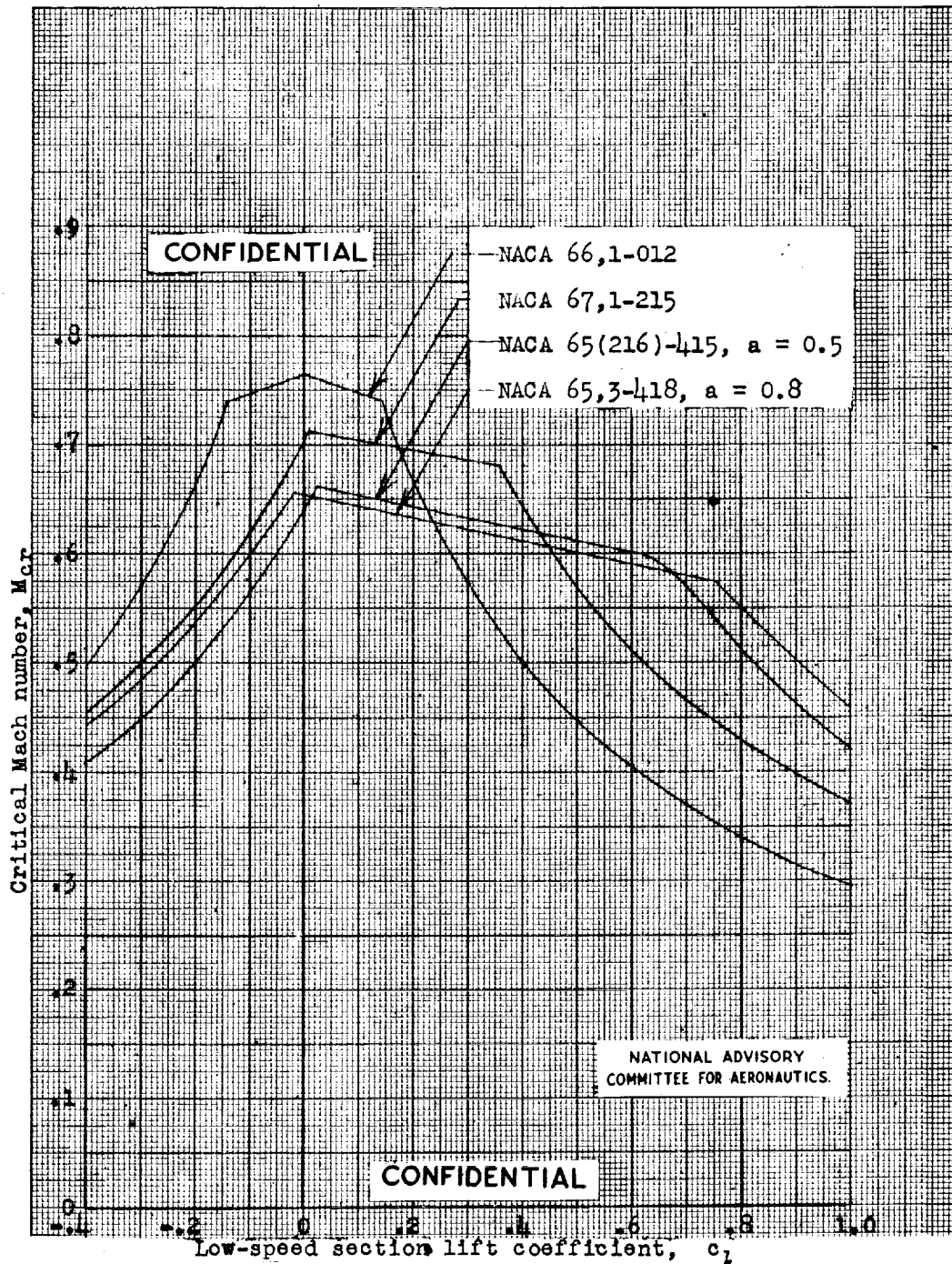
Variation of critical Mach number with low-speed section lift coefficient for two NACA 66-series airfoil sections of different thicknesses, cambered for a design lift coefficient of 0.4.





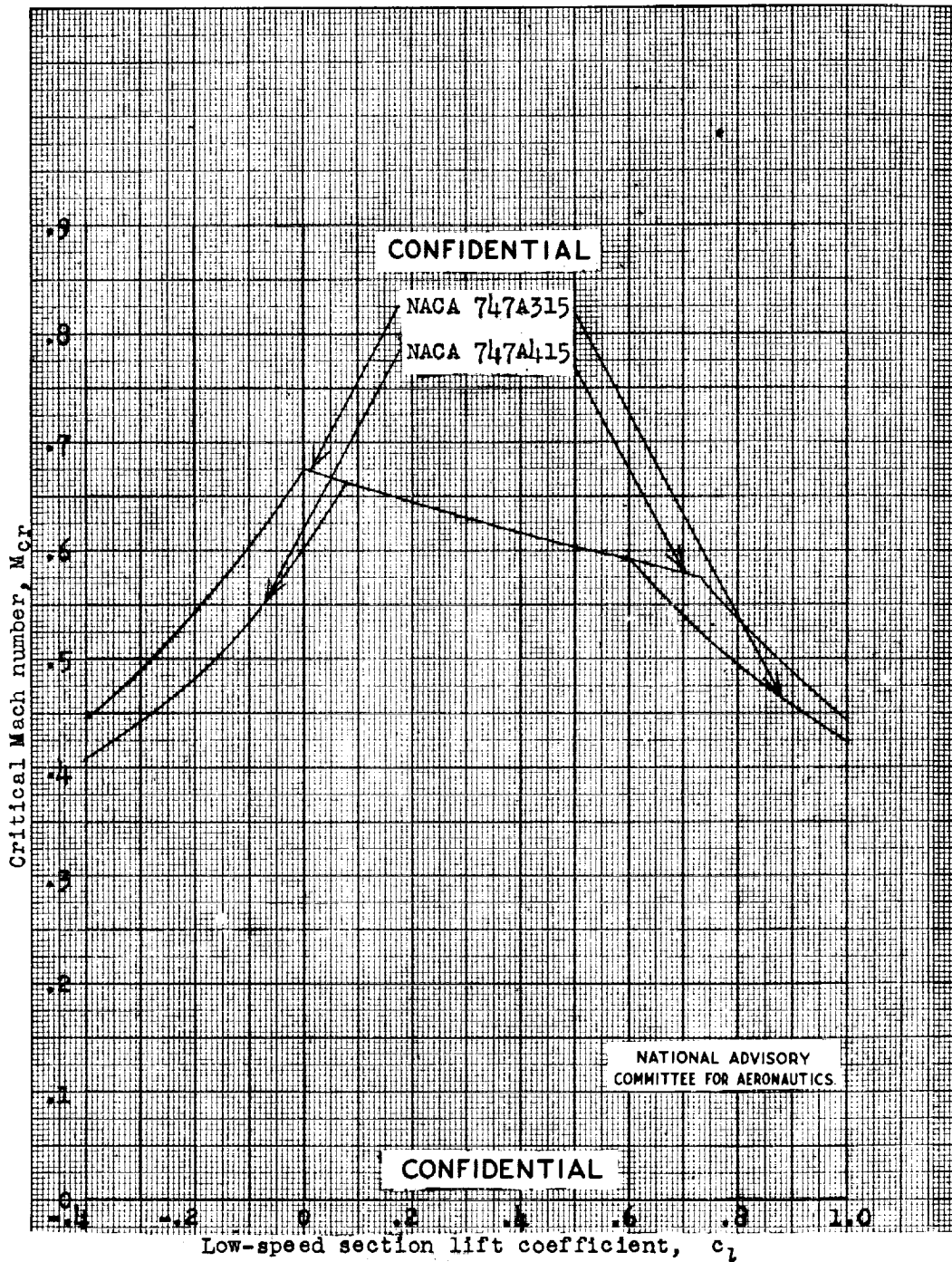
Variation of critical Mach number with low-speed section lift coefficient for several NACA 66-series airfoil sections with a thickness ratio of 0.16 and cambered for various design lift coefficients.





Variation of critical Mach number with low-speed section lift coefficient for several NACA 6-series airfoil sections with different positions of minimum pressure and various thicknesses, cambered for various design lift coefficients.

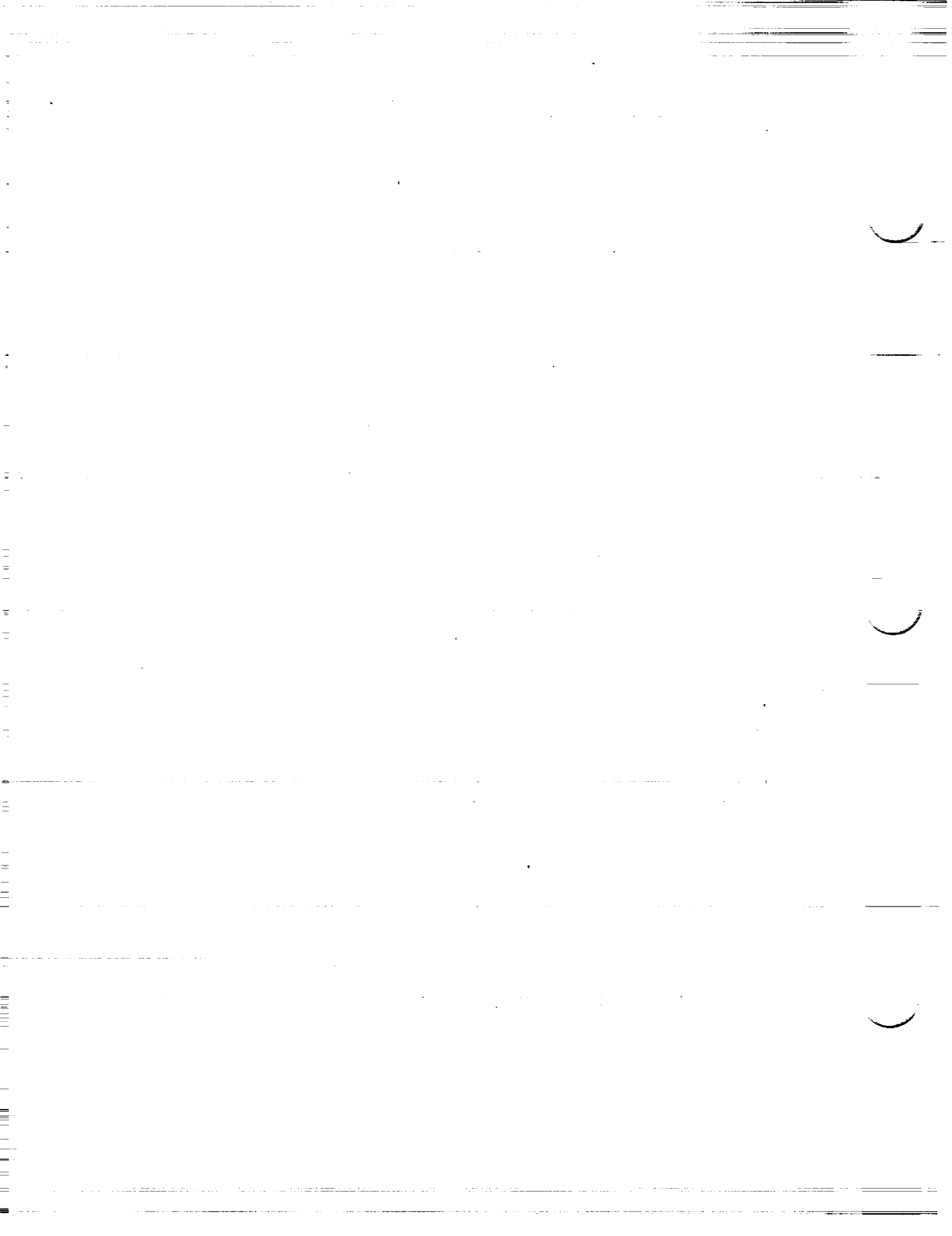




Variation of critical Mach number with low-speed section lift coefficient for two NACA 7-series airfoil sections with a thickness ratio of 0.15 and cambered for different design lift coefficients.

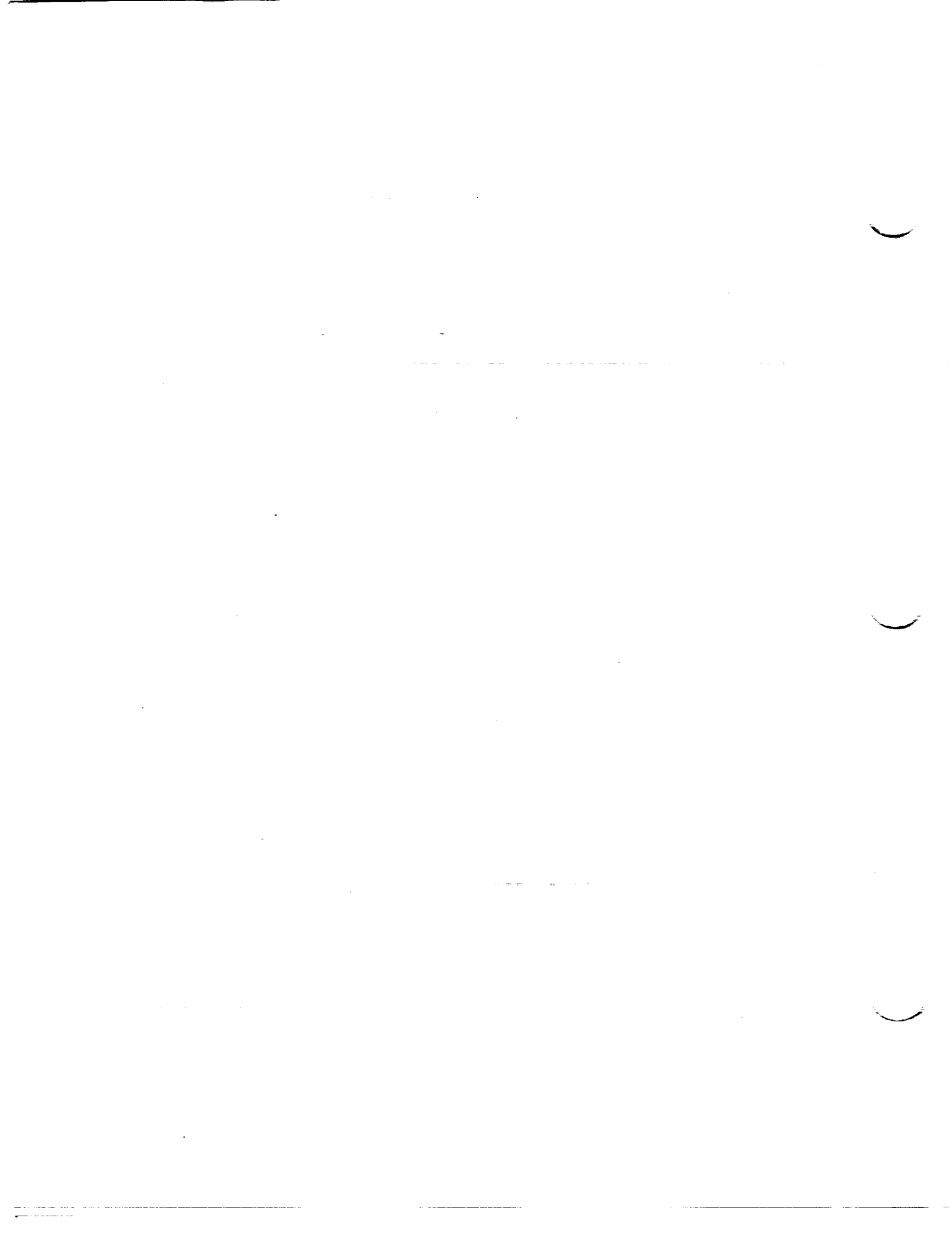


V - AERODYNAMIC CHARACTERISTICS



V - AERODYNAMIC CHARACTERISTICS

Aerodynamic characteristics of the NACA 0006 airfoil section	S115a
Aerodynamic characteristics of the NACA 0009 airfoil section	S115b
Aerodynamic characteristics of the NACA 1408 airfoil section	S115c
Aerodynamic characteristics of the NACA 1410 airfoil section	S115d
Aerodynamic characteristics of the NACA 1412 airfoil section	S115e
Aerodynamic characteristics of the NACA 2412 airfoil section	S116
Aerodynamic characteristics of the NACA 2415 airfoil section	S117
Aerodynamic characteristics of the NACA 2418 airfoil section	S118
Aerodynamic characteristics of the NACA 2421 airfoil section	S119
Aerodynamic characteristics of the NACA 2424 airfoil section	S120
Aerodynamic characteristics of the NACA 4412 airfoil section	S121
Aerodynamic characteristics of the NACA 4415 airfoil section	S122
Aerodynamic characteristics of the NACA 4418 airfoil section	S123
Aerodynamic characteristics of the NACA 4421 airfoil section	S124
Aerodynamic characteristics of the NACA 4424 airfoil section	S125



Aerodynamic characteristics of the
NACA 23012 airfoil section S126

Aerodynamic characteristics of the
NACA 23015 airfoil section S127

Aerodynamic characteristics of the
NACA 23018 airfoil section S128

Aerodynamic characteristics of the
NACA 23021 airfoil section S129

Aerodynamic characteristics of the
NACA 23024 airfoil section S130

Aerodynamic characteristics of the
NACA 63,4-420 airfoil section S131

NACA 63,4-420 airfoil section with 0.25c slotted flap
(a) Configuration S132
(b) Aerodynamic characteristics with hinge
 location 1 S133
(c) Aerodynamic characteristics with hinge
 location 2 S134

Aerodynamic characteristics of the
NACA 63,4-420, $a = 0.3$ airfoil section S135

Aerodynamic characteristics of the
NACA 63(420)-422 airfoil section S136

Aerodynamic characteristics of the
NACA 63(420)-517 airfoil section S136a

Aerodynamic characteristics of the
NACA 641-006 airfoil section S137

Aerodynamic characteristics of the
NACA 641-009 airfoil section S137a

Aerodynamic characteristics of the
NACA 641-012 airfoil section S137b

Aerodynamic characteristics of the
NACA 641-108 airfoil section S137c

Aerodynamic characteristics of the
NACA 641-110 airfoil section S137d

Aerodynamic characteristics of the
NACA 641-112 airfoil section S137e

1. The first part of the document discusses the importance of maintaining accurate records.

2. It then goes on to describe the various methods used to collect and analyze data.

3. The next section details the results of the study and the conclusions drawn from them.

4. Finally, the document concludes with a summary of the findings and recommendations for future research.

5. The authors express their gratitude to the funding agencies and the participants who made this study possible.

6. The document is organized into several sections, each covering a different aspect of the research.

7. The first section provides an overview of the research and its objectives.

8. The second section describes the methodology used in the study, including the data collection and analysis procedures.

9. The third section presents the results of the study, which are discussed in detail in the following sections.

10. The fourth section discusses the implications of the findings and offers suggestions for future research.

11. The document concludes with a final summary of the key findings and a list of references.

12. The authors hope that this study will contribute to the understanding of the topic and provide a basis for further research.

13. The document is intended for a wide audience of researchers and practitioners in the field.

14. The authors would like to thank the reviewers for their helpful comments and suggestions.

15. The document is available for free download and is intended to be a valuable resource for the community.

16. The authors are grateful to the funding agencies for their support of this research.

17. The document is a result of the collaborative efforts of the research team and the participants.

18. The authors would like to express their appreciation to the participants who provided their time and expertise.

19. The document is a testament to the power of collaborative research and the importance of sharing knowledge.

20. The authors hope that this study will inspire others to explore the topic further and contribute to the field.

Aerodynamic characteristics of the
 NACA 641-206 airfoil section S137f

Aerodynamic characteristics of the
 NACA 641-209 airfoil section S137g

Aerodynamic characteristics of the
 NACA 641-212 airfoil section S137h

Aerodynamic characteristics of the
 NACA 641-412 airfoil section S138

Aerodynamic characteristics of the
 NACA 642-215 airfoil section S138a

Aerodynamic characteristics of the
 NACA 642-415 airfoil section S139

Aerodynamic characteristics of the
 NACA 643-418 airfoil section S140

Aerodynamic characteristics of the
 NACA 644-421 airfoil section S141

Aerodynamic characteristics of the
 NACA 65,3-018 airfoil section S142

Aerodynamic characteristics of the
 NACA 65,3-418, $a = 0.8$ airfoil section S143

Aerodynamic characteristics of the
 NACA 65,3-618 airfoil section S144

Aerodynamic characteristics of the NACA 65,3-618 air-
 foil section with 0.20c sealed plain flap . . . S145

Aerodynamic characteristics of the
 NACA 65(216)-415, $a = 0.5$ airfoil section . . S146

Aerodynamic characteristics of the
 NACA 651-006 airfoil section S146a

Aerodynamic characteristics of the
 NACA 651-009 airfoil section S146b

Aerodynamic characteristics of the
 NACA 651-012 airfoil section S146c

Aerodynamic characteristics of the
 NACA 651-206 airfoil section S146d

1. The first part of the document discusses the importance of maintaining accurate records of all transactions and activities. It emphasizes that this is crucial for ensuring transparency and accountability in the organization's operations.

2. The second part of the document outlines the various methods and tools used to collect and analyze data. It highlights the need for consistent and reliable data collection processes to support effective decision-making.

3. The third part of the document focuses on the role of technology in data management and analysis. It discusses how modern software solutions can streamline data collection, storage, and reporting, thereby improving efficiency and accuracy.

4. The fourth part of the document addresses the challenges associated with data management, such as data quality, security, and privacy. It provides strategies to mitigate these risks and ensure that data is used responsibly and ethically.

5. The fifth part of the document concludes by summarizing the key findings and recommendations. It stresses the importance of ongoing monitoring and evaluation to ensure that data management practices remain effective and aligned with the organization's goals.

6. The sixth part of the document provides a detailed overview of the data collection process, including the identification of data sources, the design of data collection instruments, and the implementation of data collection procedures.

7. The seventh part of the document discusses the various methods used for data analysis, such as descriptive statistics, inferential statistics, and qualitative analysis. It explains how these methods are used to interpret the data and draw meaningful conclusions.

8. The eighth part of the document focuses on the presentation of data, including the use of tables, charts, and graphs. It provides guidelines for creating clear and concise reports that effectively communicate the results of the data analysis.

9. The ninth part of the document discusses the importance of data security and privacy. It outlines the measures that should be taken to protect sensitive data from unauthorized access, loss, or disclosure.

10. The tenth part of the document provides a final summary and concludes the report. It reiterates the key findings and emphasizes the need for continued attention to data management practices to ensure the organization's long-term success.

Aerodynamic characteristics of the NACA 65 ₁ -209 airfoil section	S146e
Aerodynamic characteristics of the NACA 65 ₁ -210 airfoil section	S147
Aerodynamic characteristics of the NACA 65 ₁ -212 airfoil section	S148
Lift and moment characteristics of the NACA 65 ₁ -212 air- foil section with 0.20c split flap	S149
Aerodynamic characteristics of the NACA 65 ₁ -410 airfoil section	S149a
Aerodynamic characteristics of the NACA 65 ₁ -412 airfoil section	S149b
Aerodynamic characteristics of the NACA 65 ₂ -415 airfoil section	S150
Aerodynamic characteristics of the NACA 65 ₂ -415, a = 0.5 airfoil section	S151
NACA 65 ₃ -118 airfoil section with 0.309c double slotted flap:	
(a) Configuration	S152
(b) Aerodynamic characteristics	S153
Aerodynamic characteristics of the NACA 65 ₃ -418 airfoil section	S154
Aerodynamic characteristics of the NACA 65 ₃ -418, a = 0.5 airfoil section	S155
Aerodynamic characteristics of the NACA 65 ₃ -618, a = 0.5 airfoil section	S156
Aerodynamic characteristics of the NACA 65 ₄ -421 airfoil section	S157
Aerodynamic characteristics of the NACA 65 ₄ -421, a = 0.5 airfoil section	S158
Aerodynamic characteristics of the NACA 65(421)-420 airfoil section	S159

Aerodynamic characteristics of the NACA 66,1-212 airfoil section	S160
Lift and moment characteristics of the NACA 66,1-212 air- foil section with 0.20c split flap	S161
Aerodynamic characteristics of the NACA 66(215)-016 airfoil section	S162
Aerodynamic characteristics of the NACA 66(215)-216 airfoil section	S163
Aerodynamic characteristics of the NACA 66(215)-216 air- foil section with 0.20c sealed plain flap	S164
Lift and moment characteristics of the NACA 66(215)-216 airfoil section with 0.20c split flap	S165
Aerodynamic characteristics of the NACA 66(215)-216 a = 0.6 airfoil section	S166
NACA 66(215)-216, a = 0.6 airfoil section with 0.30c slotted and 0.10c plain flap:	
(a) Airfoil-flap configuration	S167
(b) Flap configuration	S168
(c) Aerodynamic characteristics. Slotted flap retracted	S169
(d) Lift and moment characteristics. Slotted flap deflected 22°	S170
(e) Lift and moment characteristics. Slotted flap deflected 27°	S171
(f) Lift and moment characteristics. Slotted flap deflected 32°	S172
(g) Lift and moment characteristics. Slotted flap deflected 37°	S173
Aerodynamic characteristics of the NACA 66(215)-416 airfoil section	S174
Aerodynamic characteristics of the NACA 66 ₁ -006 airfoil section	S174a
Aerodynamic characteristics of the NACA 66 ₁ -009 airfoil section	S174b
Aerodynamic characteristics of the NACA 66 ₁ -012 airfoil section	S174c

Aerodynamic characteristics of the
NACA 66₁-206 airfoil section S174d

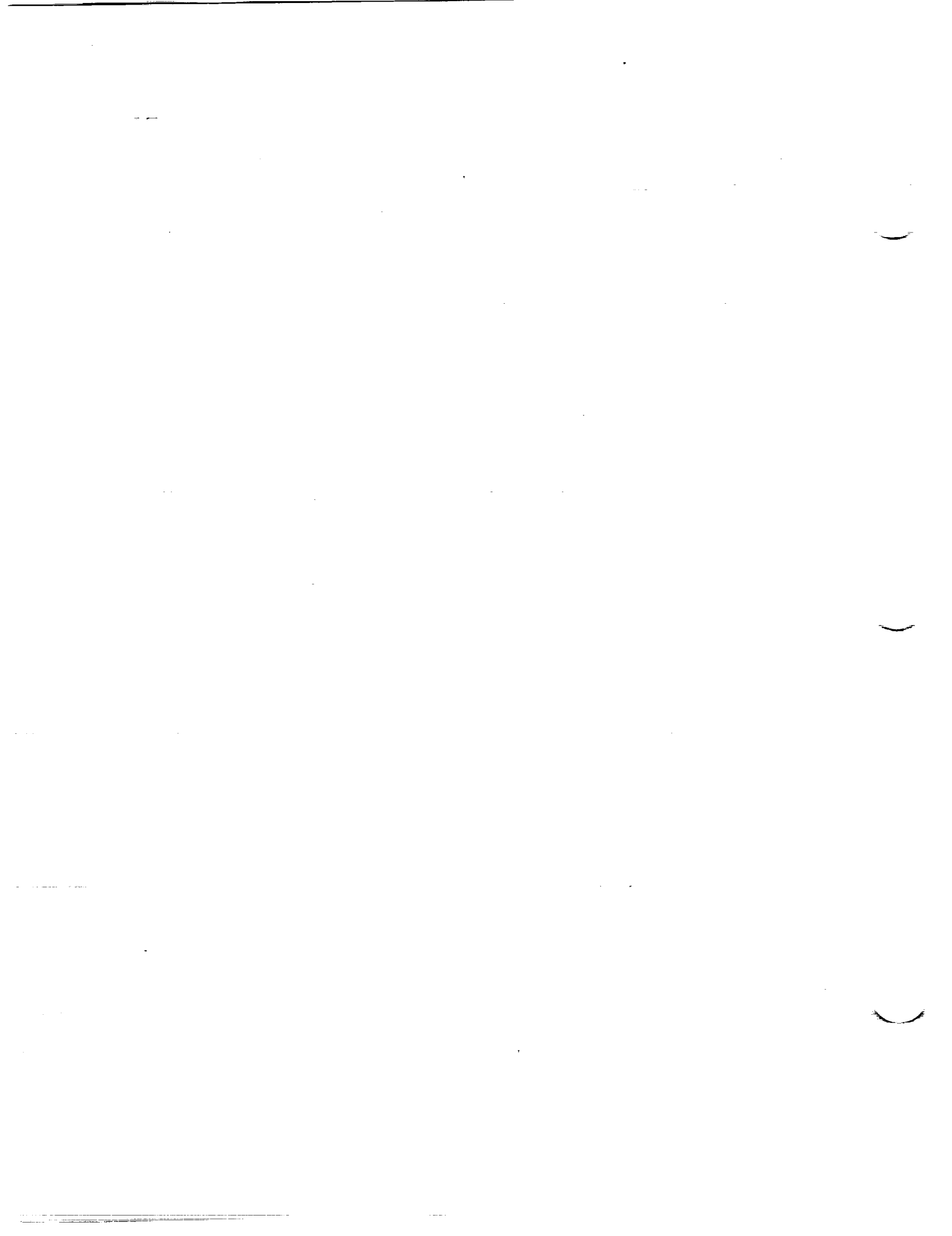
Aerodynamic characteristics of the
NACA 66₁-209 airfoil section S174e

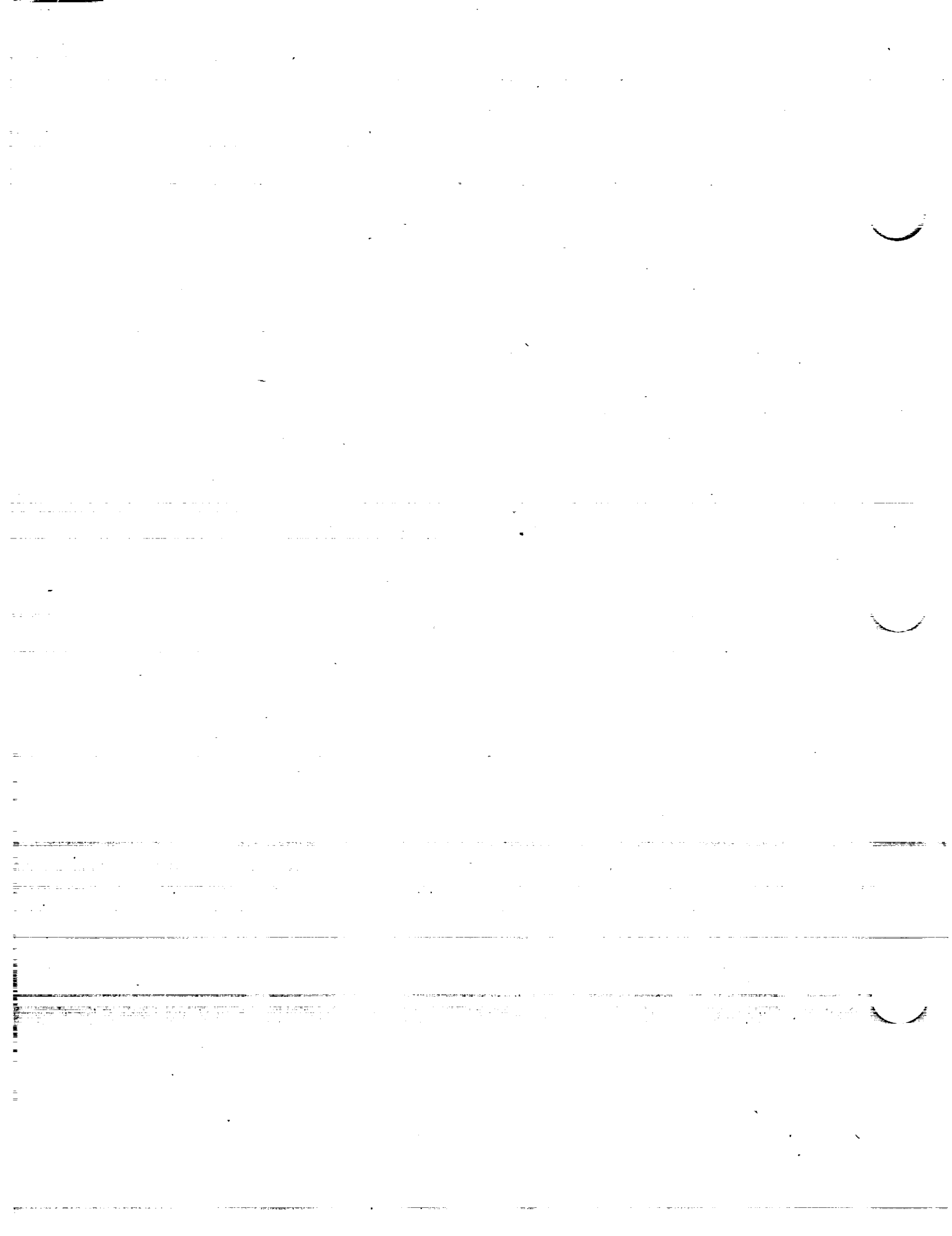
Aerodynamic characteristics of the
NACA 66₁-212 airfoil section S174f

Aerodynamic characteristics of the
NACA 67,1-215 airfoil section S175

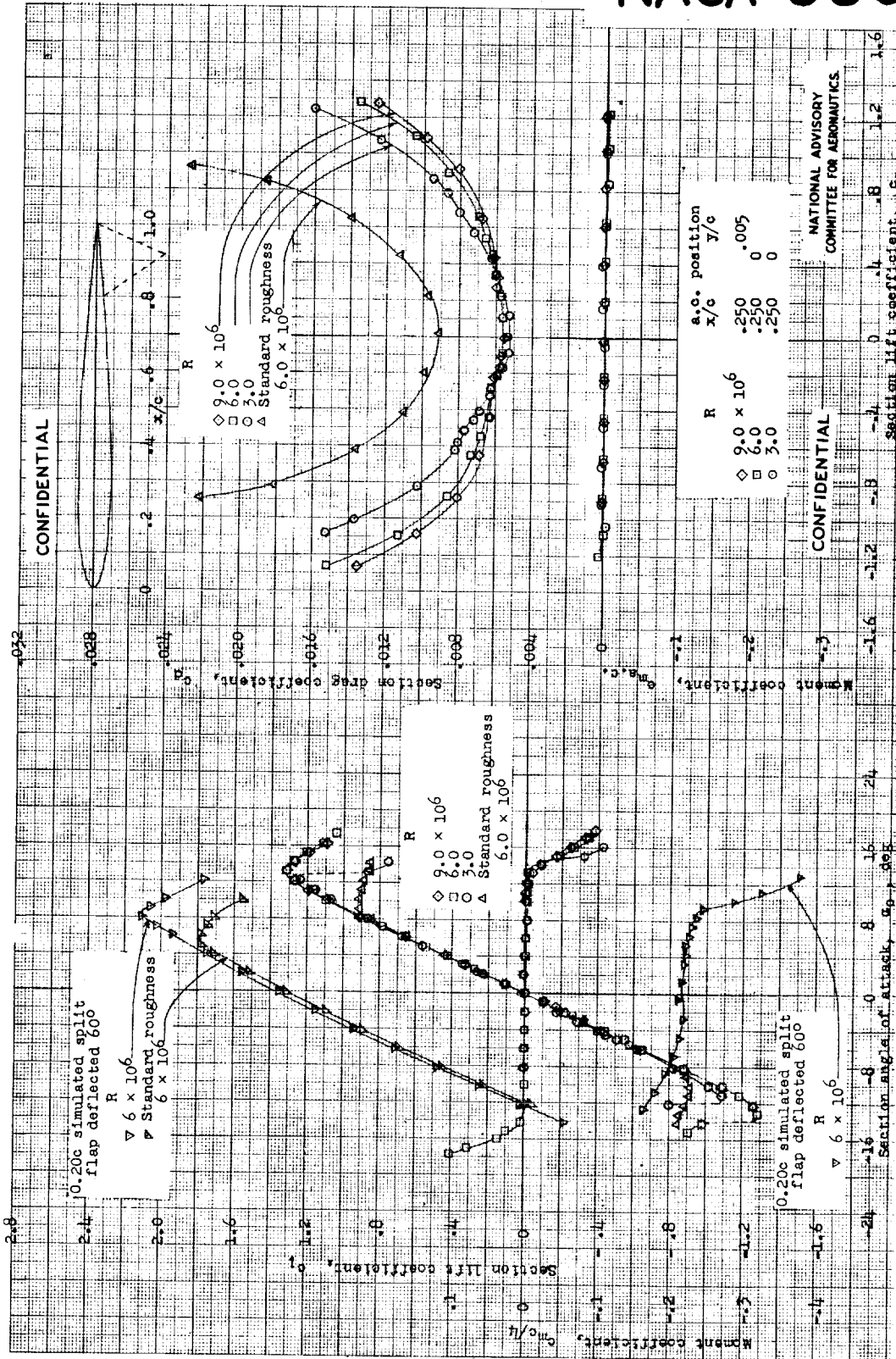
Aerodynamic characteristics of the
NACA 747A315 airfoil section S176

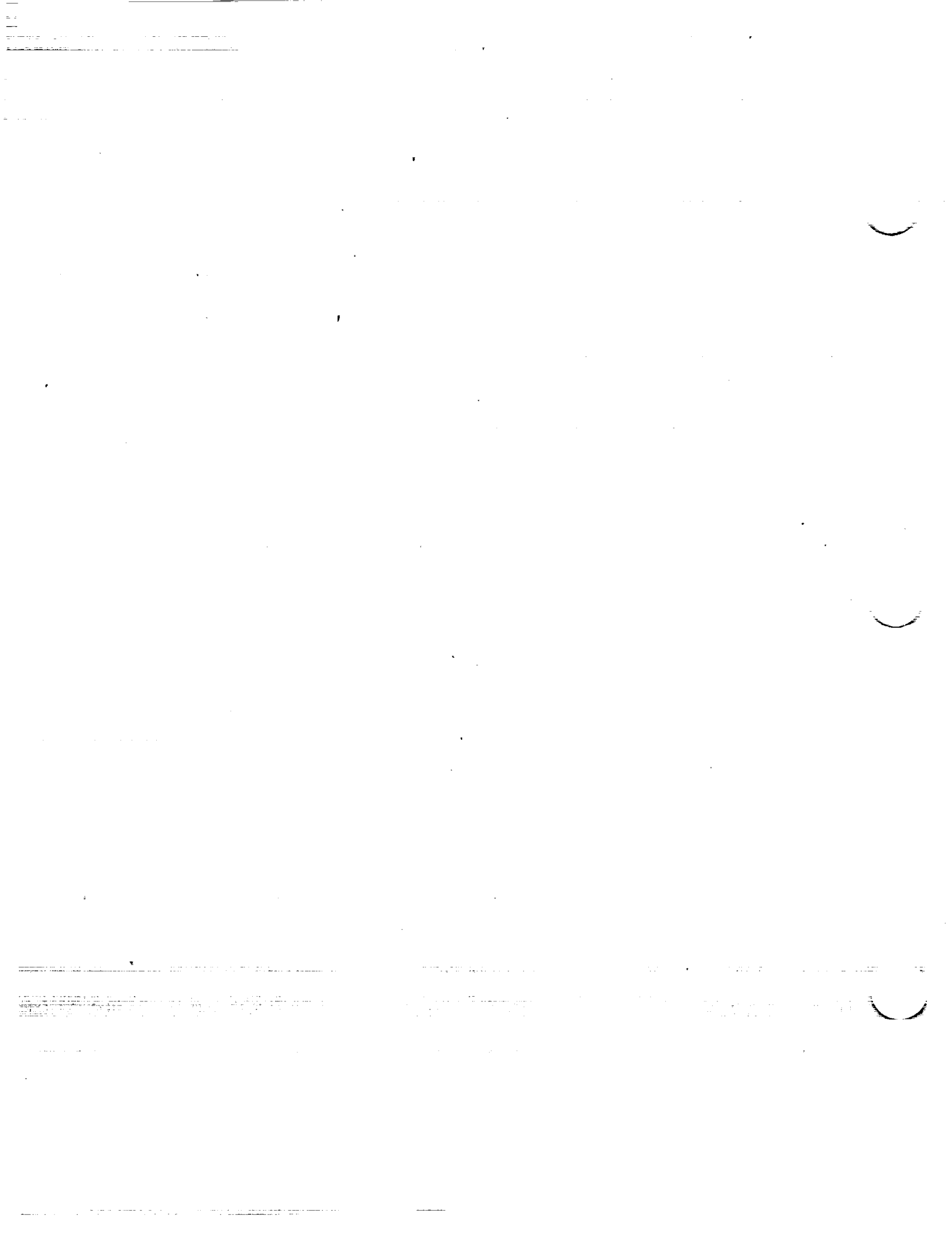
Aerodynamic characteristics of the
NACA 747A415 airfoil section S177



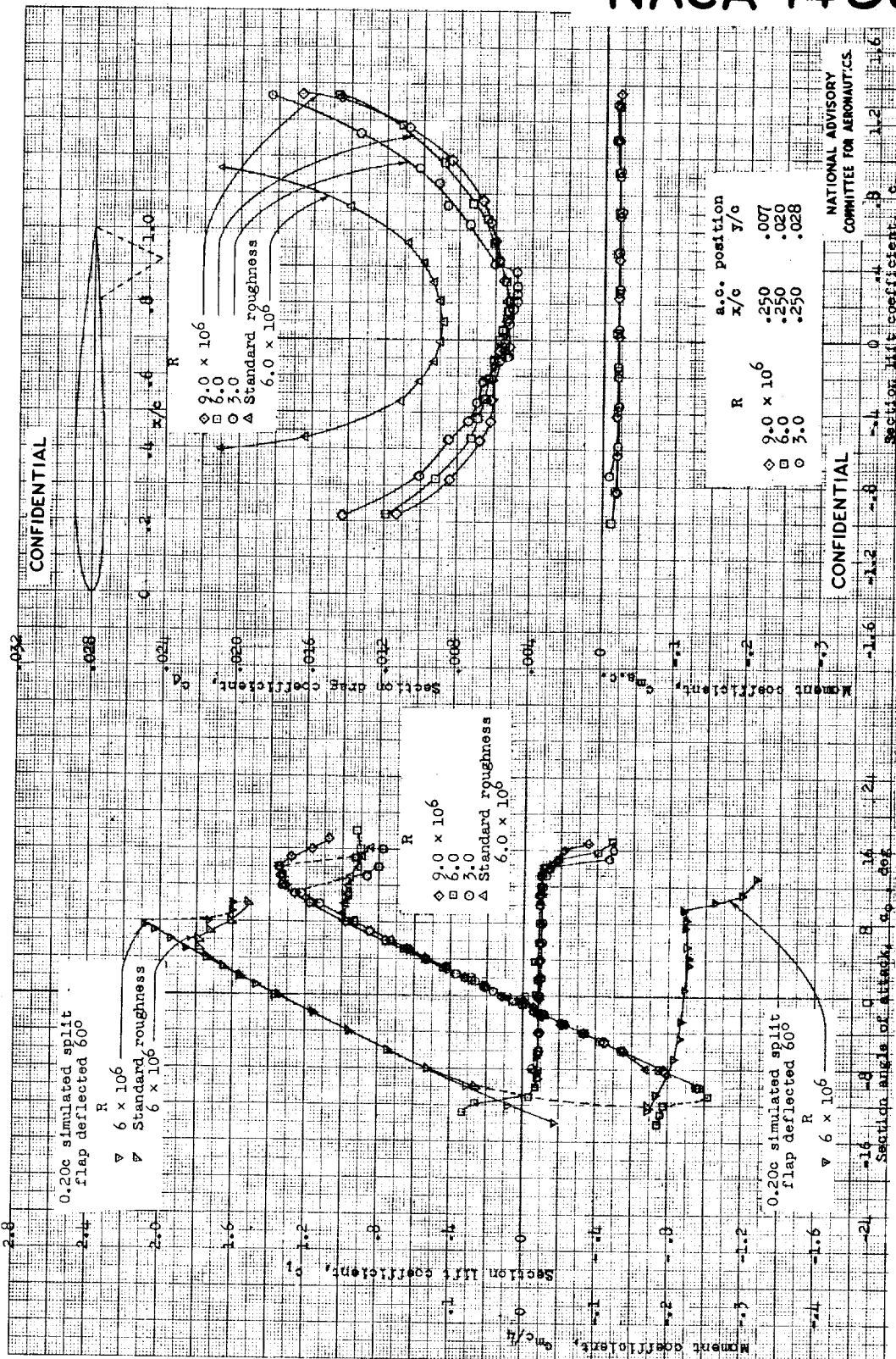


NACA 0009

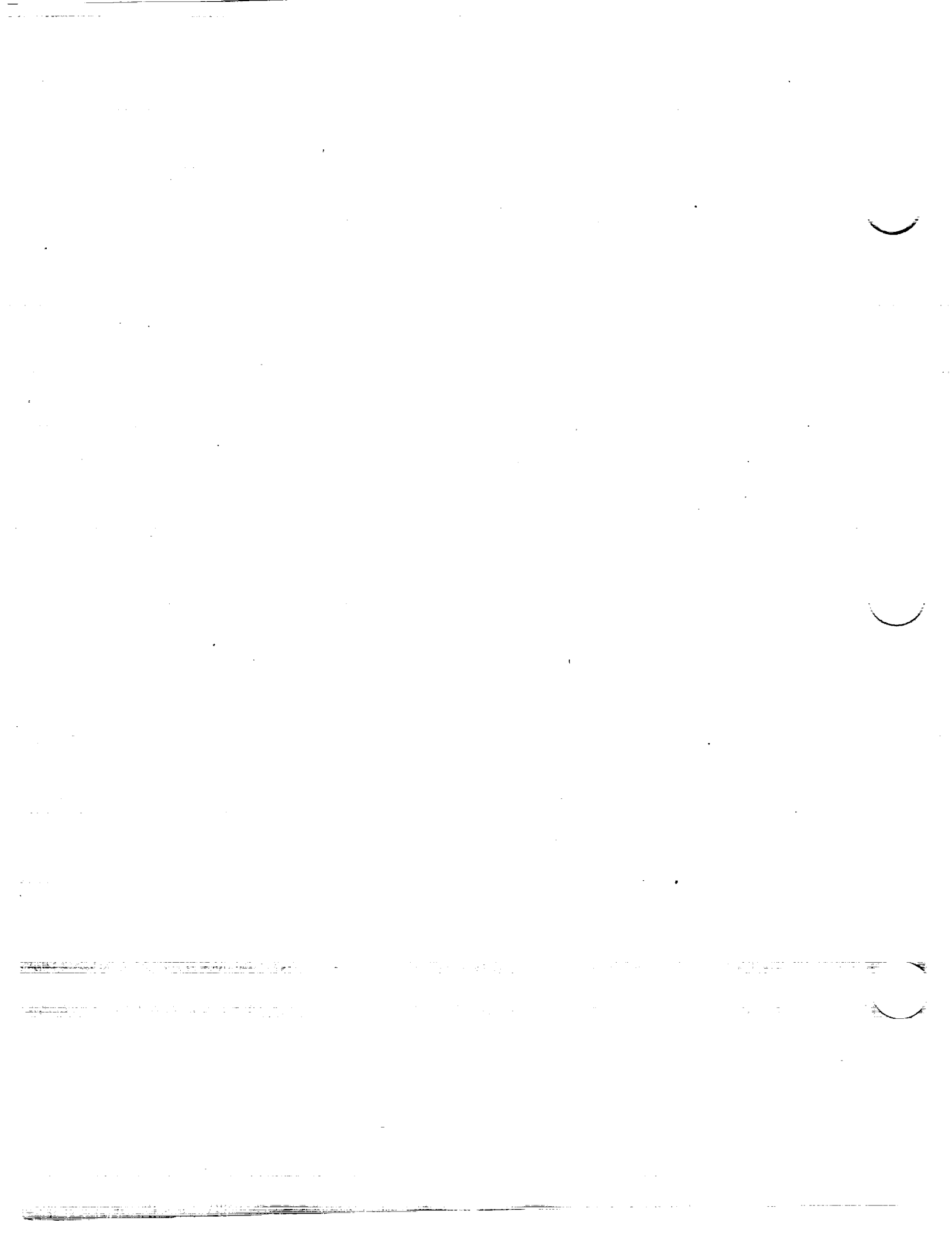




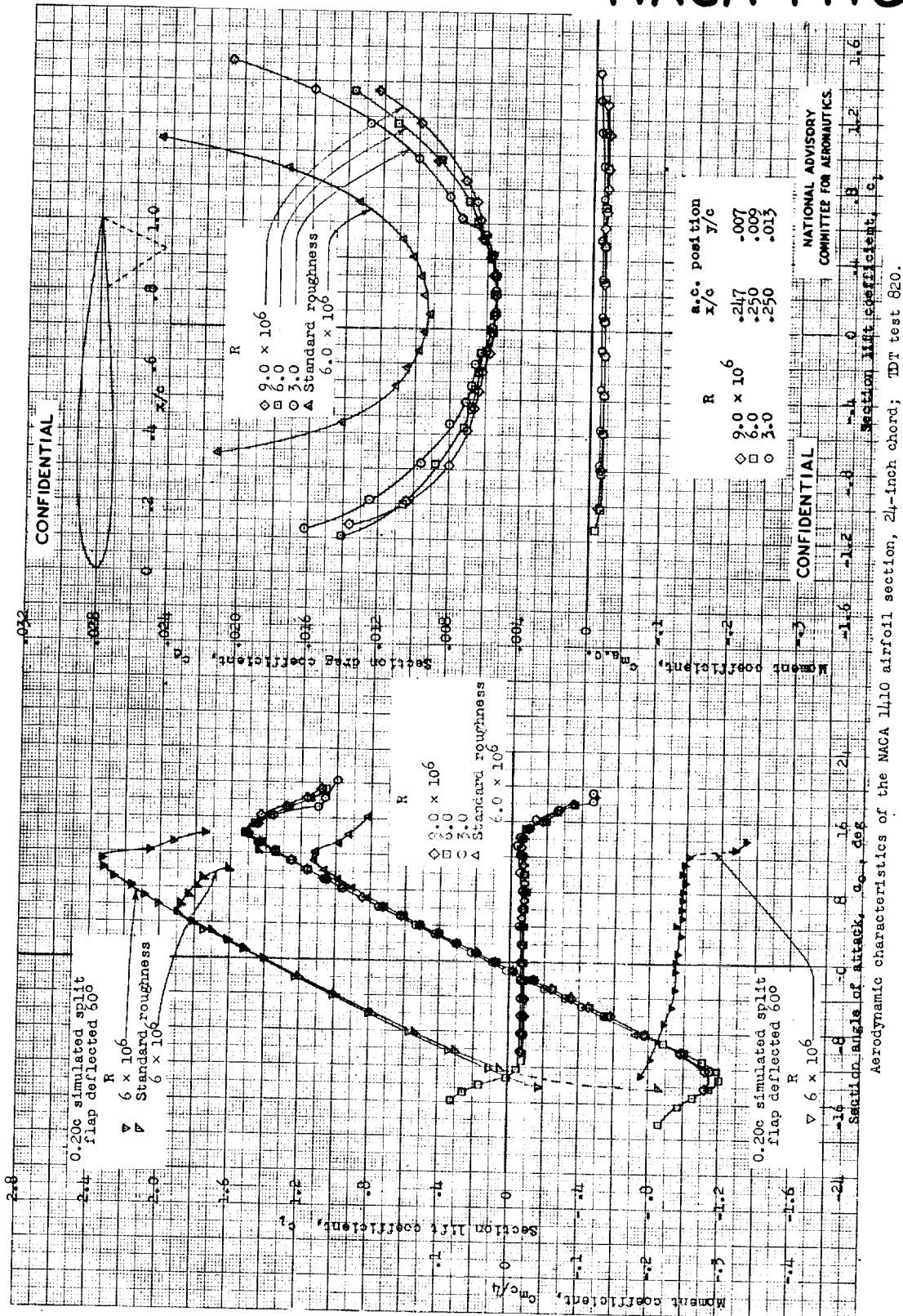
NACA 1408

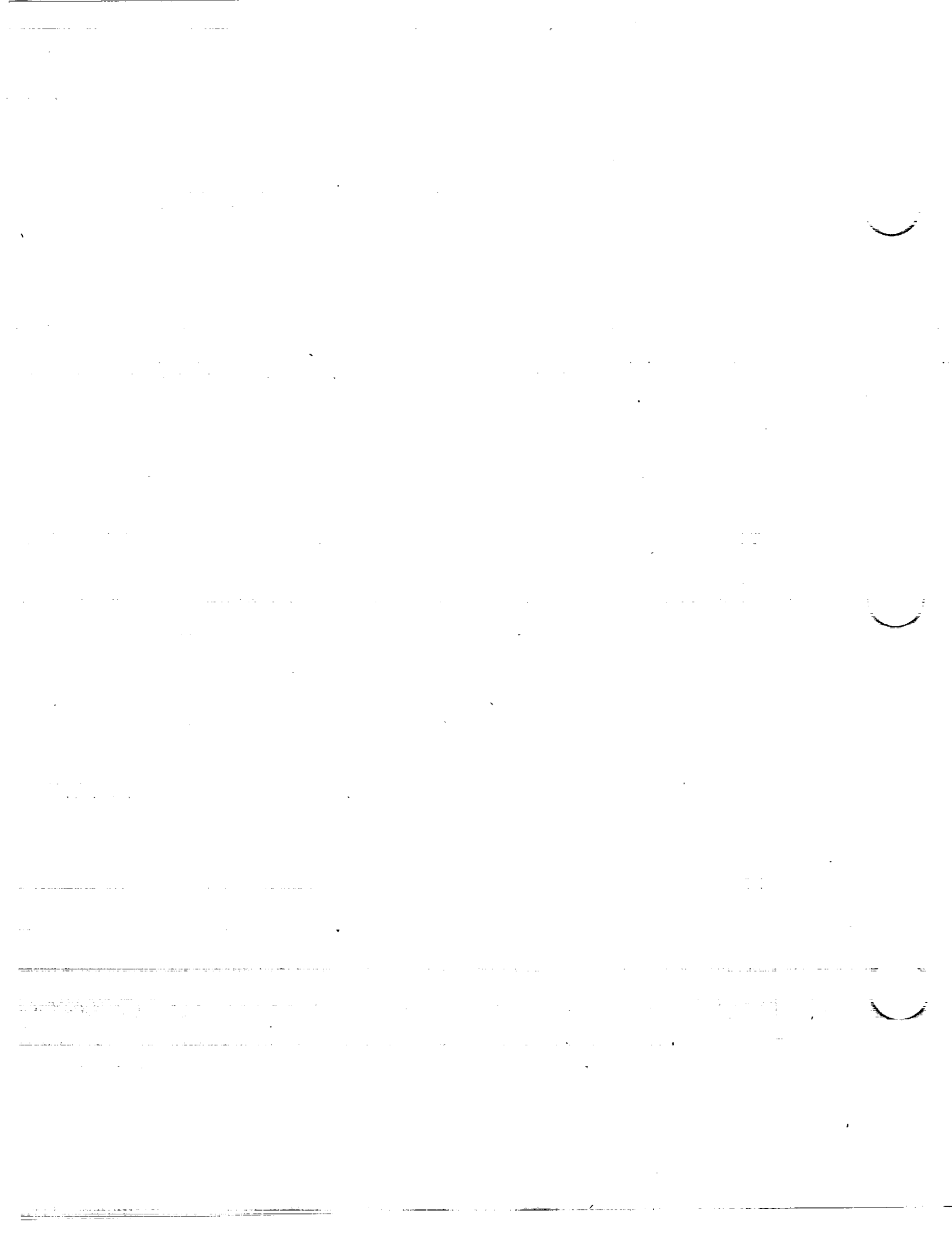


Aerodynamic characteristics of the NACA 1408 airfoil section, 24-inch chord; DT test 817.

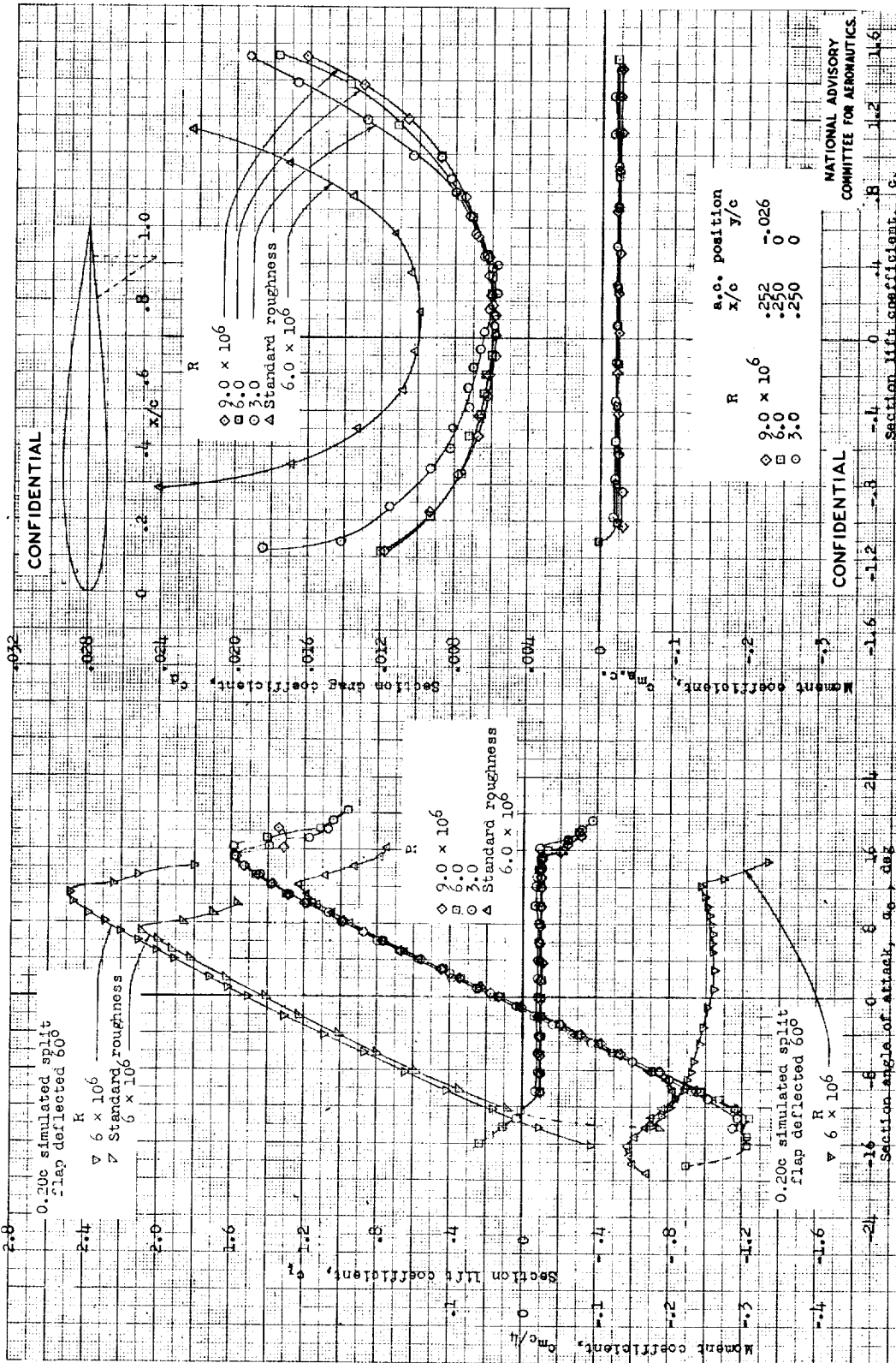


NACA 1410



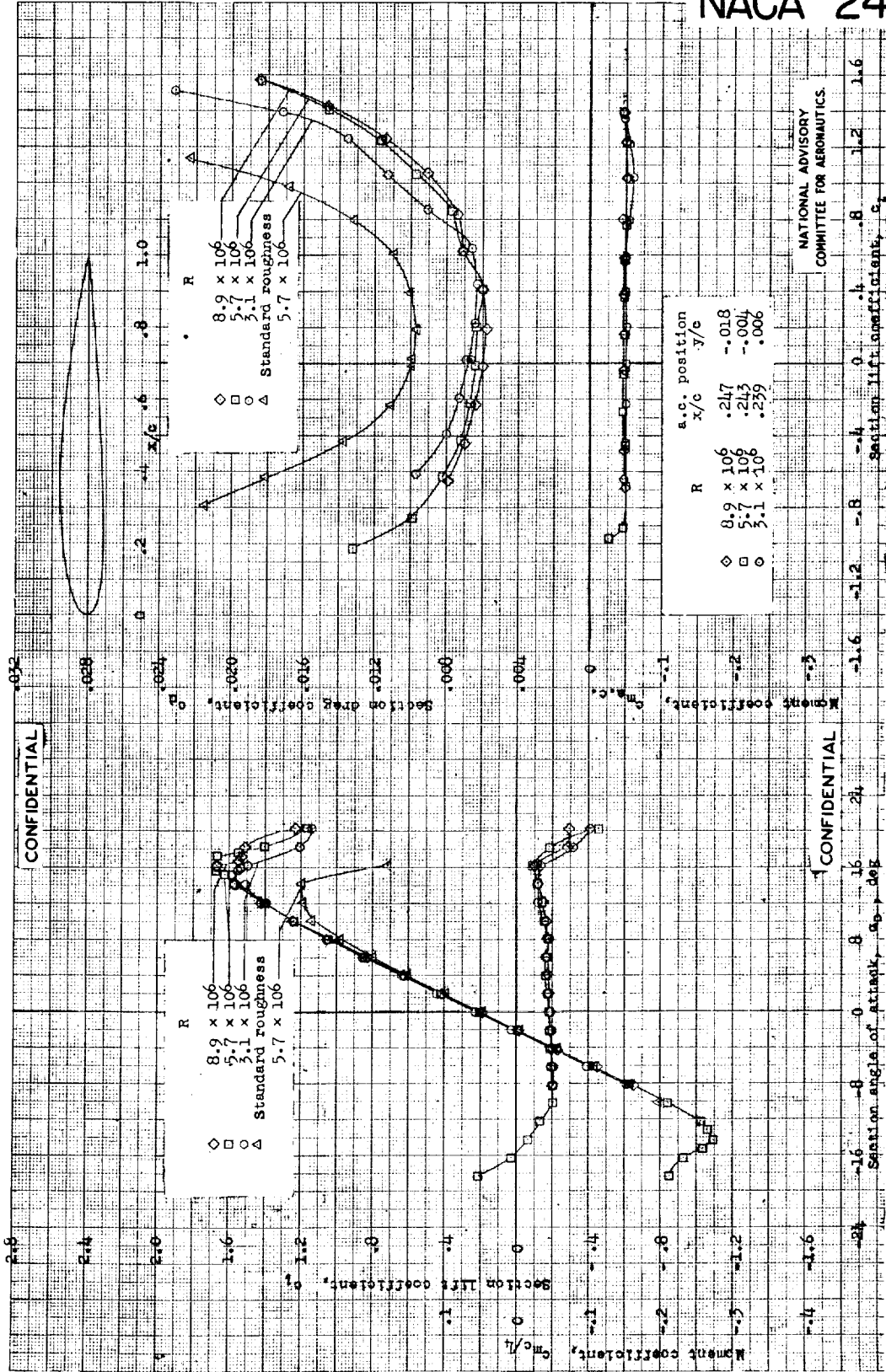


NACA 1412



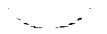


NACA 2412

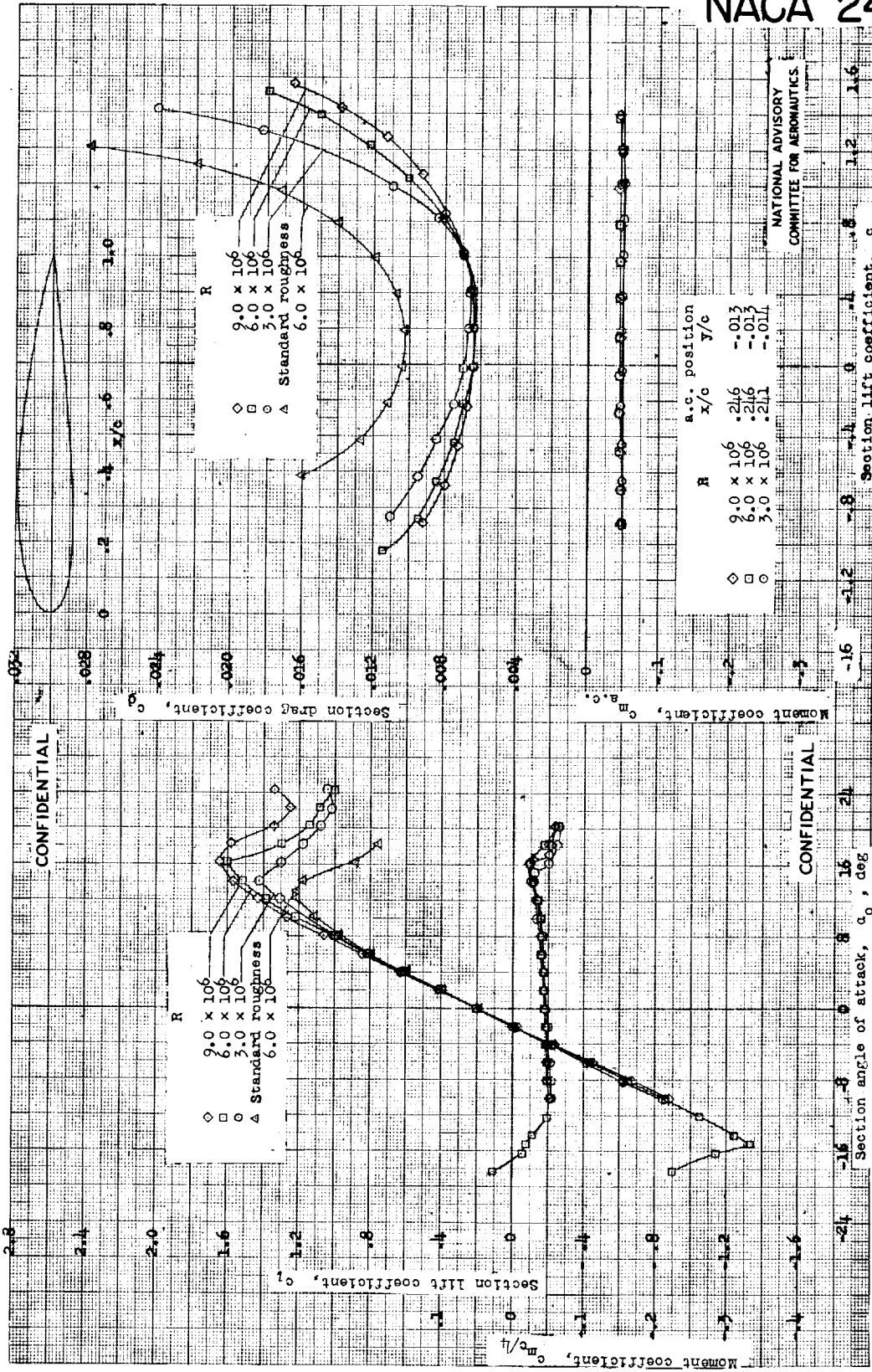


Aerodynamic characteristics of the NACA 2412 airfoil section, 24-inch chord; TDT tests 482, 508, 520, 774.

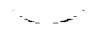
NATIONAL ADVISORY
COMMITTEE FOR AERONAUTICS



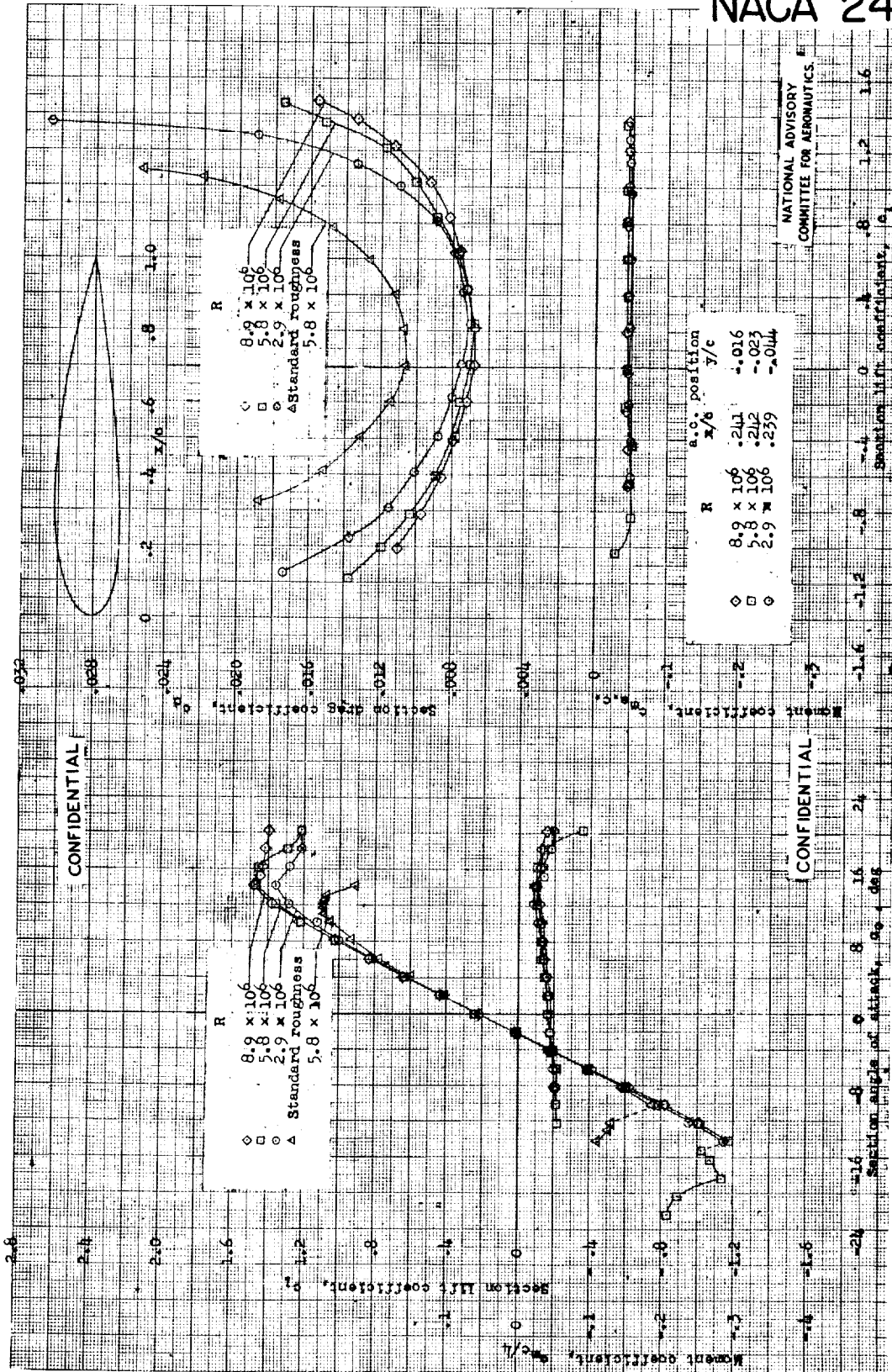
NACA 2415



Aerodynamic characteristics of the NACA 2415 airfoil section, 24-inch chord; TDT tests 464, 498, 506, 767.



NACA 2418



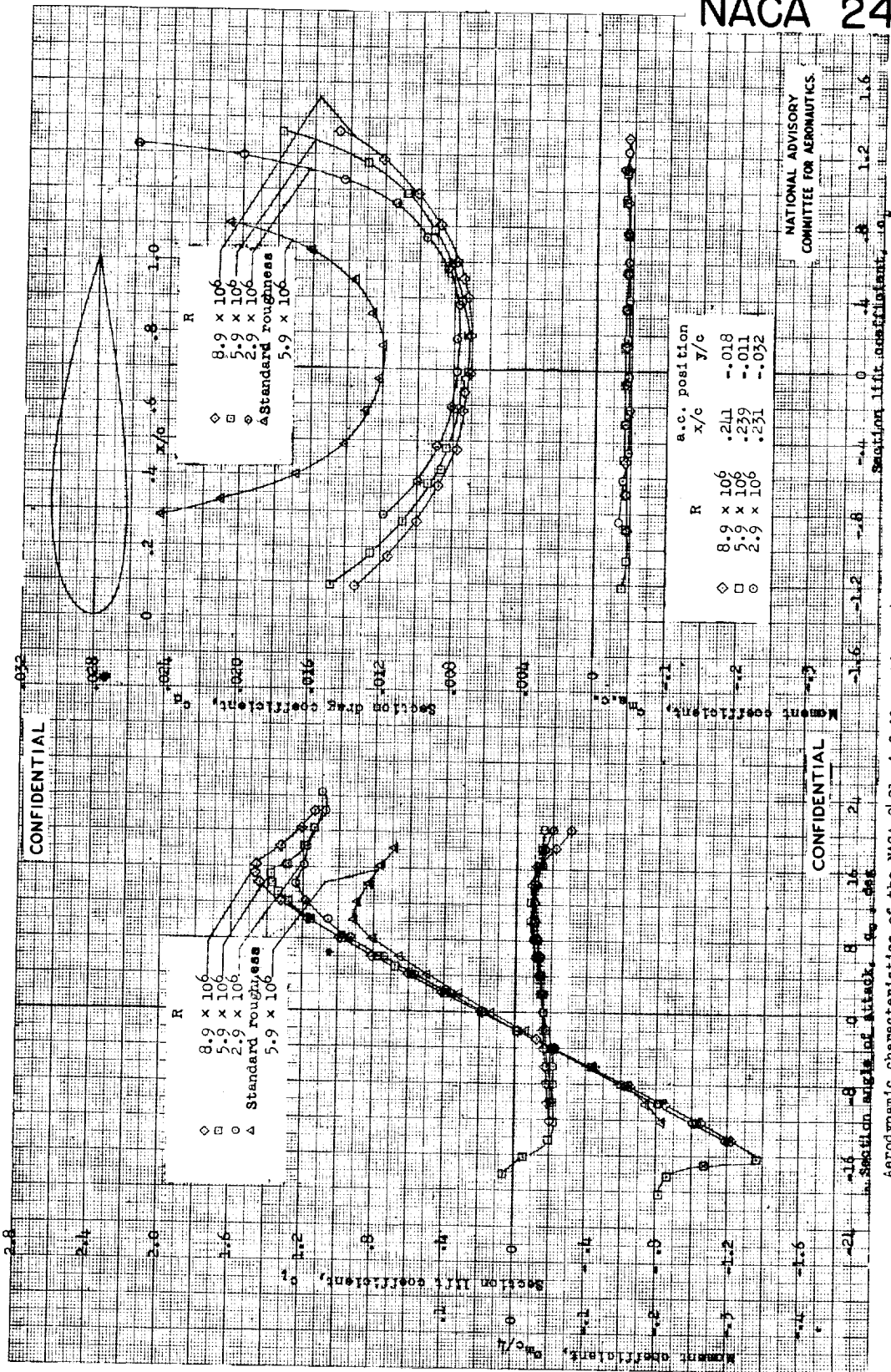
NATIONAL ADVISORY COMMITTEE FOR AERONAUTICS

Section Lift coefficient, C_l
 Section Drag coefficient, C_d
 a.c. position
 x/\bar{c} y/\bar{c}
 R 8.9×10^6 $-.016$
 5.8×10^6 $-.016$
 2.9×10^6 $-.023$
 5.8×10^6 $-.044$

Aerodynamic characteristics of the NACA 2418 airfoil section, 24-inch chord; TDT tests 465, 472, 774.

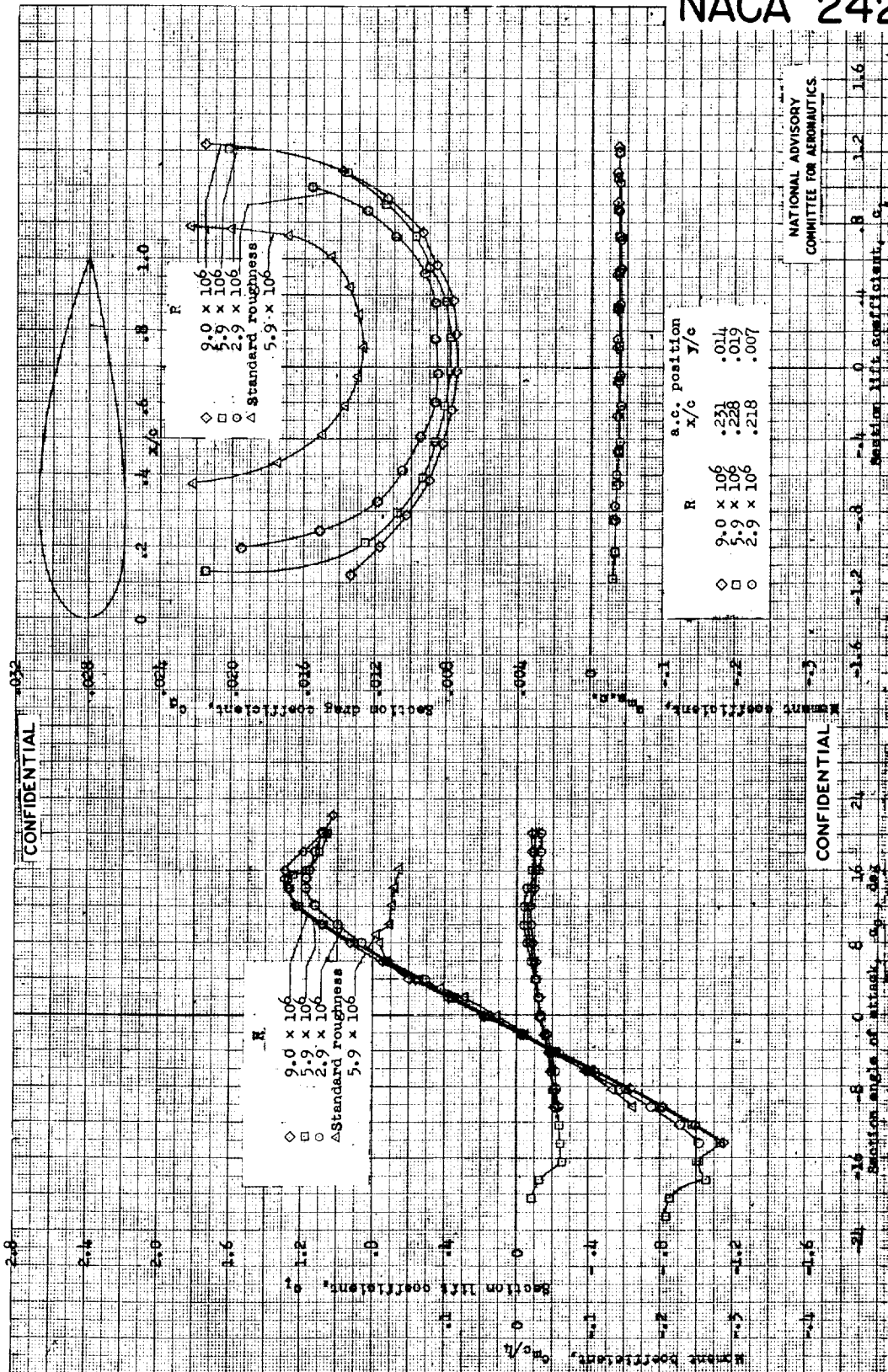


NACA 2421





NACA 2424



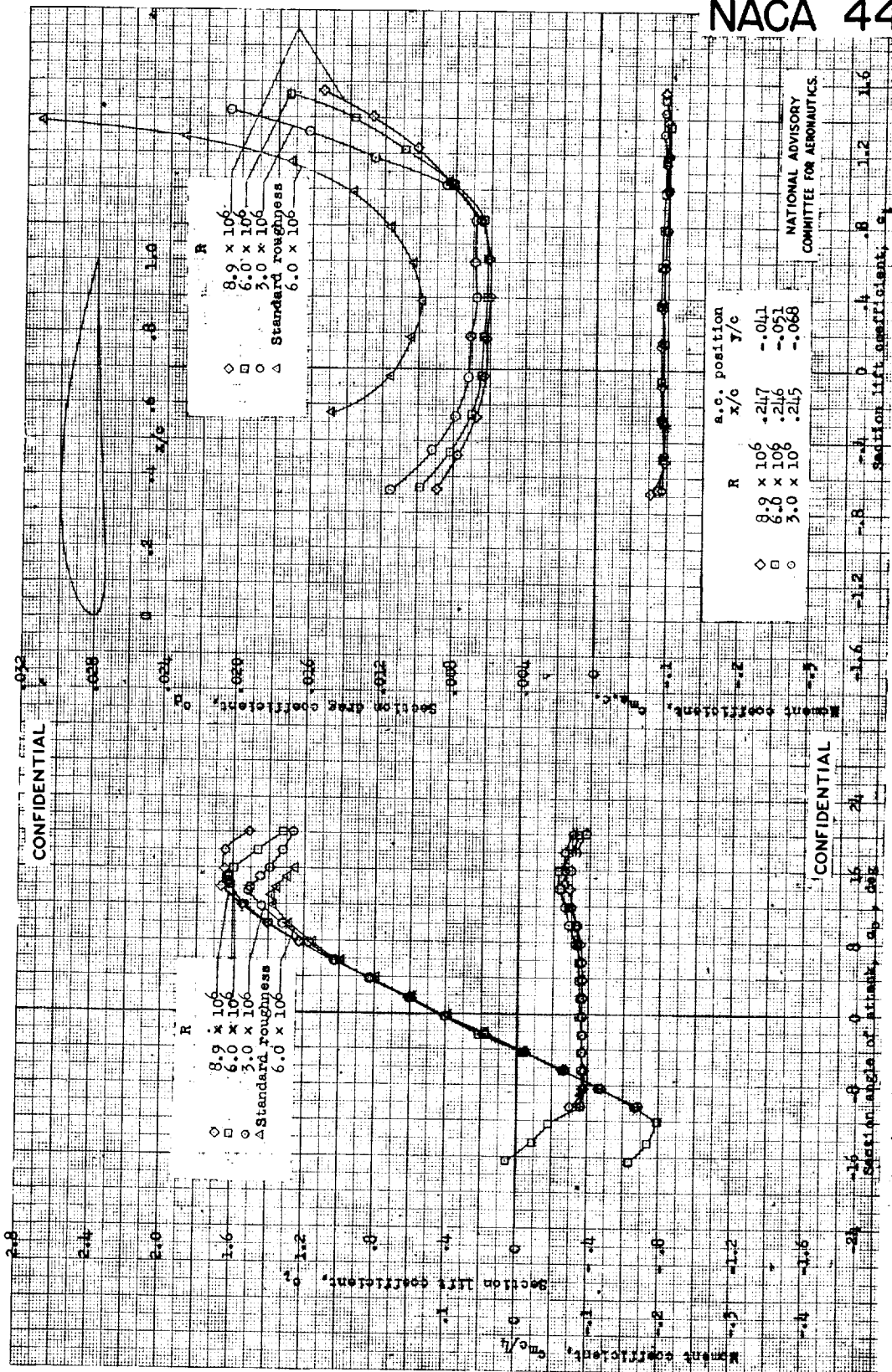
NATIONAL ADVISORY
COMMITTEE FOR AERONAUTICS

R	s.c. position x/c	y/c
9.0×10^6	.231	.014
5.9×10^6	.228	.019
2.9×10^6	.218	.007

Aerodynamic characteristics of the NACA 2424 airfoil section, 24-inch chord; TDF tests 527, 530.



NACA 4412

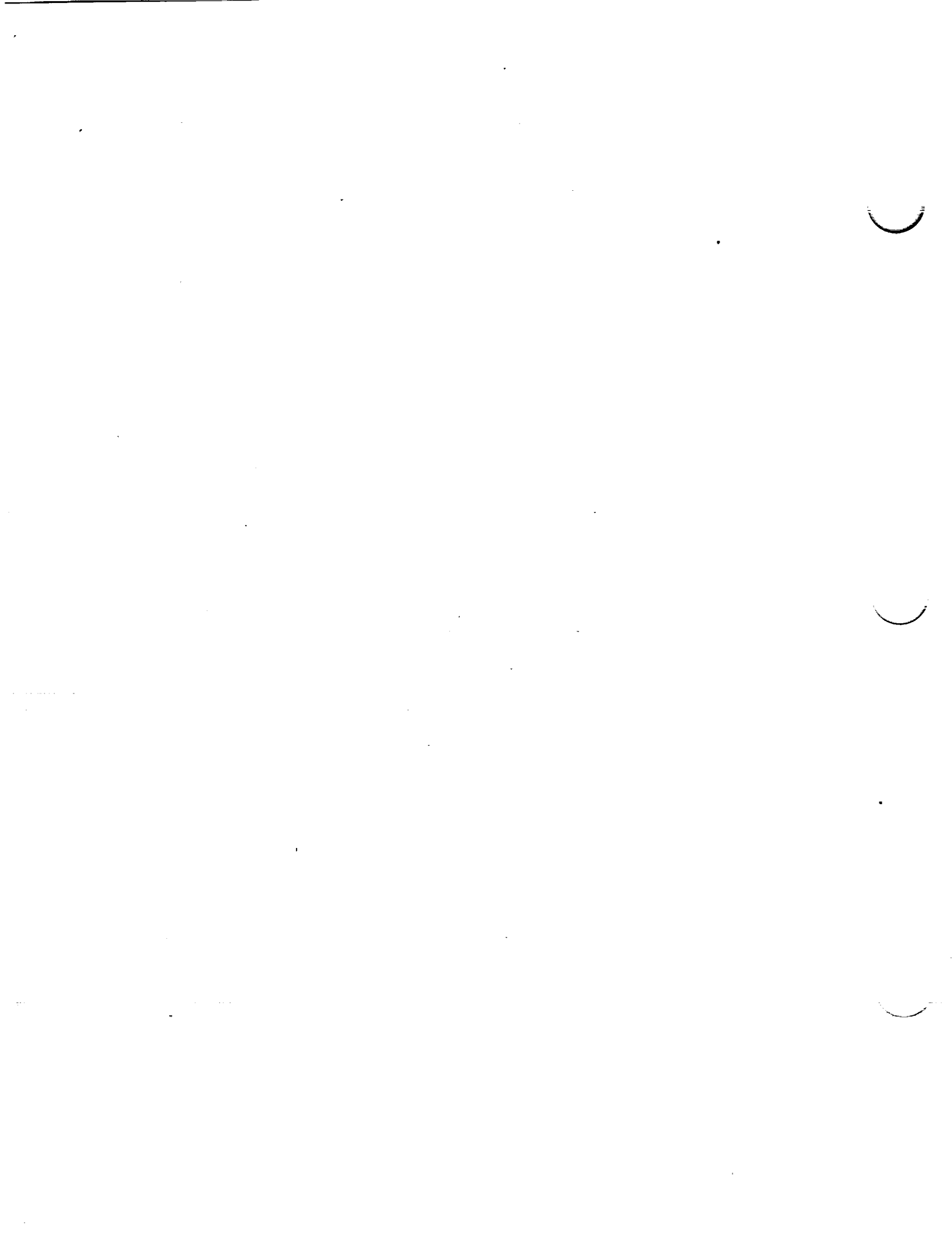


NATIONAL ADVISORY
COMMITTEE FOR AERONAUTICS

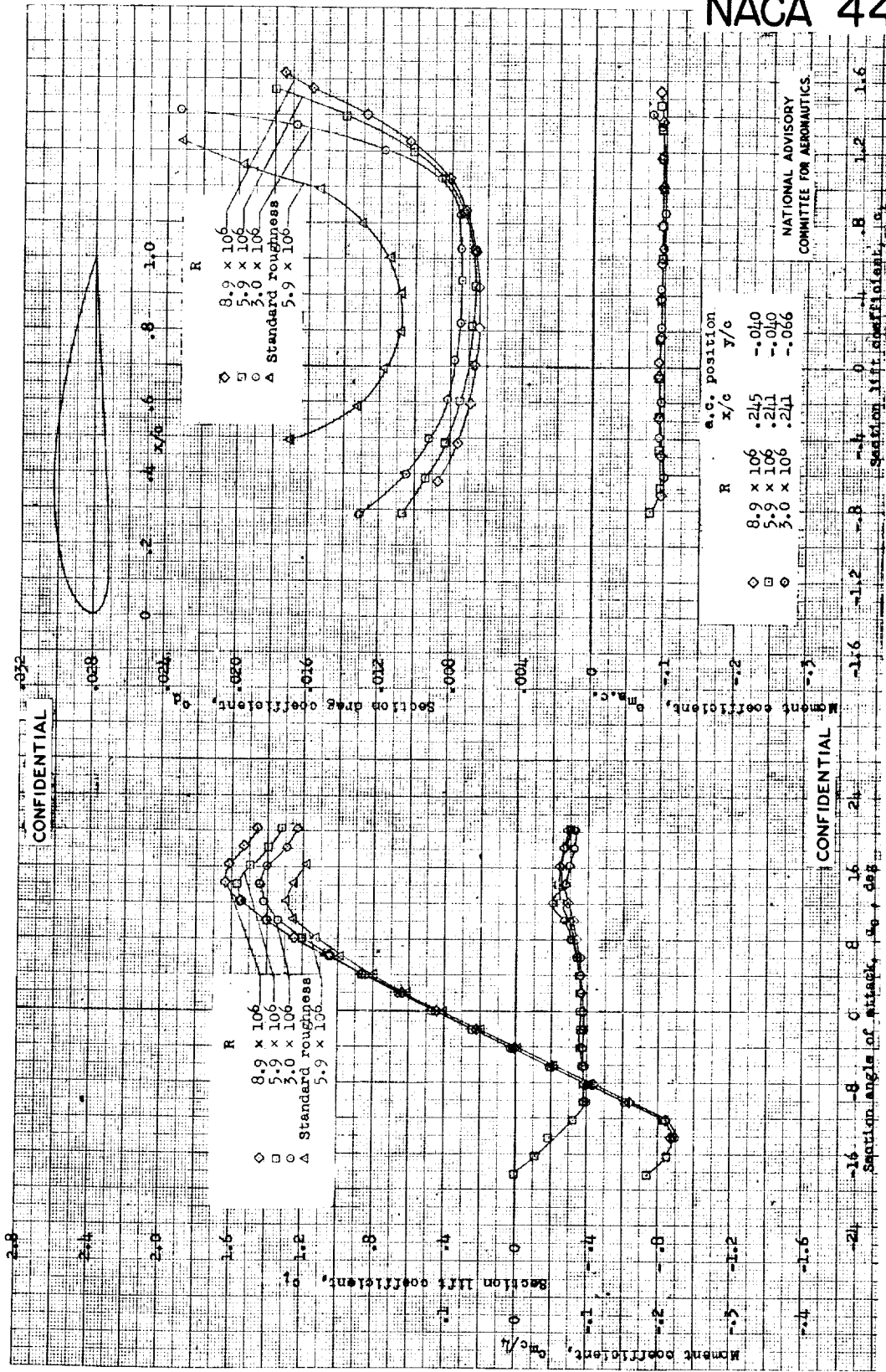
R	a.c. position x/c	y/c
8.9×10^6	.217	-.041
6.0×10^6	.246	-.051
3.0×10^6	.245	-.068

Section lift coefficient, $C_{L, sec}$
 Section drag coefficient, $C_{D, sec}$
 Section moment coefficient, $C_{M, sec}$

Aerodynamic characteristics of the NACA 4412 airfoil section, 24-inch chord; TDT tests 470, 481, 511, 784.

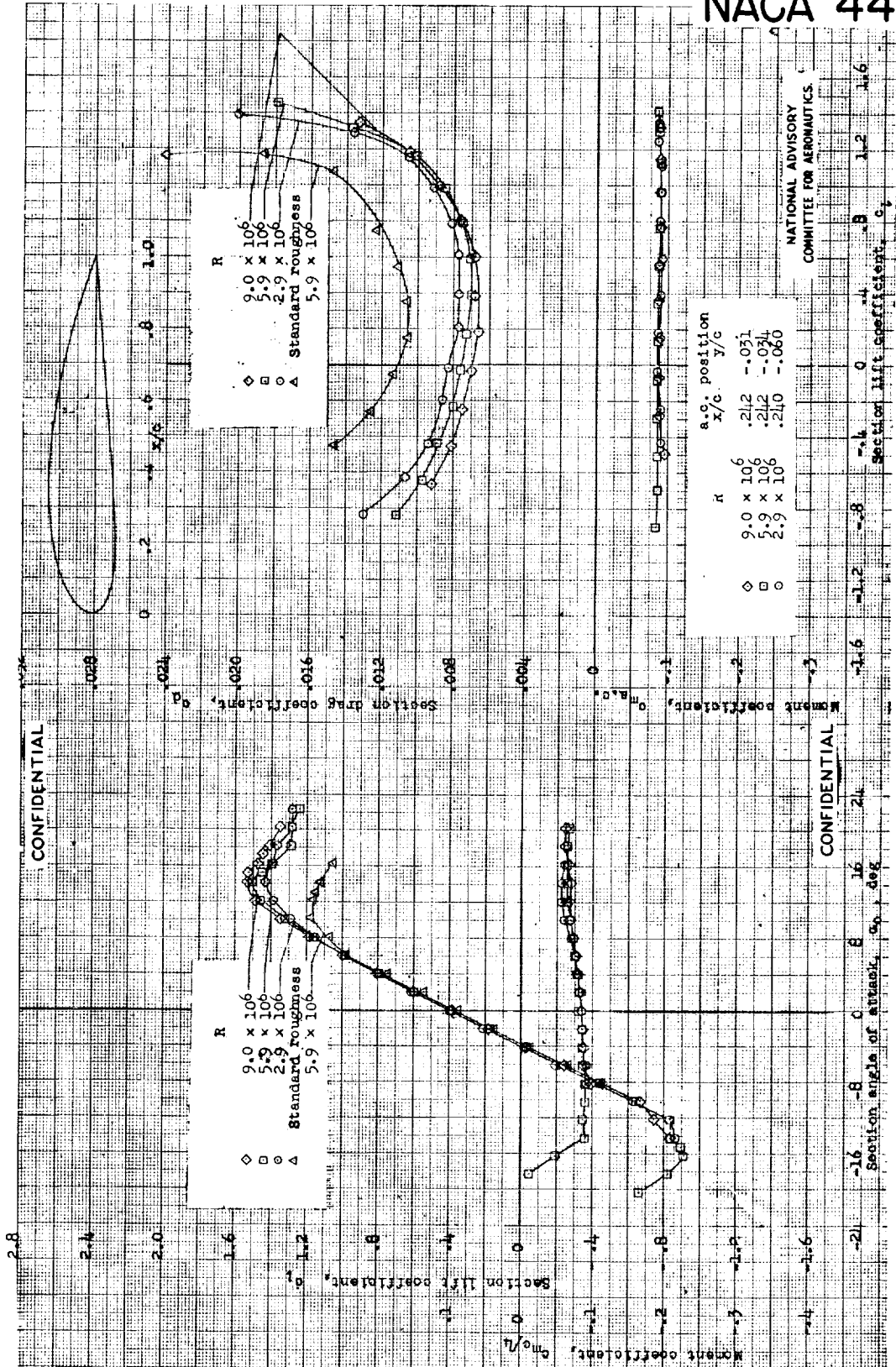


NACA 4415



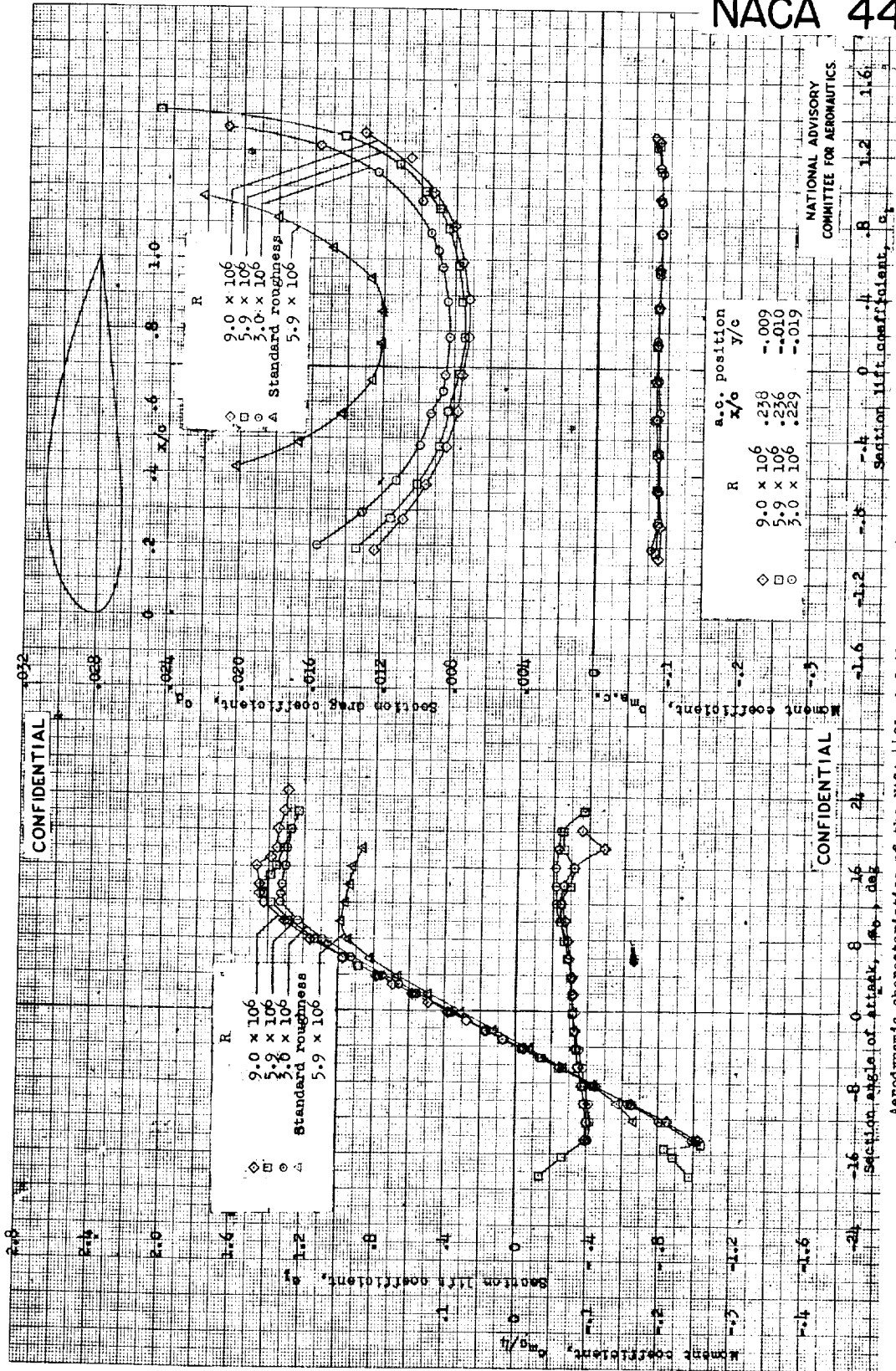


NACA 4418



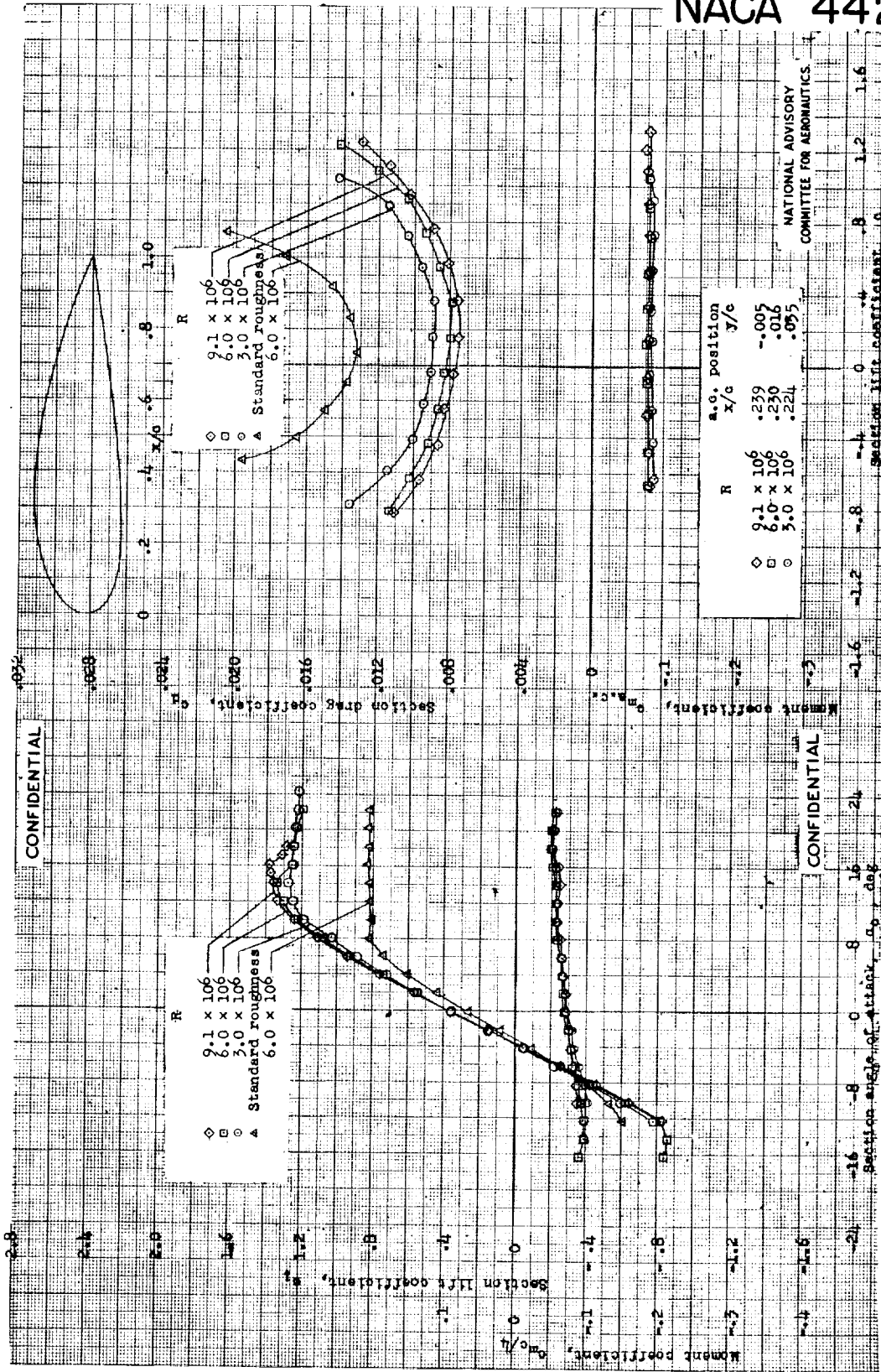


NACA 4421





NACA 4424

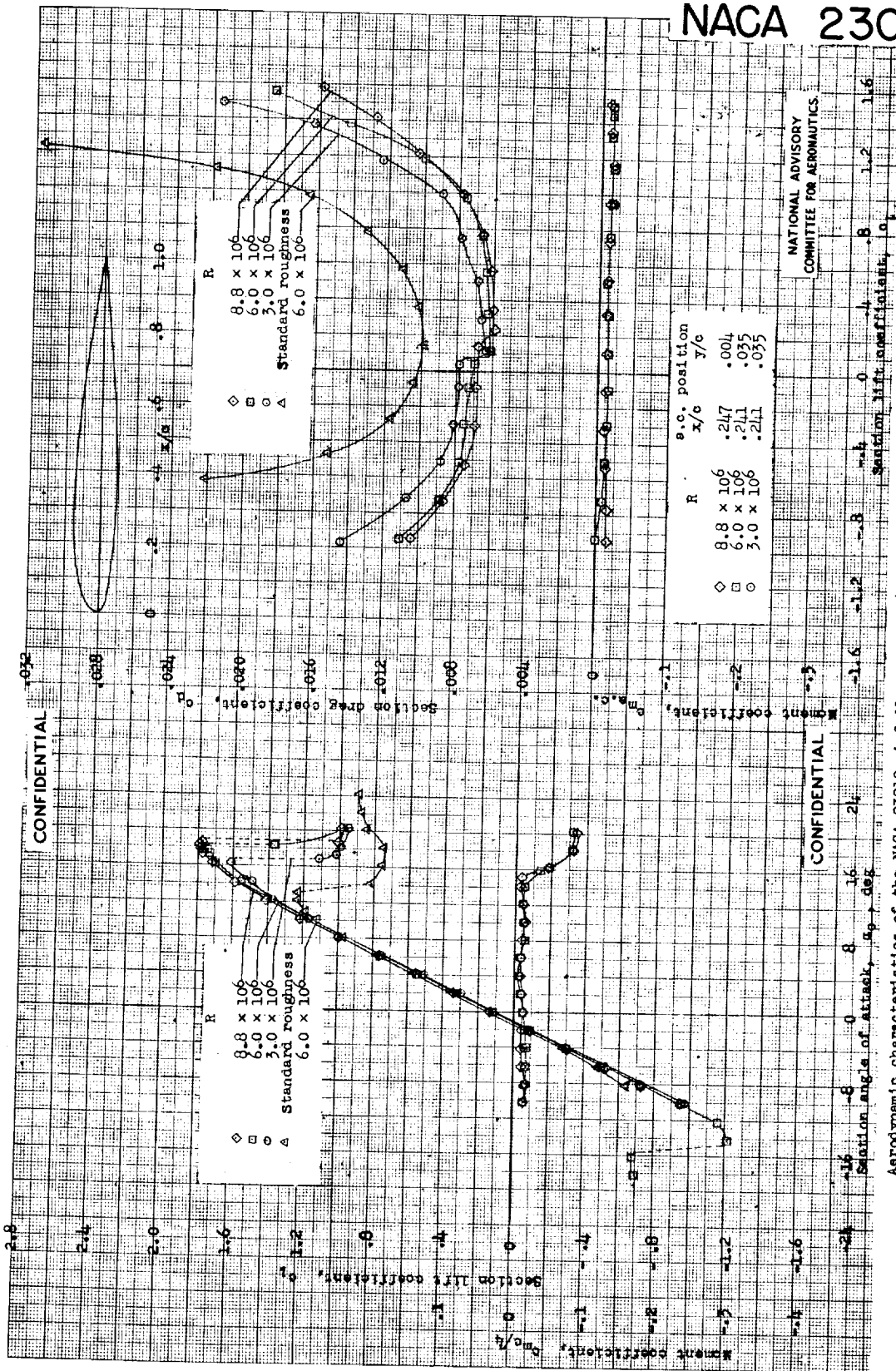


Aerodynamic characteristics of the NACA 4424 airfoil section, 24-inch chord; TDT tests 529, 532.



•

NACA 23012

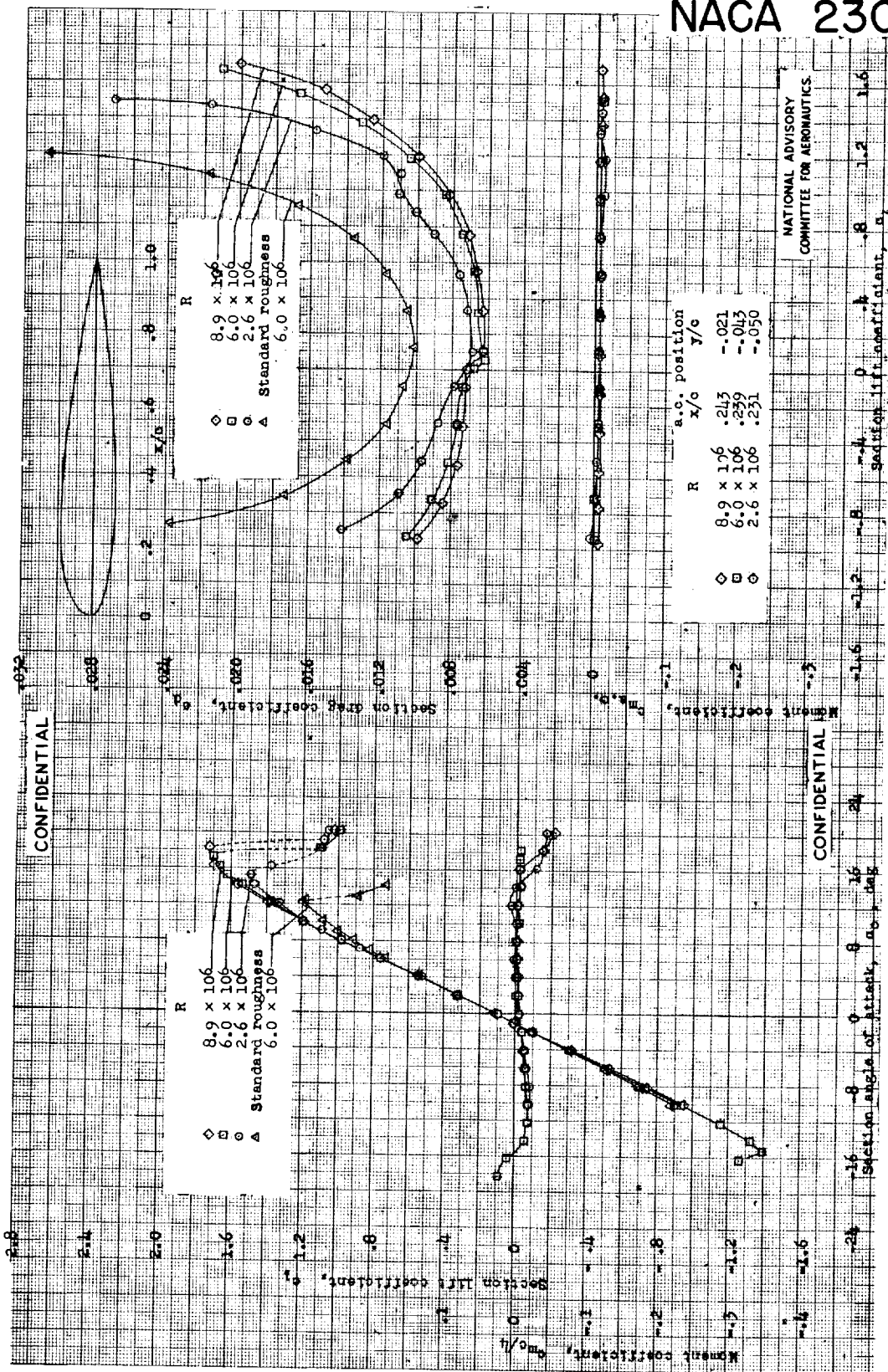


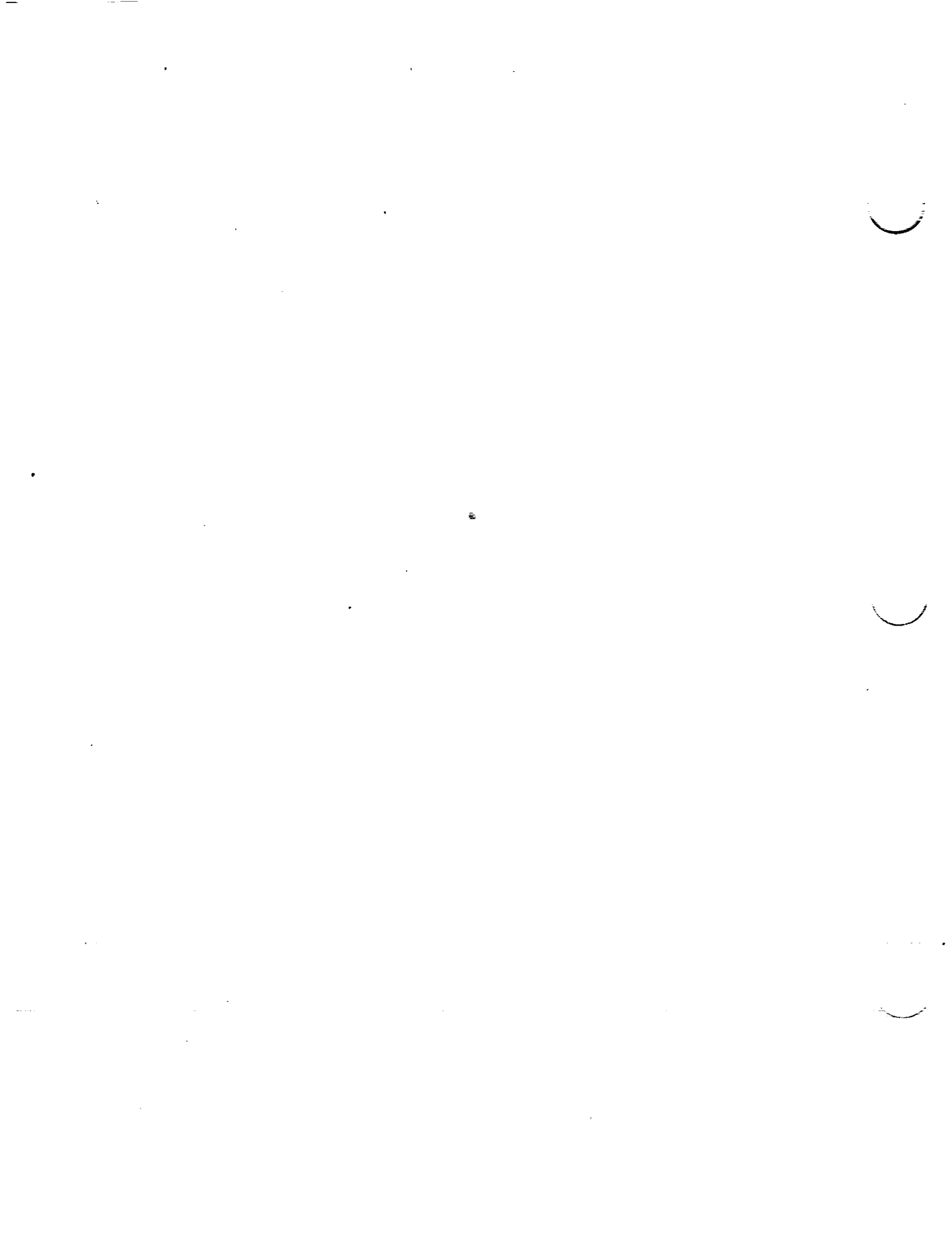
NATIONAL ADVISORY COMMITTEE FOR AERONAUTICS

Aerodynamic characteristics of the NACA 23012 airfoil section, 24-inch chord, TDT tests 494, 497, 523, 785.

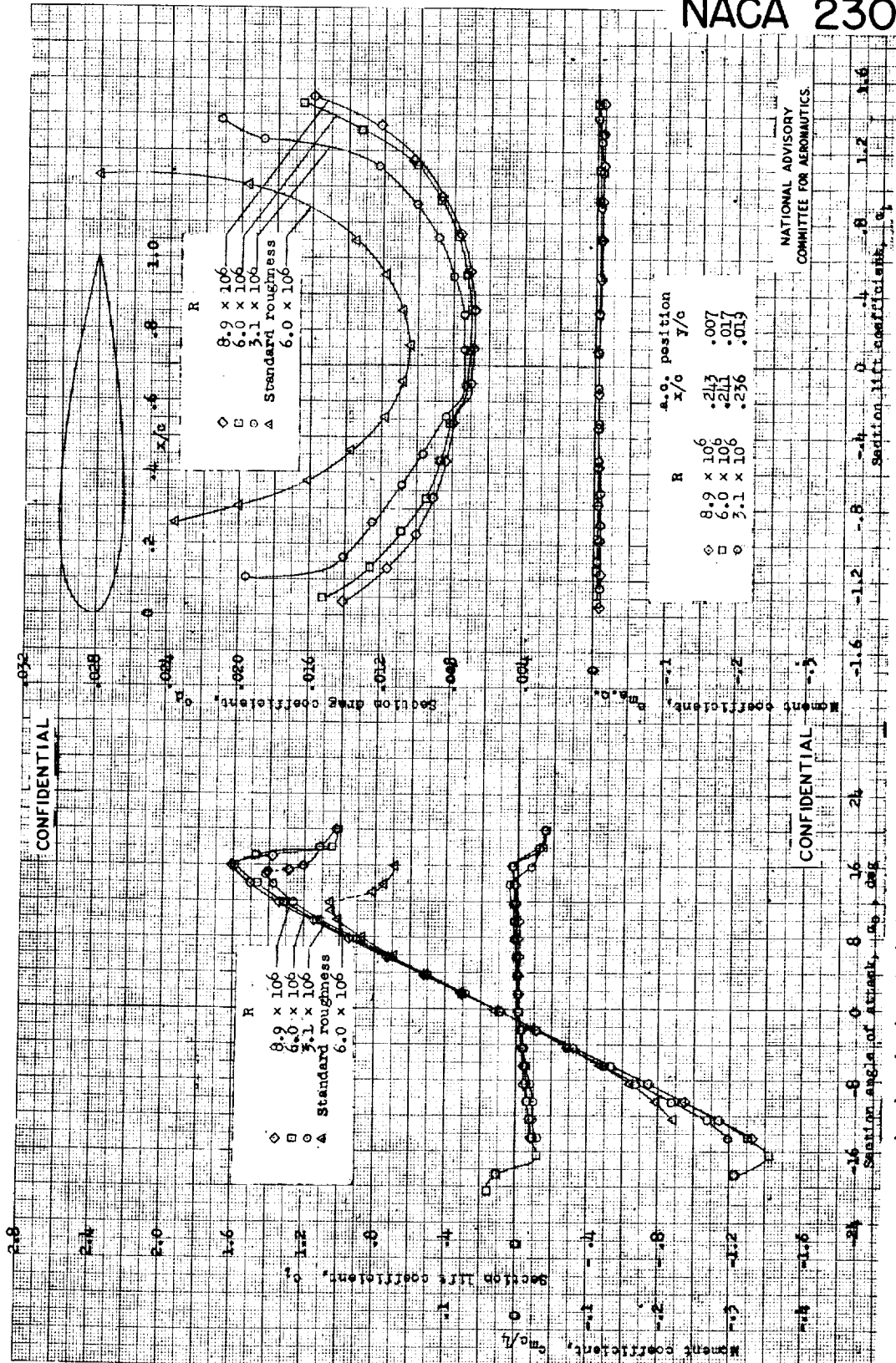


NACA 23015





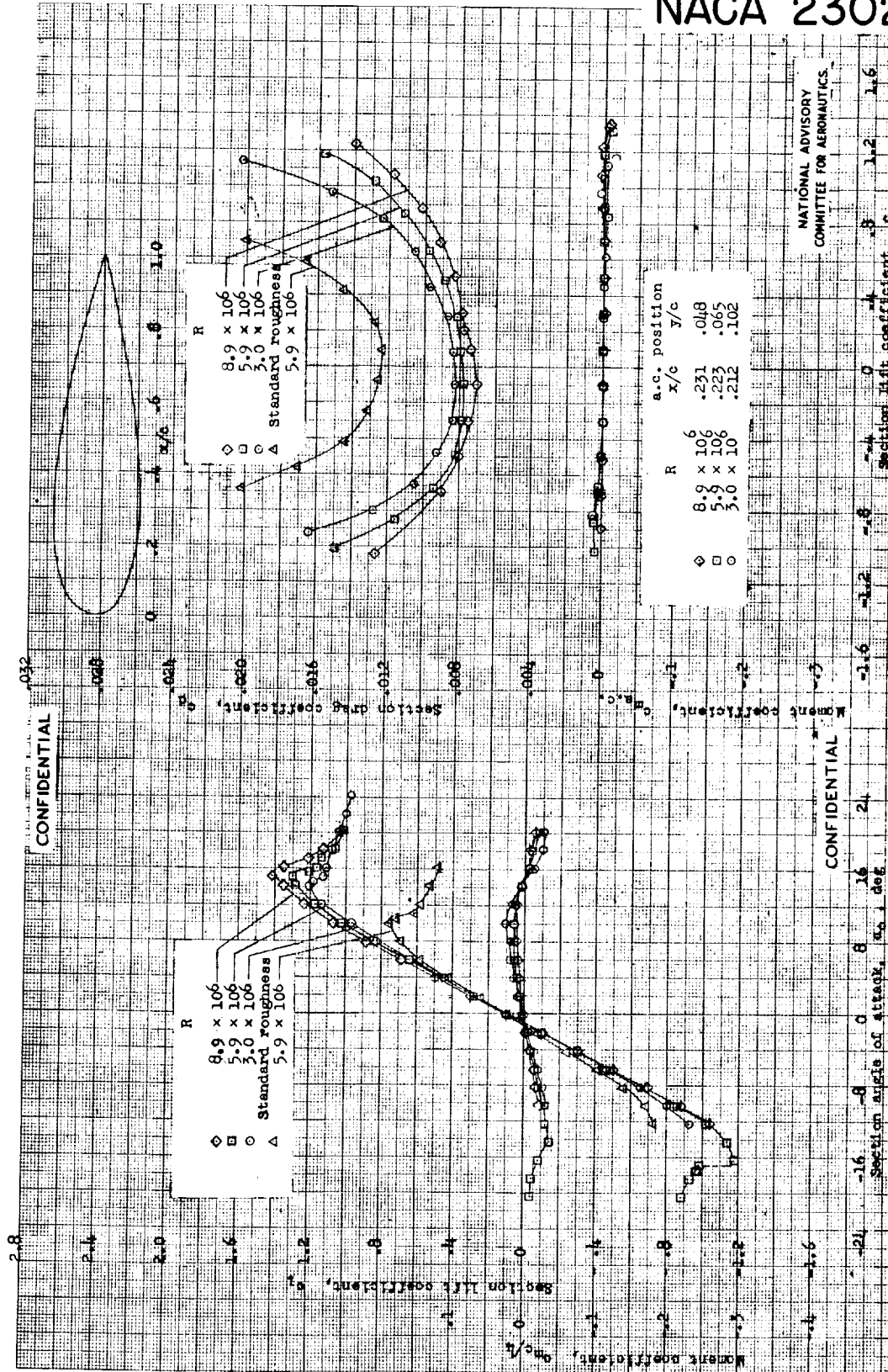
NACA 23018







NACA 23024

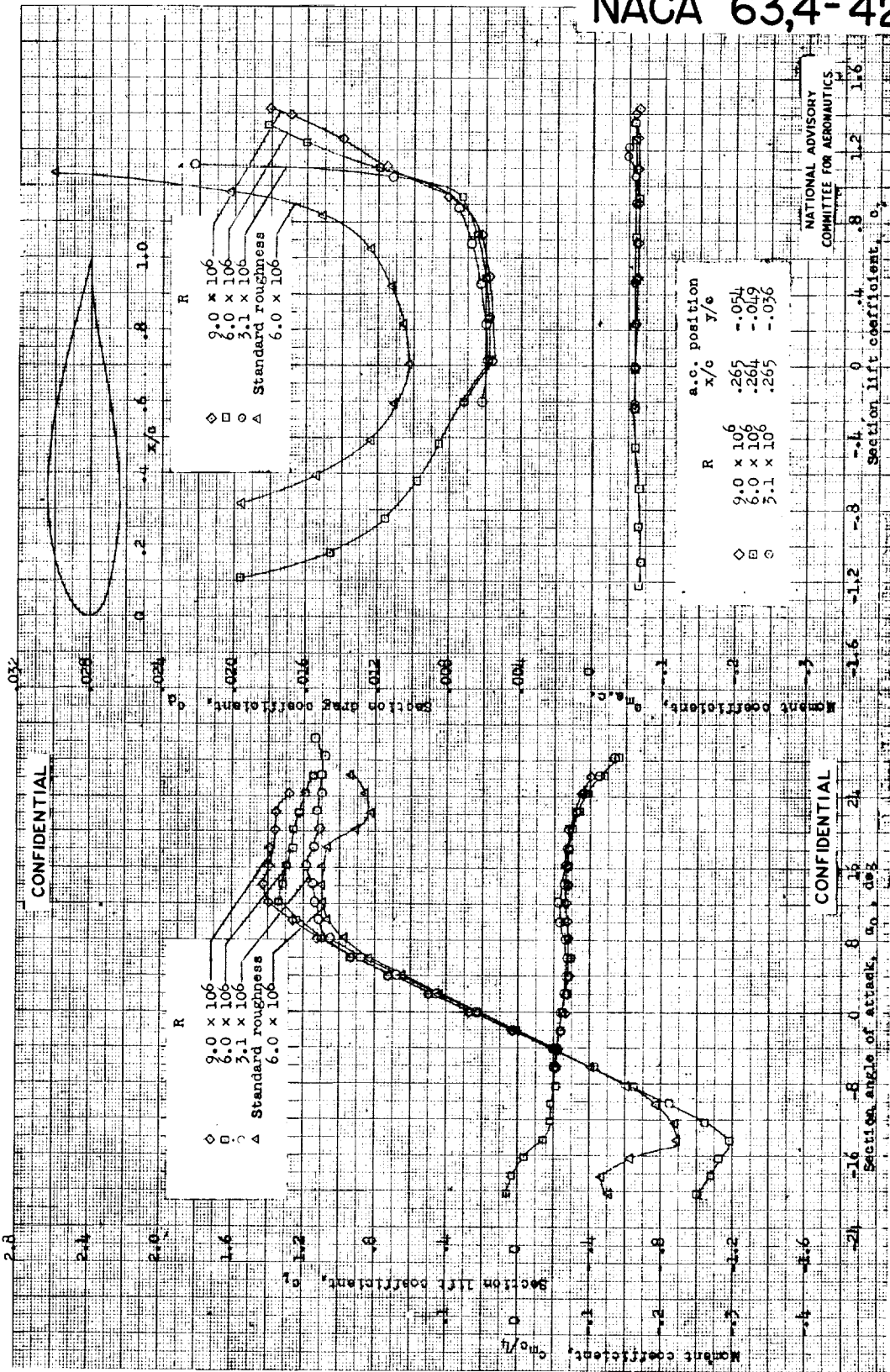


Aerodynamic characteristics of the NACA 23024 airfoil section, 24-inch chord; TDT tests 534, 536.

NATIONAL ADVISORY
COMMITTEE FOR AERONAUTICS.



NACA 63,4-420



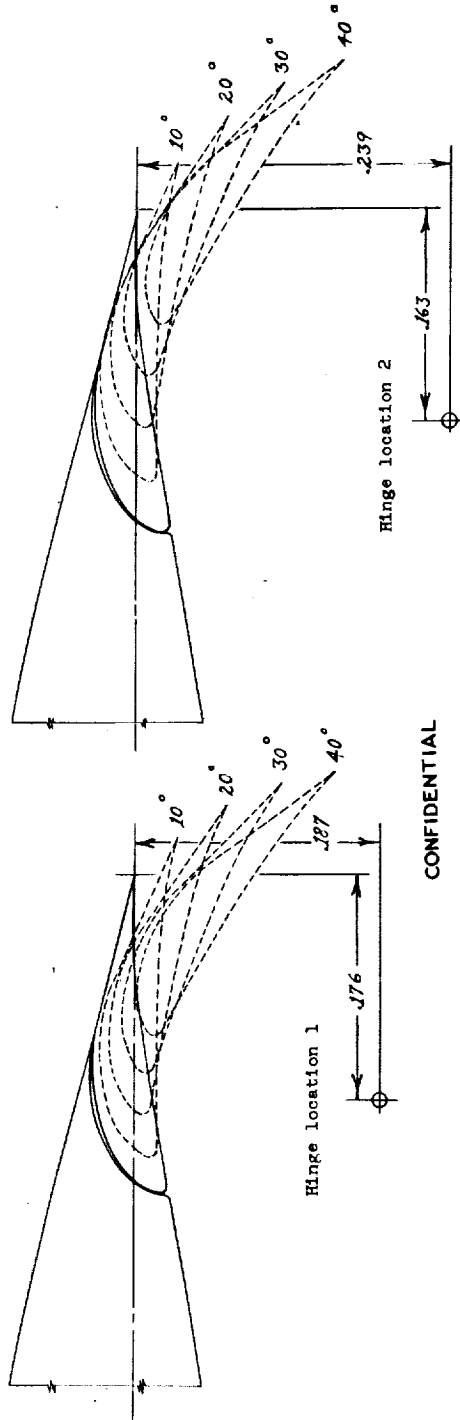
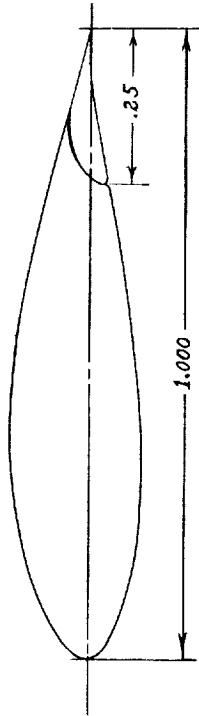
NATIONAL ADVISORY
COMMITTEE FOR AERONAUTICS

Aerodynamic characteristics of the NACA 63,4-420 airfoil section, 21-inch chord: TDT tests 241, 243.



NACA 63,4-420 WITH FLAP

CONFIDENTIAL



CONFIDENTIAL

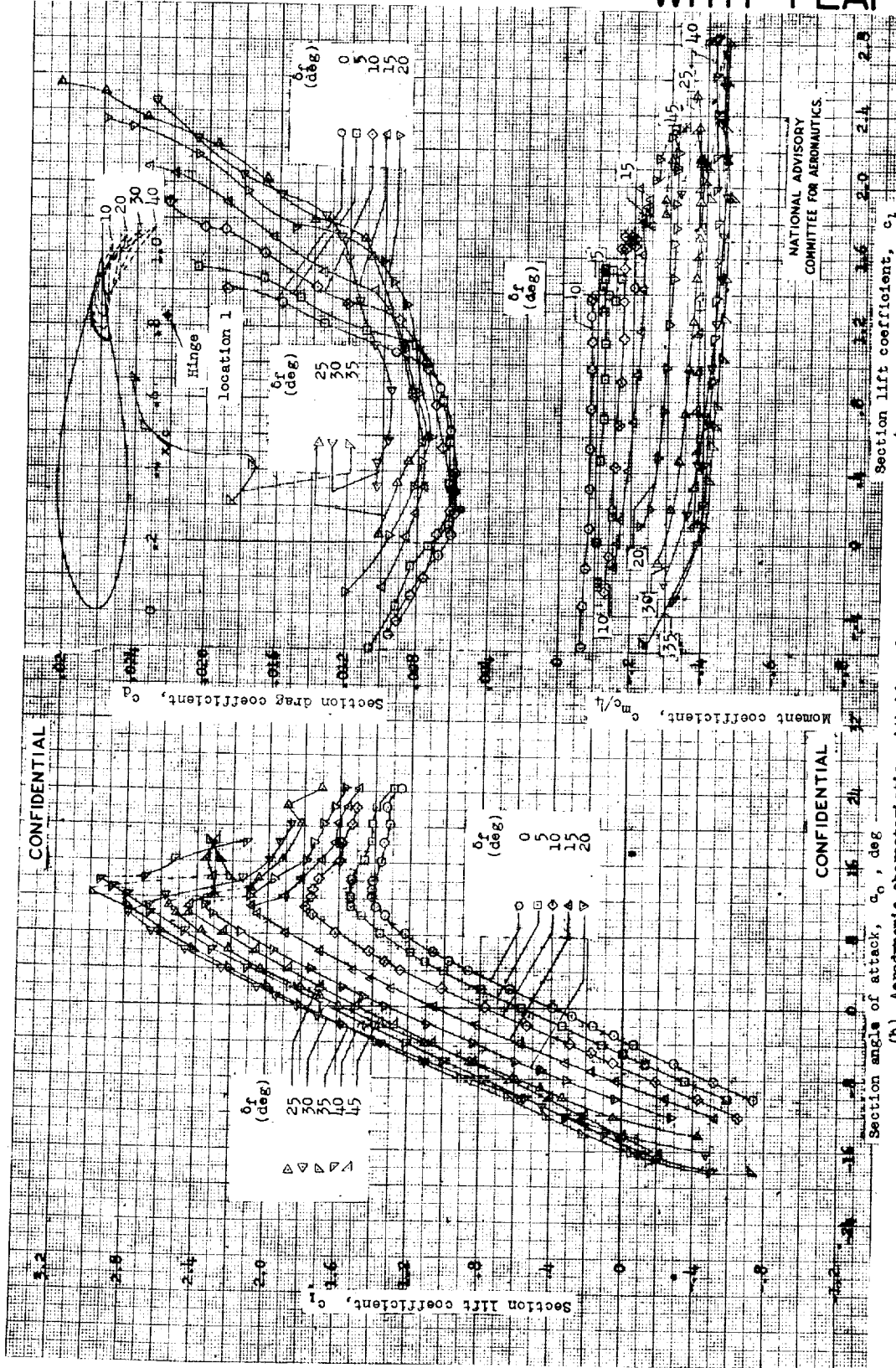
(a) Configuration.

NACA 63,4-420 airfoil section with 0.25c slotted flap.

NATIONAL ADVISORY
COMMITTEE FOR AERONAUTICS



NACA 63,4-420 WITH FLAP

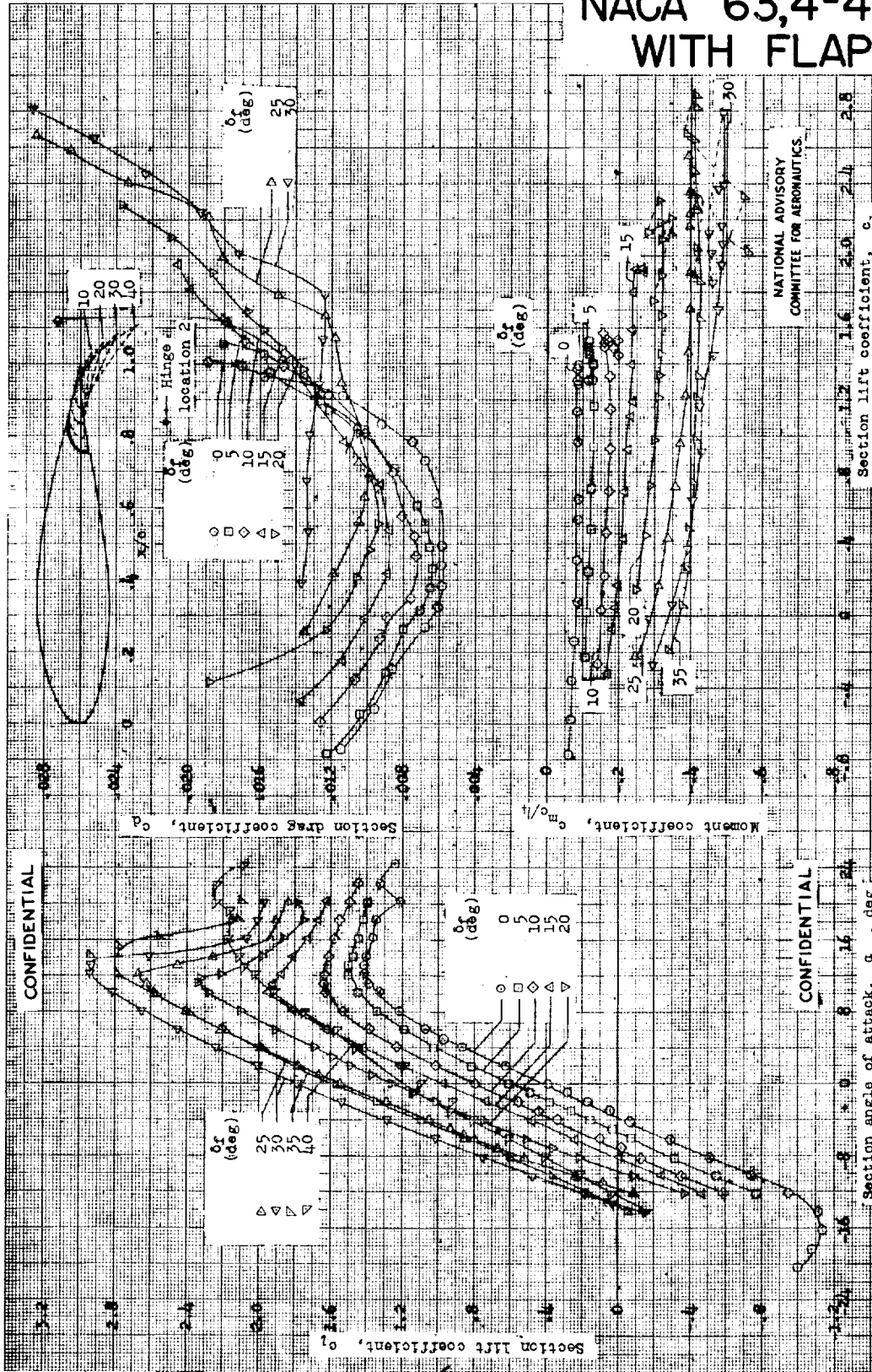


(b) Aerodynamic characteristics with hinge location 1. $R, 6 \times 10^6$; EDF tests 374, 385.

NACA 63,4-420 airfoil section with 0.25c slotted flap.



NACA 63,4-420 WITH FLAP



NATIONAL ADVISORY
COMMITTEE FOR AERONAUTICS

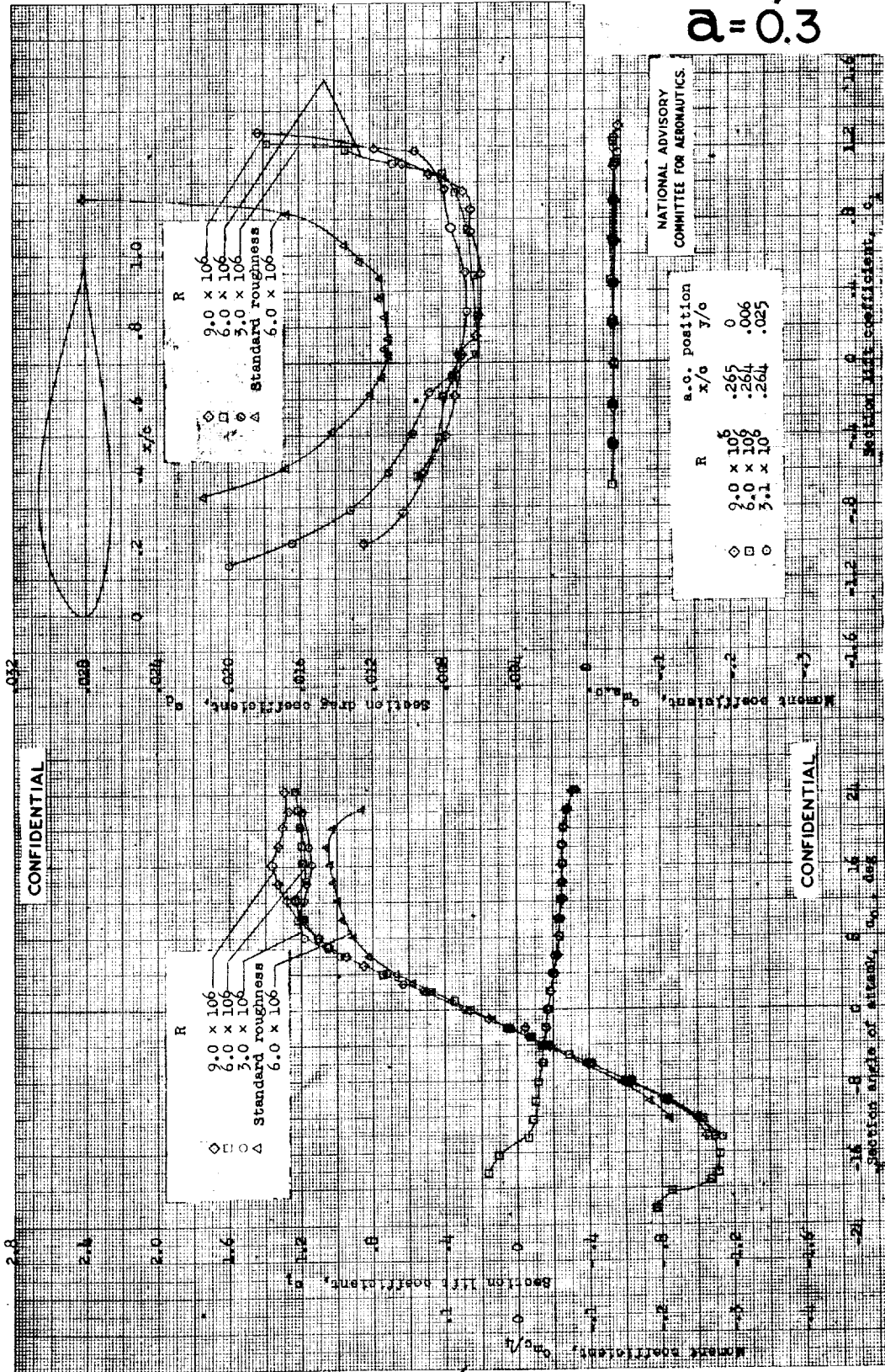
Section angle of attack, α , deg
 Section lift coefficient, C_l
 Section drag coefficient, C_d
 Moment coefficient, C_m

(c) aerodynamic characteristics with hinge location 2. $R, 6 \times 10^6$; TD7 tests
 383 and 384

NACA 63,4-420 airfoil section with 0.25c slotted flap.



NACA 63,4-420
 $\alpha = 0.3$



Aerodynamic characteristics of the NACA 63,4-420, $\alpha = 0.3$ airfoil section, 24-inch chord; TRF tests 402, 408.

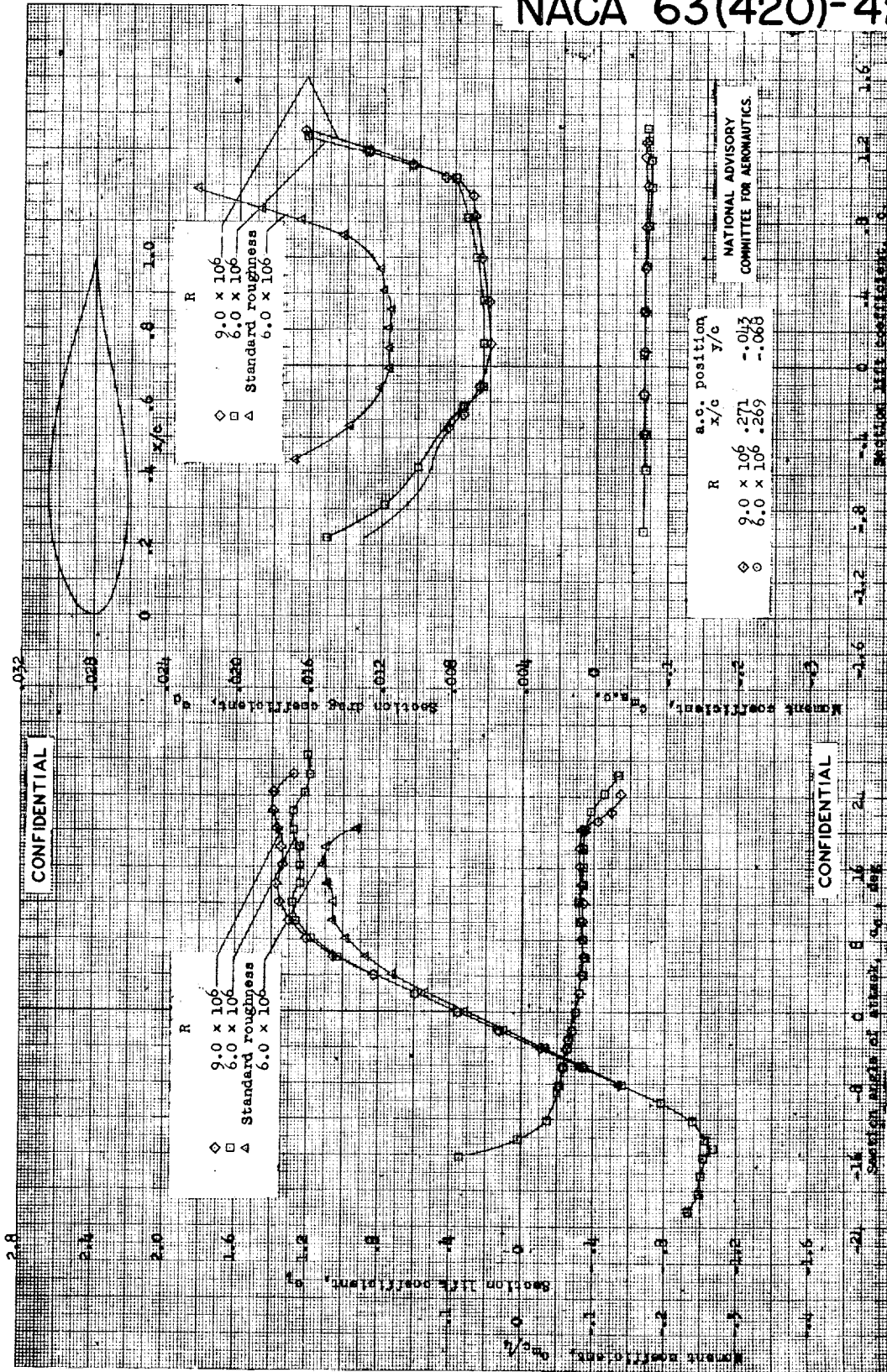
CONFIDENTIAL

CONFIDENTIAL

NATIONAL ADVISORY COMMITTEE FOR AERONAUTICS



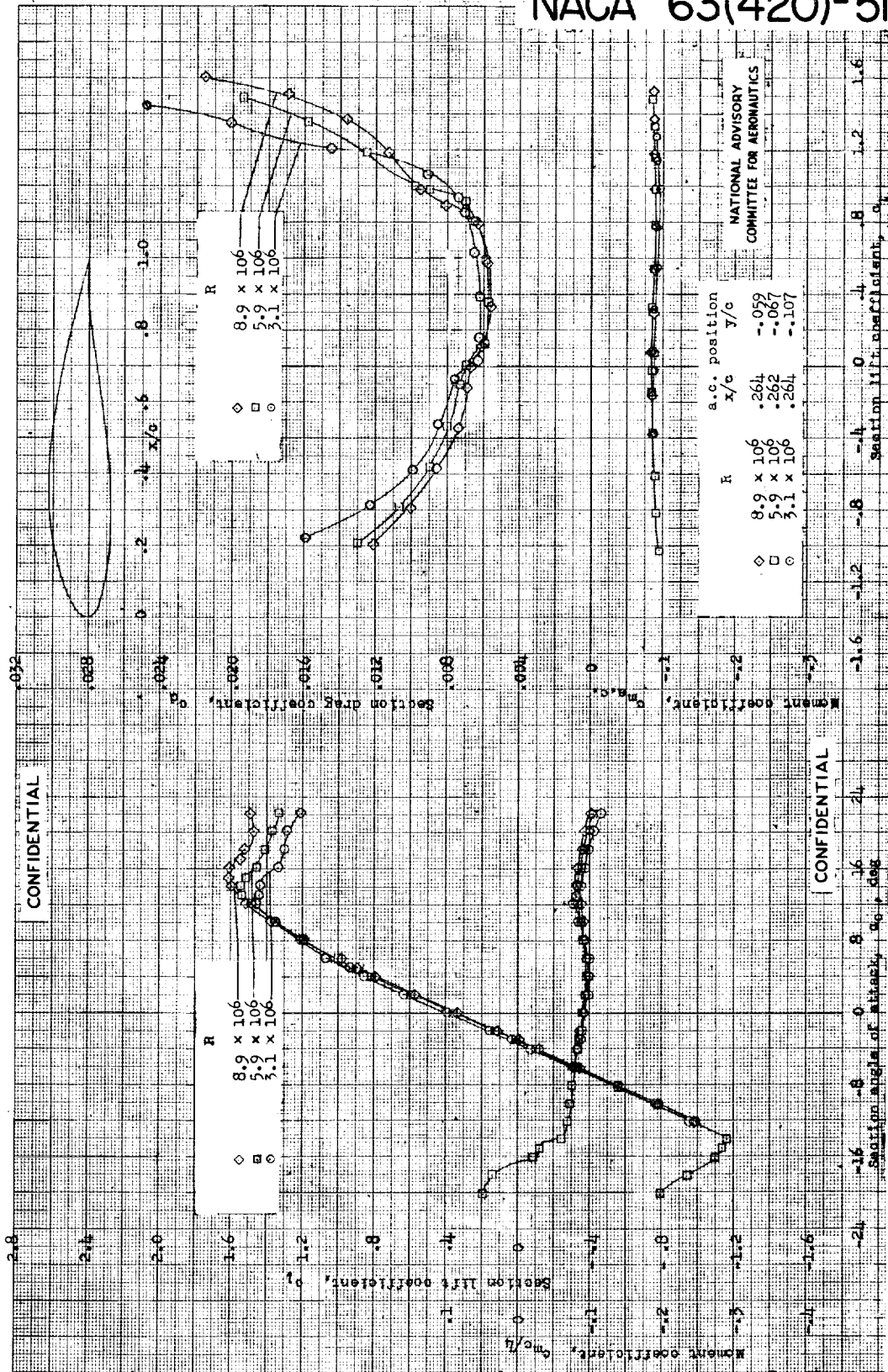
NACA 63(420)-422

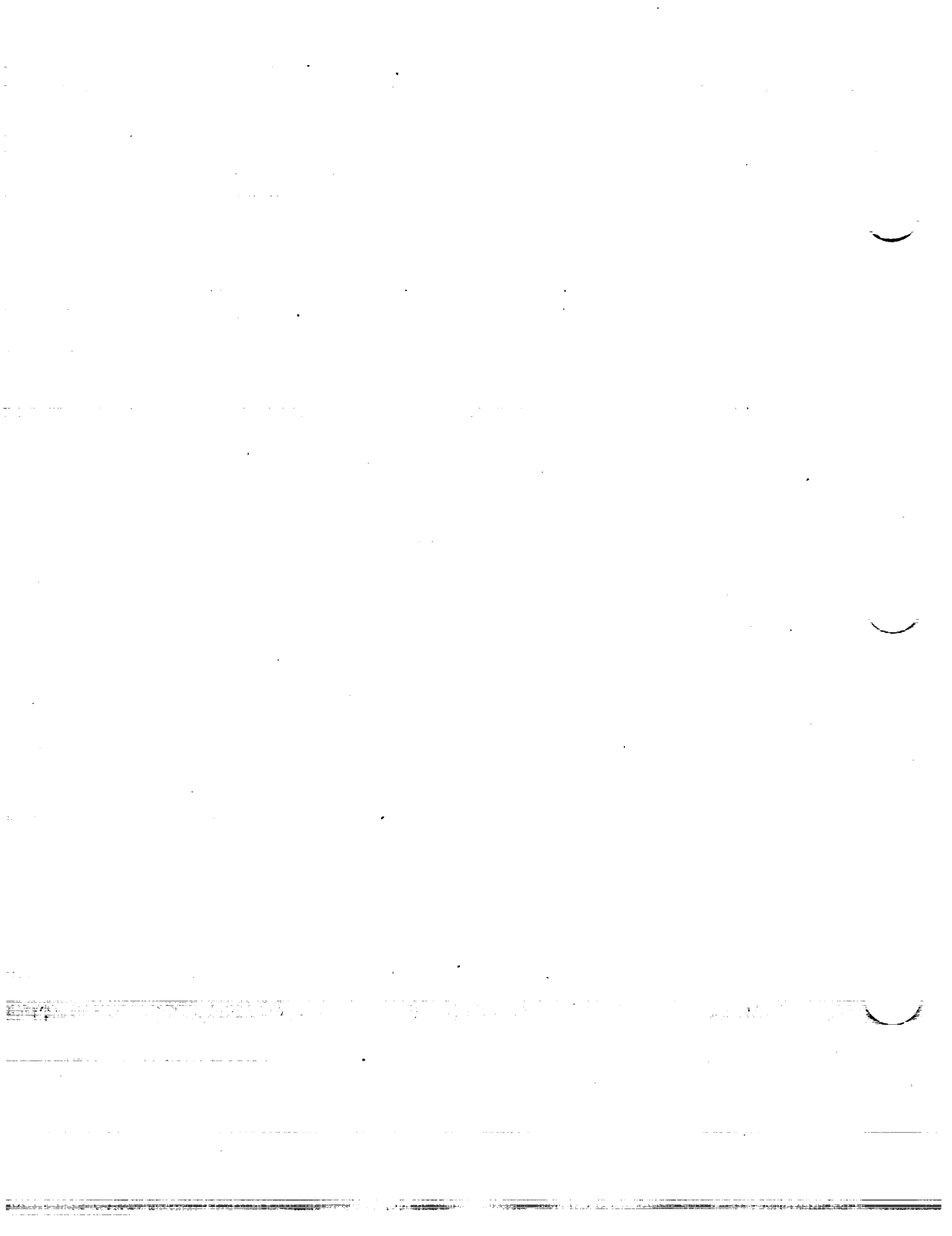


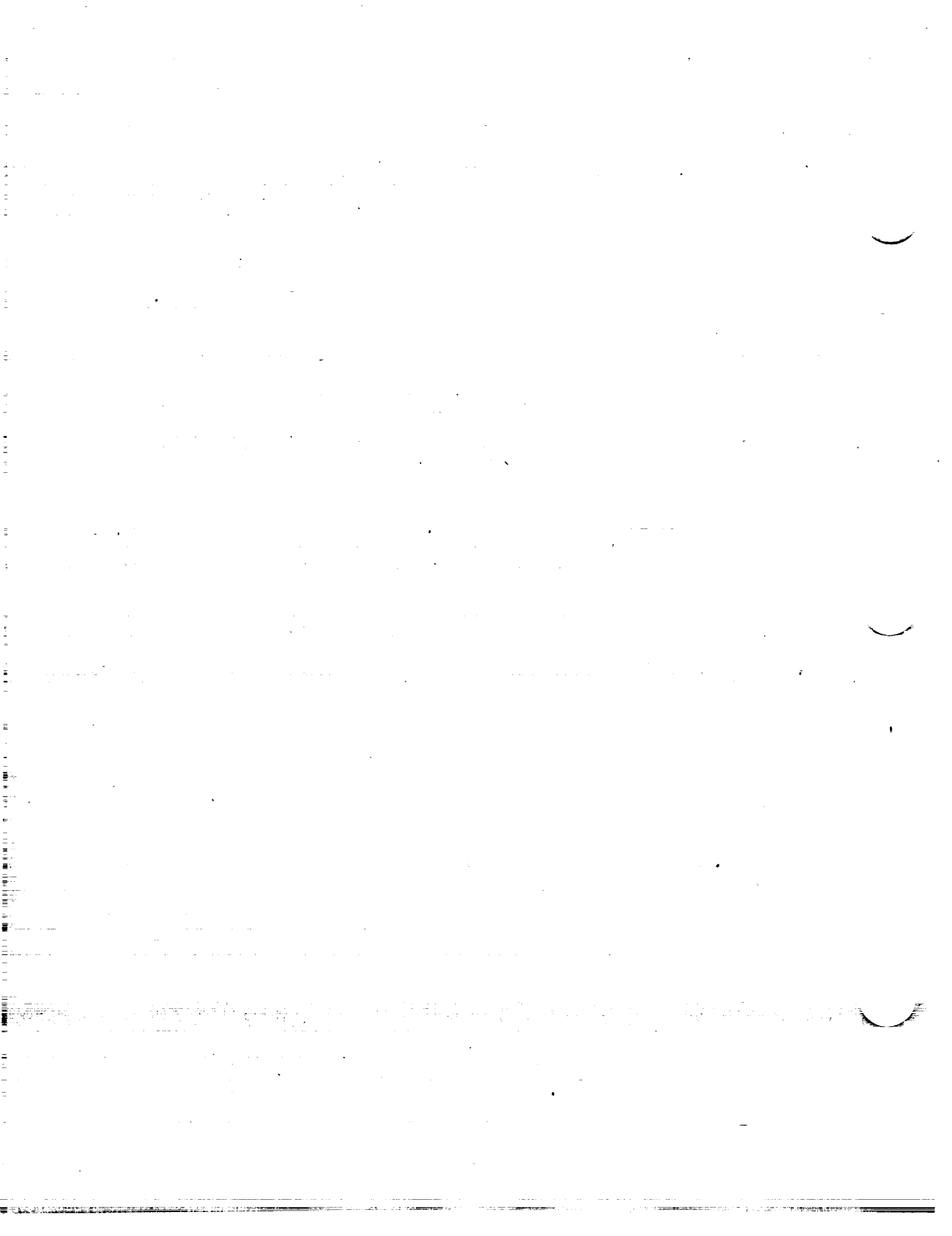
Aerodynamic characteristics of the NACA 63(420)-422 airfoil section, 24-inch chord; DT tests 228, 242.



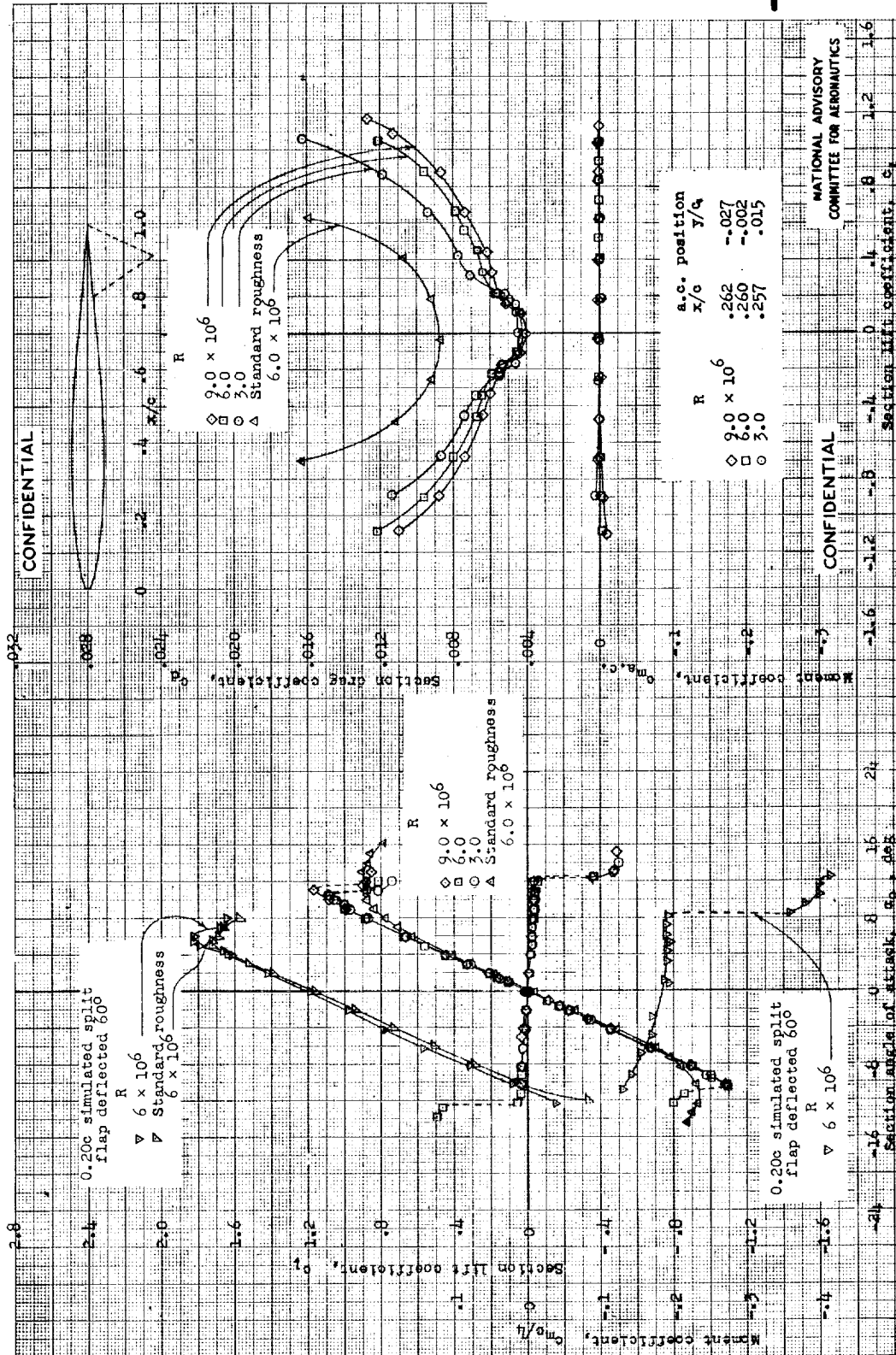
NACA 63(420)-517





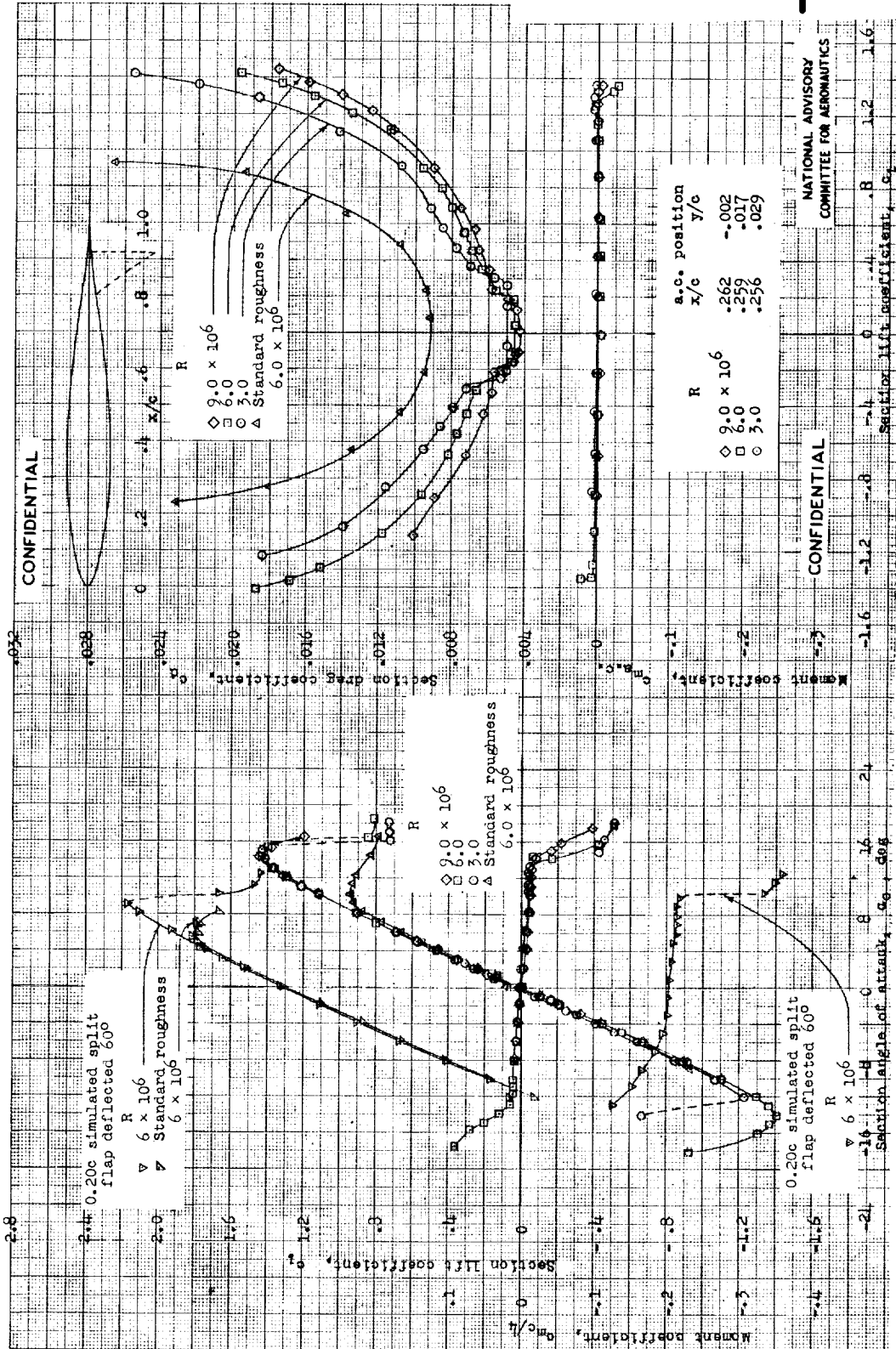


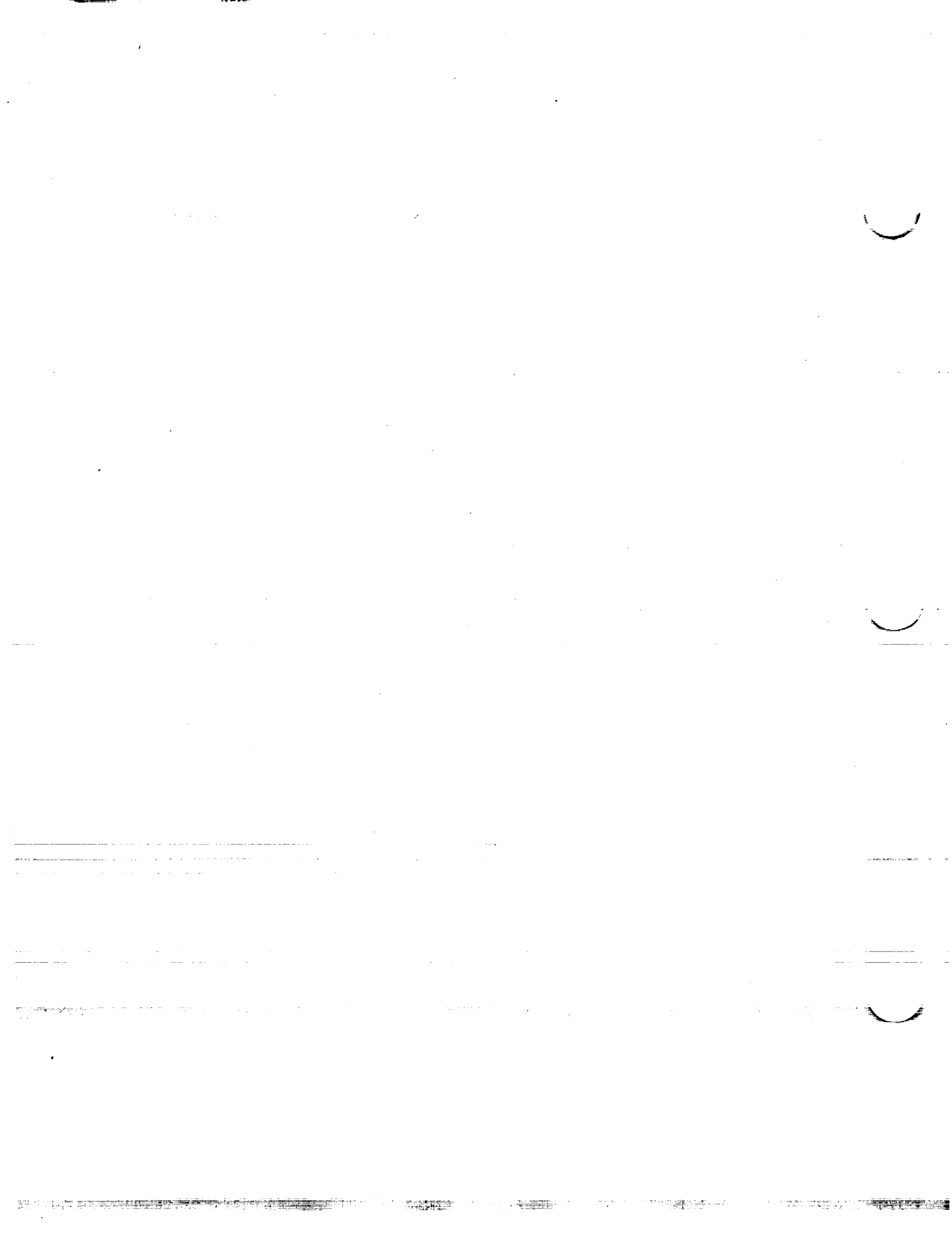
NACA 64-009





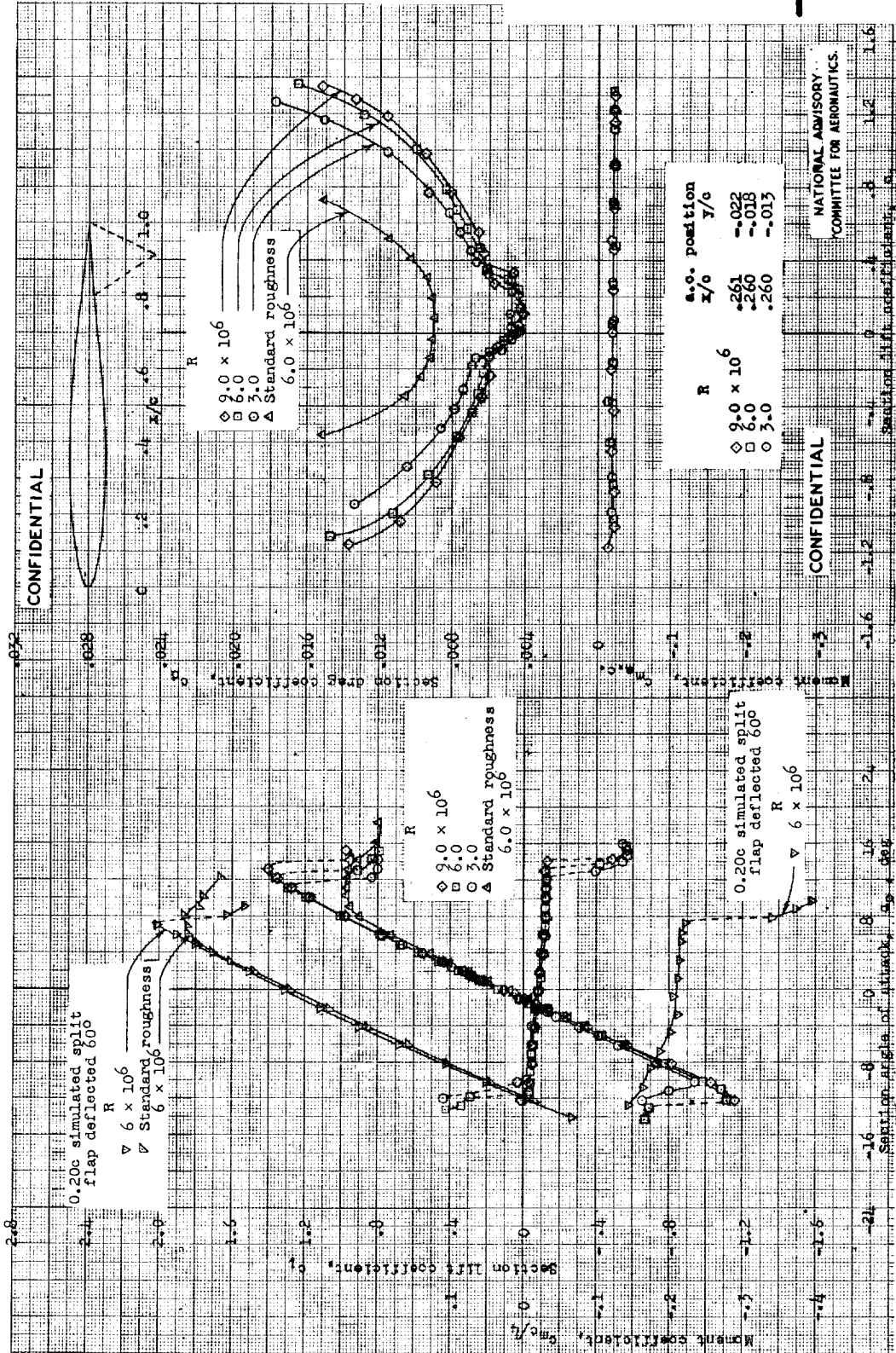
NACA 64₁-012







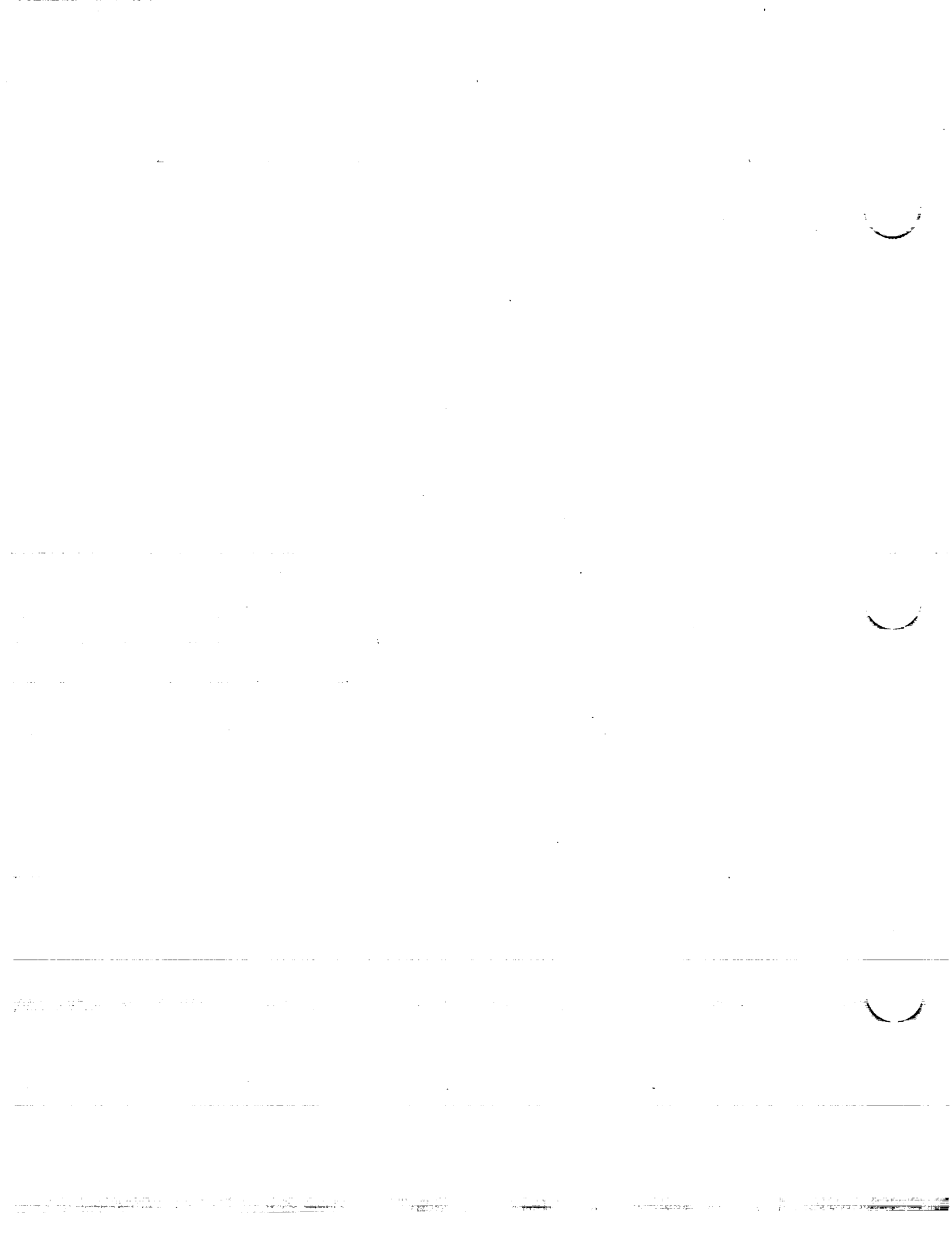
NACA 64₁-110



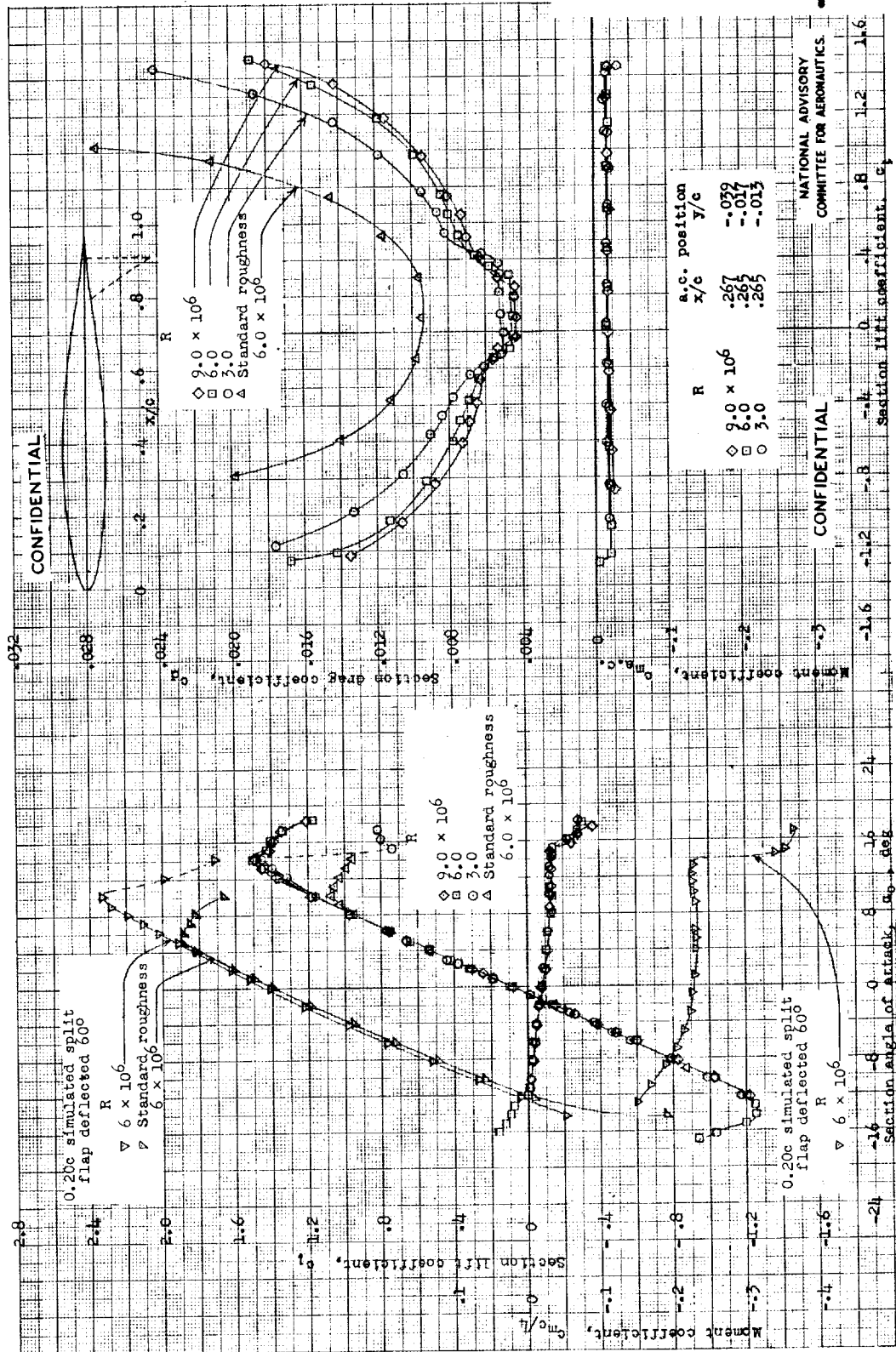
CONFIDENTIAL

CONFIDENTIAL

NATIONAL ADVISORY
COMMITTEE FOR AERONAUTICS



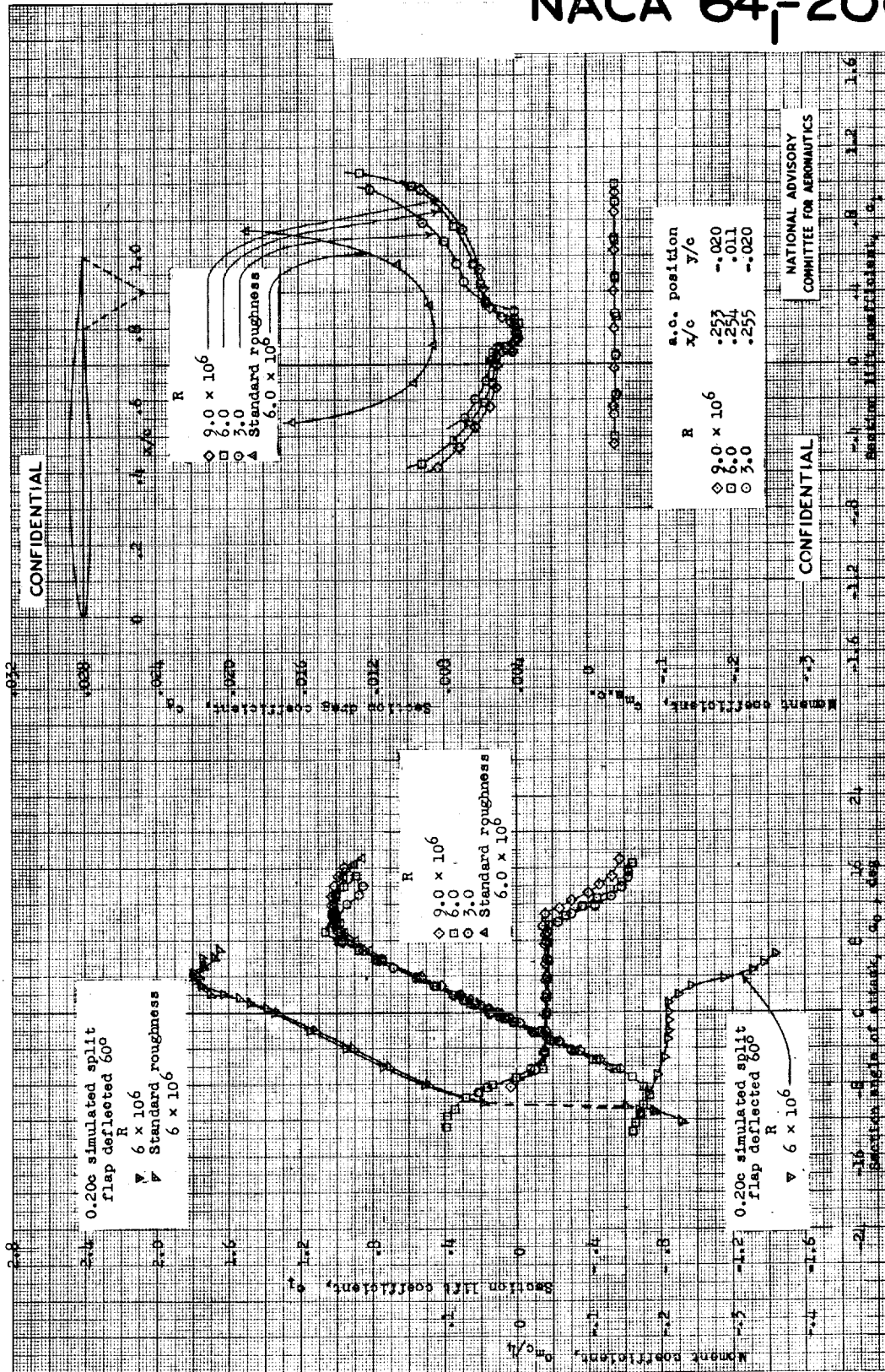
NACA 64₁-112

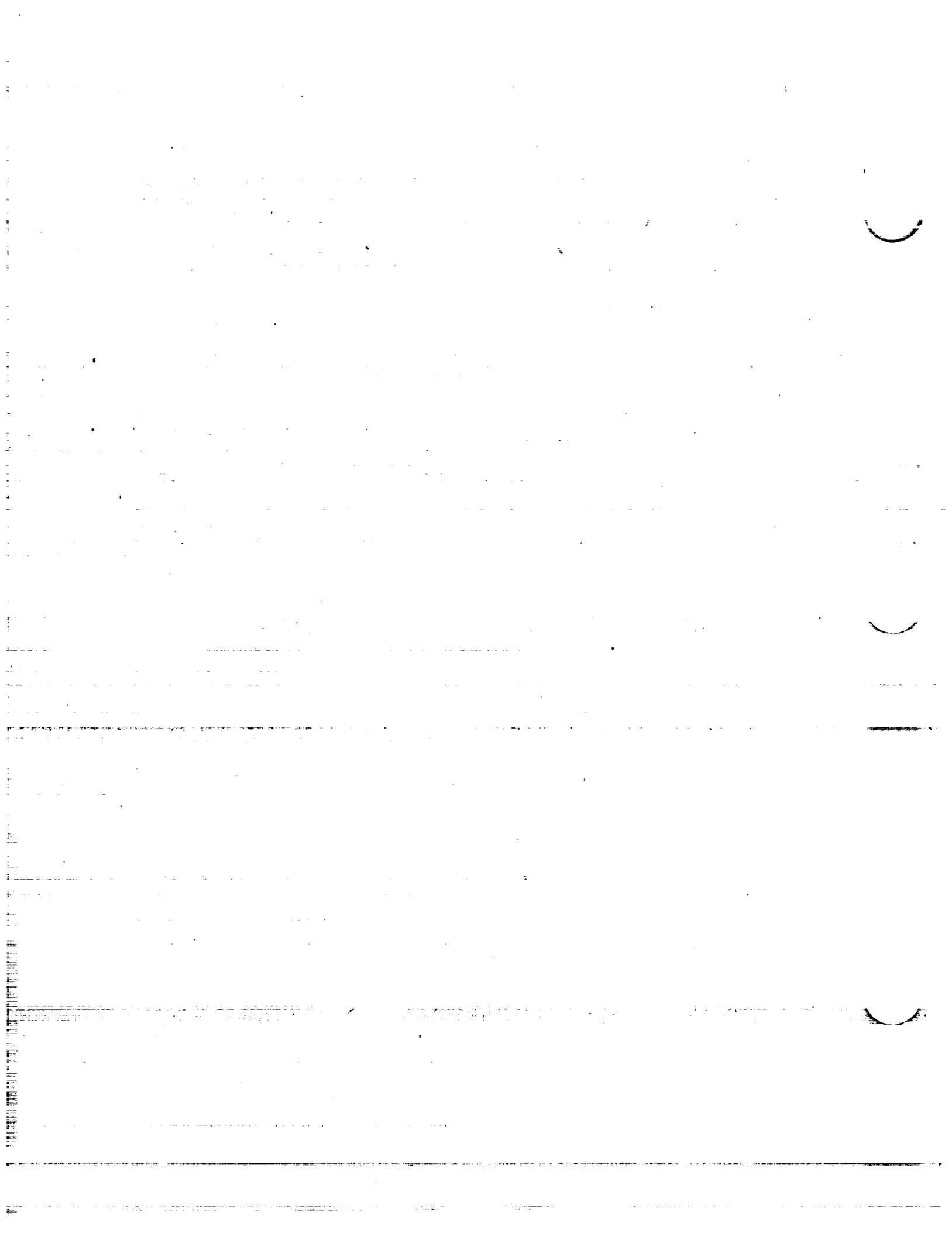


Aerodynamic characteristics of the NACA 64₁-112 airfoil section, 24-inch chord; TDT test 819.

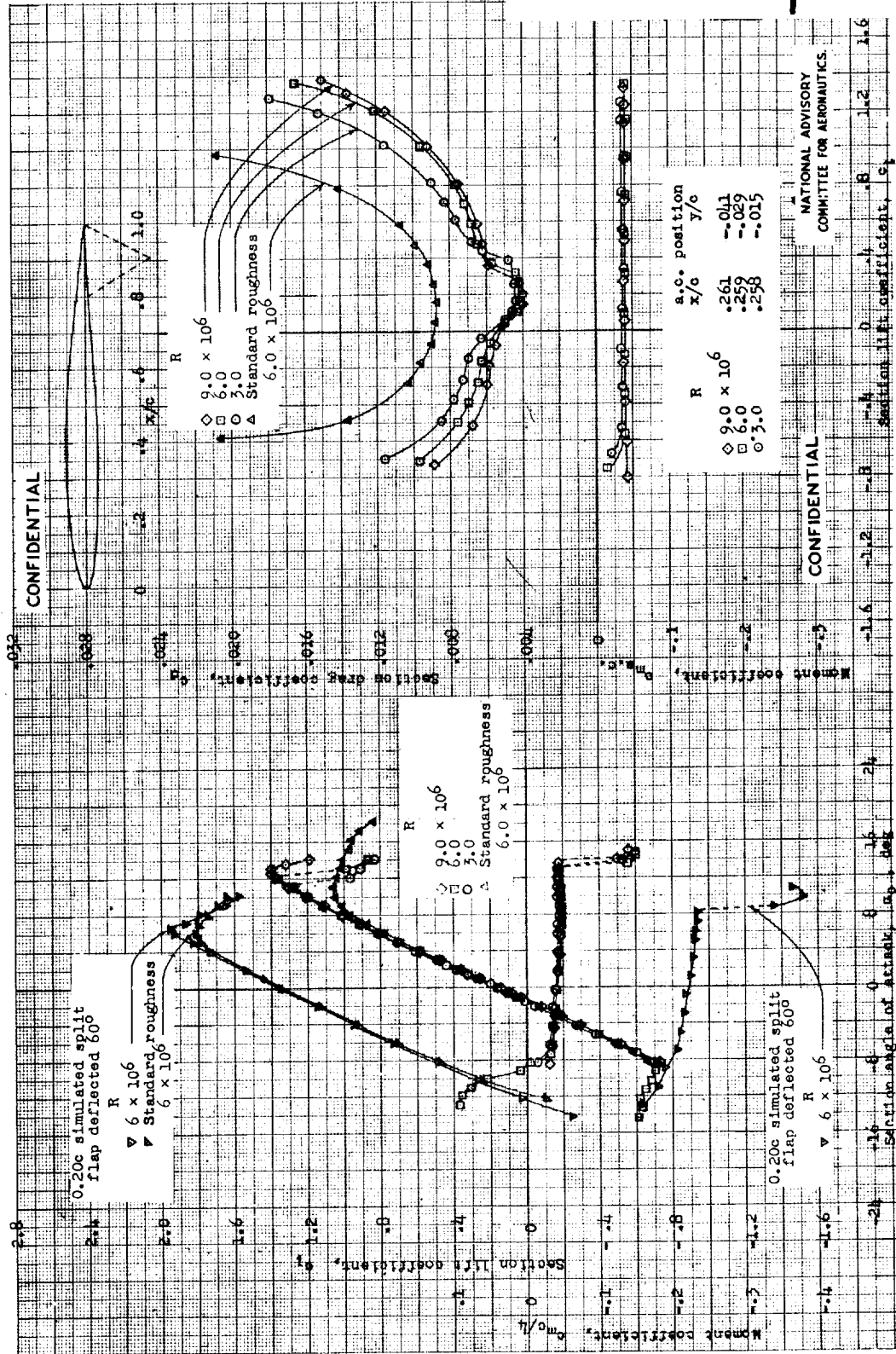


NACA 64-206



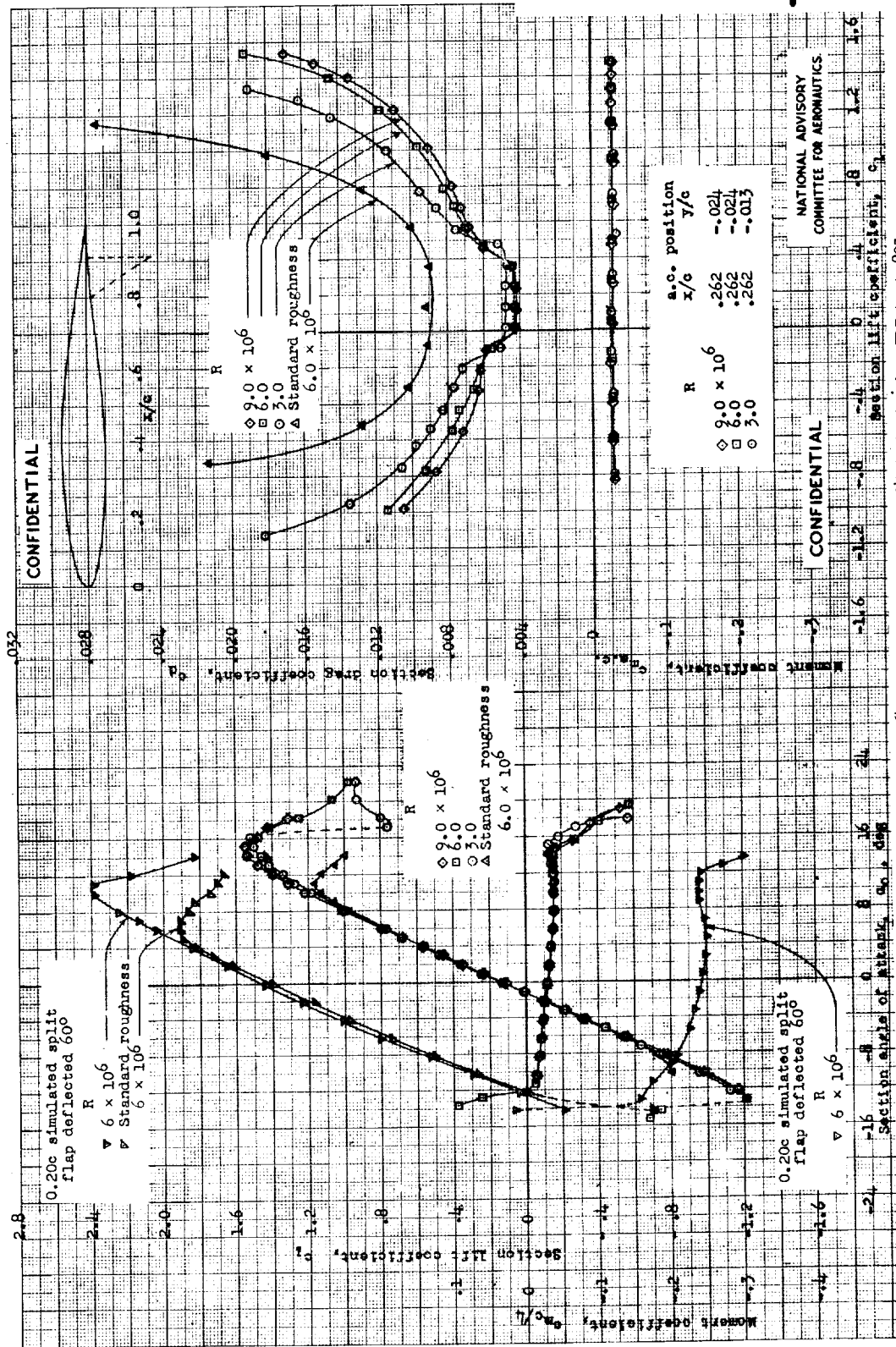


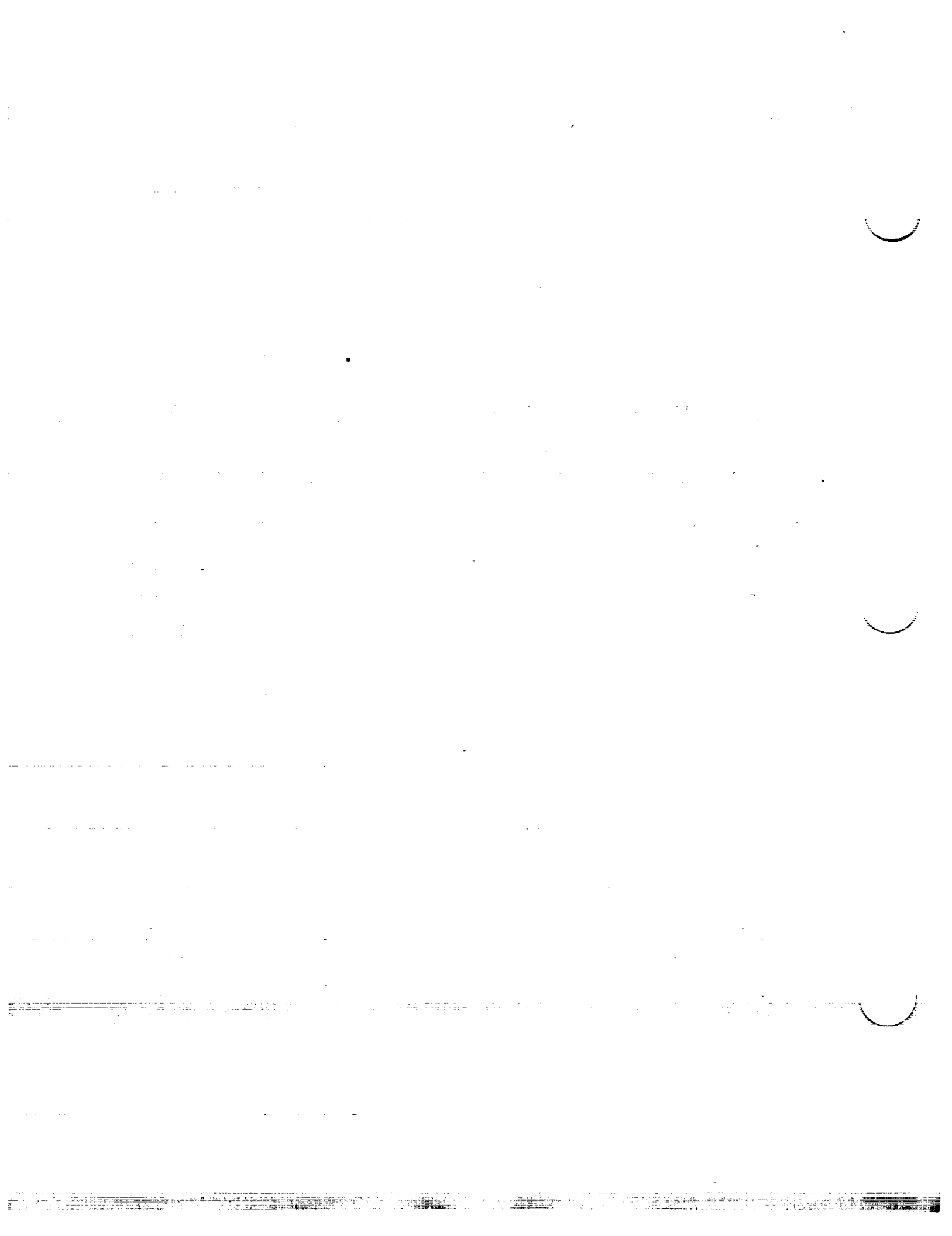
NACA 64-209



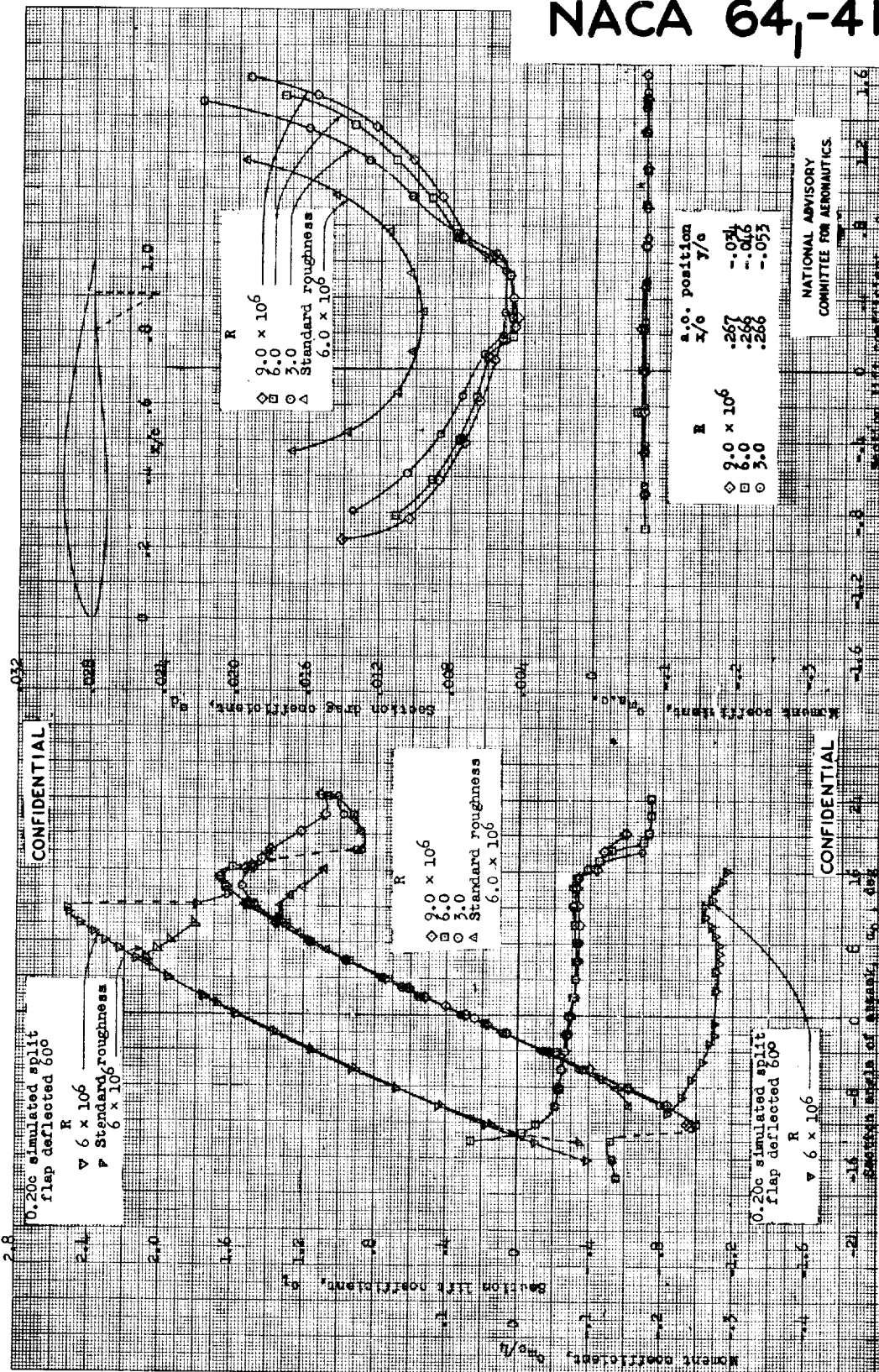


NACA 64₁-212





NACA 64₁-412

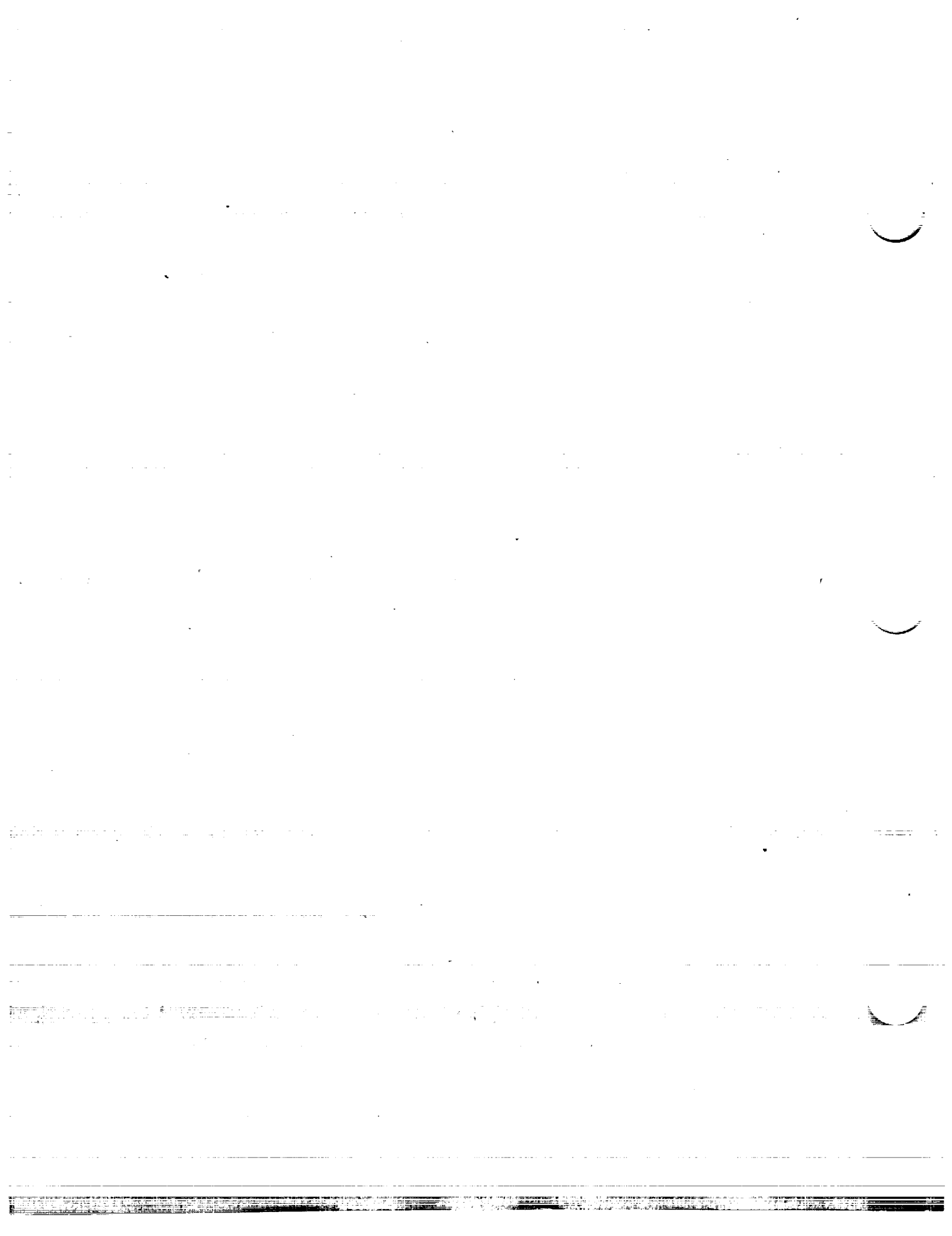


NATIONAL ADVISORY COMMITTEE FOR AERONAUTICS

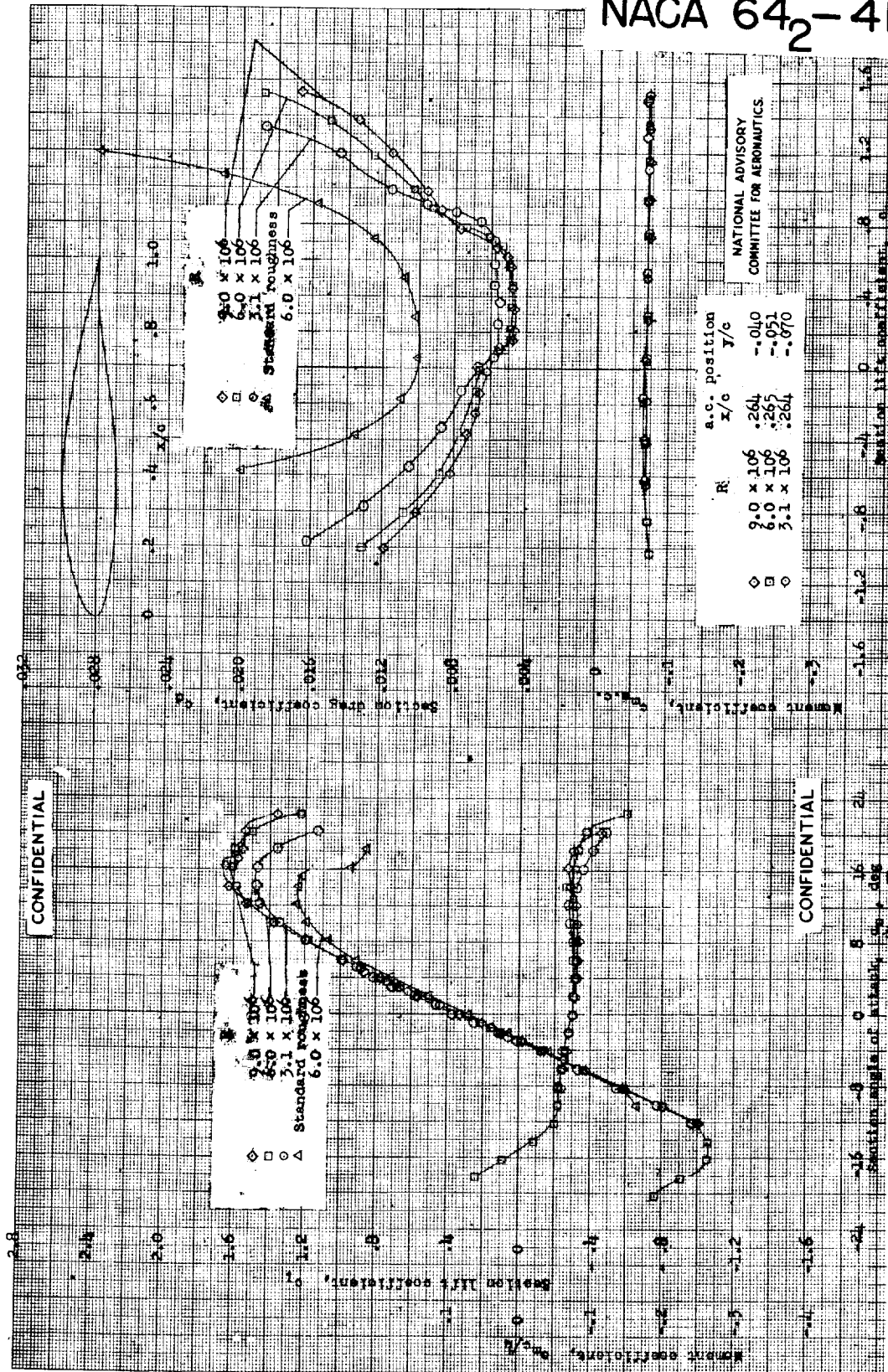
R	a.o. position x/o	y/a
◇ 2.0 x 10 ⁶	.267	-.074
□ 6.0	.266	-.016
○	.266	-.053

Aerodynamic characteristics of the NACA 64₁-412 airfoil section, 24-inch chord; TDU tests 682, 686, 831.





NACA 64₂-415



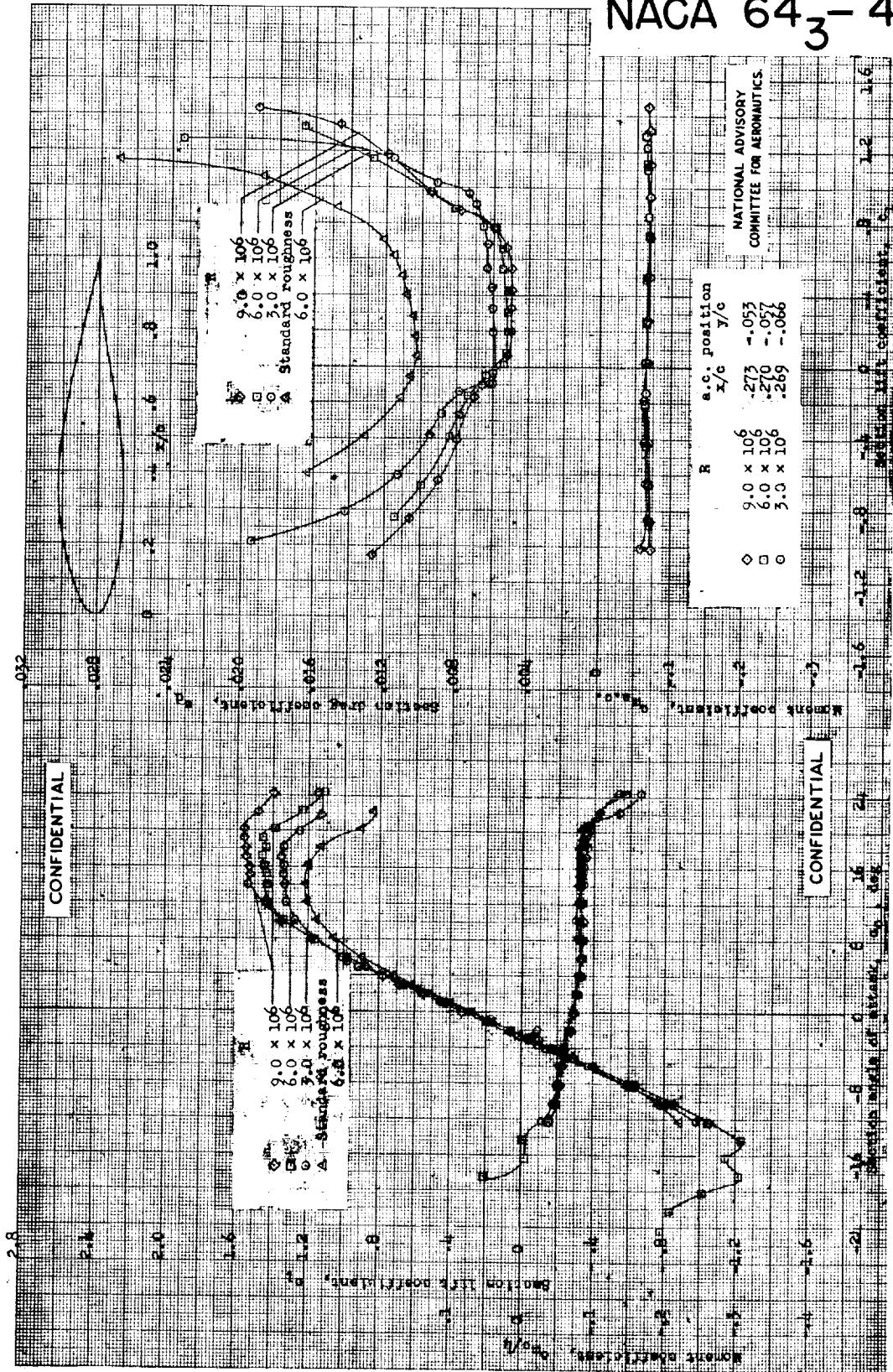
Aerodynamic characteristics of the NACA 64₂-415 airfoil section, 24-inch chord; YDF tests 656, 683, 733.

CONFIDENTIAL

CONFIDENTIAL



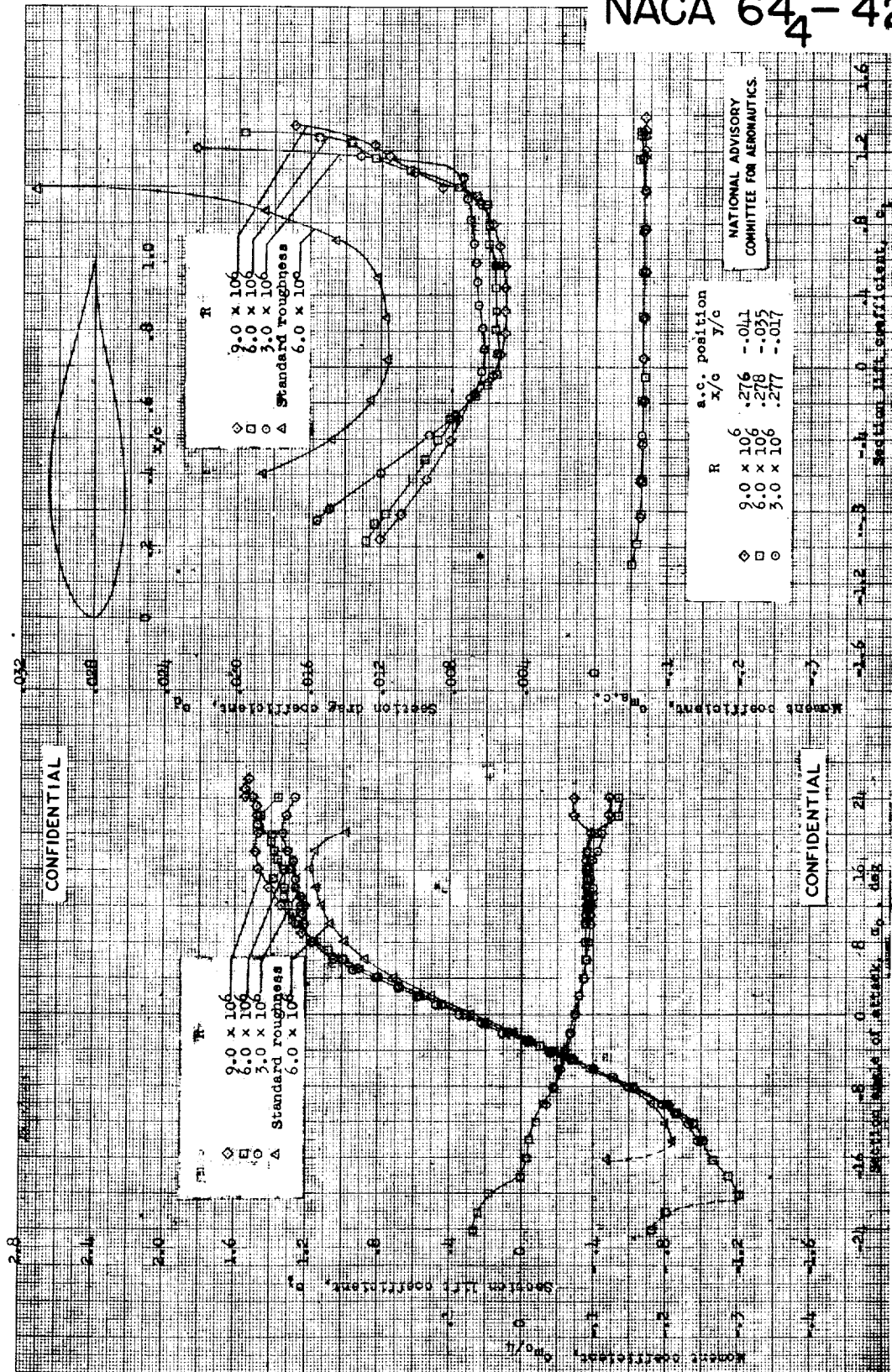
NACA 64₃-418



Aerodynamic characteristics of the NACA 64₃-418 airfoil section, 24-inch chord; DR tests 755, 756.



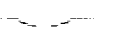
NACA 64-421

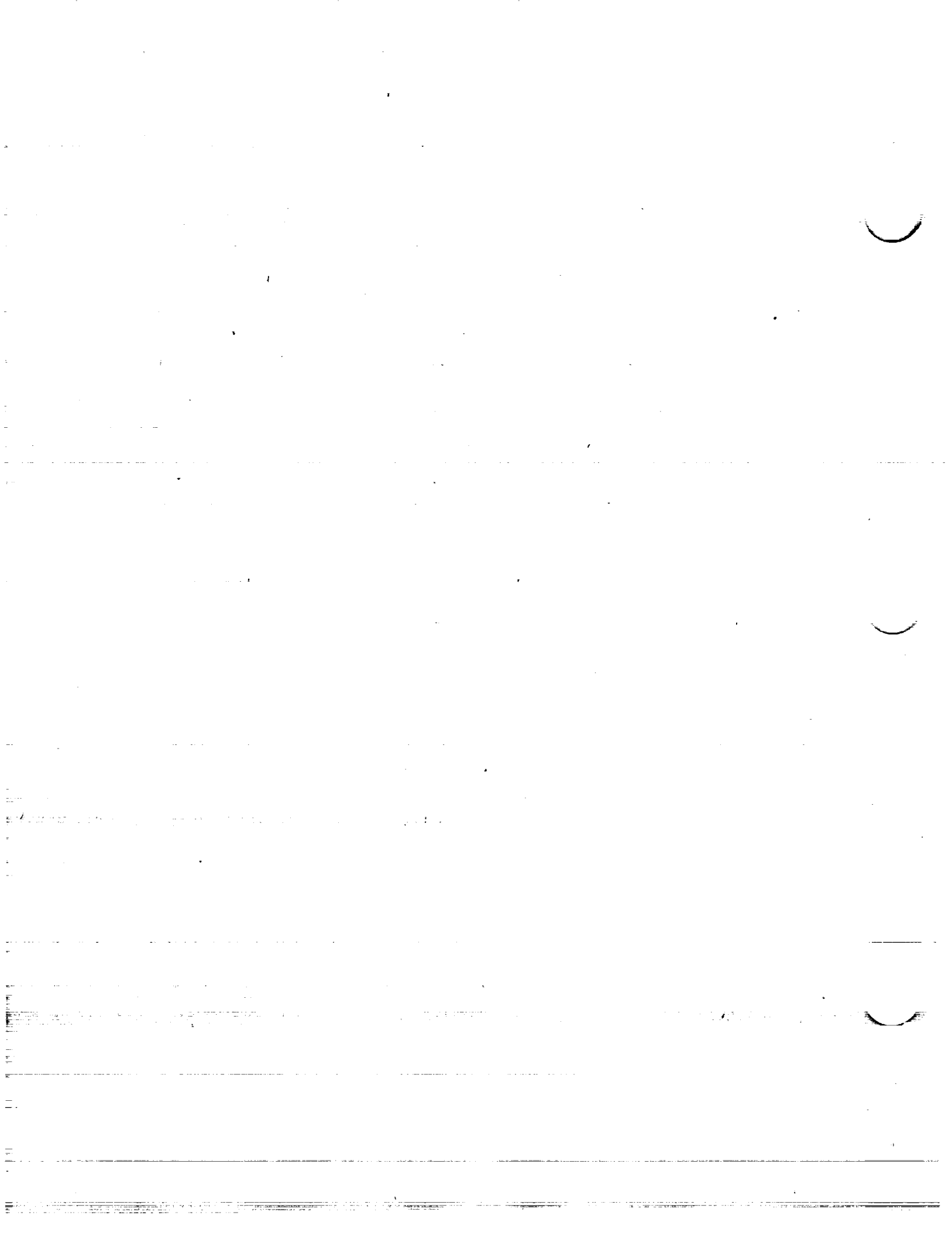


Aerodynamic characteristics of the NACA 64-421 airfoil section, 24-inch chord; TDF tests 691, 687, 727.

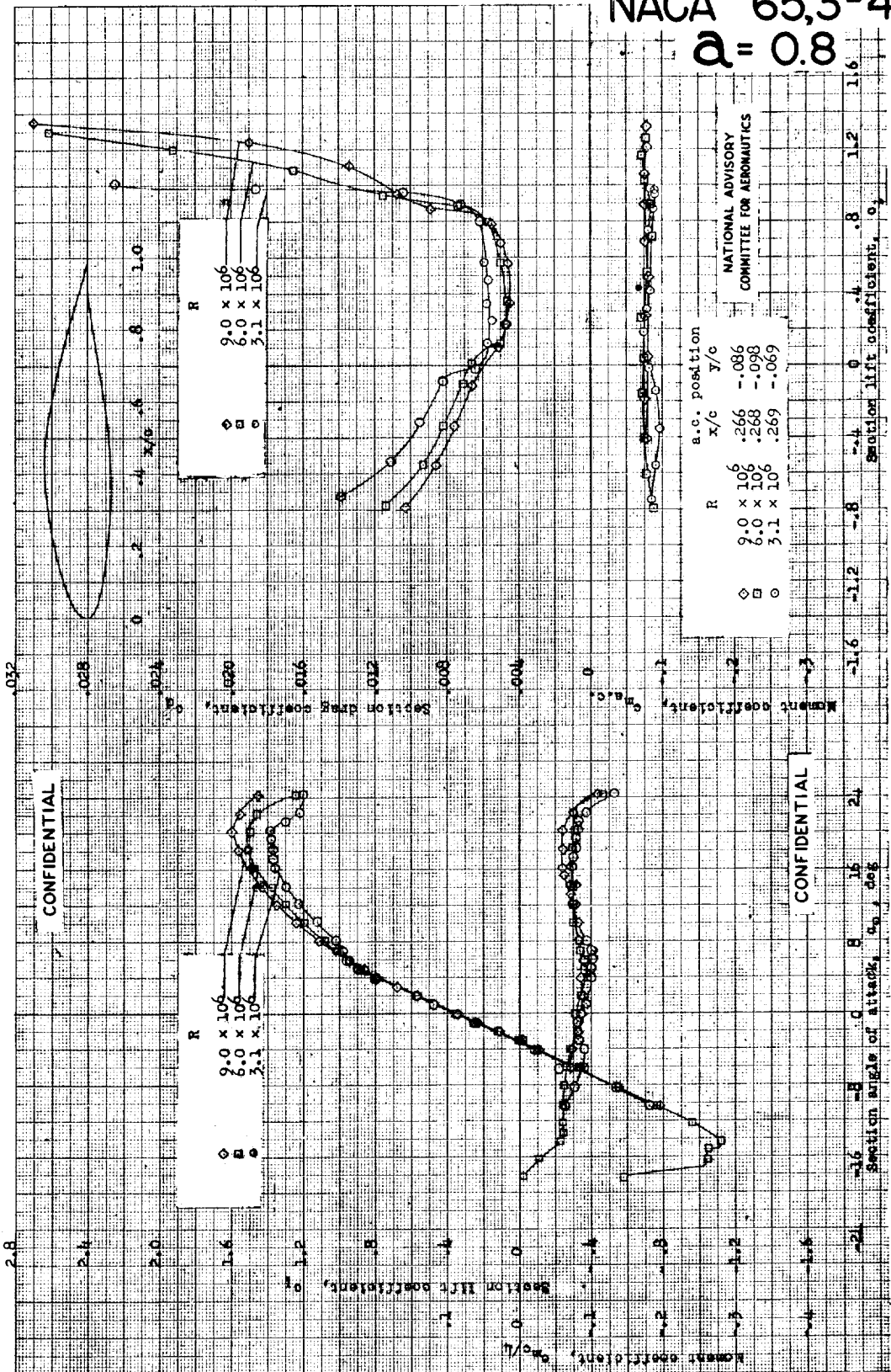
CONFIDENTIAL

CONFIDENTIAL



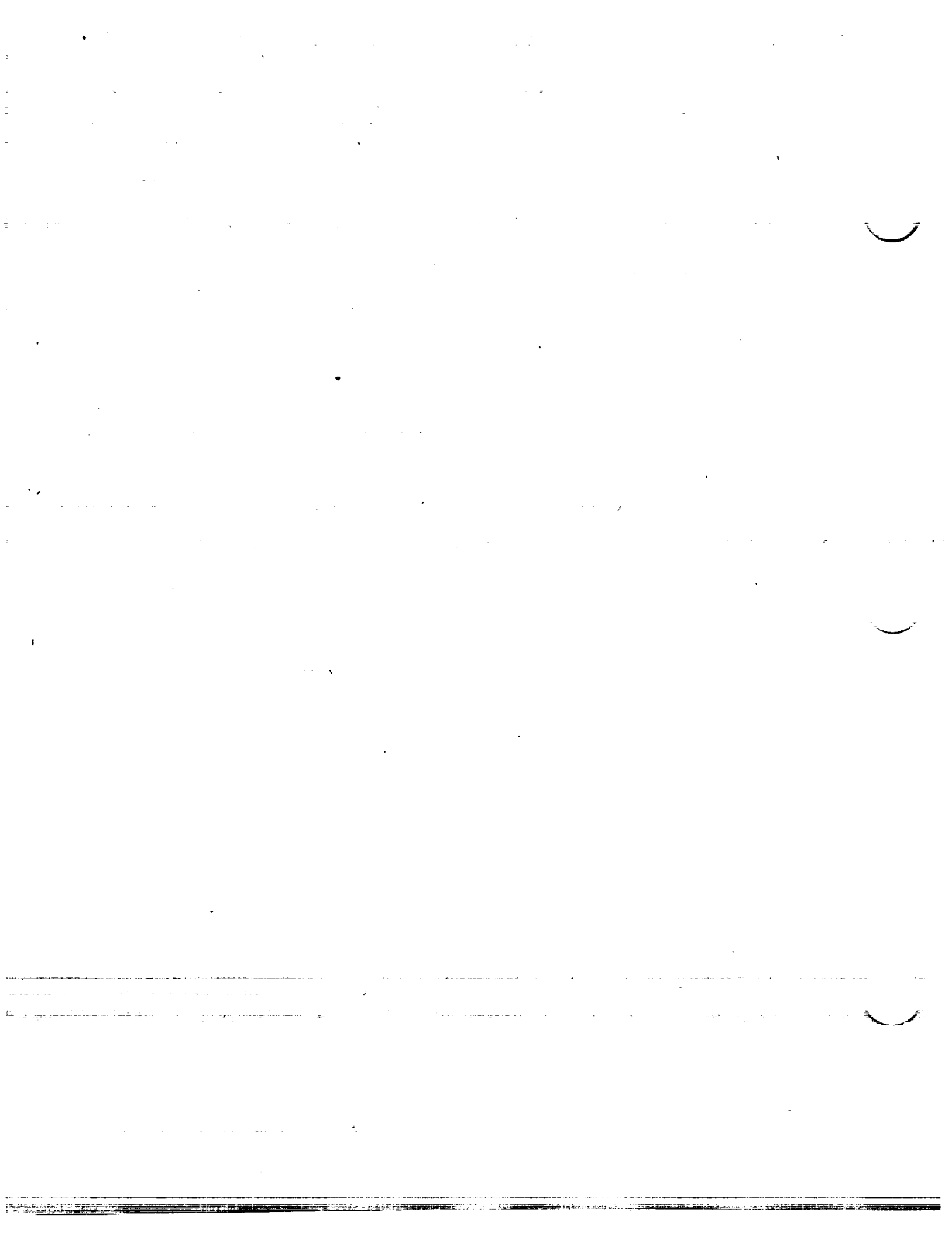


NACA 65,3-418
 $\alpha = 0.8$

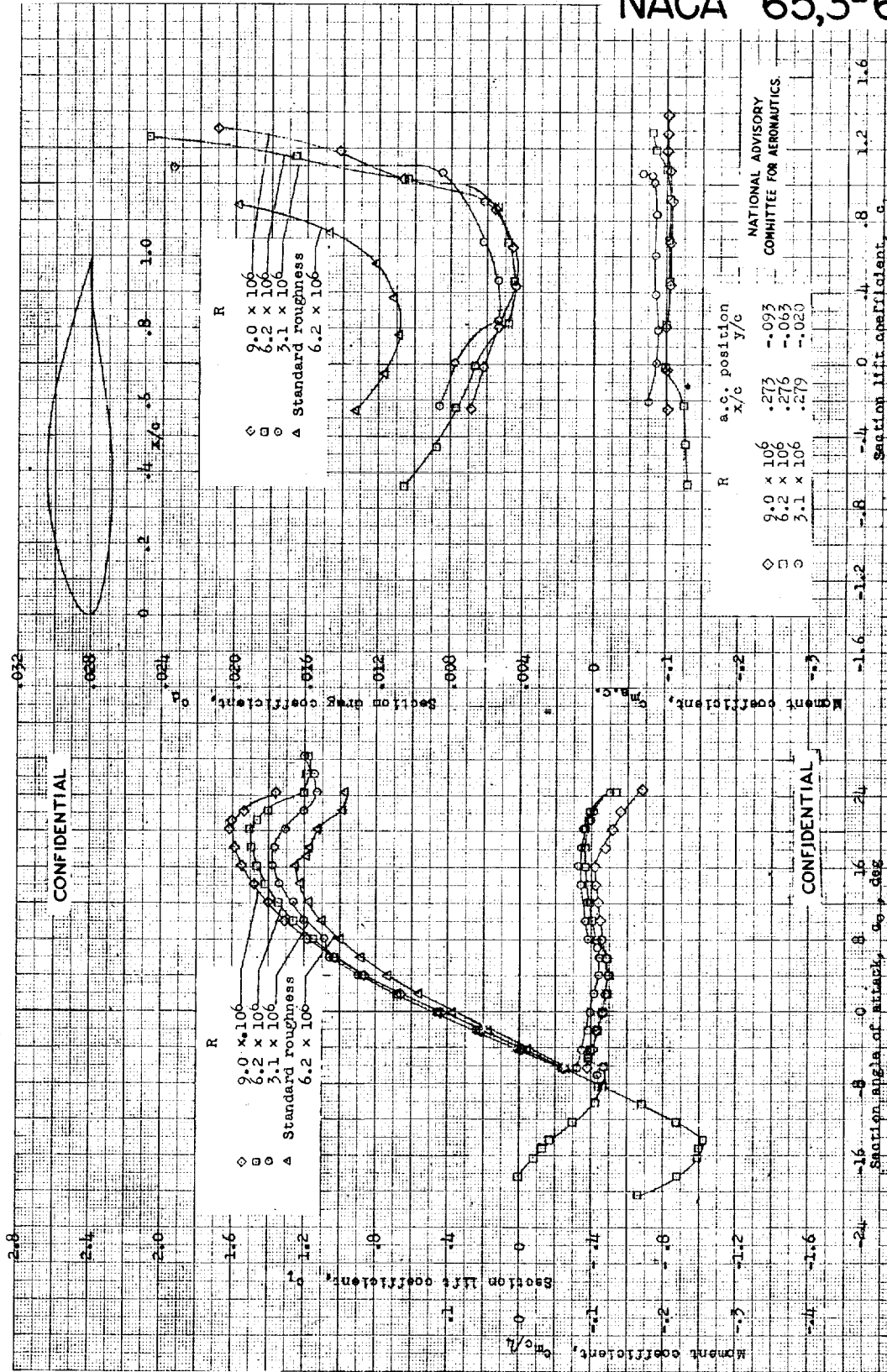


R	a.c. position	NATIONAL ADVISORY COMMITTEE FOR AERONAUTICS	
	x/c	y/c	
\diamond	9.0×10^6	.266	-.086
\square	6.0×10^6	.268	-.098
\circ	3.1×10^6	.269	-.069

Aerodynamic characteristics of the NACA 65,3-418, $\alpha = 0.8$ airfoil section, 24-inch chord; NDT tests 360, 363.



NACA 65,3-618

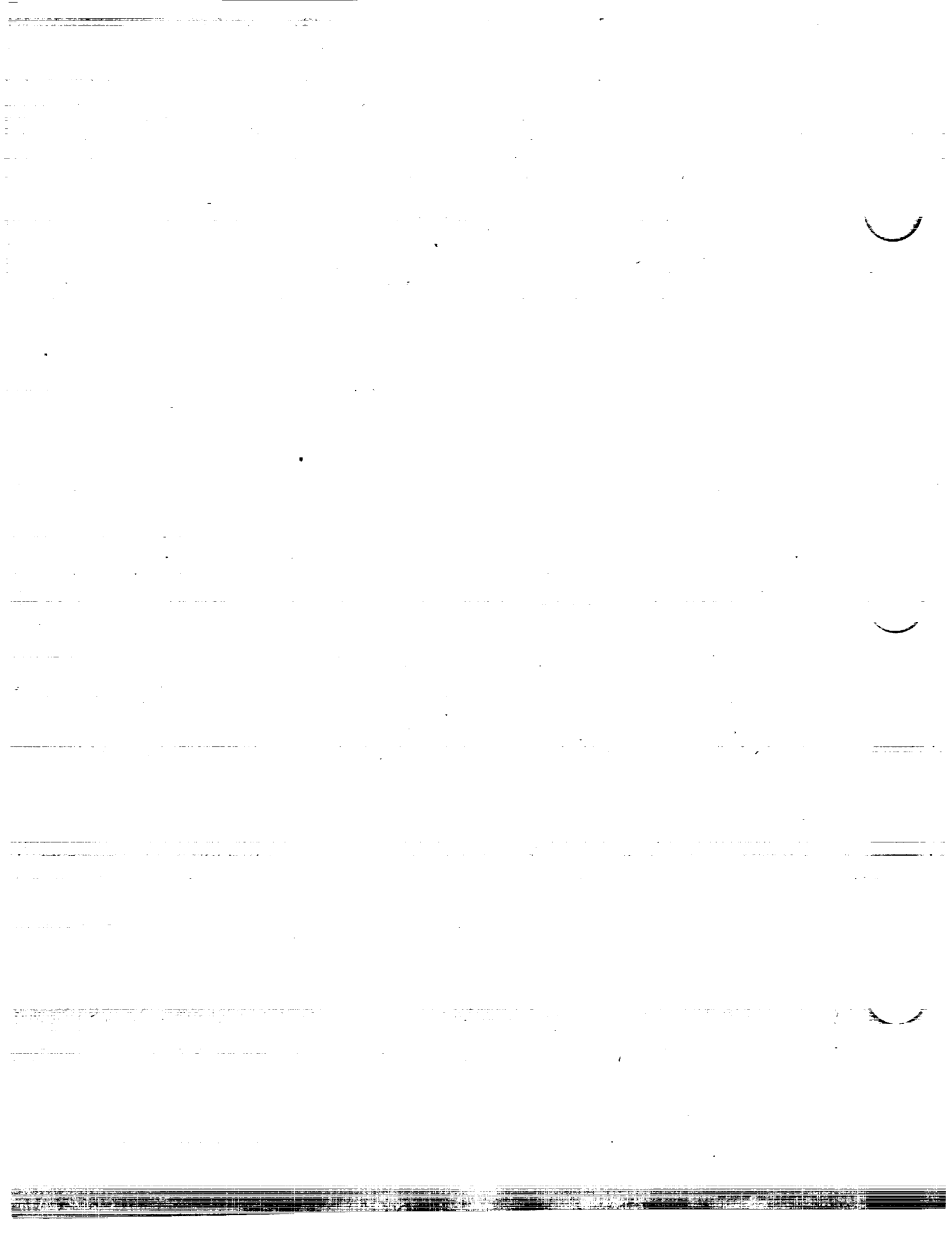


CONFIDENTIAL

CONFIDENTIAL

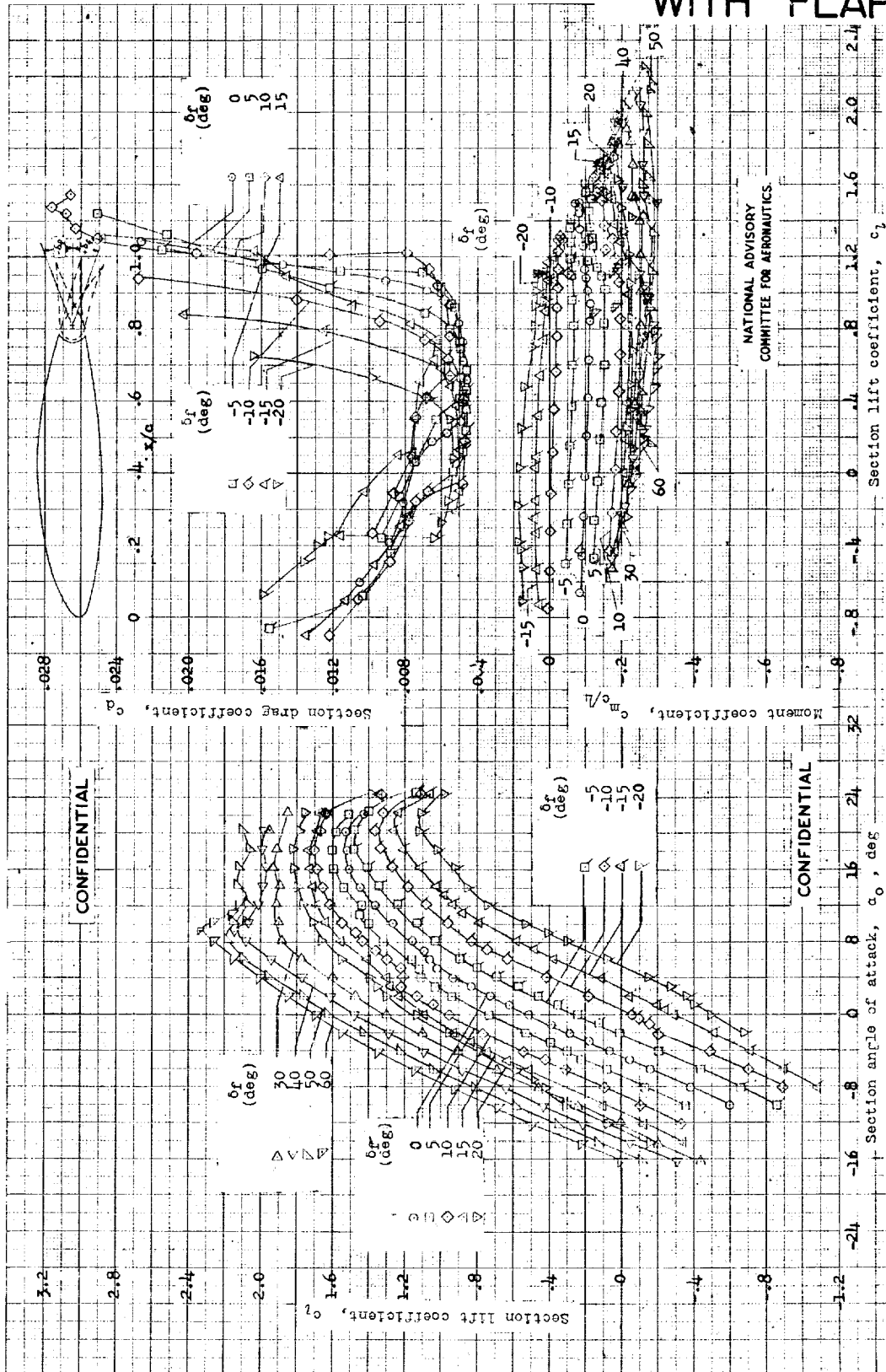
Aerodynamic characteristics of the NACA 65,3-618 airfoil section, 24-inch chord; TDT tests 195, 222.

NATIONAL ADVISORY
COMMITTEE FOR AERONAUTICS

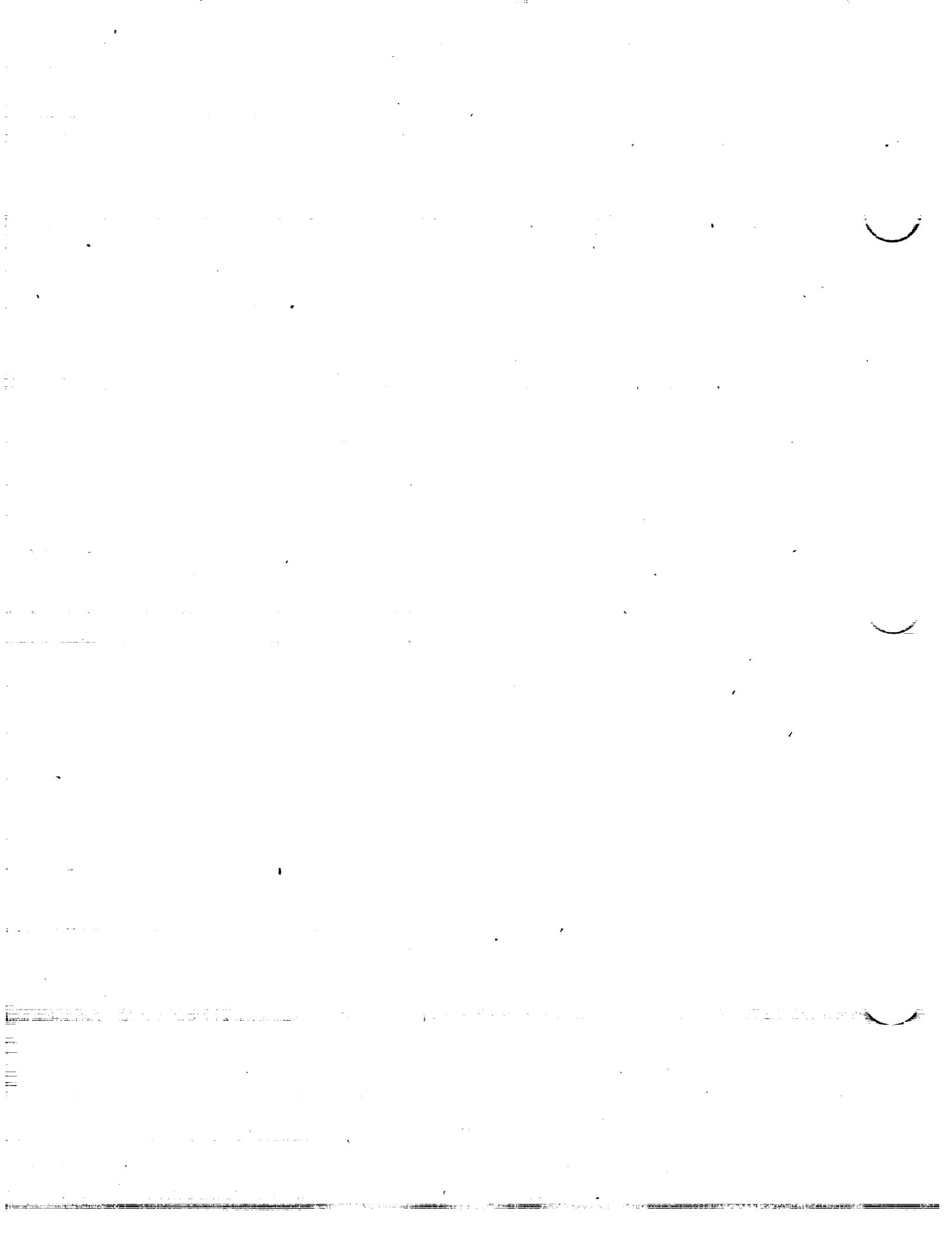


June 1, 1945

NACA 65,3-618 WITH FLAP

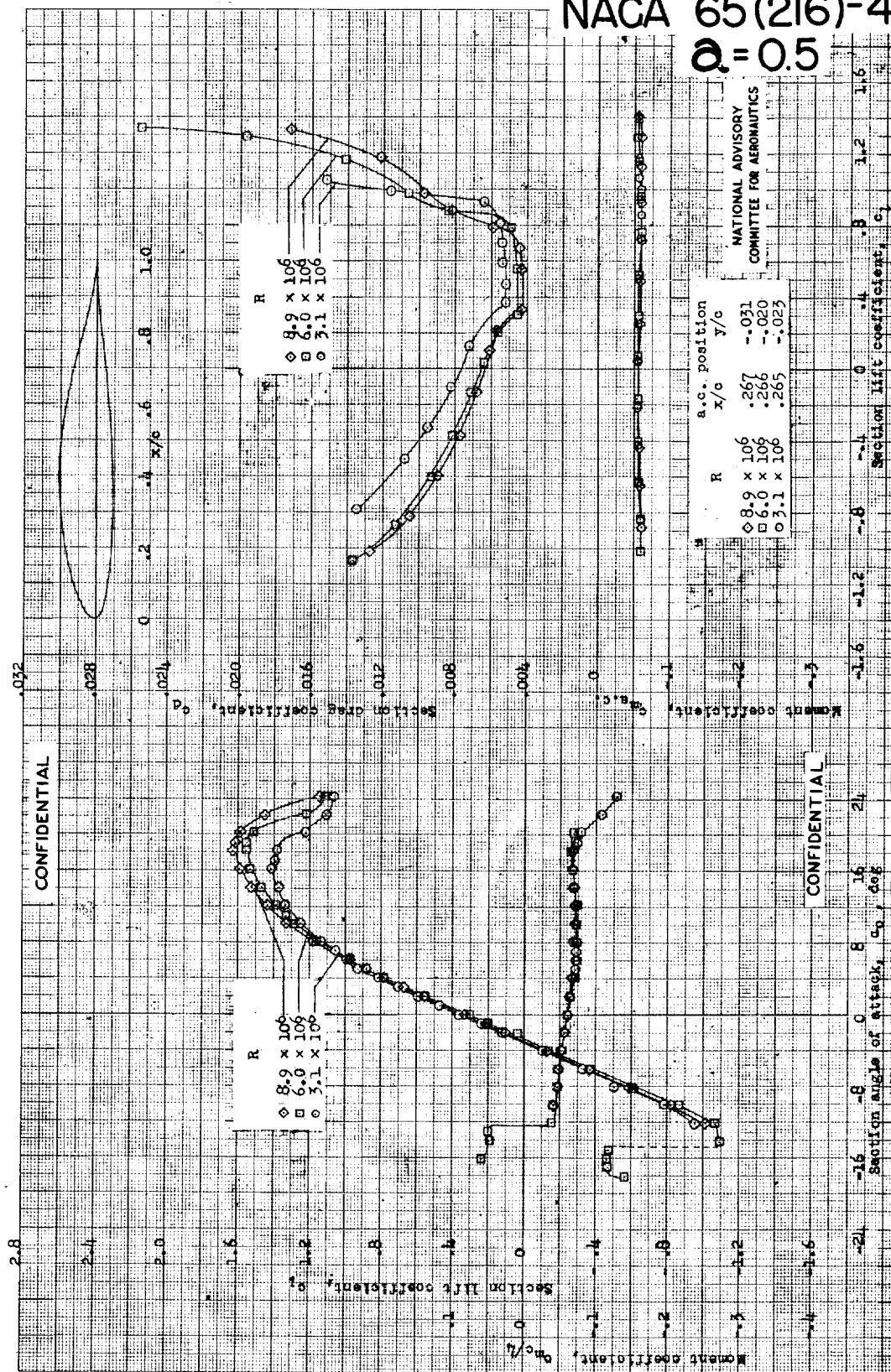


acodynamic characteristics of the NACA 65,3-613 airfoil section with 0.20c sealed plain flap. $h, 6 \times 10^6$; TDT tests 313, 315, and 317.

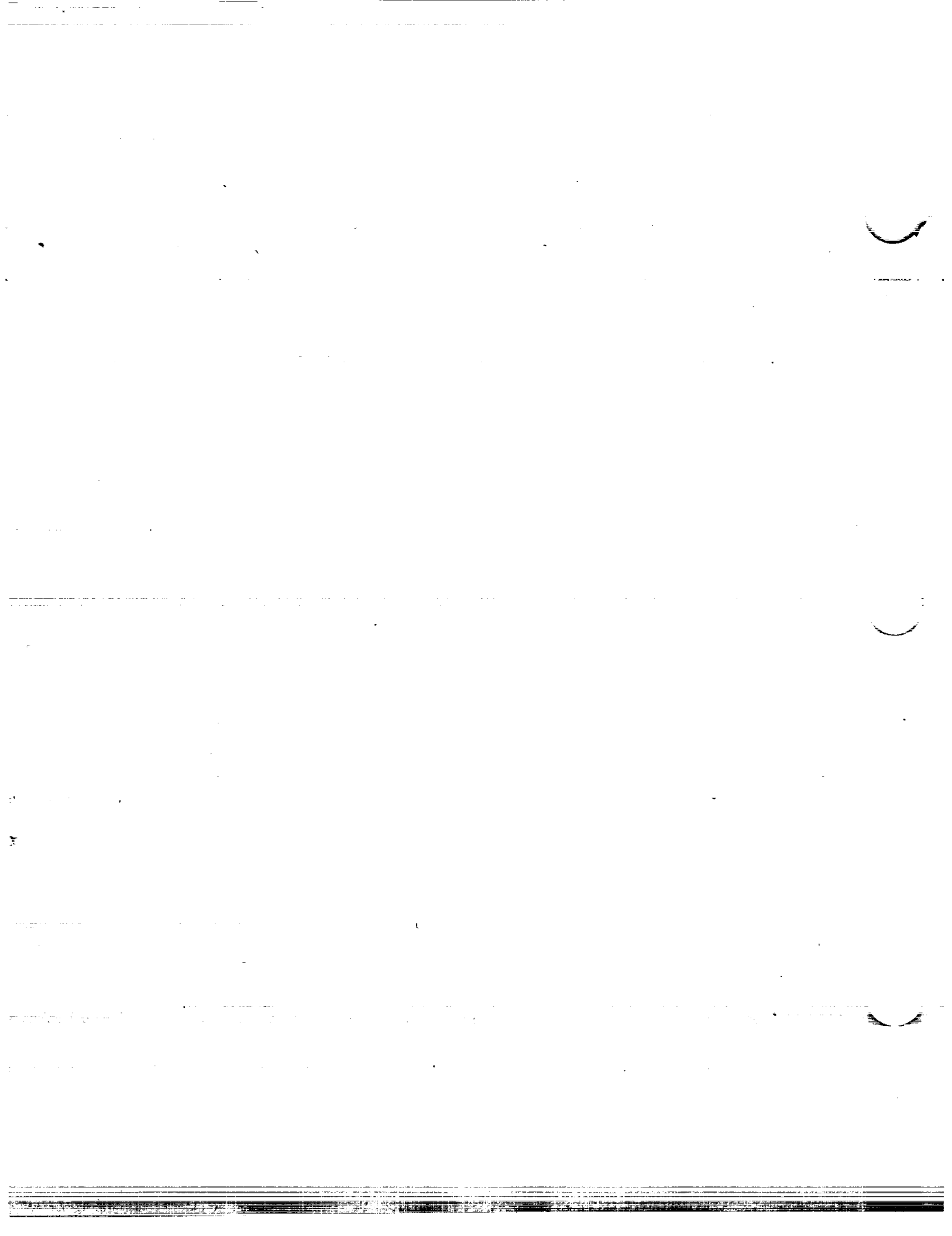


NACA 65(216)-415

$Q = 0.5$

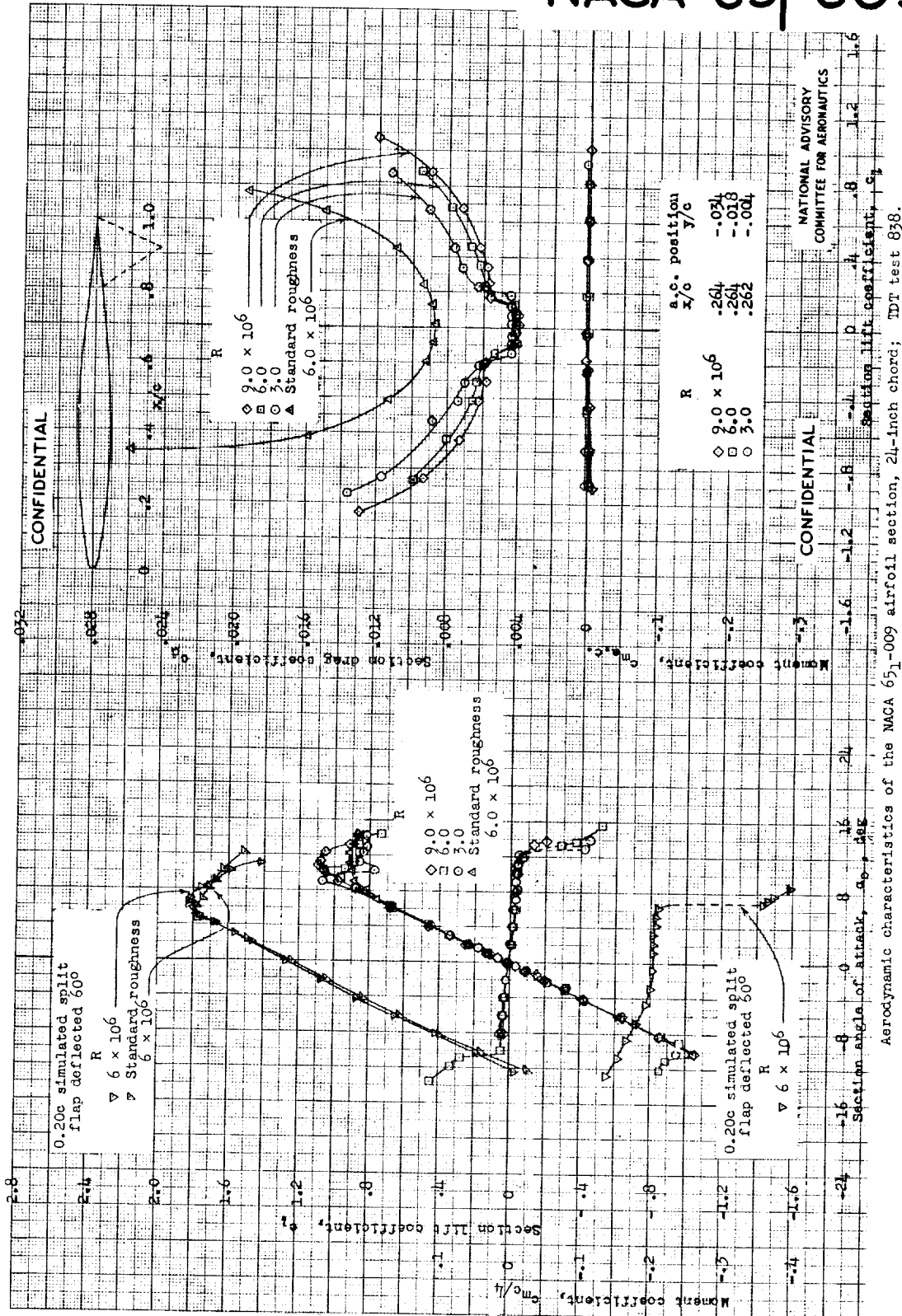


Aerodynamic characteristics of the NACA 65(216)-415, $a = 0.5$ airfoil section, 24-inch chord, MFT tests 267, 268.



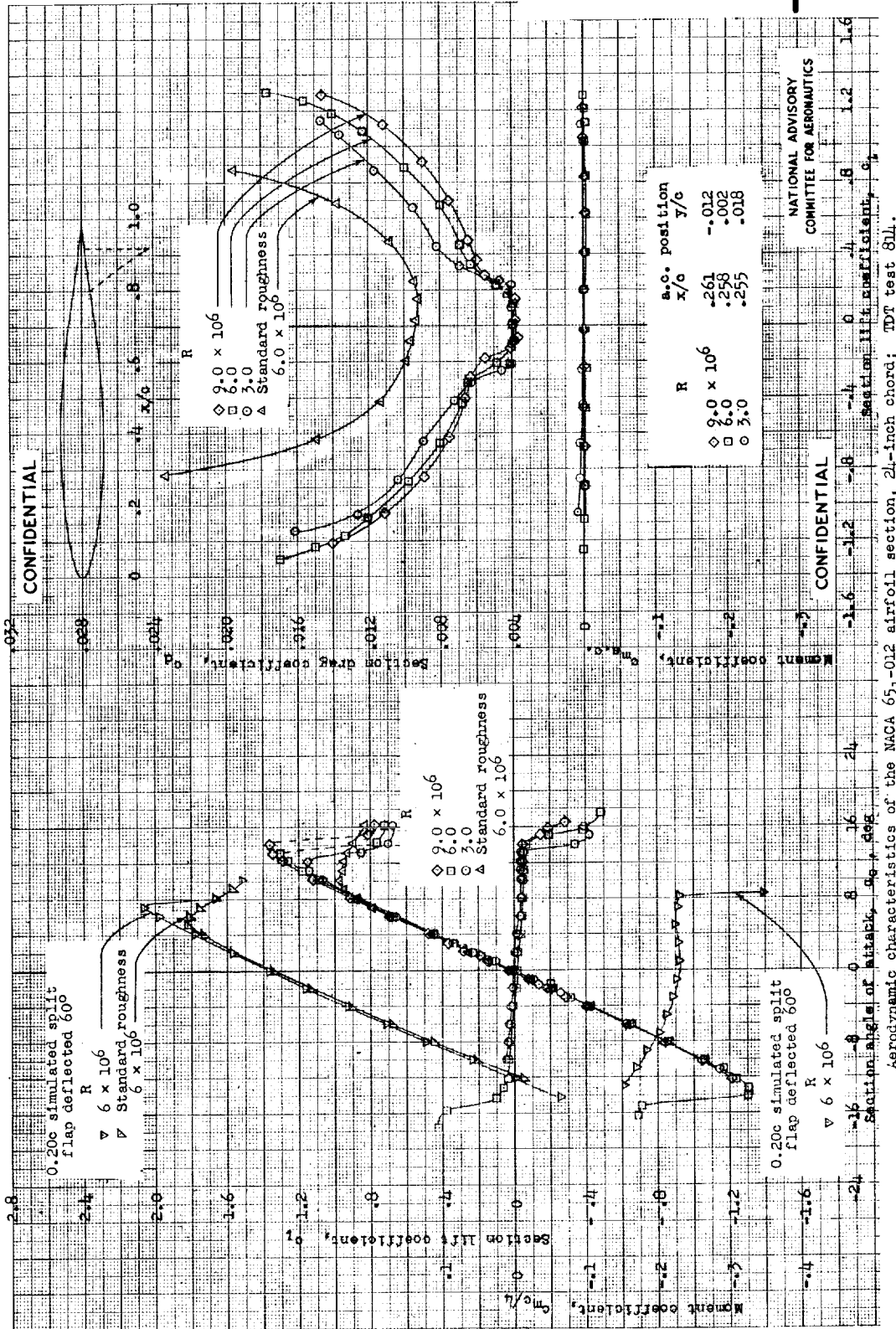


NACA 65-009



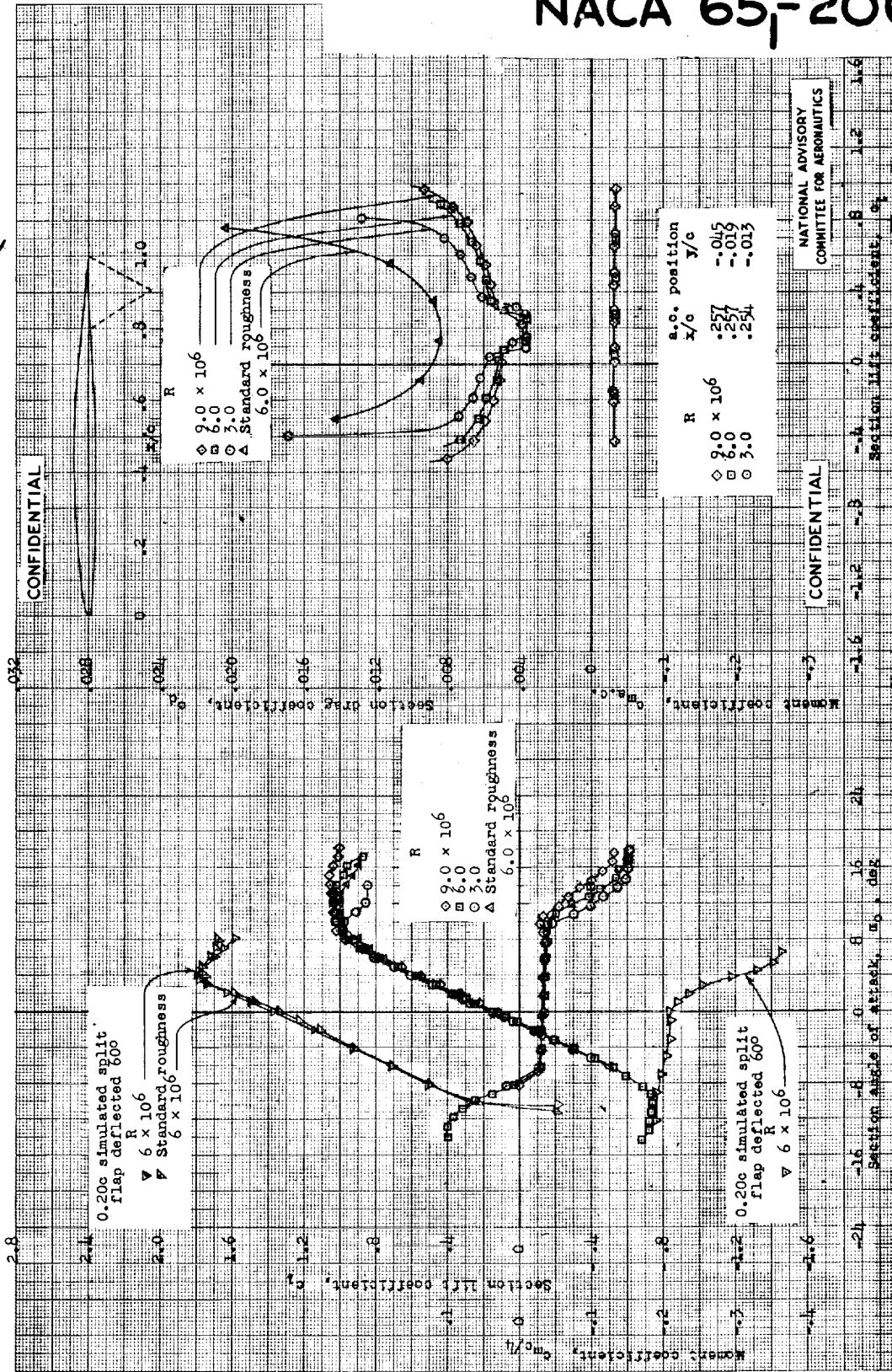


NACA 65-012





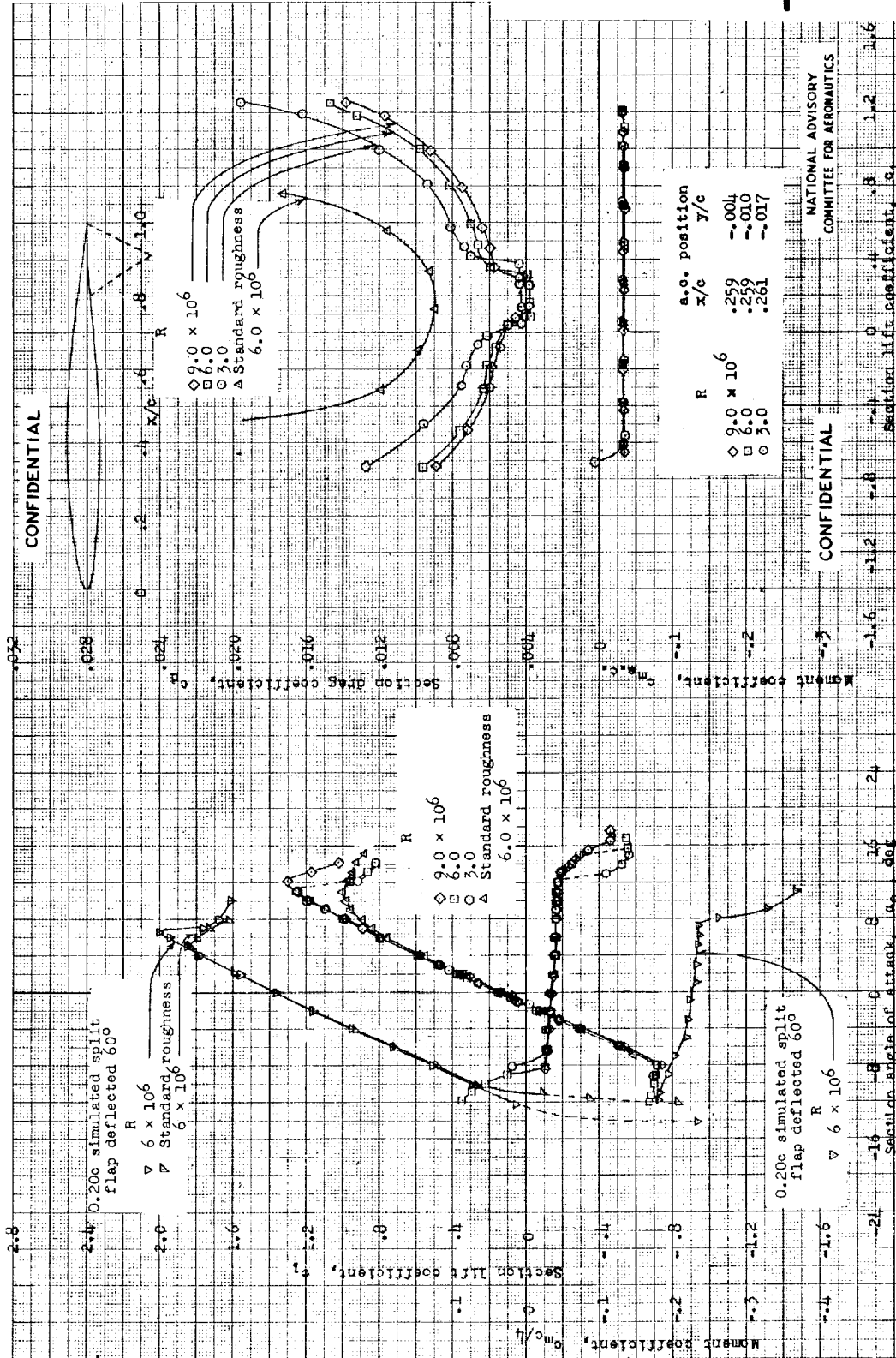
NACA 65-206



Aerodynamic characteristics of the NACA 65-206 airfoil section, 24-inch chord; TDT tests 829, 885.

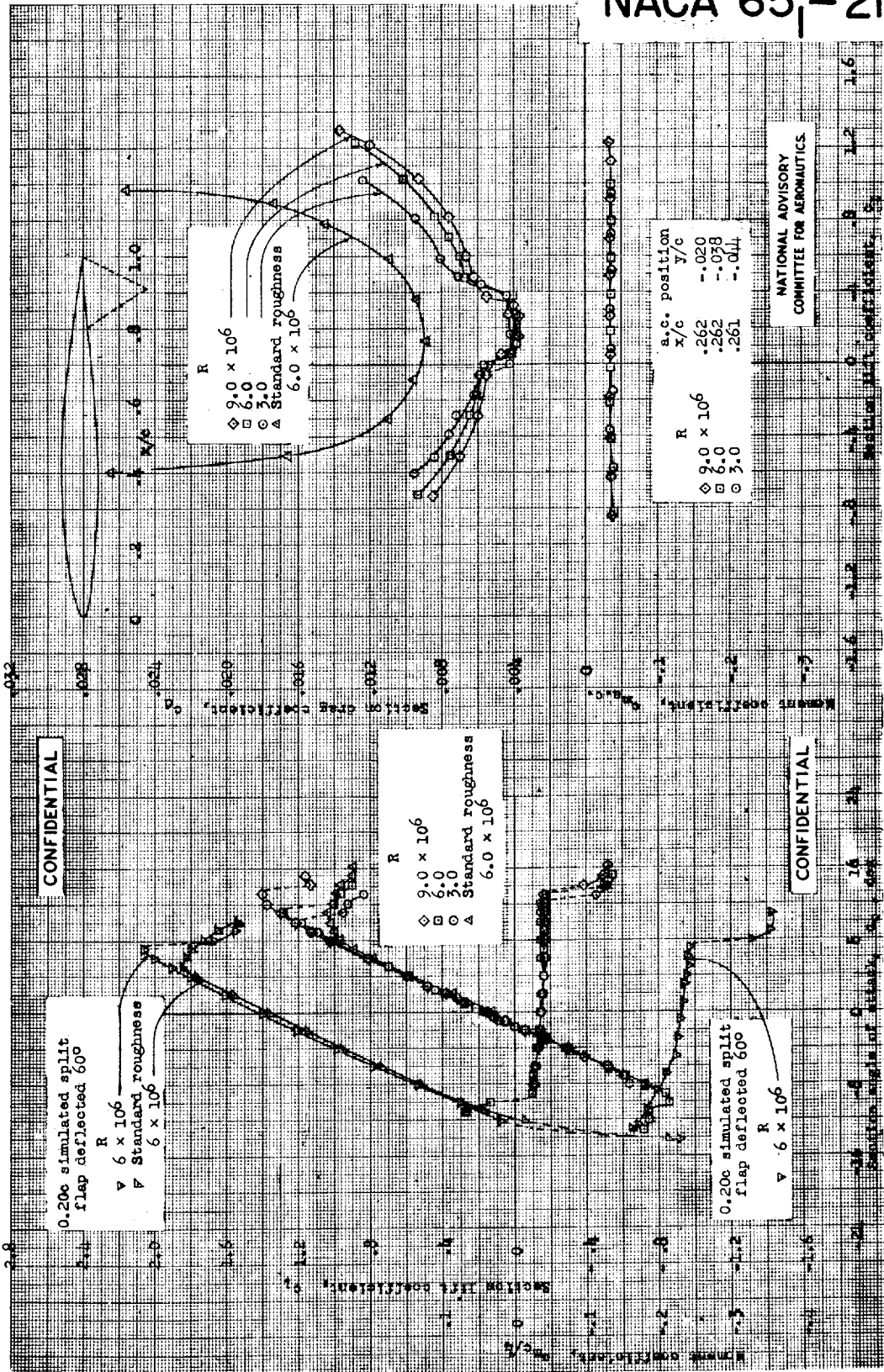


NACA 65-209



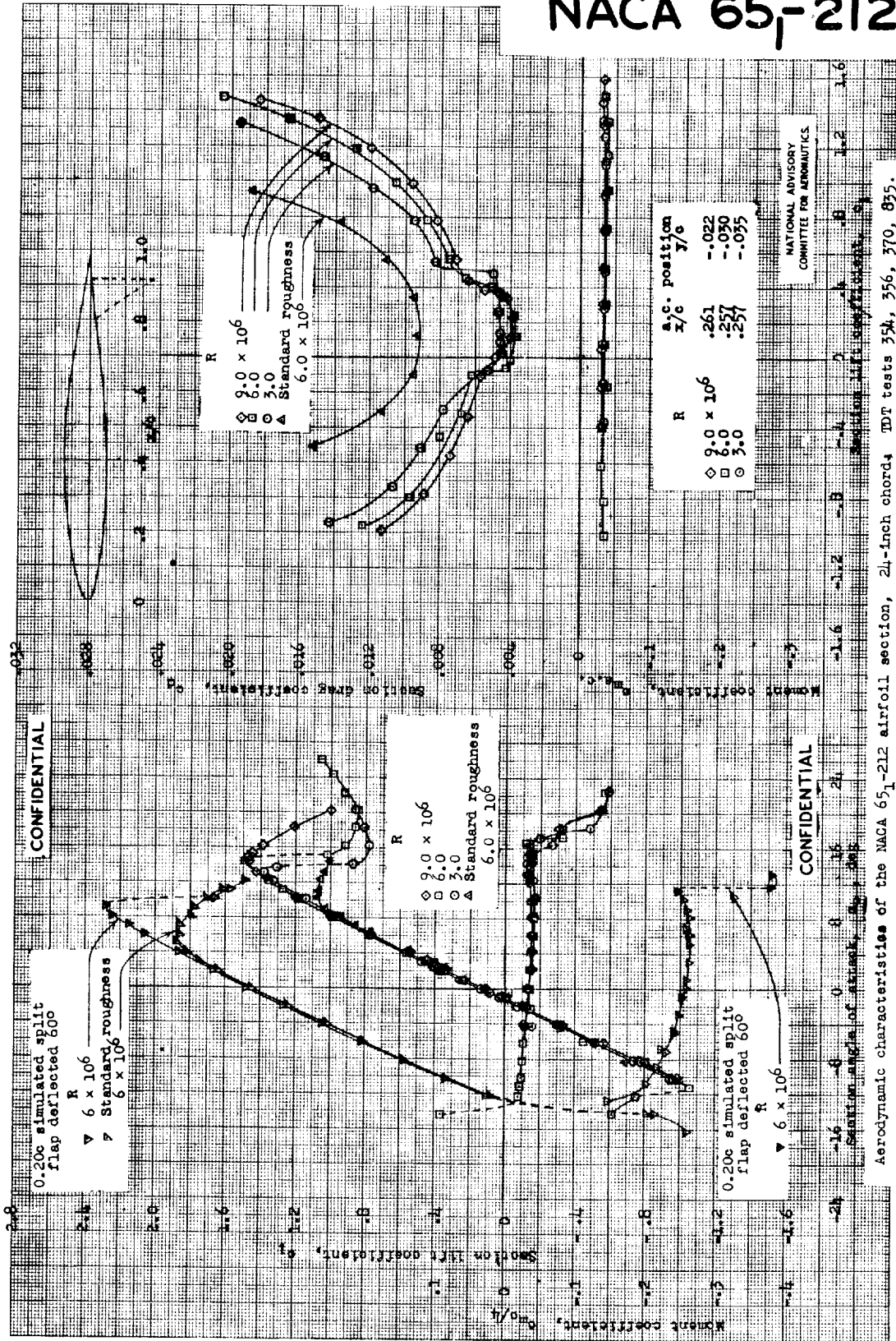


NACA 65₁-210



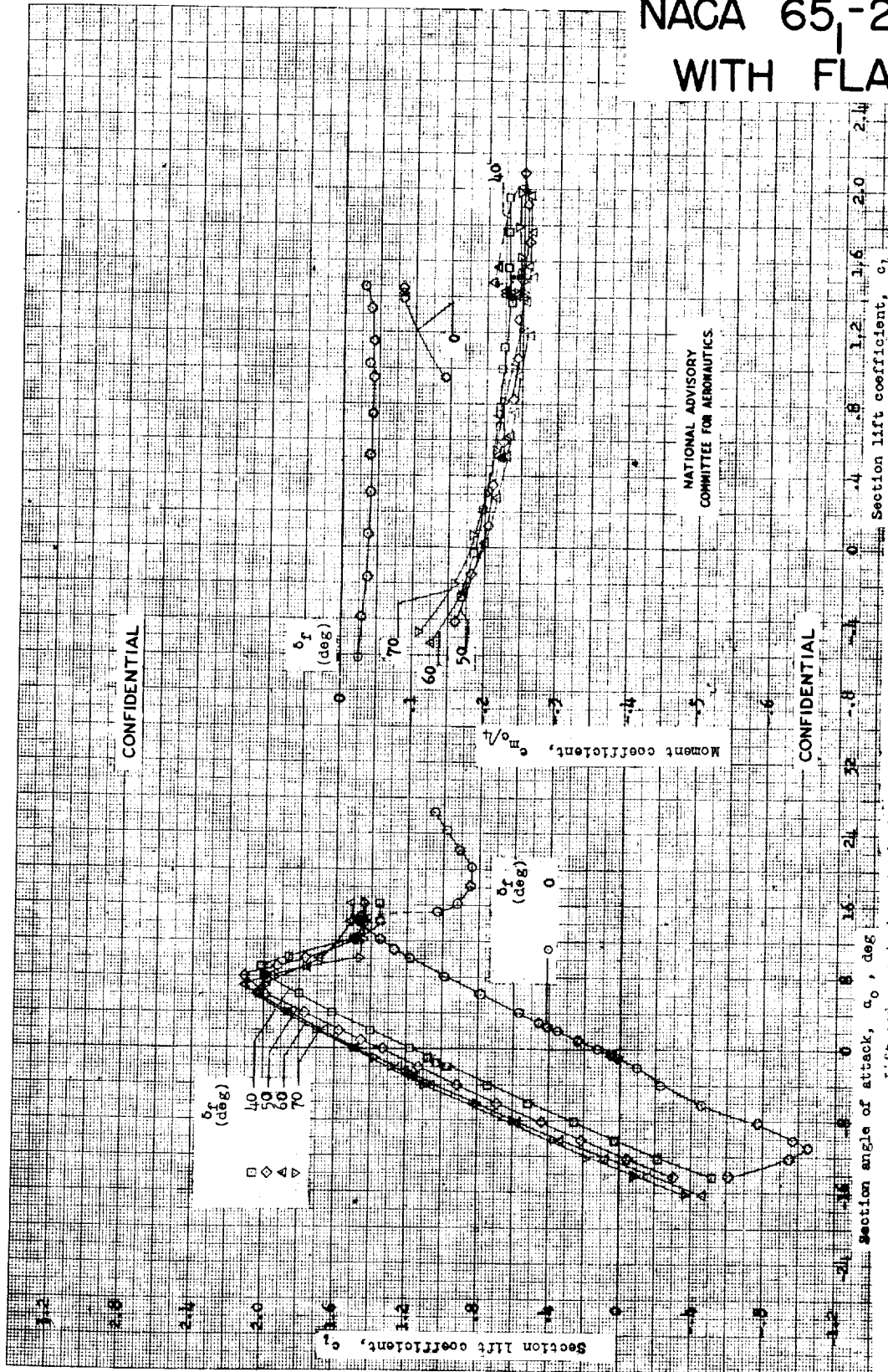


NACA 65-212





NACA 65₁-212 WITH FLAP

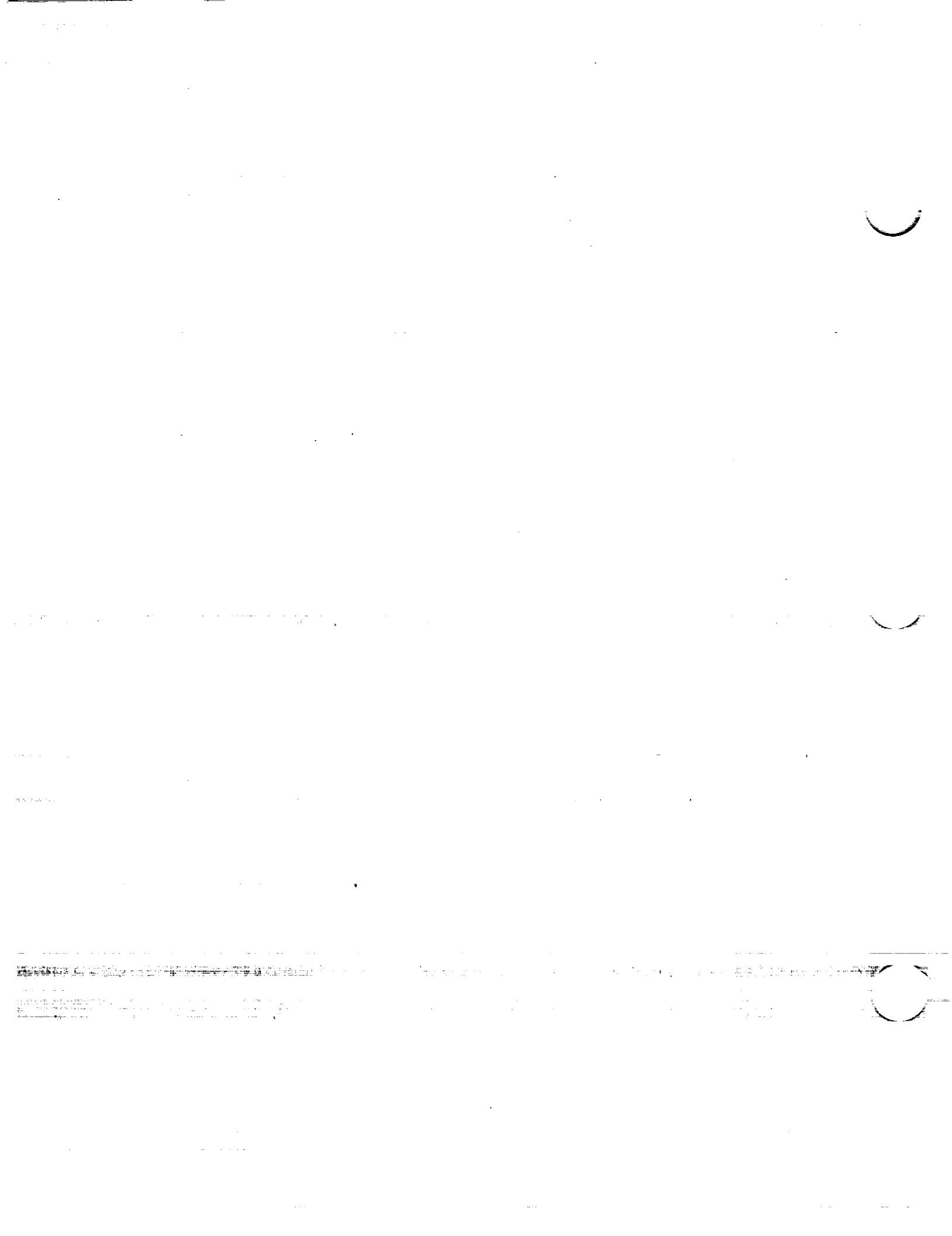


NATIONAL ADVISORY
COMMITTEE FOR AERONAUTICS

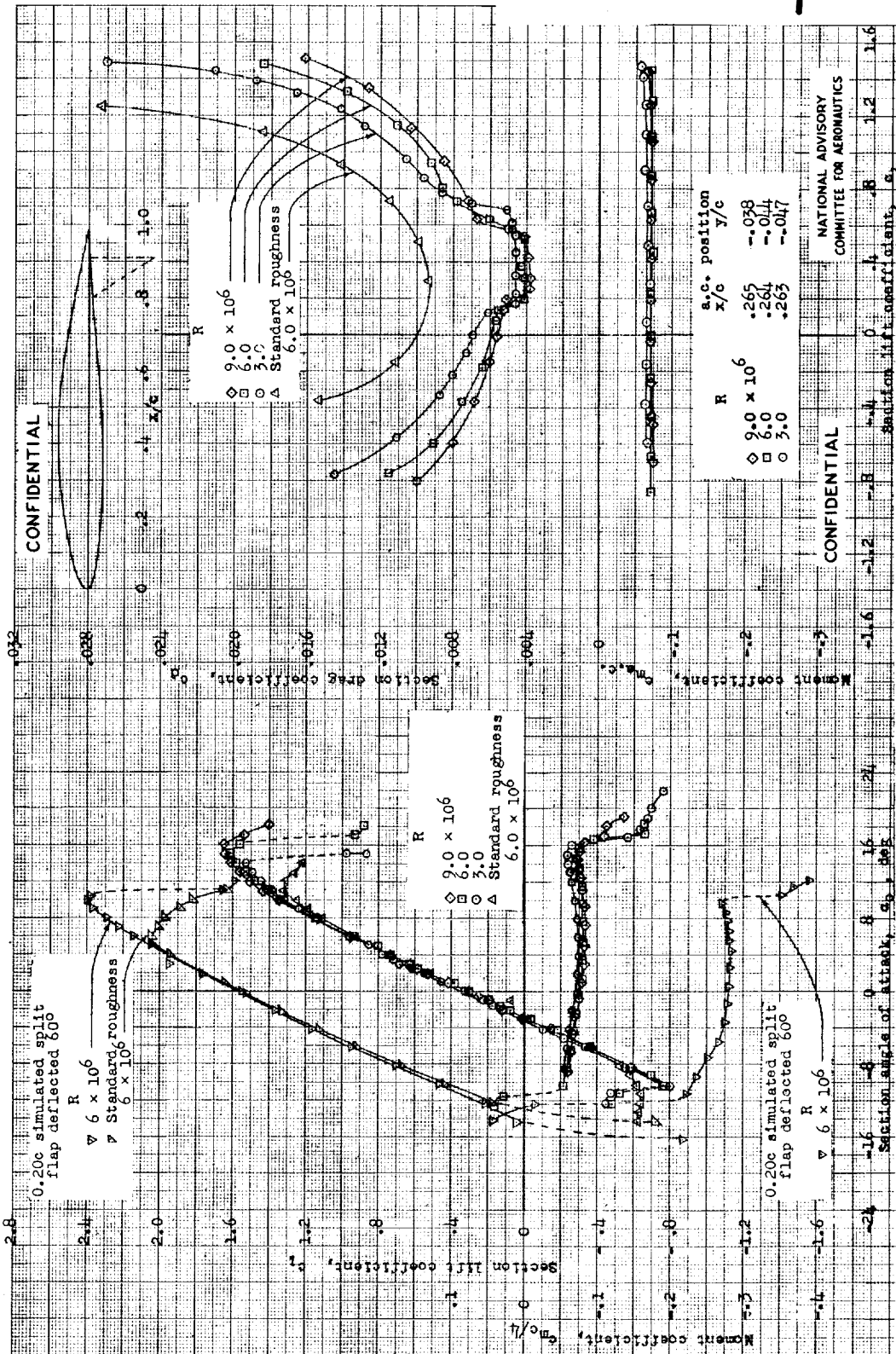
Section angle of attack, α_0 , deg
Lift and moment characteristics of the NACA 65₁-212 airfoil section with 0.20c split flap. k , 6×10^6 ; TDT tests 556, 569, and 599.

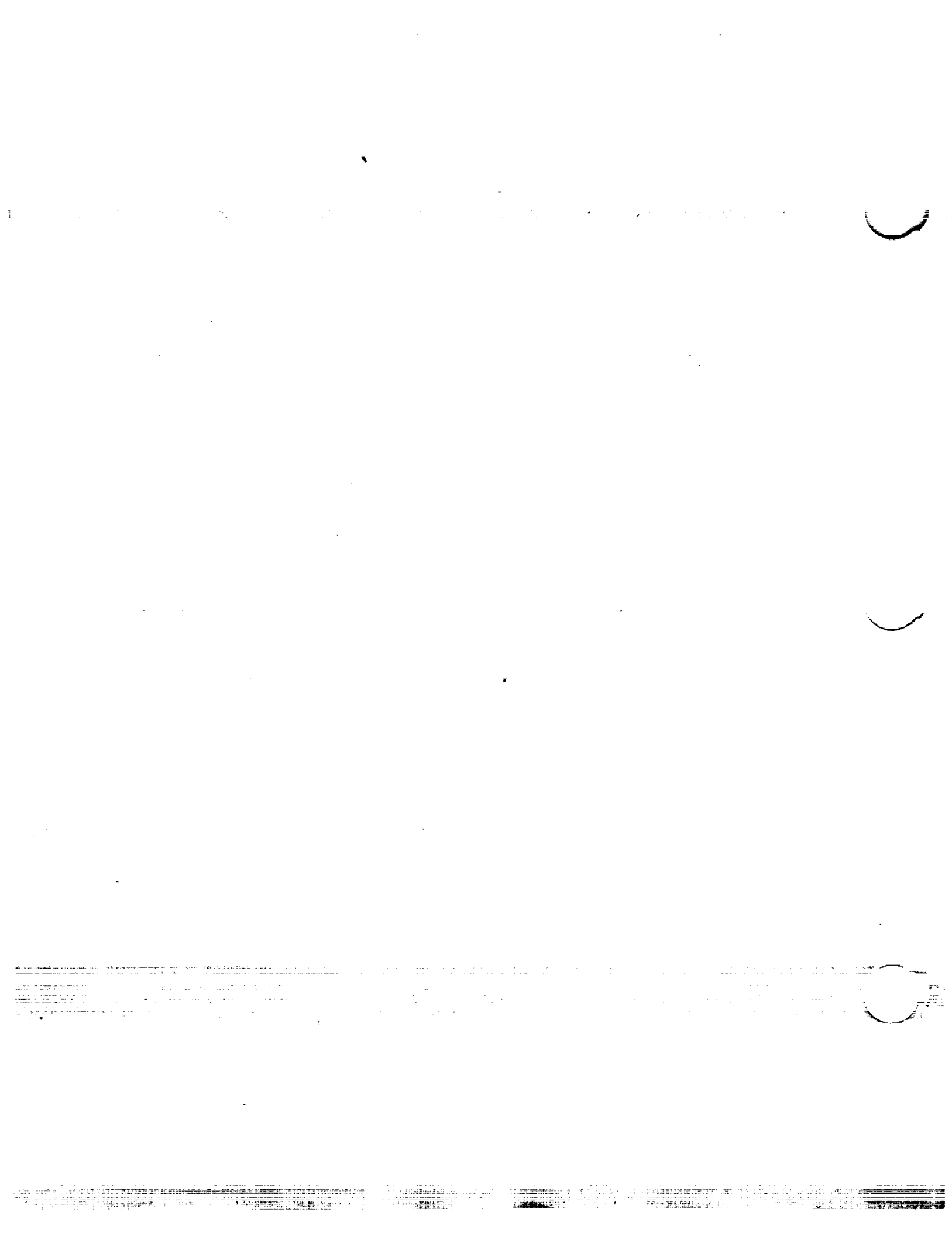


.....

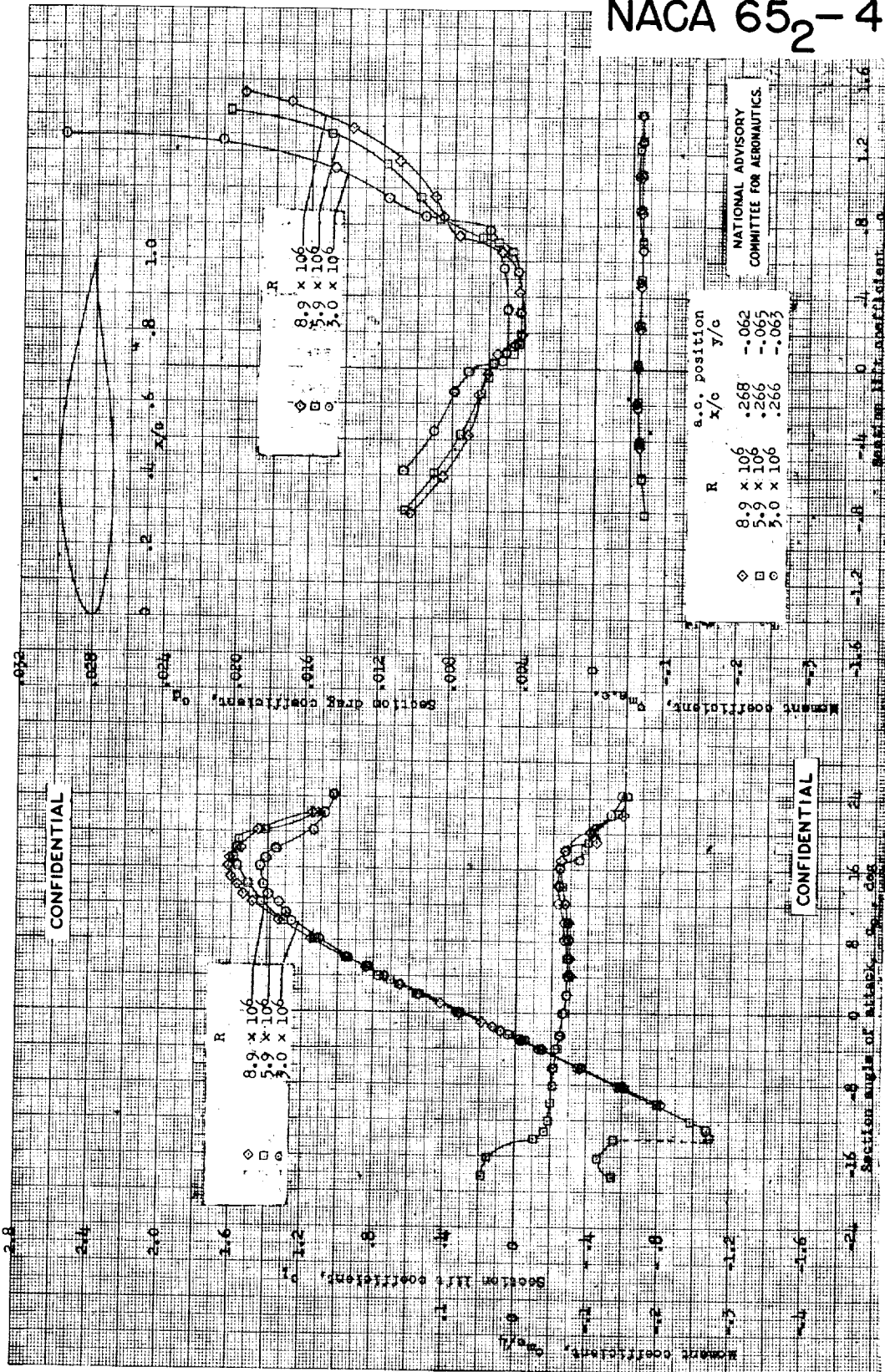


NACA 65-412





NACA 65₂-415



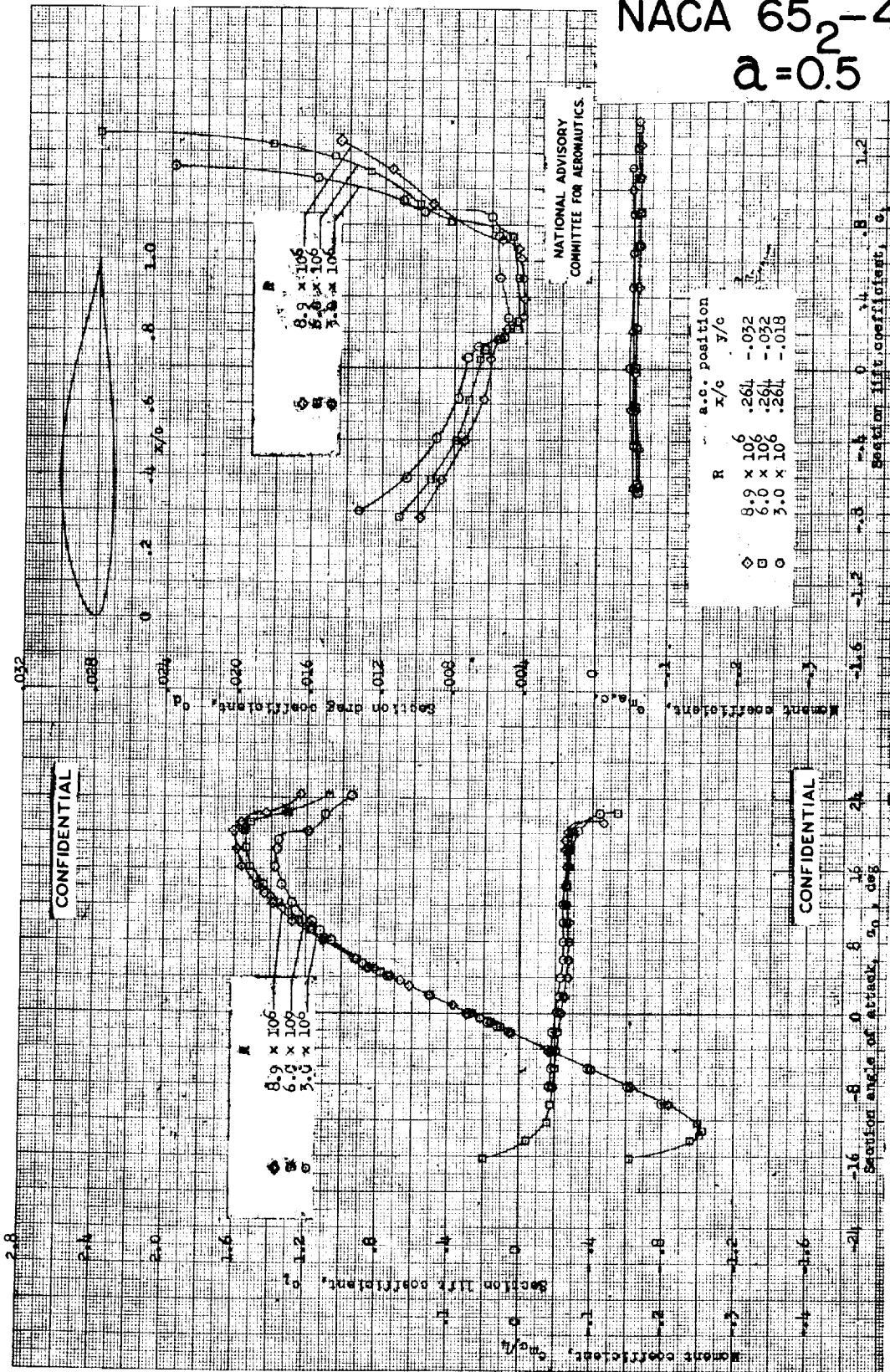
CONFIDENTIAL

CONFIDENTIAL

Aerodynamic characteristics of the NACA 65₂-415 airfoil section, 24-inch chord; DT tests 313, 318.



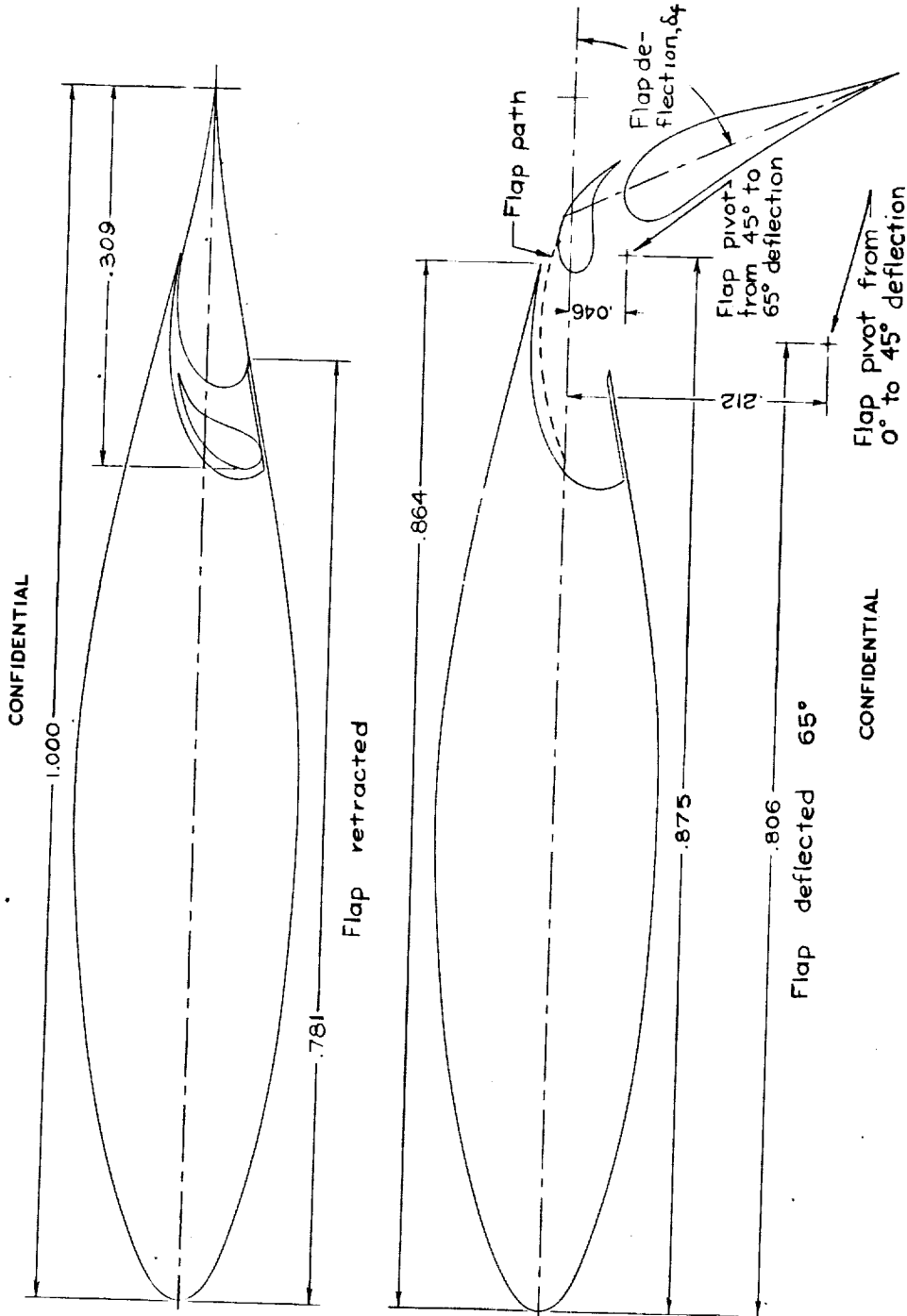
NACA 65₂-415 $\alpha = 0.5$





Faint, illegible text or markings at the bottom left corner of the page.

NACA 65₃-118 WITH FLAP



CONFIDENTIAL

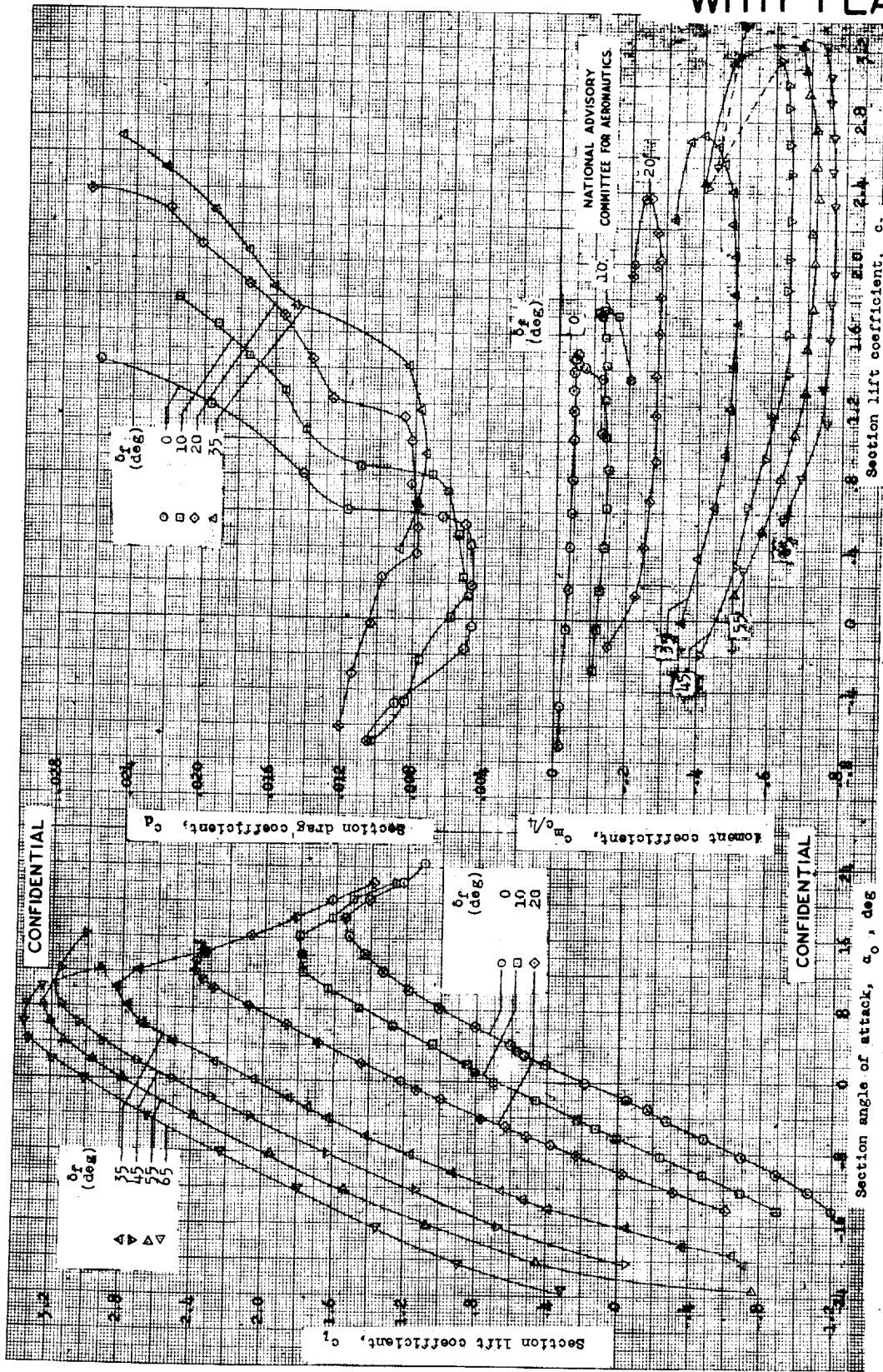
CONFIDENTIAL

(a) Configuration.
NACA 65₃-118 airfoil section with 0.309a double-slotted flap.

NATIONAL ADVISORY
COMMITTEE FOR AERONAUTICS



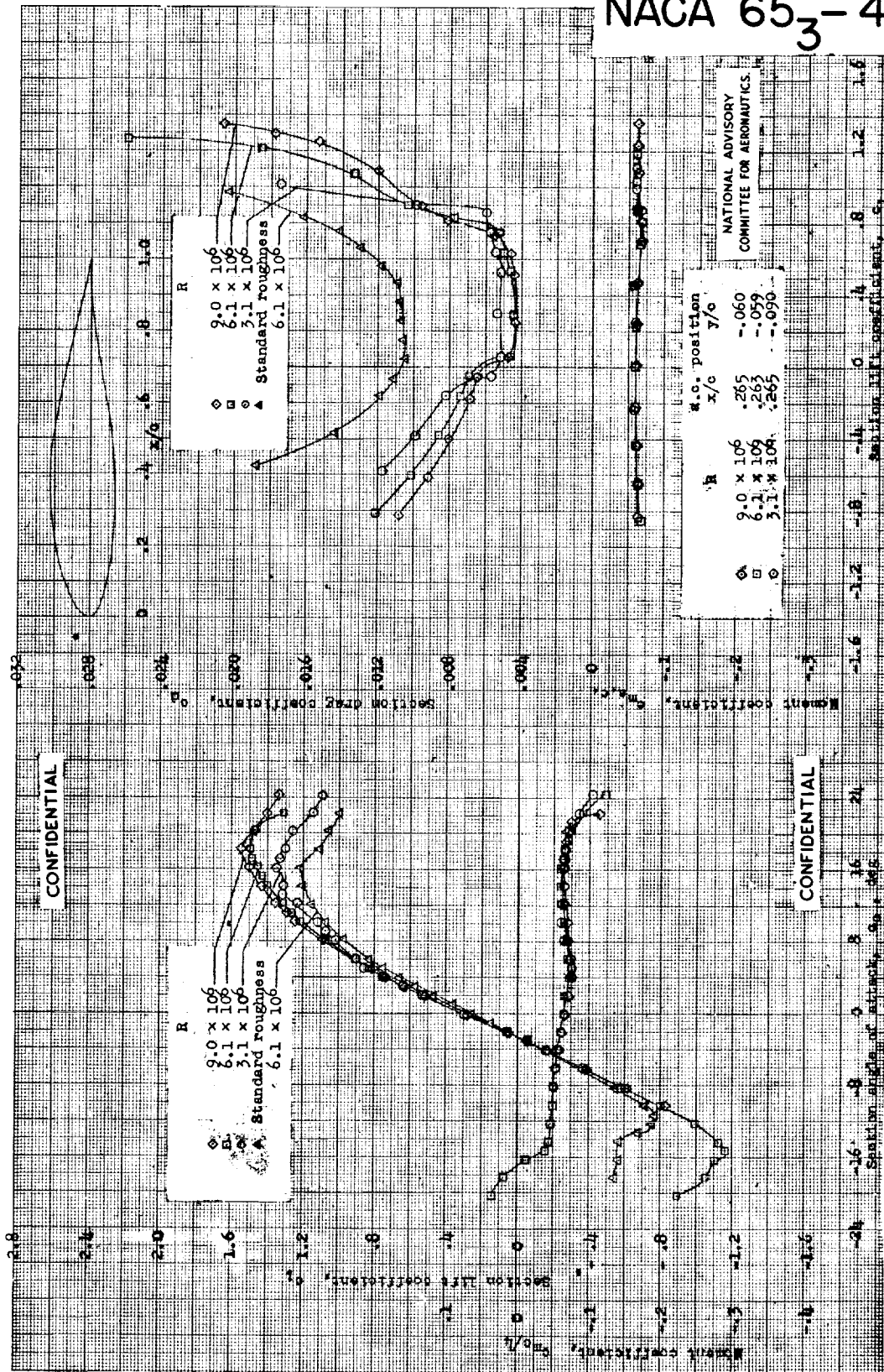
NACA 65₃-118 WITH FLAP



(b) Aerodynamic characteristics. R, 6 x 10⁶; TDT tests 399, 435, 452, 460, and 462.
NACA 65₃-118 airfoil section with 0.309c double-slotted flap.



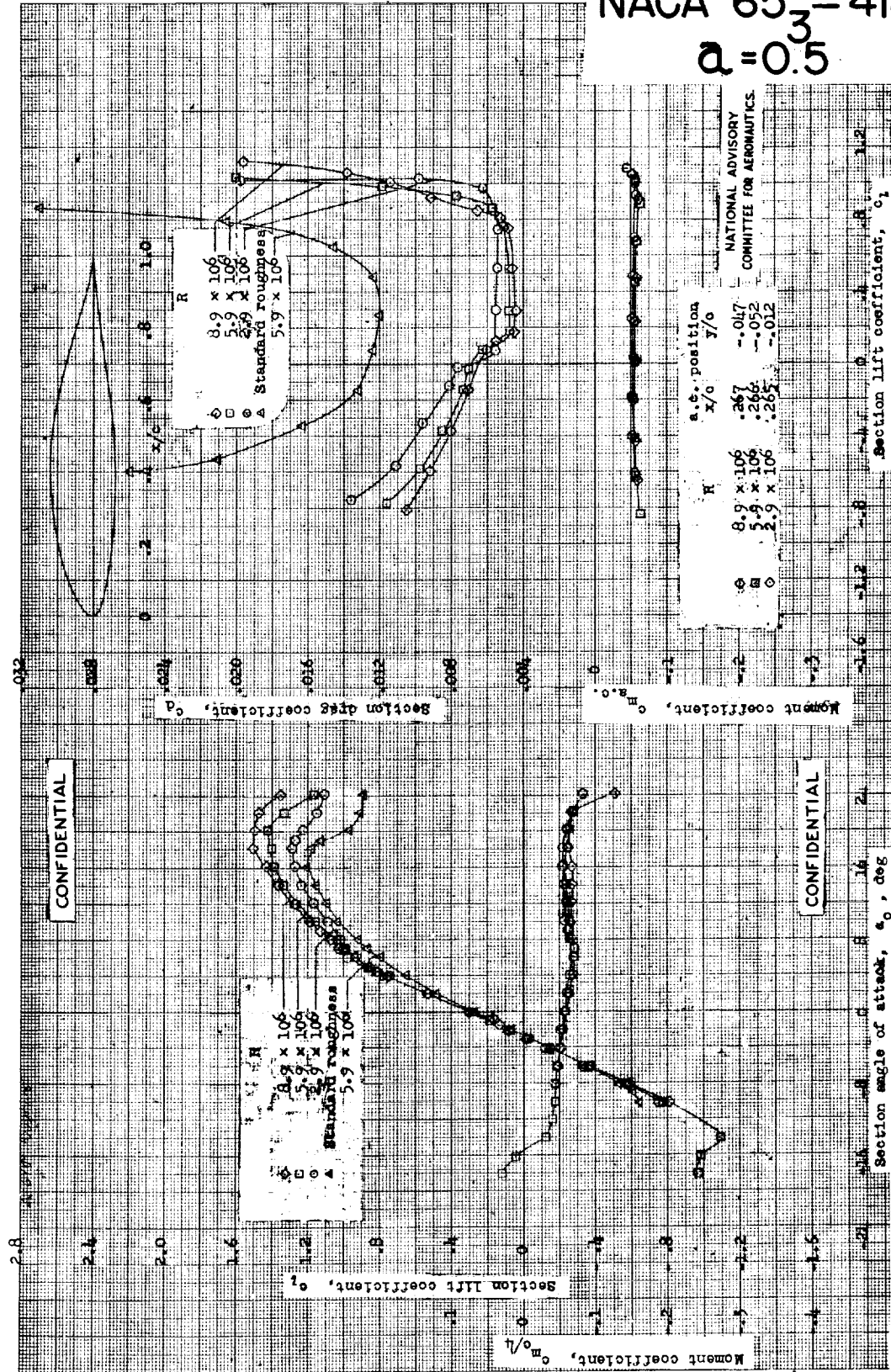
NACA 65₃-418



Aerodynamic characteristics of the NACA 65₃-418 airfoil section, 24-inch chord; TD, tests 314, 320.



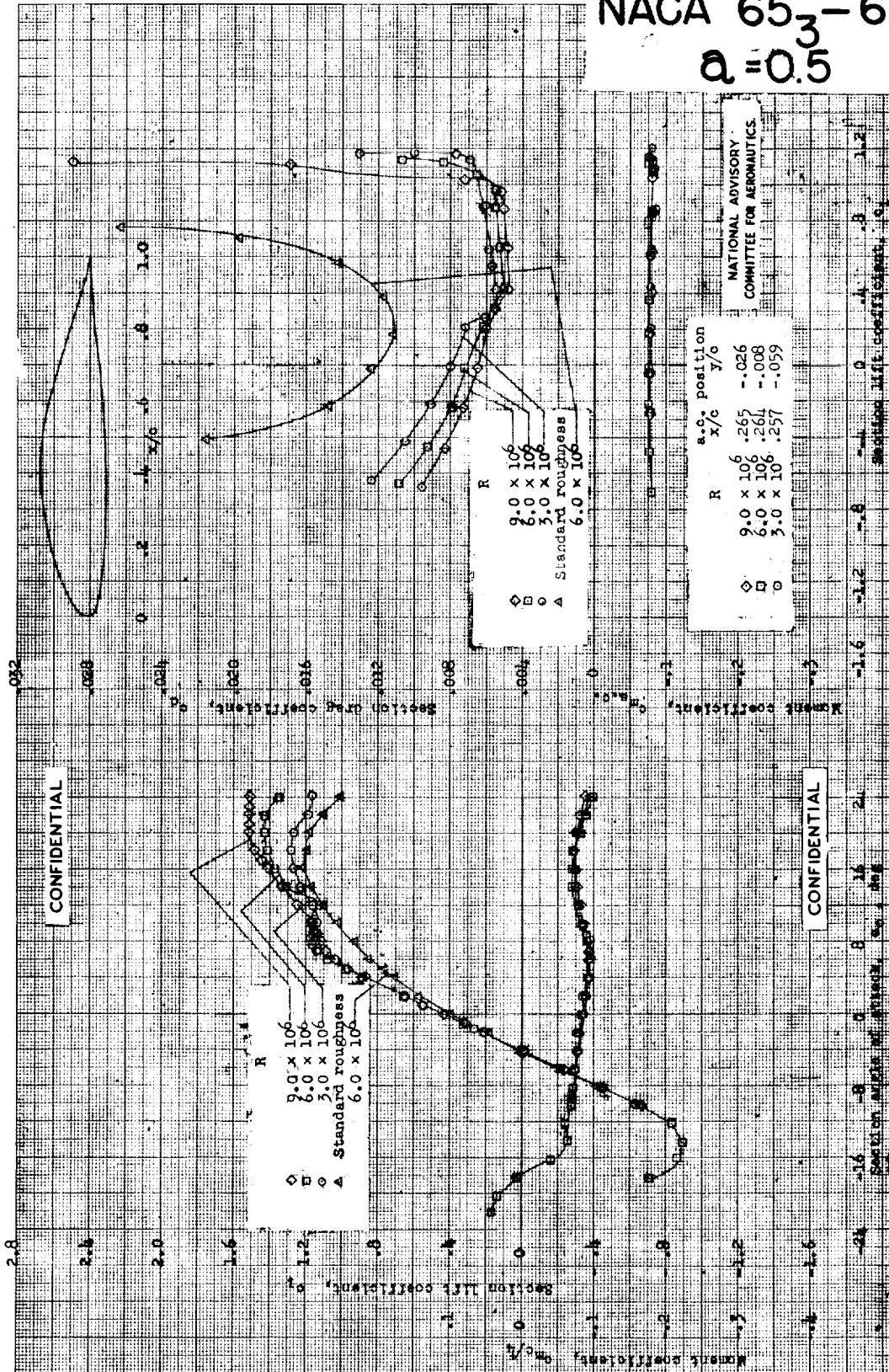
NACA 65₃-418
 $\alpha = 0.5$



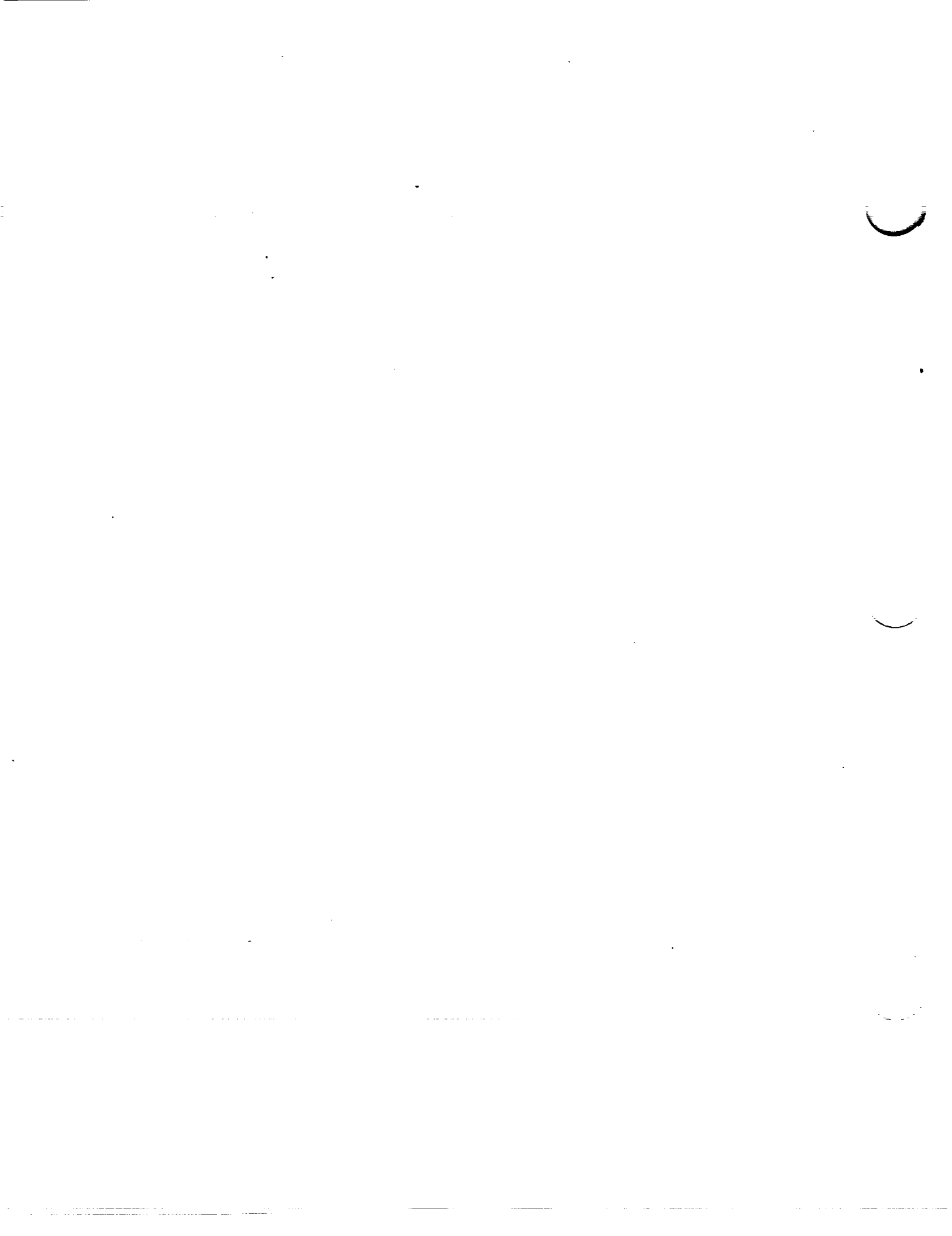
Aerodynamic characteristics of the NACA 65₃-418, $\alpha = 0.5$ airfoil section, 21-inch chord; TDT tests 406, 433, 411.



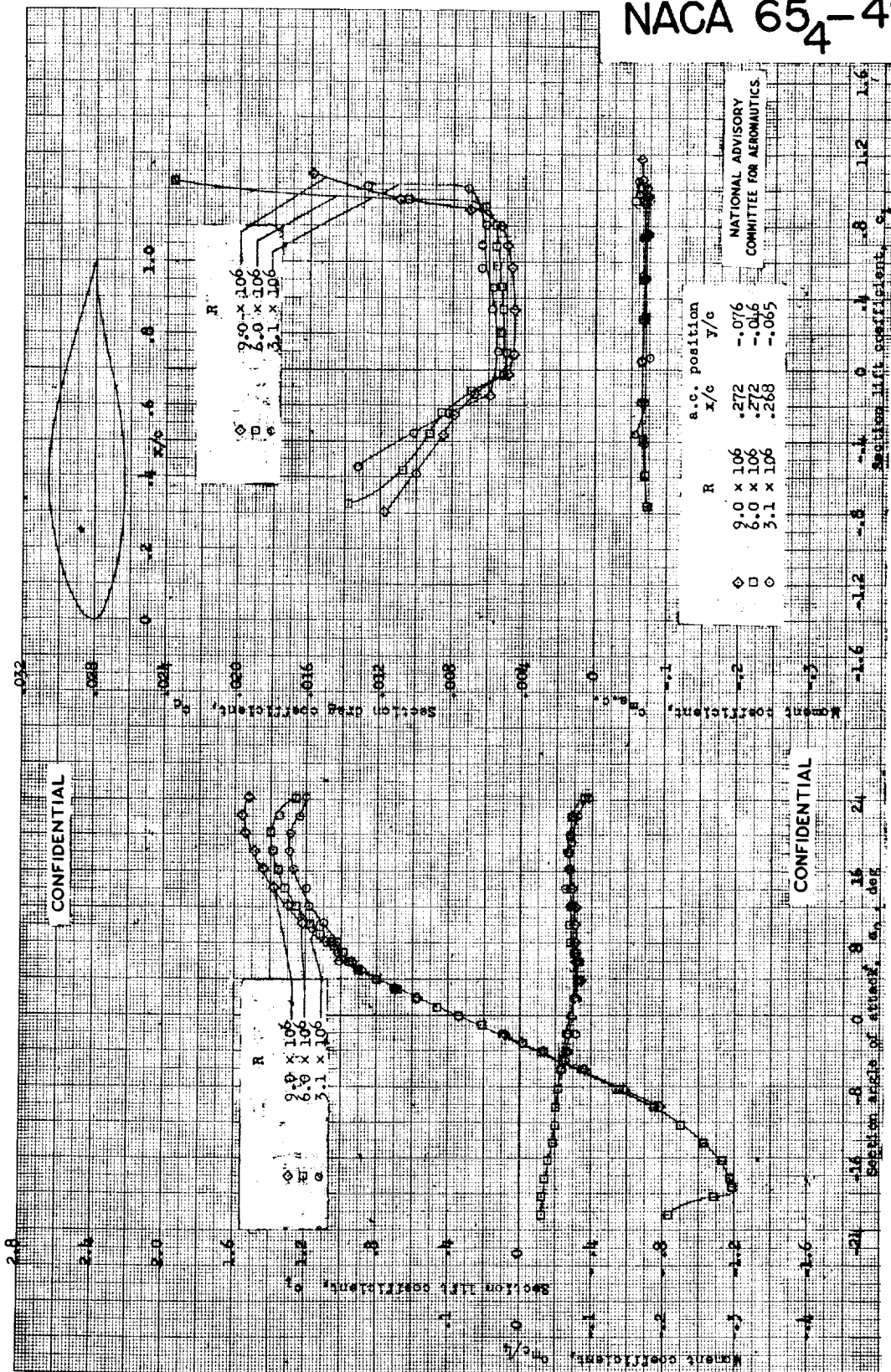
NACA 65₃-618
 $\alpha = 0.5$



Aerodynamic characteristics of the NACA 65₃-618, $\alpha = 0.5$ airfoil section, 24-inch chord; DTI tests 407, 420.



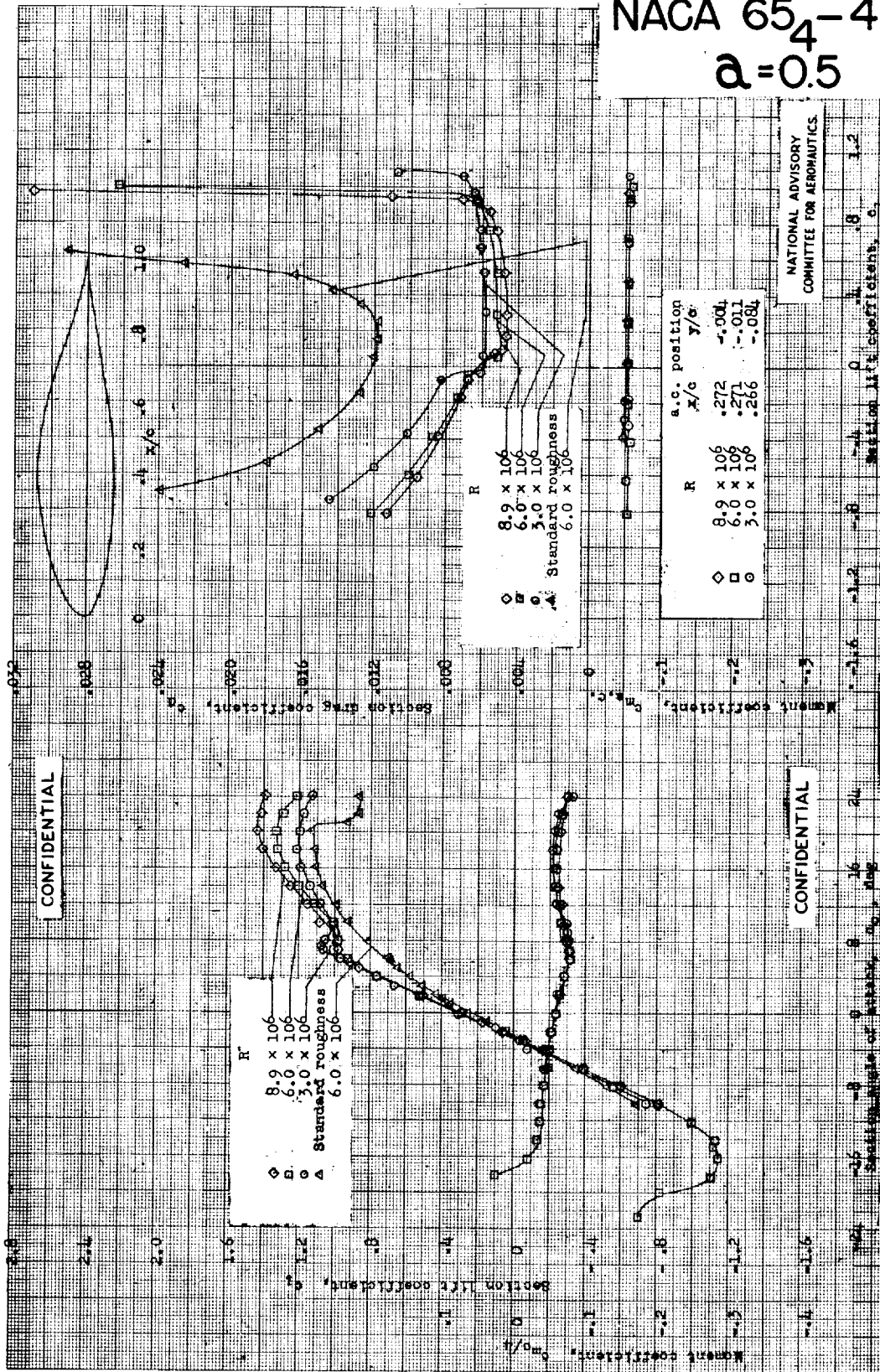
NACA 65₄-421



Aerodynamic characteristics of the NACA 65₄-421 airfoil section, 24-inch chord; TDY tests 316, 321.



NACA 65₄-421
 $\alpha = 0.5$

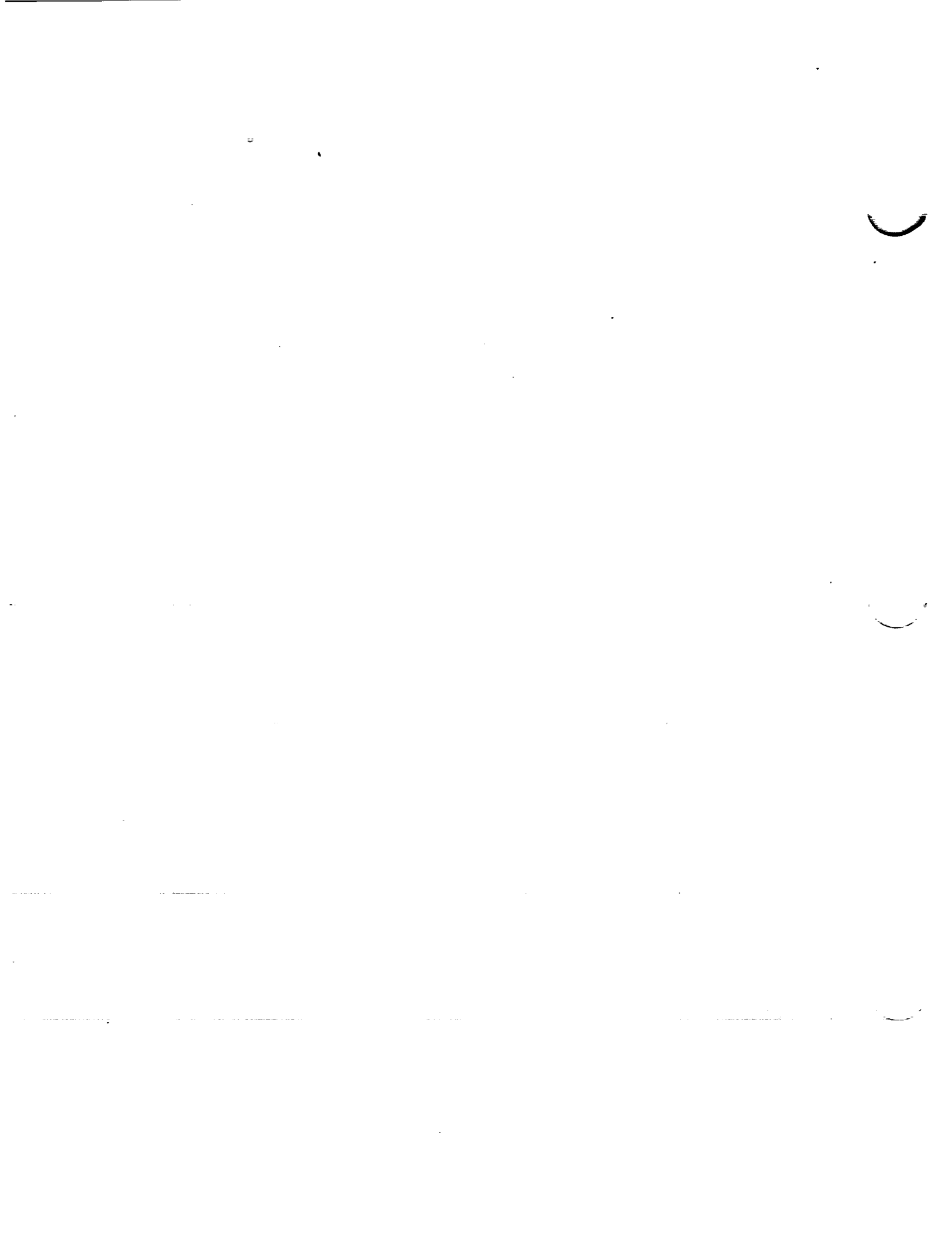


NATIONAL ADVISORY
 COMMITTEE FOR AERONAUTICS

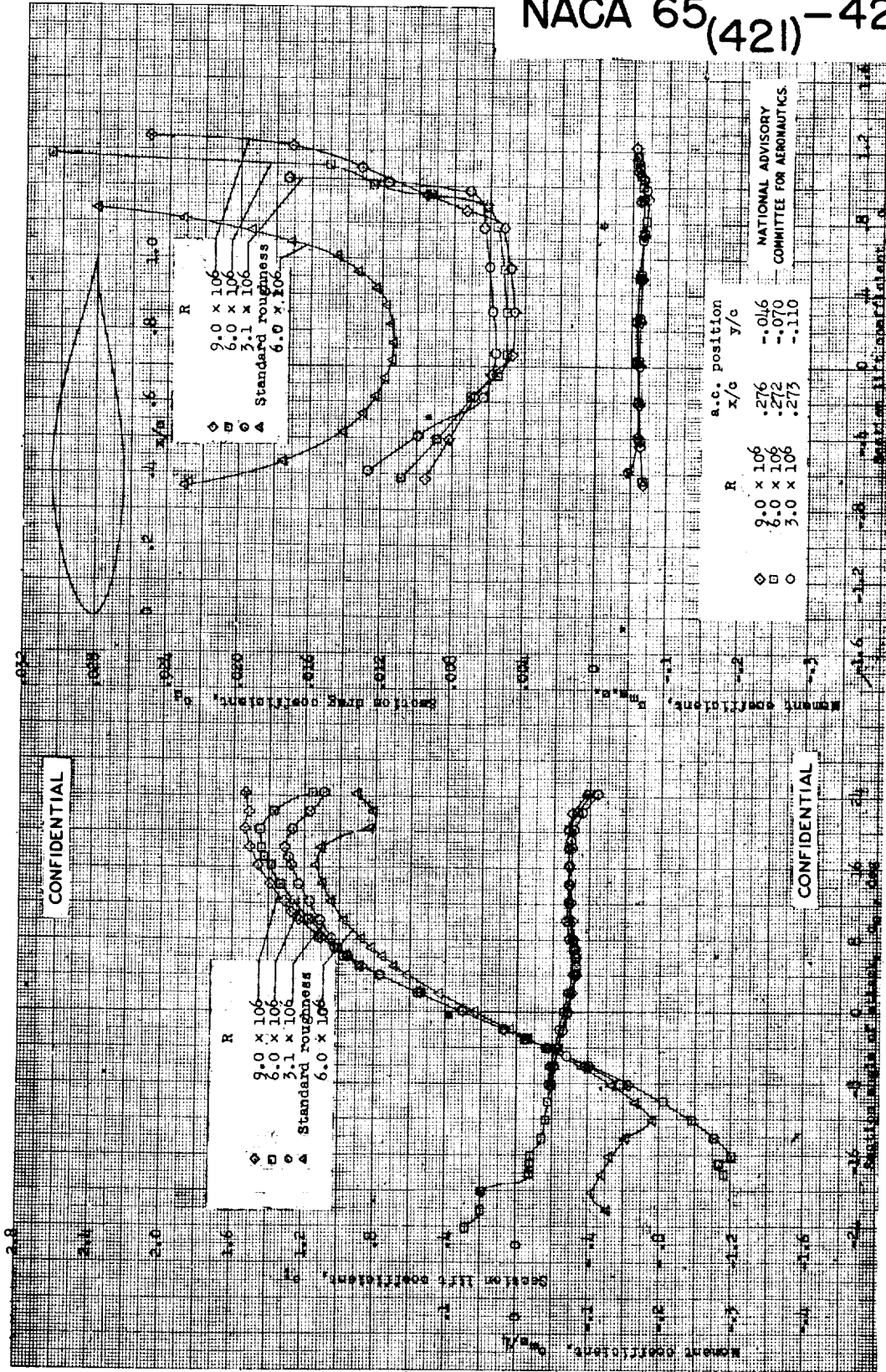
Aerodynamic characteristics of the NACA 65₄-421, $\alpha = 0.5$ airfoil section, 24-inch chord; TDT tests 403, 410, 434.

CONFIDENTIAL

CONFIDENTIAL



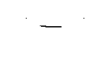
NACA 65(421)-420



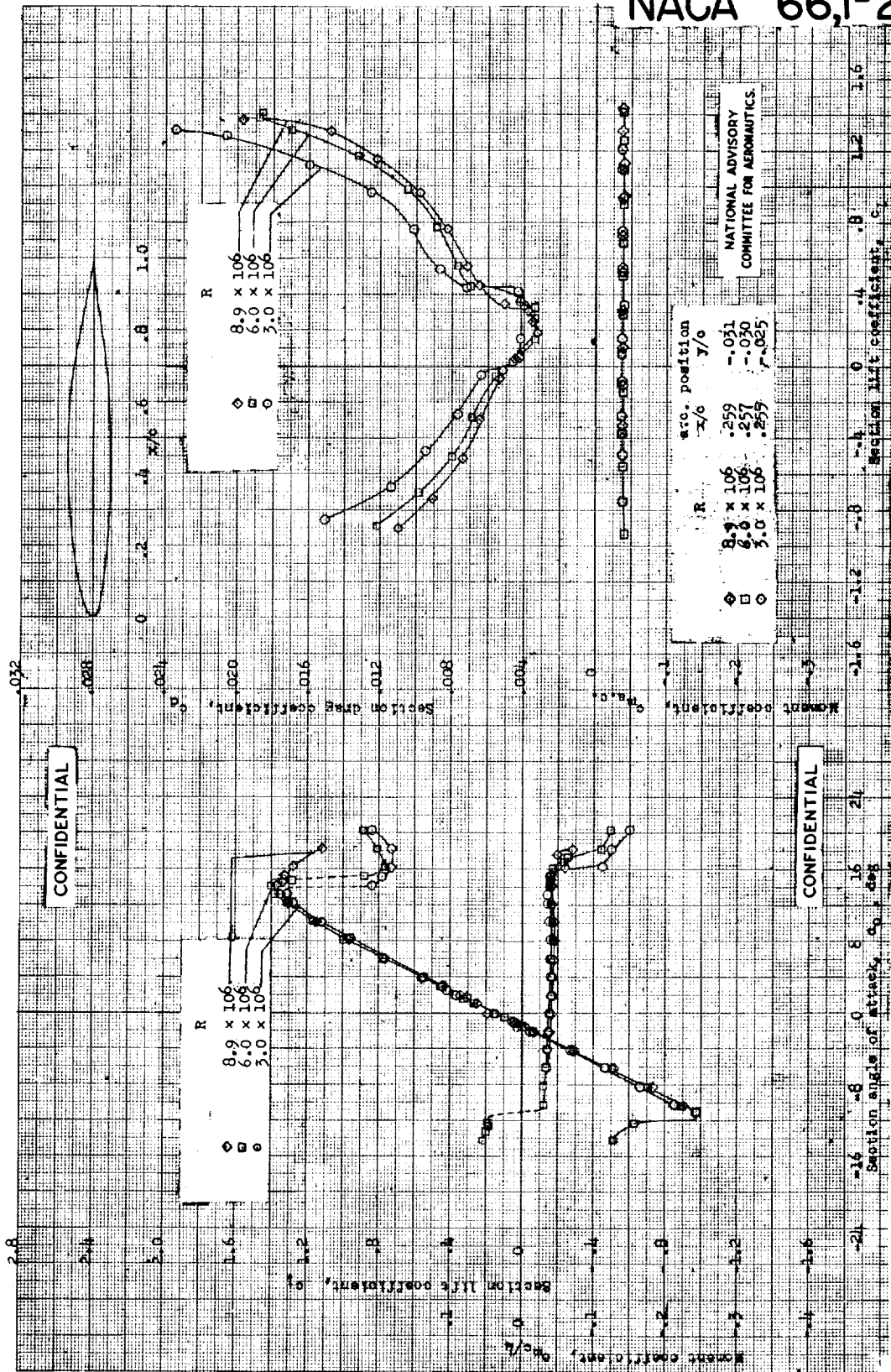
Aerodynamic characteristics of the NACA 65(421)-420 airfoil section, 24-inch chord; TDT tests 312, 322, 328.

CONFIDENTIAL

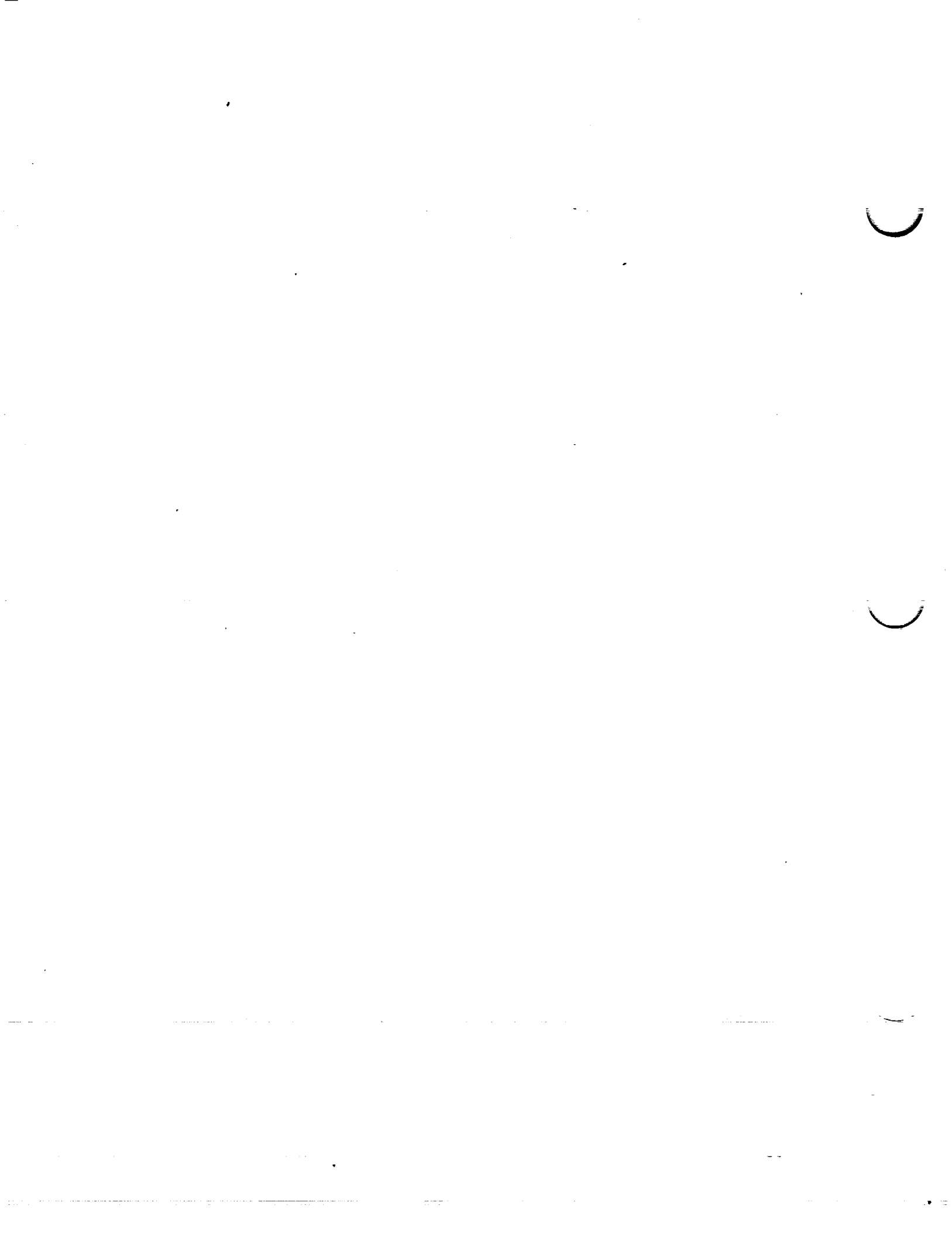
CONFIDENTIAL



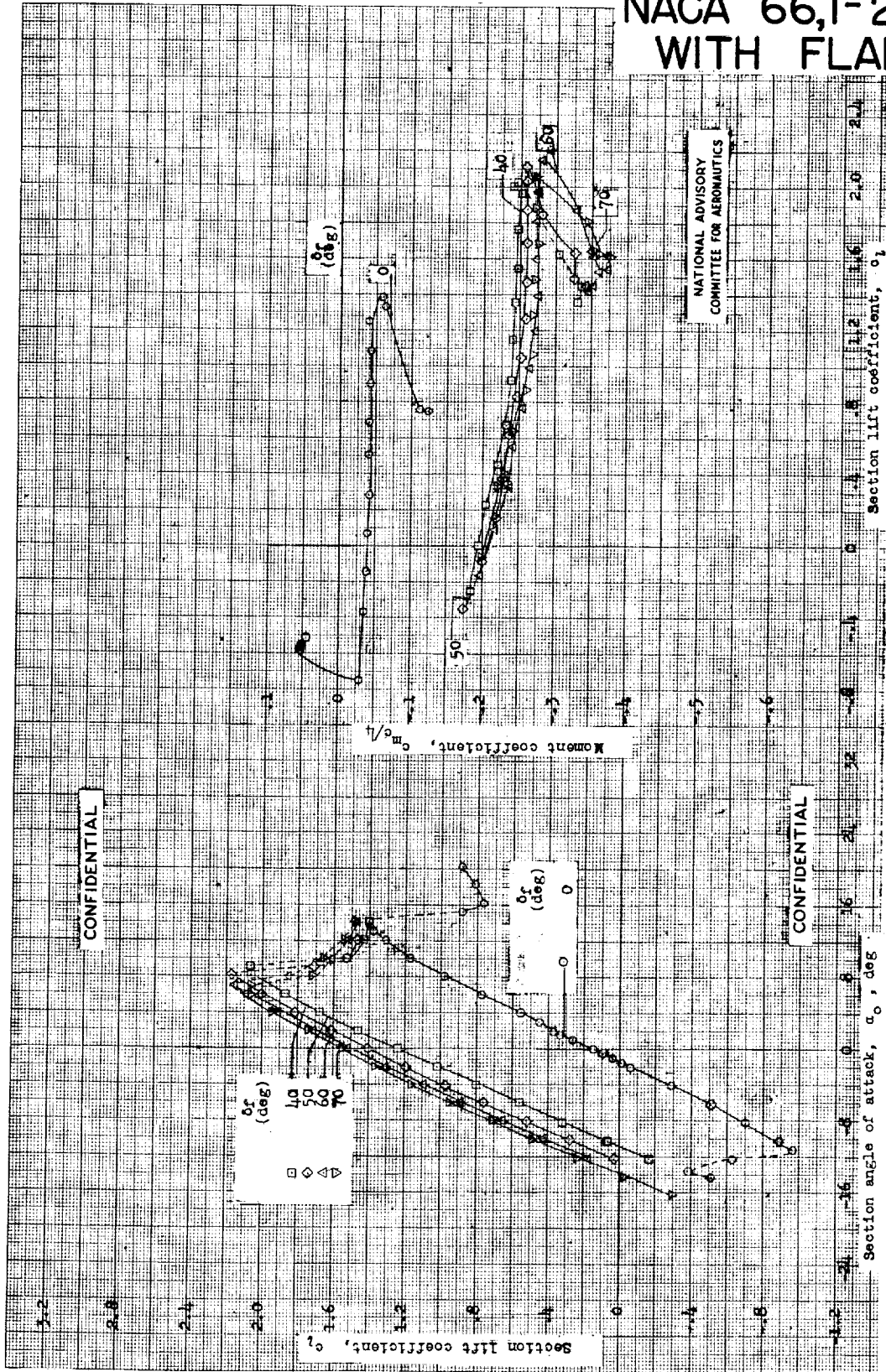
NACA 66,1-212



Aerodynamic characteristics of the NACA 66,1-212 airfoil section, 24-inch chord; TDR tests 424, 426.



NACA 66,1-212 WITH FLAP

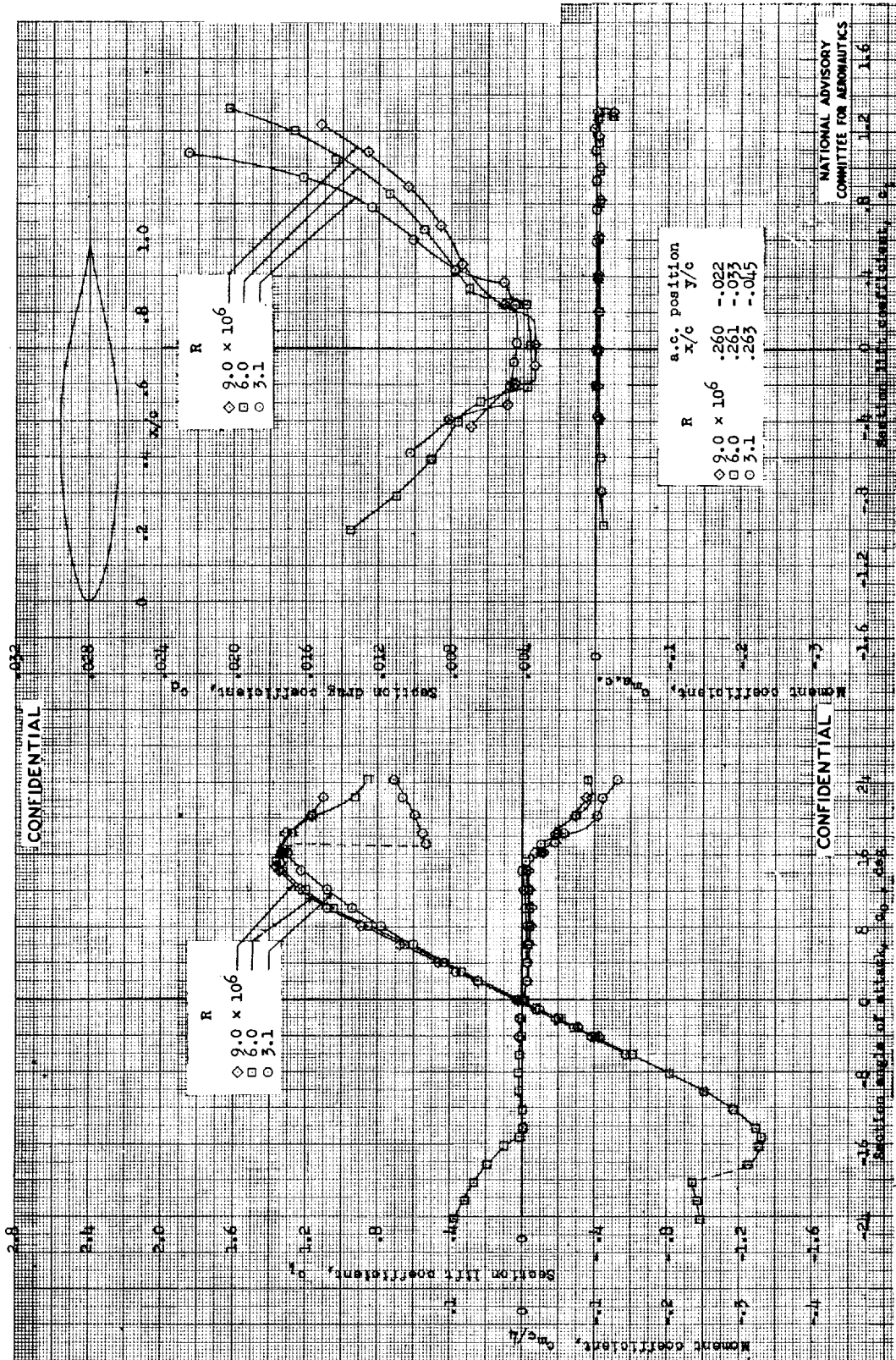


NATIONAL ADVISORY
COMMITTEE FOR AERONAUTICS

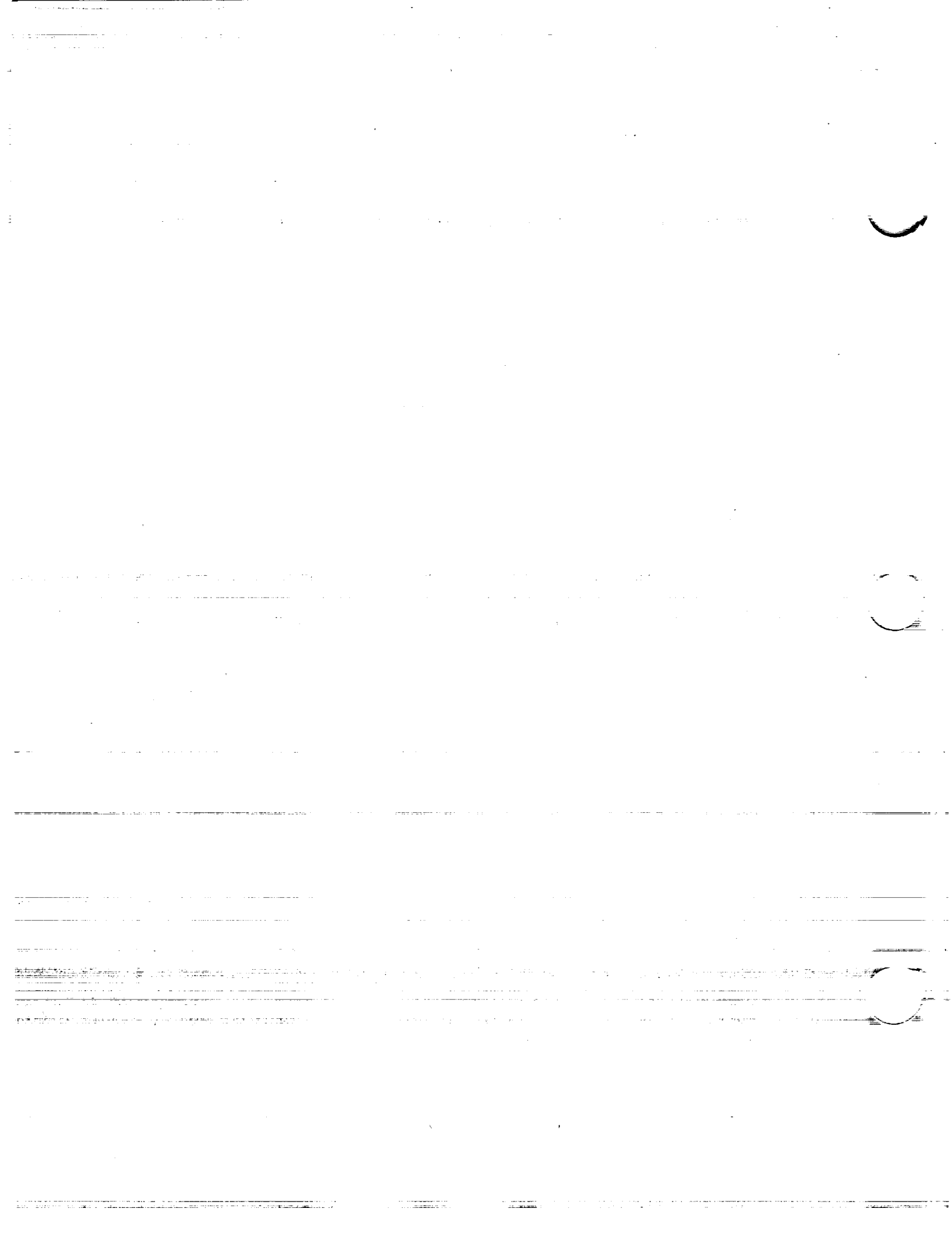
Lift and moment characteristics of the NACA 66,1-212 airfoil section with 0.20c split flap. $R, 6 \times 10^6$; TDT tests 424, 570, 576, 602.



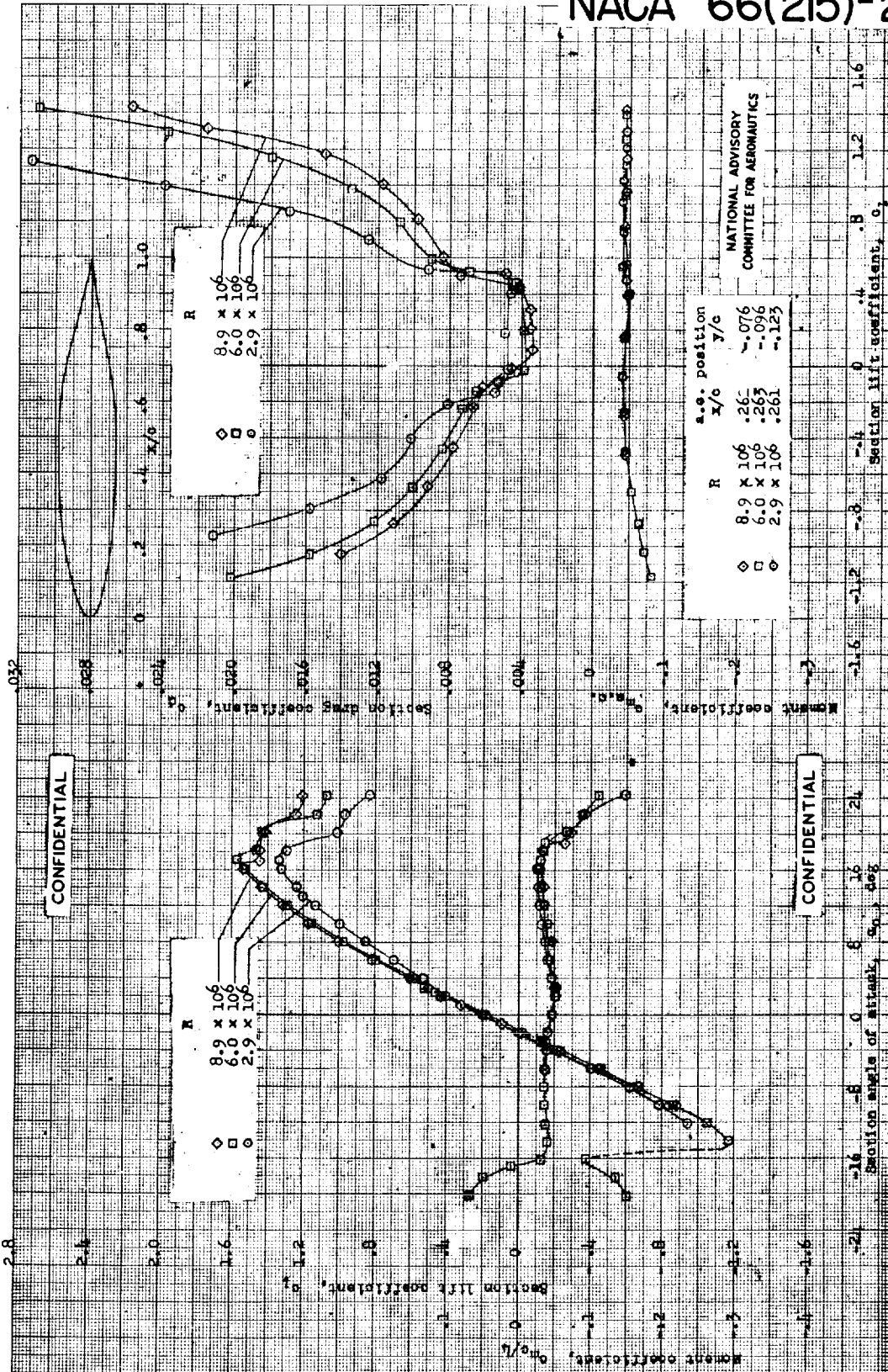
NACA 66(215)-016



Aerodynamic characteristics of the NACA 66(215)-016 airfoil section, 24-inch chord; DT test 244.



NACA 66(215)-216



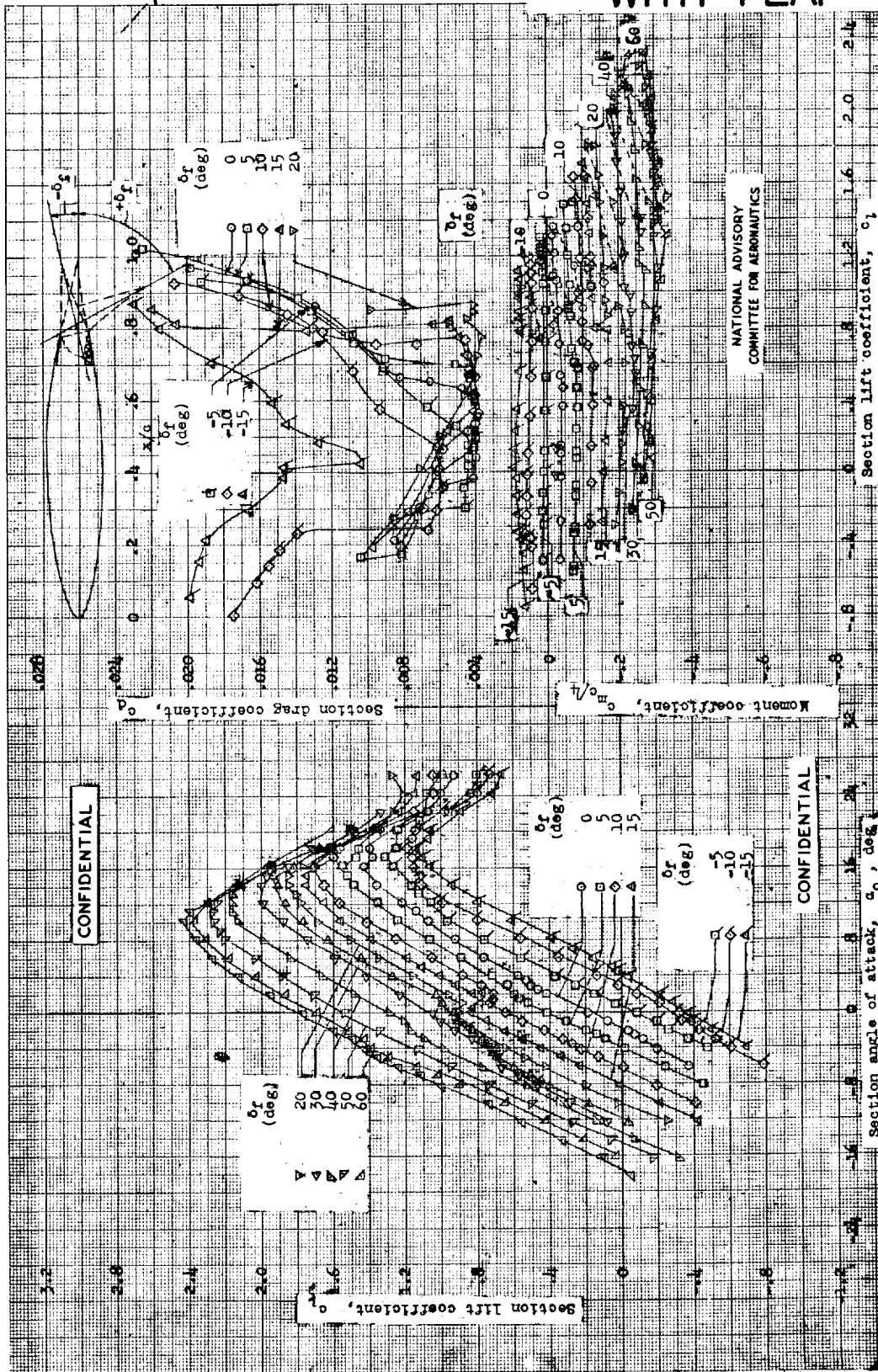
Aerodynamic characteristics of the NACA 66(215)-216 airfoil section, 24-inch chord; TDT tests 247, 249.

CONFIDENTIAL

CONFIDENTIAL



NACA 66(215)-216 WITH FLAP



CONFIDENTIAL

CONFIDENTIAL

NATIONAL ADVISORY
COMMITTEE FOR AERONAUTICS

Section lift coefficient, c_l

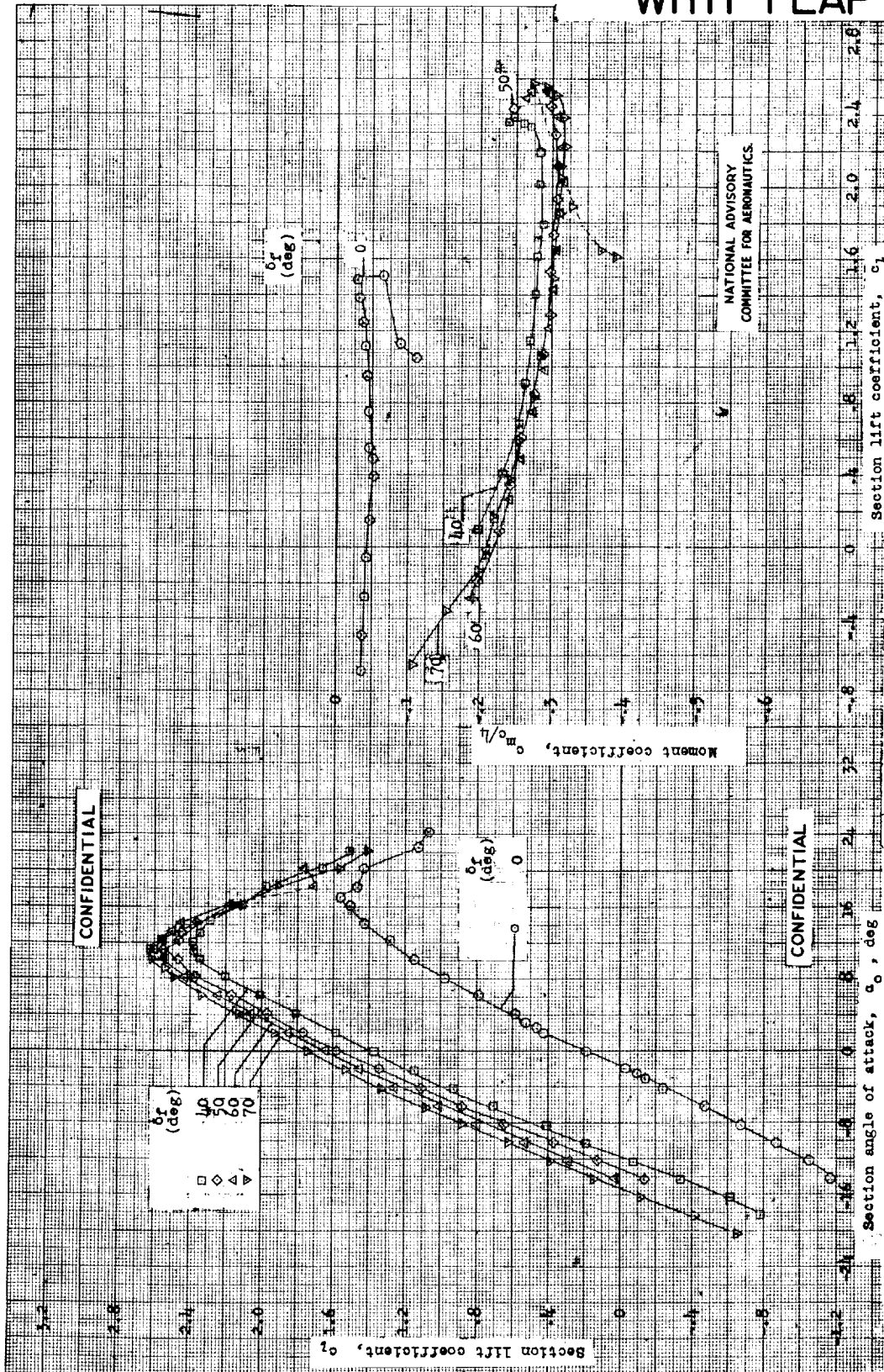
Section drag coefficient, c_d

Section angle of attack, α , deg

Aerodynamic characteristics of the NACA 66(215)-216 airfoil section with 0.20c sealed plain flap. $R = 6 \times 10^6$; MFR tests 293 and 302.

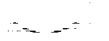


NACA 66(215)-216 WITH FLAP

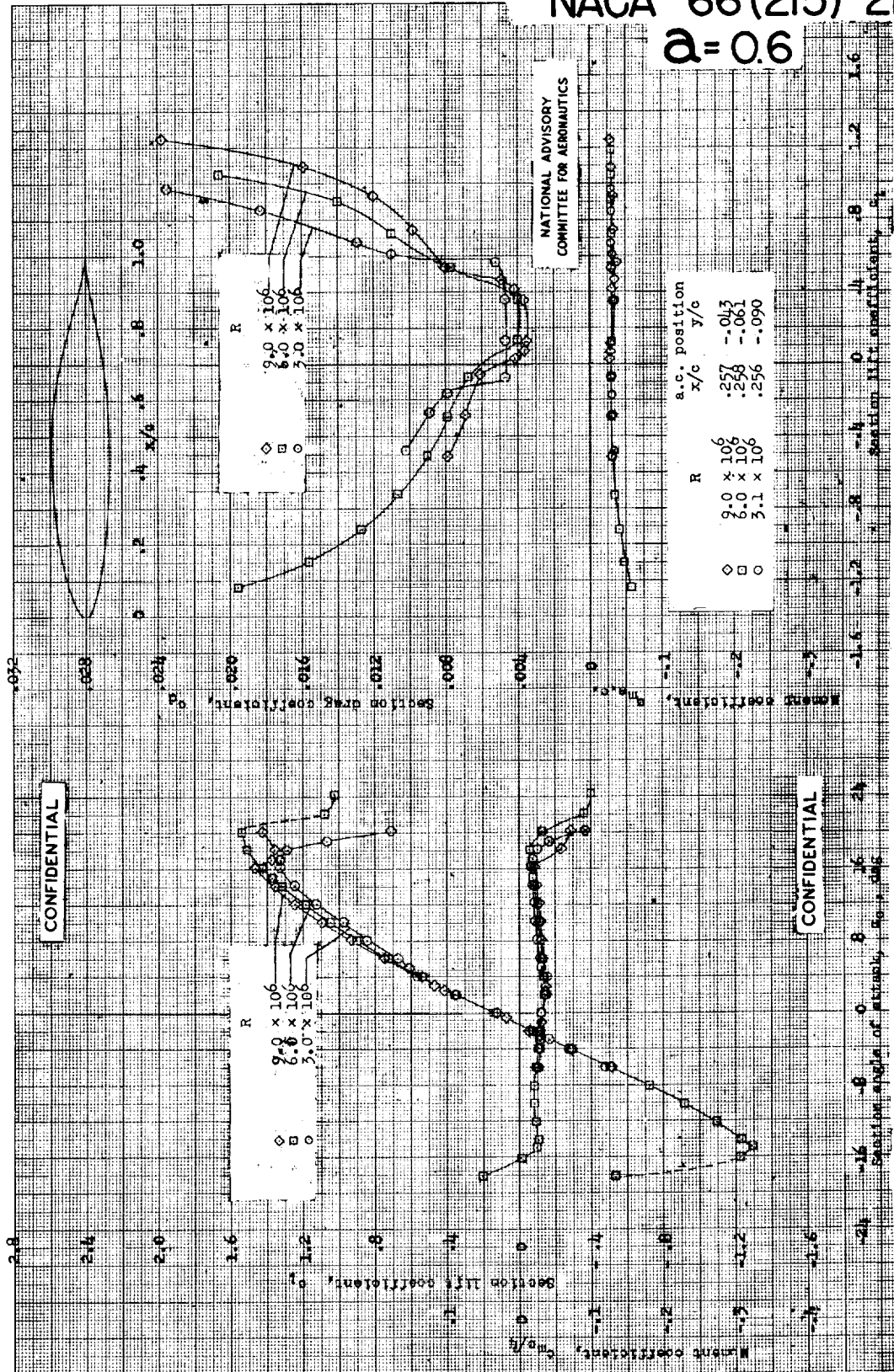


NATIONAL ADVISORY
COMMITTEE FOR AERONAUTICS.

Lift and moment characteristics of the NACA 66(215)-216 airfoil section with 0.20c split flap. R, 6×10^6 ; TDT tests 247, 568, and 571.



NACA 66(215)-216
 $\alpha = 0.6$



CONFIDENTIAL

CONFIDENTIAL

NATIONAL ADVISORY
 COMMITTEE FOR AERONAUTICS

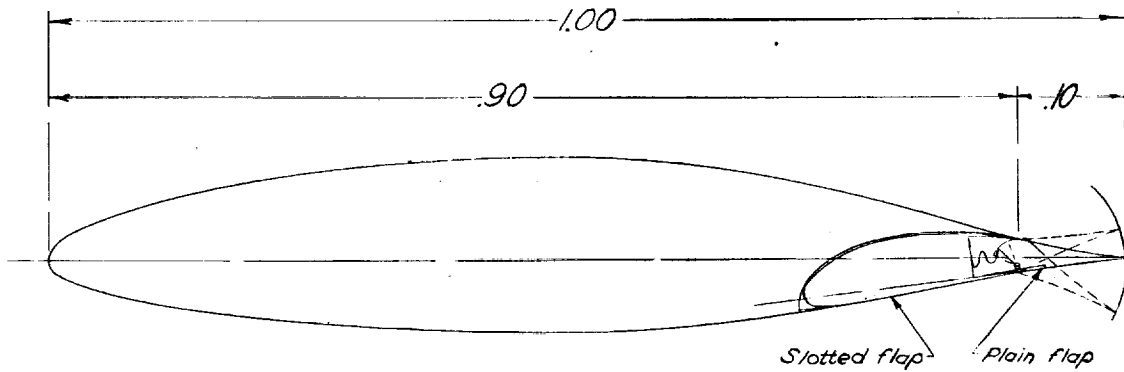
R	a.c. position x/c	y/c
\diamond 2.0×10^6	.257	-.043
\square 6.0×10^6	.258	-.061
\circ 3.1×10^6	.256	-.090

Aerodynamic characteristics of the NACA 66(215)-216, $\alpha = 0.6$ airfoil section, 24-inch chord; TDT test 215.

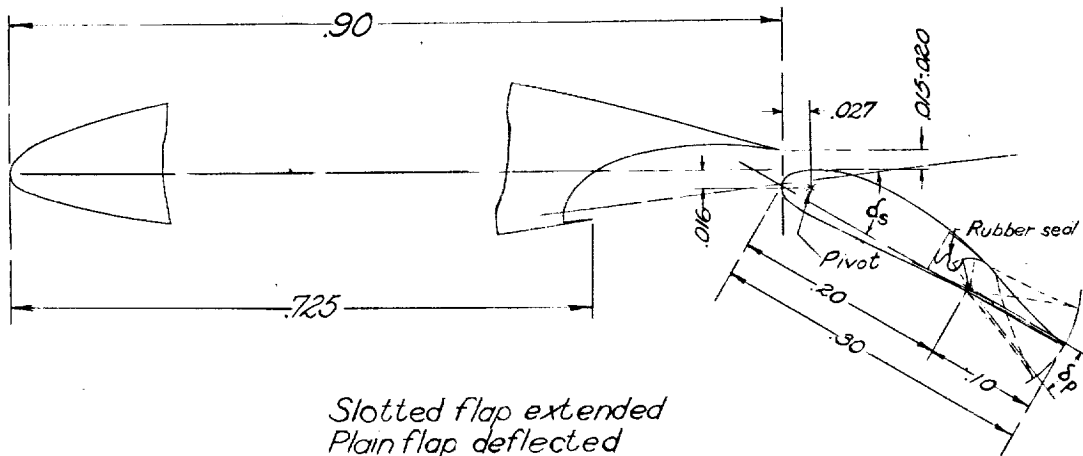


NACA 66(215)-216
 $a = 0.6$
 WITH FLAP

CONFIDENTIAL



*Slotted flap retracted
 Plain flap deflected*



*Slotted flap extended
 Plain flap deflected*

CONFIDENTIAL

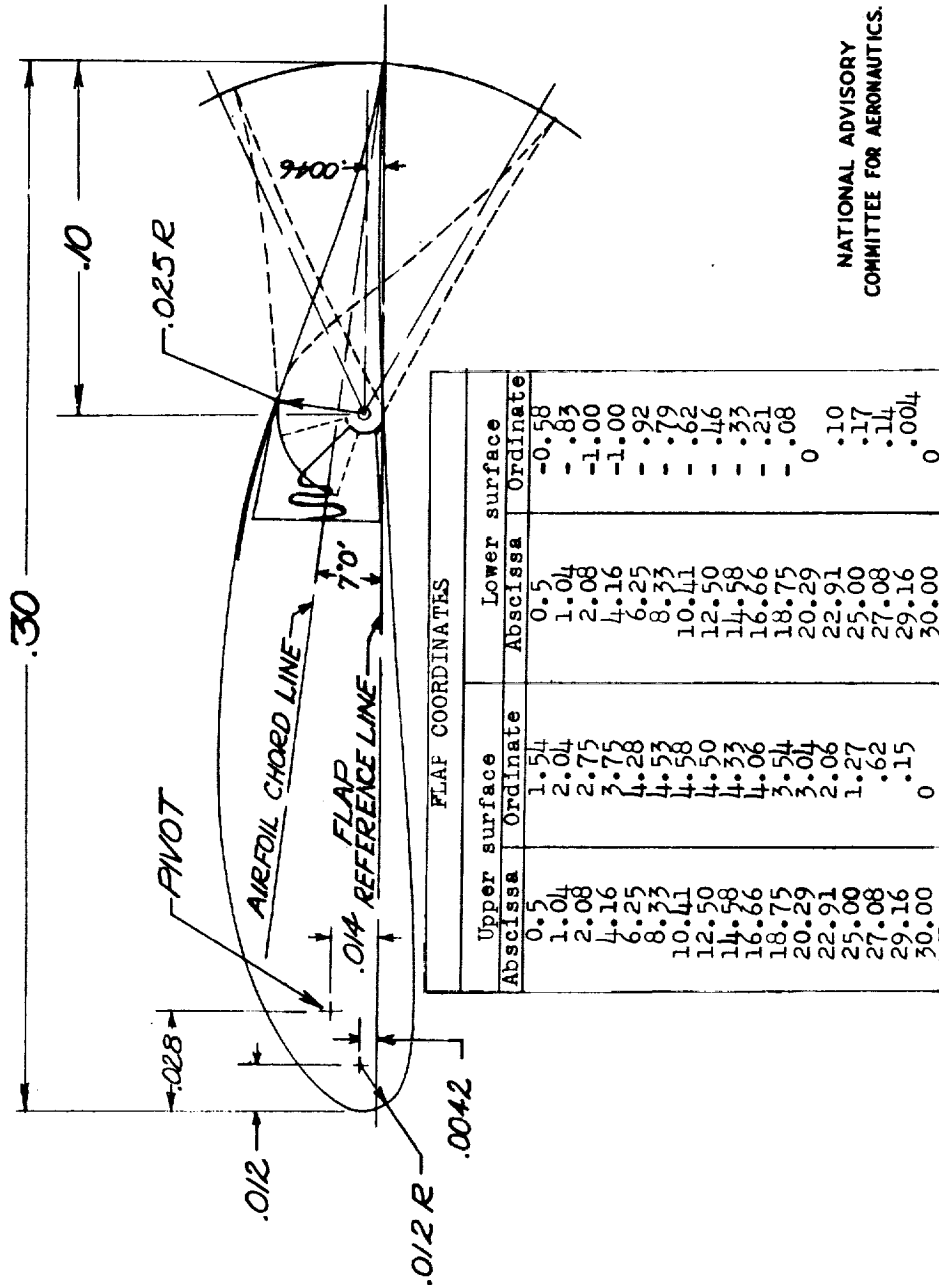
NATIONAL ADVISORY
 COMMITTEE FOR AERONAUTICS

(a) Airfoil-flap configuration.
 NACA 66(215)-216, $a = 0.6$ airfoil section with $0.30c$
 slotted and $0.10c$ plain flap.



NACA 66(215)-216 a = 0.6 WITH FLAP

CONFIDENTIAL



NATIONAL ADVISORY
COMMITTEE FOR AERONAUTICS.

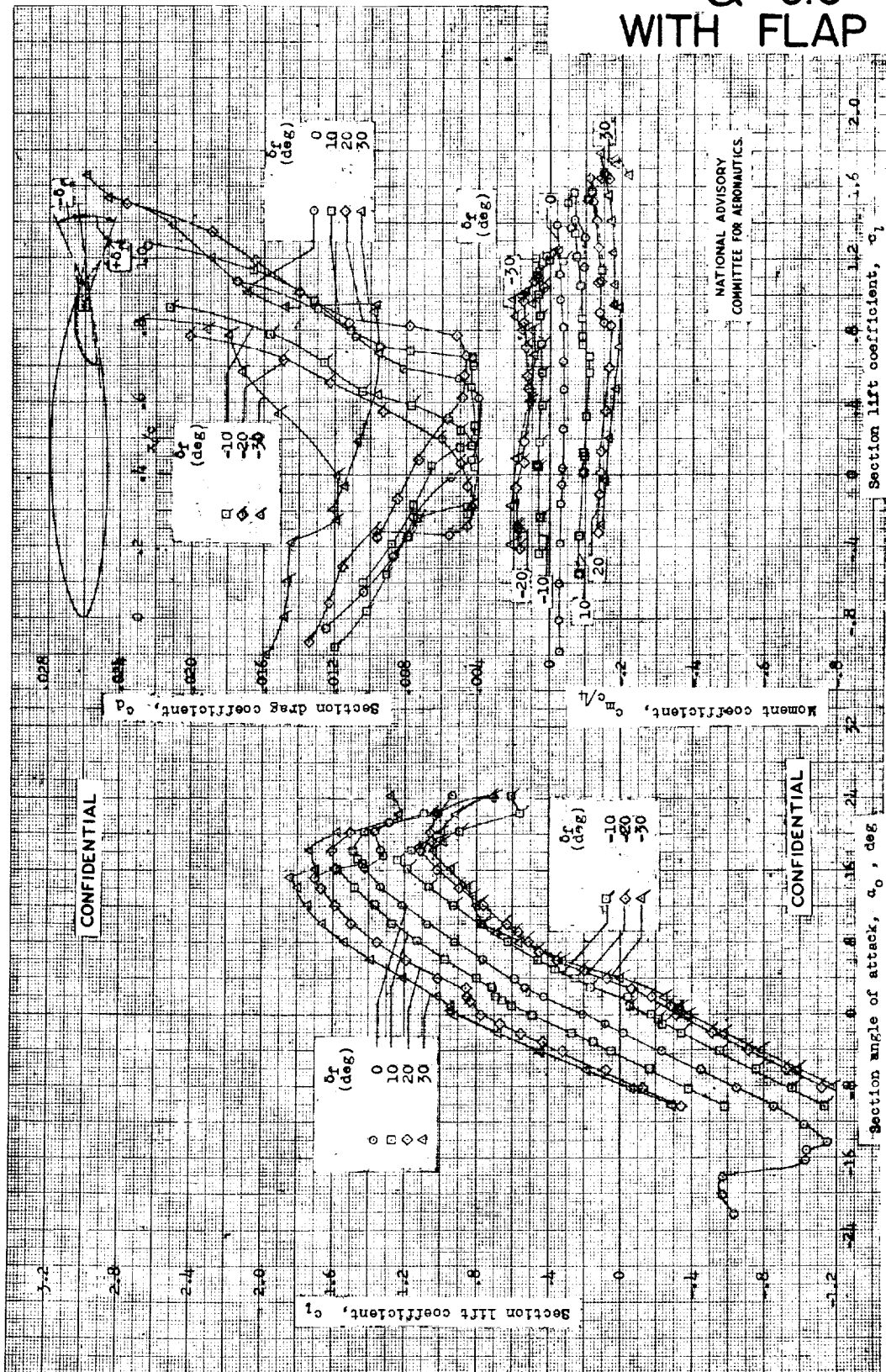
CONFIDENTIAL

(b) Flap configuration.

NACA 66(215)-216, a = 0.6 airfoil section with 0.30c slotted and 0.10c plain flap.



NACA 66(215)-216 $\alpha = 0.6$ WITH FLAP



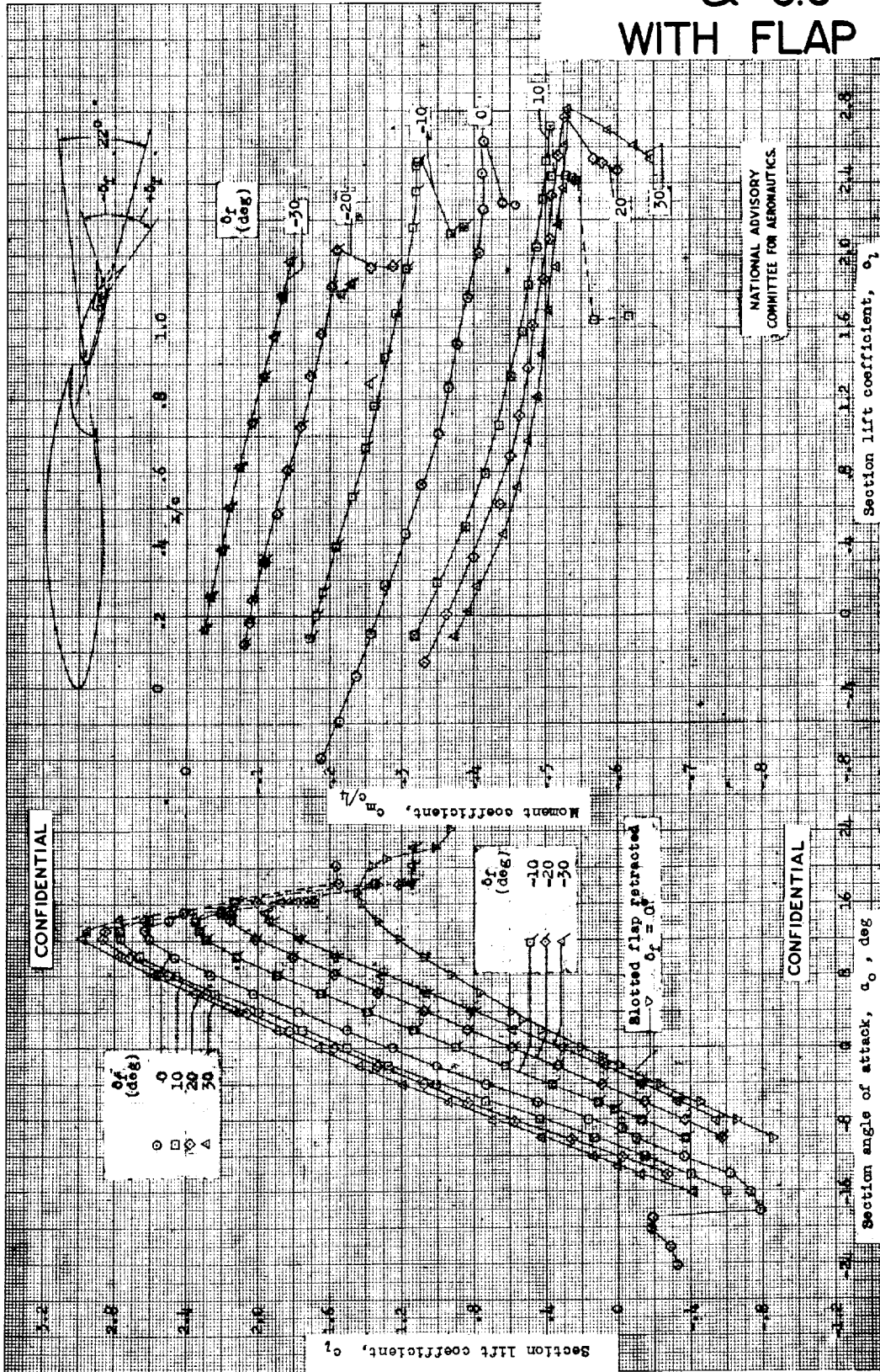
NATIONAL ADVISORY
 COMMITTEE FOR AERONAUTICS

(c) Aerodynamic characteristics. Slotted flap retracted. $R, 6 \times 10^6$. TPT tests 382 and 385.

NACA 66(215)-216, $\alpha = 0.6$ airfoil section with 0.300 slotted and 0.100 plain flap.



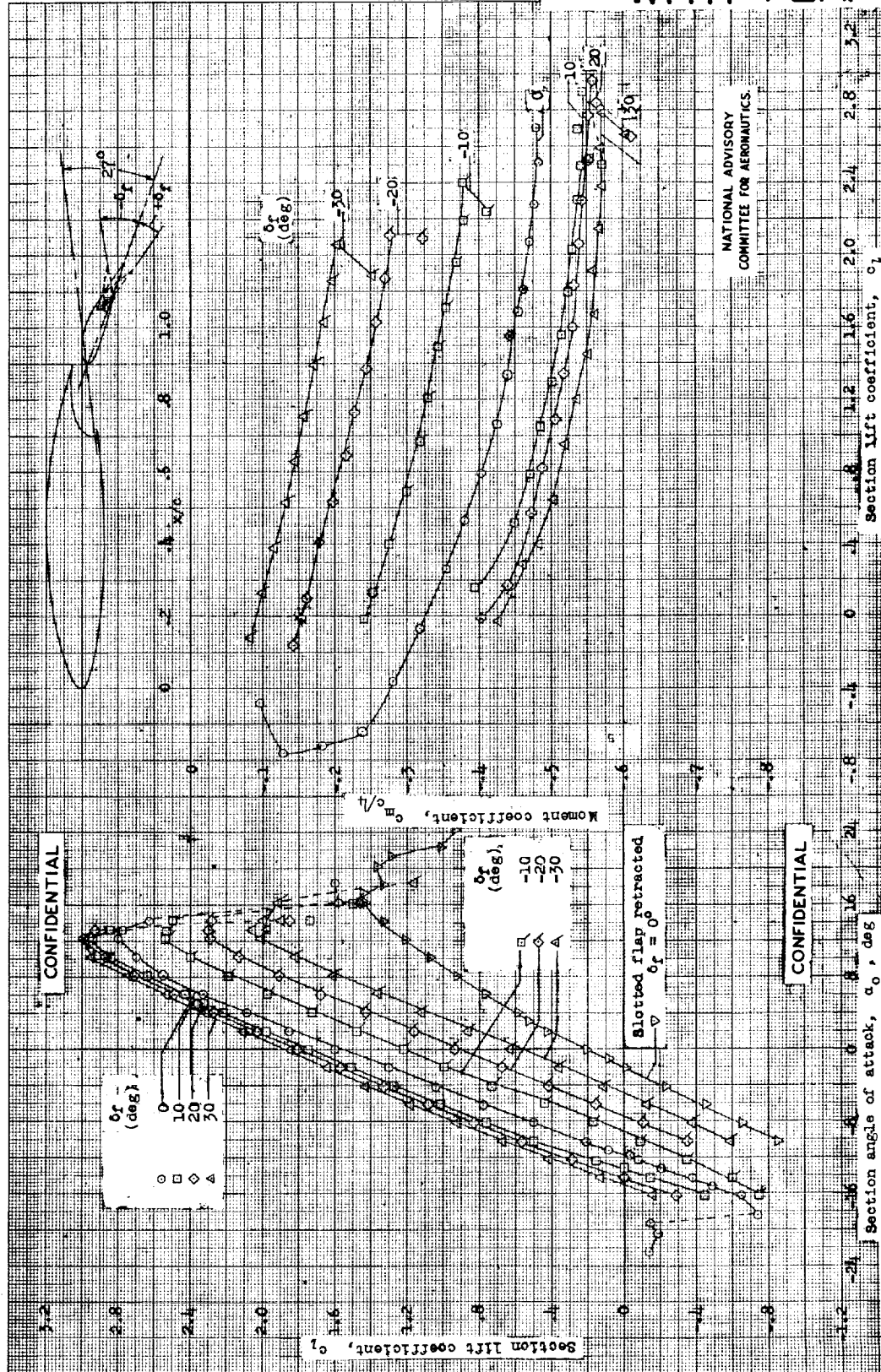
NACA 66(215)-216
 $\alpha = 0.6$
 WITH FLAP



(d) Lift and moment characteristics. Slotted flap deflected 22° . $R, 6 \times 10^6$; TDT tests 236, 352, and 382. NACA 66(215)-216, $\alpha = 0.6$ airfoil section with 0.30c slotted and 0.10c plain flap.



NACA 66(215)-216 $\alpha = 0.6$ WITH FLAP

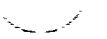


NATIONAL ADVISORY
 COMMITTEE FOR AERONAUTICS

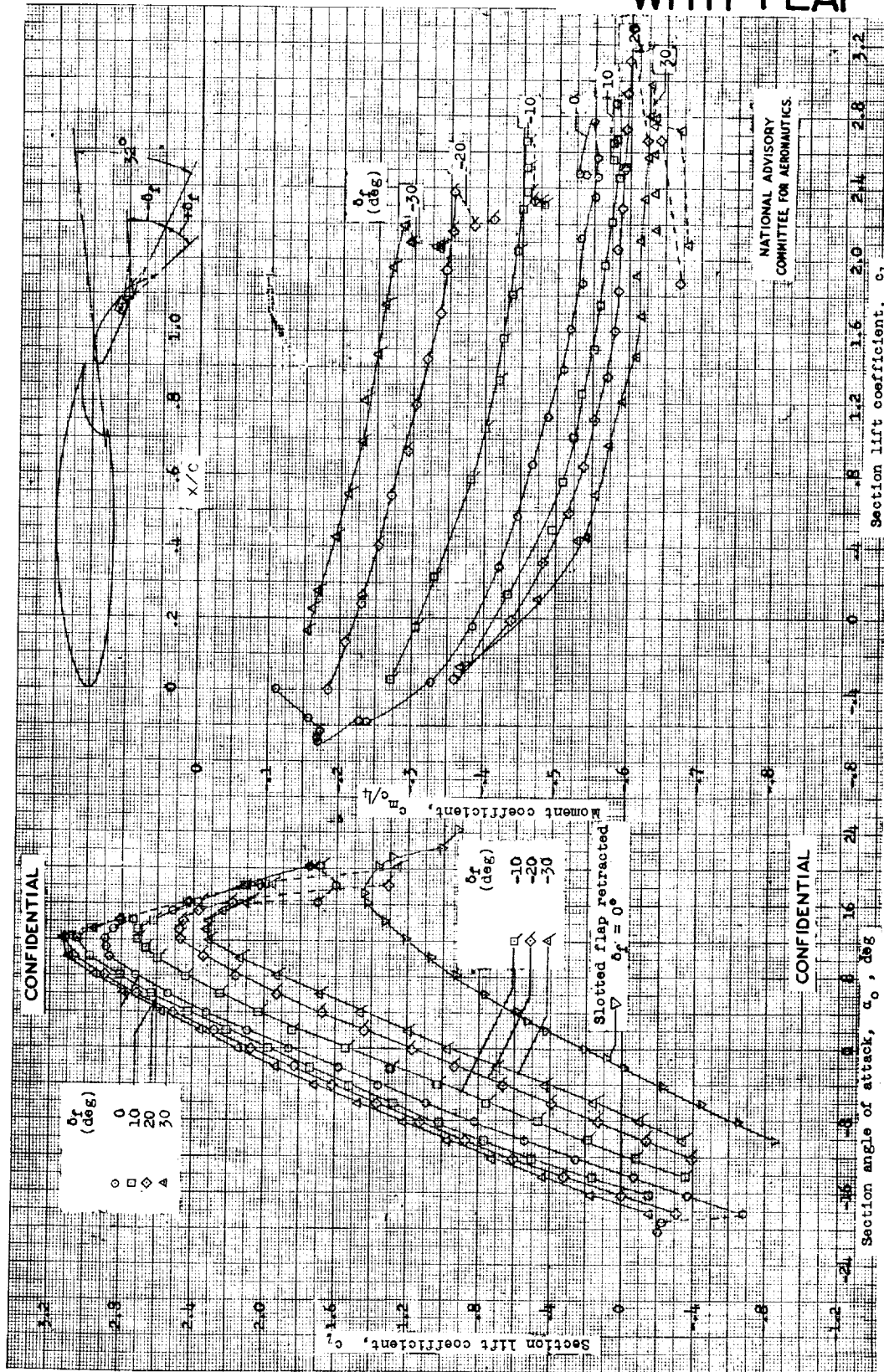
(e) Lift and moment characteristics. Slotted flap deflected 27°. $R, 6 \times 10^6$;
 NACA 66(215)-216, $\alpha = 0.6$ airfoil section with 0.30c slotted and 0.10c plain flap.

CONFIDENTIAL

CONFIDENTIAL



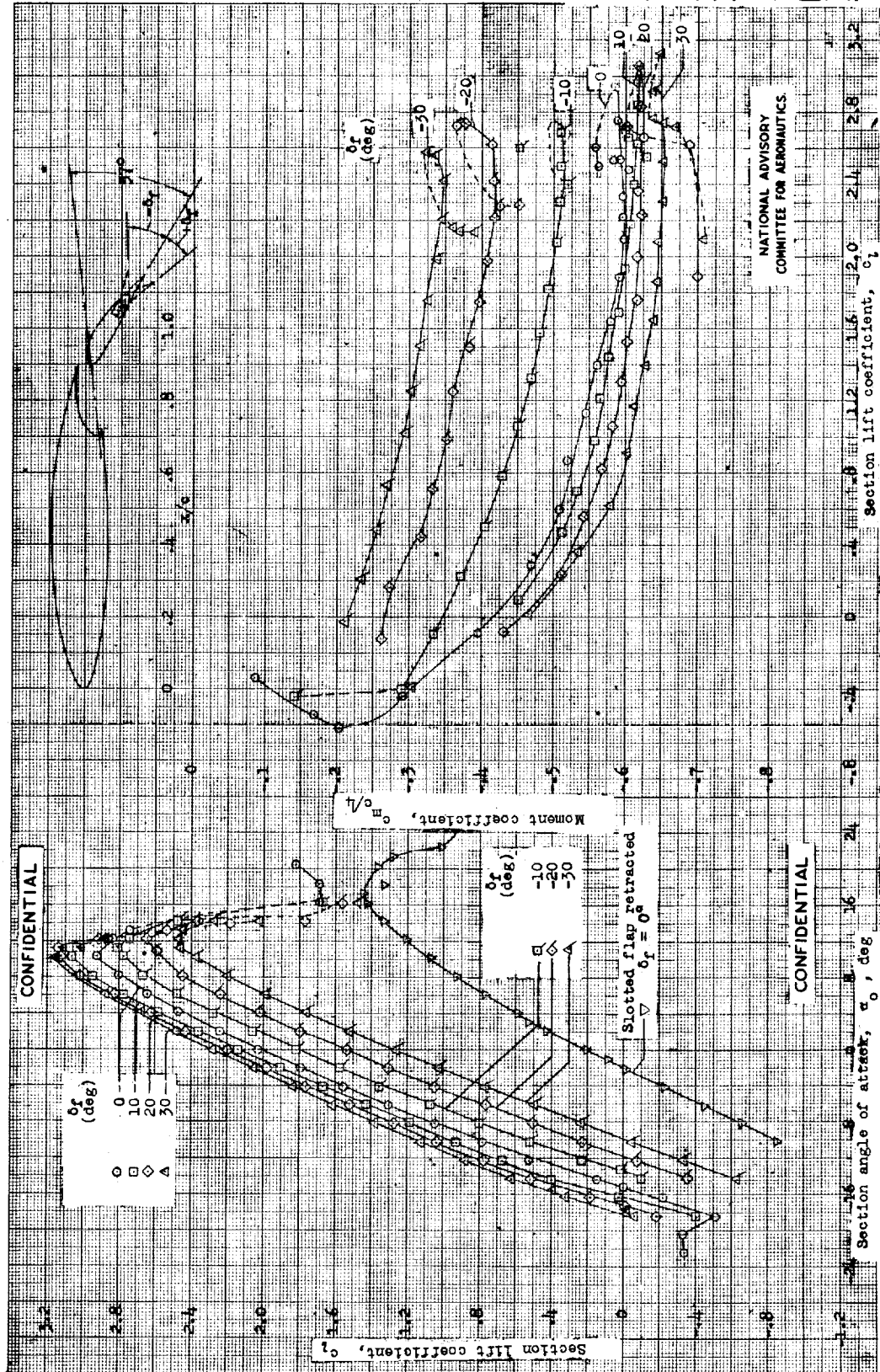
NACA 66(215)-216 $\alpha = 0.6$ WITH FLAP



(f) Lift and moment characteristics. Slotted flap deflected 32° . $R, 6 \times 10^6$; DT tests 352, 357, 359, and 382. NACA 66(215)-216, $\alpha = 0.6$, airfoil section with 0.30c slotted and 0.10c plain flap.

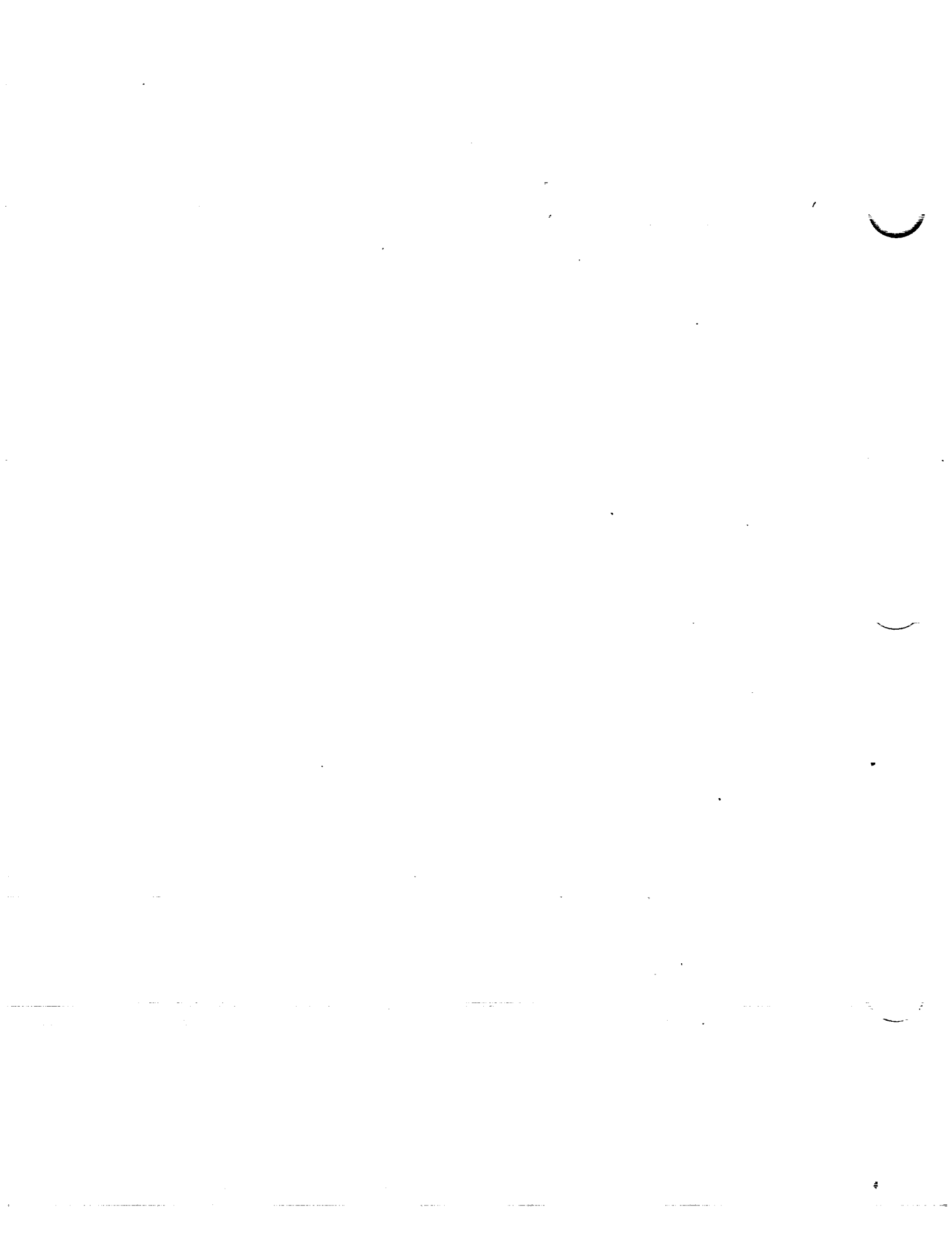


NACA 66(215)-216 a = 0.6 WITH FLAP

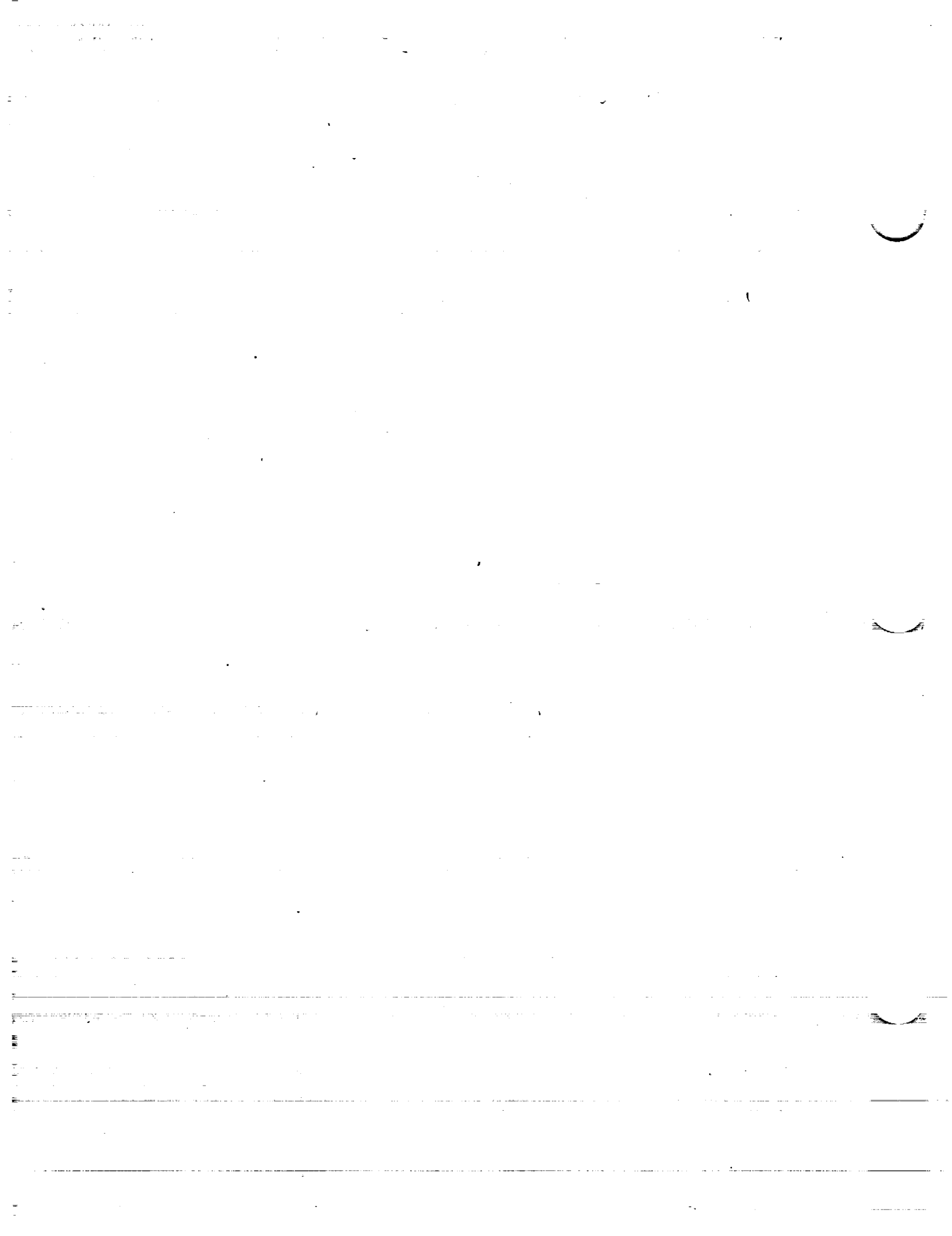


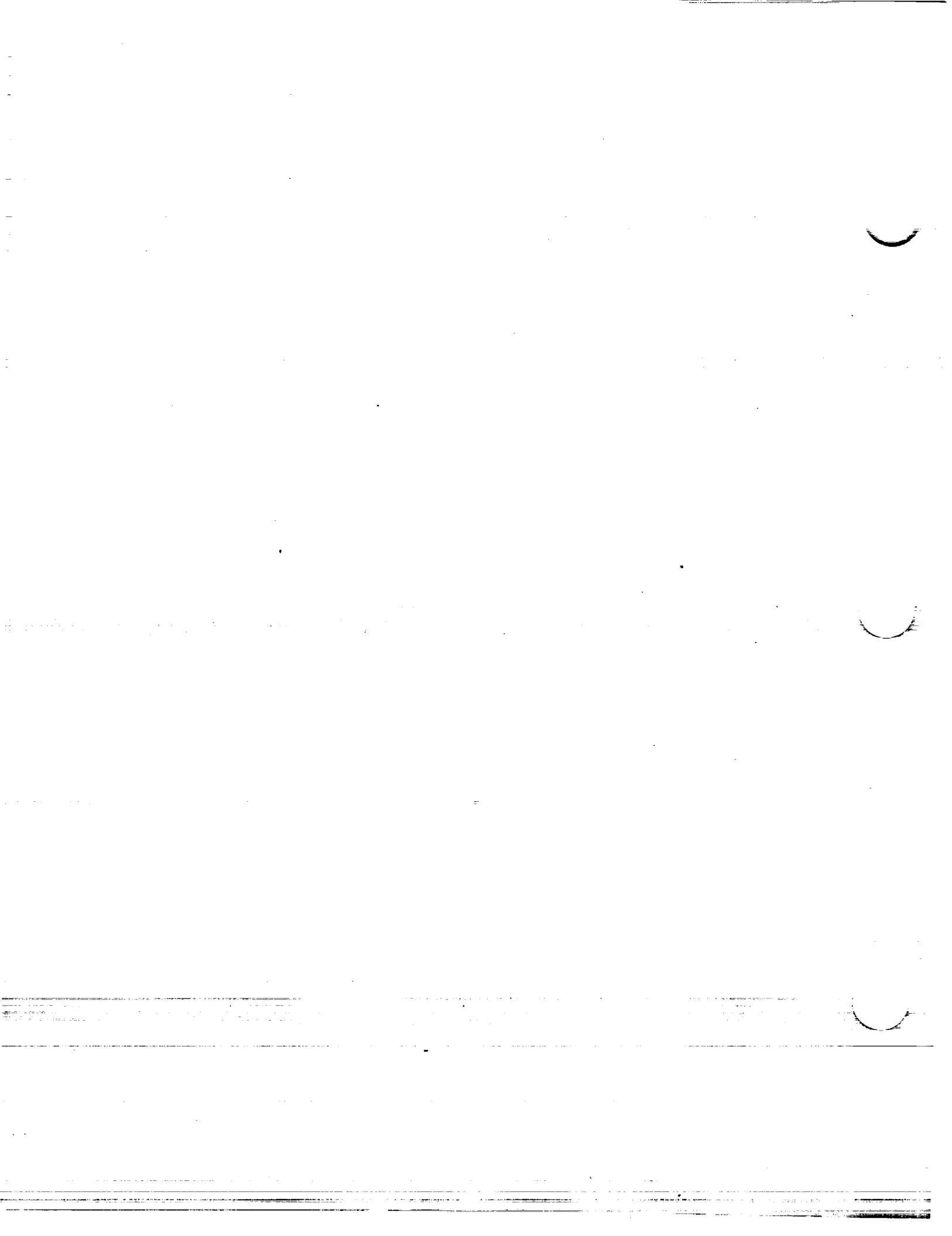
NATIONAL ADVISORY
COMMITTEE FOR AERONAUTICS

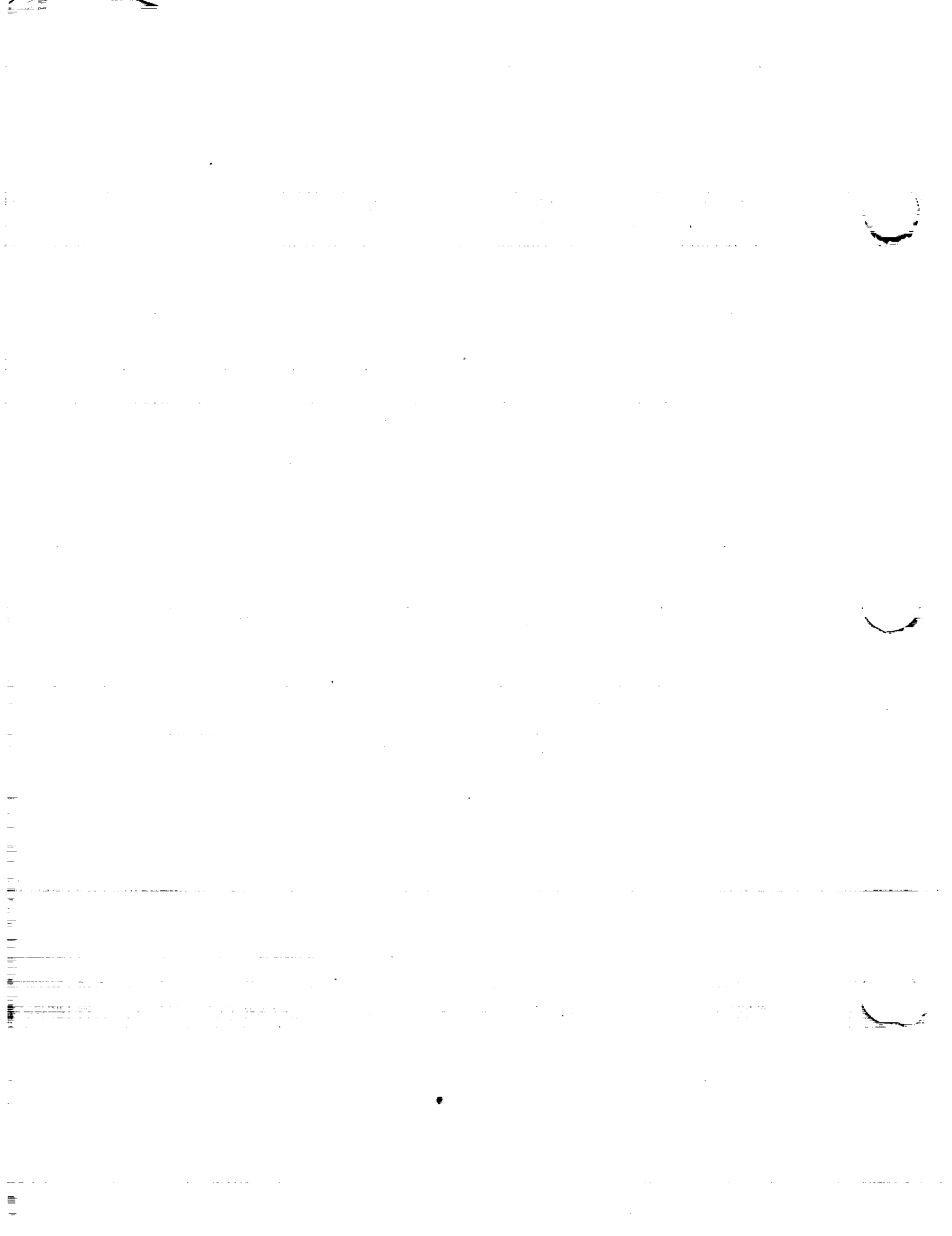
(e) Lift and moment characteristics. Slotted flap deflected 37° . $R, 6 \times 10^6$; TDT tests 236, 357, and 382. NACA 66(215)-216, $a = 0.6$ airfoil section with 0.30c slotted and 0.10c plain flap.



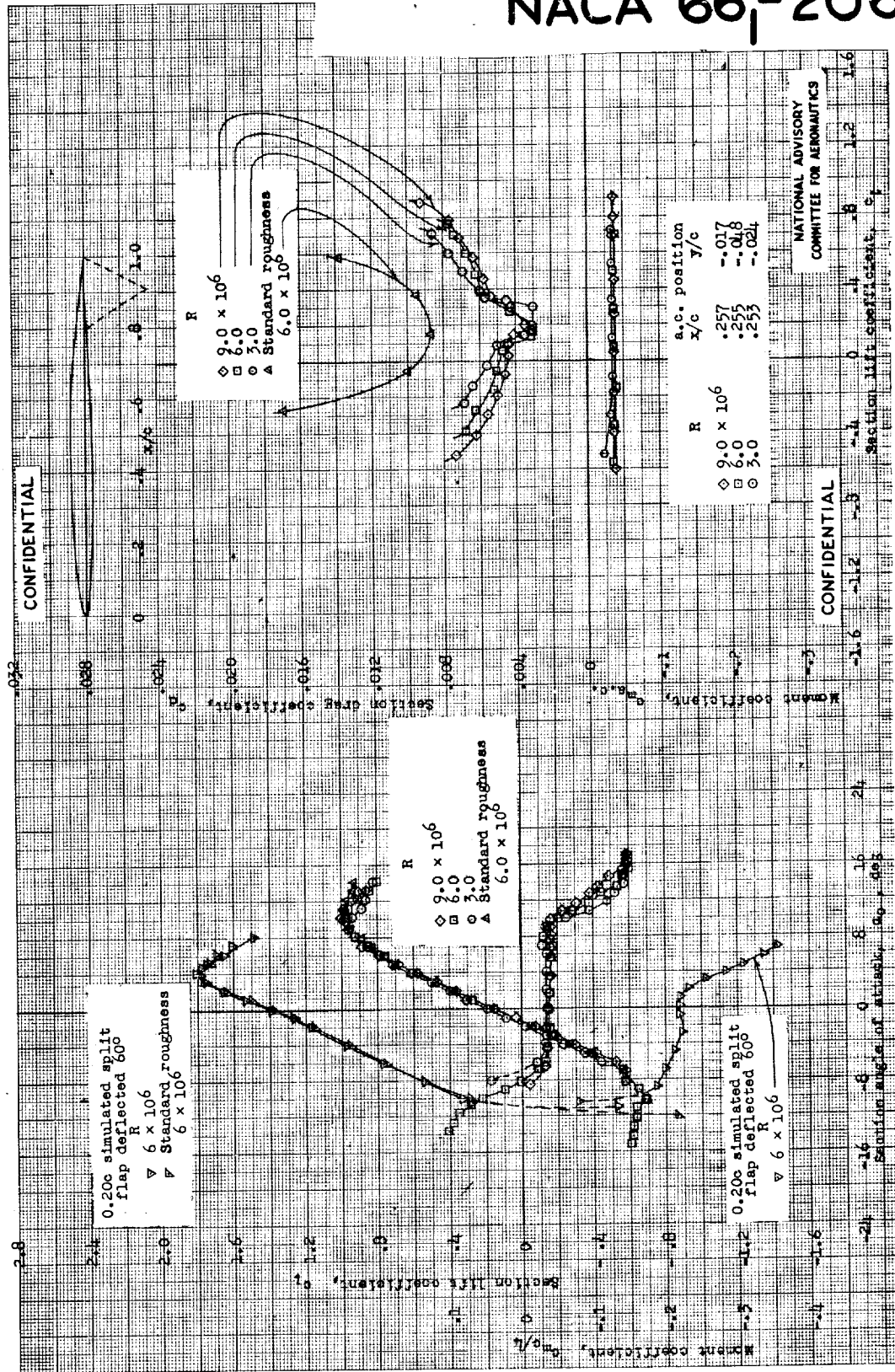




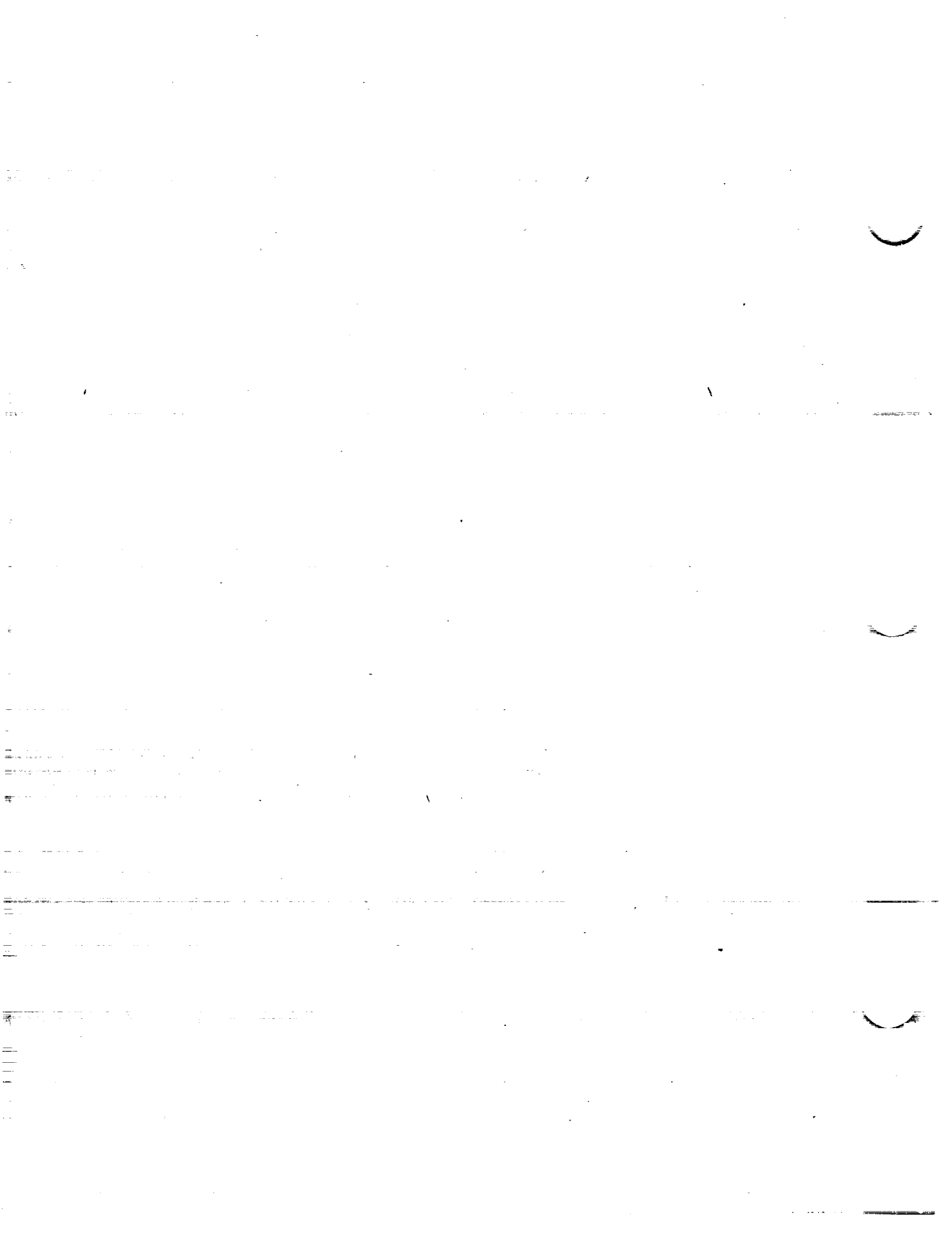




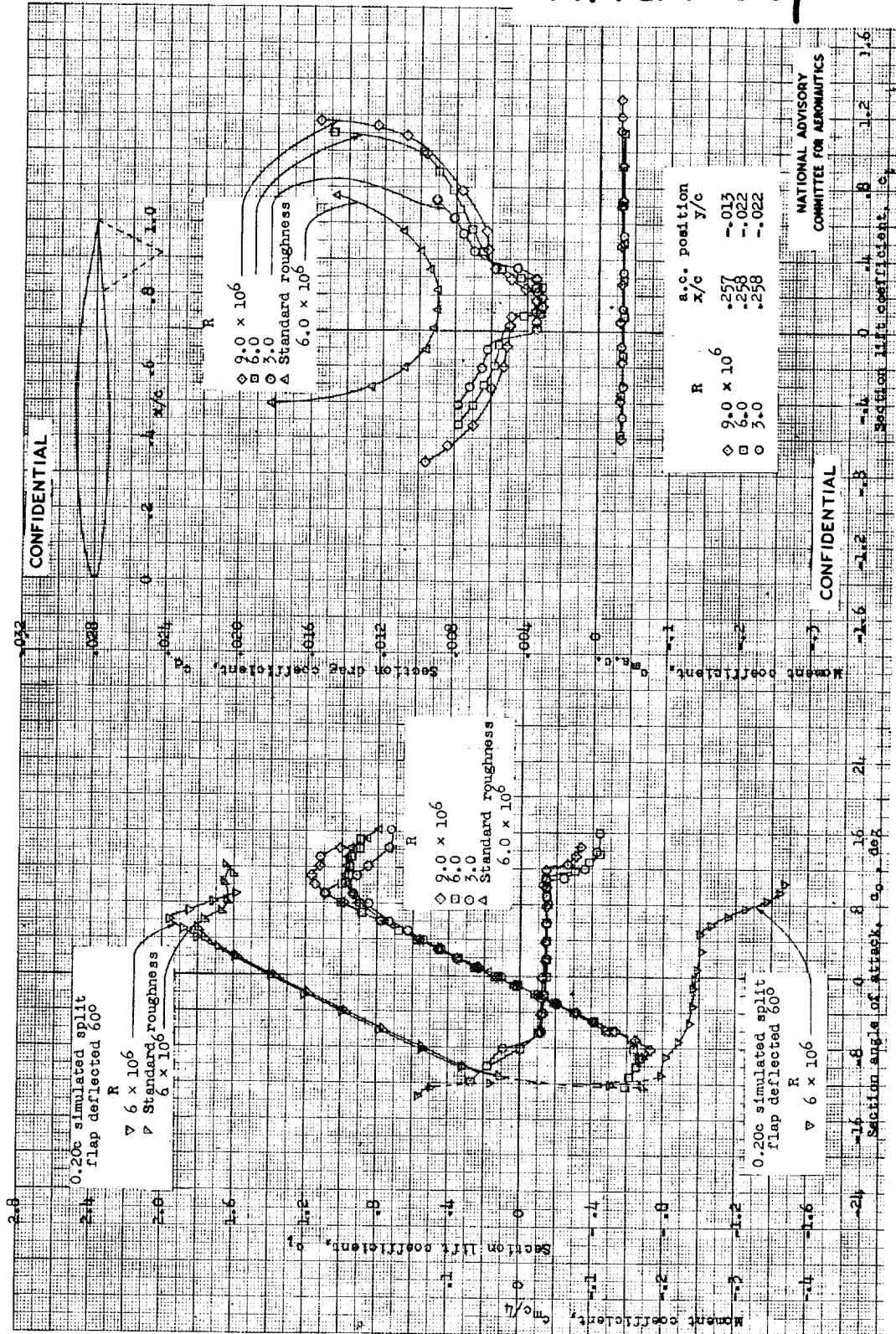
NACA 66₁-206



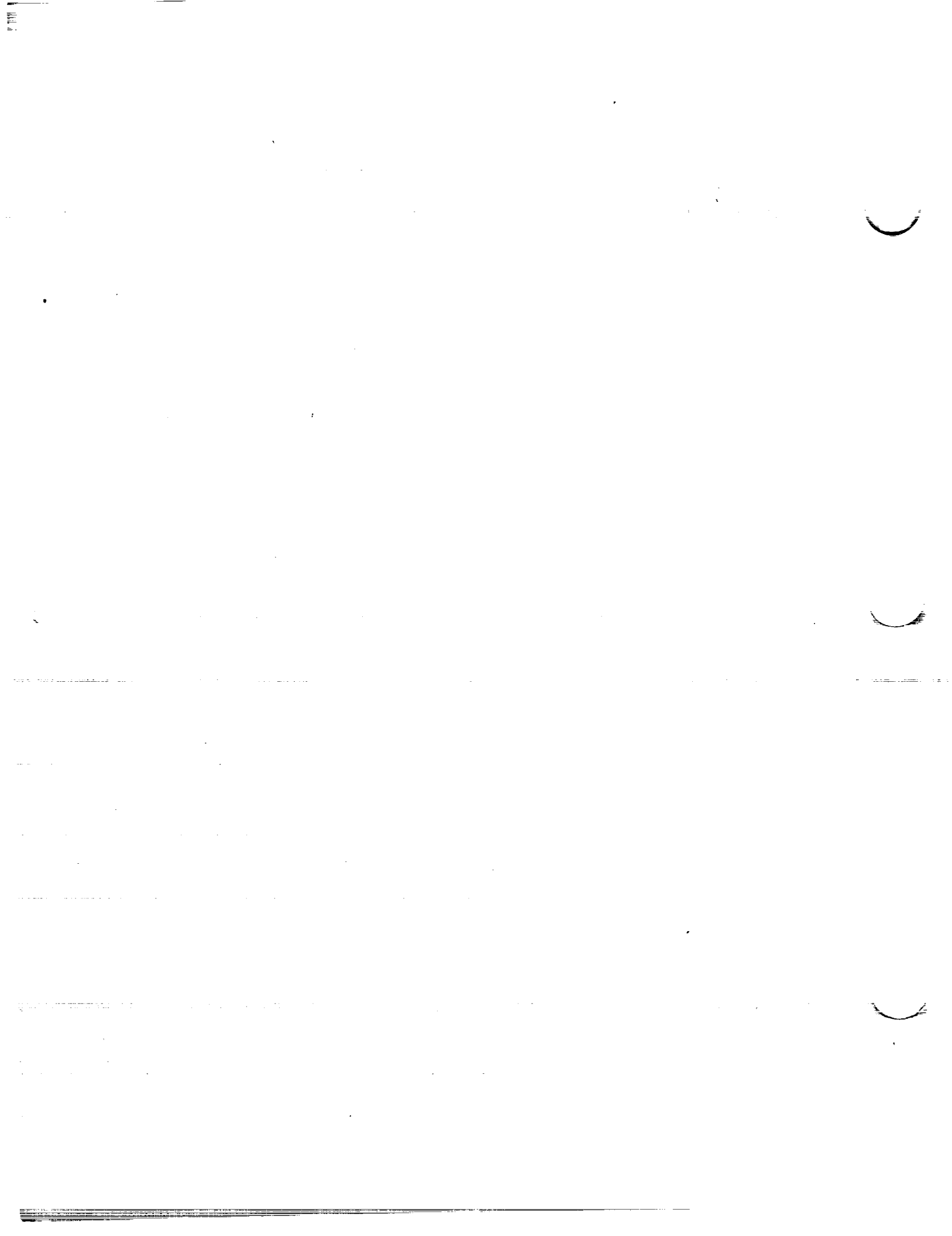
Aerodynamic characteristics of the NACA 66₁-206 airfoil section, 24-inch chord; TDT tests 806, 887.



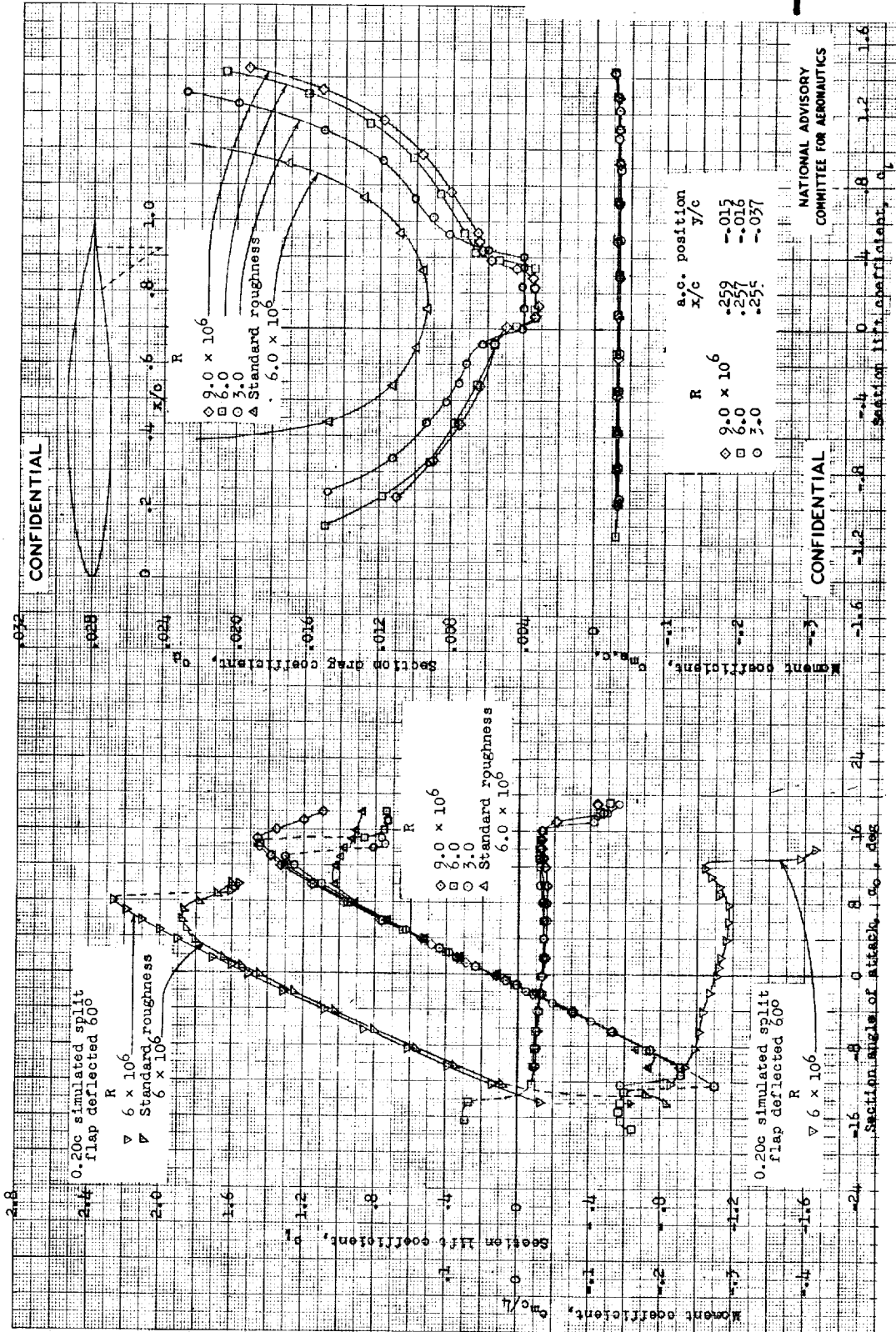
NACA 66-209



Aerodynamic characteristics of the NACA 66₁-209 airfoil section, 24-inch chord; TDR test 810.

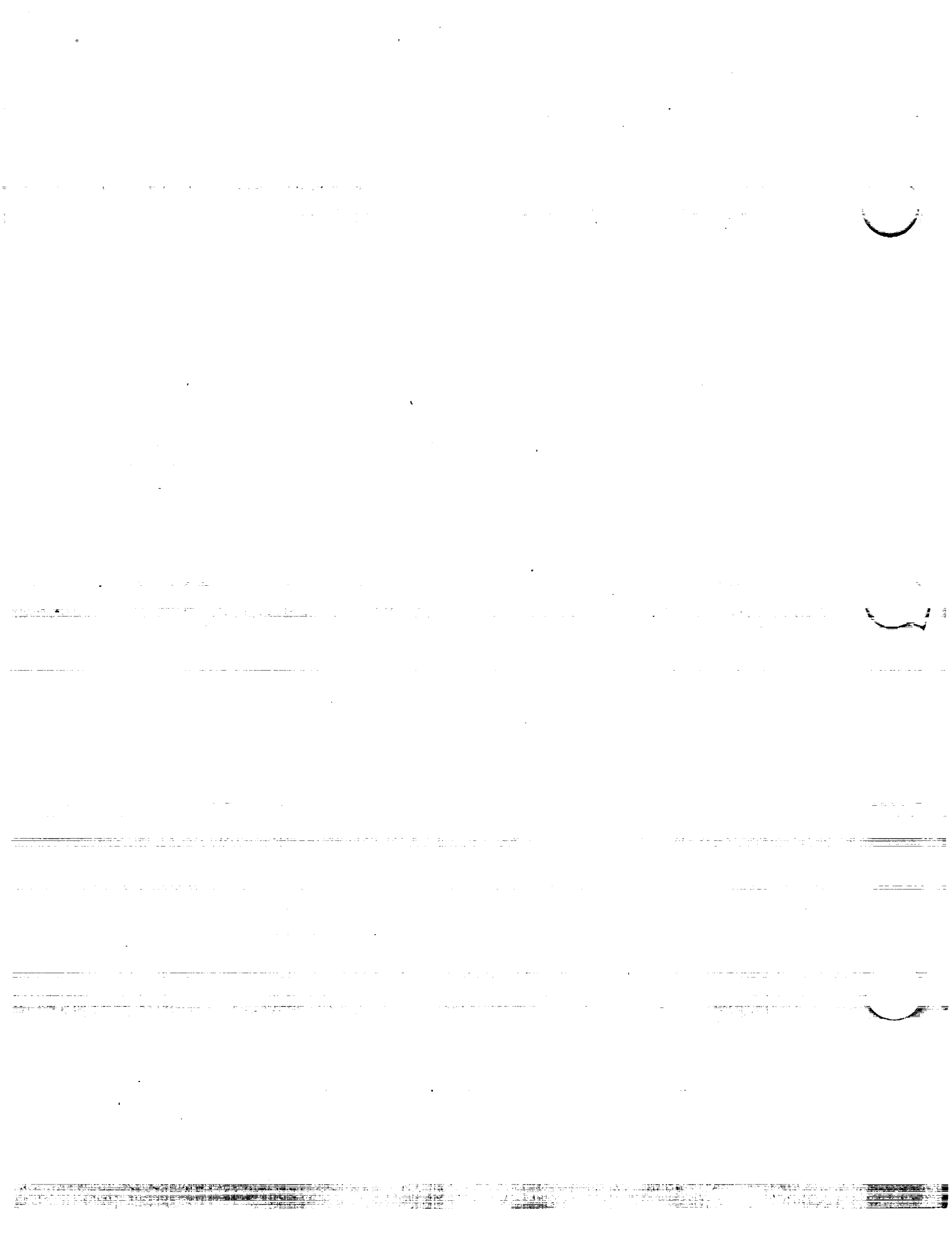


NACA 66-212

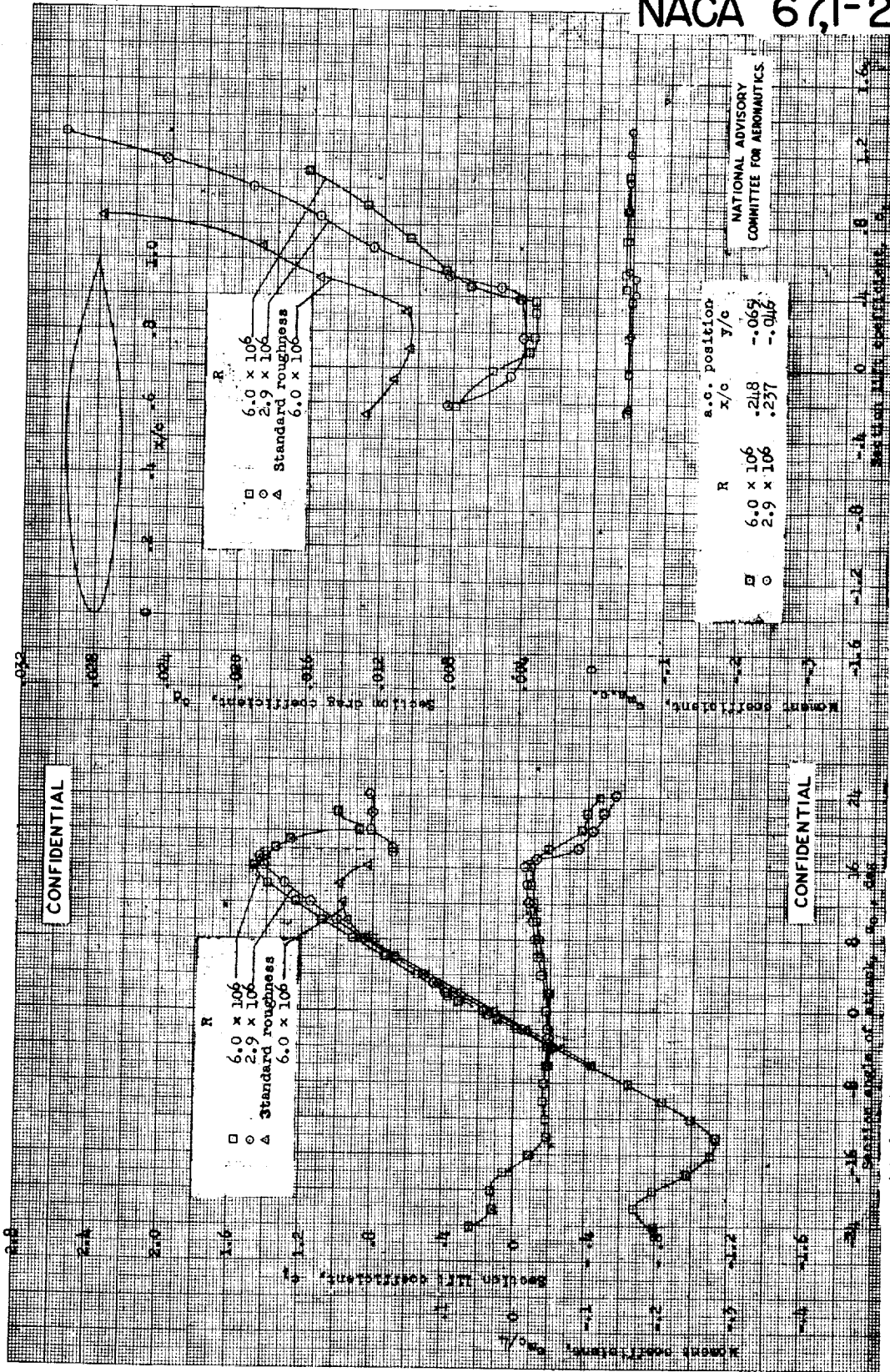


Aerodynamic characteristics of the NACA 66₁-212 airfoil section, 24-inch chord; TPR test 789.

NATIONAL ADVISORY
COMMITTEE FOR AERONAUTICS

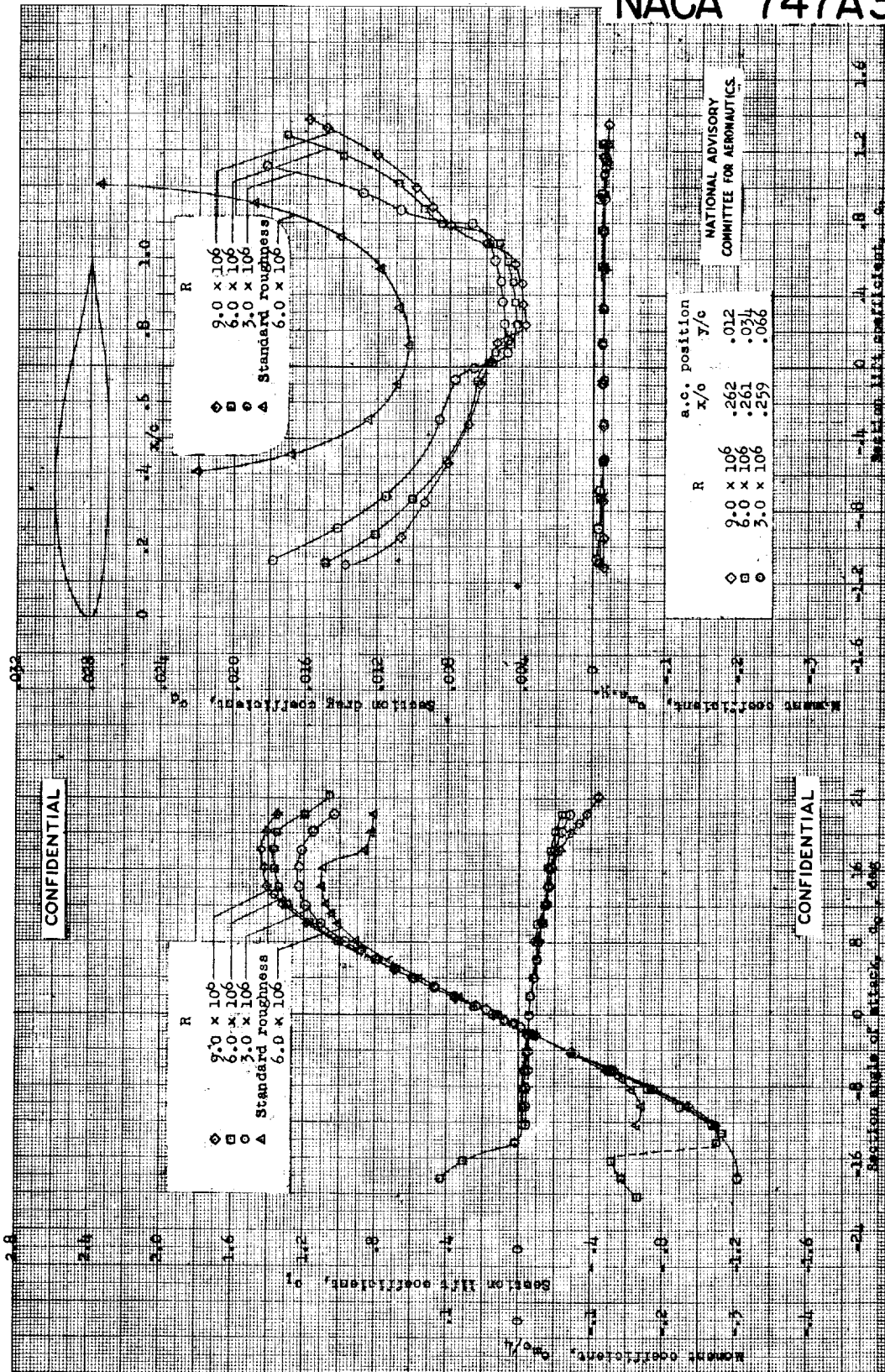


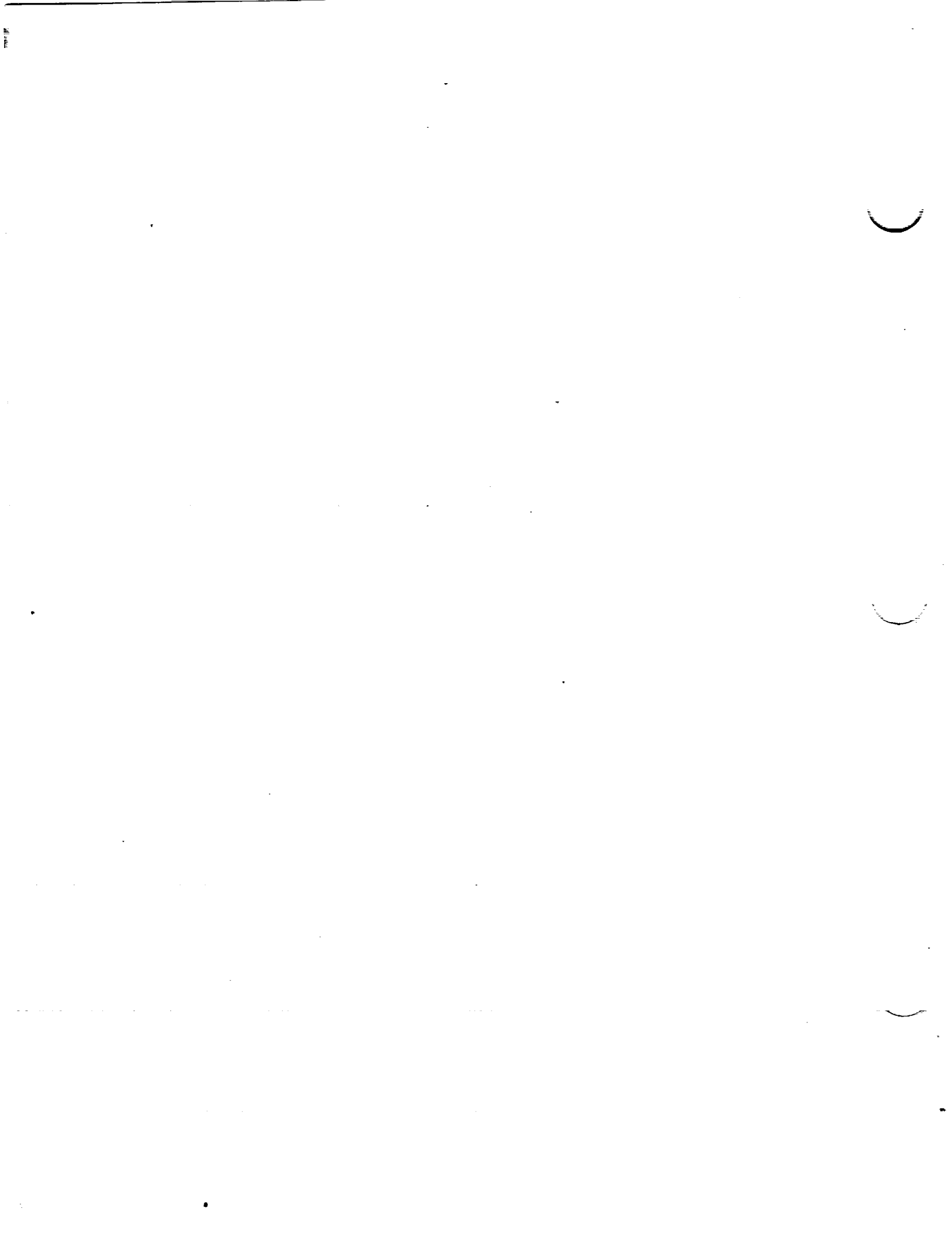
NACA 67,1-215





NACA 747A315





NACA 747A415

